รายงานวิจัยฉบับสมบูรณ์

แนวทางใหม่สำหรับการรักษากลุ่มเชื้อดื้อยา “ESKAPE”

โดยใช้โมเดล *Pseudomonas aeruginosa*

รองศาสตราจารย์ ดร. นิตยา อินทราวัฒนา

คณะเวชศาสตร์เขตร้อน

มหาวิทยาลัยมหิดล

มิถุนายน พ.ศ. 2562

สัญญาเลขที่ RSA5980048

รายงานวิจัยฉบับสมบูรณ์

แนวทางใหม่สำหรับการรักษากลุ่มเชื้อดื้อยา “ESKAPE” โดยใช้โมเดล *Pseudomonas aeruginosa*

รองศาสตราจารย์ ดร. นิตยา อินทราวัฒนา

คณะเวชศาสตร์เขตร้อน

มหาวิทยาลัยมหิดล

สนับสนุนโดยสำนักงานกองทุนสนับสนุนการวิจัย

และมหาวิทยาลัยมหิดล

กิตติกรรมประกาศ

โครงการวิจัยเรื่อง “แนวทางใหม่สำหรับการรักษากลุ่มเชื้อดื้อยา “ESKAPE” โดยใช้โมเดล Pseudomonas aeruginosa” นี้ได้รับทุนอุดหนุนจากสำนักงานกองทุนสนับสนุนการวิจัย (สกว.) และมหาวิทยาลัยมหิดล ผู้วิจัยขอขอบพระคุณให้การสนับสนุนทุนวิจัยและให้โอกาสผู้วิจัยได้ทำงานวิจัย

ผู้วิจัยขอขอบคุณบุคคลที่มีส่วนสนับสนุนจนทำให้การวิจัยของโครงการนี้สำเร็จสมบูรณ์ตามวัตถุประสงค์ที่ตั้งไว้ดังนี้ ศาสตราจารย์ ดร. วันเพ็ญ ชัยคำภา ที่ได้ช่วยให้ข้อเสนอแนะแนวทางในการดำเนินงาน ขอบคุณ นักวิจัย ผู้ช่วยวิจัย นักศึกษา และเจ้าหน้าที่ภาควิชาจุลชีววิทยาและอิมมิวโนโลยี คณะเวชศาสตร์เขตร้อนมหาวิทยาลัยมหิดลที่ร่วมทำงานในโครงการวิจัยนี้และดำเนินงานได้สำเร็จลุล่วงตามแผนที่วางไว้

Abstract

Project Code: RSA5980048

Project Title: Novel approach for combating a clique of multi-drug resistant "ESKAPE": a *Pseudomonas aeruginosa* model

Investigator: Associate Professor Dr. Nitaya Indrawattana

E-mail Address: nitaya.ind@mahidol.ac.th

Project Period: June 2016-June 2019

ESKAPE is an acronym of Enterococcus faecium, Staphylococcus aureus, Klebseilla pneumoniae, Acinetobacter baumannii, Pseudomnas aeruginosa and Enterbacter species which are common causative agents of life-threatening nosocomial infections among critically ill and immunocompromised individuals. These microorganisms are endowed with new paradigms in pathogenesis, transmission, and drug resistance. Currently, there is an urgent/immediate need of a broadly effective agent that can cope with these multi-drug resistant (MDR) pathogens. In this study a novel approach to combat with the MDR ESKAPE is proposed by using *P. aeruginosa* as a model for proving of concept. Engineered human single chain antibodies (human scFv) or humanized-nanobodies specific to the bacterial virulence factors including invasin (elastase), toxin (exotoxin A; ETA) and quorum sensing molecules (N-acyl-L-homoserine lactones; C12-HSL) were produced in vitro by using phage display technology. The HuscFv tested for their neutralizing activities by using several functional versus functional inhibition assays. Molecular mechanisms leading to the neutralizing capacity of the small antibodies were investigated by using phage mimotope search and computerized homology modeling and intermolecular docking. It is envisaged that the so-produced fully human scFv or humanized-nanobodies in their right mixture should be a safe and novel remedy for combating against the drug resistant pathogen. Similar approach can be adopted for inventing prototypic therapeutics for other members of the ESKAPE and other pathogens.

Keywords: AHLs, Biofilm, Elastase, Exotoxin A, Human monoclonal scFv/nanobodies, Pseudomonas aeruginosa, Quorum sensing

บทคัดย่อ

รหัสโครงการ: **RSA5980048**

ชื่อโครงการ: แนวทางใหม่สำหรับการรักษากลุ่มเชื้อดื้อยา “ESKAPE” โดยใช้โมเดล *Pseudomonas aeruginosa*

ชื่อนักวิจัย: รองศาสตราจารย์ ดร.นิตยา อินทราวัฒนา

อีเมล์: nitaya.ind@mahidol.ac.th

ระยะเวลาโครงการ: มิถุนายน 2559 – มิถุนายน 2561

ESKAPE คือชื่อของกลุ่มแบคทีเรียที่ประกอบด้วย *Enterococcus faecium*, *Staphylococcus aureus*, *Klebseilla pneumoniae*, *Acinetobacter baumannii*, *Pseudomnas aeruginosa* และ *Enterbacter* ซึ่งแบคทีเรียกลุ่มนี้เป็นสาเหตุที่พบได้บ่อยที่ก่อให้เกิดการติดเชื้อในผู้ป่วยในโรงพยาบาล โดยเฉพาะอย่างยิ่งผู้ป่วยที่มีภาวะภูมิคุ้มกันบกพร่อง แบคทีเรียกลุ่มนี้มีการแพร่กระจายไปทั่วโลก อีกทั้งยังมีแนวโน้มการดื้อต่อยาปฏิชีวนะที่ใช้รักษาเพิ่มขึ้นเรื่อยๆ และรวมถึงกลุ่มเชื้อแบคทีเรียที่ดื้อยาปฏิชีวนะหลายชนิด (Multi-drug resietance, MDR) ในปัจจุบันมีความต้องการเร่งด่วนและทันทีเพื่อหาวิธีการรับมือกับเชื้อโรคที่ดื้อยาปฏิชีวนะเหล่านี้ ในการศึกษาครั้งนี้ได้นำเสนอแนวทางใหม่ในการต่อสู้กับ MDR-ESKAPE โดยใช้ *P. aeruginosa* เป็นแบบจำลอง โดยทำการผลิตแอนติบอดีสายเดี่ยวของมนุษย์ (human scFv) ด้วยเทคนิค phage display library ซึ่งแอนติบอดีที่ผลิตได้นี้ความจำเพาะต่อปัจจัยความรุนแรงของแบคทีเรีย เช่น elastase (LasB), exotoxin A (ETA, recombinant ETA, recombinant-ETA-subdomains) and quorum sensing molecules (N-acyl-L-homoserine lactones; C12-HSL) ซึ่งพบว่า ETA-bound HuscFvs จำนวน 3 โคลน สามารถยับยั้ง ETA ในการเหนี่ยวนำให้เกิด apoptosis ของ mammalian cell และ C12-HSL-bound HuscFvs จำนวน 4 โคลน สามารถยับยั้ง C12-HSL ในการเหนี่ยวนำให้เกิด apoptosis ของเซลล์ด้วยเช่นกัน และ LasB-bound HuscFvs จำนวน 2 โคลน สามารถยับยั้งการทำงานของ LasB เมื่อทำการตรวจสอบโครงสร้างของ specific HuScFv กับ antigen ด้วยโปรแกรมคอมพิวเตอร์จะพบ HuScFv จับกับส่วนที่เป็น active site ของแอนติเจนจึงทำให้สามารถยับยั้งการทำงานของแอนติเจนได้ ผลจากการศึกษานี้ชี้ให้เห็นว่า HuscFvs มีประสิทธิภาพมีศักยภาพสูงและปลอดภัย ซึ่งสามารถนำมาพัฒนาเป็นวิธีการรักษาการติดเชื้อ *P. aeruginosa* และแบคทีเรียชนิดอื่นๆ ได้

Keywords: AHLs, Biofilm, Elastase, Exotoxin A, Human monoclonal scFv/nanobodies, *Pseudomonas aeruginosa*, Quorum sensing

Executive Summary

"ESKAPE" is an acronym of a clique of bacteria which are efficiently 'escaping' the bacteriocidal actions of most, if not all, currently available antibiotics. ESKAPE encompasses both Gram-positive and Gram-negative microorganisms including: ***E****nterococcus faecium*, ***S****taphylococcus aureus*, ***K****lebseilla pneumoniae*, ***A****cinetobacter baumannii*, ***P****seudomnas aeruginosa* and ***E****nterbacter* species". These bacteria are common causes of life-threatening nosocomial infections among critically ill and immunocompromised individuals. They are endowed with new paradigms in pathogenesis, transmission, and drug resistance (Rice *et al*., 2008, 2010). In 2004, The Infectious Diseases Society of America (IDSA) proposed solution in its policy report: **"Bad Bugs, No Drugs: Antibiotic R&D Stagnates, a Public Health Crisis Brews"** and more recently the IDSA issued a **"Call of Action"** to provide an update on the scope of the ESKAPE problem and the proposed solutions to fight against them. A primary objective of these IDSA reports is to encourage a community and legislative response to establish greater financial parity between the antimicrobial development (to cope with the mounting threat of the antimicrobial resistance) and the development of other drugs. However, after a decade of extensive development, a number of antibacterials produced by many major pharmaceutical companies in phase 2 or 3 of clinical trials remain disappointing. At this time, there have been no systematically administered antimicrobials in advanced development that have activity against bacteria already resistant to most or all currently available antibacterials (Boucher HW *et al.,* 2009). As such, there is an urgent/immediate need of a broadly effective agent that can cope with these multi-drug resistant (MDR) pathogens.

In this research proposal, a novel approach to combat the ESKAPE is proposing using *Pseudomonas aeruginosa* as a model for the proof of concept. The *P. aeruginosa* was chosen as the ESKAPE representative because the rates of infection by the drug resistant strains are increasing worldwide. Patients at risk include those in the intensive care units, particularly if they are ventilator dependent, and individuals with cystic fibrosis, cancers, diabetes, trauma, surgery, as well as neonatal infants. *P. aeruginosa* is the second most common cause of health care-associated pneumonia and the leading cause of pneumonia in pediatric patients in the intensive care units (Richards MJ, *et al*., 1999; Gaynes R, Edwards JS, 2005). It is also dominant Gram-negative group of bacteria which cause urosepsis, the most severe clinical manifestation of urinary tract infection (Kalra OP, Raizada A, 2009). In Thailand, the surveillance of hospital acquired infections from Khon-Kaen hospital showed that *P. aeruginosa* is the majority of clinical isolates accounting for 11.31%, followed by *S. aureus* (10.12%), and *A. baumannii* (9.52%). High prevalence of this agent was also reported from National Nosocomial Infections Surveillance (NNIS) system and the observations in Lumpang and Siriraj hospitals (Sakunee S and Khamoun P, 2007).

In this proposed research, engineered human monoclonal single chain antibody (scFv) and/or humanized-nanobodies specific to the *P. aeruginosa* virulence factors including enzyme, toxin, and quorum sensing molecules, that neutralize the respective bacterial targets will be produced. It is envisaged that the so-produced small antibodies in their right mixture should be a safe and novel remedy for combating against the drug resistant pathogen. Similar approach can be adopted for inventing therapeutics for other members of the ESKAPE and other pathogens.

Literature review

P. aeruginosa:

P. aeruginosa is a Gram-negative bacillus that is motile by a single polar flagellum. It is a common causative agent in healthcare settings which accounts for ~14% of all hospital-acquired infections and ~20% of the reported causative agents in the intensive care units (ICUs) where it is the principal cause of death among patients with cystic fibrosis, cancer, severe burns, diabetes, trauma, surgery, and neonates (Driscoll JA *et al*., 2007; Gellatly SL. and Hancock RE., 2013). The fatality rate in these patients is near to 50 percent (Todar K, 2004; Fujitani S *et al*., 2011). *P. aeruginosa* is ubiquitous in the environment, soil, water, vegetation and animals. The bacteria are found on skin and in throat and stool of normal subjects. It can be introduced into hospitals by foods, visitors, and patients referred from other clinical settings. Hospital utilities such as respiratory equipment, implanted medical devices such as intubation tubes and stents, sinks, taps, toilets, showers, and mops are reservoirs of the bacteria. Transmission occurs from patient to patient *via* the hand of healthcare worker, patients' contact with the bacterial reservoirs, and by ingestion of contaminated food and drink. *P. aeruginosa* requires minimal nutrients and can tolerate a wide variety of physical conditions. It forms biofilm on the surface which renders them refractory to antibacterial treatment and harsh environment. The prevalence of biofilm-related chronic diseases especially chronic rhinosinusitis (Prince AA *et al*., 2008) is on a rise. About 65% of bacterial infections in human are associated with biofilm forming bacteria (Post JC *et al*., 2004).

Virulence factors of *P. aeruginosa*:

P. aeruginosa can grow in various host environments and causes different types of infections due to its ability to produce a variety of virulence factors including adhesins, exotoxins, toxic enzymes, effector proteins, pigments and biofilm (Japoni A, Farshad S, and Alborzi A, 2009; Gellatly SL and Hancock RE, 2013). Some of them are mentioned below:

1. Adhesins

P. aeruginosa adheres to the epithelial cell by using its fimbriae to bind to specific receptors such as galactose, mannose, or sialic acid receptors normally present on the

epithelial cells (Prince A, 1992; Gellatly SL and Hancock RE, 2013). It may need enzymes to help in digesting away the host extracellular matrix (please see below) and expose the appropriate receptors on the epithelial cell surface. After attachment, the bacterium multiplies (colonizes) and secrete a variety of virulence factors. Tissue injury (*e.g.,* trauma, wound, surgery, some underlying conditions) may facilitate the bacterial colonization such as in the respiratory tract, eyes, and urinary tract---this step is called "Opportunistic adherence". Some strains of *P. aeruginosa,* called mucoid strains produce exopolysaccharides (repeating polymers of mannuronic acid and glucuronic acid; algenate) that have additional or alternative role as adhesin. The algenate forms a slime that makes up matrix of the bacterial **biofilm,** which protects the cells from the environmental stress, hose defenses, and antibiotics (Ramphal R *et al*., 1980; Paraje M, 2011). *P aeruginosa* strains that form biofilm are most often found in the lungs of patients with cystic fibrosis (Lee B *et al*., 2005; Sousa AM and Pereira MO, 2014).

2. Invasins

P. aeruginosa produces two proteases, namely **alkaline protease** and **elastase** which involved in the bacterial invasion and pathogenesis. Alkaline protease lyses fibrin. Both elastase and alkaline protease destroy the extracellular matrix of cornea and other structures composed of fibrin and elastin. They inactivate gamma interferon and tumor necrosis factor. Elastase is a neutral zinc metalloprotease that cleaves collagen, digests IgG and IgA and complement protein, lyses fibronectin to expose the host receptors for bacterial attachment, disrupts the respiratory epithelium and interferes with the ciliary function. This enzyme is encoded by *lasB* gene. The 33 kDa elastase is initially synthesized as a 53 kDa pre-proenzyme which is processed to mature form *via* a 51 kDa pro-elastase intermediate. Elastase has been crystallized and its three-dimensional (3D) structure was determined (Thaley MM *et al*., 1991). The enzymatic active site required for substrate interaction and catalysis are conserved, *i.e.,* Glu141, Tyr155 and His223. The zinc ligands in *P. aeruginosa* elastase are His140, His144 and Glu164 (Bever RA *et al*., 1988; McIver K *et al*., 1991). Asp189-Arg179 and Asp201-Arg205 stabilize the enzyme at the expense of catalytic activity and Glu249 is important for catalytic efficiency, stability and unfolding co-operativity of the molecule. **Figure 1** illustrates 3D structure of *P. aeruginosa* elastase (Bian F *et al*., 2015).

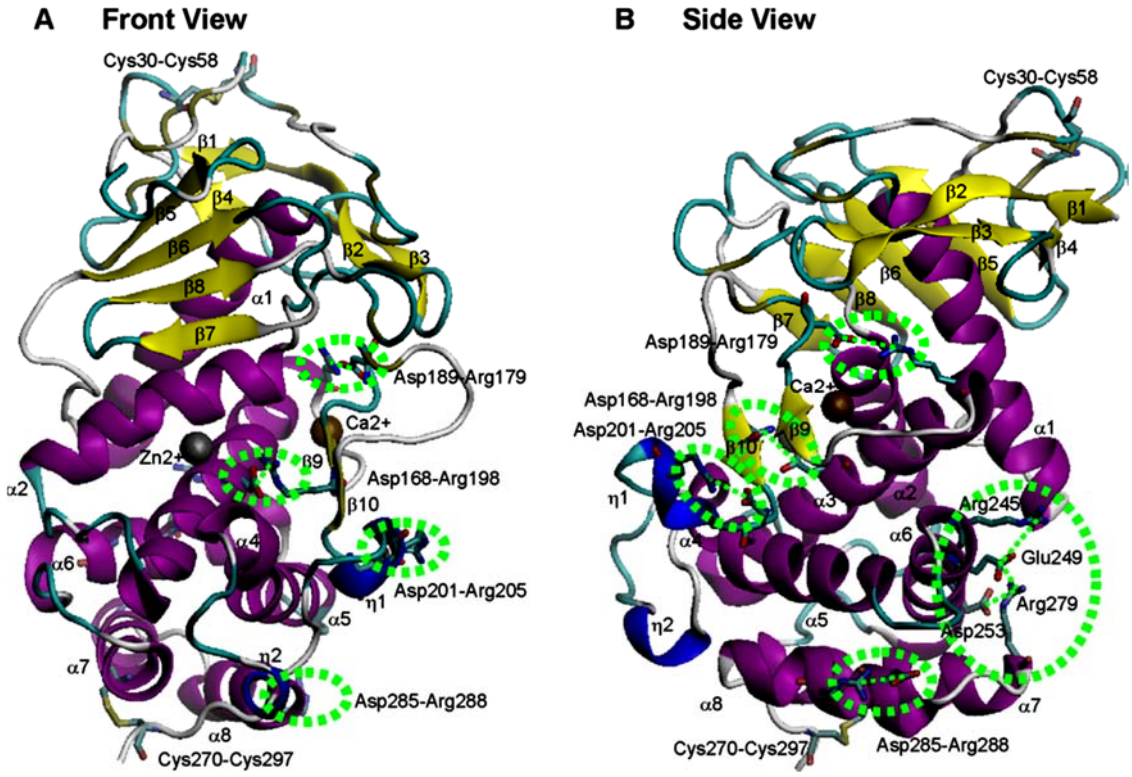

Figure 1: (A) Front view. (B) Side view of *P. aeruginosa* elastase. Green circles indicate salt bridges.

Source: Bian F *et al.* (2015)

Because of its multifunctional pathogenic activities that are detrimental to the infected patients, *P. aeruginosa* elastase is an attractive target of a therapeutic. The agent that neutralizes the enzyme should not only mitigate the symptom severity caused by the *P. aeruginosa* infection but may also restore the host immunity by rescuing both the innate (such as complement functions, respiratory epithelial barrier and ciliary movement) as well as the adaptive immunity. As far as the literature review, there has been neither drug nor inhibitor that neutralizes this enzyme and could be used as human therapeutic. Therefore, this research proposal aims to produce human single chain antibody (HuscFv) or humanized-nanobodies that neutralizes the elastase activities by targeting specifically the catalytic residues, its zinc ligands and/or other residues important for structural stability of the enzyme.

P. aeruginosa produces **pore-forming cytotoxin** that is toxic to most eukaryotic cells. It kills neutrophils in particular (Sun Y *et al*., 2012). *P. aeruginosa* produces two **hemolysins**, phospholipase and lecithinase which beak down lipid and lecithin (Ruxana T *et al*., 2005). The two hemolysins and the cytotoxins enable the bacteria to invade the host tissues through their cytotoxic effects to neutrophils, lymphocytes and other cells.

P. aeruginosa blue pigments called **pyocyanin** impairs normal function of nasal cilia, disrupt respirator epithelium and instigates proinflammatory response (Gudis D, Zhao K, and Cohen AN, 2012). Its derivative, called **pyochelin** is a siderophore that sequesters iron from the bacterial environment and permit growth of the bacteria in an iron-limited environment (Adler C *et al*. 2012).

3. Toxins

P. aeruginosa produces two extracellular toxic enzymes, *i.e*., **exoenzyme S (ExoS)** and **exotoxin A (ETA).** The **ExoS** acts as an antiphagocytiic factor that enabling the bacteria to evade the host immunity (Frithz-Lindsten E *et al*., 1997). ExoS is characterized as ADP-ribosylating enzyme which this activity is located at the C-terminus of the protein (Iglewski BH *et al.*, 1978; Knight DA *et al.*, 1995). Currently, ExoS is known as a bifunctional enzyme. It is a type-III secretion effector which includes both a GTPase-activating protein activity toward the Rho family of the small G family protein and an ADP-ribosyltransferase activity that targets multiple substrates, including low molecular weight G proteins Ras, RalA, certain Rab proteins, Rac1, and cdc42. ExoS exerts complex effects on eukayotic cell functions including inhibition of DNA synthesis, alteration of cell morphology, microvillus effacement, and loss of cellular adherence in addition to its anti-phagocytic effect.

Exotoxin A of *P. aeruginosa* (acronym ETA) belongs to the family of enzymes termed mono(ADP-ribosyl)transferases. ETA is a 66 kDa extracellular protein (Beattie BK *et al.*, 1996). It enters eukaryotic cells by receptor-mediated encocytosis (Sanyal G *et al*., 1993). Once it reaches the cytoplasm, catalyzes ADP-ribosylation of eukaryotic elongation factor-2 (eLF-2). This ADP-ribosylation inactivates the eLF-2, resulting in the inhibition of host protein synthesis and ultimately leading to cellular death (Beattie BK *et al*., 1996) which is the same mechanism as the diphtheria toxin. Nevertheless, the ETA and diphtheria toxin are antigenically distinct. The ETA causes also necrotizing activity at the site of *P. aeruginosa* colonization. Purified ETA is highly lethal to animals, including primates and humans.

The 3D structure of ETA shows that it contains three distinct functional domains: receptor-binding (domain-1), translocation (domain-2) and catalysis (domain-3) (Allured VS *et al.*, 1986; Wedekind JE *et al.*, 2001). The catalytic mechanism of the ETA has been revealed by Armstrong *et al*. in 2002 (Armstrong S *et al.*, 2002). The catalytic domain (residues 400-613) is responsible for the inactivation of the eLF-2 by catalyizing the transfer of ADP-ribosyl moiety from NAD+ to eLF-2. The important catalytic residues for ETA are Glu553, His440, Tyr 481 and Tyr470. **Figure 2** shows 3D structure of the *P. aeruginosa* exotoxin A.

In this study, human scFv or humanized nanobodies (VH/V_HH) specific to domains 1-3 of the ETA will be produced. For the ETA domain-3 (catalytic domain) that functions in cytoplasm, the human scFvs/humanized-VH/V_HH will be made into cell penetrable antibodies (transbodies) by molecular linking to the cell penetrable peptides such as nonaarginines (R9) or penetratin before use in the enzyme neutralization assay.

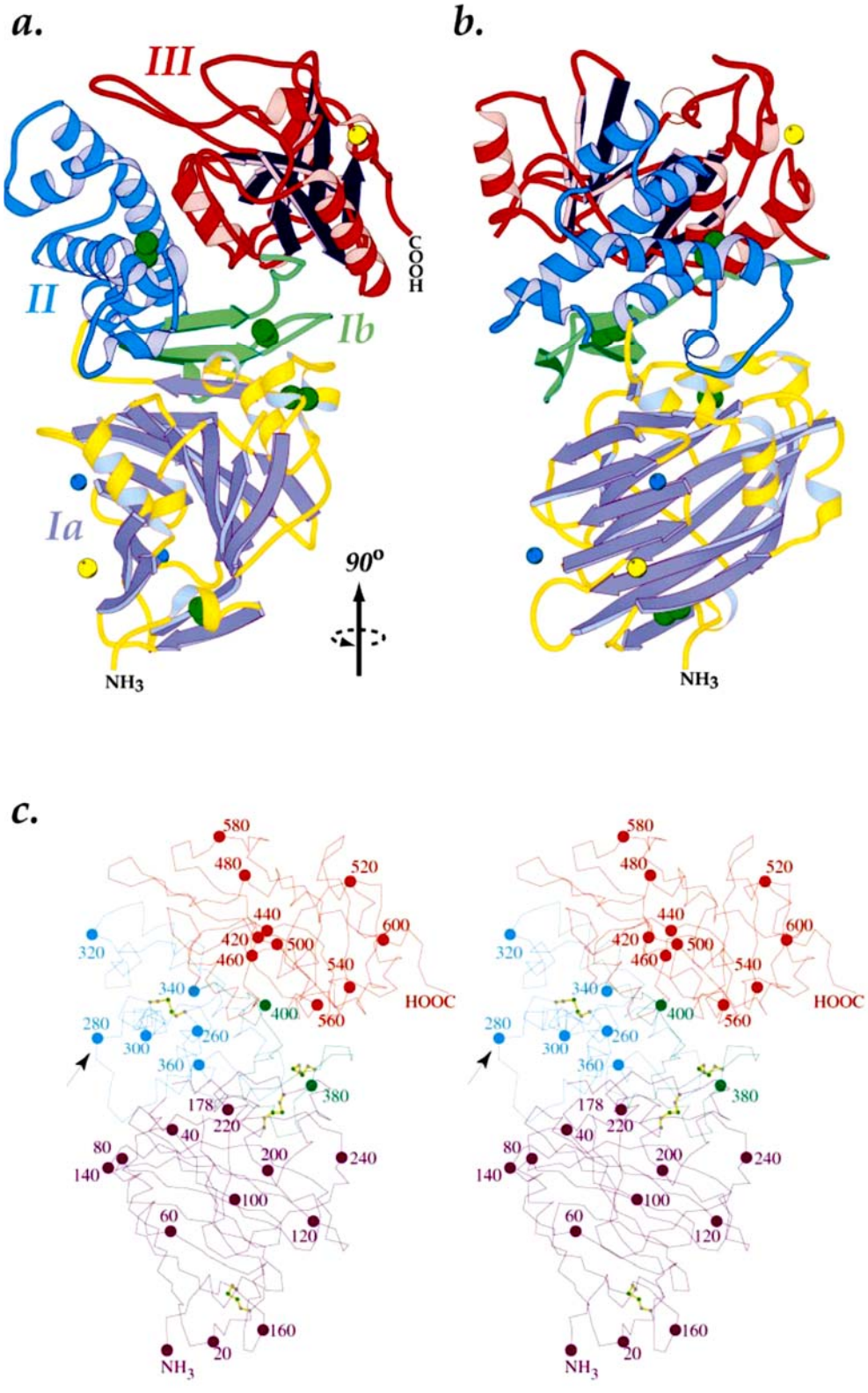
a.
III
II
Ib
Ia
COOH
NH3
90°
b.
NH3
c.
580
480
520
440
420
500
600
460
540
320
340
400
560
HOOC
280
300
260
360
380
178
220
40
80
200
240
140
100
60
120
160
20
NH3
580
480
520
440
420
500
600
460
540
320
340
400
560
HOOC
280
300
260
360
380
178
220
40
80
200
240
140
100
60
120
160
20
NH3

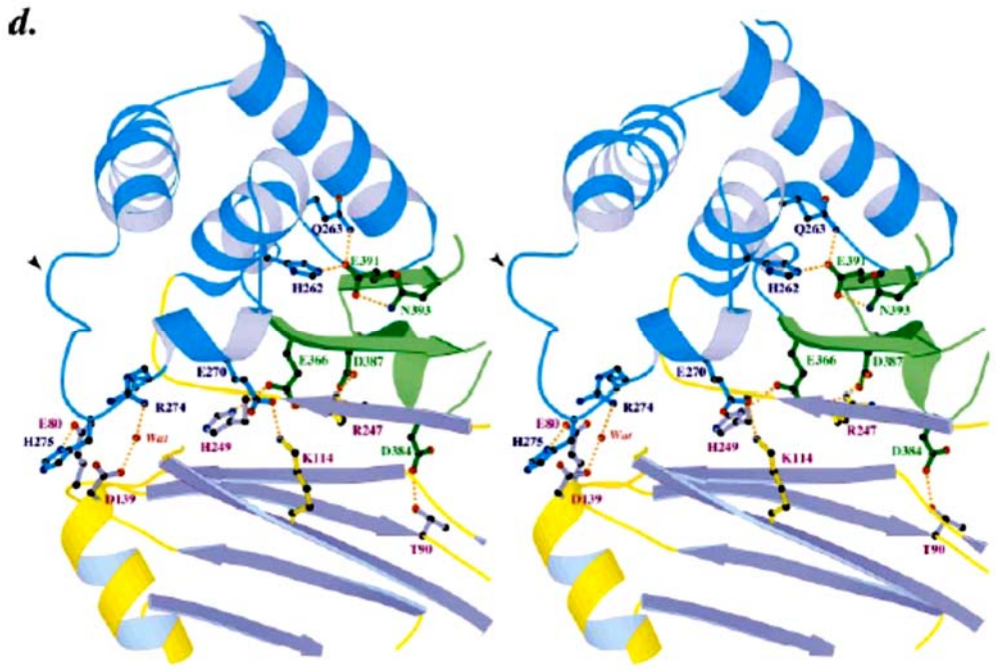

Figure 2: Three dimensiona structure of *P. aeruginosa* Exotoxin A. **(a)** Ribbon drawing of the tri-partite domain organization: domain Ia (1-252), purple β-sheet, yellow α-helices and coils; domain Ib (365-404), green β-sheet and coil; domain II (253-364), light blue β-sheet and coil; and domain III (405-613), red α-helix and coil, blue β-sheet. Cyan CPK spheres represent Na ions; yellow CPK spheres represent Cl ions; disulfide positions are indicated as green spheres. **(b)** Ribbon drawing rotated 90 degrees from orientation in (a). **(c)** Stereographic Ca representation. Spherical main-chain atom positions are numbered every 20 amino acid residues. Color scheme and orientation based on (a). Disulfide positions are indicated as ball-and-stick side-chains. Arrow heads indicate the site of furin cleavage. **(d)** Stereographic representation of the ionic (salt-bridge) interactions at the interface between domains I and II. Broken lines indicate potential ionic interactions between side-chains that are likely to be disrupted under acidic conditions. Arrow heads indicate the site of furin cleavage. The orientation and color scheme are similar to that of (a).

Source: Wedekind JE *et al*., 2001

4. Quorum sensing in *P. aeruginosa*

Quorum sensing (QS) is chemical communication process that bacteria use to regulate collective behaviors. *P. aeruginosa* uses quorum sensing to control virulence and biofilm formation. The bacteria generate small diffusible molecules called **autoinducers** for signaling the population density. The rising in numbers of the cell population leads to increased concentration of autoinducers. After a sufficient level of autoinducer is reached, it binds to transcriptional regulators and promotes the target gene expressions (Smith RS and Iglewski BH., 2003). For *P. aeruginosa,* there are two kinds of the signal molecules; one is N-acyl-L-homoserine lactones (AHLs) and another is 4-quinolones. The AHLs are the most

studied examples of quorum sensing that found in Gram-negative bacteria. They differ among bacteria but they all present the same basic part that is an acyl chain of variable length, normally from 4-16 carbons (Sharma G *et al*., 2014; Penesyan A *et al*., 2015). Blocking the quorum sensing autoinducers should limit the bacterial communication which should ultimately inhibit expressions of virulence factors and biofilm formation. **Thus, in this study, human scFvs and/or humanized nanobodies that interfere with the *P. aeromonas* quorum sensing molecules will be produced.**

Engineered antibodies

Recombinant antibodies including intact IgG or its fragments: scFv (VH-linker-VL), Fab and F(ab)'$_2$, have been used for treatment and intervention of diseases including cancers, autoimmune diseases, allergies, infections, toxemia, intoxication, and envenomation (Cheng WW and Allen TM, 2010, Li F *et al*.,2014, Wand S *et al*., 2014, Madritsch C *et al*., 2015, Chulanetra M *et al*., 2012). The advantage of the antibodies is that they use multiple complementarity determining regions (CDRs) and several amino acid residues in individual CDRs to interact with the targets molecules; thus making it difficult for the targets especially the pathogens to develop antibody resistant mutants. Nowadays, antibody engineering and molecular biology have made possible the invention of therapeutic monoclonal antibody with a desired structure, *e.g*., chimeric human-mouse antibody which the mouse Fc is replaced by human counterpart, or the use of only mouse Fab/F(ab)'$_2$ or VH-linker-VL (single chain antibody; scFv); all of which had much reduced immunogenicity in human recipients. Moreover, an antibody phage display technology has been a useful tool for producing a fully human monoclonal antibody devoid of immunogenicity in human in the form of either scFv or Fab fragments without the requirement of *in vivo* immunization (Winter *et al*., 1994). Nowadays, human single chain variable antibody fragments (human scFv/HuscFv) have been used extensively in research and therapy (Bird *et al*., 1988; Huston *et al*., 1988; Kulkeaw *et al*., 2009). Each scFv fragment (~25-35 kDa) contains complete antigen binding site of antibody, *i.e.,* VH and VL domains which are covalently linked by a flexible peptide linker usually 15-20 amino acids long, *e.g.,* $(Gly_4/Ser)_3$ (Whitlow M *et al*., 1993). The HuscFvs have broad applications in medicine (Huston JS *et al*., 1993; Hudson, 1999). The unique and highly specific antigen-binding ability of the scFv have been exploited to block toxic enzymes/toxins/venom (Indrawattana N *et al*., 2010; Danpaiboon W *et al.,* 2014; Thueng-in K *et al*., 2014).

Recently, camelid derived single domain antibodies (sdAb) and humanized-sdAbs (VHs/V_HHs or nanobodies), have proven to be forceful enzyme inhibitors (Conrath *et al*., 2001;

Lauwereys *et al*., 1998; Thanongsaksrikul *et al*., 2011; Chavanayarn *et al.*, 2012; Thueng-in *et al*., 2012; Jittavisutthikul S *et al.*, 2015). The VH and V_HH are the variable antigen-binding parts of the heavy chain of conventional four chain antibody and heavy chain antibody (HCAb), respectively. Gene coding the sdAb can be constructed and induced to express the recombinant protein in soluble form which still retains the original antigen recognition capability. The superior enzyme inhibitory mechanism of the VH/V_HH over the conventional antibodies was proved by crystallographic studies which showed that the V_HH CDRs, especially the CDR3, penetrated into the active site pockets of the enzymes which never be reached by Fv (paratope constituted by VL+CL and VH+CH1) of the conventional four chain antibody (Desmyter *et al*., 2001; De Gents E *et al*., 2006; Thanongsaksrikul *et al*., 2010). The VH and V_HH are small (~15-20 kDa) and stable molecules with improved solubility and similar target affinity to the conventional antibodies (Harmsen M and De Haard, 2007). These properties make them promisingly attractive molecules for use in prophylaxis and treatment of diseases caused by toxic enzymes.

Literature Cited

Introduction

Boucher HW, Talbot GH, Bradley JS, Edwards JE, Gilbert D, Rice LB, *et al*. Bad bugs, no drugs: no ESKAPE! An update from the Infectious Diseases Society of America. Clin Infect Dis. 2009;48(1):1-12.

Kalra OP, Raizada A. Approach to a patient with urosepsis. J Glob Infect Dis. 2009;1(1):57.

Richards MJ, Edwards JR, Culver DH, Gaynes RP. Nosocomial infections in pediatric intensive care units in the United States. Pediatrics. 1999;103(4):e39.

Rice LB. Federal funding for the study of antimicrobial resistance in nosocomial pathogens: no ESKAPE. J Infect Dis. 2008;197(8):1079-81.

Rice LB. Progress and challenges in implementing the research on ESKAPE pathogens. Infect Control. 2010;31(S1):S7-S10.

Sakunee S, Khamoun P. Nosocomial Infection in Department of Pediatrics, Khon Kaen Hospital. Khon Kaen Medical Journal 2007;31(2):143-55.

Weinstein RA, Gaynes R, Edwards JR, System NNIS. Overview of nosocomial infections caused by gram-negative bacilli. Clin Infect Dis. 2005;41(6):848-54.

Literature review

Pseudomonas aeruginosa

Driscoll JA, Brody SL, Kollef MH. The epidemiology, pathogenesis and treatment of *Pseudomonas aeruginosa* infections. Drugs 2007; 67(3): 351-68.

Fujitani S, Sun H-Y, Victor LY, Weingarten JA. Pneumonia due to *Pseudomonas aeruginosa*: part I: epidemiology, clinical diagnosis, and source. CHEST Journal. 2011;139(4):909-19.

Gellatly SL, Hancock RE. *Pseudomonas aeruginosa*: new insights into pathogenesis and host defenses. Pathog Dis. 2013; 67(3): 159-73.

Post JC, Stoodley P, Hall–Stoodley L, Ehrlich GD. The role of biofilms in otolaryngologic infections. Curr Opin Otolaryngol Head Neck Surg. 2004; 12(3): 185-90.

Prince AA, Steiger JD, Khalid AN, Dogrhamji L, Reger C, Chiu AG, et al. Prevalence of biofilm-forming bacteria in chronic rhinosinusitis. Am J Rhinol. 2008; 22(3): 239-45.

Todar K. *Pseudomonas aeruginosa*. Todar's Online Textbook of Bacteriology University of Wisconsin-Madison Department of Bacteriology [en línea]. 2004.

Virulence factors of *P. aeruginosa*

Adler C, Corbala´n SN, Seyedsayamdost RM, Pomares FM, Cristo´bal E de R, Clardy J, Kolter R, Vincent AP. Plos One. 2012;7(10):e46754.

Allured VS, Collier RJ, Carroll SF, McKay DB. Structure of exotoxin A of *Pseudomonas aeruginosa* at 3.0-Angstrom resolution. Proceedings of the National Academy of Sciences. 1986;83(5):1320-4.

Armstrong S, Yates SP, Merrill AR. Insight into the Catalytic Mechanism of *Pseudomonas aeruginosa* Exotoxin A studies of toxin interaction with eukaryotic elongation factor-2. J Biol Chem. 2002;277(48):46669-75.

Beattie BK, Prentice GA, Merrill AR. Investigation into the catalytic role for the tryptophan residues within domain III of *Pseudomonas aeruginosa* exotoxin A. Biochemistry. 1996;35(48):15134-42.

Bever RA, Iglewski BH. Molecular characterization and nucleotide sequence of the *Pseudomonas aeruginosa* elastase structural gene. J Bacteriol. 1988;170(9):4309-14.

Bian F, Yue S, Peng Z, Zhang X, Chen G, Yu J, *et al*. A comprehensive alanine-scanning mutagenesis study reveals roles for salt bridges in the structure and activity of *Pseudomonas aeruginosa* elastase. PLoS One. 2015;10(3):e0121108.

Frithz-Lindsten E, Du Y, Rosqvist R, Forsberg Å. Intracellular targeting of exoenzyme S of *Pseudomonas aeruginosa* via type III-dependent translocation induces phagocytosis resistance, cytotoxicity and disruption of actin microfilaments. Mol Microbiol. 1997;25(6):1125-39.

Gellatly SL, Hancock RE. *Pseudomonas aeruginosa*: new insights into pathogenesis and host defenses. Pathog Dis. 2013; 67(3): 159-73.

Gudis D, Zhao K, and Cohen AN.Acquired cilia dysfunction in chronic rhinosinusitis. Am J Rhinol Allergy. 2012;26(1):1–6.

Iglewski BH, Sadoff J, Bjorn MJ, Maxwell ES. *Pseudomonas aeruginosa* exoenzyme S: an adenosine diphosphate ribosyltransferase distinct from toxin A. Proceedings of the National Academy of Sciences. 1978;75(7):3211-5.

Japoni A, Farshad S, Alborzi A. *Pseudomonas aeruginosa*: Burn infection, treatment and antibacterial resistance. Iranian Red Crescent Medical Journal. 2009;2009(3):244-53.

Knight DA, Finck-Barbançon V, Kulich SM, Barbieri JT. Functional domains of *Pseudomonas aeruginosa* exoenzyme S. Infect Immun. 1995;63(8):3182-6.

Lee B, Haagensen JA, Ciofu O, Andersen JB, Høiby N, Molin S. Heterogeneity of biofilms formed by nonmucoid *Pseudomonas aeruginosa* isolates from patients with cystic fibrosis. J Clin Microbiol. 2005;43(10):5247-55.

McIver K, Kessler E, Ohman D. Substitution of active-site His-223 in *Pseudomonas aeruginosa* elastase and expression of the mutated lasB alleles in *Escherichia coli* show evidence for autoproteolytic processing of proelastase. J Bacteriol. 1991;173(24):7781-9.

Paraje M. Antimicrobial resistance in biofilms. Science against microbial pathogens: communicating current research and technological advances A Méndez-Vilas (Ed), Formatex. 2011.

Prince A. Adhesins and receptors of *Pseudomonas aeruginosa* associated with infection of the respiratory tract. Microb Pathog. 1992;13(4):251-60.

Ramphal R, Small P, Shands J, Fischlschweiger W, Small P. Adherence of P*seudomonas aeruginosa* to tracheal cells injured by influenza infection or by endotracheal intubation. Infect Immun. 1980;27(2):614-9.

Ruxana T. Sadikot, Timothy S. Blackwell, John W. Christman, and Alice S. PrincePathogen–Host Interactions in Pseudomonas aeruginosa Pneumonia. Am J Respir Crit Care Med. 2005;171(11):1209–23.

Sanyal G, Marquis-Omer D, Gress JOB, Middaugh CR. A transforming growth factor-. alpha.-*Pseudomonas* exotoxin hybrid protein undergoing pH-dependent conformational changes conducive to membrane interaction. Biochemistry. 1993;32(13):3488-97.

Sousa AM, Pereira MO. *Pseudomonas aeruginosa* diversification during infection development in cystic fibrosis lungs-a review. Pathogens. 2014;3(3):680-703.

Sun Y, Mausita Karmakar M, Taylor RP, Rietsch A, and Pearlman E. ExoS and ExoT ADP ribosyltransferase activities mediate *Pseudomonas aeruginosa* keratitis by promoting neutrophil apoptosis and bacterial survival.J Immunol.2012;188(4):1884-95.

Thayer M, Flaherty KM, McKay DB. Three-dimensional structure of the elastase of *Pseudomonas aeruginosa* at 1.5 Å resolution. J Biol Chem. 1991;266(5):2864-71.

Wedekind JE, Trame CB, Dorywalska M, Koehl P, Raschke TM, McKee M, *et al*. Refined crystallographic structure of *Pseudomonas aeruginosa* exotoxin A and its implications for the molecular mechanism of toxicity. J Mol Biol. 2001;314(4):823-37.

Quorum sensing in *P. aeruginosa*

Penesyan A, Gillings M, Paulsen IT. Antibiotic discovery: combatting bacterial resistance in cells and in biofilm communities. Molecules. 2015; 20(4): 5286-98.

Smith RS, Iglewski BH. *Pseudomonas aeruginosa* quorum sensing as a potential antimicrobial target. J Clin Invest. 2003;112(10):1460-65.

Sharma G, Rao S, Bansal A, Dang S, Gupta S, Gabrani R. *Pseudomonas aeruginosa* biofilm: potential therapeutic targets. Biologicals 2014;42(1):1-7.

Engineered antibodies

Bird RE, Hardman KD, Jacobson JW, Johnson S, Kaufman BM, Lee S-M, *et al*. Single-chain antigen-binding proteins. Science. 1988;242(4877):423-6.

Chavanayarn C, Thanongsaksrikul J, Thueng-In K, Bangphoomi K, Sookrung N, Chaicumpa W. Humanized-single domain antibodies (VH/V_HH) that bound specifically to *Naja kaouthia* phospholipase A2 and neutralized the enzymatic activity. Toxins (Basel). 2012;4(7):554-67.

Cheng WW, Allen TM.The use of single chain Fv as targeting agents for immunoliposomes: an update on immunoliposomal drugs for cancer treatment. Expert Opin Drug Deliv. 2010;7(4):461-78.

Chulanetra M, Bangphoomi K, Sookrung N, Thanongsaksrikul J, Srimanote P, Sakolvarvaree Y, Choowongkomon K, Chaicumpa W.Human ScFv that block sodium ion channel activity of tetrodotoxin. Toxicon. 2012;59(2):272-82.

Conrath KE, Lauwereys M, Galleni M, Matagne A, Frère J-M, Kinne J, et al. β-Lactamase inhibitors derived from single-domain antibody fragments elicited in the camelidae. Antimicrob Agents Chemother. 2001;45(10):2807-12.

Danpaiboon W, Reamtong O, Sookrung N, Seesuay W, Sakolvaree Y, Thanongsaksrikul J, *et al*. *Ophiophagus hannah* venom: Proteome, components bound by *Naja kaouthia* antivenin and neutralization by *N. kaouthia* neurotoxin-specific human ScFv. Toxins (Basel). 2014;6(5):1526-58.

De Genst E, Silence K, Decanniere K, Conrath K, Loris R, Kinne J, *et al*. Molecular basis for the preferential cleft recognition by dromedary heavy-chain antibodies. Proc Natl Acad Sci USA. 2006;103(12):4586-91.

Desmyter S, Vandenbussche F, Van Damme EJ, Peumans WJ. Preparation of monospecific polyclonal antibodies against *Sambucus nigra* lectin related protein, a glycosylated plant protein. Prep Biochem Biotechnol. 2001;31(3):209-16.

Filpula D. Antibody engineering and modification technologies.Biomol Eng. 2007 Jun;24(2):201-15.

Harmsen M, De Haard H. Properties, production, and applications of camelid single-domain antibody fragments. Appl Microbiol Biotechnol. 2007;77(1):13-22.

Hudson PJ. Recombinant antibody constructs in cancer therapy. Curr Opin Immunol. 1999;11(5):548-57.

Huston JS, Levinson D, Mudgett-Hunter M, Tai M-S, Novotný J, Margolies MN, *et al*. Protein engineering of antibody binding sites: recovery of specific activity in an anti-digoxin single-chain Fv analogue produced in *Escherichia coli*. Proc Natl Acad Sci USA. 1988;85(16):5879-83.

Huston JS, McCartney J, Tai M-S, Mottola-hartshorn C, Jin D, Warren F, *et al*. Medical applications of single-chain antibodies. Int Rev Immunol. 1993;10(2-3):195-217.

Indrawattana N, Sookrung N, Kulkeaw K, Seesuay W, Kongngoen T, Chongsa-nguan M, *et al*. Human monoclonal ScFv that inhibits cellular entry and metalloprotease activity of tetanus neurotoxin. Asian Pac J Allergy Immunol. 2010;28(1):85-93.

Jittavisutthikul S, Thanongsaksrikul J, Thueng-in K, Chulanetra M, Srimanote P, Seesuay W, *et al*. Humanized-V_HH Transbodies that Inhibit HCV Protease and Replication. Viruses. 2015;7(4):2030-56.

Kulkeaw K, Sakolvaree Y, Srimanote P, Tongtawe P, Maneewatch S, Sookrung N, et al. Human monoclonal ScFv neutralize lethal Thai cobra, Naja kaouthia, neurotoxin. J Proteomics. 2009;72(2):270-82.

Lauwereys M, Ghahroudi MA, Desmyter A, Kinne J, Hölzer W, De Genst E, *et al*. Potent enzyme inhibitors derived from dromedary heavy-chain antibodies. The EMBO journal. 1998;17(13):3512-20.

Li F, Meng F, Jin Q, Sun C, Li Y, Li H, Jin S.Fusion protein of single-chain variable domain fragments for treatment of myasthenia gravis.Neural Regen Res. 2014;9(8):851-6.

Madritsch C, Gadermaier E, Roder UW, Lupinek C, Valenta R, Flicker S.High-density IgE recognition of the major grass pollen allergen Phl p 1 revealed with single-chain IgE antibody fragments obtained by combinatorial cloning. J Immunol. 2015 Mar 1;194(5):2069-78.

Thanongsaksrikul J, Chaicumpa W. Botulinum neurotoxins and botulism: a novel therapeutic approach. Toxins (Basel). 2011;3(5):469-88.

Thanongsaksrikul J, Srimanote P, Maneewatch S, Choowongkomon K, Tapchaisri P, Makino S, *et al.* A V_HH that neutralizes the zinc metalloproteinase activity of botulinum neurotoxin type A. J Biol Chem. 2010;285(13):9657-66.

Thueng-in K, Thanongsaksrikul J, Jittavisutthikul S, Seesuay W, Chulanetra M, Sakolvaree Y, *et al*., editors. Interference of HCV replication by cell penetrable human monoclonal scFv specific to NS5B polymerase. mAbs; 2014: Taylor & Francis.

Thueng-In K, Thanongsaksrikul J, Srimanote P, Bangphoomi K, Poungpair O, Maneewatch S, *et al*. Cell penetrable humanized-VH/V_HH that inhibit RNA dependent RNA polymerase (NS5B) of HCV. 2012.

Wang S, Zhang P, He F, Wang JG, Sun JZ, Li ZL, Yi B, Xi J, Mao YP, Hou Q, Yuan DL, Zhang ZD, Liu WQ. Combination of specific single chain antibody variable fragment and siRNA has a synergistic inhibitory effect on the propagation of avian influenza virus H5N1 in chicken cells.Virol J. 2014;11:208.

Whitlow M, Bell BA, Feng S-L, Filpula D, Hardman KD, Hubert SL, *et al*. An improved linker for single-chain Fv with reduced aggregation and enhanced proteolytic stability. Protein Eng. 1993;6(8):989-95.

Winter G, Griffiths AD, Hawkins RE, Hoogenboom HR. Making antibodies by phage display technology. Annu Rev Immunol. 1994;12(1):433-55.

Hypothesis and Objectives

Hypotheses:

Human single chain antibodies (HuscFvs) and/or humanized-camel nanobodies that bind specifically to the critical region/residues of detrimental enzymes/toxins/signaling molecules of *P. aeruginosa* and interfere with their functions should mitigate the clinical symptom severity caused by the bacterial infection. The specific antibody fragments in their right mixture should have high potential as a safe and novel remedy for combating this deadly pathogen especially at present when a new class of antibiotics that effective against the multi-drug resistant pathogens is not yet available.

Ultimate objective: To produce human single chain antibodies/humanized-camel nanobodies that bind specifically to- and inhibit pathogenicity of- *P. aeruginosa* elastase, exotoxin A, and quorum sensing molecules, in order to test them further for human therapeutic use

Specific objectives

1. To produce recombinant *P. aeuginosa* elastase, exotoxin A (ETA) and domains 1,3 of the ETA
2. To test the inherent functional activities of the recombinant elastase and exotoxin A
3. To synthesize two different quorum sensing molecules (AHLs) of *P. aeruginosa*: biotin-labeled-N-(3-oxododecanoyl) homoserine lactone (3-oxo-C12-AHL) and biotin labeled-N-butyryl homoserine lactone (C4-AHL)
4. To select phage clones displaying human scFv/humanized-VH/V_HH that bound to the active elastase, exotoxin A, and synthetic AHLs from previously constructed human scFv/humanized-VH/V_HH phage display libraries
5. To transfect the appropriate *Escherichia coli* with the selected small antibody display phages
6. To screen the phage transformed *E. coli* for the presence antibody coding gene sequences (*huscfv/vh/*v_h*h*)
7. To express soluble human scFv/VH/V_HH from the *huscfv/vh/*v_h*h*-positive *E. coli* clones
8. To test the binding specificity of the soluble antibodies to the respective panning antigens
9. To sequence the antibody genes and determine the sequence diversity and CDRs and FRs sequences
10. To predict the residues and regions of the elastase and exotoxin A that would be bound by the human scFv by using phage mimotope search and computerized homology modeling and intermolecular docking

11. To set up the functional assays of the elastase, exotoxin A and quorum sensing molecules
12. To determine the efficiencies of the human scFv in neutralizing the bioactivities of the respective targets

Experiments and Results

1. Preparation of full length recombinant elastase, full length recombinant exotoxin A (ETA), and recombinant ETA domains 1-3

Designing the oligonucleotide primers for amplify gene fragments encoding the catalytic domain of pseudolysin (lasB) and staphylolsin (lasA)

The oligonucleotide primers for LasB gene and LasA gene (**Table 1.1**) were designed based on the sequence *Pseudomonas aeruginosa* elastase precursor (LasB) gene, complete cds, (GenBank accession no.M19472.1) (**Figure 1.1**). *Pseudomonas aeruginosa* staphylolytic protease preproenzyme LasA (LasA) gene, complete cds (GenBank accession no.U68175.1) (**Figure 1.2**). The catalytic domain of LasB and LasA have 930 bp and 570 bp in size, respectively. In this study, the researcher designs the synthetic primers which the 5'-end includes vector specific sequences and contains 3'-end overlapped with the sequence of LasB and LasA intended for cloning into the pLATE52 vector.

```
 901 tcagtgggaa ggcctggccc acgccgaggc gggcggcccc ggcggcaacc agaagatcgg
 961 caagtacacc tacggtagcg actacggtcc gctgatcgtc aacgaccgct gcgagatgga
1021 cgacggcaac gtcatcaccg tcgacatgaa cagcagcacc gacgacagca agaccacgcc
1081 gttccgcttc gcctgcccga ccaacaccta caagcaggtc aacggcgcct attcgccgct
1141 gaacgacgcg catttcttcg gcggcgtggt gttcaaactg taccgggact ggttcggcac
1201 cagcccgctg acccacaagc tgtacatgaa ggtgcactac gggcgcagcg tggagaacgc
1261 ctactgggac ggcacggcga tgctcttcgg cgacggcgcc accatgttct atccgctggt
1321 gtcgctggac gtggcggccc acgaggtcag ccacggcttc accgagcaga actccgggct
1381 gatctaccgc gggcaatcag gcggaatgaa cgaagcgttc tccgacatgg ccggcgaggc
1441 tgccgagttc tatatgcgcg gcaagaacga cttcctgatc ggctacgaca tcaagaaggg
1501 cagcggtgcg ctgcgctaca tggaccagcc cagccgcgac gggcgatcca tcgacaacgc
1561 gtcgcagtac tacaacggca tcgacgtgca ccactccagc ggcgtgtaca accgtgcgtt
1621 ctacctgttg gccaattcgc cgggctggga tacccgcaag gccttcgagg tgttcgtcga
1681 cgccaaccgc tactactgga ccgccaccag caactacaac agcggcgcct gcggggtgat
1741 tcgctcggcg cagaaccgca actactcggc ggctgacgtc acccgggcgt tcagcaccgt
1801 cggcgtgacc tgcccgagcg cgttgtaagc tcggtggtcc cggccggcac tccaggaagg
```

Figure 1.1 Nucleotide sequences of mature peptide of LasB gene of *Pseudomonas aeruginosa* that obtained from the NCBI database (GenBank accession no.M19472.1).

```
1441 gcaaccgcgt ggcccggcaa ctccaggcga aggccgcgct ggcgccgcca tccaacctga
1501 tgcaattgcc ctggcgccag ggctattcct ggcagcccaa cggagcgcat tcgaacaccg
1561 gctcgggcta tccgtactcg tccttcgatg cgtcctacga ctggccgcgc tggggcagtg
1621 cgacctacag cgtggtcgcc gcccacgccg gtacggtacg ggtgctgtcg cgctgccagg
1681 tacgggtgac ccaccccagc ggctgggcga ccaactacta ccatatggac cagatccagg
1741 tgagcaacgg ccagcaggtc agcgccgaca ccaagctcgg cgtctatgcc ggcaacatca
1801 acaccgcgct ctgcgagggt ggcagctcca ccggaccgca cctgcatttc tcgctgctct
1861 acaacggcgc cttcgtttcc ctgcagggcg ccagcttcgg tccgtaccgg atcaacgtcg
1921 gcaccagcaa ctacgacaac gactgtcgcc gctactattt ctacaaccag agcgccggca
1981 ccacccattg cgctttccgt ccgttgtaca accccggcct ggcgctctga gtcggcgcgg
```

Figure 1.2 Nucleotide sequences of mature peptide of LasA gene of *Pseudomonas aeruginosa* that obtained from the NCBI database (GenBank accession no. U68175.1).

Table 1.1 Oligonucleotide primers used for amplify pseudolysin (LasB) and staphylolsin (LasA) from *Pseudomonas aeruginosa* PAO 1 strain.

Primer name	Oligonucleotide sequences (5'-3')
F-PAO1/LasB	GGTTGGGAATTGCAAGCCGAGGCGGGCGGCCCCGGC
R-PAO1/LasB	GGAGATGGGAAGTCATTACAACGCGCTCGGGCAGGTCACGCCGACG
F-PAO1/LasA	GGTTGGGAATTGCAAGCGCCGCCATCCAACCTGATGC
R-PAO1/LasA	GGAGATGGGAAGTCATTAGAGCGCCAGGCCGGGGTTGTACAAC

Gene design and gene synthesis of Pseudomonas aeruginosa exotoxin A (eta) including the full-length and sub-domains (IA, II- IB , and III)

Gene synthesis of Pseudomonas aeruginosa exotoxinA was designed based on the sequence of exotoxin A (ETA) gene, complete cds (GenBank accession no. NC_002516.2) of Pseudomonas aeruginosa PAO1 chromosome. The design of the synthetic gene was improved to the amino initiation and termination in the coding region. This synthesized gene was optimized sequence with ETA original sequence (Figure 2.3) and alignment sequence for its protein expression in Escherichia coli. The gene was successfully designed and synthesized by GenScript (New Jercey, USA). The oligonucleotide primers used for amplification of exotoxin A gene (includes full-length and its sub-domains IA, II- IB, and III)

were also designed (Table 2.2) which their 5'-end includes vector specific sequences and contains 3'-end overlapped with the sequence of eta sub-domain IA, II- IB, III, and full-length intended for cloning into the pLATE52 vector, an expression vector which containing gene for N-terminal His-tag protein expression. The complete of ETA gene including domains IA, II- IB, III, and full-length have 756, 456, 627, and 1839 bp in size, respectively.

Original GCCGAGGAAGCCTTCGACCTCTGGAACGAATGCGCCAAGGCCTGCGTGCTCGACCTC
Optimized GCGGAAGAGGCGTTTGATTTGTGGAATGAGTGTGCGAAAGCGTGTGTGTTGGATTTG

Original AAGGACGGCGTGCGTTCCAGCCGCATGAGCGTCGACCCGGCCATCGCCGACACCAAC
Optimized AAAGATGGTGTGCGGTCGAGCCGCATGAGCGTTGATCCGGCGATTGCGGATACCAAT

Original GGCCAGGGCGTGCTGCACTACTCCATGGTCCTGGAGGGCGGCAACGACGCGCTCAAG
Optimized GGTCAGGGTGTGCTGCATTATTCGATGGTTCTGGAAGGCGGTAATGATGCATTGAAA

Original CTGGCCATCGACAACGCCCTCAGCATCACCAGCGACGGCCTGACCATCCGCCTCGAA
Optimized CTGGCGATTGATAATGCGTTGAGCATTACCAGCGATGGTCTGACCATTCGCTTGGAG

Original GGTGGCGTCGAGCCGAACAAGCCGGTGCGCTACAGCTACACGCGCCAGGCGCGCGGC
Optimized GGAGGCGTTGAACCGAATAAACCGGTGCGCTATAGCTATACTCGCCAGGCACGCGGT

Original AGTTGGTCGCTGAACTGGCTGGTGCCGATCGGCCACGAGAAGCCTTCGAACATCAAG
Optimized TCATGGTCGCTGAATTGGCTGGTGCCGATTGGTCATGAAAAACCCTCGAATATTAAA

Original GTGTTCATCCACGAACTGAACGCCGGTAACCAGCTCAGCCACATGTCGCCGATCTAC
Optimized GTGTTTATTCATGAGCTGAATGCGGGAAATCAGTTGAGCCATATGTCGCCGATTTAT

Original ACCATCGAGATGGGCGACGAGTTGCTGGCGAAGCTGGCGCGCGATGCCACCTTCTTC
Optimized ACCATTGAAATGGGTGATGAACTTCTGGCAAAACTGGCACGCGACGCGACCTTCTTT

Original GTCAGGGCGCACGAGAGCAACGAGATGCAGCCGACGCTCGCCATCAGCCATGCCGGG
Optimized GTTAGAGCACATGAAAGCAATGAAATGCAGCCGACTTTGGCGATTAGCCACGCGGGA

Original GTCAGCGTGGTCATGGCCCAGGCCCAGCCGCGCCGGGAAAAGCGCTGGAGCGAATGG
Optimized GTTAGCGTGGTTATGGCGCAGGCGCAGCCGCGCCGTGAGAAACGCTGGAGCGAGTGG

Original GCCAGCGGCAAGGTGTTGTGCCTGCTCGACCCGCTGGACGGGGTCTACAACTACCTC
Optimized GCGAGCGGTAAAGTGCTTTGTCTGTTGGATCCGCTGGATGGAGTTTATAATTATTTG

Original GCCCAGCAGCGCTGCAACCTCGACGATACCTGGGAAGGCAAGATCTACCGGGTGCTC
Optimized GCGCAGCAGCGCTGTAATTTGGATGACACCTGGGAGGGTAAAATTTATCGTGTGTTG

Original GCCGGCAACCCGGCGAAGCATGACCTGGACATCAAGCCCACGGTCATCAGTCATCGC
Optimized GCGGGTAATCCGGCAAAACACGATCTGGATATTAAACCAACTGTTATTTCACACCGC

Original CTGCATTTCCCCGAGGGCGGCAGCCTGGCCGCGCTGACCGCGCACCAGGCCTGCCAC
Optimized CTGCACTTTCCAGAAGGTGGTAGCCTGGCAGCACTGACCGCACATCAGGCGTGTCAT

Original CTGCCGCTGGAGACCTTCACCCGTCATCGCCAGCCGCGCGGCTGGGAACAACTGGAG
Optimized CTGCCGCTGGAAACCTTTACCCGGCATCGTCAGCCGCGTGGTTGGGAGCAACTGGAA

Original CAGTGCGGCTATCCGGTGCAGCGGCTGGTCGCCCTCTACCTGGCGGCGCGGCTGTCG
Optimized CAGTGTGGTTACCCGGTGCAGCGTCTGGTTGCGTTGTATCTGGCAGCACGTCTGAGT

Original TGGAACCAGGTCGACCAGGTGATCCGCAACGCCCTGGCCAGCCCCGGCAGCGGCGGC
Optimized TGGAATCAGGTTGATCAGGTGATTCGTAATGCGCTGGCGAGCCCAGGTAGCGGTGGT

Original GACCTGGGCGAAGCGATCCGCGAGCAGCCGGAGCAGGCCCGTCTGGCCCTGACCCTG
Optimized GATCTGGGTGAGGCAATTCGTGAACAGCCGGAACAGGCGCGGCTGGCGCTGACCCTG

Original GCCGCCGCCGAGAGCGAGCGCTTCGTCCGGCAGGGCACAGGCAACGACGAGGCCGGC
Optimized GCGGCAGCGGAAAGCGAACGTTTTGTTCGTCAGGGTACAGGTAATGATGAAGCGGGT

Original GCGGCCAGCGCCGACGTGGTGAGCCTGACCTGCCCGGTCGCCGCCGGTGAATGCGCG

```
Optimized GCAGCGAGCGCGGATGTGGTGAGCCTGACCTGTCCGGTTGCGGCAGGAGAGTGTGCA

Original  GGCCCGGCGGACAGCGGCGACGCCCTGCTGGAGCGCAACTATCCCACTGGCGCGGAG
Optimized GGTCCGGCAGATAGCGGTGATGCGCTGCTGGAACGTAATTACCCAACAGGTGCAGAA

Original  TTCCTCGGCGACGGCGGCGACATCAGCTTCAGCACCCGCGGCACGCAGAACTGGACG
Optimized TTTTTGGGTGATGGTGGTGATATTAGCTTTAGCACCCGCGGTACTCAGAATTGGACT

Original  GTGGAGCGGCTGCTCCAGGCGCACCGCCAACTGGAGGAGCGCGGCTATGTGTTCGTC
Optimized GTGGAACGTCTGTTGCAGGCACATCGCCAACTGGAAGAGCGCGGTTACGTGTTTGTT

Original  GGCTACCACGGCACCTTCCTCGAAGCGGCGCAAAGCATCGTCTTCGGCGGGGTGCGC
Optimized GGTTATCATGGTACCTTTTTGGAGGCCGCACAAAGCATTGTTTTTGGTGGAGTGCGC

Original  GCGCGCAGCCAGGACCTCGACGCGATCTGGCGCGGTTTCTATATCGCCGGCGATCCG
Optimized GCACGCAGCCAGGATTTGGATGCAATTTGGCGCGGATTTTACATTGCGGGTGACCCG

Original  GCGCTGGCCTACGGCTACGCCCAGGACCAGGAACCCGACGCGCGCGGCCGGATCCGC
Optimized GCACTGGCGTATGGTTATGCGCAGGATCAGGAGCCAGATGCACGCGGTCGTATTCGC

Original  AACGGTGCCCTGCTGCGGGTCTATGTGCCGCGCTCGAGTCTGCCGGGCTTCTACCGC
Optimized AATGGAGCGCTGCTGCGTGTTTACGTGCCGCGCTCGTCACTGCCGGGTTTTTATCGC

Original  ACCGGCCTGACCCTGGCCGCGCCGGAGGCGGCGGGCGAGGTCGAACGGCTGATCGGC
Optimized ACCGGTCTGACCCTGGCGGCACCGGAAGCCGCAGGTGAAGTTGAGCGTCTGATTGGT

Original  CATCCGCTGCCGCTGCGCCTGGACGCCATCACCGGCCCCGAGGAGGAAGGCGGGCGC
Optimized CACCCGCTGCCGCTGCGCCTGGATGCGATTACCGGTCCAGAAGAAGAGGGTGGACGC

Original  CTGGAGACCATTCTCGGCTGGCCGCTGGCCGAGCGCACCGTGGTGATTCCCTCGGCG
Optimized CTGGAAACCATATTGGGTTGGCCGCTGGCGGAACGCACCGTGGTGATACCATCGGCA

Original  ATCCCCACCGACCCGCGCAACGTCGGCGGCGACCTCGACCCGTCCAGCATCCCCGAC
Optimized ATTCCAACCGATCCGCGCAATGTTGGCGGTGATTTGGATCCGTCGAGCATTCCAGAT

Original  AAGGAACAGGCGATCAGCGCCCTGCCGGACTACGCCAGCCAGCCCGGCAAACCGCCG
Optimized AAAGAGCAGGCAATTAGCGCGCTGCCGGATTATGCGAGCCAGCCAGGTAAGCCGCCG

Original  CGCGAGGACCTGAAG
Optimized CGCGAAGATCTGAAA
```

Figure 1.3 Nucleotide sequences alignment of the optimized *Pseudomonas aeruginosa* exotoxin A (ETA) gene with its original form that obtained from the NCBI database (GenBank accession no. NC_002516.2).

Table 1.2 Oligonucleotide primers used for amplification of *Pseudomonas aeruginosa* exotoxin A (ETA) includes sub-domains (IA, II- IB, and III) and full-length from the synthesized ETA DNA fragment**.**

Target gene	Primer name	Oligonucleotide sequences (5'-3')	Size of PCR Product (bp)
eta sub-domainIA	F-PAO1/ETA- IA	GGTTGGGAATTGCAAGCGGAAGAGGCGTTTGATTTGTG	756
	R-PAO1/ETA- IA	GGAGATGGGAAGTCATTATTCTGGAAAGTGCAGGCGGTG	
eta sub-domainII/ IB	F-PAO1/ETA-II/ IB	GGTTGGGAATTGCAAGGTGGTAGCCTGGCAGCACTG	456
	R-PAO1/TEA-II/ IB	GGAGATGGGAAGTCATTAACCATCACCCAAAAATTCTGCACC	
eta sub-domainIII	F-PAO1/ETA- III	GGTTGGGAATTGCAAGGTGATATTAGCTTTAGCACCCGCGG	627
	R-PAO1/ETA- III	GGAGATGGGAAGTCATTATTTCAGATCTTCACGTGGCGGC	
eta full-length	F-PAO1/ETA- IA	GGTTGGGAATTGCAAGCGGAAGAGGCGTTTGATTTGTG	1839
	R-PAO1/ETA- III	GGAGATGGGAAGTCATTATTTCAGATCTTCACGTGGCGGC	

Bacterial culture and genomic DNA extraction

Bacterial culture was performed by inoculating 5 ml of Luria-Bertani (LB) broth with a single bacterial colony of *Pseudomonas aeruginosa* strain PAO1 and then incubated at 37°C with 250 rpm shaking for 12-18 hr. After that, transferred the cell suspension into 1.5 ml micro centrifuge tube and centrifuge for 1 minute at 14,000 x g. Afterwards, the cell pellet was used for perform the gram-negative DNA extraction by using the DNA extraction kit (Geneaid Biotech Ltd.) following the protocol provided by the manufacturer. The DNA extraction was performed by firstly added 180 µl of GT buffer then re-suspended the cell pellet by vortex and further added 20 µl of proteinase K. The sample mixture was incubated at 60°C for at least 10 minutes (during incubation, inverted the tube every 3 minutes). Next, proceeding with lysis step by added 200 µl of GB buffer to the sample mixture and mixed by vortex for 10 seconds. The sample mixture was incubated at 70°C for at least 10 minutes until the sample lysate is clear (during incubation, inverted the tube every 3 minutes and also pre-heated the required elution water to 70°C). Later, the DNA binding step was performed by added 200 µl of absolute ethanol to the sample lysate and mix immediately by vigorously shaking. A GD column was placed in a 2 ml collection tube and the sample mixture (including any insoluble precipitate) was transferred to the prepared GD column, then

centrifuged at 14-16,000 x g for 2 minutes. And after the 2 ml collection tube containing the flow-through was discarded, the GD column was placed in a new 2 ml collection tube. Afterwards, the washing step was done by added 400 µl of W1 buffer to the GD column and centrifuged at 14-16,000 x g for 30 seconds. And after the flow-through was discarded, the GD column was placed back in the 2 ml collection tube. The 600 µl of wash buffer was added to the GD column and centrifuged at 14-16,000 x g for 30 seconds. The flow-through was discarded and the GD column was placed back in the 2 ml collection tube. Further centrifuged again for 3 minutes at 14-16,000 x g to dry the column matrix. Finally, the elution step was performed by transferred the dried GD column to a clean 1.5 ml micro centrifuge tube. Then the 100 µl of pre-heated water was added into the center of the column matrix, let stand for at least 3 minutes to allow the water to be completely absorbed, and centrifuged at 14-16,000 x g for 30 seconds to elute the purified DNA. The concentration of the purified genomic DNA was measured by using the NanoDrop spectrophotometer at wavelengths of 260 and 280 nm.

Amplification of catalytic domain of LasB, LasA and ETA genes including the full-length and sub-domains(IA, II- IB , and III) by using polymerase chain reaction (PCR) that optimized condition

In this study, the genomic DNA of *P. aeruginosa* strain PAO1 was used as the template to amplify the catalytic domain of LasB and LasA and ETA genes including sub-domains IA, II- IB, III, and full-length with polymerase chain reaction, using Phusion High-Fidelity DNA Polymerase (Thermo Fisher Scientific). PCR amplification was performed in a total volume of 20 µl which the PCR mixture and PCR thermal cycle are shown below.

PCR mixture (20 µl)

Ingredient	**Volume (µl)**	**Final concentration**
Sterile ultrapure distilled water (UDW)	11.8	-
Phusion GC buffer (5x)	4.0	1x
dNTP (2.5 mM each)	0.4	200 µM
Forward Primer (10 µM)	1.0	0.5 µM
Reverse Primer (10 µM)	1.0	0.5 µM
DMSO	0.6	3%
Phusion DNA Polymerase	0.2	0.4 units

(1.0 units/50 µl PCR)		
DNA template	1.0	-

Thermal cycles

Initial denaturation	at 98°C for 30 seconds
35 cycles of Denaturation ,	at 98°C for 10 seconds
Annealing ,	at 65°C for LasA 75°C for LasB 70°C for exoA for 10 seconds
and Extension	at 72°C for 1 minutes
Final extension	at 72°C for 10 minutes

PCR amplicon of the catalytic domain of LasB and LasA have 930 bp and 570 bp in size as showed in **Figure 1.4.** While PCR product of exotoxin A including domains IA, II- IB, III, and full-length have 756, 456, 627, and 1839 bp in size as showed in **Figure 1.5.**

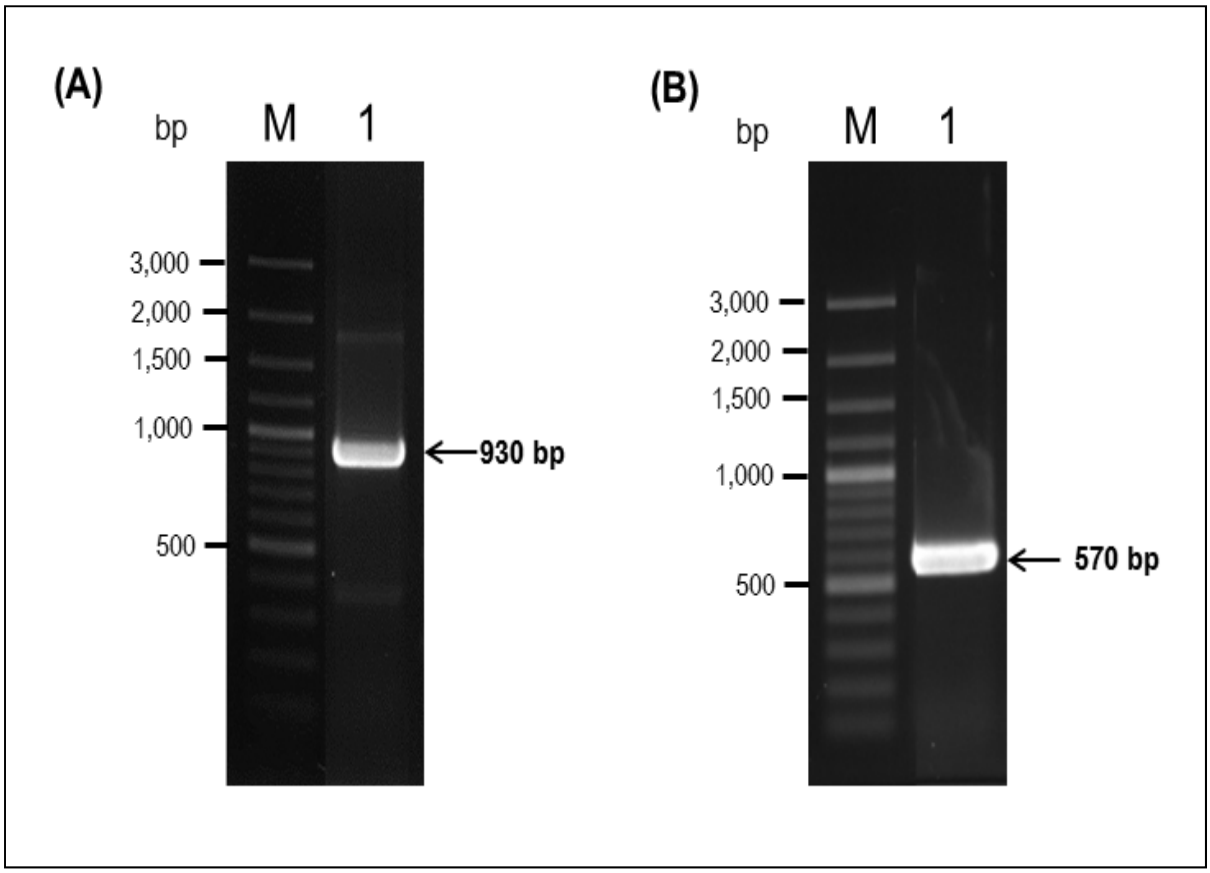

Figure 1.4 PCR product that obtained from the amplification of genomic DNA of *P. aeruginosa* using specific primers

(A) LasB-coding sequence- Lane M: GenRulerTM 100 bp DNA ladder plus, Lane 1:LasB amplicons

(B) LasA-coding sequence - Lane M : GenRulerTM 100 bp DNA ladder plus, Lane 1: LasA amplicons

The PCR product were analyzed on 1 % agarose gel electrophoresis and visualized on UV light after staining with ethidium bromide.

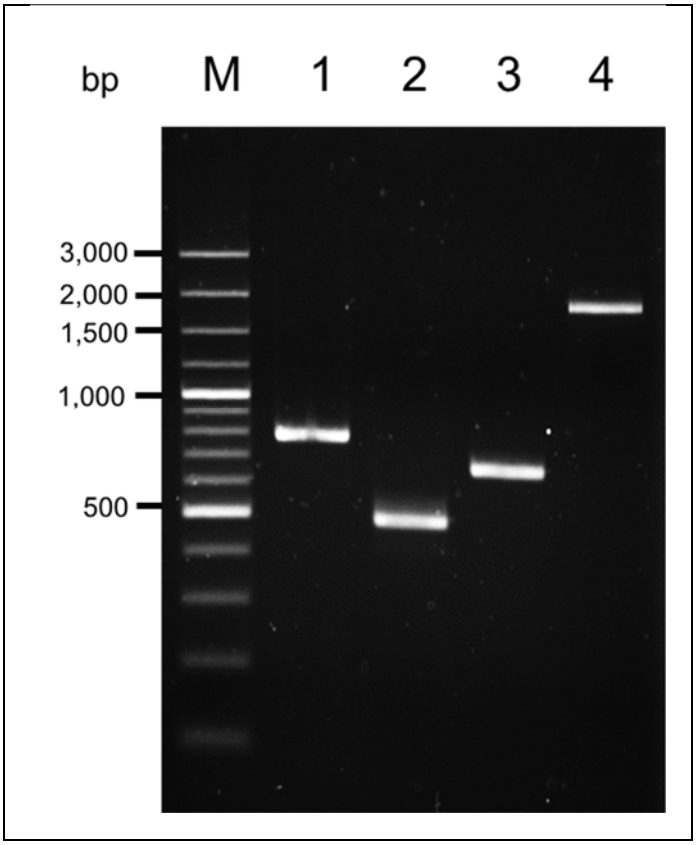

Figure 1.5 PCR product that obtained from the amplification of genomic DNA of *P. aeruginosa* using specific primers for ETA-coding sequence (including sub-domains IA, II- IB, III, and full-length)
Lane M, GenRulerTM 100 bp DNA ladder plus
Lane 1-4, ETA sub-domians IA (756 bp), II- IB (456 bp), III (627 bp), and full-length amplicons (1,839 bp), respectively
The PCR product were analyzed on 1.5% agarose gel electrophoresis and visualized on UV light after staining with ethidium bromide.

Purification of catalytic domain of LasB, LasA, ETA including the full-length and sub-domains(IA, II- IB, and III) DNA fragments

The PCR products from above were purified using the Gel/PCR DNA fragments extraction kit (Geneaid Biotech Ltd.) with a bind-wash-elute procedure to completely eliminate the incorporated primers, dNTPs, and other contaminated DNA.

Cloning of LasB, LasA, ETA gene including the full-length and sub-domains(IA, II- IB, and III) into the expression vector and analysis for the correction of the gene insert by DNA sequencing method

Individual LasB, LasA and ETA amplicons including sub-domains IA, II- IB III, and full-length were cloned into the pLATE52 expression vector (Thermo Scientific) of the LIC (ligation-independent cloning) system using the 3'-5' exonuclease and 5'-3' polymerase activities of T4 DNA polymerase and the recombinant plasmids were further introduced into the *Escherichia coli* strain JM 109, the cloning host as the gene stock. The procedure composed of two sections LIC cloning and annealing reaction. The LIC cloning was performed to generated the 5' and 3' overhangs on the purified PCR template that the following reaction were set up by mixed 2 µl of 5x LIC buffer; 4 µl of nuclease-free water; 0.1pmol of purified PCR template; T4 DNA polymerase. And after the reaction mixture were incubated at 25°C for 5 minutes, the reaction were immediately stopped by added 0.6 µl of EDTA. Then the annealing reactions were performed by added the LIC-ready pLATE52 (60g, 0.02 pmol DNA) to the reaction mixture, vortexed briefly for 3-5 seconds, and annealing proceeded at 25°C for 5 minutes. Afterwards, the bacterial transformation was done by using the Transform Aid Bacterial Transformation Kit (Thermo Scientific) to transformed the individual LasB-pLATE52, LasA- pLATE52 and eta-pLATE52 (including sub-domains IA, II- IB III, and full-length) recombinant plasmid into the competent *E. coli* strain JM109. Plating on Luira-Bertani-Amplicilin (LB-A) then colonies appearing were randomly picked and screening by direct colony PCR as following mixture and reaction (**Figure 1.6, 1.7**).

PCR mixture for direct colony PCR

Ingredient	**Volume (µl)**	**Final concentration**
Sterile ultrapure distilled water (UDW)	18.3	-
Taq DNA polymerase buffer with KCl (Fermentas) 10x	2.5	1x
MgCl2 (25mM)	1.5	1.5 mM
dNTP (2.5 mM each)	0.5	200 µM
LIC Forward primer, 10 µM	0.5	200 nM
LIC Reverse primer, 10 µM	0.5	200 nM
Taq DNA Polymerase (5.0 units/µl)	0.2	0.5 units
DNA template	1.0	-

Thermal cycles

Initial denaturation	at	98°C	for 30 seconds
35 cycles of Denaturation ,	at	98°C	for 10 seconds
Annealing ,	at	65°C	for LasA
		75°C	for LasB
		70°C	for exoA for 10 seconds
and Extension	at	72°C	for 1 minutes
Final extension	at	72°C	for 10 minutes

PCR amplicons from direct colony PCR were analyzed by agarose gel electrophoresis for the presence and size of the PCR product (**Figure 1.6** for lasB and lasA, **Figure 1.7** for ETA). For LasA and LasB, the positive clones harboring recombinant plasmid were confirmed by sequencing, for lasB seletected clone number lasB1, lasB6 and lasB7. Clone no. LasA1-3 were selected for lasA. For ETA, selected ETA sub-domian IA were clone IA-1 and IA-2, ETA sub-domian II- IB were clone IIB-1 and IIB-2 and ETA sub-domian III were clone III-1,III-2 and III-3. The positive clones were analyzed the inserted gene by using the DNA sequencing method, the pLATE52_ETA recombinant plasmid including lasA, lasB and sub-domains (IA, II- IB, III) and full-length were transformed into the competent *E. coli* strain NiCo21 (DE3) (New England Biolabs, UK), an expression host.

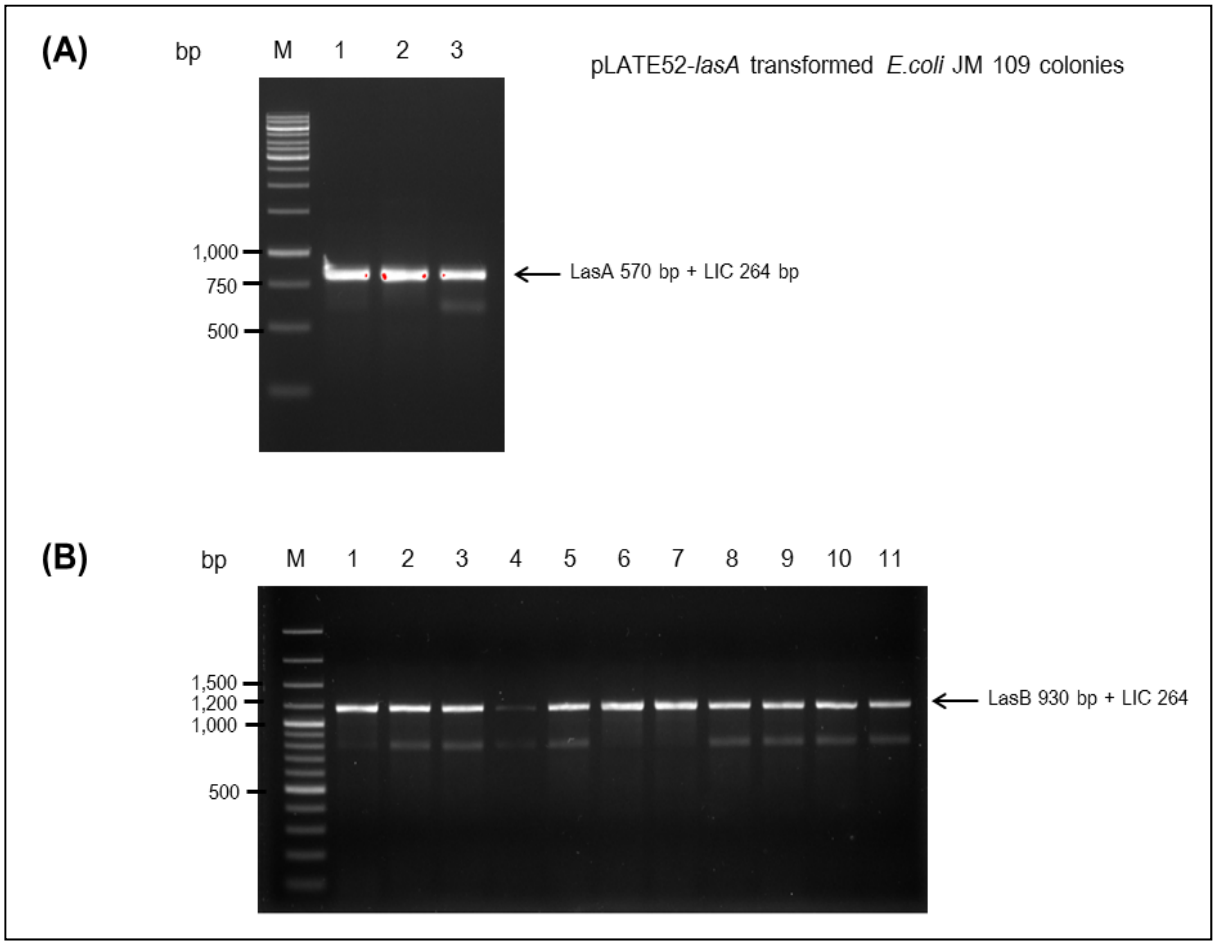

using LIC primer

(A) pLATE52-lasA transformed *E. coli* JM 109 colonies.

Lane M : GeneRuler 100 bp plus DNA Ladder

Lane 1-3: Amplicons of positive *E. coli* JM109 colonies harboring rLasA-pLATE52 plasmid

(B) pLATE52-lasB transformed *E. coli* JM 109 colonies.

Lane M : GeneRuler 100 bp plus DNA Ladder,

Lane 1-11: Amplicons of positive *E. coli* JM109 colonies harboring rLasB-pLATE52 plasmid

PCR products obtained with LIC Forward and LIC Reverse Sequencing Primers should be 264 bp (plus insert size) pLATE52 vectors .The PCR product were analyzed on 1 % agarose gel electrophoresis and visualized on UV light after staining with ethidium bromide.

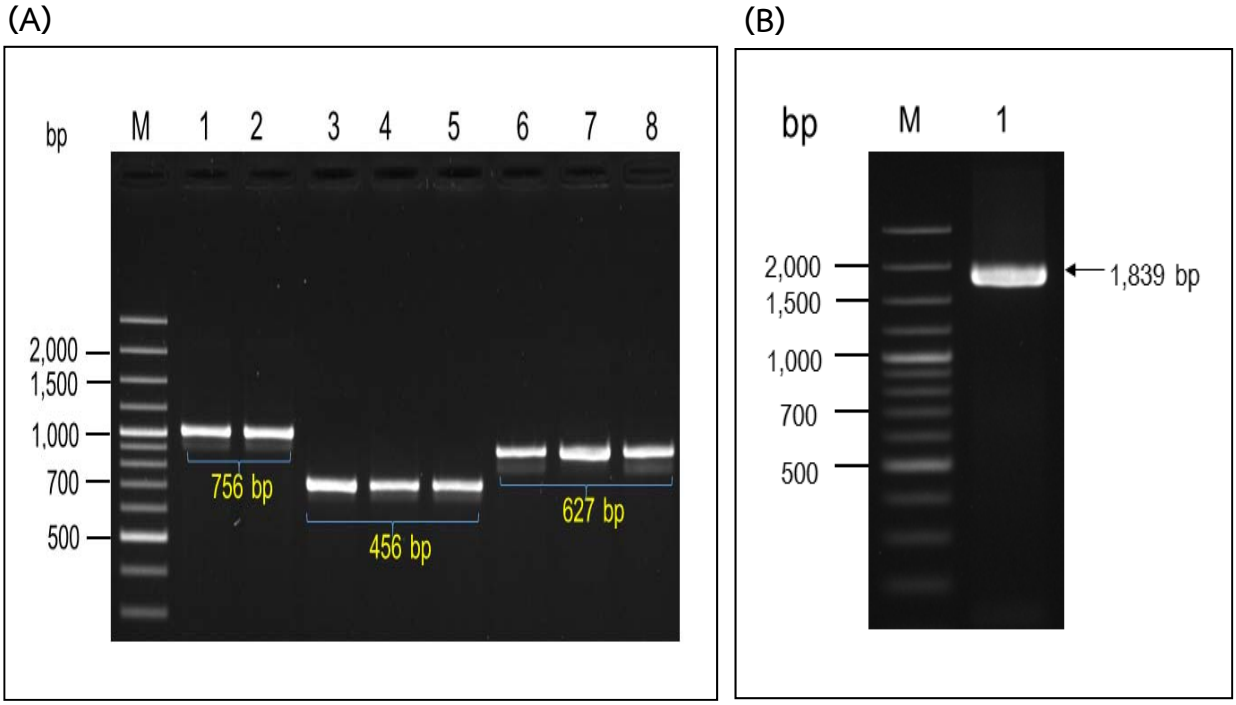

Figure 1.7 PCR amplification for screening of pLATE5_ETA (including sub-domains IA, II- IB, III, and full-length) transformed E. coli strain JM 109 colonies

(A) Lane M: GenRulerTM 100 bp DNA ladder plus
Lane 1-2: ETA sub-domian IA amplicons clone IA-1 and IA-2
Lane 3-5: ETA sub-domian II- IB amplicons clone IIB-1 and IIB-2
Lane 6-8: ETA sub-domian III amplicons clone III-1,III-2 and III-3

(B) Lane M: GenRulerTM 100 bp DNA ladder plus
Lane 1-2: ETA full gene clone Full-1

The PCR product were analyzed on 1 % agarose gel electrophoresis and visualized on UV light after staining with ethidium bromide.

Recombinant LasB, LasA and ETA protein expression and native LasB production

For protein expression, single colony of individual inserted lasA-, lasB- including sub-domain (IA, II- IB, and III)- and full-length ETA- *E. coli* clone was cultured in 5 ml LB containing 100 µg/ml amplicilin (LB-A) medium in shaking incubator at 250 rpm, 37°C for 16 hours. One hundreds microliters of starter was removed and inoculated into 1.9 ml LB-A. The cultured was shaking for 3 hours at 37 °C. Isopropyl-β-D-thiogalactopyranoside (IPTG) was added into individuals cultures to final concentration of 1 mM for expression of mature peptide then incubated in shaking at 37°C for 6 hours. Collected 1 ml by centrifugation at 10,000 x*g* for 1 minute. The cell pellets were suspended in BugBuster® protein extraction reagent incubated at RT for 10 minutes. Soluble fractions, supernatant were collected by centrifugation at 14,000 x*g* for 5 minutes. The pellets were suspended in 1:10 diluted BugBuster, then centrifugation at 14,000 x*g* for 5 minutes, discard supernatant and suspended pellet in 1:10 diluted BugBuster ,Insoluble fractions, then Analyzes by 12% SDS-PAGE (**Figure 1.8**: LasA, LasB; **Figure 1.9-1.10**: ETA) and Western blot analysis (**Figure 1.11**: LasA, LasB; **Figure 1.12**-1.**13**: ETA). The results shown desired protein expression both LasA, LasB and ETA.

In this study, the results were shown the protein expression of LasA, LasB, sub-domain IA (receptor-binding domain) and sub-main III (catalytic domain)of ETA in the insoluble fraction (inclusion body) But there have no desired protein expression for domain II- IB and the whole toxin of ETA.

Production and purified native lasB from *pseudomonas aeruginosa* PAO1

P. aeruginosa PAO1 was cultured in 250 ml LB at 37 °C for 18 hours. The supernatant was collected by centrifuge at 10,000 x*g*, 4°C for 10 minutes. For ammonium sulfate precipitation, 100 % ammonium sulfate solution was slowly added to cell-free supernatant to obtain 80% saturation and continue stirred at 4°C for overnight. Afterward, the lasB precipitated was harvested by centrifuge 15,000 x*g*, 4°C for 30 minutes and resuspended in 20 mM Tris-HCl pH 8.5. Then ammonium sulfate was removed by amicon ultracentrifuge filter (10 kDa molecular weight cut off) and LasB further purified by DEAE cellulose chromatography. The column was equilibrated and washed with 20 mM Tris-HCl pH 8.5 and eluted by linear NaCl. The lasB fractions were pooled and removed NaCl by dialysis Figure 1.8 (C.) The purified lasB was determined by SDS-PAGE and LC/MS-MS.

Determination of biological activity of native lasB from *Pseudomonas aeruginosa* PAO1

EnzChek™ elastase assay Kit was used for determining elastolytic activity of native LasB. The 100 µl of Reaction buffer was added into each well that contains 50 µl of lasB (25, 50, 100 and 200 nM), after that additional substrate, 50 µL of 100 µg/mL DQ elastin. Measure the intensity of fluorescence by a Synergy H1 Hybrid Multi-Mode Reader, Biotek, with standard fluorescence filters set for excitation at 485 ± 20 nm and emission detection at 520 ± 20. The produced native elastase was showed their biological activity (Figure 1.8D).

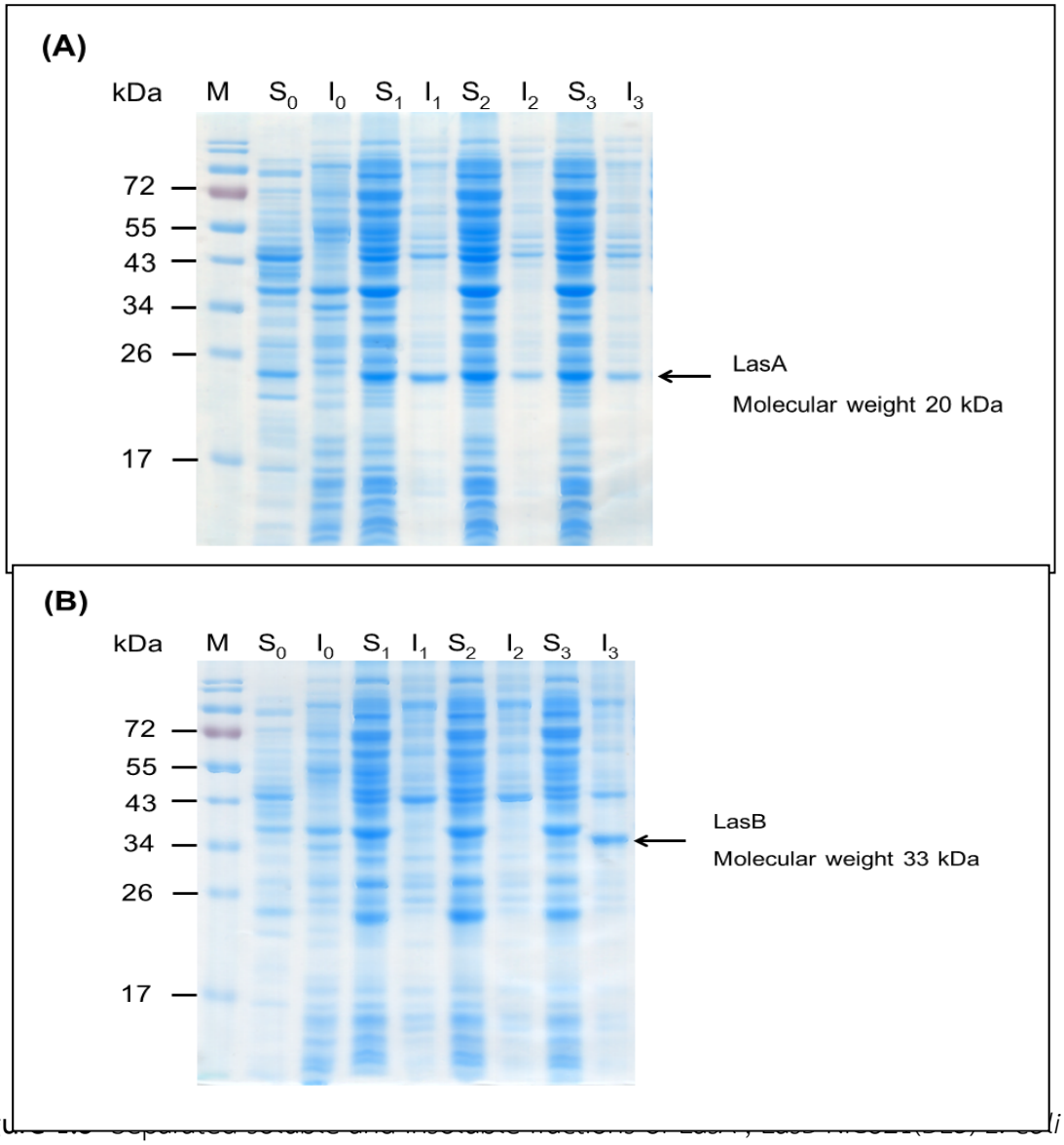

Figu[illegible] *li* expression from small scale expression by using SDS-PAGE (A.) LasA (B.) LasB

Lane M: Standard protein ladder

Lane S0: Soluble fraction of control NiCo21(DE3) *E. coli*

Lane I0: Insoluble fraction of control NiCo21(DE3) *E. coli*

Lane S1-3: Soluble fraction of clones 1-3, respectively

Lane I1-3: Insoluble fraction of clones 1-3, respectively

(C)

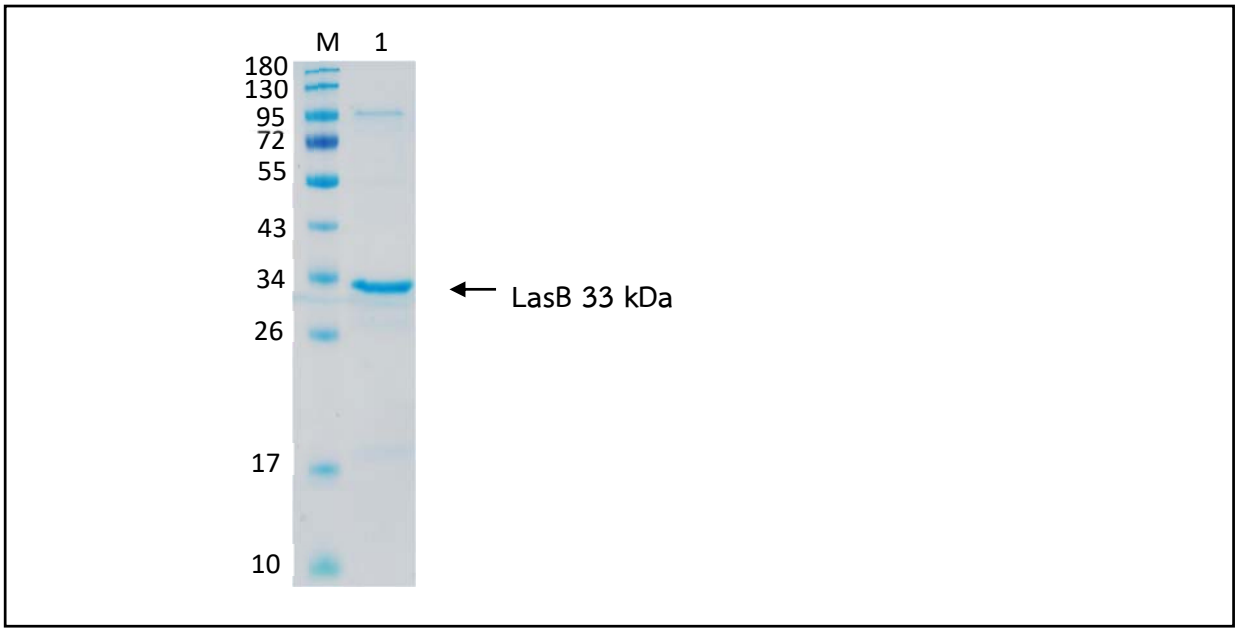

Figure 1.8 SDS-PAGE pattern of purified native LasB after stained with Coomassie Brilliant Blue G-250.
Lane M : Standard protein ladder
Lane 1: 33 kDa lasB elastase

(D)

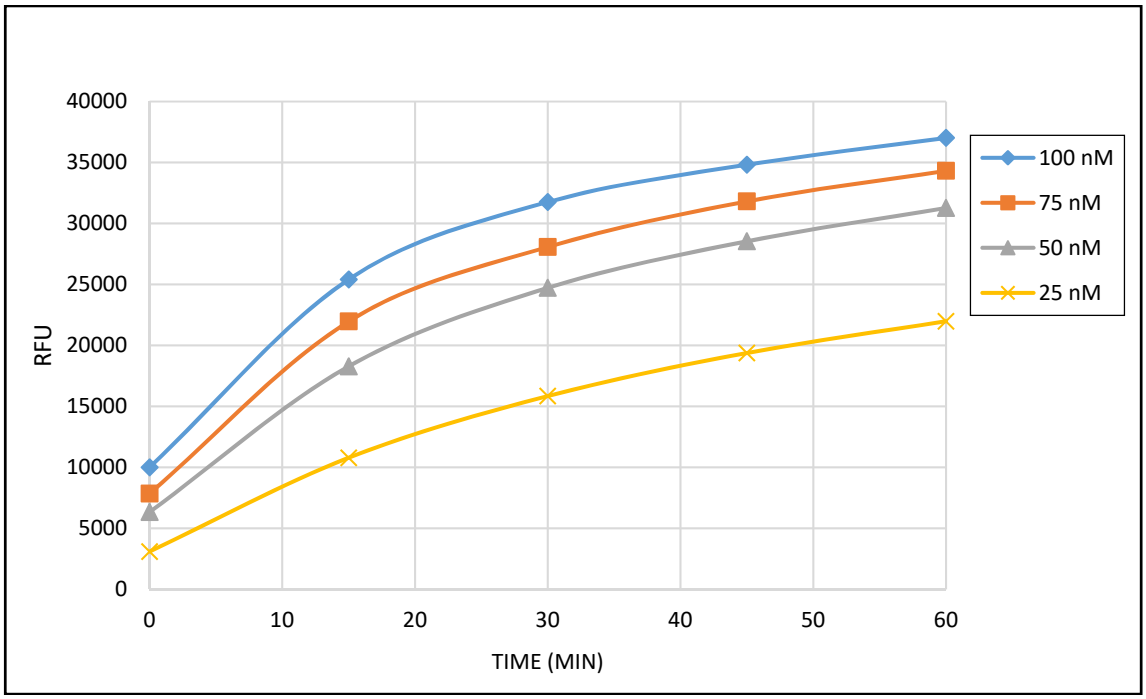

Figure 1.8 Native elastase activity was investigated by using the EnzChek™ elastase assay Kit. Samples were done in duplicate and measured fluorescence. Background fluorescence was subtracted from each value.

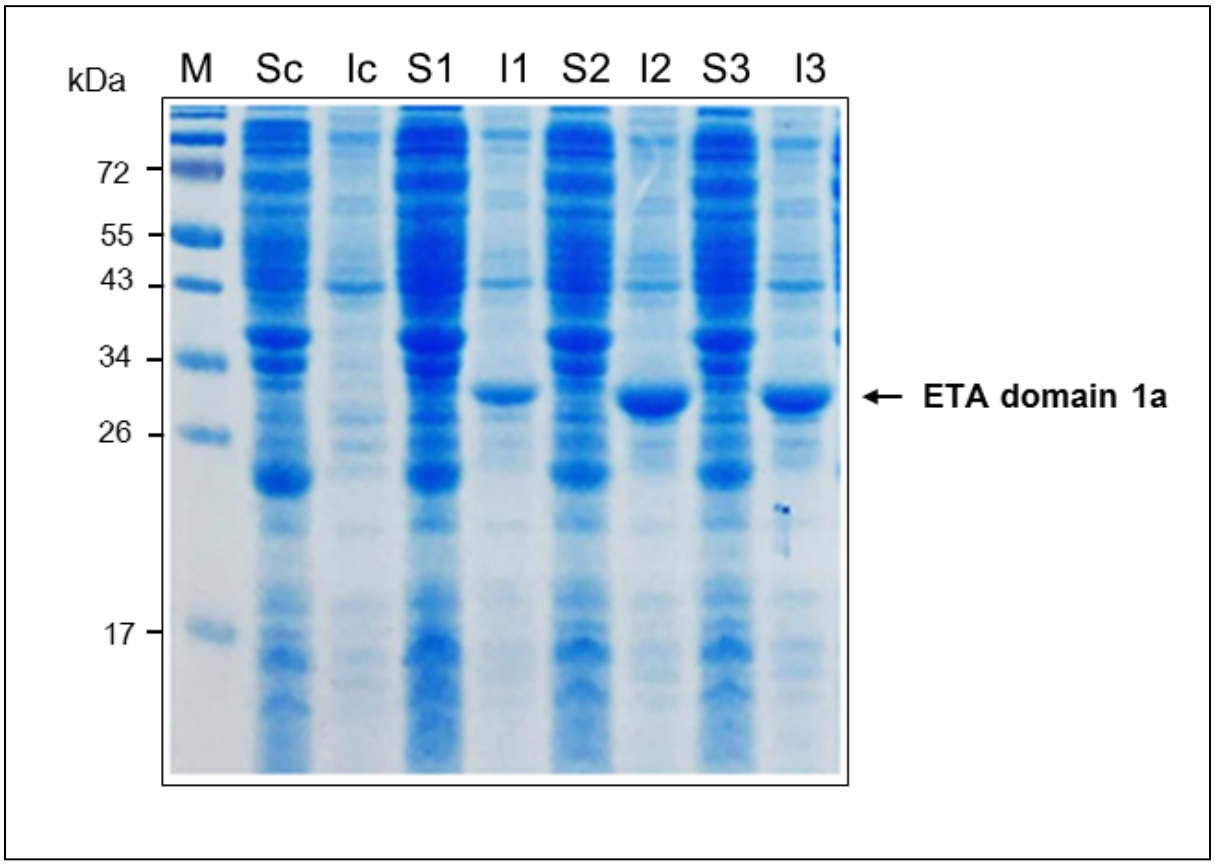

Figure 1.9 SDS-PAGE analysis of the separated soluble and insoluble fractions of the ETA sub-domain IA protein from NiCo21 (DE3) *E. coli* using 15% SDS-polyacrylamide gel.
Lane M: Standard protein ladder
Lane Sc: Soluble fraction of control [NiCo21 (DE3) E. coli]
Lane Ic: Insoluble fraction of control [NiCo21 (DE3) E. coli]
Lane S1-3: Soluble fraction of clones 1-3 of ETA sub-domain IA, respectively
Lane I1-3: Insoluble fraction of clones 1-3 of ETA sub-domain IA, respectively; protein size ~28 kDa.

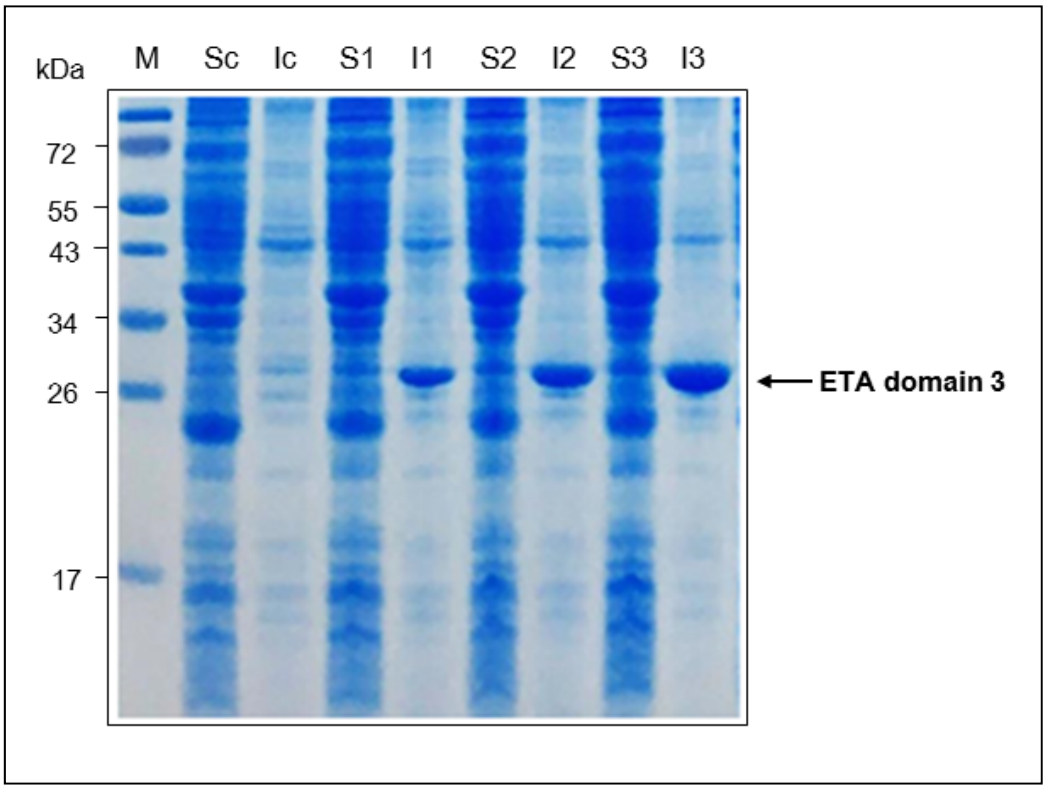

Figure 1.10 SDS-PAGE analysis of the separated soluble and insoluble fractions of the ETA sub-domain III protein from NiCo21 (DE3) E. coli using 15% SDS-polyacrylamide gel.
Lane M: Standard protein ladder
Lane Sc: Soluble fraction of control [NiCo21 (DE3) E. coli]
Lane Ic: Insoluble fraction of control [NiCo21 (DE3) E. coli]
Lane S1-3: Soluble fraction of clones 1-3 of ETA sub-domain III, respectively
Lane I1-3: Insoluble fraction of clones 1-3 of ETA sub-domain III, respectively; protein size ~23 kDa.

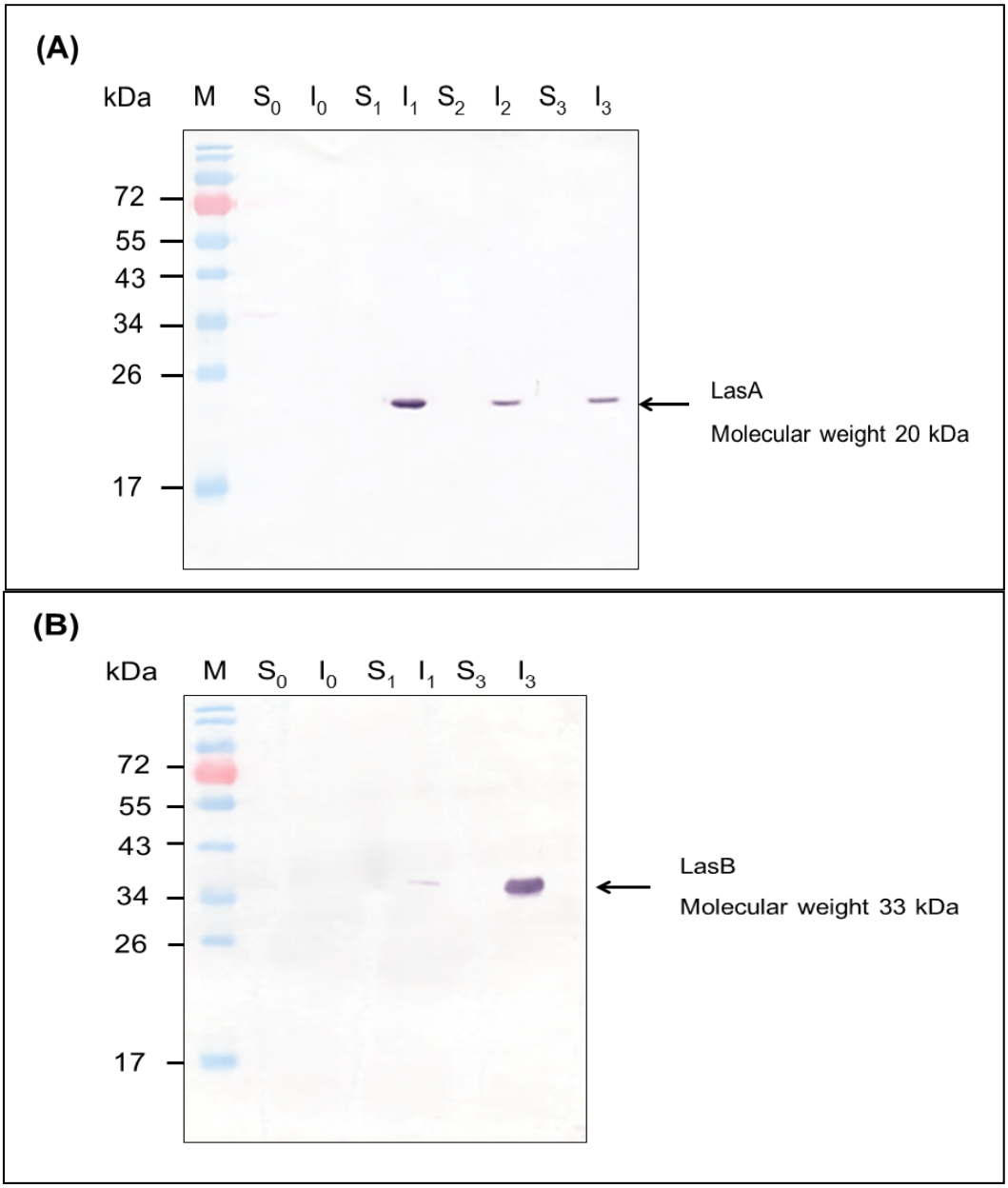

Figure 1.11 Western blot analysis for determination of NiCo21 (DE3) *E. coli* expression of (A.) LasA (B.) LasB from small scale expression.

Lane M: Standard protein ladder

Lane S0: Soluble fraction of control NiCo21(DE3) *E. coli*

Lane I0: Soluble fraction of control NiCo21(DE3) *E. coli*

Lane S1-3: Soluble fraction of clones 1-3, respectively.

Lane I1-3: Insoluble fraction of clones 1-3, respectively.

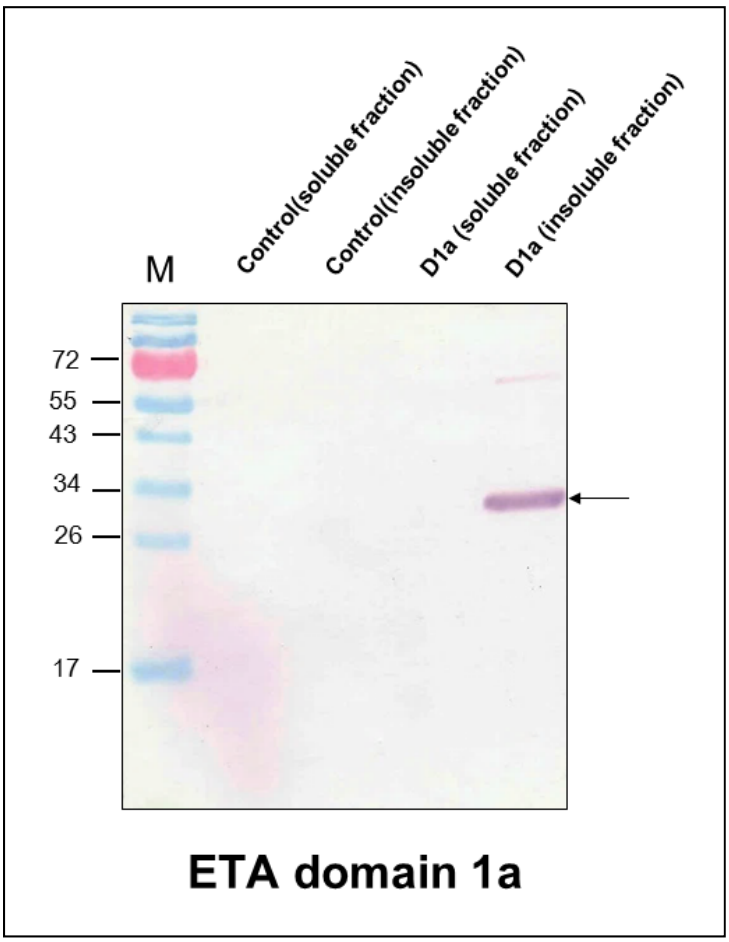

Figure 1.12 Western blot analysis of the hexa-histidine (6xHis)-tagged ETA sub-domain IA protein.
Lane M: Standard protein ladder
Lane Sc: Soluble fraction of control [NiCo21 (DE3) *E. coli*]
Lane Ic: Insoluble fraction of control [NiCo21 (DE3) *E. coli*]
Lane S1: Soluble fraction of ETA sub-domain IA
Lane I1: Insoluble fraction of ETA sub-domain IA; protein size ~28 kDa

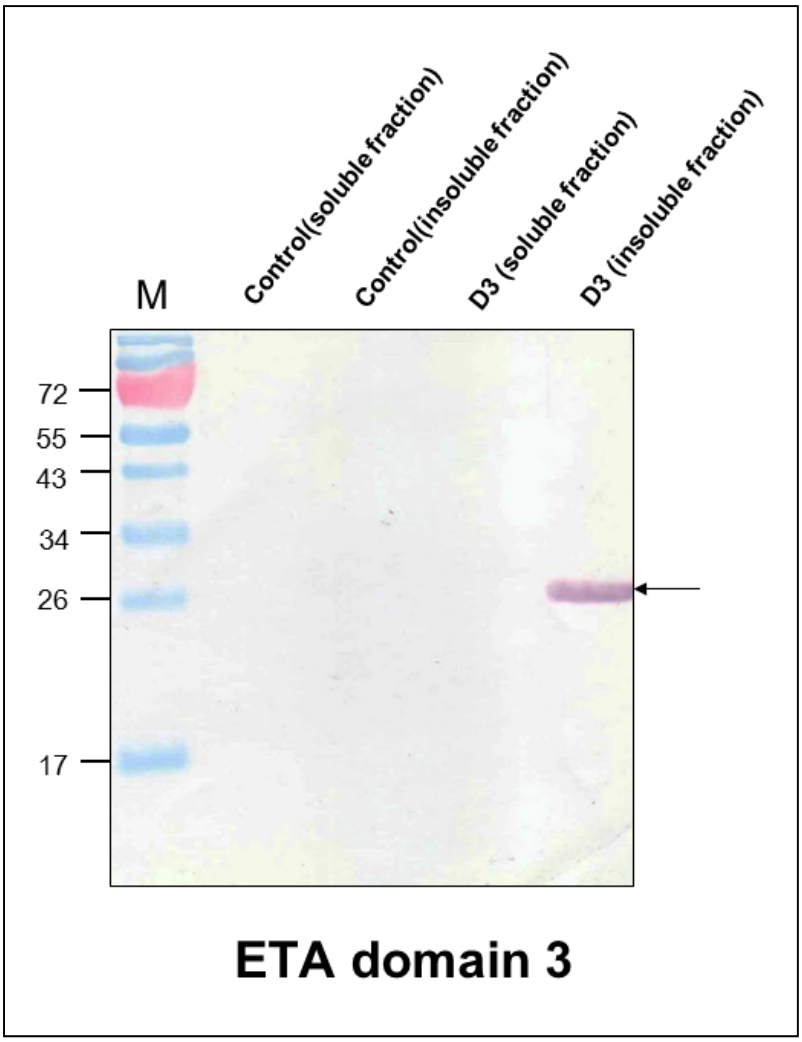

Figure 1.13 Western blot analysis of the hexa-histidine (6xHis)-tagged ETA sub-domain III protein.

Lane M: Standard protein ladder

Lane Sc: Soluble fraction of control [NiCo21 (DE3) *E. coli*]

Lane Ic: Insoluble fraction of control [NiCo21 (DE3) *E. coli*]

Lane S1: Soluble fraction of ETA sub-domain III

Lane I1: Insoluble fraction of ETA sub-domain III; protein size ~23 kDa.

Purification of recombinant protein

Recombinant protein LasB, ETA were prepared from a transformed NiCo21 (DE3) *E. coli* carrying inserted lasA-, lasB-, ETA domain I-, domain II-, domain III- pLATE52 plasmids. The IPTG induced bacterial cells were collected by centrifugation at 4,000 ×g, 4°C for 20 minutes and homogenized by sonication (LABSONIC® P, Goettingen, Germany) at 30%amplitude, 0.6 cycles for 6 minutes in a denaturing lysis buffer (1 g of bacterial cell per 10 ml of the buffer). The bacterial homogenate was centrifuged at 15,000 ×g, 4°C, 20 minutes and the supernatant was transferred to a plastic tube containing Ni-NTA™ bead (Invitrogen™, Life Technologies, NY, USA). The preparation was gently mixed by tube inverting and kept at 25°C, horizontal rocking for 10 minutes to allow protein binding to the resin. The beads were then packed into a polystyrene column and extensively washed with 20 ml washing buffer, the wash fraction also was collected. The recombinant proteins were eluted with 250 mM imidazole in equilibration buffer and each eluted fraction was collected. All eluted fractions were subjected to SDS-PAGE, followed by stained with Coomassie brilliant blue G-250 (CBB) (USB Corporation, CA, USA) staining for direct visualization of the protein band(s).

SDS-PAGE analysis of the purified recombinant protein using 12% SDS-polyacrylamide gel showed recombinant LasB, protein size ~33 kDa (**Figure 2.14**) ETA sub-domain IA; protein size ~28 kDa (**Figure 1.15**) and ETA sub-domain III; protein size ~28 kDa (**Figure 1.16**).

The purified protein was verified by LC/MS-MS. Protein content of the purified LasA, LasB, ETA domain I, and domain III were determined by Bicinchoninic acid (BCA) method. The purified recombinant proteins were kept at -80°C until use.

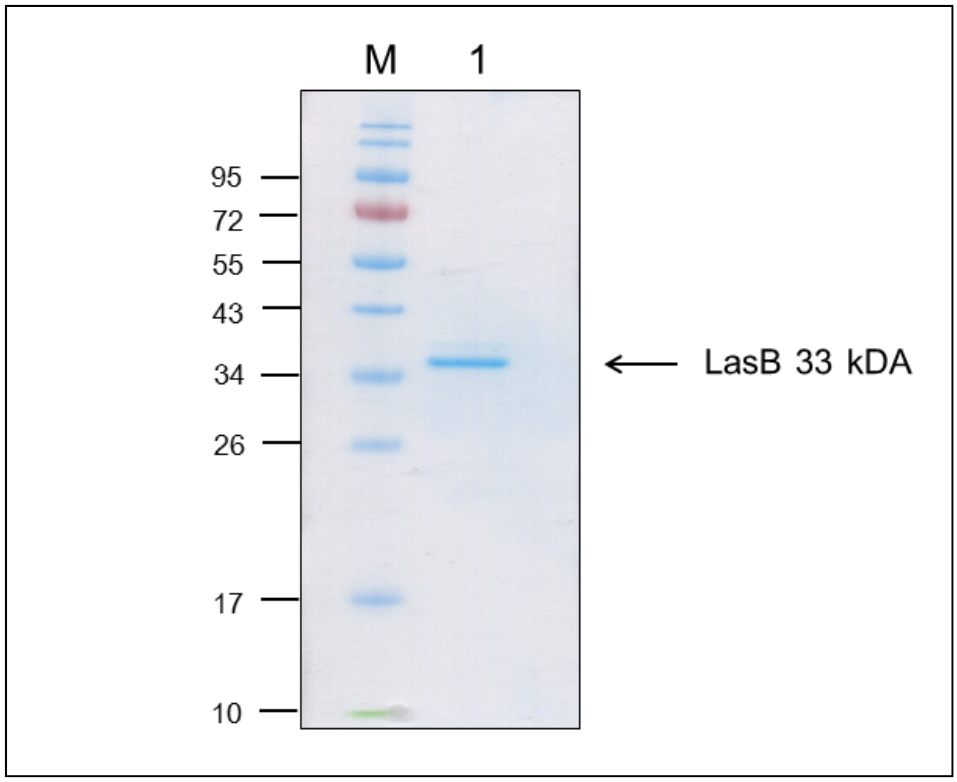

Figure 1.14 SDS-PAGE analysis of the purified inclusion bodies of the Purification recombinant LasB protein using 12% SDS-polyacrylamide gel.
Lane M : Standard protein ladder,
Lane 1 : Purified recombinant LasB, protein size ~33 kDa.

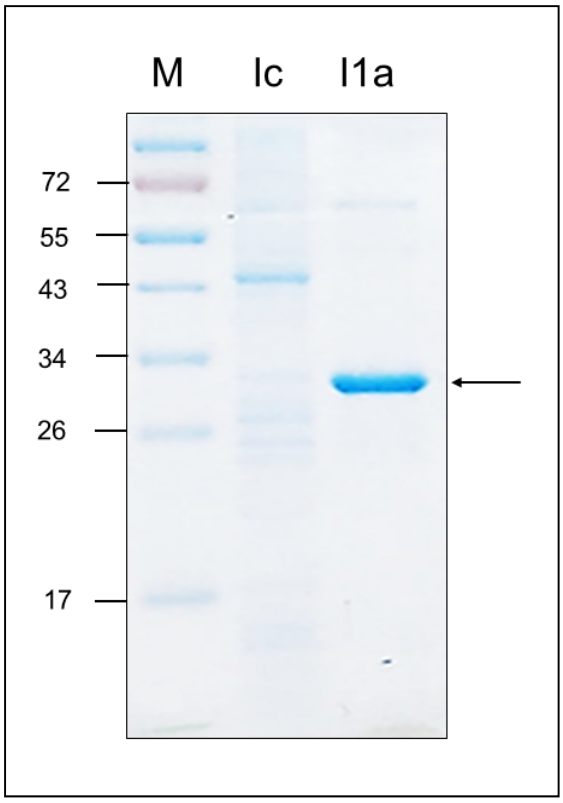

Figure 1.15 SDS-PAGE analysis of the purified inclusion bodies of the ETA sub-domain IA protein from NiCo21 (DE3) *E. coli* using 12% SDS-polyacrylamide gel.
Lane M: Standard protein ladder
Lane Ic: Insoluble fraction of control [NiCo21 (DE3) *E. coli*]
Lane I1a: Insoluble fraction of ETA sub-domain IA; protein size ~28 kDa.

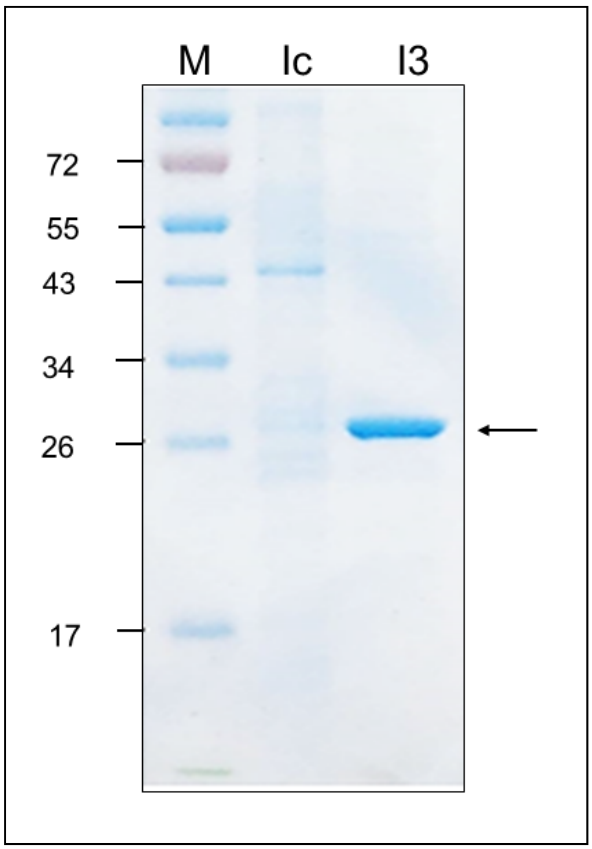

Figure 1.16 SDS-PAGE analysis of the purified inclusion bodies of the ETA sub-domain III protein from NiCo21 (DE3) *E. coli* using 12% SDS-polyacrylamide gel.
Lane M: Standard protein ladder
Lane Ic: Insoluble fraction of control [NiCo21 (DE3) *E. coli*]
Lane I1a: Insoluble fraction of ETA sub-domain III; protein size ~28 kDa.

2. To select phage clones displaying human scFv/humanized-VH/VHH that bind to the active exotoxin A, lasB from human scFv/humanized-VH/VHH phage display libraries.

Selection of human single chain variable fragment (HuscFv) displayed phage clones that bound to native *Pseudomonas aeruginosa* exotoxin A from the established human scFv phage display library

Phage bio-panning for selecting of phage clones that display HuscFv specific to native exotoxin A of *P. aeruginosa*

Purified native ETA (66 kDa) protein (Sigma-Aldrich, USA) was used as antigens in phage bio-panning to select phage clones displaying HuscFv that could bind to the respective protein. In the bio-panning process, one microgram of the native ETA (66 kDa) in a carbonate-bicarbonate buffer, pH 9.6 (coating buffer) was individually immobilized in wells of an ELISA plate. The ELISA plate was incubated at 37°C for overnight then the well was washed with PBS-T, a washing buffer. Two hundred microliters of 5% skim milk in PBS pH 7.5, a blocking solution was added into the well and incubated at room temperature for 1 hour. After that, the blocking solution was discarded from the wells and further washed three times with PBS-T. The HuscFv phage display library that kindly provided by kindly provided by Prof. Dr. Wanpen Chaicumpa (Faculty of Medicine Siriraj Hospital, Mahidol University, Bangkok, Thailand) was added into the antigen coated well and the reaction was incubated at room temperature for 1 hour. Afterwards, the fluid was discarded from the well and the reaction well was extensively washed 10 times to remove unbound phages. The mid-log phase HB2151 *E. coli* was added into the reaction well that containing phages bound to the immobilized antigen and well was incubated at 37°C for 15 minutes. Then the phages infected HB2151 *E. coli* were used to spread onto 2XYT agar plate containing ampicillin and glucose (2XYT-AG) and the plate was incubated at 37°C for 12-16 hours.

Determining of HB2151 *E. coli* clones with pCANTAB5E-huscfv phagemids

For determining the transformed HB2151 *E. coli* which carried the huscfv-phagemids, the bacterial colonies on the 2XYT-AG plate were picked to perform the colony PCR. An individual colony was selected and inoculated into the 150 µl of LB broth containing 100 µg/ml of ampicillin antibiotic, then incubated at 37°C for 2 hours with 250 rpm shaking that one microliter of each clone will be used as DNA template for checking the presence of the huscfv gene. The PCR was carried out using a pair of primers, R1 (forward primer): 5'-CCATGATTACGCCAAGCTTTGGAGCC-3' and R2 (reverse primer): 5'-GCTAGATTTCAAAACAGCAGAAAGG-3'. The 25 µl of PCR reaction mixture and PCR conditions were demonstrated as following.

PCR reaction mixture (25 µl)

Ingredients	**Volume (µl)**
Sterile ultrapure distilled water (UDW)	18.3
Taq buffer with KCl (10x)	2.5
dNTP (10 mM each)	0.5
Forward Primer (10 µM)	0.5
Reverse Primer (10 µM)	0.5
$MgCl_2$ (25 mM)	1.5
Taq DNA polymerase (5 units/1µl)	0.2
DNA template	1.0

PCR conditions

Steps	**Conditions**
Initial denaturation	at 95°C for 5 minutes
35 cycles of Denaturation ,	at 95°C for 30 seconds
Annealing ,	at 58°C for 30 seconds
and Extension	at 72°C for 1 minute
Final extension	at 72°C for 7 minutes

After PCR amplification, the PCR products were analyzed using 1.5% agarose gel electrophoresis and ethidium bromide staining.

The colonies appearing on 2XYT agar plate containing 100 µg/ml of ampicillin and 2% glucose (2XYT-AG) were picked and performed the screening for the inserted huscfv gene (the expected amplicon size ~1,000 bp) using direct colony PCR. The result shown that only 29 of the 33 selected clones (which accounted for 87.88%) derived from bio-panning with the native ETA(66kDa) were positive for huscfv segments which were clones number 1-10, 12-25, 28, 29, 31, and 32 (**Figure 2.17, 2.18,** and **2.19**).

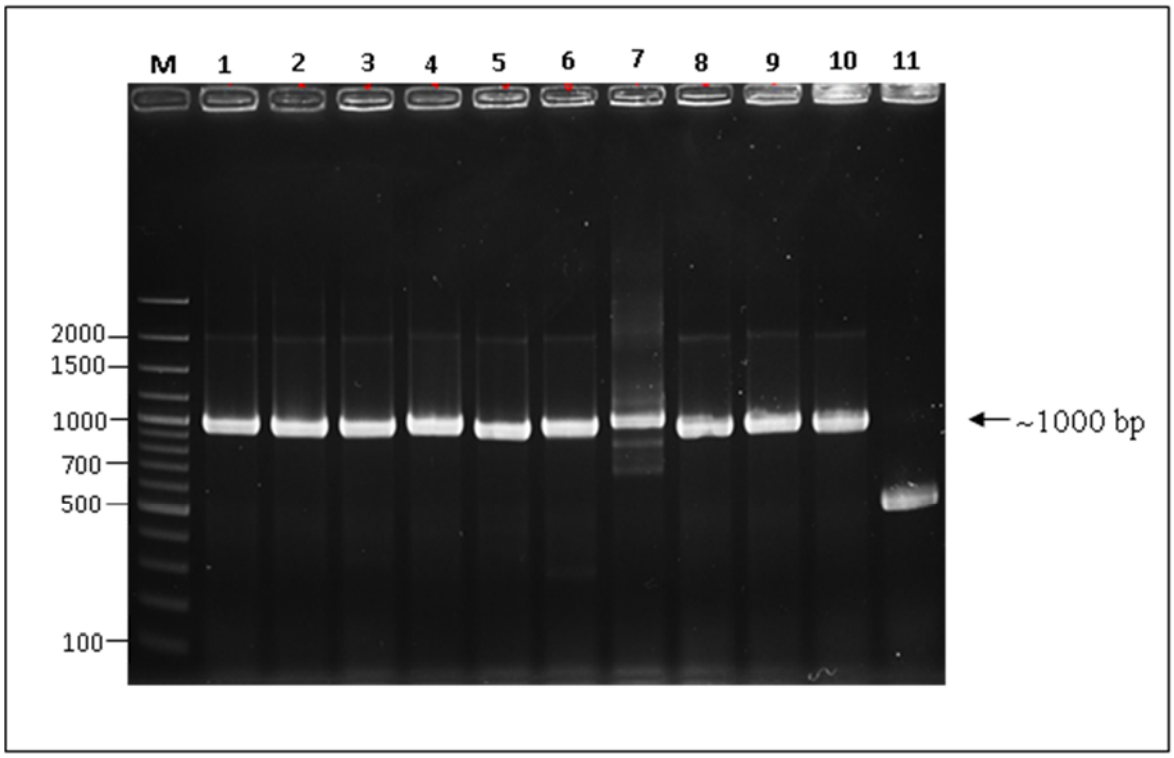

Figure 1.17 PCR amplification for screening of pCANTAB5E-ETA-huscfv phagemids (the expected amplicon size ~1,000 bp) transformed *E. coli* strain HB2151 colonies.

Lane M: GenRulerTM 100 bp DNA ladder plus

Lanes 1-11: Results of colony PCR of PCR amplicons for detecting the presence of huscfv gene transformed *E. coli* strain HB2151 colonies for clones no.1-11, respectively.

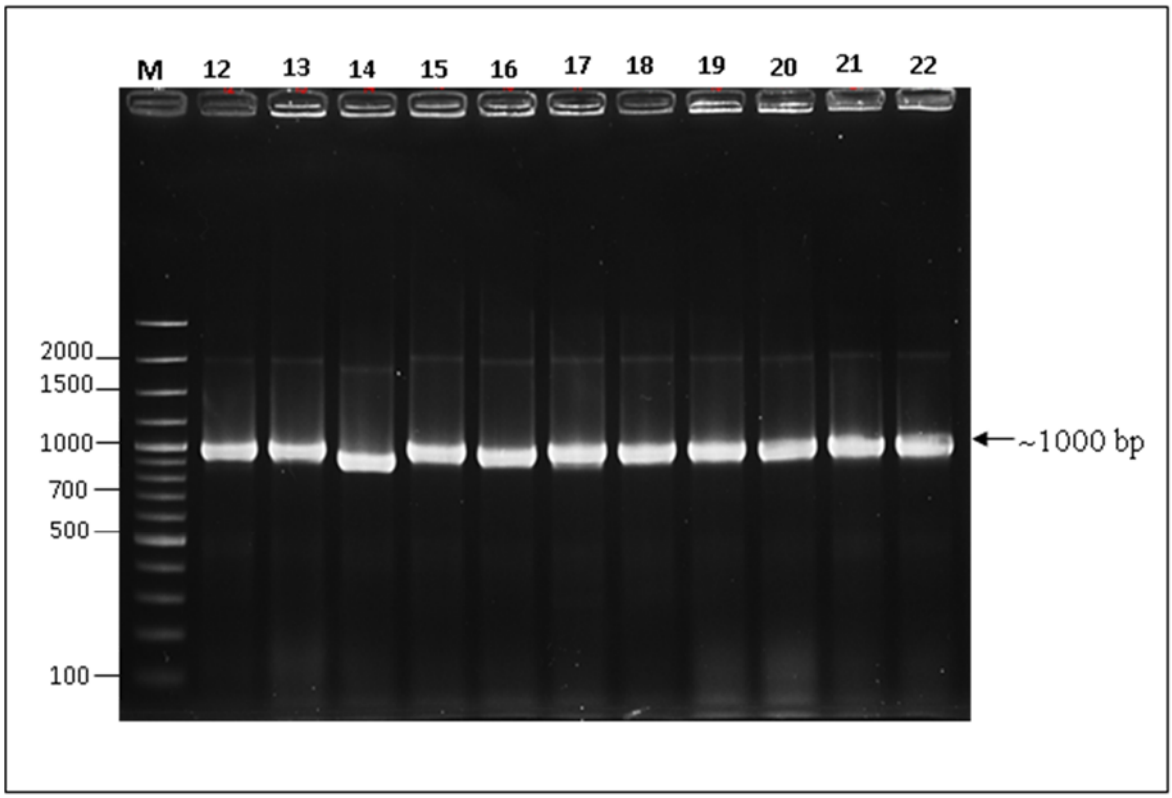

Figure 1.18 PCR amplification for screening of pCANTAB5E-ETA-huscfv phagemids (the expected amplicon size ~1,000 bp) transformed *E. coli* strain HB2151 colonies.

Lane M: GenRulerTM 100 bp DNA ladder plus

Lanes 12-22: Results of colony PCR of PCR amplicons for detecting the presence of huscfv gene transformed *E. coli* strain HB2151 colonies for clones no.12-22, respectively.

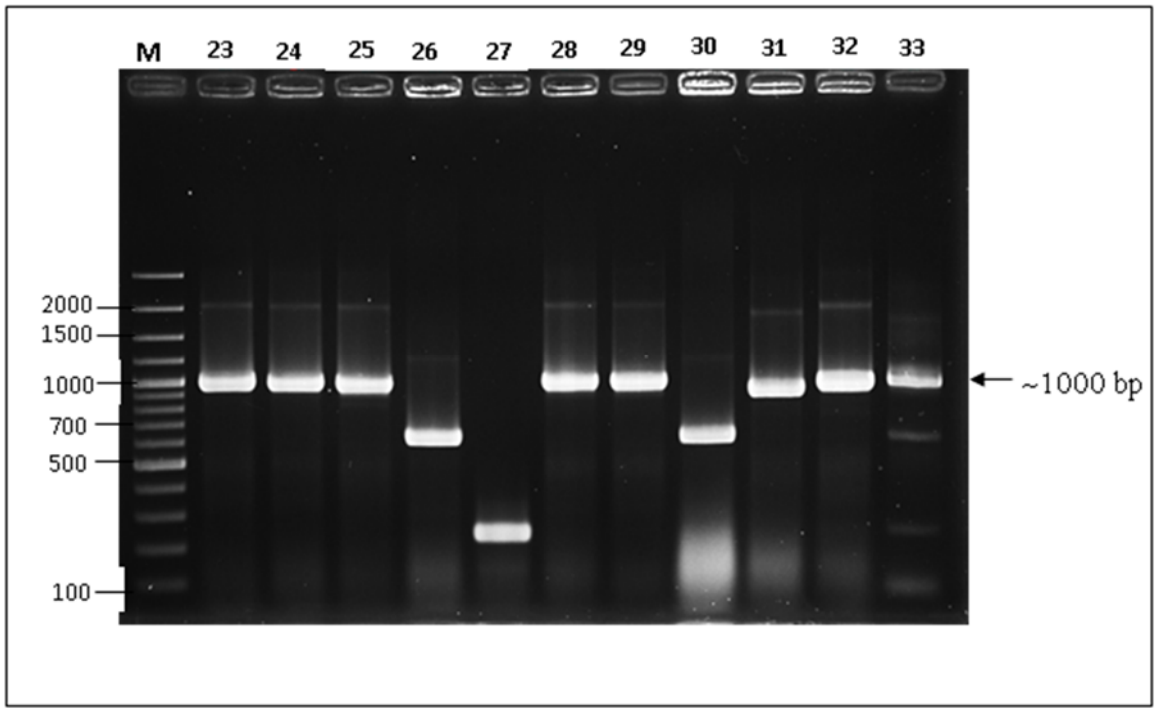

Figure 1.19 PCR amplification for screening of pCANTAB5E-ETA-huscfv phagemids (the expected amplicon size ~1,000 bp) transformed *E. coli* strain HB2151 colonies.
Lane M: GenRulerTM 100 bp DNA ladder plus
Lanes 23-33: Results of colony PCR of PCR amplicons for detecting the presence of huscfv gene transformed *E. coli* strain HB2151 colonies for clones no.23-33, respectively.

Binding of the *Escherichia coli* derived-HuscFv to exotoxin A

Verification of the HuscFvs binding activity to the native ETA (66kDa) protein antigen by indirect ELISA

The HB2151 *E. coli* clones which gave positive result for huscfv gene amplicons of the expected size ~ 1,000 bp were further performed the protein expression. In this study, HuscFv proteins were expressed by the individual clone was inoculated into 2ml of AIM (Auto Induction Medium) medium containing 100 µg/ml ampicillin antibiotic and incubated at 30°C with shaking at 250 rpm for overnight. After that, the induced bacterial cells were collected by centrifugation at 14,000 x*g* at 4°C for 1 minutes. The cell pellets of expressed soluble HuscFvs specific native ETA samples were performed the protein extraction using protein extraction kits, BugBuster® Plus Lysonase™ (Novagen, Merck, CA, USA) to separating of the soluble HB2151 *E. coli* fraction (the supernatant) that protein in this fraction was subjected to perform the binding test using an indirect ELISA for detecting the binding specificities of the soluble HuscFvs specific native ETA protein. For the indirect ELISA, Rabbit anti-E-Tag polyclonal antibody (Abcam, USA) and Goat anti-rabbit immunoglobulin-HRP conjugate (Southern Biotech, AL, USA) were used as the primary and secondary antibody, respectively. The ABTS (2,2 azino-bis [3-ethylbenzthiazoline-6-sulfonic acid]) (ZYMED CA, USA) was used as the substrate for the ELISA detection. The ELISA signal was measured at OD 405 nm using a FINSTRUMENTS® Microplate Reader.

The result of indirect ELISA shown for the representative clones that only 4 of the 29 selected clones derived from bio-panning with the native ETA (66 kDa) were gave the two times signal higher than that of BSA(control antigen) at OD 405 nm (**Figure 1.20**).

Detection of soluble HuscFvs specific native ETA (66kDa) protein expression

The Western blot analysis was used to detecting the soluble HuscFvs specific native ETA (66kDa) protein expression. The soluble HuscFvs specific native ETA clones were revealed by using the Rabbit anti-E-Tag polyclonal antibody (Abcam, USA) and Goat anti-rabbit IgG-AP conjugate (Southern Biotech, AL, USA) were used as the primary and secondary antibody, respectively. The NBT/BCIP (5-bromo-4-chloro-3-indolyl-phosphate) was used as the color development substrate.

The result of Western blot analysis shown for detecting the soluble HuscFvs specific native ETA (66kDa) protein expression that all 4 representative clones of which gave the significant signal (two times signal higher than that of control antigen at OD405nm) were expressing the HuscFv protein (the expected protein size ~25-30 kDa) (**Figure 1.21**).

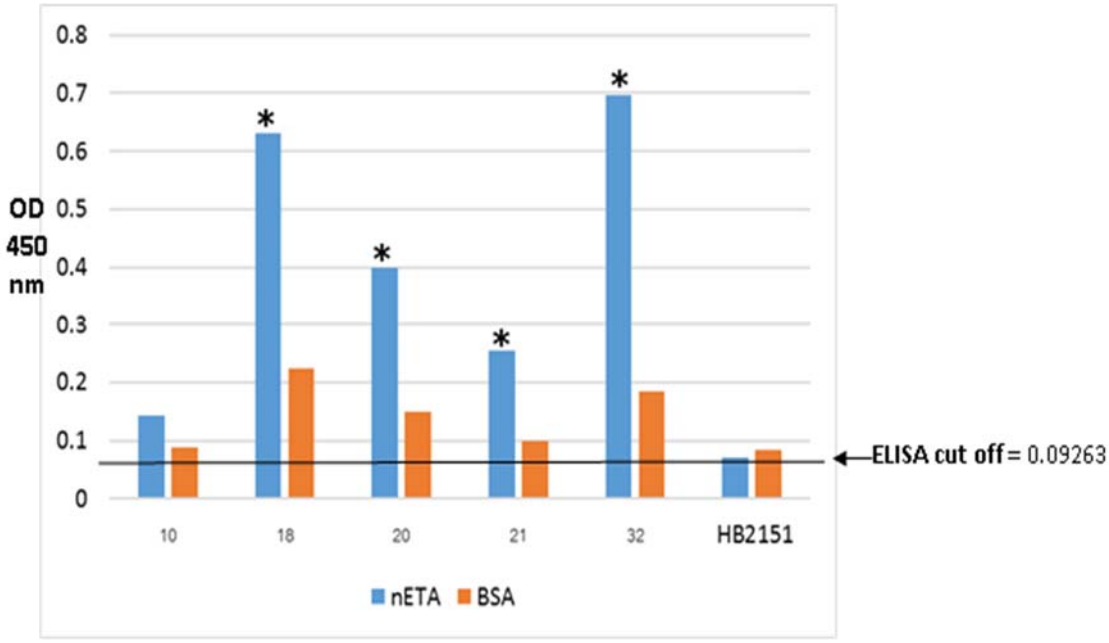

Figure 1.20 The diagram of binding test result for verifying of the HuscFvs binding activity to the native ETA (66kDa) protein antigen using indirect ELISA.

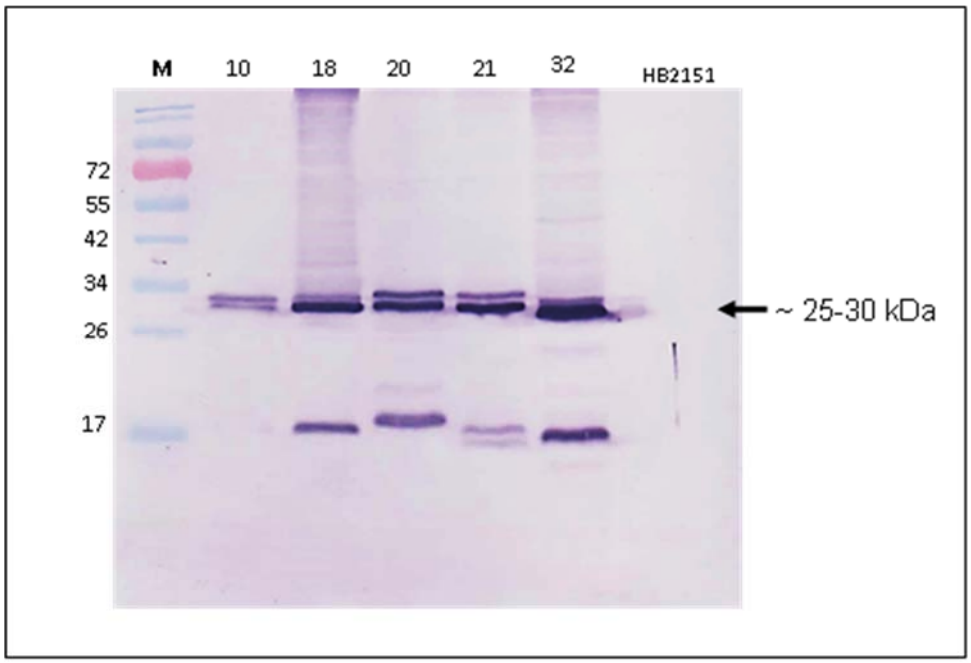

Figure 1.21 Western blot patterns of the HuscFvs specific ETA protein expressed from the huscfv positive *E. coli* clones (expected protein size ~25-30kDa).
Lane M: Standard protein ladder
Lane 10: Soluble fraction of Huscfv specific native ETA clone no.10 protein
Lane 18: Soluble fraction of Huscfv specific native ETA clone no.18 protein
Lane 20: Soluble fraction of Huscfv specific native ETA clone no.20 protein
Lane 21: Soluble fraction of Huscfv specific native ETA clone no.21 protein
Lane 32: Soluble fraction of Huscfv specific native ETA clone no.32 protein
Lane HB2151: Soluble fraction of control [HB2151 *E. coli*] protein

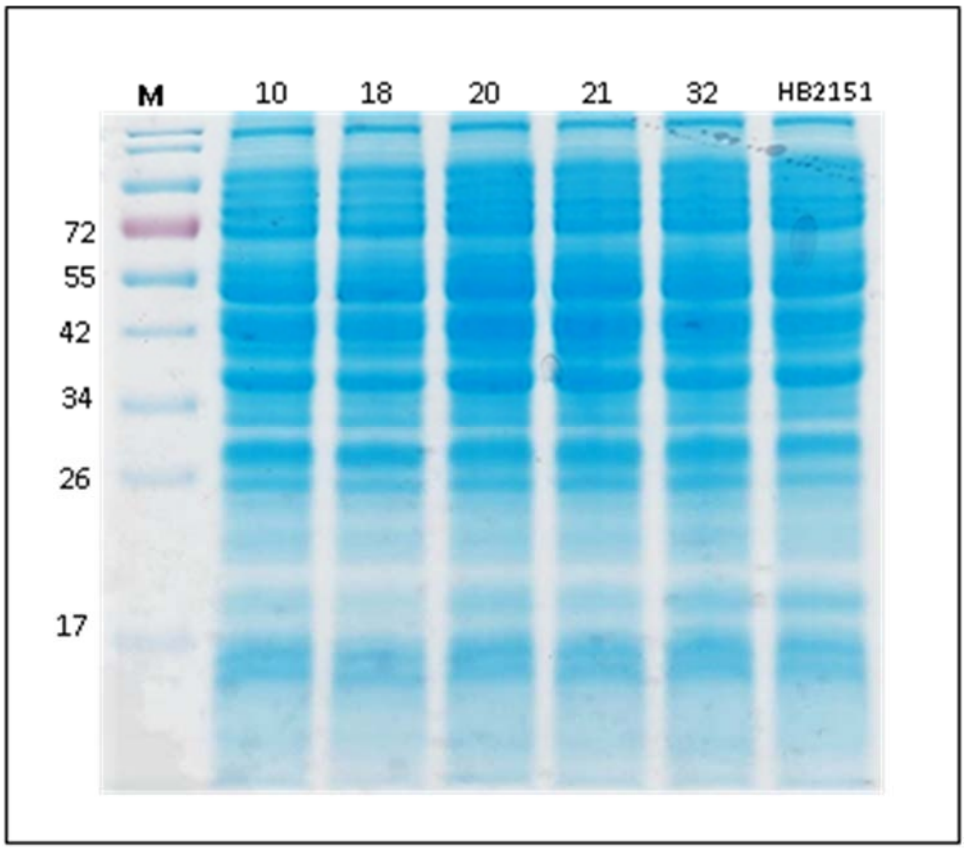

Figure 1.22 SDS-PAGE analysis of the separated soluble and insoluble fractions of the HuscFvs specific native ETA protein from HB2151 *E. coli*.
Lane M: Standard protein ladder
Lane 10: Soluble fraction of Huscfv specific native ETA clone no.10 protein
Lane 18: Soluble fraction of Huscfv specific native ETA clone no.18 protein
Lane 20: Soluble fraction of Huscfv specific native ETA clone no.20 protein
Lane 21: Soluble fraction of Huscfv specific native ETA clone no.21 protein
Lane 32: Soluble fraction of Huscfv specific native ETA clone no.32 protein
Lane HB2151: Soluble fraction of control [HB2151 *E. coli*] protein

Selection of human single chain variable fragment)HuscFv (displayed phage clones that bound to recombinant truncated *Pseudomonas aeruginosa* exotoxin A) rETA (including domain 1A and 3 from the established human scFv phage display library

Phage bio-panning for selecting of phage clones that display HuscFv specific to rETA-1A and rETA-3

Refolded rETA-1A)28kDa (and rETA-3)28kDa (were used as antigens in phage bio-panning to select phage clones displaying HuscFv that could bind to the respective protein .In the bio-panning process, 0.5 microgram of the antigens)rETA-1A and rETA-3 (in a carbonate-bicarbonate buffer, pH 9.6)coating buffer (were individually immobilized in wells of an ELISA plate)EIA/RIA 8 well strip-flat bottom, Corning, NY, USA .(The ELISA plate were incubated at 4°C for overnight then the well were washed with Distilled water .The 150 microliters of Protein-free blocking buffer were added into the well and incubated at room temperature)25°C (for 1 hour .After that, the blocking solution were discarded from the wells and further washed three times with PBS-T .The HuscFv phage display library)~ 3 x 10^{11} phage particles (that kindly provided by Prof .Dr .Wanpen Chaicumpa)Faculty of Medicine Siriraj Hospital, Mahidol University, Bangkok, Thailand (were added into the antigen coated well, and the reaction were incubated at room temperature for 1 hour .Afterwards, the fluid)unbound phages (were discarded from the well and the reaction well were extensively washed 10 times to remove unbound phages .The 100 µl of the mid-log phase HB2151 *E .coli* were added into the reaction well that containing phages bound to the immobilized antigen and well were incubated at 37°C for 10 minutes .Then the phages infected HB2151 *E .coli* were used to spread onto 2XYT agar plate containing 100 µg/ml of ampicillin and 2 %glucose)2XYT-AG (and the plate were incubated at 37°C for 12-16 hours.

Determining of HB2151 *E. coli* clones with pCANTAB5E-*huscfv* phagemids which could expressed HuscFvs specific to the respective antigens (rETA-1A and rETA-3)

For determining the transformed HB2151 *E .coli* which carried the *huscfv*-phagemids, the bacterial colonies on the 2XYT-AG plate were picked to perform the colony PCR .An individual colony was selected and inoculated into the 150 µl of LB broth containing 100 µg/ml of ampicillin antibiotic, then incubated at 37°C for 2 hours with 250 rpm shaking that one microliter of each clone will be used as DNA template for checking the presence of the *huscfv* gene .The PCR was carried out using a pair of primers, R1)forward primer : (5-' CCATGATTACGCCAAGCTTTGGAGCC-3' and R2)reverse primer :(5-' GCTAGATTTCAAAACAGCAGAAAGG-3 .'The 25 µl of PCR reaction mixture and PCR conditions were demonstrated in below, respectively .After PCR amplification, the PCR products were analyzed using 1.5 %agarose gel electrophoresis and ethidium bromide staining.

PCR reaction mixture)25 μl(

Ingredients	Volume (μl)
Sterile ultrapure distilled water (UDW)	18.3
Taq buffer with KCl (10x)	2.5
dNTPs (10 mM each)	0.5
Forward Primer (10 μM)	0.5
Reverse Primer (10 μM)	0.5
$MgCl_2$ (25 mM)	1.5
Taq DNA polymerase (5 units/1μl)	0.2
DNA template	1.0

PCR conditions

Steps	Conditions
Initial denaturation	at 95°C for 5 minutes
35 cycles of Denaturation ,	at 95°C for 30 seconds
Annealing ,	at 58°C for 30 seconds
and Extension	at 72°C for 40 seconds
Final extension	at 72°C for 7 minutes

The colonies appearing on 2XYT agar plate containing 100 μg/ml of ampicillin and 2% glucose (2XYT-AG) were picked and performed the screening for the inserted *huscfv* gene (the expected amplicon size ~1,000 bp) using direct colony PCR. The results shown that 35 of the 61 selected clones (which accounted for 57.80%) derived from bio-panning with the rETA-1A were positive for *huscfv* segments **(Figure 1.23-1.26)** and 57 of the 96 selected clones (which accounted for 59.38%) derived from bio-panning with the rETA-3 were positive for *huscfv* segments **(Figure 1.27-1.32).**

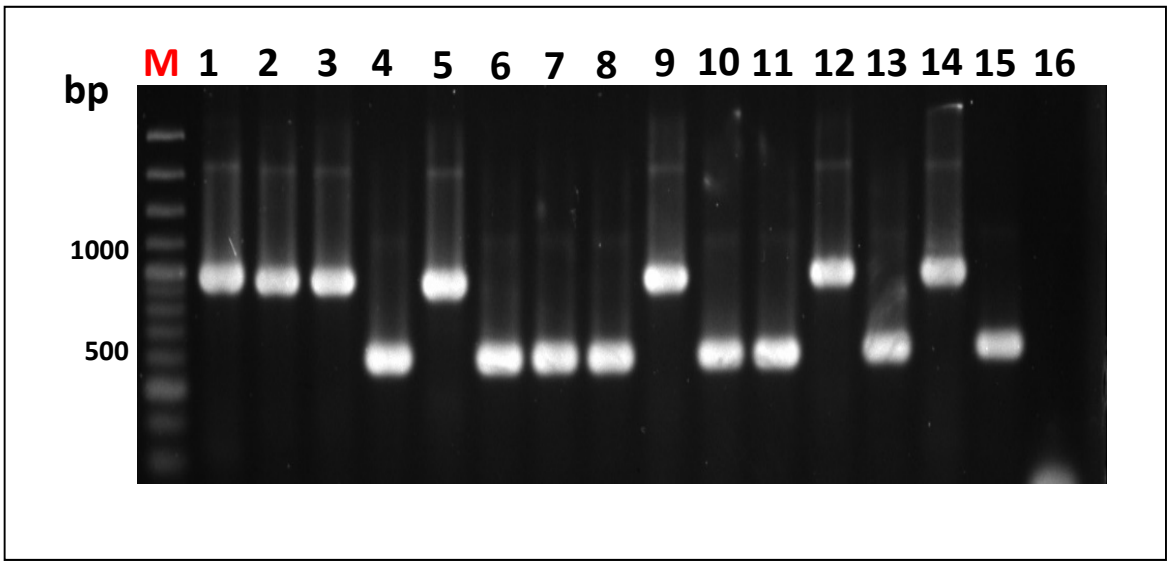

Figure 1.23 PCR amplification for screening of pCANTAB5E-*huscfv* phagemids (the expected amplicon size ~1,000 bp) transformed *E. coli* strain HB2151 colonies.

Lane M: GenRuler^{TM} 100 bp DNA ladder plus

Lanes 1-16: Results of colony PCR of PCR amplicons for detecting the presence of *huscfv* gene transformed *E. coli* strain HB2151 colonies specific for rETA-1A clone no.1-16, respectively.

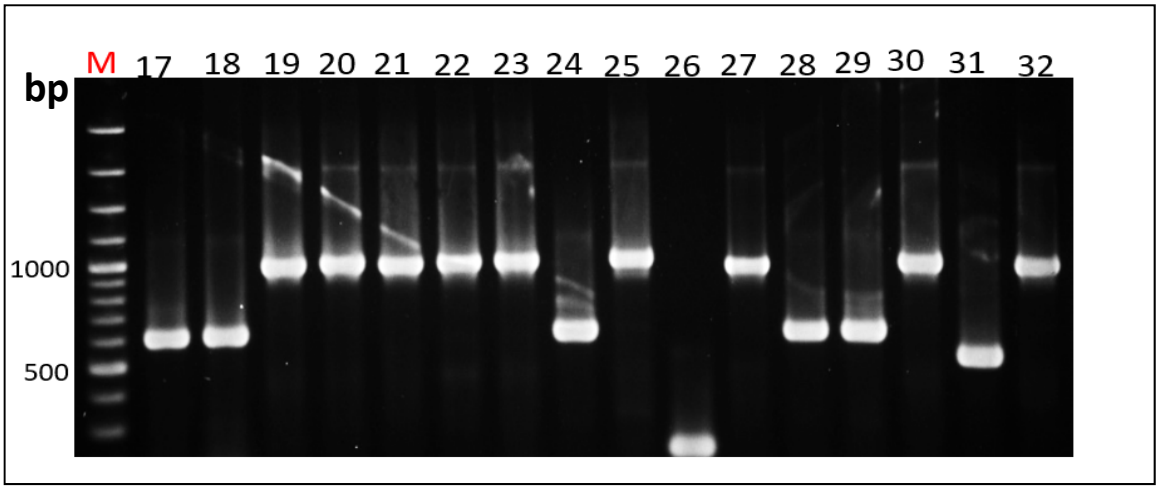

Figure 1.24 PCR amplification for screening of pCANTAB5E-*huscfv* phagemids (the expected amplicon size ~1,000 bp) transformed *E. coli* strain HB2151 colonies.

Lane M: GenRuler^{TM} 100 bp DNA ladder plus
Lanes 17-32: Results of colony PCR of PCR amplicons for detecting the presence of *huscfv* gene transformed *E. coli* strain HB2151 colonies specific for rETA-1A clones no.17-32, respectively.

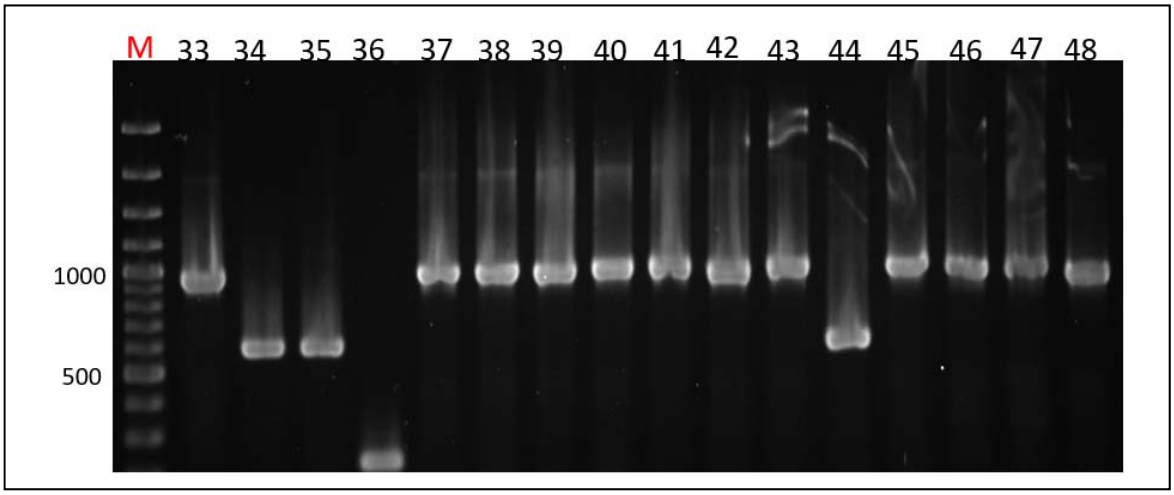

Figure 1.25 PCR amplification for screening of pCANTAB5E-*huscfv* phagemids (the expected amplicon size ~1,000 bp) transformed *E. coli* strain HB2151 colonies.

Lane M: GenRuler^{TM} 100 bp DNA ladder plus
Lanes 33-48: Results of colony PCR of PCR amplicons for detecting the presence of *huscfv* gene transformed *E. coli* strain HB2151 colonies specific for rETA-1A clones no.33-48, respectively.

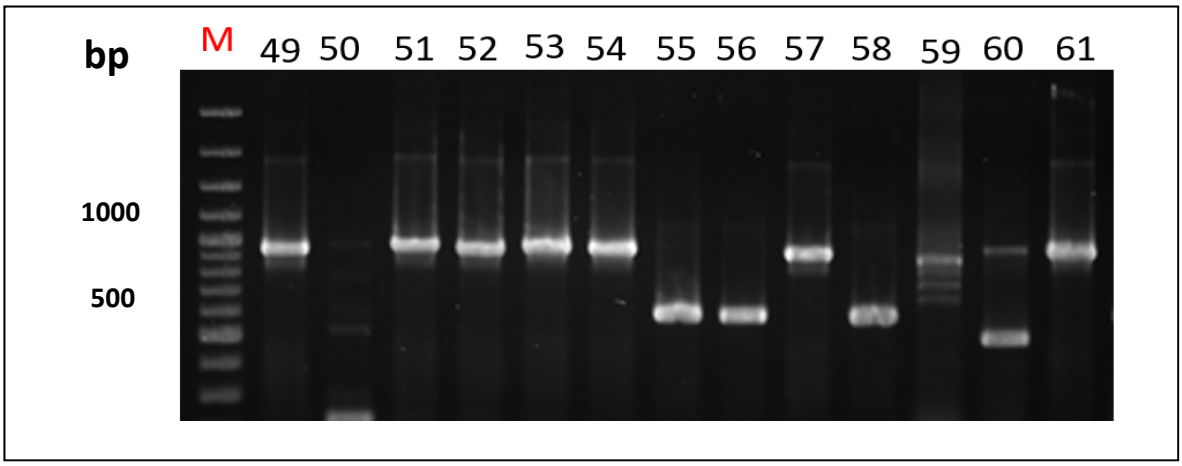

Figure 1.26 PCR amplification for screening of pCANTAB5E-*huscfv* phagemids (the expected amplicon size ~1,000 bp) transformed *E. coli* strain HB2151 colonies.
Lane M: GenRuler™ 100 bp DNA ladder plus
Lanes 49-61: Results of colony PCR of PCR amplicons for detecting the presence of *huscfv* gene transformed *E. coli* strain HB2151 colonies specific for rETA-1A clones no. 49-61, respectively.

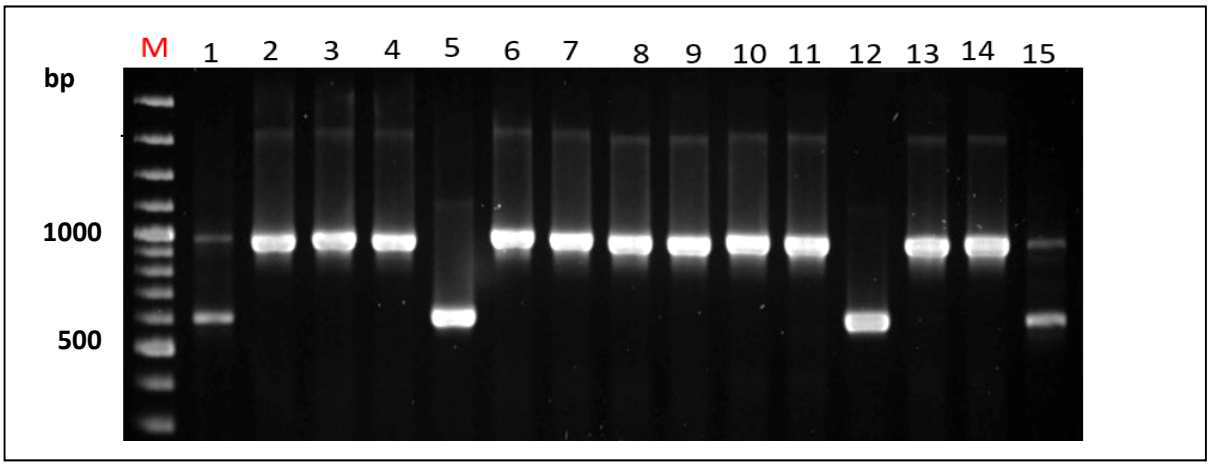

Figure 1.27 PCR amplification for screening of pCANTAB5E-*huscfv* phagemids (the expected amplicon size ~1,000 bp) transformed *E. coli* strain HB2151 colonies.

Lane M: GenRuler™ 100 bp DNA ladder plus

Lanes 1-15: Results of colony PCR of PCR amplicons for detecting the presence of *huscfv* gene transformed *E. coli* strain HB2151 colonies specific for rETA-3 clones no. 1-15, respectively.

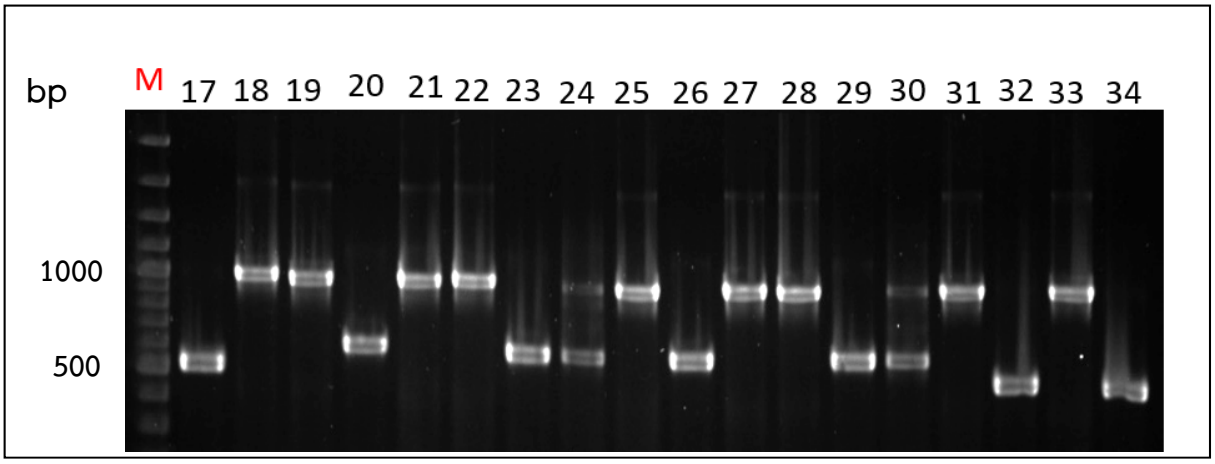

Figure 1.28 PCR amplification for screening of pCANTAB5E-*huscfv* phagemids (the expected amplicon size ~1,000 bp) transformed *E. coli* strain HB2151 colonies.
Lane M: GenRuler™ 100 bp DNA ladder plus
Lanes 17-34: Results of colony PCR of PCR amplicons for detecting the presence of *huscfv* gene transformed *E. coli* strain HB2151 colonies specific for rETA-3 clones no. 17-34, respectively.

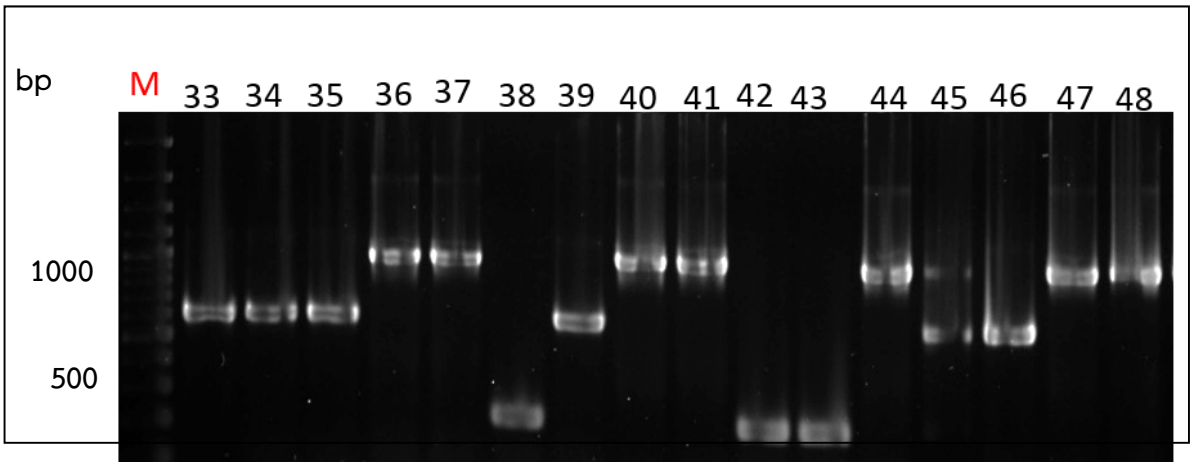

Figure 1.29 PCR amplification for screening of pCANTAB5E-*huscfv* phagemids (the expected amplicon size ~1,000 bp) transformed *E. coli* strain HB2151 colonies.
Lane M: GenRuler™ 100 bp DNA ladder plus
Lanes 33-48: Results of colony PCR of PCR amplicons for detecting the presence of *huscfv* gene transformed *E. coli* strain HB2151 colonies specific for rETA-3 clones no.33-48, respectively.

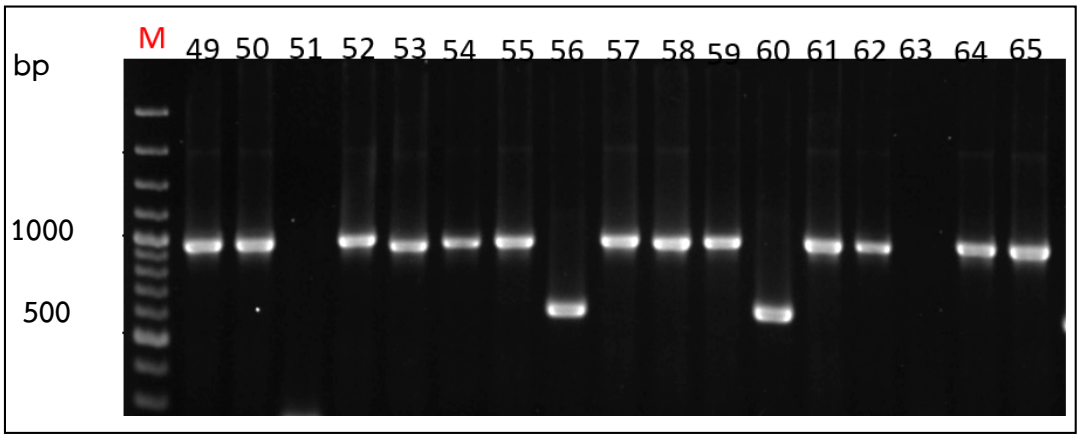

Figure 1.30 PCR amplification for screening of pCANTAB5E-*huscfv* phagemids (the expected amplicon size ~1,000 bp) transformed *E. coli* strain HB2151 colonies
Lane M: GenRuler™ 100 bp DNA ladder plus
Lanes 49-65: Results of colony PCR of PCR amplicons for detecting the presence of *huscfv* gene transformed *E. coli* strain HB2151 colonies specific for rETA-3 clones no. 49-65, respectively.

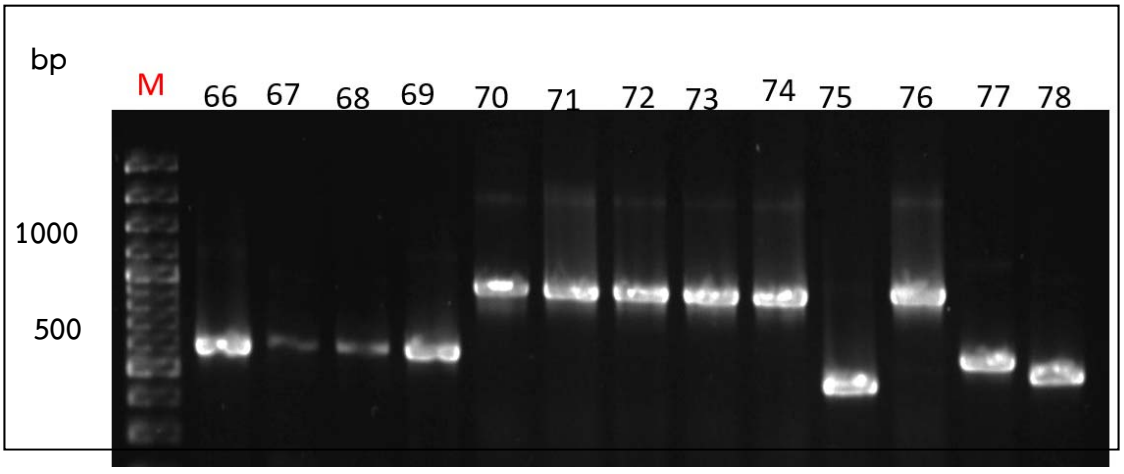

Figure 1.31 PCR amplification for screening of pCANTAB5E-*huscfv* phagemids (the expected amplicon size ~1,000 bp) transformed *E. coli* strain HB2151 colonies

Lane M: GenRuler™ 100 bp DNA ladder plus
Lanes 66-78: Results of colony PCR of PCR amplicons for detecting the presence of *huscfv* gene transformed *E. coli* strain HB2151 colonies specific for rETA-3 clones no. 66-78, respectively.

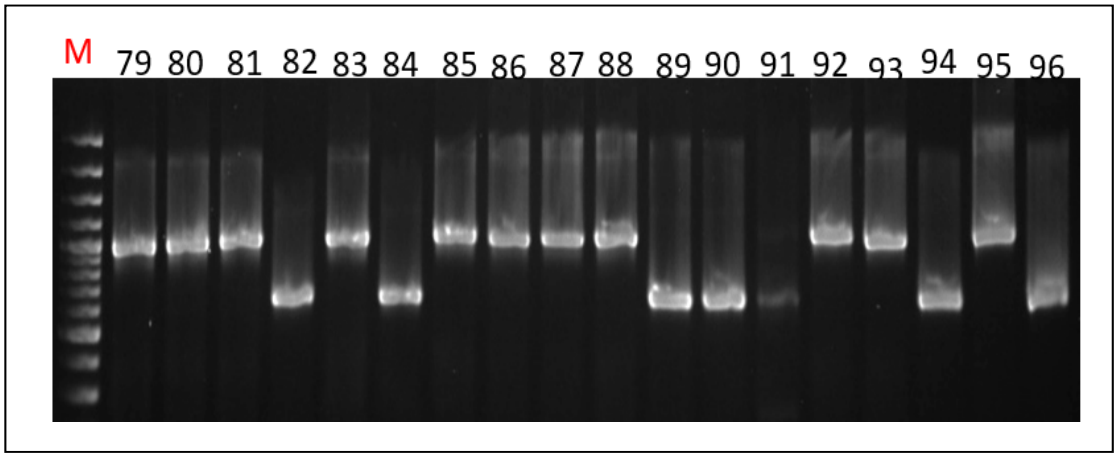

Figure 1.32 PCR amplification for screening of pCANTAB5E-*huscfv* phagemids (the expected amplicon size ~1,000 bp) transformed *E. coli* strain HB2151 colonies.

Lane M: GenRuler^{TM} 100 bp DNA ladder plus

Lanes 79-96: Results of colony PCR of PCR amplicons for detecting the presence of *huscfv* gene transformed *E. coli* strain HB2151 colonies specific for rETA-3 clones no. 79-96, respectively.

Binding of the *Escherichia coli* derived-HuscFv to exotoxin A domain 1A and 3

Verification of the HuscFvs binding activity to the respective antigens (rETA-1A and rETA-3 protein) by indirect ELISA

The HB2151 *E. coli* clones which gave positive result for *huscfv* gene amplicons of the expected size ~ 1,000 bp were further performed the protein expression. In this study, HuscFv proteins were expressed by the individual clone was inoculated into 2 ml of AIM (Auto Induction Medium) medium containing 100 µg/ml ampicillin antibiotic and incubated at 30°C with shaking at 250 rpm for overnight. After that, the induced bacterial cells were collected by centrifugation at 10,000 *x*g at 4°C for 1 minutes. The cell pellets of expressed soluble HuscFvs specific to the respective antigens (rETA-1A and rETA-3 protein) were performed the protein extraction using protein extraction kits, BugBuster® Plus Lysonase ™ (Novagen, Merck, CA, USA) to separating of the soluble HB2151 *E. coli* fraction (the supernatant) that protein in this fraction were subjected to perform the binding test using an indirect ELISA for detecting the binding specificities of the soluble HuscFvs specific native ETA protein. For the indirect ELISA, Rabbit anti-E-Tag polyclonal antibody (Abcam, USA) and Goat anti-rabbit immunoglobulin-HRP conjugate (Southern Biotech, AL, USA) was used as the primary and secondary antibody, respectively. The ABTS (2,2 azino-bis [3-ethylbenzthiazoline-6-sulfonic acid]) (ZYMED CA, USA) was used as the substrate for the ELISA detection. The ELISA signal was measured at OD405nm using a FINSTRUMENTS® Microplate Reader.

The results of indirect ELISA were shown. There are 10 positive clones for HuscFvs specific rETA-1A which are clone no. 3, 5, 9, 33, 37, 43, 45, 46, 54, 61) Figure 2.33 (and 17 positive clones for HuscFvs specific rETA-3 which are clone no. 7, 10, 14, 18, 21, 24, 41, 48, 52, 57, 58, 61, 63, 71, 80, 83, and 95) Figure 1.34.(They gave the two times signal higher than that of BSA (control antigen) at OD405nm.

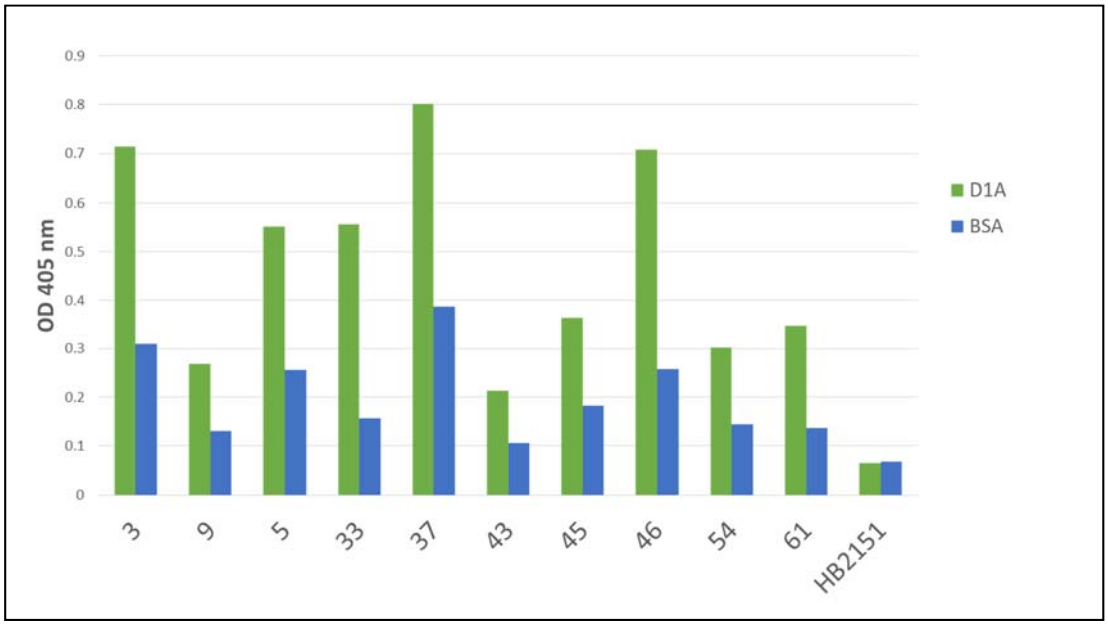

Figure 1.33 The diagram of binding test result for verifying of the HuscFvs binding activity to the rETA-1A protein antigen using indirect ELISA.

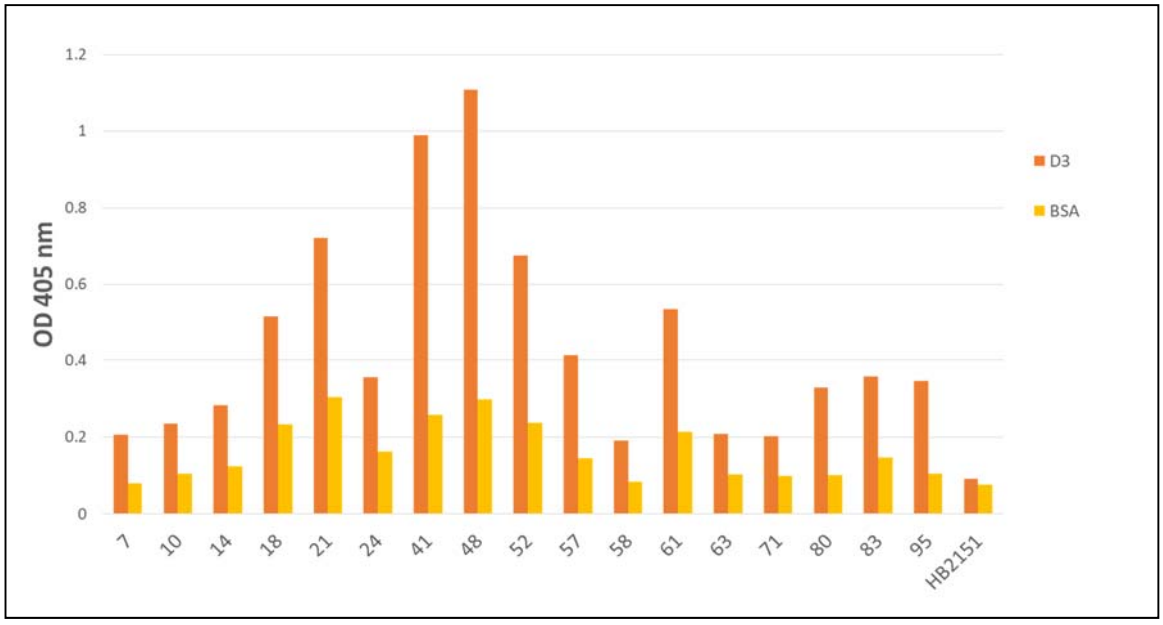

Figure 1.34 The diagram of binding test result for verifying of the HuscFvs binding activity to the rETA-3 protein antigen using indirect ELISA

Detection of soluble HuscFvs specific rETA-1A and rETA-3 protein expression

In this study, the Western blot analysis was used to detecting the soluble HuscFvs specific the rETA-1A and rETA-3 protein expression .The soluble HuscFvs specific native ETA clones were revealed by using the Rabbit anti-E-Tag polyclonal antibody)Abcam, USA (and Goat anti-rabbit IgG-AP conjugate)Southern Biotech, AL, USA (were used as the primary and secondary antibody, respectively . The NBT/ BCIP) 5- bromo- 4- chloro- 3- indolyl-phosphate (was used as the color development substrate .

The result of Western blot analysis shown for detecting the soluble HuscFvs specific the rETA-1A and rETA-3 protein expression .For the representative HuscFv clones for the rETA-1A are clone no .3, 5, 9, 33, 37, 43, 45, 46, 54 and 61 which gave the significant signal)two times signal higher than that of control antigen at OD405nm (were expressing the HuscFv protein)the expected protein size ~25-30 kDa) (Figure 1.35 .(For the representative HuscFv clones for the rETA-3 are clone no .7, 10, 14, 18, 21, 24, 41, 48, 52, 57, 58, 61, 63, 71, 80, 83, and 95)Figure 2.36 and Figure 2.37.(

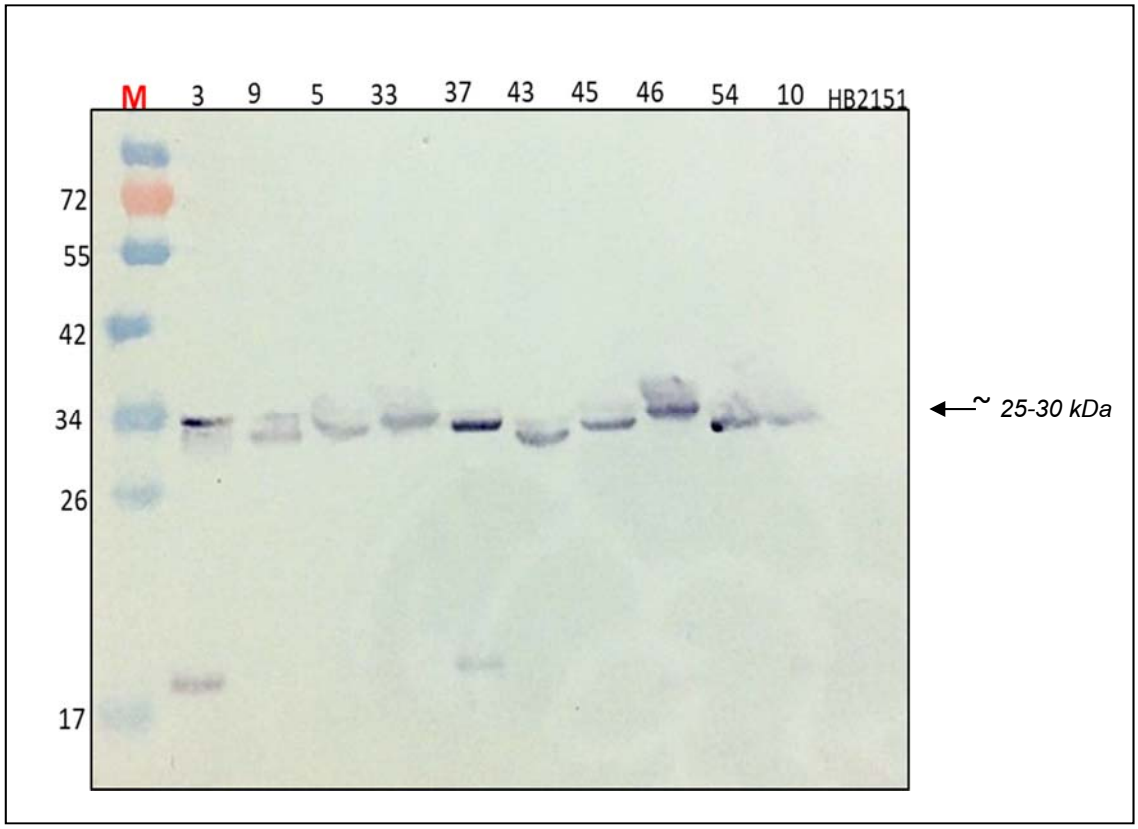

Figure 1.35 Western blot patterns of the HuscFvs specific rETA-1A protein expressed from the *huscfv* positive *E .coli* clones)expected protein size ~25-30kDa(.

Lane M :Standard protein ladder

Lane 3 :Soluble fraction of Huscfv specific rETA-1A clone no.3 protein

Lane 9 :Soluble fraction of Huscfv specific rETA-1A clone no.9 protein

Lane 5 :Soluble fraction of Huscfv specific rETA-1A clone no.5 protein

Lane 33 :Soluble fraction of Huscfv specific rETA-1A clone no.33 protein

Lane 37 :Soluble fraction of Huscfv specific n rETA-1A clone no.37 protein

Lane 43 :Soluble fraction of Huscfv specific n rETA-1A clone no.43 protein

Lane 45 :Soluble fraction of Huscfv specific n rETA-1A clone no.45 protein

Lane 46 :Soluble fraction of Huscfv specific n rETA-1A clone no.46 protein

Lane 54 :Soluble fraction of Huscfv specific n rETA-1A clone no.54 protein

Lane 10 :Soluble fraction of Huscfv specific n rETA-1A clone no.10 protein

Lane HB2151 :Soluble fraction of the negative control]HB2151 *E .coli* [protein

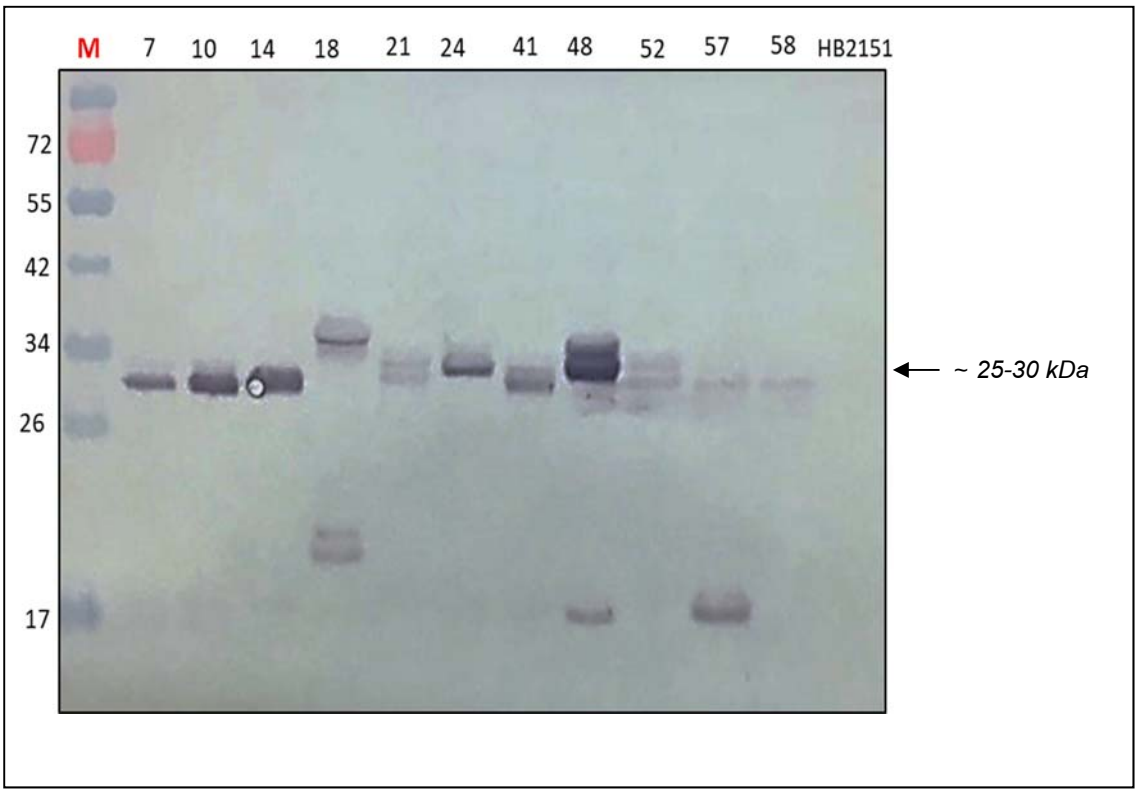

Figure 1.35 Western blot patterns of the HuscFvs specific rETA-3 protein expressed from the *huscfv* positive *E .coli* clones)expected protein size ~25-30kDa(.

Lane M :Standard protein ladder

Lane 7 :Soluble fraction of Huscfv specific rETA-3 clone no.7 protein

Lane 10 :Soluble fraction of Huscfv specific rETA-3 clone no.10 protein

Lane 14 :Soluble fraction of Huscfv specific rETA-3 clone no.14 protein

Lane 18 :Soluble fraction of Huscfv specific rETA-3 clone no.18 protein

Lane 21 :Soluble fraction of Huscfv specific rETA-3 clone no.21 protein

Lane 24 :Soluble fraction of Huscfv specific rETA-3 clone no.24 protein

Lane 41 :Soluble fraction of Huscfv specific rETA-3 clone no.41 protein

Lane 48 :Soluble fraction of Huscfv specific rETA-3 clone no.48 protein

Lane 52 Soluble fraction of Huscfv specific rETA-3 clone no.52 protein

Lane 57 :Soluble fraction of Huscfv specific rETA-3 clone no.57 protein

Lane 58 :Soluble fraction of Huscfv specific rETA-3 clone no.58 protein

Lane HB2151 :Soluble fraction of the negative control]HB2151 *E .coli* [protein

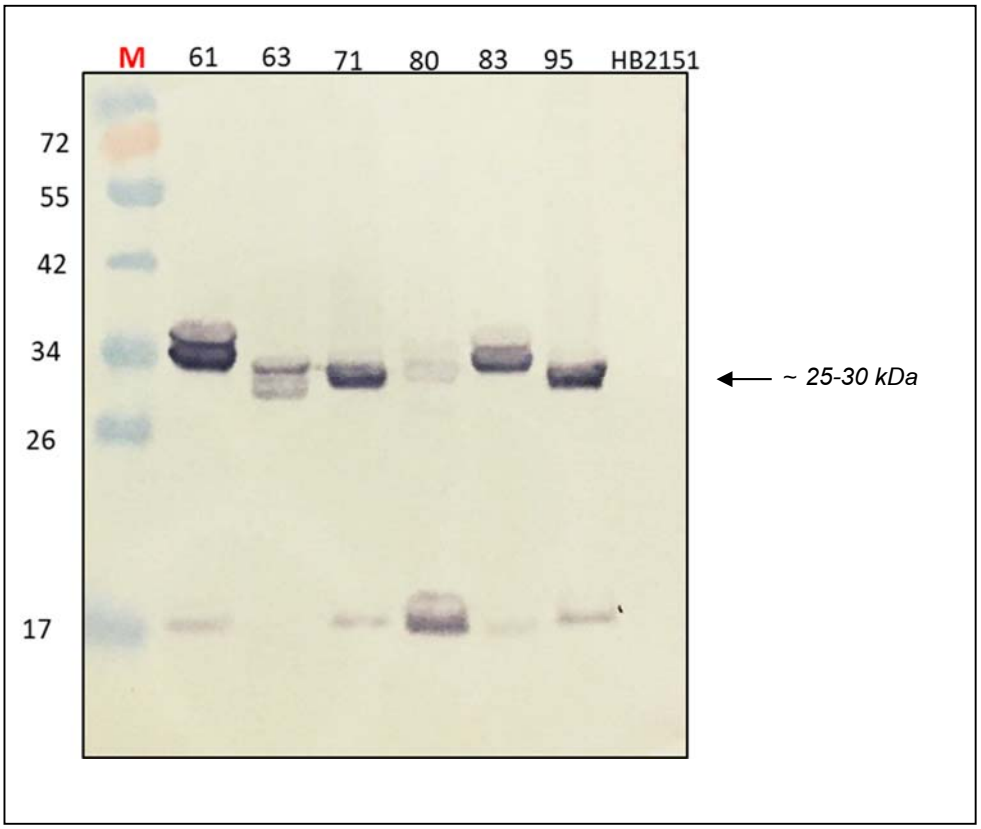

Figure 2.36 Western blot patterns of the HuscFvs specific rETA-3 protein expressed from the *huscfv* positive *E .coli* clones)expected protein size ~25-30kDa(.

Lane M :Standard protein ladder

Lane 61 :Soluble fraction of Huscfv specific rETA-3 clone no.61 protein

Lane 63 :Soluble fraction of Huscfv specific rETA-3 clone no.63 protein

Lane 71 :Soluble fraction of Huscfv specific rETA-3 clone no.71 protein

Lane 80 :Soluble fraction of Huscfv specific rETA-3 clone no.80 protein

Lane 83 :Soluble fraction of Huscfv specific rETA-3 clone no.83 protein

Lane 95 :Soluble fraction of Huscfv specific rETA-3 clone no.95 protein

Lane HB2151 :Soluble fraction of the negative control]HB2151 *E .coli* [protein

Selection of human single chain variable fragment)HuscFv (displayed phage clones that bound to catalytic peptide ETA from the established human scFv phage display library

Phage bio-panning for selecting of phage clones that display HuscFv specific to catalytic peptide ETA

The synthesized biotinylated catalytic residues of ETA peptide)M.W=.2,531.835g/mol (was used as antigens in phage bio-panning to select phage clones displaying HuscFv that could bind to the respective protein .In the bio-panning process, 0.5x binding capacity of D-biotin to the streptavidin plate .Before antigen coating, the Streptavidin Coated Plates were washed with PBS-T pH7.4 .After that, the biotinylated catalytic peptide ETA in 150 µl of Protein-free blocking buffer was individually immobilized onto the Pierce ™Streptavidin Coated Plates, Clear, 8-Well Strips .The Streptavidin Coated Plates were incubated at room temperature for 2 hours then the wells were washed with PBS-T pH7.4 for three times . The HuscFv phage display library)~ 3 x 10^{11} phage particles (that kindly provided by Prof . Dr .Wanpen Chaicumpa)Faculty of Medicine Siriraj Hospital, Mahidol University, Bangkok, Thailand (were added into the antigen coated well, and the reaction were incubated at room temperature for 1 hour .Afterwards, the fluid)unbound phages (were discarded from the well and the reaction well were extensively washed 10 times to remove unbound phages .The 20 times of the catalytic ETA-biotin concentration coated on the streptavidin well was added .The wells were incubated at room temperature for 1 hour .Afterwards, the phages bound to the 20x of antigen concentration were transferred to the clean tube . The 100 µl of the mid-log phase HB2151 *E .coli* were added into the immobilized antigen on reaction well /also the tube of phages bound to the 20x of antigen concentration and further incubated at 37°C for 10 minutes .Then the phages infected HB2151 *E .coli* were used to spread onto 2XYT agar plate containing 100 µg/ml of ampicillin and 2 % glucose)2XYT-AG (and the plate were incubated at 37°C for 12-16 hours.

3. Determining of HB2151 *E. coli* clones with pCANTAB5E-*huscfv* phagemids which could expressed HuscFvs specific to the catalytic peptide ETA

For determining the transformed HB2151 *E .coli* which carried the *huscfv*-phagemids, the bacterial colonies on the 2XYT-AG plate were picked to perform the colony PCR .An individual colony was selected and inoculated into the 150 µl of LB broth containing 100 µg/ml of ampicillin antibiotic, then incubated at 37°C for 2 hours with 250 rpm shaking that one microliter of each clone will be used as DNA template for checking the presence of the *huscfv* gene .The PCR was carried out using a pair of primers, R1)forward primer :(5-' CCATGATTACGCCAAGCTTTGGAGCC-3 'and R2)reverse primer :(5-' GCTAGATTTCAAAACAGCAGAAAGG-3 .'The 25 µl of PCR reaction mixture and PCR conditions

were demonstrated in below. After PCR amplification, the PCR products were analyzed using 1.5 %agarose gel electrophoresis and ethidium bromide staining.

PCR reaction mixture)25 µl(

Ingredients	Volume (µl)
Sterile ultrapure distilled water (UDW)	18.3
Taq buffer with KCl (10x)	2.5
dNTPs (10 mM each)	0.5
Forward Primer (10 µM)	0.5
Reverse Primer (10 µM)	0.5
$MgCl_2$ (25 mM)	1.5
Taq DNA polymerase (5 units/1µl)	0.2
DNA template	1.0

PCR conditions

Steps	Conditions
Initial denaturation	at 95°C for 5 minutes
35 cycles of Denaturation , Annealing , and Extension	at 95°C for 30 seconds at 58°C for 30 seconds at 72°C for 40 seconds
Final extension	at 72°C for 7 minutes

The colonies appearing on 2XYT agar plate containing 100 µg/ml of ampicillin and 2% glucose (2XYT-AG) were picked and performed the screening for the inserted *huscfv* gene (the expected amplicon size ~1,000 bp) using direct colony PCR. The results shown that 34 of the 51 selected clones (which accounted for 66.67%) derived from bio-panning with the biotinylated catalytic residues of ETA peptide were positive for *huscfv* segments **(Figure 1.37-1.40).**

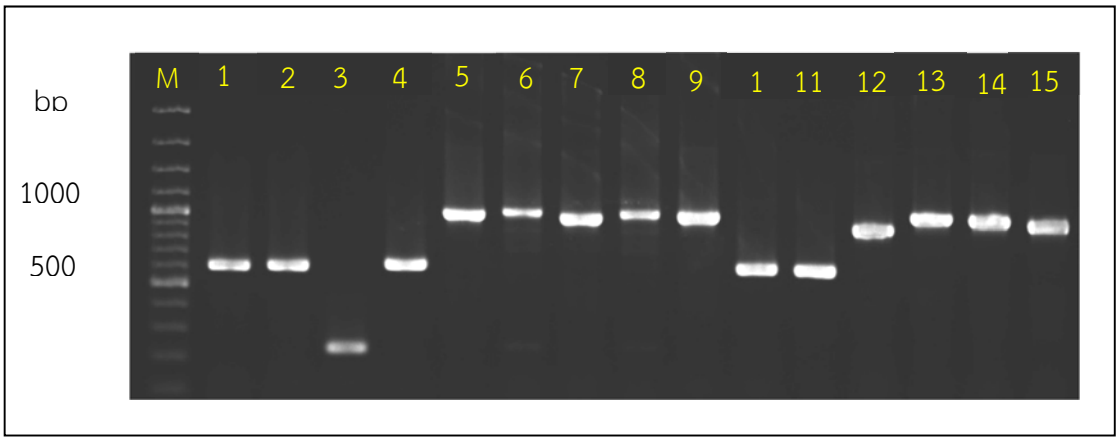

Figure 1.37 PCR amplification for screening of pCANTAB5E-huscfv phagemids (the expected amplicon size ~1,000 bp) transformed *E. coli* strain HB2151 colonies
Lane M: GenRulerTM 100 bp DNA ladder plus.

Lanes 1-15: PCR amplicons for detecting the presence of huscfv gene transformed *E. coli* strain HB2151 colonies for clones no.1-15, respectively

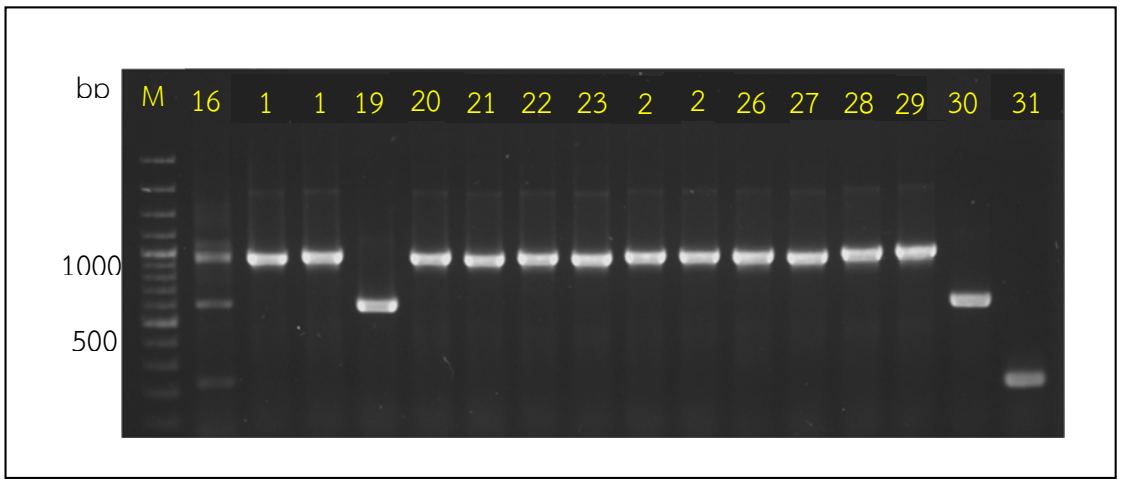

Figure1.38 PCR amplification for screening of pCANTAB5E-huscfv phagemids (the expected amplicon size ~1,000 bp) transformed *E. coli* strain HB2151 colonies.

Lane M: GenRulerTM 100 bp DNA ladder plus

Lanes 16-31: Results of colony PCR of PCR amplicons for detecting the presence of huscfv gene transformed *E. coli* strain HB2151 colonies for clones no. 16-31, respectively.

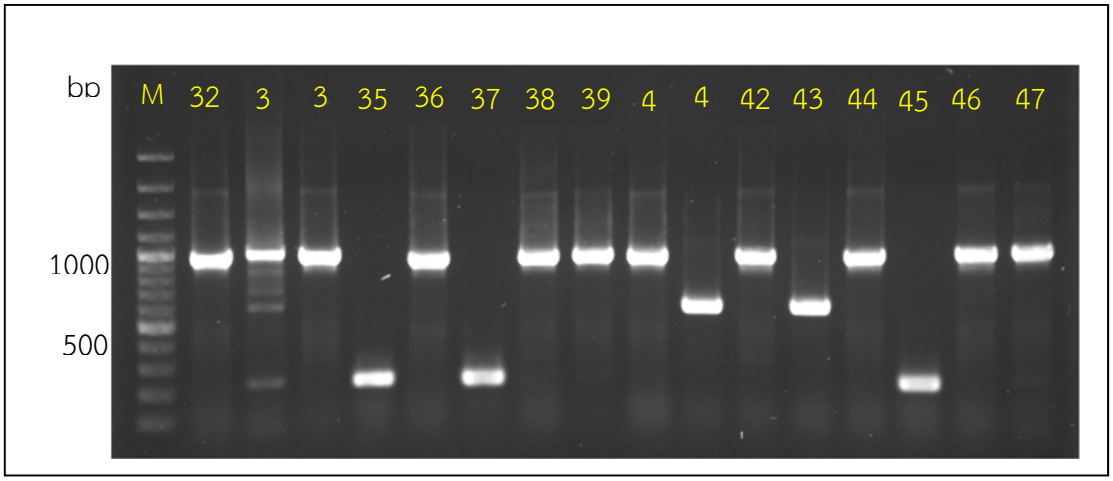

Figure 1.39 PCR amplification for screening of pCANTAB5E-huscfv phagemids (the expected amplicon size ~1,000 bp) transformed *E. coli* strain HB2151 colonies.

Lane M: GenRulerTM 100 bp DNA ladder plus

Lanes 32-47: PCR amplicons for detecting the presence of huscfv gene transformed *E. coli* strain HB2151 colonies for clones no. 32-47, respectively.

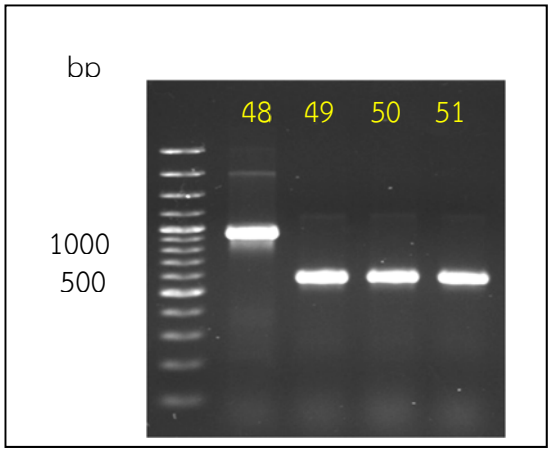

Figure 1.40 PCR amplification for screening of pCANTAB5E-huscfv phagemids (the expected amplicon size ~1,000 bp) transformed *E. coli* strain HB2151 colonies.

Lane M: GenRulerTM 100 bp DNA ladder plus

Lanes 48-51: PCR amplicons for detecting the presence of huscfv gene transformed *E. coli* strain HB2151 colonies for clones no. 48-51, respectively.

Binding of the *Escherichia coli* derived-HuscFv catalytic ETA peptide

Verification of the HuscFvs binding activity to the catalytic ETA peptide by indirect ELISA

The HB2151 *E . coli* clones which gave positive result from colony PCR screening of *huscfv* gene amplicons of the expected size ~ 1,000 bp were further performed the protein expression . In this study, HuscFv proteins were expressed by the individual clone was inoculated into 2 ml of AIM)Auto Induction Medium (medium containing 100 µg/ ml ampicillin antibiotic and incubated at 30°C with shaking at 250 rpm for overnight .After that, the induced bacterial cells were collected by centrifugation at 10,000 *x*g at 4°C for 1 minutes .The cell pellets of expressed soluble HuscFvs specific to the catalytic ETA peptide were performed the protein extraction using protein extraction kits, BugBuster® Plus Lysonase) ™Novagen, Merck, CA, USA (to separating of the soluble HB2151 *E . coli* fraction)the supernatant (that protein in this fraction were subjected to perform the binding test using an indirect ELISA for detecting the binding specificities of the soluble HuscFvs specific to the full- length native ETA protein . For the indirect ELISA, Rabbit anti- E- Tag polyclonal antibody)Abcam, USA (and Goat anti- rabbit immunoglobulin- HRP conjugate)Southern Biotech, AL, USA (was used as the primary and secondary antibody, respectively .The ABTS)2,2 azino- bis]3- ethylbenzthiazoline- 6- sulfonic acid) ([ZYMED CA, USA (was used as the substrate for the ELISA detection . The ELISA signal was measured at OD405nm using a FINSTRUMENTS® Microplate Reader.

The results of indirect ELISA were shown that 6 clones of HuscFvs specific catalytic ETA peptide which were gave the two times signal higher than that of biotin which are clone no .14, 34, 38, 40, 42, and 44)Figure 1.41 .(They gave the two times signal higher than that of BSA)control antigen (at OD405nm.

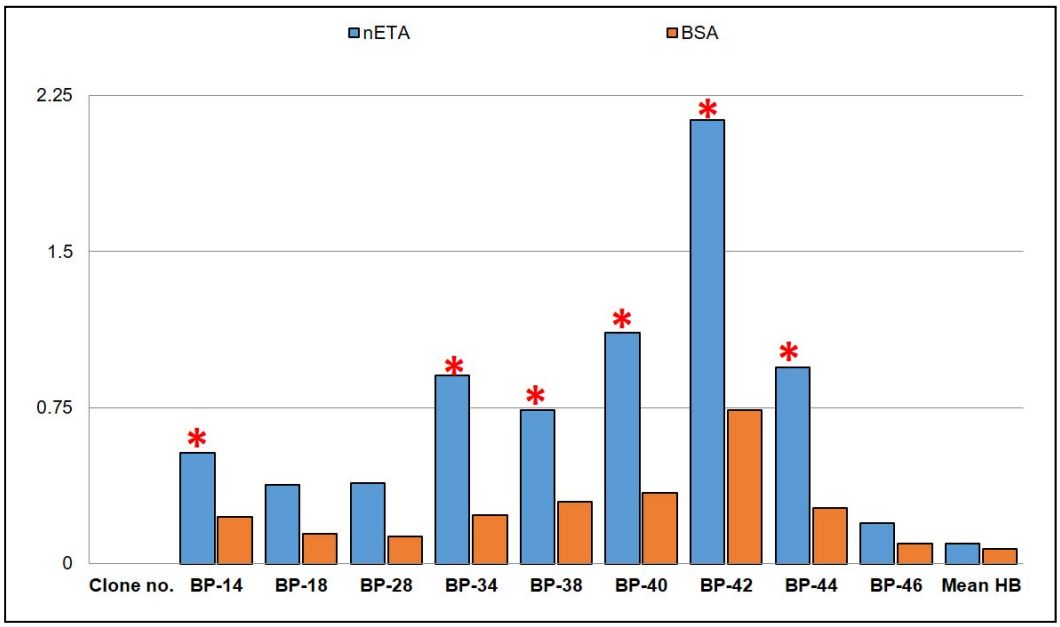

Figure 1.41 The diagram of binding test result for verifying of the HuscFvs binding activity to the biotinylated catalytic ETA peptide using indirect ELISA

4. Plasmid sequencing and characterization of the bacterial derived HuscFvs specific the native ETA (nETA), ETA domain 1A, ETA domain 3, and catalytic ETA peptide

The positive clones of bacterial derived HuscFvs specific the native ETA from the indirect ELISA and western blot analysis were further send for DNA sequencing)First BASE Laboratories Sdn .Bhd., Malaysia .(

The nucleotide sequences of the positive clones were analyzed using SnapGene Viewer program version 3.3.3 and CLC sequence viewer version 7 software .The correct huscfv reading frame in the pCANTAB5E phagemid of each clone were evaluated .Afterwards, the complementarity determining regions)CDRs (and their respective canonical immunoglobulin framework regions)FRs (of the sequenced huscfvs were predicted using an online server, the VBASE2 -the integrative germ-line V gene database)http//:www.vbase2.org.(/

The DNA sequences coding for ETA-bound HuscFvs of the 16 clones (clone numbers : N-20, N-21, N-32, 1-33, 1-46, 3-41, 3-46, 3-48, 3-61, 3-83, BP-14, BP-34, BP-38, BP-40, BP-42, and BP-44) were categorized into 7 different types based on the deduced amino acid sequences which composed of type1 (IGHV3 family and IGKV4 subgroup : N20 and BP-40, type2 (IGHV1 family and IGKV1 subgroup : N21), type3 (IGHV4 family and IGKV3 subgroup : N32), type4 (IGHV3 family and IGKV3 subgroup : 1-33, 1-46, 3-46, 3-48, 3-61, and 3-83), type5 (IGHV3 family and IGKV3 subgroup : 3-41 andBP-42), type6 (IGHV1 family and IGKV3 subgroup : BP-34), and type7 (IGHV3 family and IGKV2 subgroup : BP-14,-38, and -44). Then for clones N20, N21, N32, 1-33, 3-41, BP-34, and BP-44 were selected as the representative clones of each group for further experiments (Figure 1.42-1.48) .

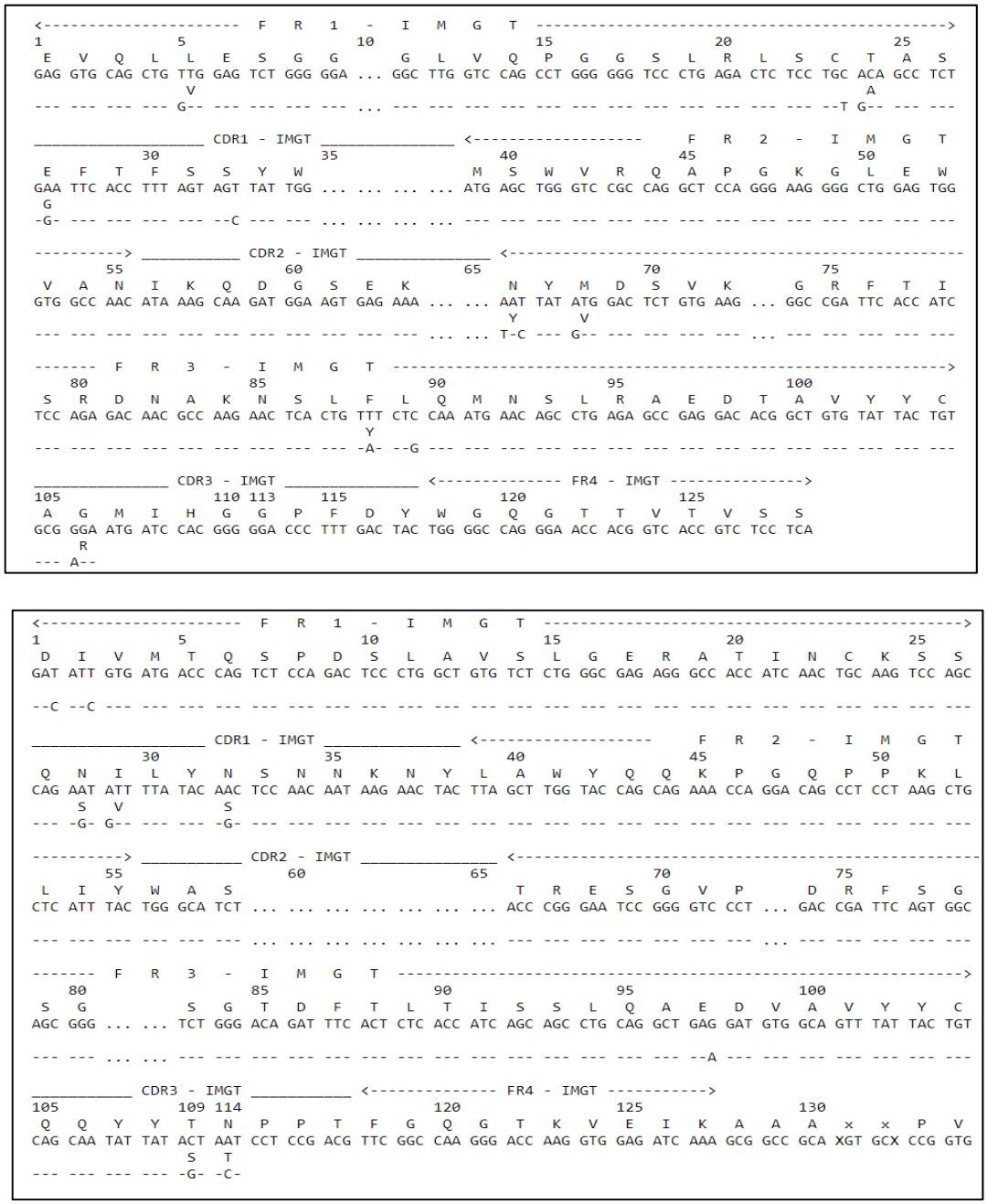

Figure .42 The CDRs and its FRs of the VH sequences)upper panel (and VL sequences)lower panel (of huscfvs specific nETA clone N20, the representative clone of IGHV3 family and IGKV4 subgroup.

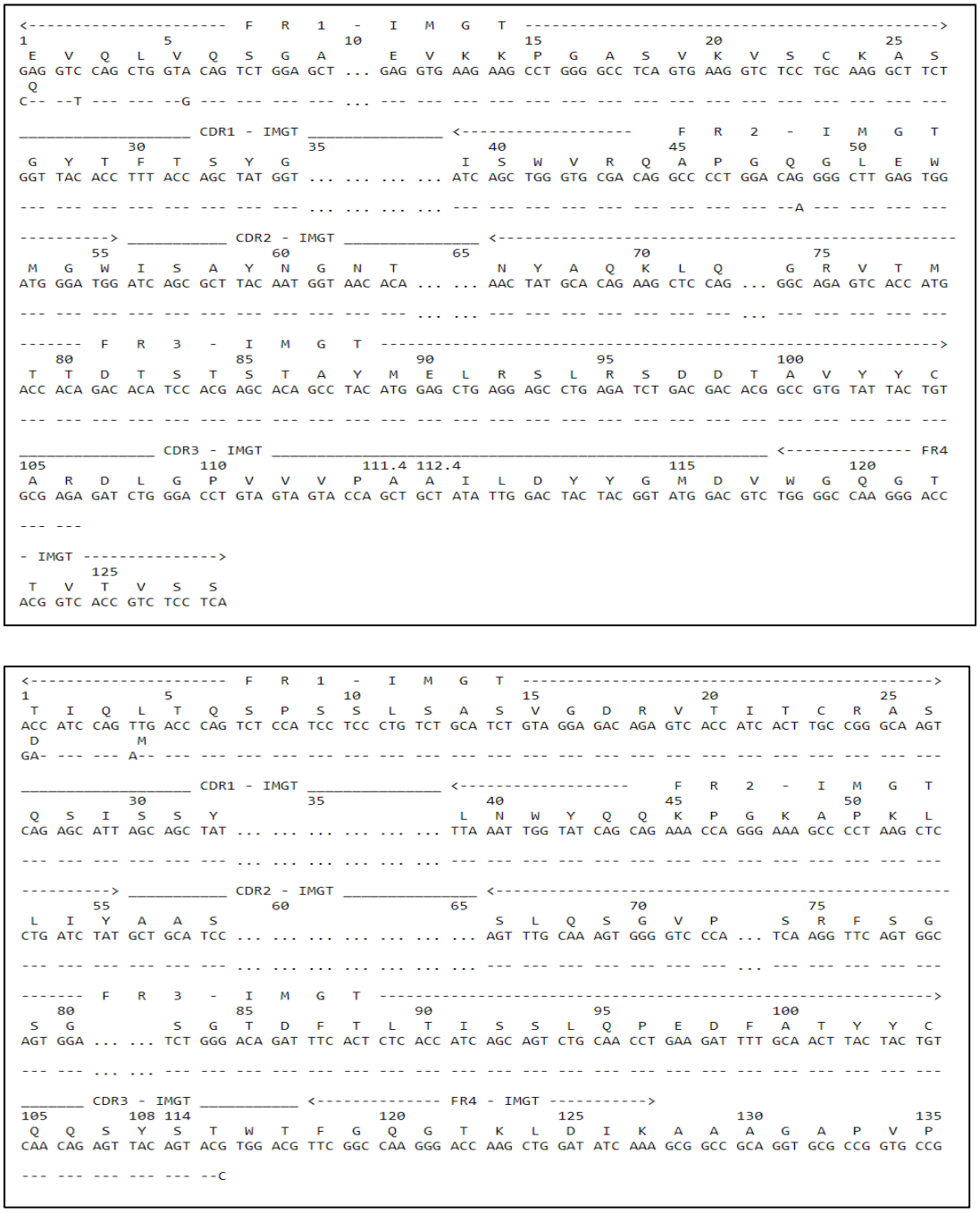

Figure 1.43 The CDRs and its FRs of the VH sequences)upper panel (and VL sequences)lower panel (of huscfvs specific nETA clone N21, the representative clone of IGHV1 family and IGKV1 subgroup.

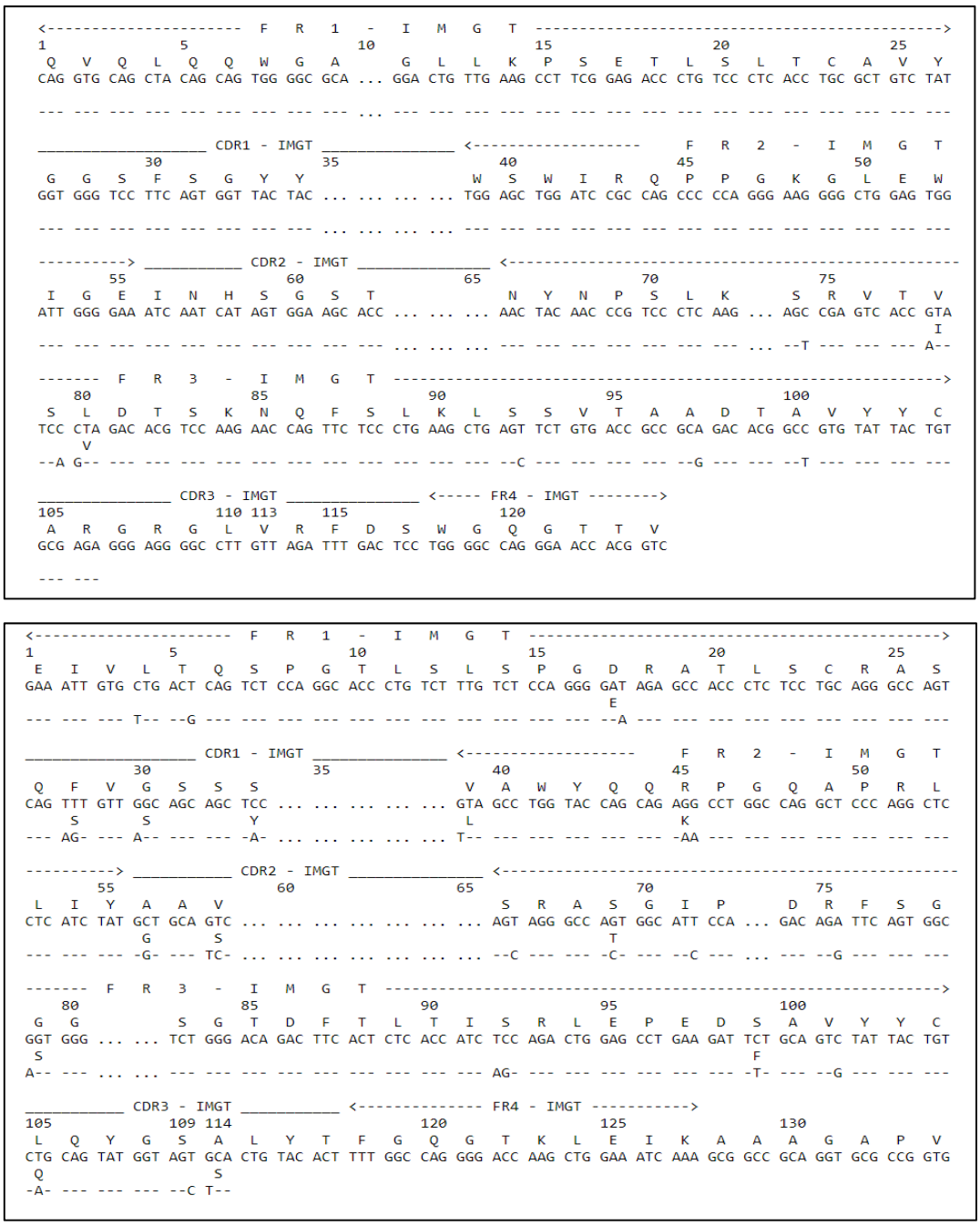

Figure 1.44 The CDRs and its FRs of the VH sequences)upper panel (and VL sequences)lower panel (of huscfvs specific nETA clone N32, the representative clone of IGHV4 family and IGKV3 subgroup.

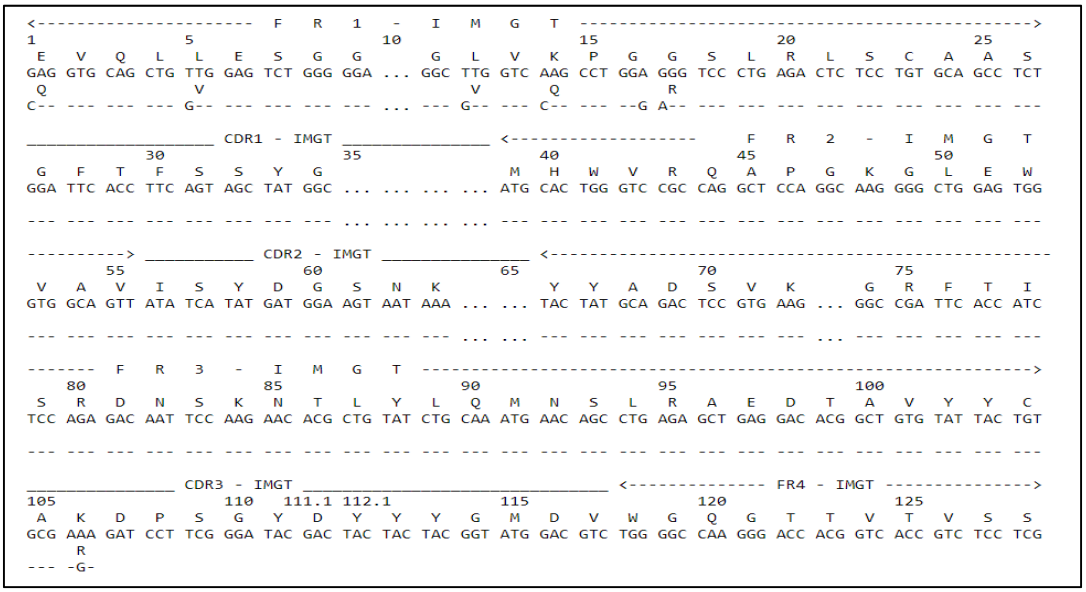

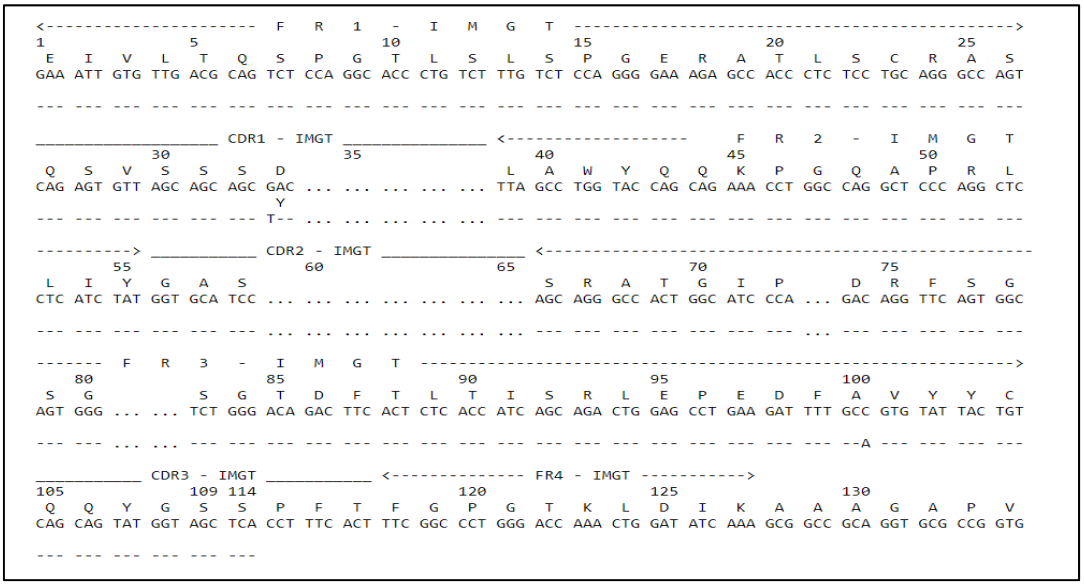

Figure 1.45 The CDRs and its FRs of the VH sequences)upper panel (and VL sequences)lower panel (of huscfvs specific nETA clone 1-33, the representative clone of IGHV3 family and IGKV3 subgroup.

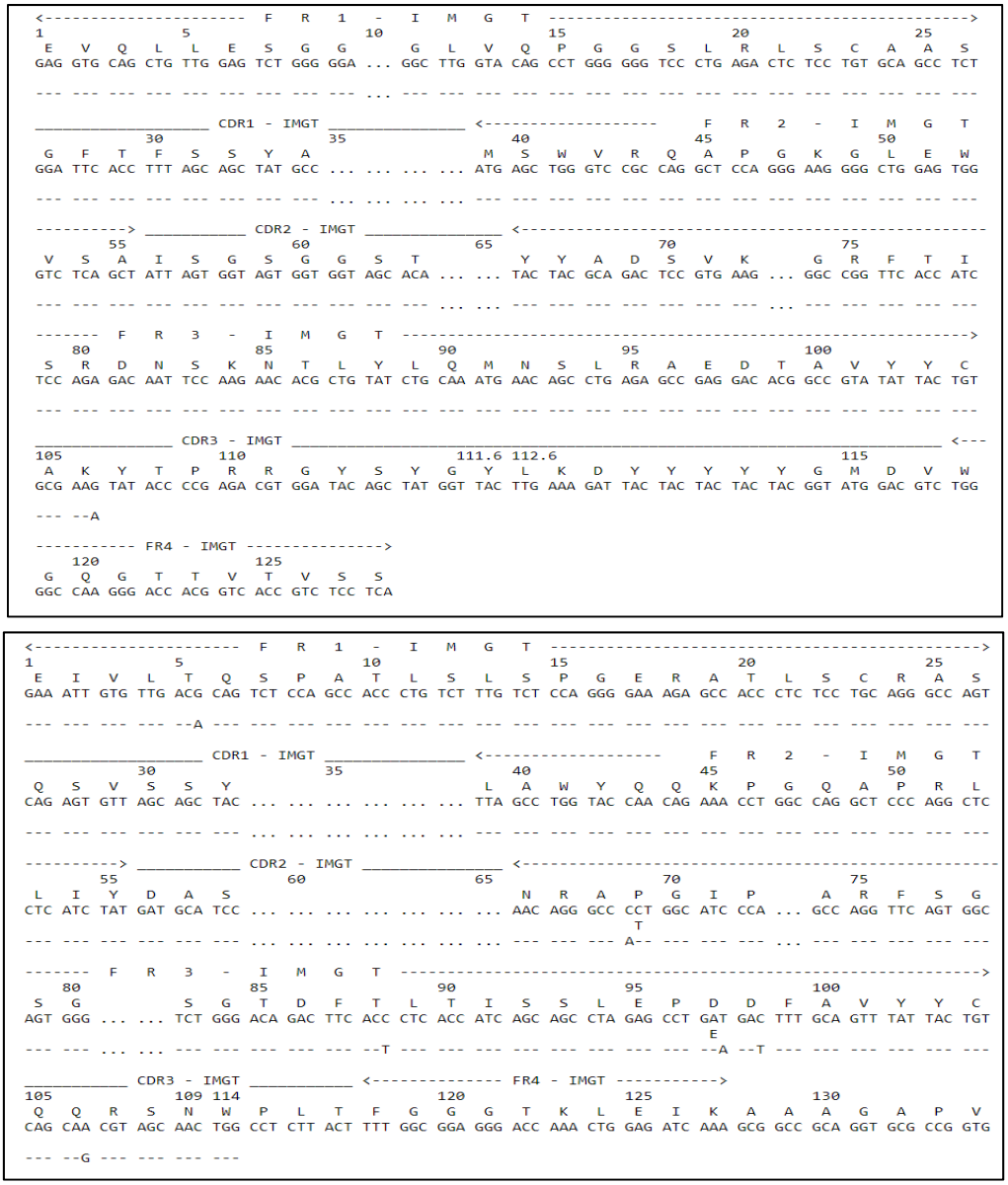

Figure 1.46 The CDRs and its FRs of the VH sequences)upper panel (and VL sequences)lower panel (of huscfvs specific nETA clone 3-41, the representative clone of IGHV3 family and IGKV3 subgroup.

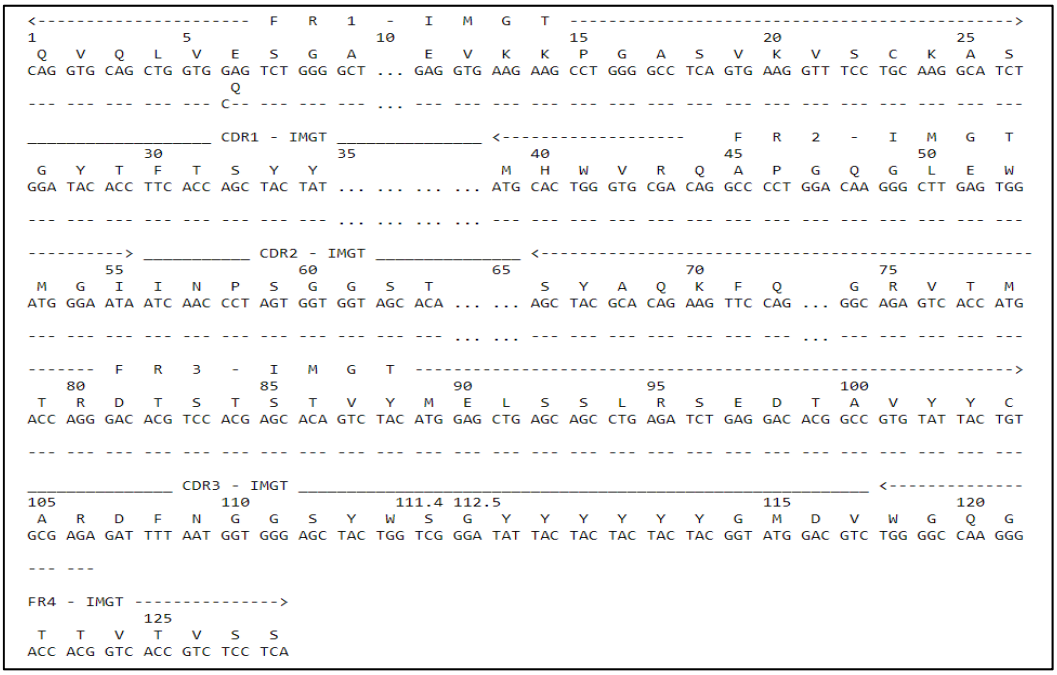

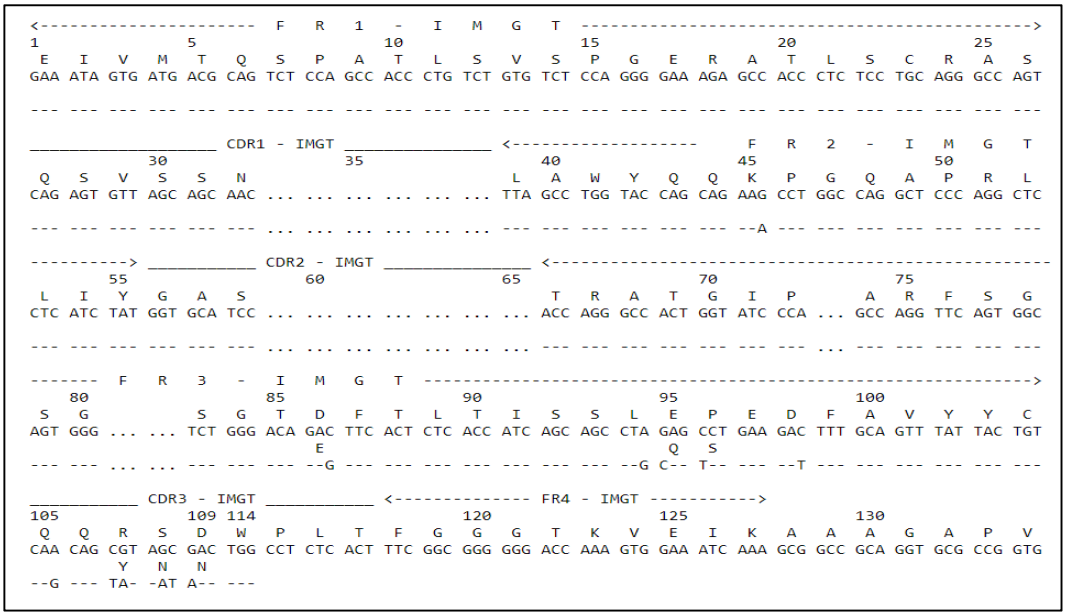

Figure 1.47 The CDRs and its FRs of the VH sequences)upper panel (and VL sequences)lower panel (of huscfvs specific nETA clone BP-34, the representative clone of IGHV1 family and IGKV3 subgroup.

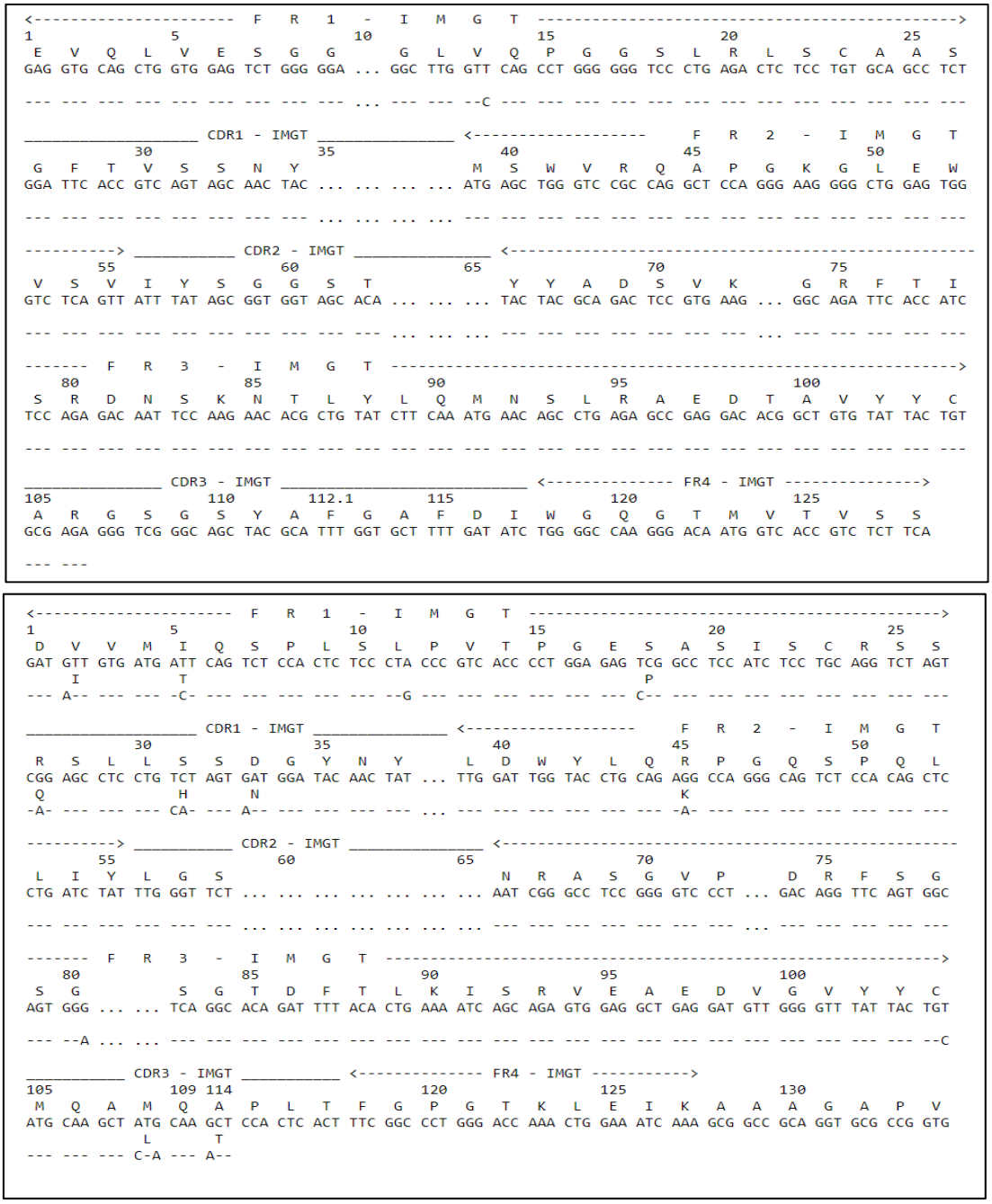

Figure 1.48 The CDRs and its FRs of the VH sequences)upper panel (and VL sequences)lower panel (of huscfvs specific nETA clone BP-44, the representative clone of IGHV3 family and IGKV2 subgroup.

5. Production of the HuscFvs that bound to the native ETA (nETA), in *E .coli* expression system

Amplification of *huscfv* insert using polymerase chain reaction)PCR (technique

In this study, the purified plasmid DNA of the HB2151 *E. coli* positive clones that could produce HuscFv specific nETA (includes the representatives clone N20, N21, N32, 1-33, 3-41, BP-34, and BP-44) were used as the template to amplify the HuscFv gene using Phusion High- Fidelity DNA Polymerase (Thermo Scientific™, USA). PCR amplification will be performed in a total volume of 25 µl which the PCR reaction mixture and PCR thermal cycle condition were provided. After that, the PCR products were verified by gel electrophoresis and ethidium bromide staining. That the PCR products were electrophoresed in 1.5% agarose gel (EMD Chemical Inc., USA) in 1x TAE buffer. The melted agarose gels were casted, allowed to solidify for around 30 minutes, and submerged in 1x TAE buffer contained in electrophoresis set (Bio-Rad, USA). DNA sample were mixed in a ratio of 10:1 with 6x DNA loading dye triple dye (Thermo Scientific™, USA). The gels were run at a constant voltage at 100 volts for 30 minutes, then the gel were stained with 0.5 µg/ml of ethidium bromide solution for 5 minutes and de-stained with distilled water for 10 minutes. Afterwards, the DNA bands were visualized under a UV Transilluminator (Molecular Imager Gel DocTM XR+ Imaging system, Bio-Rad, USA). Then size of DNA segments were estimated by comparing with the bands of known sizes of the 100 bp plus DNA ladder (Fermentas, Thermo Fisher Scientific, MA, USA) which run concurrently in the same gel (**Figure 1.49**).

PCR reaction mixture for amplification of huscfv inserts

Components	Volume (μl)	Final concentration
Sterile ultrapure distilled water (UDW)	12.4	-
Phusion HF buffer (5x)	4.0	1x
dNTP (2.5 mM each)	0.4	200 μM
Forward Primer (10 μM)	1.0	0.5 μM
Reverse Primer (10 μM)	1.0	0.5 μM
Phusion DNA Polymerase (1.0 units/50 μl PCR)	0.2	0.4 units
DNA template	1.0	10 ng/μl
Total	20	

PCR thermal cycle condition for amplification of huscfv inserts

Steps	Conditions
Initial denaturation	at 98°C for 30 seconds
35 cycles of Denaturation ,	at 98°C for 10 seconds
Annealing ,	at 60°C for 10 seconds
and Extension	at 72°C for 40 seconds
Final extension	at 72°C for 10 minutes
Hold	at 4°C for infinity

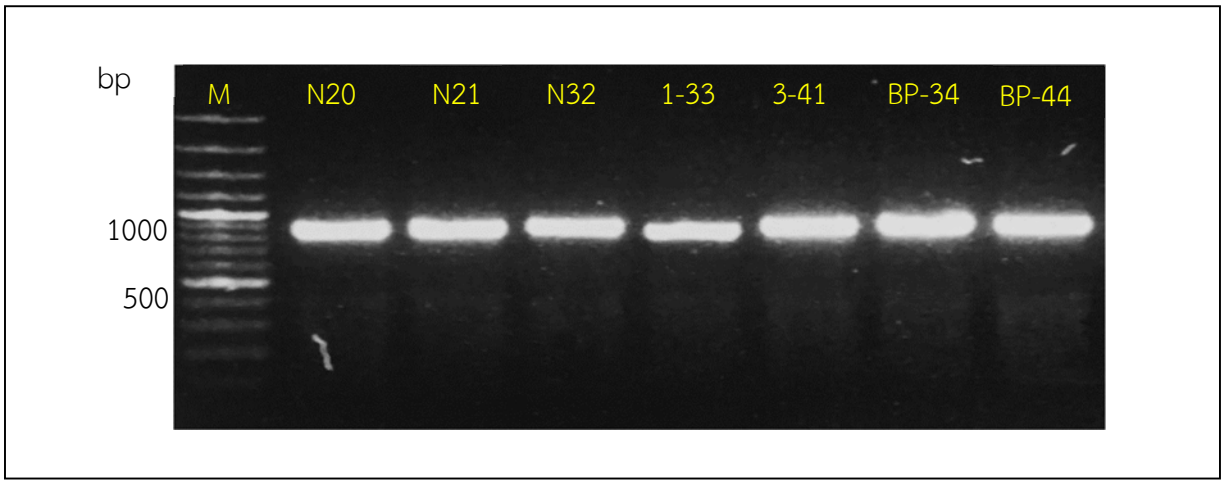

Figure 1.49 PCR products that obtained from the amplification of the *huscfv* inserts using specific LIC primers (expected amplicon size ~ 850 bp).

Lane M: GenRuler^{TM} 100 bp DNA ladder plus
Lane N20: *huscfv* amplicon from the purified plasmid DNA of the HB2151 *E. coli* positive clones that could produce HuscFv specific nETA clone no.20
Lane N21: *huscfv* amplicon from the purified plasmid DNA of the HB2151 *E. coli* positive clones that could produce HuscFv specific nETA clone no.21
Lane N32: *huscfv* amplicon from the purified plasmid DNA of the HB2151 *E. coli* positive clones that could produce HuscFv specific nETA clone no.32
Lane 1-33: *huscfv* amplicon from the purified plasmid DNA of the HB2151 *E. coli* positive clones that could produce HuscFv specific nETA clone no.1-33
Lane 3-41: *huscfv* amplicon from the purified plasmid DNA of the HB2151 *E. coli* positive clones that could produce HuscFv specific nETA clone no.3-41
Lane BP-34: *huscfv* amplicon from the purified plasmid DNA of the HB2151 *E. coli* positive clones that could produce HuscFv specific nETA clone no. BP-34
Lane BP-44: *huscfv* amplicon from the purified plasmid DNA of the HB2151 *E. coli* positive clones that could produce HuscFv specific nETA clone no.BP-44
The PCR product were analyzed on 1.5% agarose gel electrophoresis and visualized on UV light after staining with ethidium bromide.

Sub-cloning of DNAs coding for ETA-bound *huscfv* inserts into pLATE52 expression vector and bacterial transformation

The PCR products from above were be purified using the Gel/PCR DNA Fragments Extraction Kit (Geneaid Biotech Ltd., Taiwan) with a bind-wash-elute procedure to completely eliminate the incorporated primers, dNTPs, and other contaminated DNA. The purified DNA were measured for its concentration and also quality using NanoDrop™ 2000/ 2000c Spectrophotometers (Thermo Scientific™, USA) at the wavelength 260/280. The *huscfv* inserts were cloned into the pLATE52 expression vector using the aLICator LIC Cloning and Expression Kit 4 (N-terminal His-tag/WQ), #K1281 (Thermo Scientific™, USA). The LIC cloning was performed to generate the 5' and 3' overhangs on the purified PCR templates that the following reaction were set up by mixed 2 µl of 5x LIC buffer; 4 µl of nuclease-free water; 0.1 pmol of purified PCR template; T4 DNA polymerase. After that, the reaction mixture will be incubated at 25°C for 5 minutes, and then immediately stopped by adding 0.6 µl of EDTA. The annealing reactions waere performed by added the LIC-ready pLATE52 (60 g, 0.02 pmol DNA) to the reaction mixture, vortexed briefly for 3-5 seconds, and annealing proceeded at 25°C for 5 minutes.

Afterwards, the bacterial transformations were done by using the Transform Aid Bacterial Transformation Kit (Thermo Scientific™, USA) to transforming of the *huscfv*-pLATE52 recombinant plasmids into the competent *E. coli* strain JM109, a cloning host. The transformed bacterial cells were spread onto LB agar plate containing 100 µg/ml of ampicillin antibiotic (LB-A agar), and further incubated at 37°C for overnight. After overnight incubation, the individual transformed JM109 *E. coli* colonies was randomly picked and checked for the presence of the recombinant plasmids with *huscfv* inserts using the colony PCR. An individual transformed JM109 *E. coli* colonies was randomly selected and inoculated into the 150 µl of LB broth containing 100 µg/ml of ampicillin antibiotic, then incubated at 37°C for 2 hours with 250 rpm shaking that one microliter of each clone was used as DNA template. The PCR products from above were purified using the Gel/PCR DNA Fragments Extraction Kit. In this study, the two LIC primers (LIC-Forward primer: 5'-TAATACGACTCACTATAGGG-3' and LIC-reverse primer: 5'-GAGCGGATAACAATTTCACACAGG-3') were used to perform the PCR amplification of recombinant plasmid from each individual clone. The PCR reaction mixture (25 µl) was composed of 1 µl of DNA template, 0.5 µl of each primer (10 µM), 2.5 µl of 10x Taq buffer with KCl, 1.5 µl of 25 mM MgCl2, 0.5 µl of 10 mM dNTPs, 0.2 µl of 5 units/1µl *Taq* DNA polymerase (Fermentas, Thermo Fisher Scientific, USA), and 18.3 µl of UDW. PCR condition will be comprised of 1 cycle initial denaturing at 95°C for 5 minutes; 35 cycles of denaturing at 95°C for 30 seconds, annealing at 58°C for 30 seconds, and extending at 72°C for 1 minute; final extending at 72°C for 7 minutes; and holding at 4°C for infinity. The PCR products of the correct length were indicated that plasmid have been properly inserted. PCR products

obtained with LIC forward and LIC reverse primers should be approximately 1,114 bp for the recombinant plasmid. The PCR products were verified by 1.5% agarose gel electrophoresis and ethidium bromide staining. The screened positive transformed *E. coli* clones by colony PCR method were performed by extracted their plasmids using the PrestoTM Mini Plasmid Kit (Geneaid Biotech Ltd., Taiwan) following the manufacturer's instruction, and send for DNA sequencing (First BASE Laboratories Sdn. Bhd., Malaysia).

Afterwards, the positive clones from DNA sequencing were subjected to perform the plasmid extraction and further transformed into an expression host. In this study, NiCo21(DE3) pRARE2 *E. coli* (New England Biolabs, UK) cells were used as an expression host for recombinant *huscfv*-pLATE52 plasmids. Then colony PCR using the two LIC primers for screening of the positive clones of the transformed NiCo21(DE3) pRARE2 *E. coli* with the *huscfv*-pLATE52 recombinant plasmids were performed screening for the desire inserted gene.

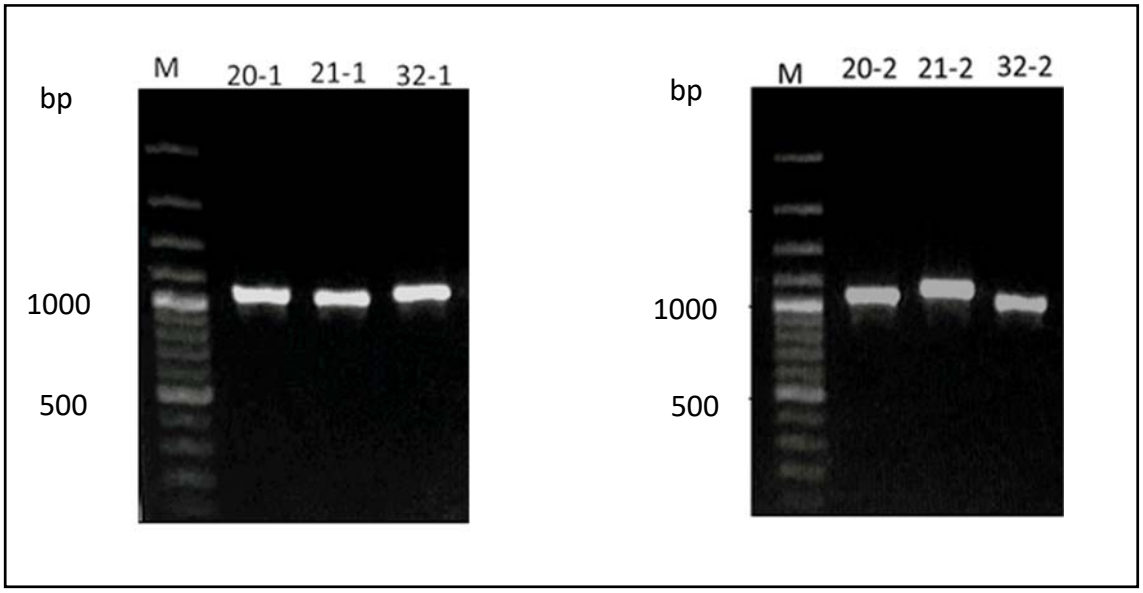

Figure 2.50 PCR amplification for screening of *huscfv*-pLATE52 transformed *E. coli* strain JM 109 colonies (expected amplicon size ~ 1,114 bp).

Lane M: GenRuler^{TM} 100 bp DNA ladder plus
Lane 20-1: *huscfv*-pLATE52 amplicon of transformed JM 109 *E. coli* clone N20 randomed colony no.1
Lane 21-1: *huscfv*-pLATE52 amplicon of transformed JM 109 *E. coli* clone N21 randomed colony no.1
Lane 32-1: *huscfv*-pLATE52 amplicon of transformed JM 109 *E. coli* clone N32 randomed colony no.1
Lane 20-2: *huscfv*-pLATE52 amplicon of transformed JM 109 *E. coli* clone N20 randomed colony no.2
Lane 21-2: *huscfv*-pLATE52 amplicon of transformed JM 109 *E. coli* clone N21 randomed colony no.2
Lane 32-2: *huscfv*-pLATE52 amplicon of transformed JM 109 *E. coli* clone N32 randomed colony no.2

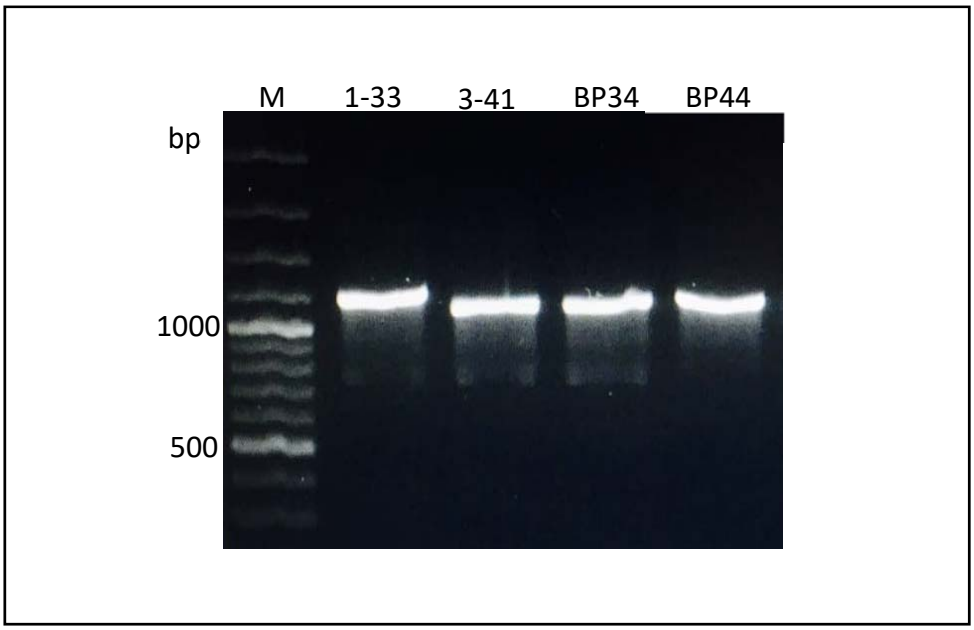

Figure 1.51 PCR amplification for screening of *huscfv*-pLATE52 transformed *E. coli* strain JM 109 colonies (expected amplicon size ~ 1,114 bp).

Lane M: GenRuler^{TM} 100 bp DNA ladder plus
Lane 1-33: *huscfv*-pLATE52 amplicon of transformed JM 109 *E. coli* clone 1-33 randomed colony no.1
Lane 3-41: *huscfv*-pLATE52 amplicon of transformed JM 109 *E. coli* clone 3-41 randomed colony no.1
Lane BP34: *huscfv*-pLATE52 amplicon of transformed JM 109 *E. coli* clone BP34 randomed colony no.1
Lane BP44: *huscfv*-pLATE52 amplicon of transformed JM 109 *E. coli* clone BP44 randomed colony no.2

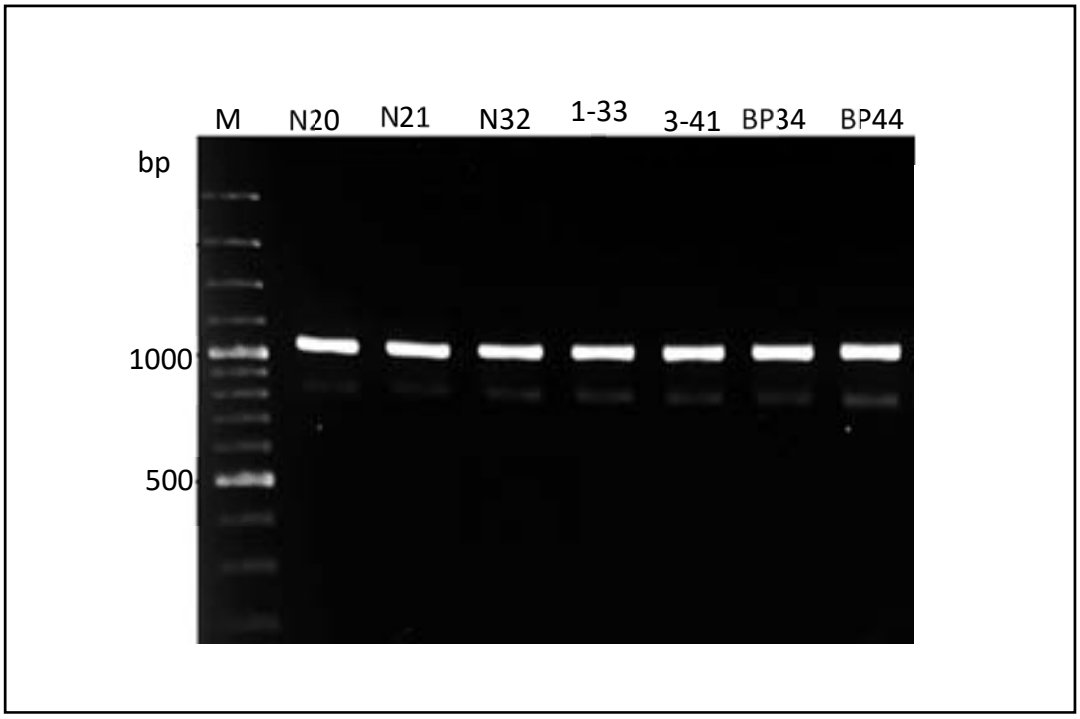

Figure 1.52 PCR amplification for screening of *huscfv*-pLATE52 transformed *E. coli* strain NiCo21(DE3) pRARE2 colonies (expected amplicon size ~ 1,114 bp)
Lane M: GenRuler^{TM} 100 bp DNA ladder plus
Lane N20: *huscfv*-pLATE52 amplicons of transformed NiCo21(DE3) pRARE2 *E. coli* clone N20
Lane N21: *huscfv*-pLATE52 amplicons of transformed NiCo21(DE3) pRARE2 *E. coli* clone N21
Lane N32: *huscfv*-pLATE52 amplicons of transformed NiCo21(DE3) pRARE2 *E. coli* clone N32
Lane 1-33: *huscfv*-pLATE52 amplicons of transformed NiCo21(DE3) pRARE2 *E. coli* clone 1-33
Lane 3-41: *huscfv*-pLATE52 amplicons of transformed NiCo21(DE3) pRARE2 *E. coli* clone 3-41
Lane BP34: *huscfv*-pLATE52 amplicons of transformed NiCo21(DE3) pRARE2 *E. coli* clone BP34
Lane BP44: *huscfv*-pLATE52 amplicons of transformed NiCo21(DE3) pRARE2 *E. coli* clone BP44

Recombinant ETA-huScFv protein expression and expressed protein analysis

The representative NiCo21(DE3) pRARE2 *E. coli* clones carrying *huscfv*- pLATE52 recombinant plasmid were tested for their ability to express the recombinant HuscFv protein. For HuscFv protein expression, single colony of each positive *E. coli* clone was individually cultured in 2 ml of LB broth containing 100 ug/ml ampicillin in shaking incubator at 37°C with shaking at 250 rpm until the culture reached the bacterial log phase growth (OD600nm ~0.5). The bacterial cells were induced for their recombinant protein expression by adding 1 mM isopropyl beta-D-1-thiogalactopyranoside (IPTG) into the individual cultures and further the incubation of the cultures at 30°C with shaking at 250 rpm for 6 hours. The induced bacterial cells were collected by centrifugation at 10,000 *xg* at 4°C for 5 minutes. The cell pellets of HuscFv specific nETA (including clone no. 18, 20, 21, and 32) samples were performed protein extraction using protein extraction kits, BugBuster® Plus Lysonase™ (Novagen, Merck, CA, USA) to separating of the soluble and insoluble *E. coli* fractions that proteins in both fractions were analyzed by SDS-PAGE.

In this study, the results were shown the over-expression of protein for HuscFv specific native ETA including clone no. N20, N21, N32, 1-33, 3-41, BP34, and BP44 that were expressed in the insoluble fraction (inclusion body). So these representatives were further subjected to perform protein purification and refolding.

Protein purification and refolding of the inclusion bodies provided the recombinant HuscFv specific nETA proteins

Recombinant HuscFvs specific nETA (nos. N20, N21, N32, 1-33, 3-41, BP34, and BP44) proteins were further performed the large scale protein expression by preparation of the transformed NiCo21 (DE3) *E. coli* pRARE2 host that carrying the inserted *huscfv*-pLATE52 plasmids. The bacterial cells were induced using 1mM IPTG and were further collected the cell pellets by centrifugation at 4,000 *xg*, 4°C for 20 minutes and the cell pellets were kept at -20°C until use.

The inclusion bodies of the induced NiCo21 (DE3) *E. coli* pRARE2 clones were isolate from the bacterial pellets using the BugBuster® Protein Extraction Reagent Plus Lysonase™ kit (Novagen, Merck, CA, USA) and the inclusion bodies were then washed with Wash-100, Wash- 114, Wash- solvent reagent, and Milli-Q water by shaking at high speed shaking platform and harvested the inclusion bodies by centrifugation. The wet inclusion bodies pellet were re-suspended in the Milli-Q water containing 0.02 % (w/v) NaN_3. The inclusion bodies were characterized using SDS-PAGE and Western blot analysis

For recombinant HuscFvs inclusion bodies refolding, 5 ml of buffer [50 mM CAPS, pH 11.0; 0.3% (w/v) N-Lauryl sarcosine; and 1 mM DTT] were added to reconstitute 5 mg of each purified IBs and kept at 4°C for 16 hours. After dissolving completely, the protein was separately loaded into the Slide- A- Lyzer® 2K Dialysis Cassettes G2 (Thermo Fisher Scientific), and the cassette were individually subjected to dialysis against 750 ml of a refolding buffer (20 mM Imidazole, pH 8.5, supplemented with 0.1 mM DTT) at 4°C with slow stirring. After 3 hours, the buffers were individually changed to fresh refolding buffer, and the dialysis were continued for 16 hours. The refolded proteins were consequently dialyzed against the dialysis buffer (20 mM Imidazole without DTT) with slow stirring at 4°C for 16 hours. The preparations were filtered through a 0.2- μm low protein binding Acrodisc® Syringe Filter (Pall, NY, USA) before adding 60mM Trehalose dihydrate. Protein concentration of the refolded representative HuscFvs were measured using Pierce® BCA Protein Assay, while quality and purity of the proteins were determined by SDS-PAGE and and Western blot (**Figure 1.53** and **Figure 1.54**).

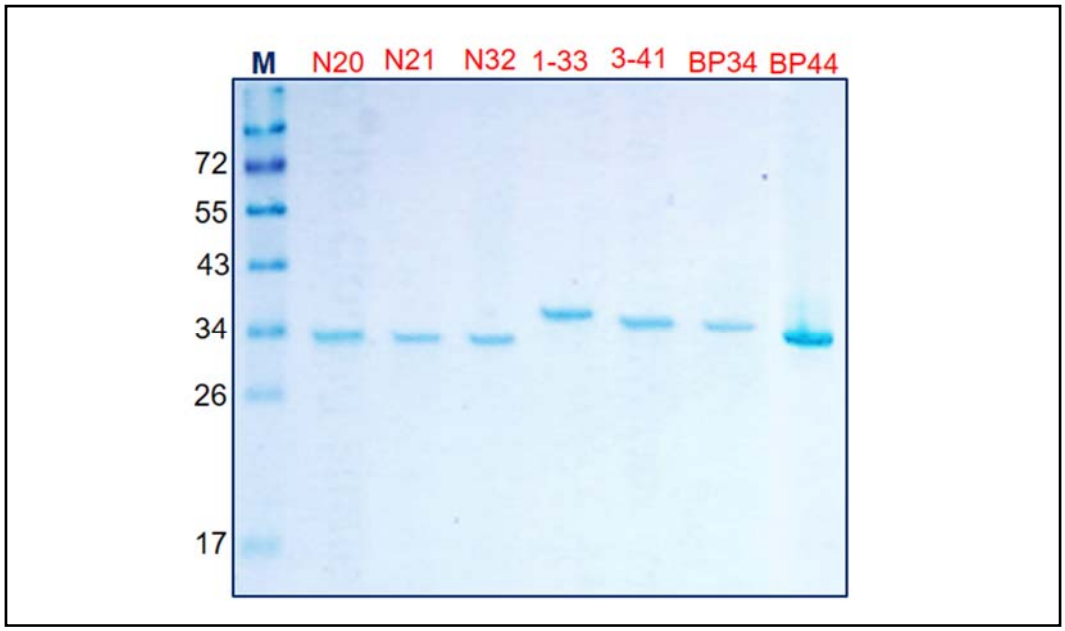

Figure 1.53 SDS-PAGE analysis of the purified inclusion bodies of the HuscFv specific native ETA proteins from NiCo21)DE3(*E . coli* pRARE2 using 12 %SDS-polyacrylamide gel (protein size ~25-35 kDa).

Lane M :Standard protein ladder

Lane N20 :Insoluble fraction of HuscFv clone N20

Lane N21 :Insoluble fraction of HuscFv clone N21

Lane N32 :Insoluble fraction of HuscFv clone N32

Lane 1-33 :Insoluble fraction of HuscFv clone 1-33

Lane 3-41 :Insoluble fraction of HuscFv clone 3-41

Lane BP-34 :Insoluble fraction of HuscFv clone BP-34

Lane BP-44 :Insoluble fraction of HuscFv clone BP-44

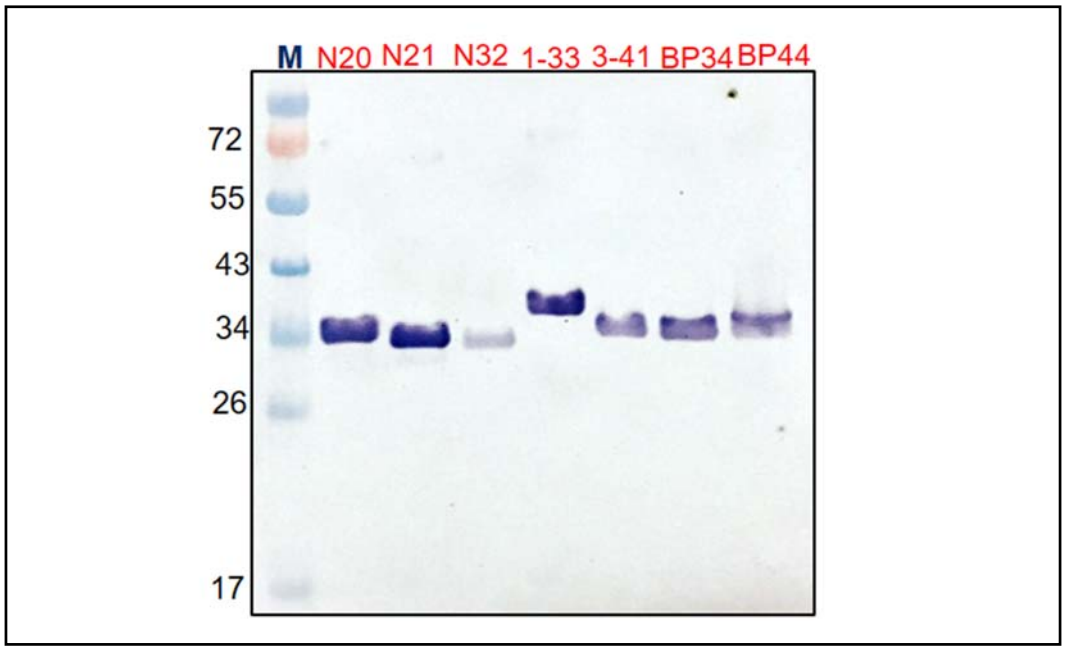

Figure 1.54 Western blot analysis of the purified inclusion bodies of the HuscFv specific native ETA proteins from NiCo21)DE3(*E .coli* pRARE2 using 12 %SDS-polyacrylamide gel.
Lane M :Standard protein ladder
Lane N20 :Insoluble fraction of HuscFv clone N20
Lane N21 :Insoluble fraction of HuscFv clone N21
Lane N32 :Insoluble fraction of HuscFv clone N32
Lane 1-33 :Insoluble fraction of HuscFv clone 1-33
Lane 3-41 :Insoluble fraction of HuscFv clone 3-41
Lane BP-34 :Insoluble fraction of HuscFv clone BP-34
Lane BP-44 :Insoluble fraction of HuscFv clone BP-44

Selection of human single chain variable fragment (HuscFv) displayed phage clones that bound to native *Pseudomonas aeruginosa* lasB from the established human scFv phage display library

Phage bio-panning for selecting of phage clones that display HuscFv specific to native native LasB of *P. aeruginosa*

The native and recombinant LasB were coated on microtiter well. Then, added BSA to block the free space. The HuscFv phage display library was added to individually well and incubated at 37°C for 1 hour. Unbound phage was washed away. One hundred microliters of *E.coli* HB2151 was added to each well. Then, incubated at 37 °C for 20 minutes. The *E. coli* was plated onto a 2xYT-AG plate. *E.coli* colonies grown on the plate were used as DNA template for checking the presence of HuscFv gene by PCR using R1 and R2 primer. Seventy-three colonies of native LasB and fifty-one colonies of recombinant lasB were picked to perform direct colony PCR. PCR mixture and thermal cycle are shown in previously part (Determining of HB2151 E. coli clones with pCANTAB5E-huscfv phagemids part). There 32 of 73 colonies of native LasB and 11 of 51 colonies of recombinant lasB that were positive for HuscFv gene (**Figure 1.55**). Then, the positive clones will test the specificity of binding with respective antigens.

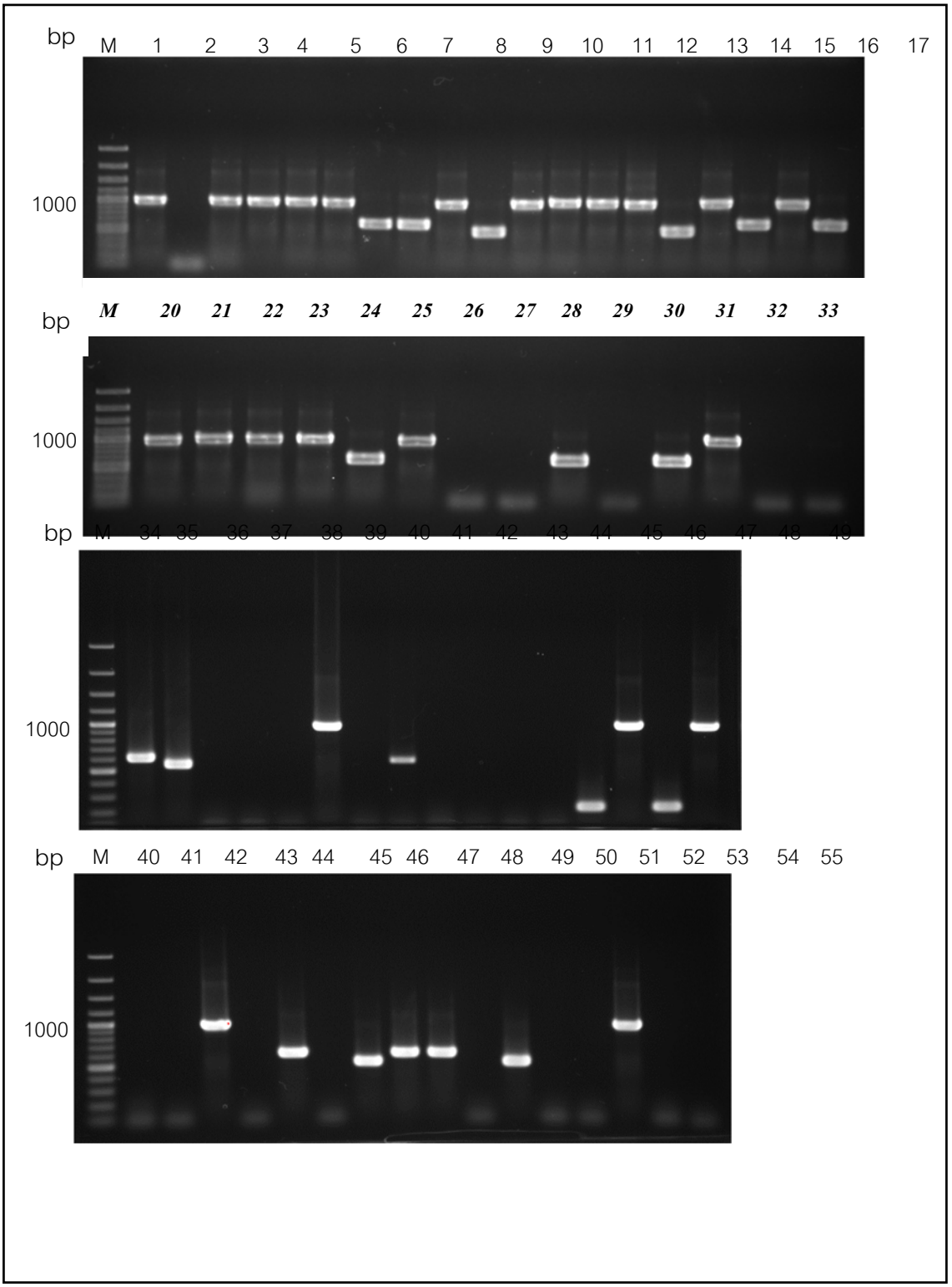
bp
M 1 2 3 4 5 6 7 8 9 10 11 12 13 14 15 16 17
1000
bp
M 20 21 22 23 24 25 26 27 28 29 30 31 32 33
1000
bp
M 34 35 36 37 38 39 40 41 42 43 44 45 46 47 48 49
1000
bp
M 40 41 42 43 44 45 46 47 48 49 50 51 52 53 54 55
1000

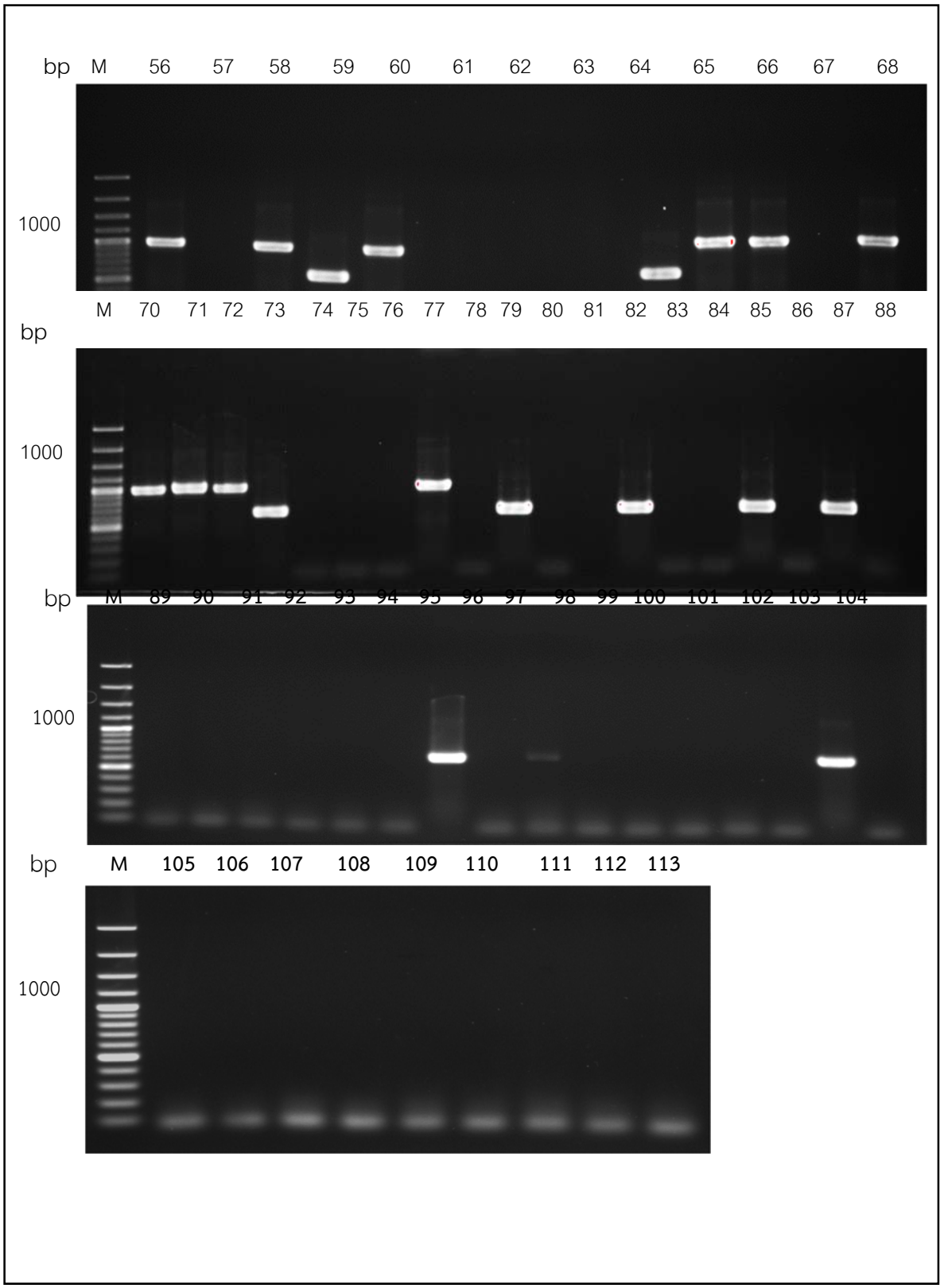
bp M 56 57 58 59 60 61 62 63 64 65 66 67 68
1000
M 70 71 72 73 74 75 76 77 78 79 80 81 82 83 84 85 86 87 88
bp
1000
bp M 89 90 91 92 93 94 95 96 97 98 99 100 101 102 103 104
1000
bp M 105 106 107 108 109 110 111 112 113
1000

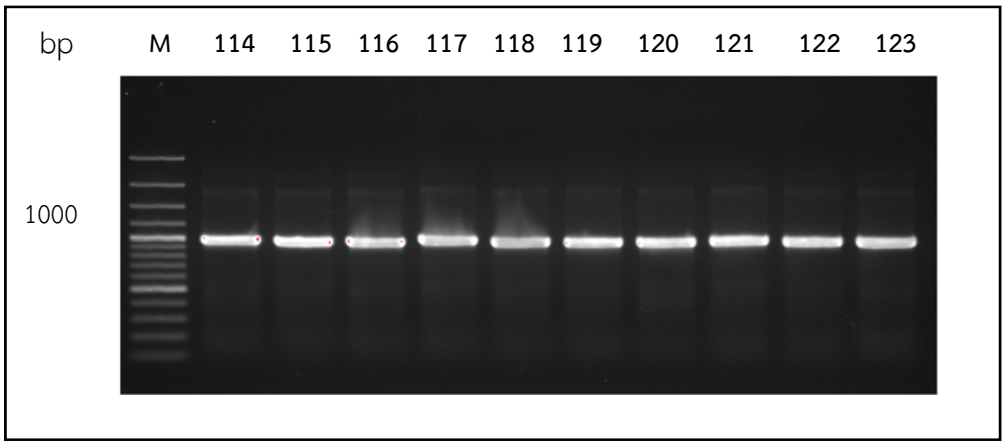

Figure 1.55 PCR product for screening of *huscfv* representative colonies of the phagemid transformed HB2151 *E.coli* using R1 and R2 primer. The expected size was around1000 bp.

Lane M: GeneRuler 100 bp plus DNA Ladder

Lane 1-73 : clones of naive *LasB* number BN2.1 to BN 2.73 respectively

Lane 74- 123 : clones of recombinant *LasB* number BR3.1 to BR 3.50 respectively

Production of HuscFvs that bound to the respective antigens and the cell penetrable HuscFv to critical residue of LasB in *E. coli* system

Sub-cloning of huscfv inserts into pLATE52 vector for production of HuscFvs that bound to the respective antigens

The huscfv-phagemids was used as a template for PCR. PCR amplification was performed in a total volume of 25 μl which the PCR mixture and PCR thermal cycle program are shown below.

PCR mixture (25 μl)

Ingredient	Volume (μl)	Final concentration
Sterile ultrapure distilled water (UDW)	15.75	-
Phusion GC buffer (5x)	5.0	1x
dNTP (2.5 mM each)	0.5	200 μM
Forward Primer (10 μM)	1.25	0.5 μM
Reverse Primer (10 μM)	1.25	0.5 μM
Phusion DNA Polymerase (1.0 units/50 μl PCR)	0.25	0.4 units
DNA template	1.0	-

Thermal cycles

Initial denaturation	at 98°C for 30 seconds
35 cycles of Denaturation ,	at 98°C for 10 seconds
Annealing ,	at 72°C for 10 seconds
and Extension	at 72°C for 15 seconds
Final extension	at 72°C for 5 seconds

The PCR product were analyzed on 1.2 % agarose gel electrophoresis and visualized on UV light after staining with ethidium bromide. The expected size of PCR product is ~ 850 bp **(Figure 1.56**).

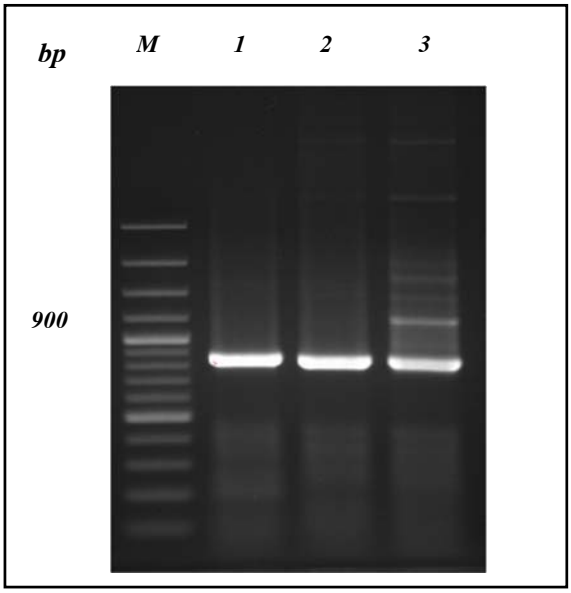

Figure 1.56 PCR product that obtained from the amplification of huscfv-phagemids.
Lane M: GeneRuler 100 bp plus DNA Ladder
Lane 1-3: clone BR1.2
Lane 2: clone BR2.7
Lane 3: clone BR2.10

Cloning of huscfv insert into the expression vector and bacterial transformation

The HuscFv-phagemid were cloned into the pLATE52 expression vector (Thermo Scientific) and then HuscFv-phagemid were introduced into the *E. coli* JM 109. The process comprise of two sections LIC cloning and annealing reaction. The LIC cloning were set up by mixed 2 μl of 5x LIC buffer; 4 μl of nuclease-free water; 0.1 pmol of purified PCR template; T4 DNA polymerase. Then the reaction mixture were incubated at 25°C for 5 minutes, the reaction were stopped by EDTA. Then the annealing reactions were generated by added the LIC-ready pLATE52 to the reaction mixture. Afterwards, the bacterial transformation was performed by using the Transform Aid Bacterial Transformation Kit (Thermo Scientific) to transform the huscFv-phagemid into the competent *E. coli* JM109. The positive clones were identified by colony PCR as below. The PCR product were analyzed on 1.2 % agarose gel electrophoresis and visualized on UV light after staining with ethidium bromide. The expected size of PCR product is ~ 1,000 bp **(Figure 1.57**).

PCR mixture (25 μl)

Ingredient	Volume (μl)	Final concentration
Sterile ultrapure distilled water (UDW)	18.3	-
Taq DNA polymerase buffer with KCl (Fermentas) 10x	2.5	1x
MgCl2 (25mM)	1.5	1.5 mM
dNTP (2.5 mM each)	0.5	200 μM
LIC Forward Sequencing primer, 10 μM	0.5	200 nM
LIC Reverse Sequencing primer, 10 μM	0.5	200 nM
Taq DNA Polymerase (5.0 units/μl)	0.2	0.5 units
DNA template	1.0	-

Thermal cycles

Initial denaturation	at 95°C for 5 minutes
35 cycles of Denaturation ,	at 95°C for 1 minutes
Annealing ,	at 54°C for 30 seconds
and Extension	at 72°C for 30 seconds
Final extension	at 72°C for 30 seconds

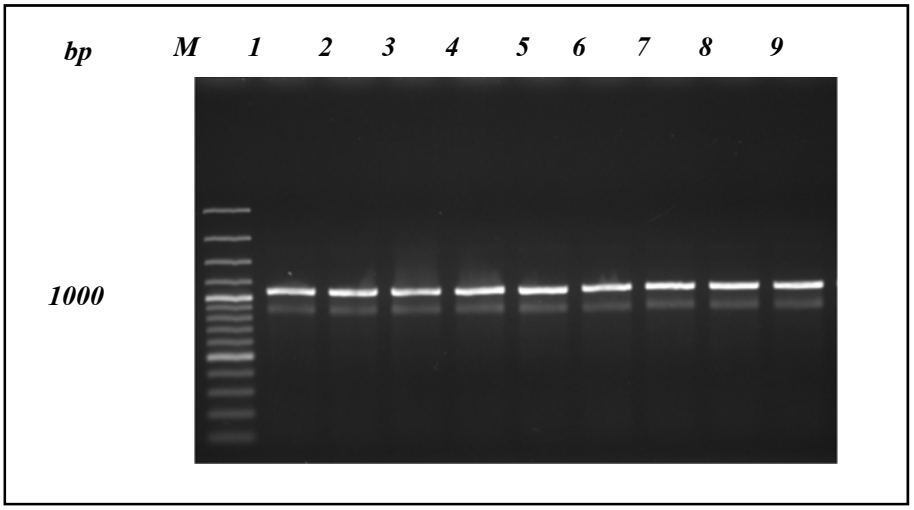

Figure 1.57 PCR product for screening of JM109 *E.coli* clones *carrying huscfv*-pLATE52. PCR products obtained with LIC primer should be show amplicon ~1000 bp in size. The PCR product were analyzed on 1 % agarose gel electrophoresis and visualized on UV light after staining with ethidium bromide.
Lane M: GeneRuler 100 bp plus DNA Ladder
Lane 1-3: clone BR1.2
Lane 4-6: clone BR2.7
Lane 7-9: clone BR2.10

Screening of transformed *E.coli* clones expressing HuscFv bound to recombinant LasB and native LasB

Dilute the protein to be coated to a concentration of 1 µg in a coating buffer pH 9.6 and add 100µL of this solution per well. Incubated until dry at 37°C. 3. BSA was used as antigen control. Unbound antigen were removed by washing with PBS-T. Block unoccupied binding sites with a blocking buffer and incubate at 37°C for 1 hour. Wash wells three times with PBS-T. Then, added 100 µl of *E.coli* lysate containing HuscFv or lysate of HB2151 *E.coli*, used as negative binding control and kept at room temperature for 1 hours with rocking. After washing, Rabbit polyclonal antibody to E tag (diluted 1:3000) was added to each wells and incubated at room temperature for 1 hours with rocking. Detected by Goat Anti-Rabbit immunoglobulin-HRP conjugate (diluted 1:3000) and ABTS peroxidase substrate was used to detect reaction product and measure the absorbance at 405 nm. The HuscFv expressing *E.coli* clones that provided ELISA signals twofold higher than the signal of the same lysates to BSA were selected. The result shown that only HuscFv bound only recombinant LasB (Figure 1.58).

(A.)

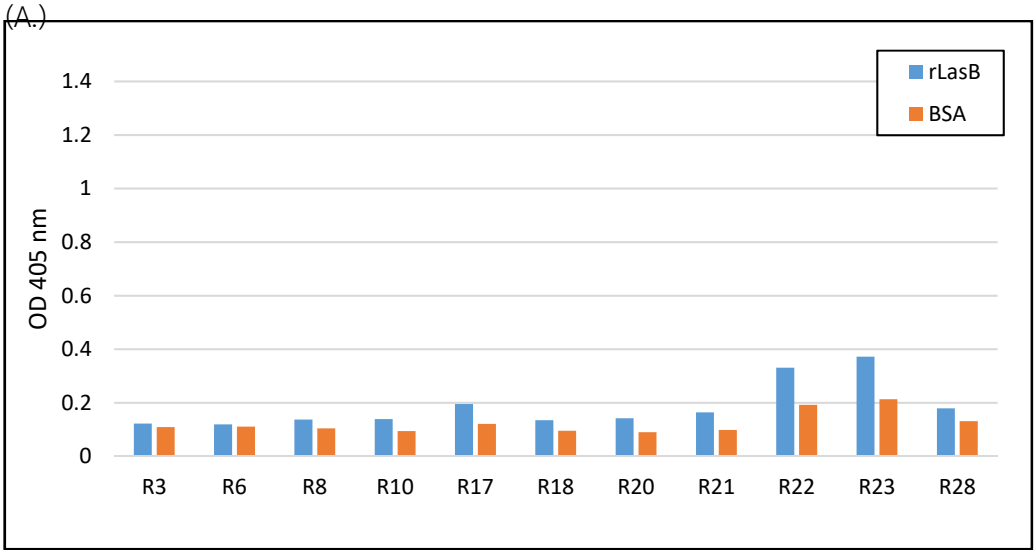

(B.)

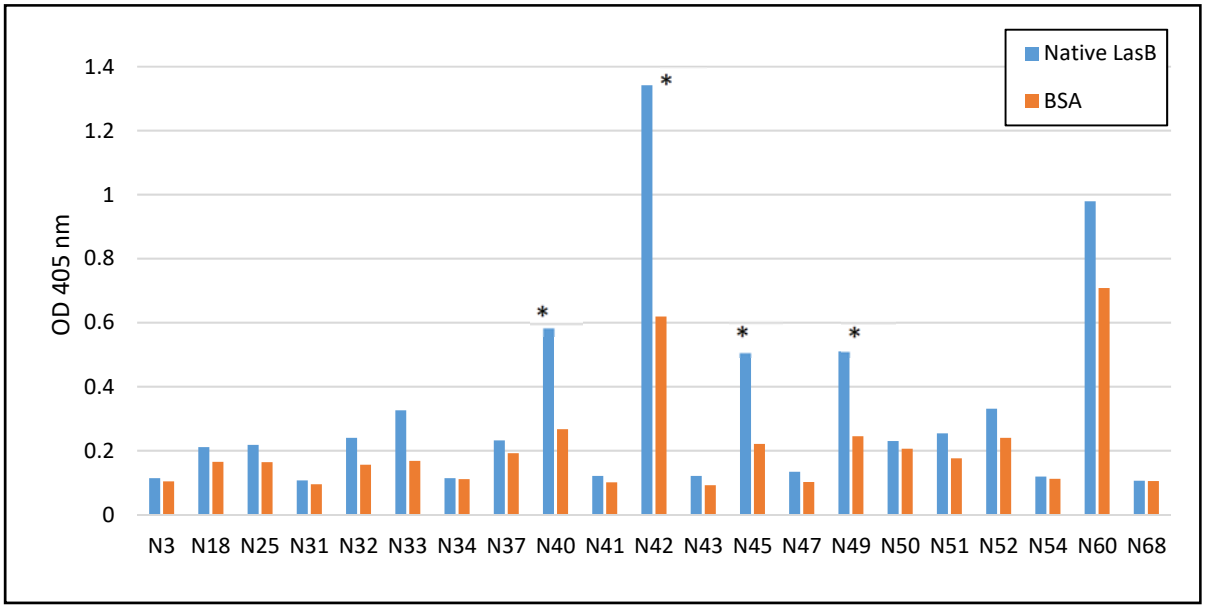

Figure 1.58 Indirect ELISA for specific binding of HuscFv in lysates of the transformed HB2151 *E.coli* clones to native LasB (A) and recombinant LasB (B)
Positive *E.coli* clone that the lysates gave absorbance at 405 nm two times higher than BSA (control antigen)

Production of HuscFvs that bound to the respective antigens to critical residue of LasB in *E. coli* system

Sub-cloning of huscfv inserts into pLATE52 vector for production of HuscFvs that bound to the respective antigens

The huscfv-phagemids were used as a template for PCR amplification, performed in a total volume of 25 μl**.** The PCR mixture and thermal cycle program were shown below. The expected PCR amplicom is ~ 850 bp in size (**Figure 1.59**).

PCR mixture (25 μl)

Ingredient	Volume (μl)	Final concentration
Sterile ultrapure distilled water (UDW)	15.75	-
Phusion GC buffer (5x)	5.0	1x
dNTP (2.5 mM each)	0.5	200 μM
Forward Primer (10 μM)	1.25	0.5 μM
Reverse Primer (10 μM)	1.25	0.5 μM
Phusion DNA Polymerase (1.0 units/50 μl PCR)	0.25	0.4 units
DNA template	1.0	-

Thermal cycles

Initial denaturation	at 98°C for 30 seconds
35 cycles of Denaturation ,	at 98°C for 10 seconds
Annealing ,	at 72°C for 10 seconds
and Extension	at 72°C for 15 seconds
Final extension	at 72°C for 5 seconds

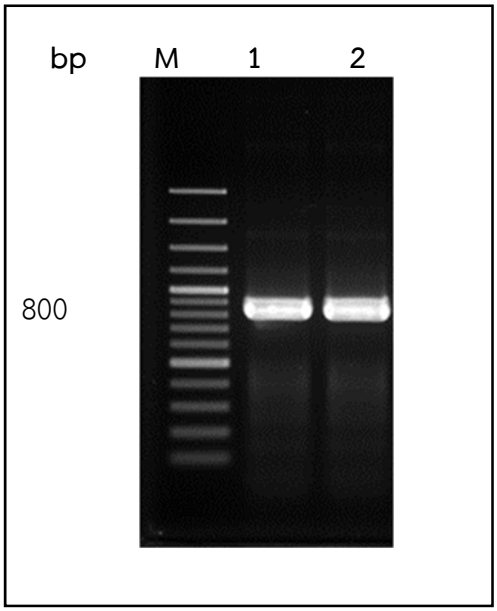

Figure 1.59 PCR product that obtained from the amplification of huscfv-phagemids. The expected size ~ 850 bp.The PCR product were analyzed on 1.2 % agarose gel electrophoresis and visualized on UV light after staining with ethidium bromide.
Lane M: GeneRuler 100 bp plus DNA Ladder
Lane 1: clone N42
Lane 2: clone N45

Cloning of LasB-huscfv insert into the expression vector and bacterial transformation

The LasB-HuscFv-phagemids were cloned into the pLATE52 vector and then introduced into the *E. coli* JM 109. The procedure starts with the LIC cloning was set up by mixing 2 μl of 5x LIC buffer; 4 μl of nuclease-free water; 0.1pmol of purified PCR template; T4 DNA polymerase and then the reaction mixture was incubated at 25°C for 5 minutes, Followed by the annealing reactions were created by added the LIC-ready pLATE52. After that, the huscFv-phagemid was transformed into the *E. coli* JM109 by using the Transform Aid Bacterial Transformation Kit (Thermo Scientific) The positive clones were identified by colony PCR (**Figure 1.60**) and transformed into expression host, *E. coli* NiCo21 (DE3). The colony PCR was used to check the clones that carrying recombinant plasmids by using LIC primer.

PCR mixture (25 μl)

Ingredient	Volume (μl)	Final concentration
Sterile ultrapure distilled water (UDW)	18.3	-
Taq DNA polymerase buffer with KCl (Fermentas) 10x	2.5	1x
MgCl2 (25mM)	1.5	1.5 mM
dNTP (2.5 mM each)	0.5	200 μM
LIC Forward Sequencing primer, 10 μM	0.5	200 nM
LIC Reverse Sequencing primer, 10 μM	0.5	200 nM
Taq DNA Polymerase (5.0 units/μl)	0.2	0.5 units
DNA template	1.0	-

Thermal cycles

Initial denaturation	at 95°C for 5 minutes
35 cycles of Denaturation ,	at 95°C for 1 minutes
Annealing ,	at 54°C for 30 seconds
and Extension	at 72°C for 30 seconds
Final extension	at 72°C for 30 seconds

t

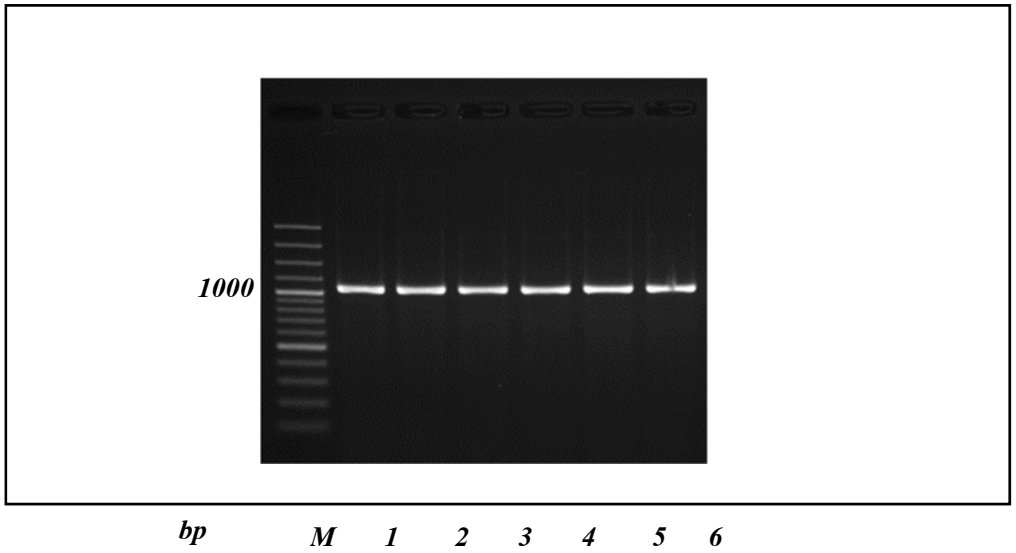

Figure 1.60 Product for the screening of JM109 *E.coli* clones carrying LasB-huscfv-pLATE52. PCR products were analyzed with 1.2 % agarose gel electrophoresis and should be showed amplicon about 1000 bp in size.
Lane M: GeneRuler 100 bp plus DNA Ladder
Lane 1-3: clone N42
Lane 4-6: clone N45

LasB-ScFv protein expression and protein analysis

The small expression was performed in LB broth with 100 μg / ml ampicillin. IPTG was added to each culture and incubated in a shaker at 37 ° C for 6 hours and Cell pellets were collected by centrifugation at 10,000 x g for 1 minute. The pellets were resuspended in BugBuster® protein extraction solution. Soluble fractions were collected by centrifugation at 14,000 x g for 5 minutes. The Insoluble fractions were suspended in diluted BugBuster and harvested by centrifugation. Then, the expression of the protein was analyzed by 12% SDS-PAGE (**Figure 1.61**). The results showed that the expression of the protein in the insoluble part, which should be approximately 27 to 35 kDa in size. Subsequently scale up expression was performed in 250 mL LB-A and further extracted by using BugBuster® protein extraction reagent with Lysonase™ Bioprocessing Reagent. Inclusion bodies were collected and washed by wash-100 reagent, wash-114 reagent and MilliQ water. The inclusion bodies were re-suspended in milliQ water with 0.02% (w/v) sodium azide. For protein refolding, inclusion bodies were dissolved at concentration 0.5 mg/ml in 50 mM CAPs, pH11 supplemented with 0.3% sarkosyl and 1 mM DTT and stored at 4 ℃ for overnight. Solubilized protein was dialyzed against 20 mM Tris-HCl, pH 8.3 addition with 1mM β-mercaptoethanol and stirred for 3 hours at 4 ℃. The dialysis buffer was changed and dialyzed further for 16-18 hours. Bicinchoninic acid (BCA) assay was used to evaluate concentration of total protein. The refolded LasB-HuscFv was analyzed using 12% SDS-PAGE and western blot analysis.

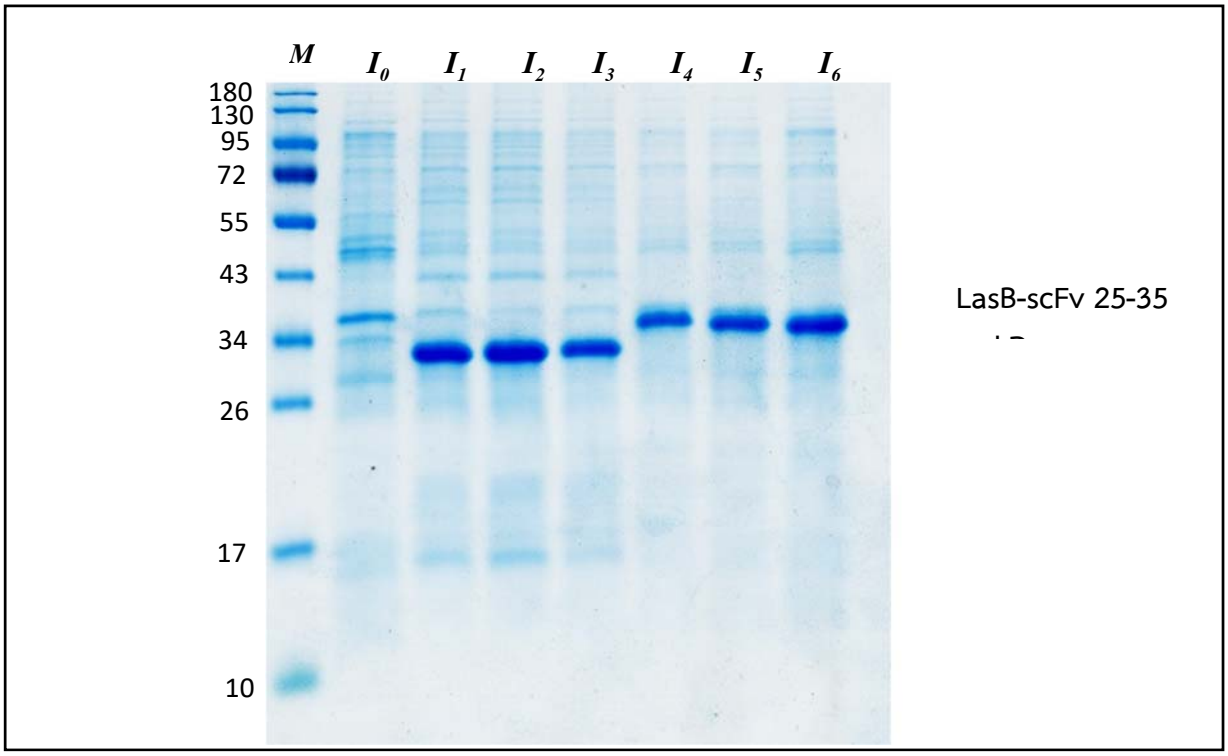

Figure 1.61 Separated insoluble fractions (LasB-scFv) of NiCo21 (DE3) *E.coli* expression from small scale expression by using SDS-PAGE

Lane M: Standard protein ladder

Lane I_0: Soluble fraction of control NiCo21 (DE3) *E.coli*

Lane I_{1-3}: Insoluble fraction of clones N42-1, N42-2 and N42-3respectively

Lane I_{4-6}: Insoluble fraction of clones N45-1, N45-2 and N45-3, respectively

6. Homology modeling and intermolecular docking

Homology modeling and intermolecular docking for predicting the presumptive residues of the ETA interacted with the HuscFvs

Computerized simulation was performed for predicting catalytic residues of ETA that formed interface contact with the HuscFvs. *Pseudomonas* exotoxin A (1IKQ) was used. Amino acid sequences coding for HuscFvs were modeled by the I-TASSER server. The top 10 treading templates used to model the HuscFvN20, HuscFv N21, HuscFv N32, HuscFv 1-33, HuscFv 3-41, HuscFv BP34, and HuscFv BP44 by I-TASSER and the top 10 identified structural analogs of the HuscFvs in the PDB. After that, the physical quality of the I-TASSER predicted 3D models were improved using Mod-Refiner algorithm, the low free-energy conformations were further refined by full-atomic simulations using Fragment Guide Molecular Dynamics Simulation (FG-MD). The FG-MD as a molecular dynamics-based algorithm for atomic-level protein structure modification refined the protein 3D models to be closer to their native structures. Also by using the FG-MD, the steric clash was avoided and the hydrogen binding network was improved. The antibody mode of ClusPro 2.0 antibody-protein docking was used. The largest cluster size with minimal local energy and protein conformation near to native state were subjected further for antibody-protein interaction simulation (Molecular Dynamics program). Pymol software (PyMOL Molecular Graphics System, Version 1.3r1 edu, Schrodinger, LLC) was used for building and visualizing the intermolecular interaction.

The three-dimensional (3D) structure of ETA (PDB 1IKQ) and modeled-HuscFvs were subjected to intermolecular docking. **Figure 1.62** show predicted ETA residues and domains that formed contact interface with HuscFvs of E. coli clones C41, E44 and P32. By the in silico docking, HuscFv-C41 uses VH-CDR1-3, VL-CDR2 as well as VL-FR2 and VL-FR3 to form contact with critical residues on the ETA-catalytic domain including Y481, Q485, R490, G491, E546, E547, E548, G549, R551, E553, N577, V578, G579, G580, and D581 of which Y481, E546, E547 and E553 are NAD+ binding site. The E553 is the ETA residue pivotal for the toxin enzymatic activity in transferring ADP-ribose to the eEF-237,38,39. Y481 is the NAD+-binding site of hydrophobic cavity of the toxin catalytic domain; the ETA uses the phenol ring of Y481 to tether the nicotinamide ring of NAD+ substrate, i.e., ADP-ribosyl group of NAD+, in order to transfer the substrate to eEF-240. The D461, Q485, E546, E547 and E553 formed the edge of the ETA-NAD+ binding cavity and participated in hydrogen bonding with two ribose moieties of the NAD+ molecule41. Moreover, previous study indicated that the ETA epitopes recognized by murine monoclonal antibody clone B7 (MAbB7) which displayed strong neutralizing capacity on ETA cytotoxicity were mapped to the C-terminal residues

575-595 of the toxin42. Although the results of ETA-HuscFv interaction by computerize simulation needs experimental validation, it is pluasible that the effectiveness of HuscFv-C41 in neutralizing the apoptotic activity of ETA is through interfering with the catalytic activity and inhibition of ADP-ribose transfer from NAD+ to eEF2.

The HuscFv-E44 was predicted to use VL-CDR2 and VL-FR3 to interact with Q310, R313 and A317 of ETA-2 (translocation domain); this binding should not involve in the HuscFv-mediated-neutralization of the ETA cytotoxicity. The HuscFv-E44 also used VH-CDR2, VH-CDR3, VH-FR1, VL-CDR1, VL-CDR2 and VL-FR2 to bind to D461 and E547 which are NAD+ binding site, and Q485, E486, E548, G549, D581, D583, and P584 of ETA-3 of the catalytic domain. The HuscFv-P32 interacted with residues of the ETA-catalytic domain including S515, A519, P545, E547 (NAD+ binding site), E548, G550 and D581 by using VH-CDR1-3 and VL-CDR1. Based on the computerized results of the protein-antibody docking, the ETA bound-HuscFvs of the three *E. coli* clones presumptively formed contact interface with critical residues for ETA-mediated ADP-ribosylation. HuscFv-C41 was more effective than the HuscFv-E44 and HuscFv-P32 in inhibiting the ETA cytotoxicity. This might be because the HuscFv-C41 interact with several more residues critical for catalytic activity and ADP-ribosylation reaction than the other two cognates.

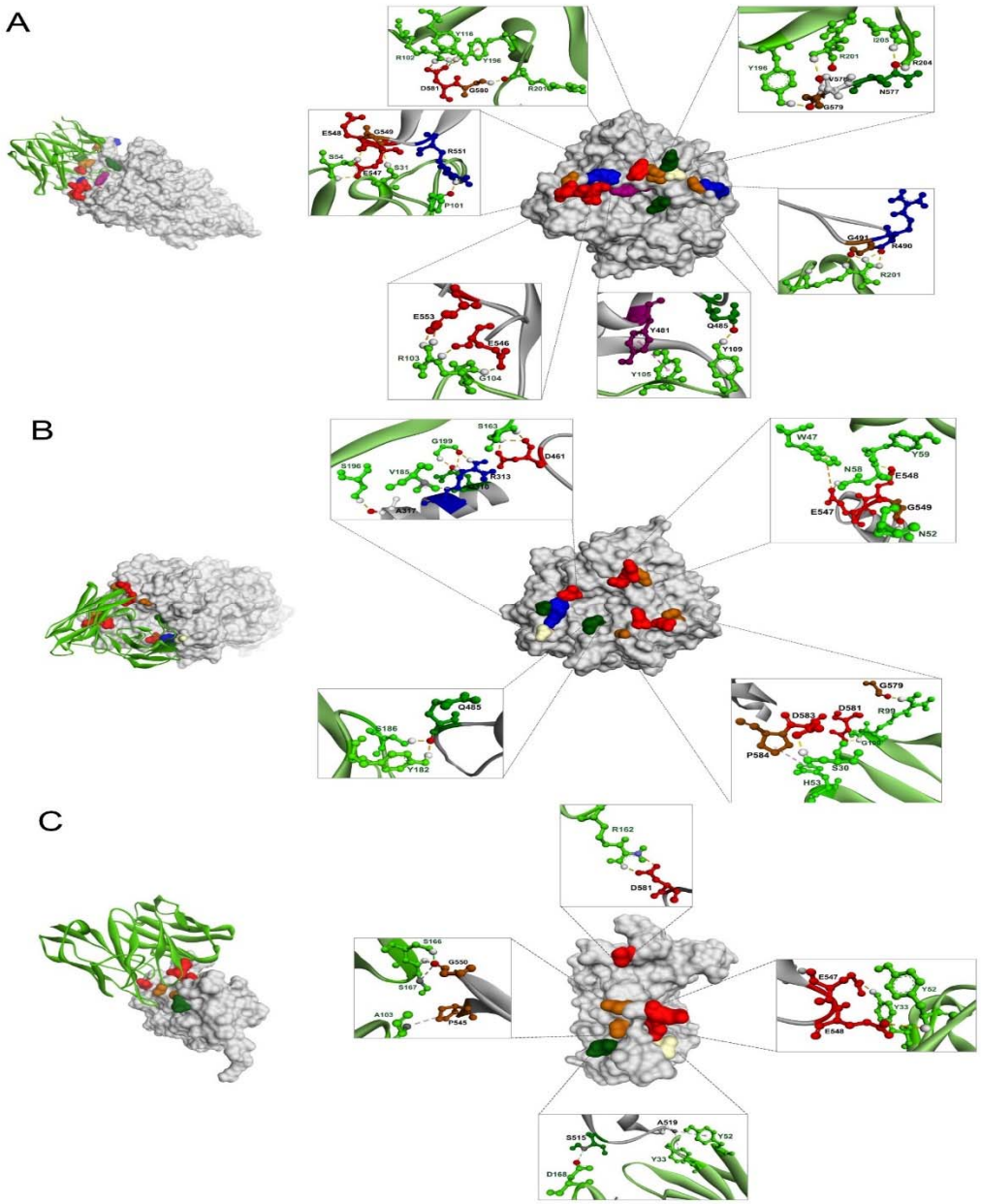

Figure 1.62 Computerized interaction of modeled-ETA and HuscFvs and residues that were predicted to form contact interface between them. Left side of Panels A-C, interactions of ETA (grey) with several residues near/or in the catalytic site of the respective HuscFvs (light green). Right side of Panels A-C, contact residues between ETA and HuscFv-C41, HuscFv-E44, and HuscFv-P32, respectively. The ETA amino acids are colored according to CINEMA color scheme: polar negative D and E are red; polar positive H and R are blue; polar neutral S, N, and Q are dark green; non-polar aromatic Y is purple/magenta; non-polar aliphatic A and V are white, P and G are brown.

Homology modeling and intermolecular docking for predicting the presumptive residues of the LasB interacted with the HuscFvs

The 3D structure of huscFv was created and refined by I-Tasser sever and improved to close the native states using cluspro 2.0 antibody-antigen docking. LasB-HuscFv complexes were built and visualized using Pymol software (**Figure 1.63**). The huscFv42 was predicted had interaction with catalytic residues of LasB (PDB 1EZM) that consistent with inhibition test by EnzChek™ elastase assay Kit.

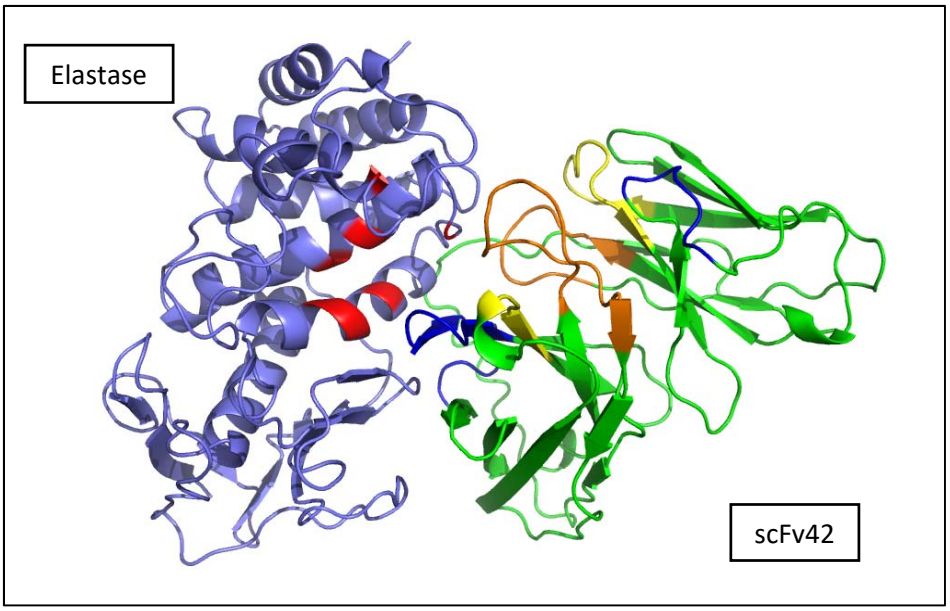

Figure 1.63 Interface interaction between the LasB and the scFv42 by molecular docking.

7. Neutralization assay for HuscFvs against ETA and LasB

Inhibition of elastolytic activity by EnzChek™ elastase assay Kit

The inhibition of HuscFv on elastolytic activity of LasB was evaluated by using the EnzChek ™ elastase assay Kit. The scFv42 diluted at concentrations 10, 7.5, 5 and 2.5 μM were incubated at 37 ℃ for 1 h with 25 nM of native elastase. Then, DQ elastin as fluorogenic substrates was added into each well and incubated for 30 minutes. Measure the fluorescence intensity in a fluorescence microplate reader equipped with standard fluorescein filters. The excitation and emission wavelengths were 485 ± 20 and 520 ± 20 nm, respectively. The result showed that scFv42 was able to decrease the fluorescence activity of native elastase (**Figure 1.64**).

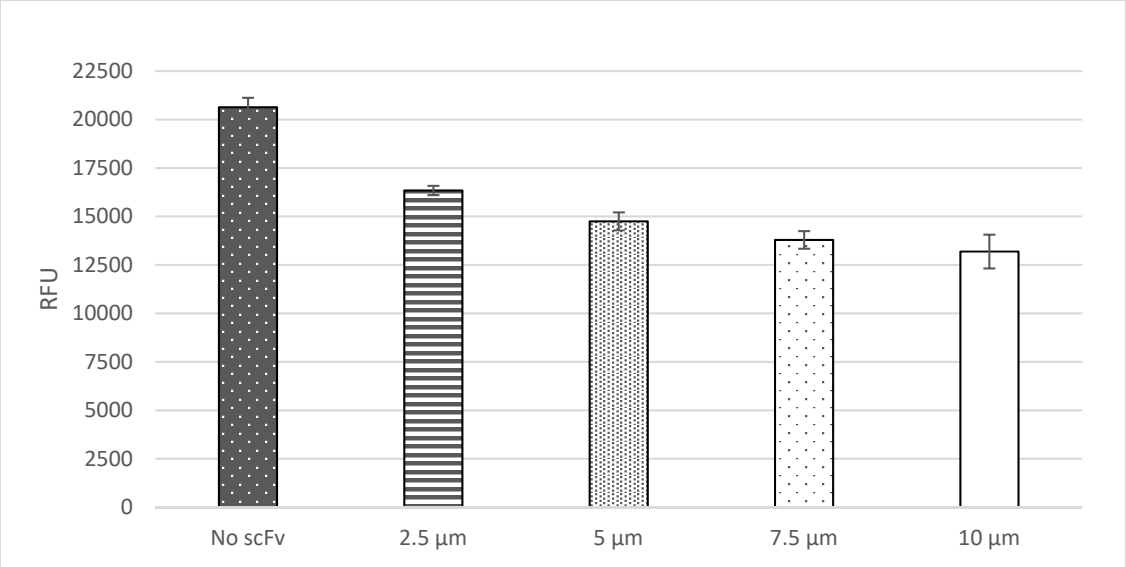

Figure 1.64 Graph of the relative fluorescence unit (RFU) and the concentration of scFV42.

The biological activities of recombinant full-length ETA on mammalian cell line

Optimization of the conditions for ETA treated HeLa cells apoptosis to detecting the flipped phosphatidyl serine using AnnexinV-FITC and PI staining

In this study, we use HeLa cells as the model for characterizing the ability of *Pseudomonas* Exotoxin A to cause mammalian cell death. HeLa cells were cultured and maintained in serum supplemented-DMEM in T75 flask. The HeLa cells monolayer in individual wells of a 24-well tissue culture plate (1×10^5 cells/well) were washed with sterile PBS, added with 100-1,000 ng/well of recombinant ETA in complete DMEM, and incubated for 24 h at 37°C in 5% CO_2 atmosphere. Controls were cells in the medium alone (negative control for cell death) and cells added with 3% H_2O_2 (positive control for cell death) were included. After 24 h, culture supernatants and the trypsinized cells in the wells of each treatment and controls were collected separately to perform flow cytometry through the FITC Annexin V Apoptosis Detection Kit manufacturer's instructions (BD Biosciences). The results showed in **Figure 1.65**.

Figure1.65 Cytotoxicity of the rETA-FL (ability of the rETA-FL to induce mammalian cells apoptosis). The rETA-FL at 100, 250, 500, 750, and 1000ng/well activated HeLa cell

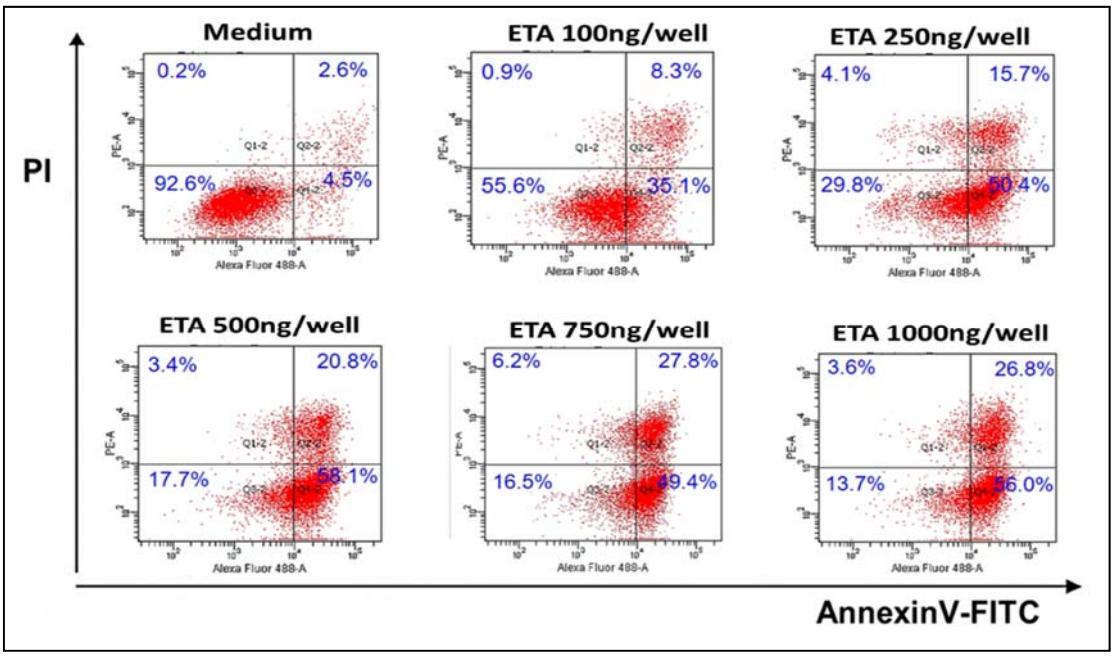

line to progress apoptosis compared with the cells in medium alone.

The optimal concentration of rETA-FL to induce HeLa cells apoptosis. By varying the toxin concentration from 100, 250, 500, 750, and 1000ng per well, the results demonstrated that the apoptotic populations were 43.4%, 66.1%, 78.9%, 77.2%, and 82.8%, respectively compared to the cells culture with medium alone revealed 3.1% of apoptotic populations. The LD50 was 109.203 ng (**Figure 1.66**).

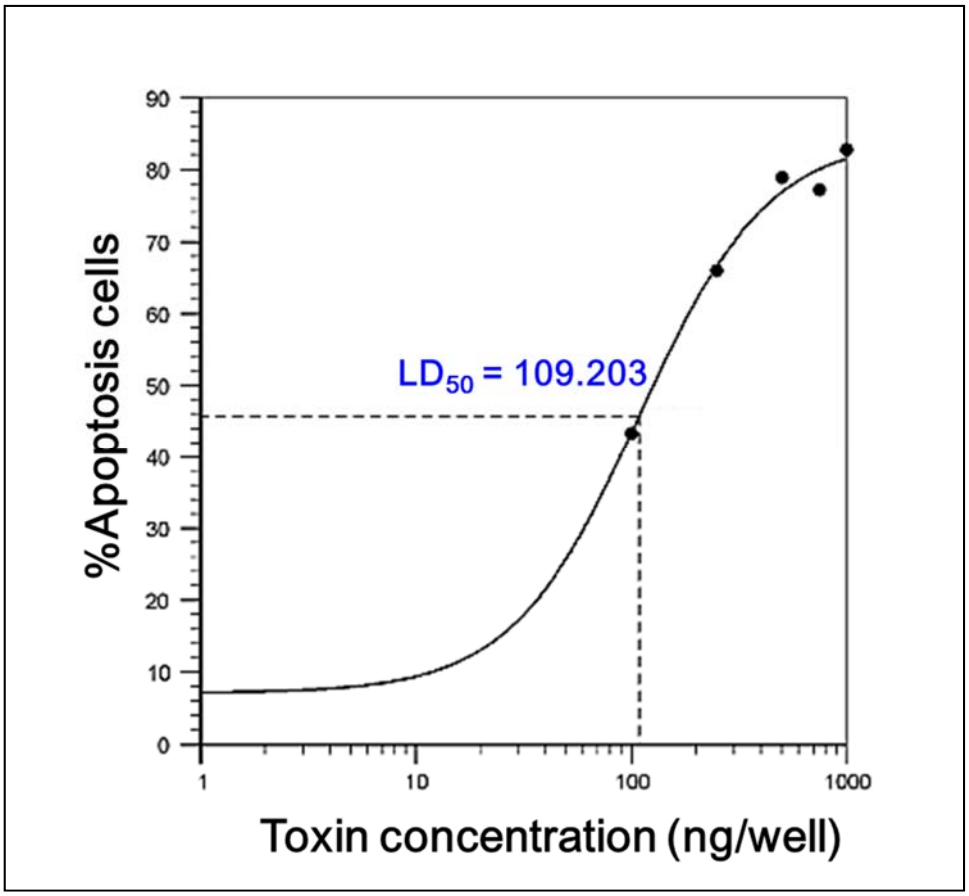

Figure 1.66 Cytotoxicity of the rETA-FL (ability of the rETA-FL to induce mammalian cells apoptosis).

Detection of apoptotic cells using Acridine orange/Ethidium bromide Staining

Morphologically characterized of apoptotic cells ETA induced HeLa cells apoptosis using ethidium bromide (EB) and acridine orange (AO) staining. HeLa cells were cultured with/without ETA for 24 hr in the completed DMEM. Following trypsinization, the detached cells were washed with 1X Dulbecco's Phosphate (DPBS) pH 7.4, then centrifuged at 3,000 rpm at 4°C for 10 mins and then collected. The cell pellets were then resuspended in 50 μL of culture medium. The resuspended cells were stained with 100 μg/mL of EB and 100 μg/ml AO with a cell to fluorescent dye ratio of 2:1 (v/v). All of the staining procedures were performed on an ice-cold container. Then the stained cell suspensions were further drop on the glass slide covered with a coverslip and observed under the fluorescence microscope. The results showed in **Figure 1.67**.

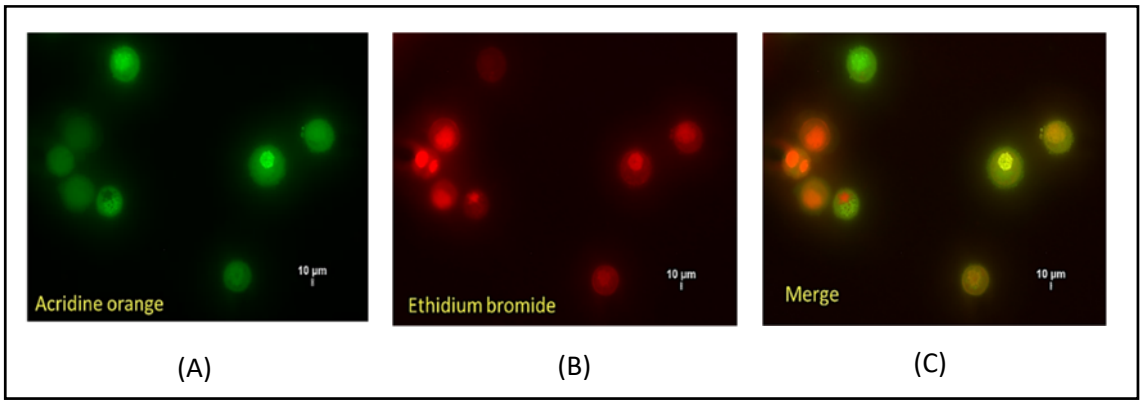

Figure 1.67 Dual acridine orange/ethidium bromide staining of apoptotic cells induced by rETA-FL using fluorescence microscopy. Acridine orange staining HeLa cells (A), Ethidium bromide staining HeLa cells (B), and dual AO/EB staining HeLa cells (C).

Determination of apoptotic cells using AnnexinV/PI binding assay by flow cytometry

The rETA-FL mediated 37.15% HeLa cells apoptotic cells. After treatment with HuscFvBP44, HuscFvN32, and HuscFvD341, percent apoptosis cells were reduced to 8.18%, 21.24%, and 7.94%, respectively. The inhibitory activities of HuscFv clone BP44 and D341 were higher than the HuscFv clone N32 (**Figure 1.68** and **1.69**).

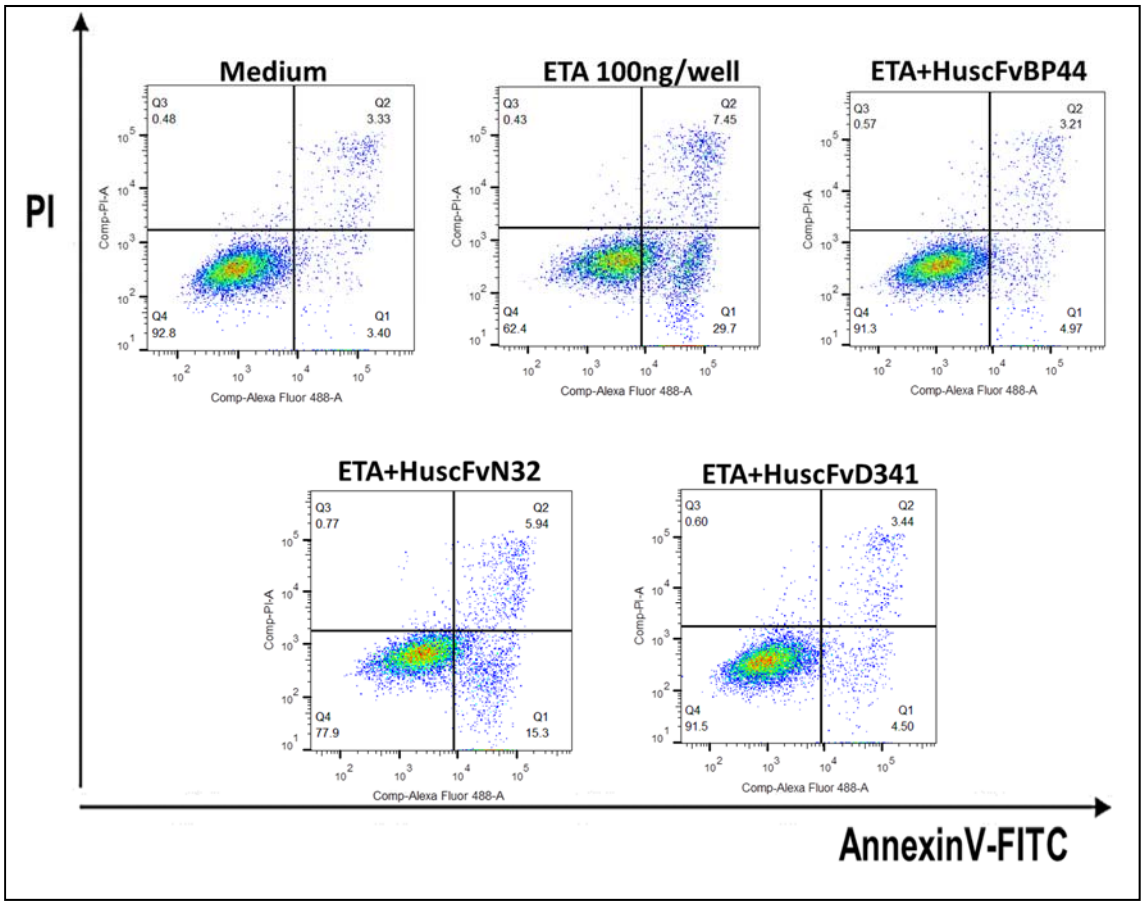

Figure 1.68 Cytoprotective effect of HuscFvs against Pseudomonas exotoxin A. The rETA-FL at 100 ng/well activated HeLa cell line with/without HuscFvs compared with the cells in medium alone.

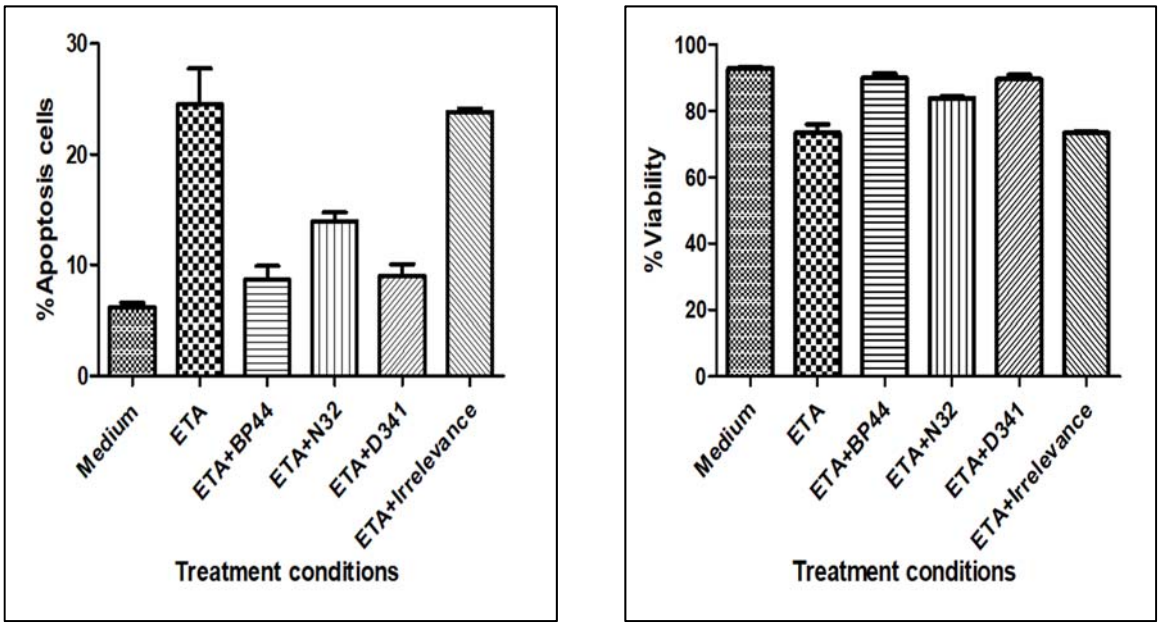

(A) (B)

Figure 1.69 Percentage of apoptotic cells (A) and viability (B) of HeLa cells induced by ETA. The bar graph exhibited the difference in the number of apoptotic cells and viability of cells in each treatment conditions.

Detection of expression of apoptosis-related genes (cas3 and p53) by reverse transcription-polymerase chain reaction (RT-PCR).

Total RNA were extracted from ETA-exposed-HeLa cells that had been treated with HuscFvs and controls for 12 h, by using a GeneJET RNA Purification Kit (Thermo Fisher Scientific). The quality of RNAs were determined at OD260nm and OD280nm using NanoDrop™ 2000/2000c Spectrophotometers. After DNase treatment using RNase-free-DNase I (Thermo Fisher Scientific), the RNAs were used to generate cDNA using RevertAid First Strand cDNA Synthesis Kit (Thermo Fisher Scientific). Real-time RT-PCR was performed on KAPA SYBR® FAST qPCR (Kapa Biosystems, Cape Town, South Africa). Each reaction mixture (20 µl) contained 10 µl of 2× KAPA SYBR® FAST qPCR Master Mix Universal, 200 nM final concentration each of forward and reverse primers, and 20 ng of cDNA template in nuclease-free PCR-grade water. The reaction was performed in a CFX96 Touch™ Real-Time PCR Detection System (Bio-Rad Laboratories). The following thermal cycles was used: initial denaturation at 95 °C for 3 min and 40 cycles at 95 °C for 30 s, 53 °C for 30 s, and 72 °C for 30 s. A dissociation curve was generated from a thermal profile consisting of 95 °C for 1 min, 55 °C for 30 s, and 95 °C (0.5 °C/s). Each sample was amplified in triplicate. Gene expressions relative to the normal cells were analyzed using the **Δ**CT method. Amounts of casp3 and p53 were normalized to the internal control, i.e., GAPDH. Primer used in this experiments are shown in Table 2. The ETA-exposed-HeLa cells treated with the HuscFvs had significant decreases of expressions of apoptosis-related genes including cas3 and p53 compared to the control HuscFv-treated (Irre) cells and the cells in medium alone **(Figure 1.70 A and B).**

Table 2. Primers for study the expression of apoptosis-related genes (cas3 and p53).

Primer	Primer sequence (5´– 3´)
cas3 forward	TGG TTC ATC CAG TCG CTT TG
cas3 reverse	ATT CTG TTG CCA CCT TTC G
p53 forward	ACT AAG CGA GCA CTG CCC AA
p53 reverse	ATG GCG GGA GGT AGA CTG AC
GAPDH forward	CTG GGC TAC ACT GAG CAC C
GAPDH reverse	AAG TGG TCG TTG AGG GCA ATG

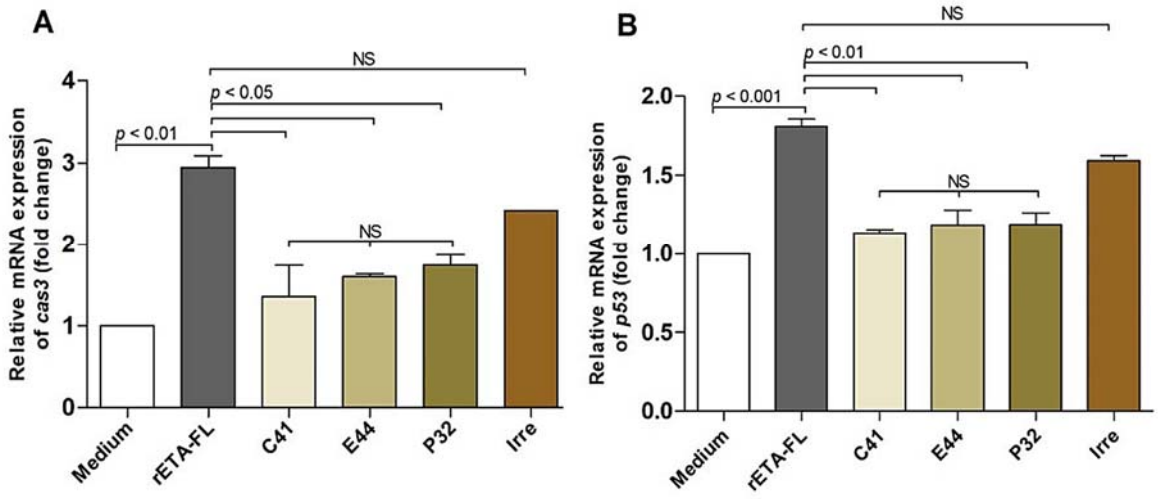

Figure 1.70 Expression of apoptosis-related genes (*cas3* and *p53*) as determined by real-time RT-PCR. A, the relative mRNA expression of *cas3*; B, the relative mRNA expression of *p53* in ETA-exposed-HeLa cells treated with ETA-bound-HuscFvs, control HuscFv (Irre) or medium alone for 12 h. GAPDH mRNA was used as an internal control. Data are from triplicate experiments.

8. Cytoprotective effects of quorum quenching single-chain antibodies against 3-oxo-C12-HSL

N-3-oxo-dodecanoyl-L-homoserine lactone (C12-HSL) was purchased from Cayman Chemical (Michigan, USA) was dissolved in dimethyl sulfoxide (DMSO) as 5 mg/ml stocks.

C12-HSL induced HeLa cells apoptosis

Cell culture

The HeLa cell line (human cervical cancer cell) were maintained at 37 °C in 5% CO2 in Dulbecco's Modified Eagle Medium(DMEM) supplemented with 10% (v/v) Fetal Bovine Serum and 1% (v/v) penicillin antibiotics.

Flow cytometry analysis of C12-HSL induced HeLa cells apoptosis

Cells were seeded in 24-well plates (1 × 105 cells/well) and incubate at 37 °C in 5% CO2 for 24 hr. Cells were treated with N-3-oxo-dodecanoyl-L-homoserine lactone in various concentration (10 µM, 25 µM, 50 µM, 75 µM, and 100 µM) for 18 hr. HeLa cell apoptosis was evaluated by FITC Annexin V Apoptosis Detection Kit I (BD Biosciences, USA) according to the manufacturer's protocol. Briefly, the floating cells were collected and also the attached cells were harvested by trypsinization using 0.05% Trypsin/EDTA. The whole operation process was protected from light. In brief, cells washed with ice-cold phosphate buffered saline (DPBS pH 7.4) were re-suspended in binding buffer (approximately 1×105 cells/100 µl buffer solution). The cell suspension supplemented with Annexin V-FITC and PI incubated for 15 min at room temperature. The apoptotic cells were identified by flow cytometer.

Production of scFvs that could neutralize C12-HSL bioactivities

The scFvs that could neutralize the AHL bioactivities were selected from a HuscFv phage display library previously constructed (Kulkeaw K. *et al.,* 2009) by *in silico* docking and structural homology to the quorum quenching antibody (mAb RS2-1G9) (Kaufmann G.F. *et al.,* 2008). The selected clones of bacterial derived scFvs were further send for DNA sequencing (First BASE Laboratories Sdn. Bhd., Malaysia). The nucleotide sequences of the positive clones were analyzed using SnapGene Viewer program version 3.3.3 and CLC sequence viewer version 7 software.

The correct *scfv* reading frame in the pCANTAB5E phagemid of each clone were evaluated. Afterwards, the complementarity determining regions (CDRs) and their respective canonical immunoglobulin framework regions (FRs) of the sequenced huscfvs were predicted using an online server, the VBASE2 - the integrative germ-line V gene database (http://www.vbase2.org/). After that, purified plasmid DNA of the HB2151 *E. coli* positive clones that could produce scFv (includes the representatives clone F15 and F19) were used as the template to amplifythe scFv gene using Phusion High-Fidelity DNA Polymerase (Thermo Scientific™, USA). PCR amplification was performed in a total volume of 25 µl which the PCR reaction mixture and PCR thermal cycle condition were provided. After that, the PCR products were verified by gel electrophoresis and ethidium bromide staining.

To Sub-cloning of DNAs coding for AHL-bound scfv inserts into pLATE52 expression vector and bacterial transformation, the PCR products from above were be purified using the Gel/PCR DNA Fragments Extraction Kit (Geneaid Biotech Ltd., Taiwan) with a bind-wash-elute procedure to completely eliminate the incorporated primers, dNTPs, and other contaminated DNA. The purified DNA were measured for its concentration and also quality using NanoDrop™2000/2000c Spectrophotometers (Thermo Scientific™, USA) at the wavelength 260/280. The scfv inserts were cloned into the pLATE52 expression vector using the aLICator LIC Cloning and Expression Kit 4 (N-terminal His-tag/WQ), #K1281 (Thermo Scientific™, USA). The LIC cloning was performed to generate the 5’ and 3’ overhangs on the purified PCR templates as previously described. Afterwards, the bacterial transformations were done by using the Heat-shock method to transforming of the *scfv*-pLATE52 recombinant plasmids into the competent *E. coli* strain JM109, a cloning host. The transformed bacterial cells were spread onto LB agar plate containing 100 µg/ml of ampicillin antibiotic (LB-A agar), and further incubated at 37 °C for overnight. The individual transformed JM109 *E. coli* colonies was randomly picked and checked for the presence of the recombinant plasmids with *scfv* inserts using the colony PCR. An individual transformed JM109 *E. coli* colonies was randomly selected and inoculated into the 150 µl of LB broth containing 100 µg/ml of ampicillin antibiotic, then incubated at 37 °C for 2 hours with 250 rpm shaking that one microliter of each clone was used as DNA template.

The PCR products from above were purified using the Gel/PCR DNA Fragments Extraction Kit. In this study, the two LIC primers (LIC-Forward primer: 5'-TAATACGACTCACTATAGGG-3' and LIC-reverse primer: 5'-GAGCGGATAACAATTTCACACAGG-3') were used to perform the PCR amplification of recombinant plasmid from each individual clone. The PCR reaction mixture (25 µl) was composed of 1 µl of DNA template, 0.5 µl of each primer (10 µM), 2.5 µl of 10 × *Taq* buffer with KCl, 1.5 µl of 25 mM $MgCl_2$, 0.5 µl of 10 mM dNTPs, 0.2 µl of 5 units/1µl *Taq* DNA polymerase (Fermentas, Thermo Fisher Scientific, USA), and 18.3 µl of UDW. PCR condition comprised of 1 cycle initial

denaturing at 95 °C for 5 minutes; 35 cycles of denaturing at 95 °C for 30 seconds, annealing at 58 °C for 30 seconds, and extending at 72 °C for 1 minute; final extending at 72 °C for 7 minutes; and holding at 4 °C for infinity. The PCR products of the correct length were indicated that plasmid have been properly inserted. PCR products obtained with LIC forward and LIC reverse primers showed approximately 850 bp for the recombinant plasmid. The PCR products were verified by 1.5% agarose gel electrophoresis and ethidium bromide staining (Figure 1.71).

The screened positive transformed *E. coli* clones by colony PCR method were performed by extracted their plasmids using the PrestoTM Mini Plasmid Kit (Geneaid Biotech Ltd., Taiwan) following the manufacturer's instruction, and send for DNA sequencing (First BASE Laboratories Sdn. Bhd., Malaysia). Afterwards, the positive clones from DNA sequencing were subjected to perform the plasmid extraction and further transformed into an expression host. In this study, NiCo21(DE3) *E. coli* (New England Biolabs, UK) cells were used as an expression host for recombinant *scfv*-pLATE52 plasmids. Then colony PCR using the two LIC primers for screening of the positive clones of the transformed NiCo21(DE3) *E. coli* with the *scfv*-pLATE52 recombinant plasmids were performed screening for the desire inserted gene.

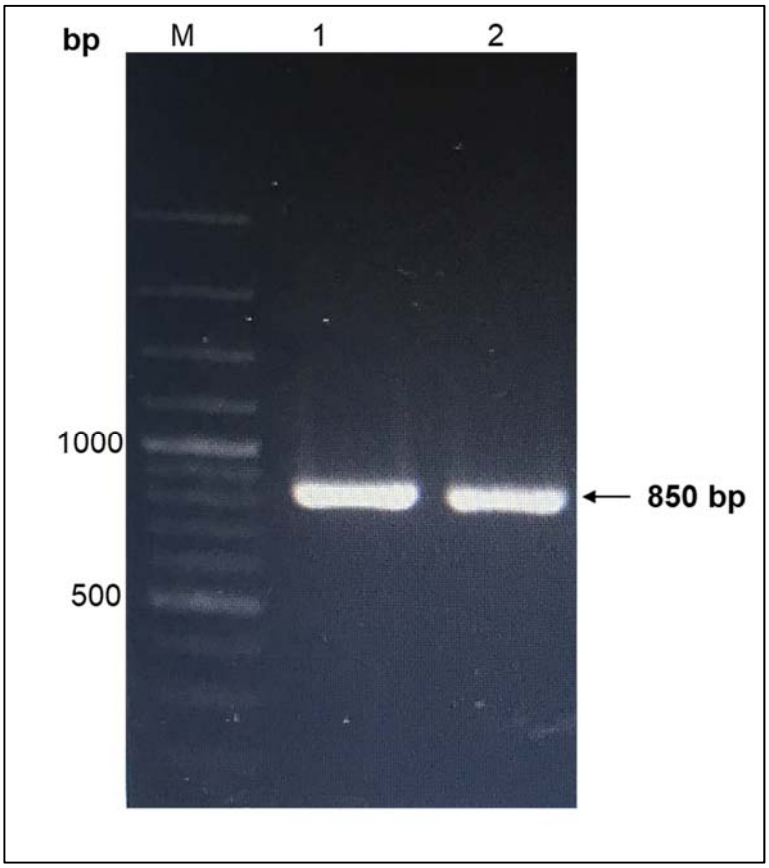

Figure 1.71 PCR products that obtained from the amplification of the *huscfv* inserts using specific LIC primers (expected amplicon size ~ 850 bp).

Lane M: GenRuler^{TM} 100 bp DNA ladder plus

Lane N20: *huscfv* amplicon from the purified plasmid DNA of the HB2151 *E. coli* positive clones that could produce HuscFv specific nETA clone no.20

Lane N21: *huscfv* amplicon from the purified plasmid DNA of the HB2151 *E. coli* positive clones that could produce HuscFv specific nETA clone no.21

Lane N32: *huscfv* amplicon from the purified plasmid DNA of the HB2151 *E. coli* positive clones that could produce HuscFv specific nETA clone no.32

The PCR product were analyzed on 1.5% agarose gel electrophoresis and visualized on UV light after staining with ethidium bromide.

To express the recombinant scFv protein, the representative NiCo21(DE3) *E. coli* clones carrying *scfv*-pLATE52 recombinant plasmid were verified. An individual single colony of each positive *E. coli* clone was individually cultured in 2 ml of LB broth containing 100 ug/ml ampicillin in shaking incubator at 37°C with shaking at 250 rpm until the culture reached the bacterial log phase growth (OD_{600nm} ~0.5). The bacterial cells (HuscFv specific native ETA including clone no. N20, N21, N32, 1-33, 3-41, BP34, BP44, F15 and F19) that were expressed in the insoluble fraction (inclusion body). So these representatives were further subjected to perform protein purification and refolding.were induced for their recombinant protein expression by adding 1 mM IPTG into the individual cultures and further the incubation of the cultures at 30 °C with shaking at 250 rpm for 6 hours. The induced bacterial cells were collected by centrifugation at 10,000 *×g* at 4°C for 5 minutes. These scFv were further subjected to perform protein purification and refolding and were analyzed by SDS-PAGE. **Figure 1.72** showed recombinant scFvs clone F15 and F19 which not previously present. The scFvs expected size is about 25-35 kDa.

Flow cytometry analysis of neutralizing ability of scFvs to C12-HSL using Annexin V/PI staining of apoptotic cells

HeLa cells were seeded in 24-well plates (1 × 105 cells/well) and incubate at 37 °C in 5% CO2 for 24 hr. The AHL induced cells with 25 μM was treated with scFv clone F15, F19, C41, and E44 for 18 hr. Then, HeLa cell apoptosis was evaluated by FITC Annexin V Apoptosis Detection Kit I (BD Biosciences, USA) according to the manufacturer's protocol. The rETA-FL mediated 14% HeLa cells apoptotic cells. After treatment with HuscFv F15, F19, and E44, percent apoptosis cells were reduced to 8%, 6%, and 8%, respectively. The inhibitory activities of HuscFv clone F19 was higher than the HuscFv clone N15 and E44 (Figure 1.73).

Homology modeling and intermolecular docking for predicting the presumptive residues of the AHL, C12HSL, interacted with the HuscFvs

The 3D structure of huscFv was created and refined by I-Tasser sever and improved to close the native states using cluspro 2.0 antibody-antigen docking. C12HSL-HuscFv complexes were built and visualized using AutodockVina software. The huscFv clone no.F15, F19, BP44 and C41 were predicted had interaction with catalytic residues of C12HSL (**Figure 1.74**).

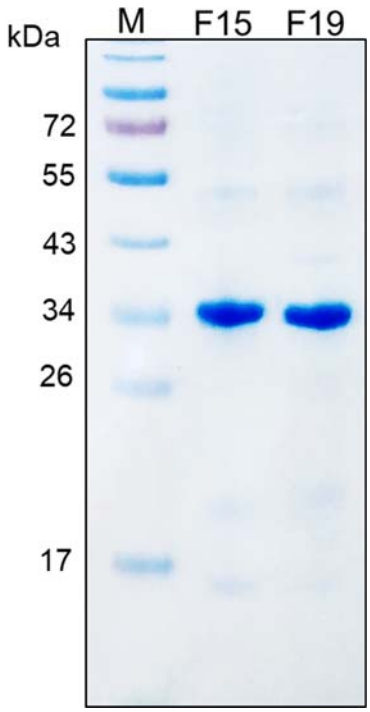

Figure 1.72 Stained SDS-PAGE-separated-purified and refolded recombinant scFvs clone F15 and F19.

M, pre-stained protein ladder

Lane F15, purified scFv clone F15

Lane F19, purified scFv clone F19

Numbers at the left represent the protein molecular masses in kDa . The scFvs expected size is about 25-35 kDa.

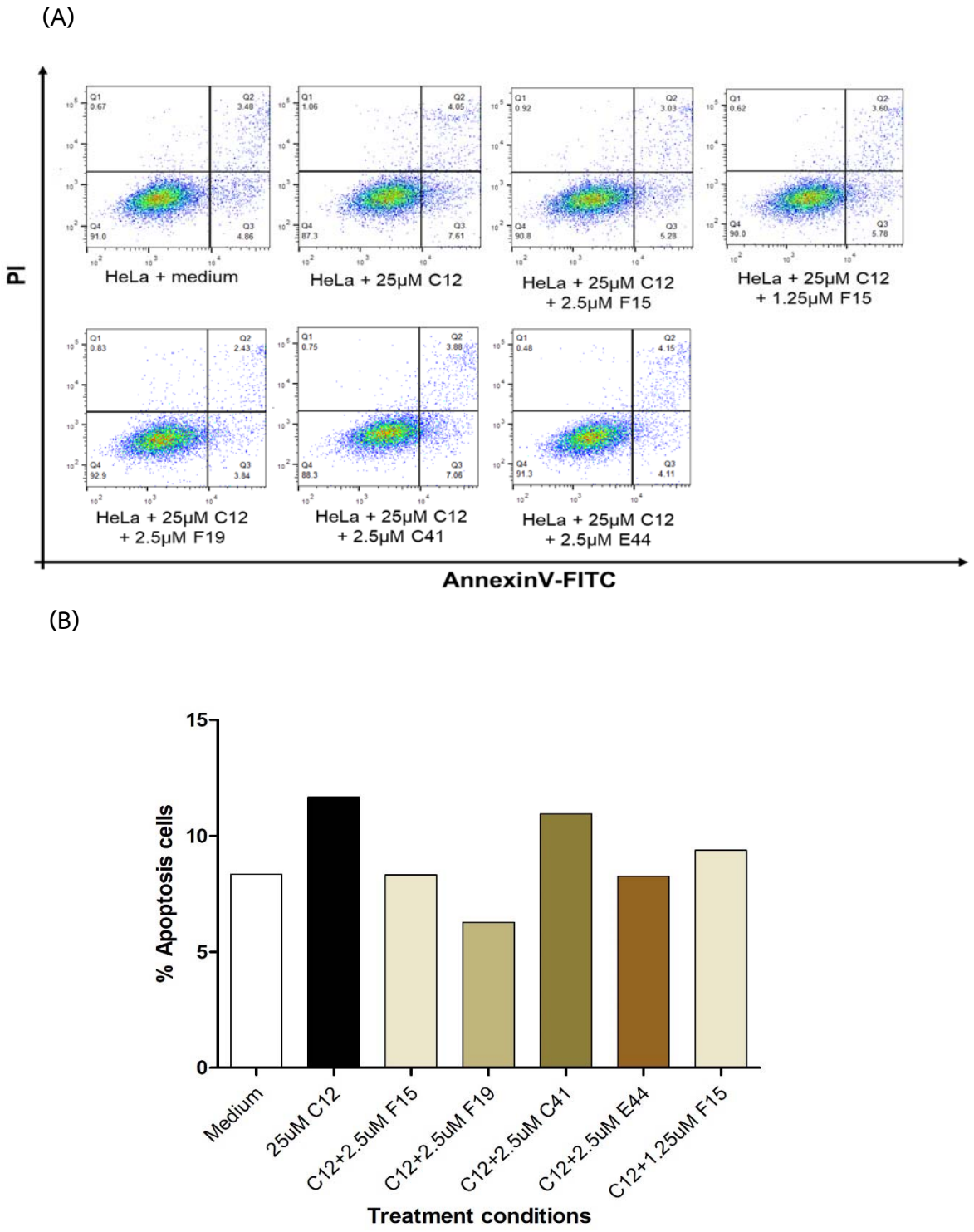

Figure 1.73 A, Apoptotic analysis of Annexin V/PI stained-ETA-exposed-HeLa cells after treatment with ETA-bound HuscFvs/control HuscFv (Irre) at HuscFv to ETA molar ratio 50:1 and medium alone. B, Bar graphs that represent statistical comparison of the averaged percentages of ETA induced-HeLa cells apoptosis after different treatments. The data shown are representative of three independent experiments. The significant difference from control is indicated by $p < 0.05$. Triplicate

experiments were performed. C, Scanning electron microscopic appearances of ETA-exposed HeLa cells after treatment with ETA-bound HuscFvs, control HuscFv (Irre) and medium alone. C, Normal HeLa cells (a); ETA- exposed HeLa cells (b); cells exposed to ETA treated with HuscFv-C41 (c); cells exposed to ETA treated with control HuscFv (d).

F15

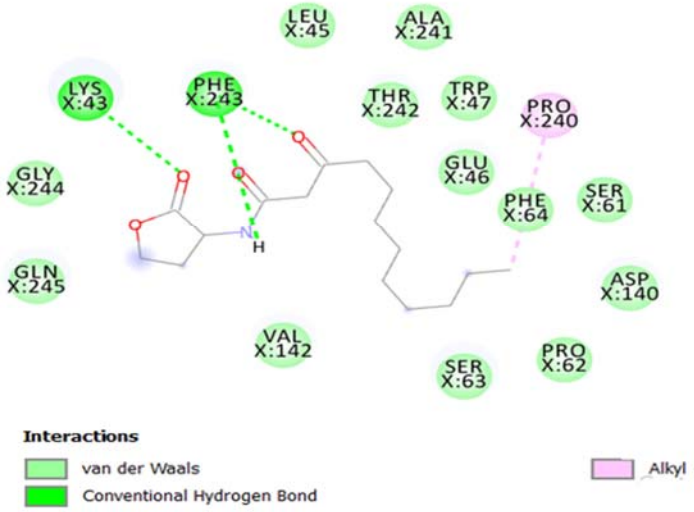
LEU X:45
ALA X:241
LYS X:43
PHE X:243
THR X:242
TRP X:47
PRO X:240
GLY X:244
GLU X:46
PHE X:64
SER X:61
GLN X:245
ASP X:140
VAL X:142
PRO X:62
SER X:63
Interactions
van der Waals
Conventional Hydrogen Bond
Alkyl

F19

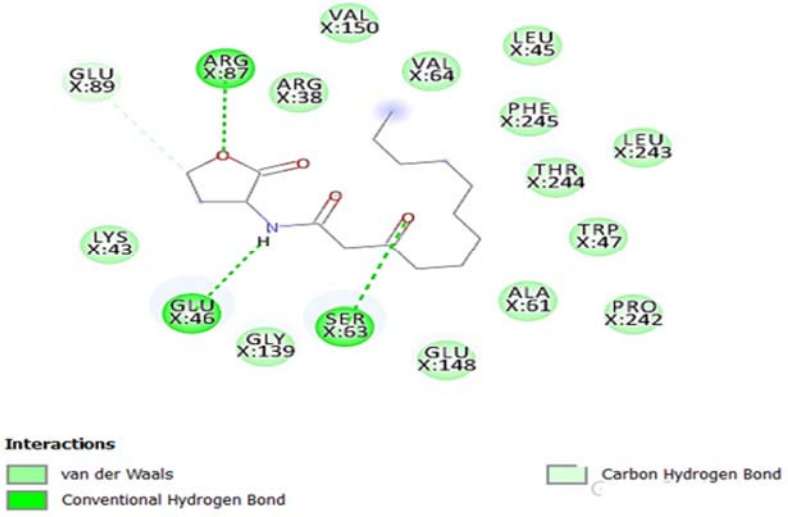
VAL X:150
LEU X:45
ARG X:87
VAL X:64
GLU X:89
ARG X:38
PHE X:245
LEU X:243
THR X:244
LYS X:43
TRP X:47
ALA X:61
GLU X:46
SER X:63
PRO X:242
GLY X:139
GLU X:148
Interactions
van der Waals
Conventional Hydrogen Bond
Carbon Hydrogen Bond

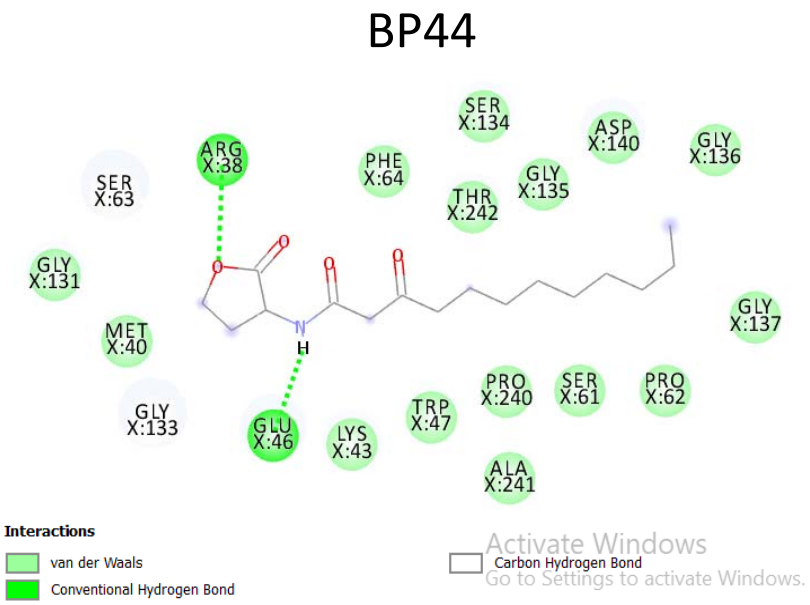

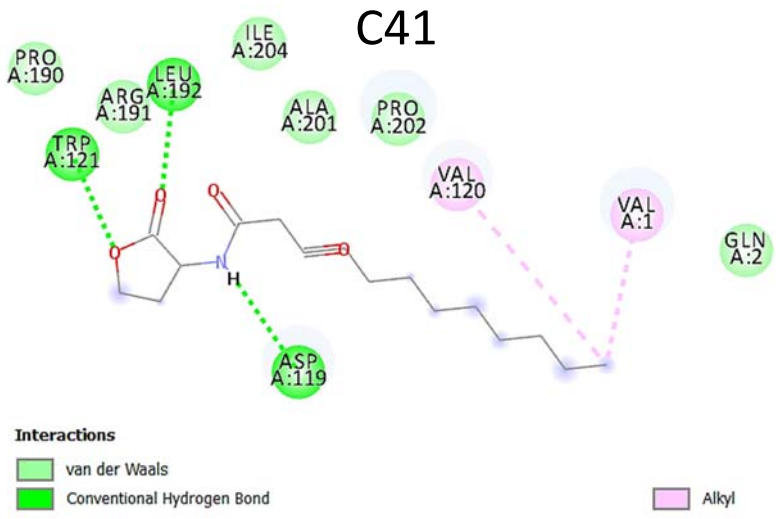

Figure 1.74 In silico study of Huscfvs to C12HSL.

Discussion

ESKAPE is an acronym of *Enterococcus faecium*, *Staphylococcus aureus*, *Klebseilla pneumoniae*, *Acinetobacter baumannii*, *Pseudomnas aeruginosa* and *Enterbacter* species which are common causative agents of life-threatening nosocomial infections among critically ill and immunocompromised individuals. These microorganisms are endowed with new paradigms in pathogenesis, transmission, and drug resistance. Currently, there is an urgent/immediate need of a broadly effective agent that can cope with these multi-drug resistant (MDR) pathogens.

Targeting bacterial virulence factors directly provides a new paradigm for intervention and treatment of bacterial diseases. *Pseudomonas aeruginosa* produces a myriad of virulence factors to cause fatal diseases in human. In this study a novel approach to combat with the MDR ESKAPE is proposed by using *P. aeruginosa* as a model for proving of concept. Engineered human single chain antibodies (human scFv) or humanized-nanobodies specific to the bacterial virulence factors including invasin (elastase, LasB), toxin (exotoxin A; ETA) and quorum sensing molecules (N-acyl-L-homoserine lactones; AHLs) were produced in vitro by using phage display technology.

Recombinant ETA domain-1A (ETA-1A), domain-3 (ETA-3), and full-length-ETA (ETA-FL), LasB were successfully produced by cloning technique. After purification and refolding, the recombinant protein of each preparation revealed only one protein band by SDS-PAGE and Coomassie Brilliant Blue G-250 (CBB) staining and Western blot analysis. LC-MS/MS verified that the purified recombinant proteins were *P. aeruginosa* proteins. The recombinant proteins were further characterized using Far-UV Circular Dichroism (CD) measurements. They were found to acquire predominantly alpha-helical structure (Fig. 2) which are characteristic of the ETA protein; the protein structures are conformed to that of the RCSB Protein database.

The effect of recombinant ETA-FL (rETA-FL) on mammalian (HeLa) cells were determined using dual acridine orange/ethidium bromide (AO/EB) fluorescent staining, flow cytometric analysis, and ultrastructural studies by means of scanning electron microscopy (SEM) and transmission electron microscopy (TEM). The results revealed that rETA-FL induced apoptosis of the HeLa cells as characterized by morphological changes and staining patterns, i.e., the early apoptotic cells showed green fluorescence with nuclear fragmentation or condensed chromatin, cellular blebbing and cytoplasmic vacuolization, while the late apoptotic cells exhibited condensed chromatin. A total of 241 colonies of HB2151 *E. coli*

transfected with ETA-bound phages were obtained from the HuscFv-phage display library by phage bio-panning using rETA-1A (binding domain; B), rETA-3 (catalytic domain; C), ETA-FL (E) and commercially synthesized biotinylated peptide of ETA catalytic site (ADAITGPEEEGGRLETILGW; P) as the antigens. These clones were categorized into 7 different types, based on the deduced amino acid sequences and numbering according to the Kabat and Chothia scheme. *huscfvs* of the *E. coli* clones C41, E44 and P32 that their HuscFvs showed high binding signal to native ETA by indirect ELISA were subcloned from pCANTAB5E phagemids into pLATE52 vectors and the recombinant plasmids were used to transform NiCo21 (DE3) *E. coli* for large-scale production of the respective HuscFvs.

The protective effect of HuscFvs on ETA-exposed cells was demonstrated through Annexin V/PI staining and flow cytometric analysis. ETA-induced early apoptosis of mammalian (HeLa) cells by 16.53 ±4.22% (quadrant 1; Annexin V+/PI-stained cells) and late apoptosis of the cells by 8.55 ± 0.46% (quadrant 2; Annexin V+/PI+-stained cells); hence, a total of 25.08 ±4. 51% of apoptotic cells (quadrant 1 + quadrant 2; average of three- independent experiments). After treatment with HuscFv-C41, HuscFV-E44, and HuscFv-P32, the average percentages of cellular apoptosis from three-independent experiments was significantly reduced. The inhibitory activities of the HuscFv-C41 were significantly higher than the HuscFv-E44 and HuscFv-P32. The ETA-exposed-HeLa cells treated with the HuscFvs had significant decreases of expressions of apoptosis-related genes including cas3 and p53 compared to the control HuscFv-treated (Irre) cells and the cells in medium alone. The three-dimensional (3D) structure of ETA (PDB 1IKQ) and modeled-HuscFvs were subjected to intermolecular docking. , the ETA bound-HuscFvs of the three *E. coli* clones presumptively formed contact interface with critical residues for ETA-mediated ADP-ribosylation. HuscFv-C41 was more effective than the HuscFv-E44 and HuscFv-P32 in inhibiting the ETA cytotoxicity. This might be because the HuscFv-C41 interact with several more residues critical for catalytic activity and ADP-ribosylation reaction than the other two cognates.

The effect of recombinant and native LasB were evaluated by EnzChek ™ elastase assay Kit. The results showed native LasB has high enzyme activity better than recombinant protein. A total of 98 colonies of HB2151 *E. coli* transfected with LasB-bound phages were obtained from the HuscFv-phage display library by phage bio-panning. The HuscFv expressing *E.coli* clones that provided ELISA signals twofold higher than the signal of the same lysates to BSA were selected. HuscFv bound recombinant LasB has high has binding signal when compared to native protein. The LasB-HuscFv-phagemids no. 42 and 49 were cloned into the pLATE52 vector and then introduced into the *E. coli* JM 109. The 3D structure of huscFv was

created and refined by I-Tasser sever and improved to close the native states using cluspro 2.0 antibody-antigen docking. LasB-HuscFv complexes were built and visualized using Pymol software. The huscFv42 was predicted had interaction with catalytic residues of LasB (PDB 1EZM) that consistent with inhibition test by EnzChek™ elastase assay Kit.

N-3-oxo-dodecanoyl-L-homoserine lactone (C12-HSL), the quorum sensing signaling molecule, produced by *P. aeruginosa* not only participate in the quorum sensing circuit that control the virulence expression but render the cytotoxicity in mammalian cells. In this study, we characterized four single-chain quorum quenching antibodies (F15, F19, C41, and E44) whether they provide the cytoprotective effect against apoptosis and cell cycle arrest induced by C12-HSL of human epithelial cells. All four HuscFvs recognize a conformational regions of bacterial ligand by in silico docking and structural alignment between HuscFvs and mAb RS2-1G9 (previous described quorum quenching antibody) (Kaufmann GF, 2008) demonstrated that the structure of selected HuscFvs intensely resembles the quorum quenching RS2-1G9 in their overall features and topology. As a results, HuscFvs exhibited the quorum quenching abilities to neutralize/mitigate the biological activities of AHL conferring bacterial pathogenesis in human host cells, as a result of the reduced in sub-G1 population, apoptotic cells, and p53 mRNA expression level, also restored of nuclear condensation and DNA fragmentation, moreover, increased in bcl-2, anti-apoptotic gene expression. These human single-chain antibodies provide a hopeful therapeutic strategy combating the *P. aerugionosa* virulence and pathogenesis via QS-based signaling also have a high potential for developing further in clinical application.

Future direction

In this study, engineered human monoclonal single chain antibody (scFv) and/or humanized-nanobodies specific to the *P. aeruginosa* virulence factors including enzyme, toxin, and quorum sensing molecules, that neutralize the respective bacterial targets was successfully produced. The so-produced antibodies should be tested further, step-by-step, towards the clinical use (e.g., GMP production, pre-clinical trial as well as different phases of clinical trials), as a safe immunotherapeutic against virulence factors of the difficult to treat *P. aeruginosa* infection. It is envisaged that the so-produced small antibodies in their right mixture should be a safe and novel remedy for combating against the drug resistant pathogen. Similar approach can be adopted for inventing therapeutics for other members of the ESKAPE and other pathogens.

Research Outputs

Publications

Related to this project

1. Santajit S, Seesuay W, Mahasongkram K, Sookrung N, Ampawon Sg, Reamtong O, Diraphat P, Chaicumpa W, **Indrawattana N**. Human single-chain antibodies that neutralize *Pseudomonas aeruginosa*-exotoxin A-mediated cellular apoptosis. Submitted to Scientific Reports (Revision). (Corresponding Author, IF=4.011) (เอกสารแนบหมายเลข 1)

2. Pumipuntu N, Tunyong N, Chantratita N, Diraphat P, Pumirat P, Sookrung N, Chaicumpa W, **Indrawattana N**. *Staphylococcus* spp. associated with subclinical bovine mastitis in central and northeast provinces of Thailand. PeerJ. 2019 Mar 14;7:e6587. doi: 10.7717/peerj.6587. eCollection 2019. (Corresponding Author, IF=2.353) (เอกสารแนบหมายเลข 2)

3. **Indrawattana N**, Pumipuntu N, Suriyakhun N, Jangsangthong A, Kulpeanprasit S, Chantratita N, Sookrung N, Chaicumpa W, Buranasinsup S. *Staphylococcus argenteus* from rabbits in Thailand. Microbiologyopen. 2019 Apr;8(4):e00665. doi: 10.1002/mbo3.665. . (First Author, IF=2.738) (เอกสารแนบหมายเลข 3)

4. Shutipen Buranasinsup, Suphang Kulpeanprasit, Thida Kong-ngoen, Arunee Jangsangthong, Nitat Sookrung, Wanpen Chaicumpa and **Nitaya Indrawattana**. Prevalence of the multi-drug resistance of shiga toxin-producing *Escherichia coli* isolated from pigs in central Thailand. Chaingmai Journal of Science 2018: 45(1); 21 – 32. (Corresponding Author, IF=0.342). (เอกสารแนบหมายเลข 4)

5. Pumipuntu N, Kulpeanprasit S, Santajit S, Tunyong W, Kong-Ngoen T, Hinthong W, **Indrawattana N**. Screening method for Staphylococcus aureus identification in subclinical bovine mastitis from dairy farms. Vet World. 2017 Jul;10(7):721-726. doi: 10.14202/vetworld.2017.721-726. (Corresponding Author, Citescore=1.29) (เอกสารแนบหมายเลข 5)

6. Pumirat P, Vanaporn M, Boonyuen U, **Indrawattana N**, Rungruengkitkun A, Chantratita N. Effects of sodium chloride on heat resistance, oxidative susceptibility, motility, biofilm and plaque formation of *Burkholderia pseudomallei*. Microbiologyopen. 2017 Aug;6(4). doi: 10.1002/mbo3.493. (IF=2.738) (เอกสารแนบหมายเลข 6)

7. Hinthong W, Pumipuntu N, Santajit S, Kulpeanprasit S, Buranasinsup S, Sookrung N, Chaicumpa W, Aiumurai P, **Indrawattana N**. Detection and drug resistance profile of

Escherichia coli from subclinical mastitis cows and water supply in dairy farms in Saraburi Province, Thailand. PeerJ. 2017 Jun 13;5:e3431. doi: 10.7717/peerj.3431. (Corresponding Author, IF=2.353). (เอกสารแนบหมายเลข 7)

8. Rukkawattanakul T, Sookrung N, Seesuay W, Onlamoon N, Diraphat P, Chaicumpa W, **Indrawattana N**. Human scFvs That Counteract Bioactivities of Staphylococcus aureus TSST-1. Toxins (Basel). 2017 Feb 17;9(2). pii: E50. doi: 10.3390/toxins9020050. (Corresponding Author, IF=3.895). (เอกสารแนบหมายเลข 8)

9. Santajit S, Indrawattana N. Mechanisms of Antimicrobial Resistance in ESKAPE Pathogens. Biomed Res Int. 2016;2016:2475067. doi: 10.1155/2016/2475067. (Corresponding Author, IF=2.583). (เอกสารแนบหมายเลข 9)

ภาคผนวก

Human single-chain antibodies that neutralize *Pseudomonas aeruginosa*-exotoxin A-mediated cellular apoptosis

Sirijan Santajit[1], Watee Seesuay[2], Kodchakorn Mahasongkram[2], Nitat Sookrung[2,3], Sumate Ampawong[4], Onrapak Reamtong[5], Pornphan Diraphat[6], Wanpen Chaicumpa[2], Nitaya Indrawattana[1]

[1]Department of Microbiology and Immunology, [4]Department of Tropical Pathology, and [5]Department of Tropical Molecular Biology and Genetics, Faculty of Tropical Medicine, Mahidol University, Bangkok, Thailand. [2]Center of Research Excellence on Therapeutic Proteins and Antibody Engineering, Department of Parasitology, Faculty of Medicine Siriraj Hospital, Mahidol University, Bangkok, Thailand. [3]Biomedical Research Incubator Unit, Department of Research, Faculty of Medicine Siriraj Hospital, Mahidol University, Bangkok, Thailand University, Bangkok, Thailand. Faculty of Tropical Medicine, Mahidol University, Bangkok, Thailand. [6]Department of Microbiology, Faculty of Public Health, Mahidol University, Bangkok, Thailand. Correspondence and requests for materials should be addressed to N.I. (email: nitaya.ind@mahidol.ac.th)

KEYWORDS: Exotoxin A (ETA)/ Human monoclonal single-chain antibody variable fragments (HuscFvs)/ *Pseudomonas aeruginosa*/ Apoptosis/ Phage display technology

Abstract

Targeting bacterial virulence factors directly provides a new paradigm for intervention and treatment of bacterial diseases. *Pseudomonas aeruginosa* produces a myriad of virulence factors to cause fatal diseases in human. In this study, human single-chain antibodies (HuscFvs) that bound to *P. aeruginosa* exotoxin A (ETA) were generated by phage display technology using recombinant ETA, ETA-subdomains and synthetic peptide of the ETA-catalytic site as baits for selecting ETA-bound-phages from the human-scFv phage display library. ETA-bound HuscFvs derived from three phage-transfected *E. coli* clones neutralized the ETA-induced mammalian cell apoptosis. Computerized simulation demonstrated that these HuscFvs used several residues in their complementarity determining regions (CDRs) to form contact interface with critical residues in ETA-catalytic domain essential for ADP-ribosylation of eukaryotic elongation factor 2 which should consequently rescue the ETA-exposed-cells from apoptosis. The HuscFv-treated ETA-exposed cells also had decrement of apoptosis-related genes, *i.e.*, *cas3* and *p53*. The effective HuscFvs have high potential for future evaluation in animal models and clinical trials as a safe novel remedy for amelioration of exotoxin A-mediated pathogenesis. The HuscFvs may be used either singly or in combination with their HuscFv cognates that target other *P. aeruginosa* virulence factors as alternative therapeutic regime for the difficult to treat infection.

Introduction

Pseudomonas exotoxin A (ETA) is one of the most potent bacterial virulence factors produced by *Pseudomonas aeruginosa*, an opportunistic Gram-negative bacterium, which belongs to the clique of difficult to treat multi-drug resistant ESKAPE pathogens. *P. aeruginosa* is the common cause of life-threatening nosocomial infections, which endows a new paradigm in pathogenesis, transmission, and drug resistance, worldwide[1]. Infections caused by this ubiquitous pathogen can occur in any part of the body, causing otitis media folliculitis (hot-tub folliculitis), otitis externa (swimmer's ear), keratitis (corneal infection), bacteremia, endocarditis, pneumonia, urosepsis, etc.[2,3,4,5,6,7,8,9]. The infections could be fatal in individuals who are already very ill, such as those in the intensive care units, particularly the ventilator-dependent subjects and patients with cystic fibrosis, cancers, diabetes, trauma, surgery, as well as neonatal infants[10,11,12]. *P aeruginosa* causes diseases by using numerous virulence elements, such as enzymes (elastase, proteases), pyocyanin, cytotoxins and biofilm[13,14,15].

ETA is an NAD^+-diphthamide ADP-ribosyl transferase (EC 2.4.2.36). This toxin catalyzes the transfer of ADP-ribose moiety from NAD^+ to the diphthamide residue (a post-translationally modified histidine residue) on eukaryotic elongation factor-2 (eEF-2) through the covalent attachment. This reaction results in termination of protein synthesis and eventually leads to cell death[16,17]. ETA is a heat-labile, 613 amino acids protein (66-kDa) which is released to the extracellular environment[18]. It is the most intoxicating virulence factor of *P. aeruginosa,* which is remarkably toxic to mammalian cell with a single toxin molecule[19]. It is extremely lethal, *i.e.*, possessing an LD_{50} of 0.2 μg per mouse upon intraperitoneal injection[20]. The toxin molecule

62 comprises three distinct domains, *i.e.*, receptor-binding domain or ETA domain-1A (residues 1-
63 252), translocation domain or ETA domain-2 (residues 253-384), and catalytic domain or ETA
64 domain-3 (residues 385-613)[21]. ETA domain-1A (ETA-1A) binds its cognate receptor called the
65 heavy chain of low-density lipoprotein receptor-related protein/alpha 2-macroglobulin on
66 eukaryotic cell; then the toxin-receptor complex internalizes *via* clathrin-dependent
67 endocytosis. In the early endosome, the toxin is exposed to acidic environment and
68 consequently cleaved between R279 and G280 within the domain-2 by the host furin
69 protease[22,23]. The cleaved-off-C-terminal (37-kDa) portion exits into cytoplasm and transported
70 *via* the Golgi apparatus to the endoplasmic reticulum (ER). C-terminal KDEL of the
71 enzymatically active 37-kDa fragment binds to the protein retention receptor-1 (KDELR1) on
72 ER membrane, and subsequently translocated back to cytosol where it inhibits protein synthesis
73 by catalyzing the transfer of the ADP-ribosyl moiety of the oxidized NAD onto eEF-2[24,25,26].
74 The catalytic 37-kDa fragment and also the full-length-ETA (ETA-FL) have been shown to
75 induce cellular apoptosis by causing depolarization of the mitochondrial membrane resulting in
76 cytochrome c release; activation of caspases- 9 and 3; and inactivation of DNA repair enzyme
77 [poly(ADP-ribose) polymerase (PARP)] in several physiological events including chromatin de-
78 condensation, DNA replication and repair, gene expression (*e.g.*, *p53*, *cas3*, *cdc2*, *cyclin-B*, and
79 *bcl-2*) and cellular differentiation[27,28,29,30,31].

80 Besides targeting the bacteria by using the traditional anti-bacterial drugs, an alternative
81 therapeutic strategy is to target bacterial virulence factors pivotal for pathogenesis in host. The
82 later approach provides many benefits such as maintaining the host endogenous microbiome
83 and creating less selective pressure to the bacteria *per se* which potentially bring about

84 diminution of drug resistance[33]. At present, there has been no novel antimicrobials in advanced
85 development that are active against bacteria already resistant to most or all currently available
86 anti-bacterial drugs. Thus, there is an urgent need of a broadly effective agent that can cope with
87 the multi-drug resistant (MDR) pathogens. In this study, engineered fully human single-chain
88 antibody variable fragments (HuscFvs) specific to *P. aeruginosa* ETA were produced *in vitro* by
89 using phage display technology. The HuscFvs effectively neutralized the ETA-mediated
90 mammalian cell apoptosis. It is envisaged that the antibody fragments may be used either singly
91 or in combination with other anti-bacterial agent as a novel remedy/protocol for fighting against
92 the drug-resistant pathogen. The strategy reported herein may be applied for inventing
93 prototypic therapeutics for other members of the ESKAPE and other pathogens.
94
95 ## Results and discussions
96 **Recombinant ETA domain-1A (ETA-1A), domain-3 (ETA-3), and full-length-ETA (ETA-**
97 **FL).** Amplicons of the *ETA-1A* and *ETA-3* are shown in Fig. 1A; and *ETA-FL* amplicon is in Fig.
98 1D. The *E. coli* clones carrying recombinant plasmids with the *ETA-1A*, *ETA-3* and *ETA-FL*
99 inserts were grown under 1 mM IPTG induction; the recombinant proteins were successfully
100 expressed. After purification and refolding, the recombinant protein of each preparation
101 revealed only one protein band by SDS-PAGE and Coomassie Brilliant Blue G-250 (CBB)
102 staining and Western blot analysis, with molecular weights of approximately 28, 26, and 66.7
103 kDa, respectively (Fig. 1B, 1C, 1E and 1F). LC-MS/MS verified that the purified recombinant
104 proteins were *P. aeruginosa* proteins (Supplementary Table 1). The recombinant proteins were
105 further characterized using Far-UV Circular Dichroism (CD) measurements. They were found

106 to acquire predominantly alpha-helical structure (Fig. 2) which are characteristic of the ETA
107 protein; the protein structures are conformed to that of the RCSB Protein database, 3B82[34,35].

108 **Biological activities of recombinant ETA-FL**. The effect of recombinant ETA-FL (rETA-FL)
109 on mammalian (HeLa) cells were determined using dual acridine orange/ethidium bromide
110 (AO/EB) fluorescent staining, flow cytometric analysis, and ultrastructural studies by means of
111 scanning electron microscopy (SEM) and transmission electron microscopy (TEM). The results
112 revealed that rETA-FL induced apoptosis of the HeLa cells as characterized by morphological
113 changes and staining patterns, *i.e.*, the early apoptotic cells showed green fluorescence with
114 nuclear fragmentation or condensed chromatin, cellular blebbing and cytoplasmic
115 vacuolization, while the late apoptotic cells exhibited orange-red fluorescence with condensed
116 chromatin (Fig. 3). Results of the ultrastructural studies of the ETA-treated cells by SEM and
117 TEM are shown in Fig. 4 and Fig. 5, respectively. Percentages of apoptotic cells after treated
118 with various amounts of ETA as determined by the Annexin V/PI staining and flow cytometric
119 analysis are shown in Fig. 6A. Percent dead cells increased in ETA-dose-dependent manner, *i.e.*,
120 43.4, 66.1, 78.9, and 82.8% for 200, 500, 1000 and 2,000 ng ETA/ml, respectively. The
121 background apoptotic HeLa cells in medium alone was 7.1%. LD_{50} of the rETA-FL on the HeLa
122 cells was 218.405 ng/ml (3.27 nM) based on Annexin V/PI and flow cytometric analysis (Fig.
123 6B).

124 **Production of ETA bound-HuscFvs**. A total of 241 colonies of HB2151 *E. coli* transfected
125 with ETA-bound phages were obtained from the HuscFv-phage display library by phage bio-
126 panning using rETA-1A (binding domain; B), rETA-3 (catalytic domain; C), ETA-FL (E) and

commercially synthesized biotinylated peptide of ETA catalytic site (ADAITGPEEEGGRLETILGW; P) as the antigens. They were 61, 96, 51, and 33 clones from panning with B, C, E and P, respectively. From the 241 clones, 155 clones were positive for genes coding for HuscFvs (*huscfvs*), *i.e.*, PCR amplicons at ~1000 bp, which representatives are shown in Fig. 7A. Lysates of 37 of 155 clones produced soluble HuscFvs that bound to native ETA (Sigma, St. Louis, Mo., USA) using BSA as control antigen; representative binders to native ETA are shown in Fig. 7B. After nucleotide sequencing, 16 clones (B33, B46, C41, C46, C48, C61, C83, E14, E34, E38, E40, E42, E44, P20, P21 and P32) showed complete sequences of single-chain antibodies, *i.e.*, the *huscfv* contains contiguous sequences coding for immunoglobulin (Ig)-VH, peptide linker $(Gly_4Ser1)_3$, and Ig-VL. These clones were categorized into 7 different types, based on the deduced amino acid sequences and numbering according to the Kabat and Chothia scheme[36]. They were type-1 (IGHV3 family and IGKV4 subgroup: P20 and E40), type-2 (IGHV1 family and IGKV1 subgroup: P21), type-3 (IGHV4 family and IGKV3 subgroup: E44), type-4 (IGHV3 family and IGKV3 subgroup: B33, B46, C46, C48, C61, and C83), type-5 (IGHV3 family and IGKV3 subgroup: C41 and E42), type-6 (IGHV1 family and IGKV3 subgroup: E34), and type-7 (IGHV3 family and IGKV2 subgroup: E14, E38, and P32). Subsequently, *huscfvs* of the *E. coli* clones C41, E44 and P32 that their HuscFvs showed high binding signal to native ETA by indirect ELISA (Fig. 7B; asterisks) were subcloned from pCANTAB5E phagemids into pLATE52 vectors and the recombinant plasmids were used to transform NiCo21 (DE3) *E. coli* for large-scale production of the respective HuscFvs. Inclusion bodies (IB) containing N-terminal 6× His-tagged-HuscFvs were purified from homogenates of individual *E. coli* clones grown under IPTG induction, and refolded. SDS-PAGE and Western

149 blot patterns of purified HuscFvs of clones C41, E44 and P32 are shown in Fig. 7C and 7D,
150 respectively.

151 **HuscFvs protected mammalian cells from ETA-mediated cellular apoptosis.** Fig. 8A shows
152 results of one of the three independent-experiments to demonstrate the protective effect of
153 HuscFvs on ETA-exposed cells. Annexin V/PI staining and flow cytometric analysis
154 demonstrated that ETA-induced early apoptosis of mammalian (HeLa) cells by 16.53 ±4.22%
155 (quadrant 1; Annexin V+/PI-stained cells) and late apoptosis of the cells by 8.55 ± 0.46% (quadrant
156 2; Annexin V+/PI+-stained cells); hence, a total of 25.08 ±4.51% of apoptotic cells (quadrant 1 +
157 quadrant 2; average of three-independent experiments) (Table 2). After treatment with HuscFv-
158 C41, HuscFV-E44, and HuscFv-P32, the average percentages of cellular apoptosis from three-
159 independent experiments was significantly reduced to 9.85 ± 1.09, 11.09 ± 0.98 and 15.78 ±
160 1.13, respectively (Table 2). Bar graphs for statistical comparisons of the averaged percentages
161 of cellular apoptosis among different treatment groups of the three-independent experiments
162 are shown in Fig. 8B. The inhibitory activities of the HuscFv-C41 were significantly higher than
163 the HuscFv-E44 and HuscFv-P32. Control HuscFv (Irre) showed averaged percent apoptotic
164 cells at 23.8 ± 0.52%, which was not different from the ETA-exposed cells in medium alone.
165 Normal HeLa cells had 6.97 ± 0.02% background apoptosis (average of three experiments also).
166 The ultrastructural studies by SEM confirmed that the HuscFvs could neutralize the ETA-
167 induced cellular apoptosis (Fig. 8C).

168 The ETA-exposed-HeLa cells treated with the HuscFvs had significant decreases of
169 expressions of apoptosis-related genes including *cas3* and *p53* compared to the control HuscFv-
170 treated (Irre) cells and the cells in medium alone (Fig. 9A and 9B).

171 **Computerized simulation for determining presumptive residues and domains of ETA**
172 **that formed contact interface with the HuscFvs.** In order to have some insight into the
173 mechanisms of the HuscFvs in rescuing the cells from ETA-mediated cytotoxicity,
174 computerized simulation was performed to predict the presumptive residues of the toxin that
175 were interacted by the effective HuscFvs.

176 The three-dimensional (3D) structure of ETA (PDB 1IKQ) and modeled-HuscFvs were
177 subjected to intermolecular docking. Fig. 10 and Table 1 show predicted ETA residues and
178 domains that formed contact interface with HuscFvs of *E. coli* clones C41, E44 and P32. By the
179 *in silico* docking, HuscFv-C41 uses VH-CDR1-3, VL-CDR2 as well as VL-FR2 and VL-FR3 to
180 form contact with critical residues on the ETA-catalytic domain including Y481, Q485, R490,
181 G491, E546, E547, E548, G549, R551, E553, N577, V578, G579, G580, and D581 of which
182 Y481, E546, E547 and E553 are NAD^+ binding site. The E553 is the ETA residue pivotal for
183 the toxin enzymatic activity in transferring ADP-ribose to the eEF-2[37,38,39]. Y481 is the NAD^+-
184 binding site of hydrophobic cavity of the toxin catalytic domain; the ETA uses the phenol ring
185 of Y481 to tether the nicotinamide ring of NAD^+ substrate, *i.e.*, ADP-ribosyl group of NAD^+, in
186 order to transfer the substrate to eEF-2[40]. The D461, Q485, E546, E547 and E553 formed the
187 edge of the ETA-NAD^+ binding cavity and participated in hydrogen bonding with two ribose
188 moieties of the NAD^+ molecule[41]. Moreover, previous study indicated that the ETA epitopes
189 recognized by murine monoclonal antibody clone B7 (MAbB7) which displayed strong

neutralizing capacity on ETA cytotoxicity were mapped to the C-terminal residues 575-595 of the toxin[42]. Although the results of ETA-HuscFv interaction by computerize simulation needs experimental validation, it is pluasible that the effectiveness of HuscFv-C41 in neutralizing the apoptotic activity of ETA is through interfering with the catalytic activity and inhibition of ADP-ribose transfer from NAD^+ to eEF2.

The HuscFv-E44 was predicted to use VL-CDR2 and VL-FR3 to interact with Q310, R313 and A317 of ETA-2 (translocation domain); this binding should not involve in the HuscFv-mediated-neutralization of the ETA cytotoxicity. The HuscFv-E44 also used VH-CDR2, VH-CDR3, VH-FR1, VL-CDR1, VL-CDR2 and VL-FR2 to bind to D461 and E547 which are NAD^+ binding site, and Q485, E486, E548, G549, D581, D583, and P584 of ETA-3 of the catalytic domain. The HuscFv-P32 interacted with residues of the ETA-catalytic domain including S515, A519, P545, E547 (NAD^+ binding site), E548, G550 and D581 by using VH-CDR1-3 and VL-CDR1. Based on the computerized results of the protein-antibody docking, the ETA bound-HuscFvs of the three *E. coli* clones presumptively formed contact interface with critical residues for ETA-mediated ADP-ribosylation. HuscFv-C41 was more effective than the HuscFv-E44 and HuscFv-P32 in inhibiting the ETA cytotoxicity. This might be because the HuscFv-C41 interact with several more residues critical for catalytic activity and ADP-ribosylation reaction than the other two cognates.

Taken all together, this study successfully generated human single-chain antibodies that effectively neutralize the ETA activity. The so-produced antibodies should be tested further, step-by-step, towards the clinical use (*e.g.*, GMP production, pre-clinical trial as well as different

phases of clinical trials), as a safe immunotherapeutic against ETA of the difficult to treat *P. aeruginosa* infection.

Materials and methods

Cell culture. In this study, HeLa cells (human cervical epithelial cancer cells) were grown in Dulbecco's Modified Eagle's Medium (DMEM) supplemented with 10% fetal bovine serum (FBS) and 1% penicillin/streptomycin at 37 °C in a humidified 5% CO_2 atmosphere.

Production of recombinant ETA domain-1A (rETA-1A), domain-3 (rETA-3), and full-length-ETA (rETA-FL). In this study, the synthesized DNA of *P. aeruginosa* ETA (GenScript, New Jercey, USA) was used as the template to amplify the ETA genes including *ETA-1A*, *ETA-3* and *ETA-FL* by PCR using Phusion High-Fidelity DNA polymerase (Thermo Fisher Scientific). Specific primers for the respective gene amplification were designed according to the deduced amino acids of *P. aeruginosa* full-length ETA gene sequence (Gene Bank accession no. NC_002516.2) (Supplementary Table 2). The PCR amplicons were inserted appropriately into the pLATE52 expression vector, and the recombinant vectors were introduced into expression host, *i.e.*, NiCo21 (DE3) *E. coli* (New England Biolabs, UK). The appropriately transformed bacterial colonies were grown in LB broth contained 100 µg/ml ampicillin until an OD_{600nm} was 0.5; then expressions of the recombinant proteins were induced by adding 1 mM isopropyl-β-D-1-thiogalactopyranoside (IPTG) to individual cultures at 37 °C for 4 h. Thereafter, the bacterial cells were harvested by centrifugation and lysed by using the BugBuster® Protein Extraction Reagent (Novagen, Merck KGaA, Darmstadt, Germany) supplemented with 10 microliters of Lysonase™ Bioprocessing Reagent (Novagen) per gram of bacterial cell pellet.

232 The bacterial inclusion bodies (IBs) containing the recombinant proteins in the pellets were
233 collected after centrifugation of the *E. coli* homogenates. The IBs were washed sequentially with
234 Wash-100 buffer [50 mM sodium phosphate buffer, pH 8.0; 500 mM NaCl; 5 mM EDTA; 8%
235 w/v glycerol and 1% v/v Triton X-100], Wash-114 buffer [50 mM Tris buffer, pH 8.0; 300 mM
236 NaCl and 1% v/v Triton X-114], Wash-Solvent buffer [50 mM Tris buffer, pH 8.0 and 60% v/v
237 isopropanol], and finally with Milli-Q® water (Merck Millipore). The pellets collected after
238 centrifugation were added with small volumes of ultrapure-water and stored at 4 °C. Quality of
239 the preparations was analyzed by a 12% SDS-PAGE and Western blotting and the quantities
240 were determined by Pierce™ BCA Protein Assay Kit (Thermo Fisher Scientific, Rockford, IL,
241 USA). LC-MS/MS was used to verified the recombinant proteins. Afterwards, the purified IBs
242 containing rETA-1A, rETA-3, and rETA-FL were separately solubilized at 0.5 mg/ml in 5 ml of
243 50 mM CAPS, pH 11.0; 0.3% w/v N-lauryl sarcosine and 1 mM DTT and kept at 4 °C until they
244 were completely dissolved. The proteins were refolded by dialysis at 4 °C with slow stirring
245 against 750 ml of 20 mM Tris-HCl, pH 8.5 supplemented with 0.1 mM DTT for 3 h then the
246 dialysis buffer was changed to 20 mM Tris-HCl, pH 8.5 containing 0.1 mM DTT at 4 °C
247 overnight. The refolded ETA-1A and ETA-3 were finally dialyzed against 20 mM Tris-HCl, pH
248 8.5, while the ETA-FL preparation was dialyzed against 20 mM imidazole, pH 8.5. All
249 preparations were then filtered through 0.2 µm low protein binding Acrodisc® syringe filter
250 (Pall, Port Washington, NY, USA). Protein contents were determined using a BCA assay before
251 keeping in 8% (w/v) glycerol at -80 °C until use.
252 Folding of the refolded-rETA-1A, rETA-3 and rETA-FL were determined by using Far-UV
253 Circular Dichroism (CD) measurements. Briefly, 400 µl of the proteins (0.25 mg/ml) were

254 subjected for CD measurements on a JASCO J-815 spectropolarimeter equipped with Peltier
255 temperature controller system (Jasco Co., Ltd., Tokyo, Japan). The refolded protein spectra were
256 recorded in a 0.1 cm path-length quartz cuvette in 20 mM Tris-HCl, pH 8.5. The proteins were
257 scanned from 190 and 260 nm at a speed of 50 nm/min at 25 °C. The average of three scans was
258 used to generated the CD spectra of each protein.
259
260 **Biological activities of rETA-FL.** Morphological characteristics of HeLa cells treated with ~
261 LD50 of rETA-FL were evaluated by electron microscopy (EM) and dual AO/EB staining. For
262 AO/EB staining, cells were trypsinized, washed three times with PBS, pH 7.4 and the pellets
263 were resuspended in 50 µl of culture medium. The cells were stained in an ice-cold container
264 with 100 µg/ml of AO and 100 µg/ml of EB [cells to dye ratio of 2:1 (v/v)]. The stained cell
265 suspensions were dropped on glass slides, covered with coverslips, and observed under a
266 fluorescence microscope.
267 SEM and TEM were used for studying ultrastructure of the cells after exposure to ETA and
268 the ETA-exposed cells treated with HuscFvs. For SEM, HeLa cells grown on coverslips for 24
269 h were fixed with 2.5% glutaraldehyde at room temperature for 1 h, washed with sucrose
270 phosphate buffer (SPB) three times, followed by fixing with 1% osmium tetroxide in 0.1 M SPB
271 for 1 h and washed again. They were then dehydrated in ethanol gradients, and allowed air-dried
272 overnight. The coverslips were mounted on an aluminum stub and coated with a gold film (20
273 nm-thickness) using the sputter coater (EMITECH K550, UK). They were examined under a
274 scanning electron microscope (JEOL JSM-6610LV, Japan) with 15 kV acceleration voltages.
275 For TEM, the ethanol-dehydrated cells were infiltrated with LR white embedded medium

276 (EMS, USA.) in 70% ethanol, then embedded in a capsule beam and kept in a 65 °C incubator
277 for 48 h. Ultra-thin sections (90-100 nm thickness) of the preparations were placed on a 200
278 square-mesh copper grids and stained with uranyl acetate and lead citrate. The fine cell
279 morphology were examined under a transmission electron microscope (Hitachi; model
280 HT7700, Japan).
281
282 **Flow cytometry analysis.** Apoptotic cells were revealed by doubly staining with Annexin V/PI
283 using FITC-Annexin V Apoptosis Detection Kit (BD Biosciences) according the manufacturer's
284 instructions. HeLa cells (1×10^5 cells in 500 µl completed culture medium) were incubated with
285 different concentrations of rETA-FL (200-2000 ng/ml) for 24 h. Cells in medium alone were
286 included in the experiments. After incubation, the cells were trypsinized, harvested and washed
287 with ice-cold PBS, pH 7.4. One hundred microliters of the cell suspension (~1 x 10^5 cells) were
288 transferred to a 5-ml culture tube. The cells were stained by adding 5 µl each of FITC-Annexin
289 V and PI working solutions and incubated at 25 °C for 15 min in the dark. The preparation was
290 diluted with 500 µl of 1× binding buffer and the stained cells were immediately analyzed by
291 flow cytometry. The EC_{50} graphs of HeLa cells treated with various concentrations of the rETA-
292 FL was generated using EC_{50} calculator.
293
294 **Production of ETA-bound HuscFvs.** The refolded rETA-1A, rETA-3, rETA-FL and
295 commercially synthesized (GenScript, New Jercey, USA) biotinylated peptide containing ETA
296 catalytic residues (biotin-6-aminohexanoic acid-ADAITGPEEEGGRLETILGW) were used as
297 the panning antigens. The refolded rETA-1A, rETA-3 and rETA-FL (0.5 µg in 100 µl of coating

298 buffer) were used to coat separate wells of EIA/RIA 8-well strips and kept at 4 °C overnight.
299 For biotinylated-ETA peptide, 2.5 μM of the peptide in 100 μl PBS were added to well of a
300 streptavidin plate (Pierce™ Streptavidin Coated Plates, Clear Well Strips, Rockford, IL, USA)
301 and kept at room temperature for 1 h. After blocking with Pierce™ Protein-Free (PBS) Blocking
302 Buffer (Thermo Fisher Scientific, Rockford, IL, USA) and washed with PBS containing 0.01%
303 Tween-20 (PBST), the previously constructed HuscFv-phage display library[43] were added to
304 individual antigen coated wells. Binding of HuscFv-display phages to the immobilized antigens
305 were allowed at room temperature for 1 h on a rocking platform. Antigen-unbound phages were
306 removed by washing thoroughly with PBST. Aliquots of log phase-grown HB2151 *E. coli*
307 culture was added to each phage-containing well. In case of biotinylated-ETA peptide bound
308 phages, 50 μM of peptide were added for competitive elution of the phages before adding with
309 the bacteria. The phage-transformed *E. coli* were plated onto the 2× YT agar containing 2%
310 glucose and 100 μg/ml ampicillin. After overnight incubation, the bacterial colonies grown on
311 the selective agar were screened for the clones carrying pCANTAB5E-*huscfv* phagemids by
312 colony PCR using R1 (forward primer): 5'-CCA TGA TTA CGC CAA GCT TTG GAG CC-3'
313 and R2 (reverse primer): 5'-GCT AGA TTT CAA AAC AGC AGA AAG G-3'. The *E. coli* clones
314 with *huscfv* amplicons (~1000 bp) were grown in 2 ml of auto-induction medium containing
315 100 μg/ml ampicillin at 30 °C with shaking at 250 rpm overnight. The presence of HuscFvs in
316 the E. coli homogenates were checked by Western blotting using anti-E tag antibody as the
317 HuscFv tracer. *E. coli* homogenates containing soluble HuscFvs were tested for binding to
318 native ETA (Sigma, St. Louis, Mo., USA) (test antigen) by indirect ELISA using BSA as control
319 antigen. *E. coli* clones that the HuscFvs in their homogenates gave ELISA signal at OD_{405nm}

above mean + 3 SD of the background binding control (lysate of original *E. coli* HB2151) and more than two times higher than to the control antigen were selected. Nucleotides of the *huscfvs* coding for the ETA-bound-HuscFvs were sequenced, deduced, and the complementarity determining regions (CDRs) and their respective canonical immunoglobulin framework regions (FRs) were determined using an online server, the VBASE2- the integrative germ-line V gene database (http://www.vbase2.org/).

To produce ETA-bound HuscFvs in large scale, the *huscfvs* of the selected HB2151 *E. coli* were subcloned from the pCANTABE5E phagemids to pLATE52™ expression vector by using ligation independent cloning (LIC) system (Thermo Fisher Scientific) and the recombinant plasmids were introduced into JM109 *E. coli*. The recombinant pLATE52-*huscfv* plasmids were individually used to further transform into NiCo21 (DE3) *E. coli*. The selected transformed bacterial colonies were grown under 1 mM IPTG induction in LB medium containing 100 µg/ml ampicillin and each bacterial pellet was suspended in BugBuster®Protein Extraction buffer (5 ml/g of bacterial wet weight) (Novagen) supplemented with 20 µl of Lysonase™ Bioprocessing Reagent (Novagen) and kept at 25 °C with agitation. Each preparation was added with Lysonase™ Bioprocessing reagent (10 µl/g of bacteria) and agitated further for 20 min. The inclusion bodies (IBs) were harvested by centrifugation at 8,000 × *g* at 4 °C for 30 min, washed twice with Wash-100 solution, twice with Wash-114 buffer and once with Wash-Solvent. The preparations were shaken vigorously during the washings followed by centrifugation as above. The preparations were added with 20 ml of Milli-Q® water (Merck Millipore), placed on a shaker at 25 °C for 20 min, and centrifuged at 8,000 × *g* for 20 min. The IBs were solubilized in buffer [50 mM CAPS, pH 11.0; 0.3% (w/v) N-lauryl sarcosine; 1 mM DTT] and kept at 4 °C

342 for 16 h or until completely dissolved. Each preparation was dialyzed in the Slide-A-Lyzer® 2K
343 Dialysis Cassettes G2 (Thermo Fisher Scientific, Rockford, IL, USA) at 4 °C with slow stirring
344 against refolding buffer [20 mM imidazole, pH 8.5, supplemented with 0.1 mM DTT], filtered
345 through 0.02 μm low protein binding Acrodisc® syringe filter (Pall, Port Washington, NY,
346 USA), and kept in water-bath at 30 °C for 3 h before adding with 60 mM trehalose. Protein
347 quantity and quality were determined using a Pierce BCA™ Protein Assay (Thermo Fisher
348 Scientific) and SDS-PAGE and protein staining, respectively. All preparations were stored at -
349 80 °C until use. The refolded-HuscFvs were retested for binding to native ETA by indirect
350 ELISA.

351 **Computerized simulation for determining presumptive residues and domains of ETA**
352 **bound by the HuscFvs.** Homology modeling and intermolecular docking were used for
353 predicting the presumptive residues of the ETA that were bound by the HuscFvs. The three-
354 dimensional (3D) structure of wild type *P. aeruginosa* ETA was retrieved from RCSB PDB
355 1IKQ. The 3D structures of the ETA-bound-HuscFvs were modeled by the I-TASSER
356 server[44,45]. The physical quality of each I-TASSER predicted 3D model was further refined by
357 high-resolution protein structure refinement, *i.e.*, ModRefiner[46]. Subsequently their low free-
358 energy conformations which were closer to their native structures were improved by removing
359 the steric clashes and improved the torsion angles and the hydrogen-binding networks by
360 molecular dynamics (MD) based algorithm, full-atomic simulations using Fragment Guide
361 Molecular Dynamics Simulation (FG-MD)[47]. The ETA-HuscFv complexes were built on the
362 automated ClusPro 2.0 antibody-protein docking server[48]. All models were analyzed and

363 visualized by using program Discovery studio 3.5 and PyMol software (PyMol Molecular
364 Graphics System, Version 2 edu, Schrodinger, LLC).
365
366 **Determination of HuscFv capability in rescuing cells from ETA-mediated apoptosis.** For
367 staining and flow cytometric analysis, ETA-exposed HeLa cells were stained by annexin V/PI
368 and analyzed by flow cytometry as described above. Ultrastructural studies of the cells of all
369 treatments were investigated by SEM.
370
371 **Detection of expression of apoptosis-related genes (*cas3* and *p53*) by quantitative reverse**
372 **transcription-polymerase chain reaction (qRT-PCR).** Total RNA were extracted from ETA-
373 exposed-HeLa cells that had been treated with HuscFvs and controls for 12 h, by using a
374 GeneJET RNA Purification Kit (Thermo Fisher Scientific). The quality of RNAs were
375 determined at OD_{260nm} and OD_{280nm} using NanoDrop™ 2000/2000c Spectrophotometers. After
376 DNase treatment using RNase-free-DNase I (Thermo Fisher Scientific), the RNAs were used to
377 generate cDNA using RevertAid First Strand cDNA Synthesis Kit (Thermo Fisher Scientific).
378 Real-time RT-PCR was performed on KAPA SYBR® FAST qPCR (Kapa Biosystems, Cape
379 Town, South Africa). Each reaction mixture (20 µl) contained 10 µl of 2× KAPA SYBR® FAST
380 qPCR Master Mix Universal, 200 nM final concentration each of forward and reverse primers,
381 and 20 ng of cDNA template in nuclease-free PCR-grade water. The reaction was performed in
382 a CFX96 Touch™ Real-Time PCR Detection System (Bio-Rad Laboratories). The following
383 thermal cycles was used: initial denaturation at 95 °C for 3 min and 40 cycles at 95 °C for 30

s, 53 °C for 30 s, and 72 °C for 30 s. A dissociation curve was generated from a thermal profile consisting of 95 °C for 1 min, 55 °C for 30 s, and 95 °C (0.5 °C/s). Each sample was amplified in triplicate. Gene expressions relative to the normal cells were analyzed using the ΔC_T method. Amounts of *casp3* and *p53* were normalized to the internal control, *i.e.*, GAPDH. Primer used in this experiments are shown in Supplementary Table 2.

Statistical analysis. GraphPad Prism version 5 (La Jolla, CA, USA) was used to compare the results of all tests. Statistically significance differences were determined using one-way ANOVA and Bonferroni test. *P*-value < 0.05 was statistically significant.

References

1. Rice, L. B. Federal funding for the study of antimicrobial resistance in nosocomial pathogens: no ESKAPE. *J. Infect. Dis.* **197**, 1079□1081 (2008).
2. Richards, M. J., Edwards, J. R., Culver, D. H. & Gaynes, R. P. Nosocomial infections in medical intensive care units in the United States. *Crit. Care Med.* **27**, 887□892 (1999).
3. Weinstein, R. A., Gaynes, R., Edwards, J. R. & National Nosocomial Infections Surveillance System. Overview of nosocomial infections caused by gram-negative bacilli. *Clin. Infect. Dis.* **41**, 848□854 (2005).
4. Paterson, D. L. The epidemiological profile of infections with multidrug-resistant *Pseudomonas aeruginosa* and *Acinetobacter* species. *Clin. Infect. Dis.* **43**, S43□S48 (2006).

405 5. Parker, C. M. *et al.* Ventilator-associated pneumonia caused by multidrug-resistant
406 organisms or *Pseudomonas aeruginosa*: prevalence, incidence, risk factors, and
407 outcomes. *J. Cri. Care* **23**, 18□26 (2008).
408 6. Kalra, O. P. & Raizada, A. Approach to a patient with urosepsis. *J. Glob. Infect. Dis.* **1**, 57
409 (2009).
410 7. Zhanel, G. G. *et al.* Prevalence of antimicrobial-resistant pathogens in Canadian
411 hospitals: results of the Canadian Ward Surveillance Study (CANWARD 2008).
412 *Antimicrob. Agents Chemother.* **54**, 4684□4693 (2010).
413 8. Wahab, A. A., & Rahman, M. M. *Pseudomonas aeruginosa* bacteremia secondary to
414 acute right leg cellulitis: case of community-acquired infection. *EXCLI J.* **12**, 997 (2013).
415 9. Shaukat, A. *et al. Pseudomonas aeruginosa* bacteremia in ICU: clinical presentation and
416 outcome, emergence of MDR strains. *J. Infect. Dis. Med. Microbiol.* **2**, (2018).
417 10. Cao, B., Wang, H., Sun, H., Zhu, Y. & Chen, M. Risk factors and clinical outcomes of
418 nosocomial multi-drug resistant *Pseudomonas aeruginosa* infections. *J. Hosp. Infect.* **57**,
419 112□118 (2004).
420 11. Aloush, V., Navon-Venezia, S., Seigman-Igra, Y., Cabili, S. & Carmeli, Y. Multidrug-
421 resistant *Pseudomonas aeruginosa*: risk factors and clinical impact. *Antimicrob. Agents*
422 *Chemother.* **50**, 43□48 (2006).
423 12. Kim, Y. J. *et al.* Risk factors for mortality in patients with *Pseudomonas aeruginosa*
424 bacteremia; retrospective study of impact of combination antimicrobial therapy. *BMC*
425 *Infect. Dis.* **14**, 161 (2014).

426 13. van Delden, C. Virulence factors in *Pseudomonas aeruginosa*. In: Virulence and Gene
427 Regulation. Springer, Boston, MA. 3□45 (2004).
428 14. Strateva, T. & Mitov, I. Contribution of an arsenal of virulence factors to pathogenesis
429 of *Pseudomonas aeruginosa* infections. *Ann. Microbiol.* **61**, 717□732 (2011).
430 15. Gellatly, S. L., & Hancock, R. E. *Pseudomonas aeruginosa*: new insights into
431 pathogenesis and host defenses. *Pathog. Dis.* **67**, 159□173 (2013).
432 16. Althaus, F. R. & Richter, C. Poly (ADP-ribose) biosynthesis. Springer, Berlin, Heidelberg.
433 12□37 (1987).
434 17. Durand, É., Bernadac, A., Ball, G., Lazdunski, A., Sturgis, J. N. & Filloux, A. Type II
435 protein secretion in *Pseudomonas aeruginosa*: the pseudopilus is a multifibrillar and
436 adhesive structure. *J. Bacteriol.* **185**, 2749□2758 (2003).
437 18. Lory, S., Tai, P. C. & Davis, B. D. Mechanism of protein excretion by gram-negative
438 bacteria: *Pseudomonas aeruginosa* exotoxin A. *J. Bacteriol.* **156**, 695□702 (1983).
439 19. Weldon, J. E. & Pastan, I. A guide to taming a toxin-recombinant immunotoxins
440 constructed from *Pseudomonas* exotoxin A for the treatment of cancer. *FEBS J.* **278**,
441 4683□4700 (2011).
442 20. Wick, M. J., Frank, D. W., Storey, D. G. & Iglewski, B. H. Structure, function, and
443 regulation of *Pseudomonas aeruginosa* exotoxin A. *Annu. Rev. Microbiol.* **44**, 335□363
444 (1990).
445 21. Allured, V. S., Collier, R. J., Carroll, S. F. & McKay, D. B. Structure of exotoxin A of
446 *Pseudomonas aeruginosa* at 3.0-Angstrom resolution. *Proc. Natl. Acad. Sci. USA.* **83**,
447 1320□1324 (1986).

448 22. Kounnas, M. Z., Morris, R. E., Thompson, M. R., FitzGerald, D. J., Strickland, D. K. &
449 Saelinger, C. B. The alpha 2-macroglobulin receptor/low density lipoprotein receptor-
450 related protein binds and internalizes *Pseudomonas* exotoxin A. *J. Biol. Chem.* **267**,
451 12420□12423 (1992).
452 23. Chiron, M. F., Fryling, C. M. & FitzGerald, D. J. Cleavage of *Pseudomonas* exotoxin and
453 diphtheria toxin by a furin-like enzyme prepared from beef liver. *J. Biol. Chem.* **269**,
454 18167□18176 (1994).
455 24. Yates, S. P. & Merrill, A. R. A catalytic loop within *Pseudomonas aeruginosa* exotoxin
456 A modulates its transferase activity. *J. Biol. Chem.* **276**, 35029□35036 (2001).
457 25. Wedekind, J. E. *et al.* Refined crystallographic structure of *Pseudomonas aeruginosa*
458 exotoxin A and its implications for the molecular mechanism of toxicity. *J. Mol. Biol.*
459 **314**, 823□837 (2001).
460 26. Capitani, M. & Sallese, M. The KDEL receptor: new functions for an old protein. *FEBS*
461 *Lett.* **583**, 3863□3871 (2009).
462 27. Jenkins, C. E., Swiatoniowski, A., Issekutz, A. C. & Lin, T. J. *Pseudomonas aeruginosa*
463 exotoxin A induces human mast cell apoptosis by a caspase-8 and-3-dependent
464 mechanism. *J. Biol. Chem.* **279**, 37201□37207 (2004).
465 28. Pastrana, D. V. & FitzGerald, D. J. A nonradioactive, cell-free method for measuring
466 protein synthesis inhibition by *Pseudomonas* exotoxin. *Anal. Biochem.* **353**, 266□271
467 (2006).

468 29. Chang, J. H., & Kwon, H. Y. Expression of 14-3-3δ, cdc2 and cyclin B proteins related
469 to exotoxin A-induced apoptosis in HeLa S3 cells. *Int. J. Immunopharmacol.* **7**, 1185–
470 1191 (2007).
471 30. Du, X., Youle, R. J., FitzGerald, D. J. & Pastan, I. *Pseudomonas* exotoxin A-mediated
472 apoptosis is Bak dependent and preceded by the degradation of Mcl-1. *Mol. Cell. Biol.*
473 **30**, 3444–3452 (2010).
474 31. Risberg, K., Fodstad, Ø. & Andersson, Y. Immunotoxins: a promising treatment
475 modality for metastatic melanoma? *Ochsner. J.* **10**, 193–199 (2010).
476 32. Boucher, H. W. *et al.* Bad bugs, no drugs: no ESKAPE! An update from the Infectious
477 Diseases Society of America. *Clin. Infect. Dis.* **48**, 1–12 (2009).
478 33. Clatworthy, A. E., Pierson, E. & Hung, D. T. Targeting virulence: a new paradigm for
479 antimicrobial therapy. *Nat. Chem. Biol.* **3**, 541 (2007).
480 34. Kelly, S. M., Jess, T. J. & Price, N. C. How to study proteins by circular dichroism.
481 *Biochim. Biophys. Acta* **1751**, 119–139 (2005).
482 35. Jørgensen, R., Wang, Y., Visschedyk, D. & Merrill, A. R. The nature and character of
483 the transition state for the ADP-ribosyltransferase reaction. *EMBO Rep.* **9**, 802–809
484 (2008).
485 36. Abhinandan, K. R. & Martin, A. C. Analysis and improvements to Kabat and structurally
486 correct numbering of antibody variable domains. *Mol. Immunol.* **45**, 3832–3839 (2008).
487 37. Lukac, M., & Collier, R. J. Restoration of enzymic activity and cytotoxicity of mutant,
488 E553C, *Pseudomonas aeruginosa* exotoxin A by reaction with iodoacetic acid. *J. Bio.*
489 *Chem.* **263**, 6146–6149 (1988).

490 38. Carroll, S. F. & Collier, R. J. Active site of *Pseudomonas aeruginosa* exotoxin A.
491 Glutamic acid 553 is photolabeled by NAD and shows functional homology with
492 glutamic acid 148 of diphtheria toxin. *J. Biol. Chem.* **262**, 8707□8711 (1987).
493 39. Douglas, C. M., & Collier, R. J. Exotoxin A of *Pseudomonas aeruginosa*: substitution of
494 glutamic acid 553 with aspartic acid drastically reduces toxicity and enzymatic activity.
495 *J. Bacteriol.* **169**, 4967□4971 (1987).
496 40. Yates, S. P. & Merrill, A. R. A catalytic loop within *Pseudomonas aeruginosa* exotoxin
497 A modulates its transferase activity. *J. Biol. Chem.* **276**, 35029□35036 (2001).
498 41. Han, X. Y., & Galloway, D. R. Active site mutations of *Pseudomonas aeruginosa*
499 exotoxin A analysis of the His440 residue. *J. Biol. Chem.* **270**, 679□684 (1995).
500 42. Shang, H. F., Yeh, M. L., Lin, C. P. & Hwang, J. Characterization of monoclonal antibody
501 B7, which neutralizes the cytotoxicity of *Pseudomonas aeruginosa* exotoxin A. *Clin.*
502 *Diagn. Lab. Immunol.* **3**, 727□732 (1996).
503 43. Kulkeaw, K., *et al.* Human monoclonal ScFv neutralize lethal Thai cobra, *Naja*
504 *kaouthia*, neurotoxin. *J. Proteom.* **72**, 270□282 (2009).
505 44. Zhang, Y. I-TASSER server for protein 3D structure prediction. *BMC Bioinformatics* **9**,
506 40 (2008).
507 45. Yang, J., Yan, R., Roy, A., Xu, D., Poisson, J. & Zhang, Y. The I-TASSER Suite: protein
508 structure and function prediction. *Nat. Methods.* **12**, 7 (2015).
509 46. Xu, D. & Zhang, Y. Improving the physical realism and structural accuracy of protein
510 models by a two-step atomic-level energy minimization. *Biophys. J.* **101**, 2525□2534
511 (2011).

512 47. Zhang, J., Liang, Y., & Zhang, Y. Atomic-level protein structure refinement using
513 fragment-guided molecular dynamics conformation sampling. *Structure*. **19**, 1784–
514 1795 (2011).
515 48. Kozakov, D. *et al*. The ClusPro web server for protein-protein docking. *Nat. Protoc*. **12**,
516 255 (2017).

517

518 **Acknowledgements**

519 This work was supported by the Thailand Research Fund (grants no. RSA5980048 to NI) and
520 the NSTDA Chair Professor grant funded by the Crown Property Bureau of Thailand (Grant
521 no. P-1450624) to WC. SS received the Royal Golden Jubilee Ph.D. scholarship (Grant No.
522 PHD/0073/2558) from the Thailand Research Fund. Dr. Pornpan Pumirat provided the HeLa
523 cells and she is acknowledged with thanks.

524

525 **Contributions**

526 SS and NI planned and designed the study. SS and WS did experiments on recombinant
527 proteins production. SA performed electron microscopic experiments. OR identified proteins
528 by LC-MS/MS. SS and KM did flow cytometric analysis. SS, NI, NS, PD, and WC performed
529 data analysis. NS and WC provided consultation and coordination. SS and NI drafted the
530 manuscript; WC edited the draft and finalized the manuscript. All authors approved the final
531 manuscript.

Competing Interests

The authors declare no competing interests.

Corresponding author

Correspondence to Nitaya Indrawattana.

Exotoxin A protein		HuscFv-C41		Interactive bond(s)
Residue	**Domain**	**Residue**	**Domain(s)**	
Y481	Catalytic (NAD+ binding site)	Y105	VH-CDR3	Hydrophobic (π-π stacking)
Q485	Catalytic	Y109	VH-CDR3	Hydrogen
R490	Catalytic	R201	VL-CDR2	Hydrogen
G491	Catalytic	R201	VL-CDR2	Hydrogen
E546	Catalytic (NAD+ binding site)	R103/G104	VH-CDR3	Hydrogen
E547	Catalytic (NAD+ binding site)	S54	VH-CDR2	Hydrogen
E548	Catalytic	S54	VH-CDR2	Hydrogen
G549	Catalytic	S31	VH-CDR1	Hydrogen
R551	Catalytic	P101	VH-CDR3	Hydrogen
E553	Catalytic (NAD+ binding site)	R103	VH-CDR3	Salt bridge
N577	Catalytic	G204/I205	VL-FR3	Hydrogen
V578	Catalytic	R201	VL-CDR2	Hydrogen
G579	Catalytic	Y196	VL-FR2	Hydrogen
G580	Catalytic	R201	VL-CDR2	Hydrogen
D581	Catalytic	R102/Y116/Y196	VH-CDR3/VH-CDR3/VL-FR2	Salt bridge/Hydrogen/Anionic π

Exotoxin A protein		HuscFv-E44		Interactive bond(s)
Residue	**Domain**	**Residue**	**Domain(s)**	
Q310	Translocation (ETA-2)	G199	VL-FR3	Hydrogen
R313	Translocation	V185/G199	VL-CDR2/VL-FR3	Hydrophobic (alkyl)/Hydrogen
A317	Translocation	S196	VL-FR3	Hydrogen
D461	Catalytic (NAD+ binding site)	S163	VL-CDR1	Hydrogen
Q485	Catalytic	Y182/S186	VL-FR2/VL-CDR2	Hydrogen
E486	Catalytic	S186	VL-CDR2	Hydrogen
E547	Catalytic (NAD+ binding site)	W47/N58	VH-FR2/VH-CDR2	Anionic π/Hydrogen
E548	Catalytic	Y59	VH-CDR2	Hydrogen

G549	Catalytic	N52/R99	VH-CDR2/VH-CDR3	Hydrogen
D581	Catalytic	G100	VH-CDR3	Hydrogen
D583	Catalytic	S30	VH-FR1	Hydrogen
P584	Catalytic	H53	VH-CDR2	Hydrophobic (π-alkyl)
Exotoxin A protein		**HuscFv-P32**		**Interactive bond(s)**
Residue	**Domain**	**Residue**	**Domain(s)**	
S515	Catalytic	D168	VL-CDR1	Hydrogen
A519	Catalytic	Y33/Y52	VH-CDR1/VH-CDR2	Hydrophobic (π-alkyl)
P545	Catalytic	A103	VH-CDR3	Hydrophobic (alkyl)
E547	Catalytic (NAD^+ binding site)	Y33	VH-CDR1	Hydrogen
E548	Catalytic	Y52	VH-CDR2	Hydrophobic (π-alkyl)
G550	Catalytic	S166/S167	VL-CDR1	Hydrogen
D581	Catalytic	R162	VL-CDR1	Salt bridge

Table 1. Residues and domains of *P. aeruginosa* exotoxin A (ETA) that were predicted by computerized simulation to be interacted by the effective human single-chain antibodies, *i.e.*, HuscFv-C41, HuscFV-E44 and HuscFv-P32.

551 **Table 2.** Results of Annexin V-FITC/PI staining for apoptotic cells after treatment of the ETA-exposed

HeLa cells treated with	Percent cellular apoptosis	Percent cell survival
Medium	6.97 ± 0.02	92.27 ± 0.25
rETA-FL	25.08 ± 4.51	73.03 ± 4.18
rETA-FL + HuscFv- C41	9.85 ± 1.09	89.07 ± 1.70
rETA-FL + HuscF-E44	11.09 ± 0.98	87.77 ± 0.97
rETA-FL + HuscFv-P32	15.78 ± 1.13	83.27 ± 1.19
rETA-FL + control HuscFv (Irre)	23.80 ± 0.52	73.37 ± 0.93

552 cells with HuscFv-C41, HuscFv-E44 and HuscFv-P32 compared to control HuscFv (Irre), ETA-exposed
553 cells inmedium alone and normal cells. Data represent the means ± standard deviations from three
554 independent-experiments

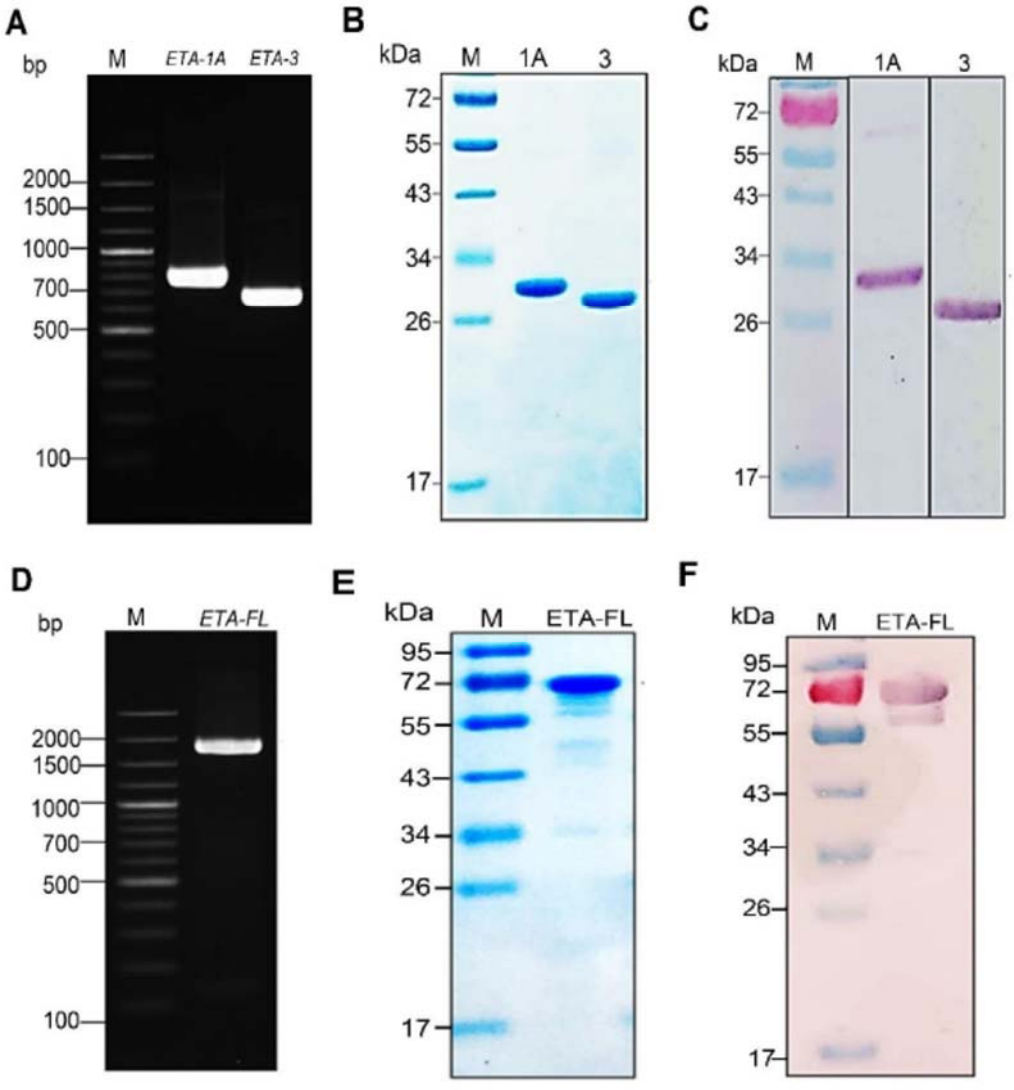

Figure 1. Production of recombinant ETA-1A, ETA-3 and ETA-FL. Panels A, amplicons of *ETA-1A* (756 bp) and *ETA-3* (627 bp). Panel B, stained SDS-PAGE-separated rETA-1A (28 kDa) and rETA-3 (26 kDa) and Panel C, Western blot patterns of rETA-1A and rETA-3. Panel D, amplicon of *ETA-FL* (1839 bp). Panels E and F, stained SDS-PAGE-separated rETA-FL (66.7 kDa) and the Western blot pattern of rETA-FL, respectively. Numbers at the left of panels A and C, DNA molecular size marker in base pairs (bp). Numbers at the left of Panels B, C, E and F are protein molecular masses in kDa.

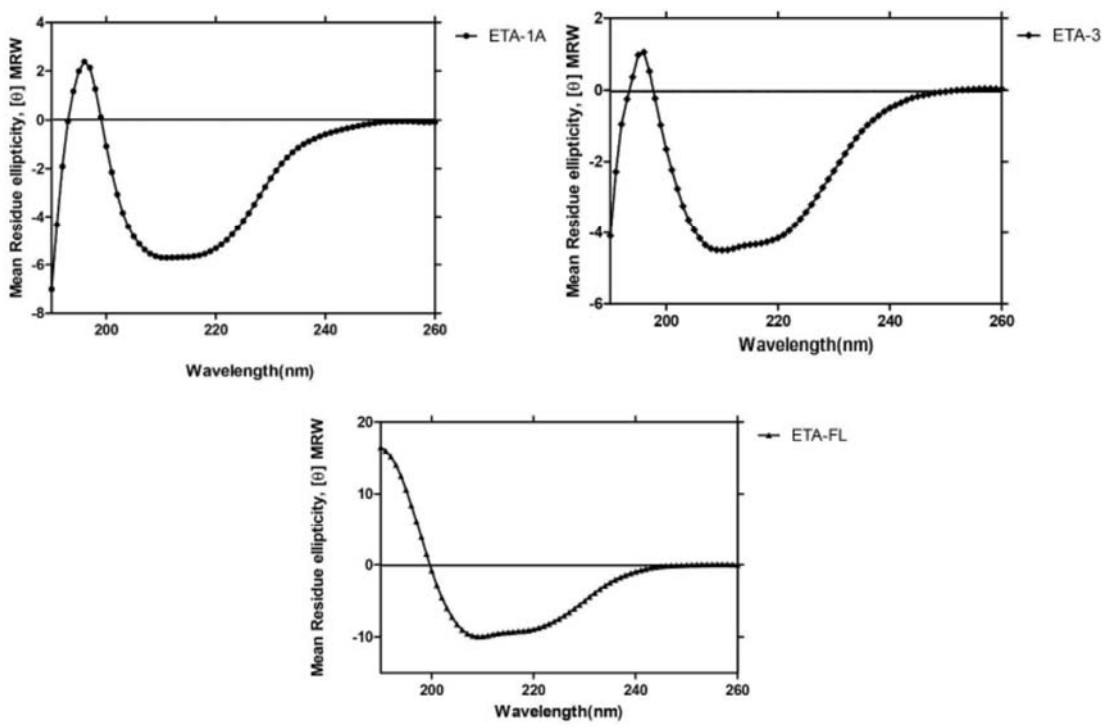

Figure 2. CD spectra in far-UV region of the refolded rETA-1A, rETA-3, and rETA-FL.

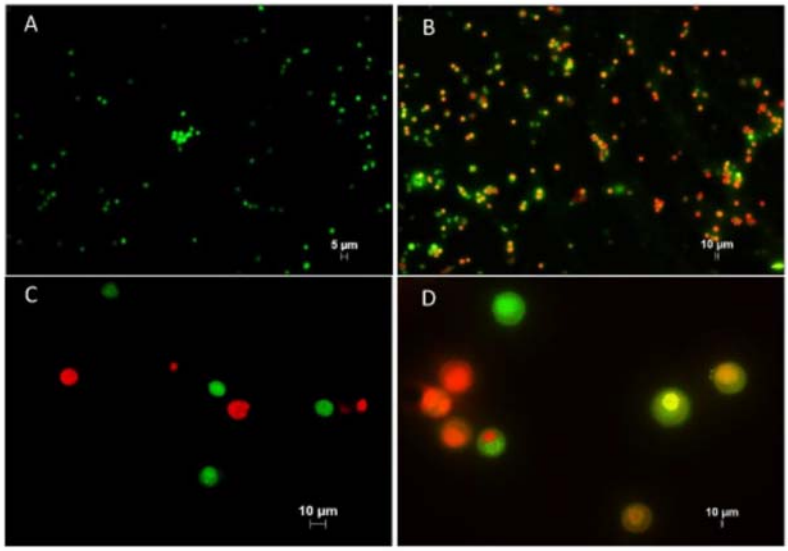

Figure 3. ETA-exposed-HeLa cells stained with AO/EB. Panel A shows normal HeLa cells without prominent apoptosis (10× magnification). Panels B, C and D are HeLa cells treated with ~LD_{50} of rETA-FL for 24 h at 10×, 20× and 40× magnifications, respectively.

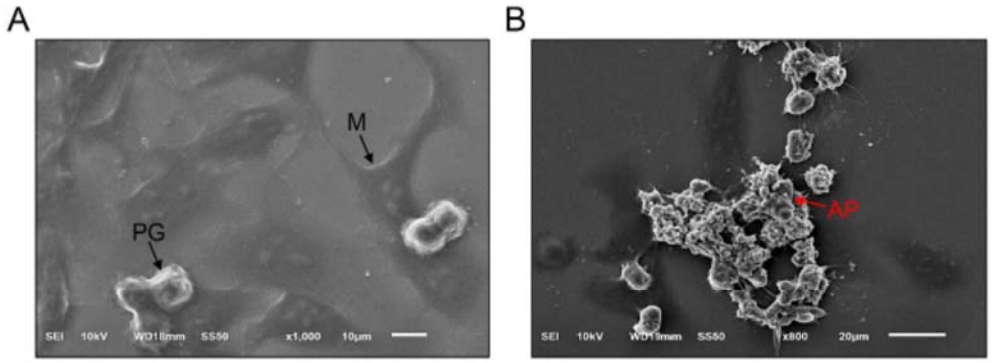

Figure 4. Scanning electron microscopic appearance of HeLa cells. Panel A, normal cells; the typical mature form without granule (M), and the progenitor form consisted of small and rounded cells with a smooth regular membrane (PG). Panel B, after exposure to ~ LD_{50} of recombinant full-length ETA for 24 h; apoptotic cell (AP) appears as the shrunken cell with numerous vacuolated membranes.

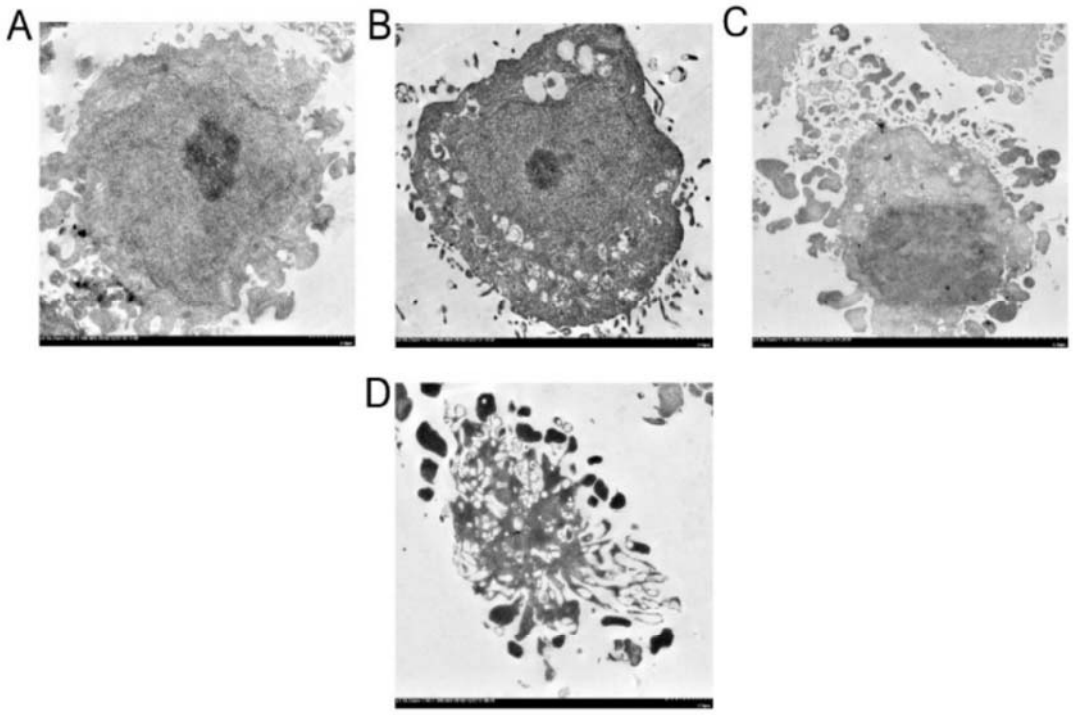

Figure 5. Transmission electron microscopic appearance of HeLa cells exposed to ~LD_{50} of rETA-FL for 24 h. A, Normal cell; B, early apoptotic.

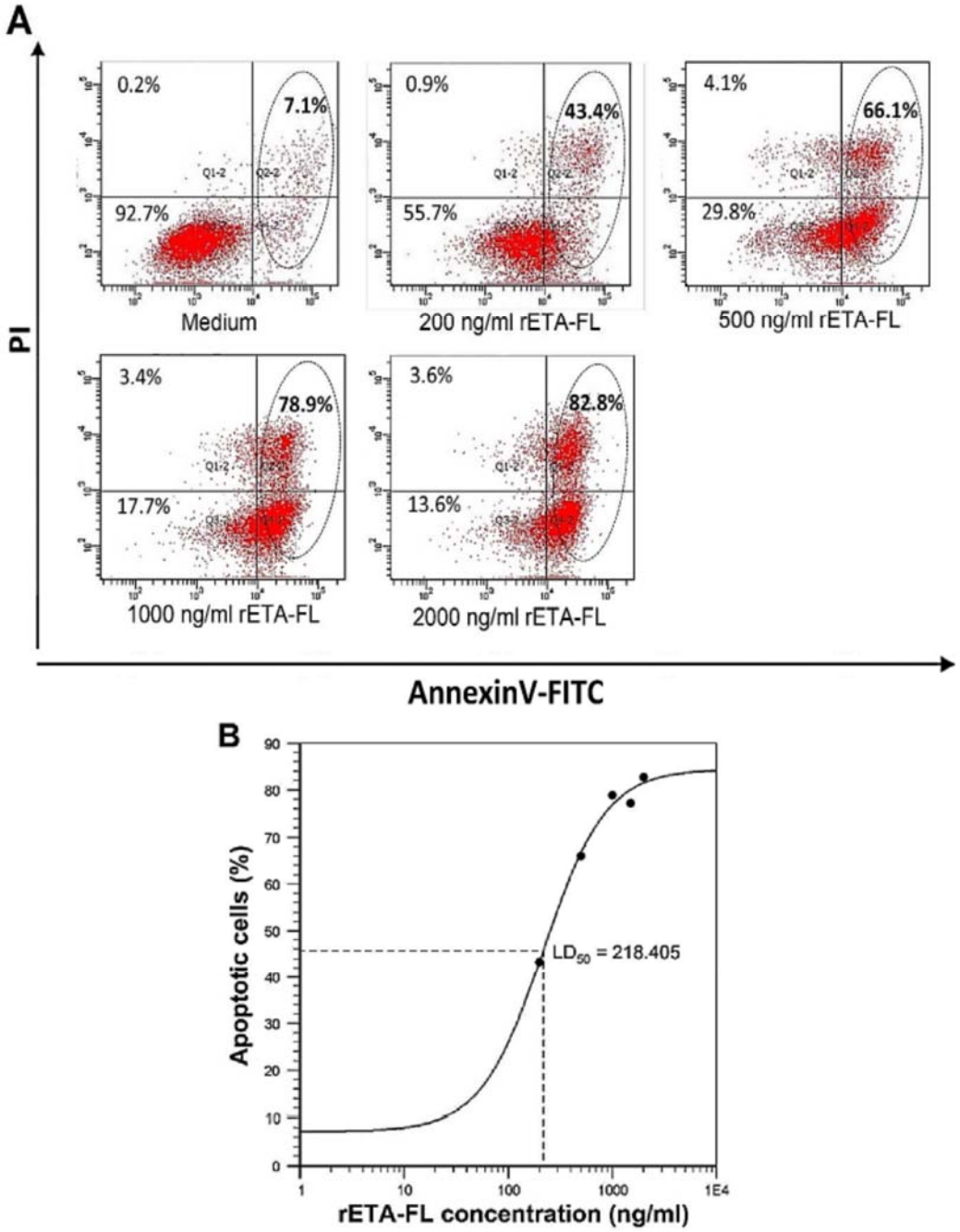

686

687 **Figure 6**. Cytotoxic effect of rETA-FL on HeLa cells revealed by staining the ETA-exposed

688 cells with Annexin V/PI stains and flow cytometric analysis. A, Percentages of Annexin V-

689 FITC+PI+ in the HeLa cells treated with various concentrations of rETA-FL for 24 h. B, LD_{50}

690 of rETA-FL on HeLa cells.

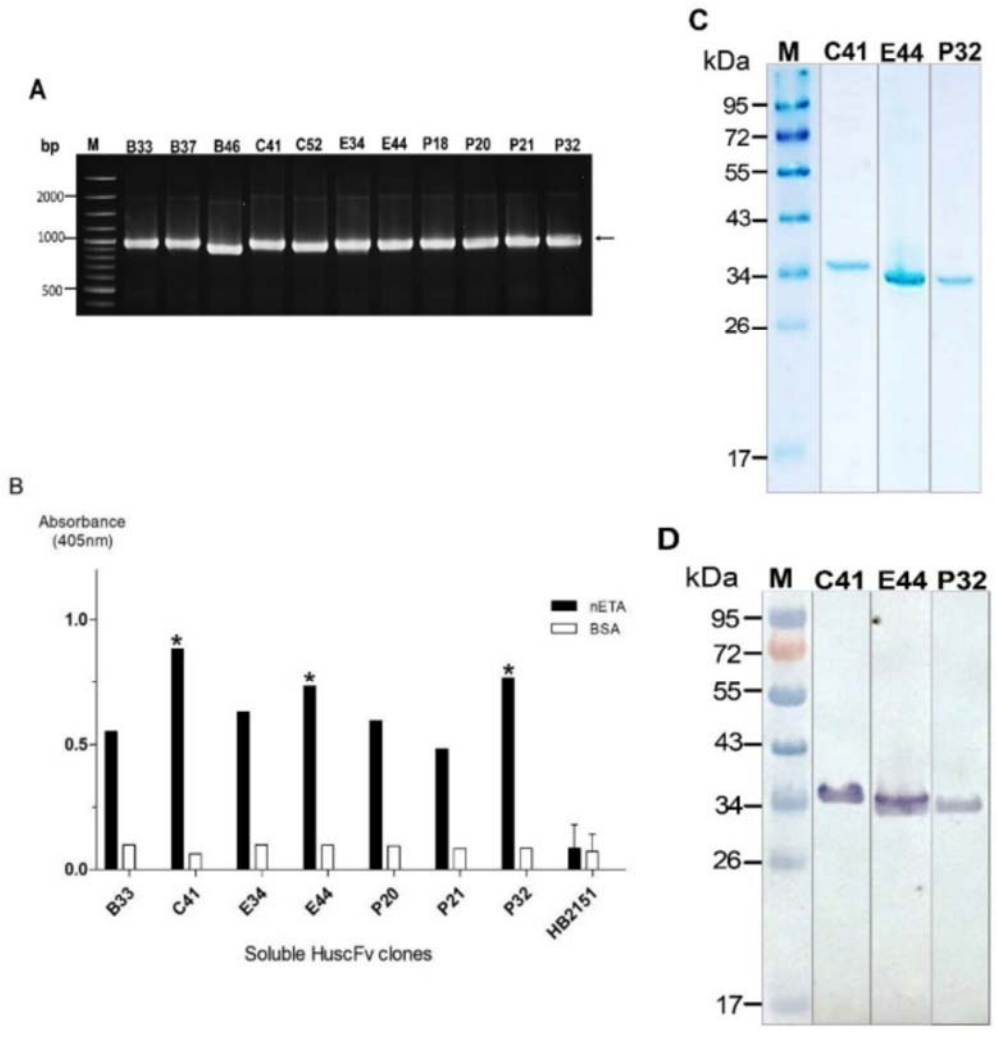

Figure 7. Production of ETA-bound HuscFvs. A, Amplicons of HuscFv gene (~1000 bp) from representative phage-transformed HB2151 *E. coli* clones. B, Indirect ELISA results for determining the binding of HuscFvs in lysate of the representative phage-transformed-HB2151 *E. coli* clones to the native ETA (1 µg/well) and BSA (control antigen). C, Stained SDS-PAGE-separated-purified and refolded rETA-bound HuscFvs (~34 kDa or slightly higher) from transformed NiCo21 (DE3) *E. coli* (1 µg per lane). D, Western blot patterns of the representative ETA-bound HuscFvs from transformed NiCo21 (DE3) *E. coli* (1 µg per lane). Numbers at the left of A, DNA sizes in bp; numbers at the left of C and D, protein molecular masses in kDa.

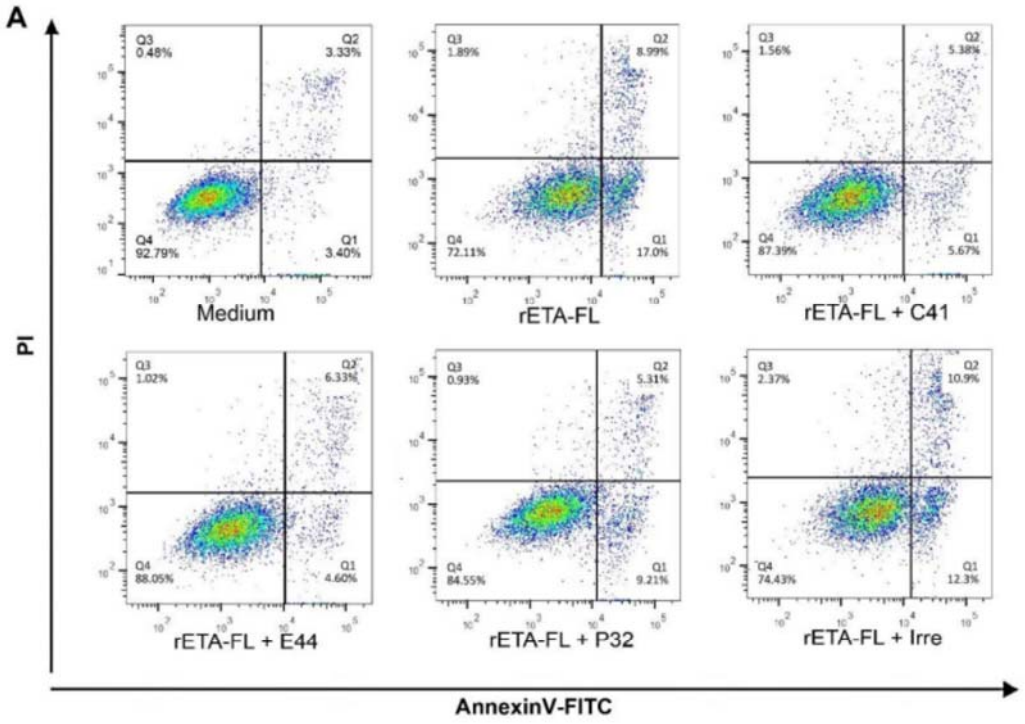
A
PI
AnnexinV-FITC
Medium
rETA-FL
rETA-FL + C41
rETA-FL + E44
rETA-FL + P32
rETA-FL + Irre
Q3 0.48%
Q2 3.33%
Q4 92.79%
Q1 3.40%
Q3 1.89%
Q2 8.99%
Q4 72.11%
Q1 17.0%
Q3 1.56%
Q2 5.38%
Q4 87.39%
Q1 5.67%
Q3 1.02%
Q2 6.33%
Q4 88.05%
Q1 4.60%
Q3 0.93%
Q2 5.31%
Q4 84.55%
Q1 9.21%
Q3 2.37%
Q2 10.9%
Q4 74.43%
Q1 12.3%

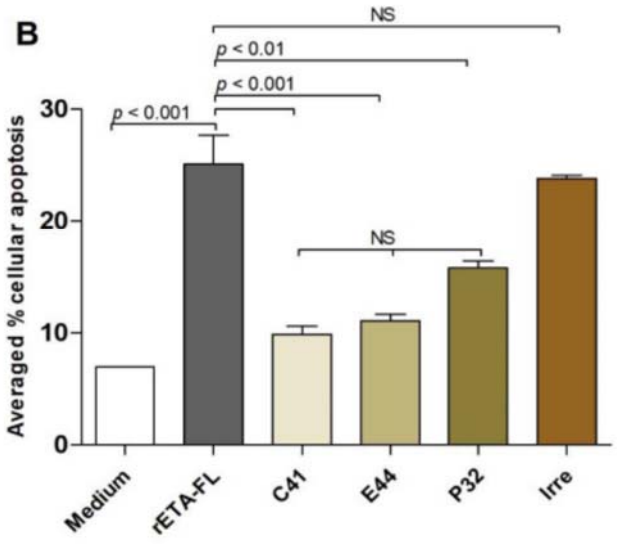
B
Averaged % cellular apoptosis
30
20
10
0
NS
p < 0.01
p < 0.001
p < 0.001
NS
Medium
rETA-FL
C41
E44
P32
Irre

C

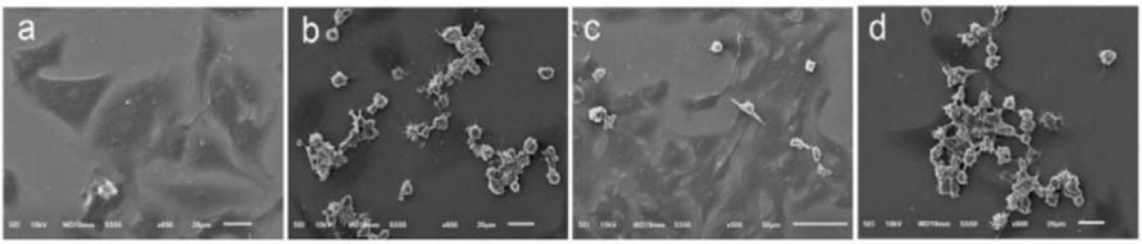
a
b
c
d

137

Figure 8. A, Apoptotic analysis of Annexin V/PI stained-ETA-exposed-HeLa cells after treatment with ETA-bound HuscFvs/control HuscFv (Irre) at HuscFv to ETA molar ratio 50:1 and medium alone. B, Bar graphs that represent statistical comparison of the averaged percentages of ETA induced-HeLa cells apoptosis after different treatments. The data shown are representative of three independent experiments. The significant difference from control is indicated by $p < 0.05$. Triplicate experiments were performed. C, Scanning electron microscopic appearances of ETA-exposed HeLa cells after treatment with ETA-bound HuscFvs, control HuscFv (Irre) and medium alone. C, Normal HeLa cells (a); ETA- exposed HeLa cells (b); cells exposed to ETA treated with HuscFv-C41 (c); cells exposed to ETA treated with control HuscFv (d).

PeerJ

Staphylococcus spp. associated with subclinical bovine mastitis in central and northeast provinces of Thailand

Natapol Pumipuntu[1,2], Witawat Tunyong[1], Narisara Chantratita[1,3], Pornphan Diraphat[4], Pornpan Pumirat[1], Nitat Sookrung[5], Wanpen Chaicumpa[6] and Nitaya Indrawattana[1]

[1] Department of Microbiology and Immunology/Faculty of Tropical Medicine, Mahidol University, Bangkok, Thailand
[2] One Health Research Unit/Faculty of Veterinary Sciences, Maha Sarakham University, Maha Sarakham, Thailand
[3] Mahidol-Oxford Tropical Medicine Research Unit/Faculty of Tropical Medicine, Mahidol University, Bangkok, Thailand
[4] Department of Microbiology/Faculty of Public Health, Mahidol University, Bangkok, Thailand
[5] Biomedical Research Incubator Unit/Department of Research/Faculty of Medicine Siriraj Hospital, Mahidol University, Bangkok, Thailand
[6] Center of Excellence on Therapeutic Proteins and Antibody Engineering/Department of Parasitology/Faculty of Medicine Siriraj Hospital, Mahidol University, Bangkok, Thailand

Submitted 12 November 2018
Accepted 10 February 2019
Published 14 March 2019

Corresponding author
Nitaya Indrawattana,
nitaya.ind@mahidol.ac.th

Academic editor
Steven Tong

Additional Information and Declarations can be found on page 16

DOI 10.7717/peerj.6587

ABSTRACT

Background: *Staphylococcus* spp. are major cause of bovine mastitis (BM) worldwide leading to economic damage to dairy farms and public health threat. Recently, a newly emerged *Staphylococcus argenteus* has been found as a human and animal pathogen. Molecular characteristics, virulence and antibiotic resistant phenotypes of bacteria causing BM in Thailand are rare. This study aimed to investigated *Staphylococcus* spp. associated with subclinical bovine mastitis (SCM) in Thailand.
Methods: Milk samples were collected from 224 cows of 52 dairy herds in four central and northeast provinces. Total somatic cell counts (SCC) and California mastitis test (CMT) were used to identify SCM cows. Milk samples were cultured for *Staphylococcus* spp. Coagulase-positive isolates were subjected to pulsed-field gel electrophoresis (PFGE) and multilocus sequence typing (MLST). Organisms suspected as *S. argenteus* were verified by detecting nonribosomal peptide synthetase gene. All isolates were checked for antibiograms and the presence of various virulence genes.
Results: From the 224 milk samples of 224 cows, 132 (59%) were positive for SCM by SCC and CMT and 229 staphylococcal isolates were recovered. They were 32 coagulase-positive (24 *S. aureus* and eight *S. argenteus*) and 197 coagulase-negative. PFGE of the *S. aureus* and *S. argenteus* revealed 11 clusters and a non-typeable pattern. MLST of representatives of the 11 PFGE clusters, three PFGE non-typeable *S. aureus* isolates from different locations and *S. argenteus* showed 12 sequence types. The eight *S. argenteus* isolates belonged to ST1223 (three isolates), ST2250 (two isolates), and ST2793 (two isolates). The antimicrobial tests identified 11 (46%) methicillin-resistant *S. aureus* and 25 (13%) methicillin-resistant coagulase-negative isolates, while seven *S. argenteus* were methicillin-susceptible and one isolate was methicillin-resistant. All of the 229 isolates were multiply resistant to other antibiotics. The most prevalent virulence genes of the 24 *S. aureus* isolates were *clfA*, *coa* and

How to cite this article Pumipuntu N, Tunyong W, Chantratita N, Diraphat P, Pumirat P, Sookrung N, Chaicumpa W, Indrawattana N. 2019. *Staphylococcus* spp. associated with subclinical bovine mastitis in central and northeast provinces of Thailand. PeerJ 7:e6587
DOI 10.7717/peerj.6587

spa (X and IgG-binding region) (100%), *hla* (96%), *pvl* (96%) and *sec* (79%). Six *S. argenteus* isolates carried one enterotoxin gene each and other virulence genes including *coa, clfA, hla/hlb, spa, tsst* and *pvl*, indicating their pathogenic potential. **Conclusion and perspective:** This is the first report on the *S. argenteus* from cow milk samples with SCM. Data on the molecular characteristics, virulence genes and antibiograms of the *Staphylococcus* spp. obtained from the present study showed a wide spread and increasing trend of methicillin-resistance and multiple resistance to other antibiotics. This suggests that the "One Health" practice should be nurtured, not only at the dairy farm level, but also at the national or even the international levels through cooperation of different sectors (dairy farmers, veterinarians, medical and public health personnel and scientists) in order to effectively combat and control the spread of these pathogens.

Subjects Agricultural Science, Microbiology
Keywords *Staphylococcus aureus*, Coagulase-negative staphylococci, *Staphylococcus argenteus*, Bovine mastitis, Antimicrobial susceptibility, Virulence genes

INTRODUCTION

Bovine mastitis (BM) is an inflammation of the mammary gland caused mainly by bacteria that made incursion of the udder through the teat canal. The disease has negative economic impact to the dairy producers as it causes reduction of not only the milk yield and quality (change of milk composition and palatable leading to un-salability of the milk), but also the cow fertility by causing irregular/extended estrus cycle and hence the calving problem. Mastitis also incurs the expense on treatment, intervention and control of the infection in the herd (*Rollin, Dhuyvetter & Overton, 2015*). BM can be classified based on clinical manifestations into clinical mastitis (CM) and subclinical bovine mastitis (SCM); of which the latter is the more common entity (*Islam et al., 2011*). In the CM case, the affected udder shows inflammation including heat, swelling, discoloration as well as abnormal secretion; the infected cow may exhibit systemic reactions such as fever, loss of appetite and sometimes death (*Kibebew, 2017*). The SCM cases usually do not show any visible sign of inflammation or infection; but can be recognized by either high somatic cell counts (SCC) (predominantly neutrophils) in the milk samples as a result of the host immune response (*Östensson, Hageltorn & Aström, 1988*; *Harmon, 1994*; *Kehrli & Shuster, 1994*) or positive gelation of the milk samples caused by DNA of the infiltrating somatic cells, as tested by a California mastitis/milk test (CMT) (*White et al., 2005*).

Staphylococcus spp., including *S. aureus* and coagulase-negative staphylococci (CoNS) are the most common pathogens associated with SCM (*Harmon, 1994*; *Djabri et al., 2002*). Surveillance of epidemiology, prevalence and incidence of bacteria causing BM, particularly the *Staphylococcus* spp. is essential to develop programs and strategies for preventing economic loss for dairy producers (*Xu et al., 2015*), and also for safeguarding of human health based on the "One Heath" policy. In Thailand, the prevalence of the SCM in dairy cows was ~62.8% in a northeastern province, that is, Khon-Kaen (*Jarassaeng et al., 2012*) and ~54% in a northern province, that is, Chiang-mai

(*Suriyasathaporn, 2011*). Nevertheless, data on the pathogens causing/associating with the SCM in other provinces/regions where there are many more dairy farms are lacking.

Thus, the aim of this study was to investigate the presence of both coagulase-positive *Staphylococcus aureus* and *S. argenteus* as well as CoNS in milk samples of cows with SCM from 52 dairy farms in two northeast and two central provinces of Thailand. Particular attention has been made to the *S. argenteus* because this bacterium has emerged in many countries as a human pathogen causing nosocomial infections, serious morbidity, and/or death, especially in patients with underlying diseases, such as diabetes mellitus and renal diseases (*Thaipadungpanit et al., 2015*). *S. argenteus* has been isolated also from animals, for example, ape (*Schuster et al., 2017*) and rabbit (*Indrawattana et al., 2018*) but so far, there has been no report on isolation of the *S. argenteus* from CM or SCM milk samples. Phenotypically, *S. argenteus* is highly similar to *S. aureus*, that is, Gram-positive cocci, which are positive by catalase- and coagulase- tests, and both shows β-hemolysis on blood agar (*Becker et al., 2003*; *El-Sayed et al., 2005*; *Indrawattana et al., 2013*). Therefore, *S. argenteus* bacteria isolated from infected humans have been frequently misidentified as *S. aureus* (*Chantratita et al., 2016*). Nevertheless, *S. argenteus* shows white colonies (non-pigmented appearance) on blood agar due to the lack of staphyloxanthin, which is a carotenoid pigment providing yellowish or golden colour for *S. aureus* colonies (*Holt et al., 2011*). Moreover, by using multilocus sequence typing (MLST) method and single-genome sequencing, *S. aureus* and *S. argenteus* could be molecularly differentiated (*Indrawattana et al., 2018*). Besides the colony characteristics, biochemical test results, and DNA sequence types (STs) (*Becker et al., 2003*; *El-Sayed et al., 2005*; *Tong et al., 2015*; *Chantratita et al., 2016*), the staphylococcal isolates suspected to be the newly emerged *S. argenteus* can be verified by using nonribosomal peptide synthetase (NRPS) gene amplification (*Zhang et al., 2016*). The *Staphylococcus* spp. isolated from SCM milk samples in this study were characterized molecularly by using pulsed-field gel electrophoresis (PFGE) and MLST, which enabling recognition of their diversity. Antibiograms against methicillin and other antibiotics were investigated. Virulence genes of the bacterial isolates including enterotoxins, toxic shock syndrome toxin (*tsst*), Panton-Valentine leukocidin (PVL) toxin (*pvl*), hemolysins (*hla*, *hlb*), clumping factor A (*clfA*), coagulase (*coa*) and protein A (*spa* X-region and *spa* IgG biding region) were also determined.

MATERIALS AND METHODS

Study area

Milk samples were collected from 52 dairy farms from eight districts of four provinces in central (Kaeng Khoi, Muak Lek and Wang Muang districts of Saraburi province; Pattananikom district of Lopburi province) and northeast (Muang, Kantarawichai and Borabue districts of Maha-Sarakham province; and Pak-Chong district of Nakorn-Ratchasima province) Thailand.

Milk samples, time of collection and identification of subclinical bovine mastitis

All animal procedures were approved by the Faculty of Tropical Medicine–Animal Care and Use Committee (FTM-ACUC), Mahidol University, Thailand (Reference number FTM-ACUC 002/2016). A total of 224 milk samples were collected from 224 cows with SCM (as tested by CMT and SCC); one sample was a pool of equal volume of milk collected from four udder quarters. The milk collection was performed by a qualified veterinarian using aseptic technique (*National Mastitis Council (U.S.) et al., 2004*; *Abebe et al., 2016*). Sample collection was carried-out during September 2015 and April 2016. All samples were primarily submitted to CMT and categorized by CMT scores (0, T, 1, 2 and 3) (*Philpot & Nickerson, 1999*). The positive CMT samples (CMT score: T, 1, 2 or 3) were subsequently measured for SCC (*Schwarz et al., 2010*). An SCC > 2×10^5 cells/ml was taken as positivity for BM. The milk samples were then transported at 4–10 °C to the Microbiology Laboratory, Faculty of Tropical Medicine, Mahidol University, within 12 h after sampling, and subjected immediately to bacterial culture upon the laboratory arrival.

Bacterial culture

Columbia blood agar supplemented with nalidixic acid and colistin sulphate (Oxoid Ltd, Basingtoke, UK) was used as a selective medium for *Staphylococcus* spp. Cultures were incubated at 37 °C for 24 h. For each sample, up to six colonies grown on the plate that were suspected to be *Staphylococcus* bacteria were examined further by Gram staining, catalase test, mannitol salt agar selectivity, DNase selectivity test, coagulase test, and agglutination test by using Staphaurex™ Plus kit (Remel Europe Ltd., Dartford, UK) (*Indrawattana et al., 2013*).

Amplification of nonribosomal peptide synthetase gene

Coagulase-positive isolates suspected as *S. argenteus* were subjected to NRPS gene amplification using the primer sequences (Table 1) and PCR protocol described previously (*Zhang et al., 2016*). The PCR reaction mixture (25 µl) contained 1 × *Taq* buffer, 2.5 mM MgCl2, 0.2 mM of dNTP, 0.4 µM of each primer, one unit *Taq* DNA polymerase (Thermo-Scientific, Darmstadt, Germany) and 100 ng of bacterial genomic DNA. PCR reaction was initially denatured at 94 °C for 4 min; 35 cycles of 94 °C for 30 s, 53 °C for 30 s, 72 °C for 40 s; and final extension at 72 °C, 10 min (BioRad Thermal Cycler, CA, USA). PCR amplicons were analysed by 1.5% agarose gel electrophoresis and ethidium bromide (Sigma, MO, USA) staining. The DNA bands were observed under a Gel Doc XR+ System. *S. aureus* ATCC 25923 and *S. argenteus* DS-003 (*Thaipadungpanit et al., 2015*) were used as references in the experiment.

Pulsed-field gel electrophoresis

Chromosomal DNA of all *S. aureus* and *S. argenteus* isolates were digested with *Sma*I restriction endonuclease. The PFGE patterns were then determined by electrophoretic separation of the digested DNA in a CHEF-DR II system (Bio-Rad, CA, USA) at six Volts/cm, 14 °C, for 27 h using the 25 K–800 K automatic program (initial Sw Tm: 1.79 s;

Table 1 Specific oligonucleotide primers for amplification of virulence and housekeeping genes of staphylococci.

Target gene	Sequence (5′–3′)	Amplicon size (bp)	Reference
sea	F: GAAAAAAGTCTGAATTGCAGGGAACA R: CAAATAAATCGTAATTAACCGAAGGTTC	560	*Wu et al. (2011)*
seb	F: ATTCTATTAAGGACACTAAGTTAGGGA R: ATCCCGTTTCATAAGGCGAGT	404	
sec	F: CTTGTATGTATGGAGGAATAACAAAACATG R: CATATCATACCAAAAAGTATTGCCGT	275	
sed	F: GAATTAAGTAGTACCGCGCTAAATAATATG R: GCTGTATTTTTCCTCCGAGAGT	492	
see	F: CAAAGAAATGCTTTAAGCAATCTTAGGC R: CACCTTACCGCCAAAGCTG	482	
tsst	F: TTCACTATTTGTAAAAGTGTCAGACCCACT R: TACTAATGAATTTTTTTATCGTAAGCCCTT	180	*Wu et al. (2011)*
coa	F: CGAGACCAAGATTCAACAAG R: AAAGAAAACCACTCACATCA	410, 740, 910, 970	*Aslantas et al. (2007)*
clfA	F: ATTGGCGTGGCTTCAGTGCT R: CGTTTCTTCCGTAGTTGCATTTG	292	*Tristan et al. (2003)*
hla	F: CTGATTACTATCCAAGAAATTCGATTG R: CTTTCCAGCCTACTTTTTTATCAGT	209	*Jarraud et al. (2002)*
hlb	F: GTGCACTTACTGACAATAGTGC R: GTTGATGAGTAGCTACCTTCAGT	309	*Jarraud et al. (2002)*
spa (X-region)	F: CAAGCACCA AAAGAGGAA R: CACCAGGTTTAACGACAT	320	*Fre´nay et al. (1996)*
spa (IgG-biding region)	F: CACCTGCTGCAAATGCTGCG R: GGCTTGTTGTTGTCTTCCTC	920	*Seki et al. (1998)*
pvl	F: ATCATTAGGTAAAATGTCTGGACATGATCCA R: GCATCAASTGTATTGGATAGCAAAAGC	433	*Jarraud et al. (2002)*
arc	F: TTGATTCACCAGCGCGTATTGTC R: AGGTATCTGCTTCAATCAGCG	456	*Enright et al. (2000)*
aroE	F: ATCGGAAATCCTATTTCACATTC R: GGTGTTGTATTAATAACGATATC	456	
glpF	F: CTAGGAACTGCAATCTTAATCC R: TGGTAAAATCGCATGTCCAATTC	465	
gmk	F: ATCGTTTTATCGGGACCATC R: TCATTAACTACAACGTAATCGTA	429	
pta	F: GTTAAAATCGTATTACCTGAAGG R: GACCCTTTTGTTGAAAAGCTTAA	474	
tpi	F: TCGTTCATTCTGAACGTCGTGAA R: TTTGCACCTTCTAACAATTGTAC	402	
yqiL	F: CAGCATACAGGACACCTATTGGC R: CGTTGAGGAATCGATACTGGAAC	516	
nrps	F: TTGARWCGAC ATTACCAGT R: AT WR CRTACAT Y TC RTTAT C	160, 340	*Zhang et al. (2016)*

final Sw Tm: 1 min, 33.69 s). Then, the gels were stained with ethidium bromide and visualized using the Gel Doc System (Bio-Rad, Hercules, CA, USA). DNA fragment patterns were analyzed for similarity and phylogenetic relatedness by the GeneTools and

Directory Application version 2.01.00, Copyright 2000–2008 (Synoptics Ltd., Cambridge, UK). The percent similarity of the bacterial isolates was based on Dice coefficients and derived from the unweighted-pair group method with arithmetic averages (UPGMA). A coefficient similarity of 80% was set to arrange PFGE clusters. Band position tolerance was set at 1.0%.

Multilocus sequence typing

Multilocus sequence typing was accomplished based on the technique described previously (*Enright et al., 2000*) using seven primer pairs to amplify seven housekeeping genes of *S. aureus* and suspected *S. argenteus* (Table 1). All DNA amplicons were purified by using GenepHlow™ Gel/PCR purification kit (Geneaid, New Taipei, Taiwan) and the DNA were sequenced. Allelic number queries and allelic profile queries or STs derived from DNA sequencing of each gene were defined using the *S. aureus* MLST database (https://pubmlst.org/saureus/). Information for assumed novel alleles or queried allelic profiles of novel STs were sent to the curator of the database website for assigning novel alleles or novel ST numbers and the data were added to the database.

Antimicrobial susceptibility testing

Staphylococcus aureus, S. argenteus and CoNS isolates were analyzed for antimicrobial phenotypes by disc diffusion method according to the Clinical & Laboratory Standards Institute guidelines (*CLSI, 2016*). A total of 15 antibiotics were used, that is, cefoxitin (30 µg), ciprofloxacin (five µg), clindamycin (two µg), erythromycin (15 µg), gentamicin (10 µg), kanamycin (30 µg), levofloxacin (five µg), linezolid (30 µg), novobiocin (five µg), oxacillin (one µg), penicillin G (10 units), rifampin (five µg), sulfamethoxazole plus trimethoprim (23.75/1.25 µg), teicoplanin (30 µg), and tetracycline (30 µg). Antibiotic susceptibility was determined on Mueller–Hinton agar (Oxoid, Basingstoke, UK). Methicillin resistance (MR) was investigated by disc diffusion method using cefoxitin (30 µg).

Detection of staphylococcal enterotoxin genes, TSST-1 gene and other virulence genes

The genomic DNA of individual bacterial isolates were extracted using a DNA extraction kit (Geneaid, New Taipei City, Taiwan) following the protocol for Gram-positive bacteria. The extracted DNA was quantified and amplified for 13 virulence genes including enterotoxins (*sea*, *seb*, *sec*, *sed* and *see*), *tsst*, *coa*, *spa* x and *spa* IgG-binding regions, *hla* and *hlb*, *clfA* and *pvl*. Specific oligonucleotide primers (*Fre´nay et al., 1996*; *Seki et al., 1998*; *Jarraud et al., 2002*; *Tristan et al., 2003*; *Aslantas et al., 2007*; *Wu et al., 2011*) are shown in Table 1. Each PCR reaction mixture (25 µl) contained 10 mM of each forward/reverse primer, 0.2 mM dNTPs, two mM $MgCl_2$, one unit *Taq* DNA polymerase, 1 × *Taq* reaction buffer and 100 ng DNA template. PCR was carried-out using a T100™ ThermalCycler (Bio-Rad, Hercules, CA, USA) with initial denaturation at 95 °C for 10 min, followed by 35 cycles of 95 °C for 30 s, 55 °C for 30 s, and 72 °C for 30 s, and a final extension at 72 °C for 10 min. PCR amplicons were subjected to 1.5% agarose gel electrophoresis and staining with ethidium bromide. The DNA bands were observed under a Gel Doc XR+ System (Bio-Rad, Hercules, CA, USA). The control bacterial DNA templates included

S. aureus strains ATCC 19095 (*sea*, *sec* and *tsst*), ATCC 14458 (*seb*), ATCC 23235 (*sed*), ATCC 27664 (*see*) and ATCC 13565 (*coa*, *clfA*, *hla*, *hlb*, *spa* x region, *spa* IgG-binding region, *arcC*, *aroE*, *glpF*, *gmk*, *pta*, *pta* and *yqiL*). For *tsst* and *pvl*, the PCR amplicons were subjected to nucleotide sequencing and sequence analysis for gene confirmation (accession numbers: KX371630.1 and AB084255.1, respectively).

Statistical analysis

Chi-square test and Fisher's exact test of independence were performed using the SPSS statistics program (version 22) to analyze the differences of the detected virulence genes between MR and methicillin sensitivity groups. A probability value (p-value) <0.05 was considered statistically significant. Dice coefficients and the UPGMA were used to arrange PFGE clusters with a coefficient similarity of 80% and a tolerance at 1.0% (GeneTools and Gene Directory Application, version 2.01.00).

RESULTS

Staphylococcus spp. in milk samples

From 224 milk samples from 224 cows, 132 were positive for *Staphylococcus* spp. And these samples had also elevated SCC; thus, the results gave an overall prevalence of SCM at 59%. From the 132 samples, 229 staphylococcal isolates were recovered; they were 32 (14%) coagulase-positive from 29 milk samples and 197 (86%) CoNS from 121 milk samples. Among the 32 coagulase-positive isolates, 24 were *S. aureus* and eight were *S. argenteus* (as identified by colony morphology and later by MLST and NRPS gene amplification). Some milk samples contained all three types of the bacteria, that are, *S. aureus, S. argenteus* and CoNS, while the others contained two or one (Table 2).

PFGE types

Figure 1 shows UPGMA dendrogram derived from *Sma*I-PFGE and MLST of 24 *S. aureus* and eight *S. argenteus*. The bacteria with at least 80% coefficient similarity were placed in the same PFGE cluster. Among the 32 isolates, 21 isolates could be classified into 11 PFGE clusters, while 11 isolates fell into a non-typeable group (their genomic DNA could not be digested readily by the *Sma*I). Milk samples from Muak Lek district of Saraburi province yielded 10 isolates: seven isolates were PFGE cluster 2 which is the predominant pattern, two isolates (two *S. argenteus*) belonged to clusters 8, and 1 *S. aureus* was in cluster 6. The next most common PFGE pattern was cluster 1, which comprised three isolates (three *S. argenteus*) from Borabue district of Maha Sarakharm province; another isolate from Borabue sample fell in cluster 5. Two isolates (two *S. argenteus*) from Pak Chong district, Nakorn Ratchasima province belonged to cluster 4. Two isolates from Panatnikom district, Lopburi province were in clusters 3 and 9. One isolate each of Kantarawichai district, Maha Sarakharm province were clusters 10 and 11.

MLST

A total of 14 of coagulase-positive isolates, that is, 11 representatives of PFGE clusters 1–11 (M226, M185, M125, M159, M222, M196, M77, M185, M124, M89 and M85) and three isolates from different areas that showed the non-typeable PFGE pattern

Table 2 Coagulase-positive and coagulase-negative staphylococci (CoNS) isolated from subclinical bovine mastitis (SCM) and their antimicrobial phenotypes and virulence genotypes.

Study area	CoNS (*N* = 197)	*S. aureus* isolate no. (*N* = 32)	Methicillin resistance (R)/ susceptibility (S)	Antimicrobial phenotype	Virulence genes												
					sea	*seb*	*sec*	*sed*	*see*	*tsst*	*coa*	*clfA*	*hla*	*hlb*	*spa (X)*	*spa (IgG)*	*pvl*
Lopburi Pattananikom	25	(2) M124	S	P, RA	+	−	+	+	−	+	+	+	+	+	+	+	+
		M125	S	S	−	−	+	+	−	−	+	+	+	+	+	+	+
Maha Sarakham																	
Borabue	6	(4) M222	S	S	−	−	−	−	+	−	+	+	+	+	+	+	+
		M226	S	S	−	−	+	−	+	−	+	+	+	−	+	+	+
		M227	S	S	−	−	+	−	−	−	+	+	−	−	+	+	+
		M228	S	S	−	−	+	+	−	−	+	+	+	−	+	+	+
Kantarawichai	55	(3) M77	S	P	−	−	−	+	−	−	+	+	+	+	+	−	−
		M85	S	S	−	−	−	+	−	+	+	+	+	+	+	+	+
		M89	S	S	−	−	+	+	−	+	+	+	+	+	+	+	+
Muang	15	(11) M129	R	CIP[(I)], CN, DA, E, FOX, K, NV, OX, P, TE	−	−	+	+	−	+	+	+	+	−	+	+	+
		M136	R	CN, DA, E, FOX, K, LZD, NV, OX, P, RA, TE	−	−	+	+	−	+	+	+	+	−	+	+	+
		M137	R	CN, DA, E, FOX, K, NV, OX, P, RA, TE	+	−	+	+	−	+	+	+	+	+	+	+	+
		M138	R	CN, DA, E, FOX, K, NV, OX, P, RA, TE	+	−	+	+	−	+	+	+	+	+	+	+	+
		M140	R	CN, DA, E, FOX, K, NV, OX, P, RA, TE	+	−	+	+	−	+	+	+	+	+	+	+	+
		M141	R	CN, DA, E, FOX, K, NV, OX, P, RA, TE	−	−	+	+	−	−	+	+	+	−	+	+	+
		M142	R	CN, DA, E, FOX, K, LZD, NV, OX, P, RA, TE	−	−	+	+	+	+	+	+	+	−	+	+	+
		M146	R	CN, DA, E, FOX, K, NV, OX, P, RA, TE	+	−	+	+	−	+	+	+	−	+	+	+	+
		M147	R	CN, DA, E, FOX, K, NV, OX, P, RA, TE	−	−	+	+	−	−	+	+	+	−	+	+	+

Table 2 (continued).

Study area	CoNS (N = 197)	*S. aureus* isolate no. (N = 32)	Methicillin resistance (R)/ susceptibility (S)	Antimicrobial phenotype	Virulence genes												
					sea	*seb*	*sec*	*sed*	*see*	*tsst*	*coa*	*clfA*	*hla*	*hlb*	*spa (X)*	*spa (IgG)*	*pvl*
		M148	R	CN, DA, E, FOX, K, NV, OX, P, RA, TE	–	–	+	+	–	–	+	+	+	–	+	+	+
		M149	R	CN, DA, E, FOX, K, NV, OX, P, RA, TE	–	–	+	+	–	+	+	+	+	–	+	+	+
Pak Chong	13	(2) M152	R	DA, E, P, FOX, LZD, NV, OX, RA	–	–	–	–	+	+	+	+	–	–	+	+	–
		M159	S	NV, OX(I)	–	–	–	–	–	–	+	+	–	–	+	+	–
Saraburi																	
Kaeng Khoi	38	(0)	–	ND	ND	ND	ND	ND	ND	ND	ND	ND	ND	ND	ND	ND	ND
Muak Lek	31	(10) M183	S	DA(I), NV	–	–	+	–	–	–	+	+	+	+	+	+	+
		M185	S	S	–	–	+	–	–	–	+	+	+	+	+	+	+
		M186	S	S	–	–	+	–	–	–	+	+	+	+	+	+	+
		M187	S	S	–	–	–	–	–	–	+	+	+	+	+	+	+
		M188	S	K(I), NV, P, TE	–	–	–	+	–	–	+	+	+	–	+	–	–
		M192	S	NV, P	–	–	–	–	–	–	+	+	–	–	+	+	–
		M196	S	S	–	–	–	–	–	–	+	+	+	+	+	+	+
		M198	S	NV, P	–	–	–	–	–	–	+	+	+	+	+	+	+
		M213	S	S	–	–	+	–	–	–	+	+	+	+	+	+	+
		M219	S	E, P	–	–	+	–	–	–	+	+	+	+	+	+	–
Wang Muang	14	(0)	ND	ND	ND	ND	ND	ND	ND	ND	ND	ND	ND	ND	ND	ND	ND

Notes:
CIP, ciprofloxacin; CN, gentamicin; DA, clindamycin; E, erythromycin; FOX, cefoxitin; I, intermediate sensitivity; K, kanamycin; LZD, linezolid; ND, not determine NV, novobiocin; OX, oxacillin; P, penicillin; R, resistant; RA, rifampin; S, susceptible; TE, tetracycline; spa(X), spa x-region; spa (Ig), spa IgG biding region; –, not found; *S. argenteus* isolates are underlined (M226, M227, M228, M77, M152, M159, M188 and M192).

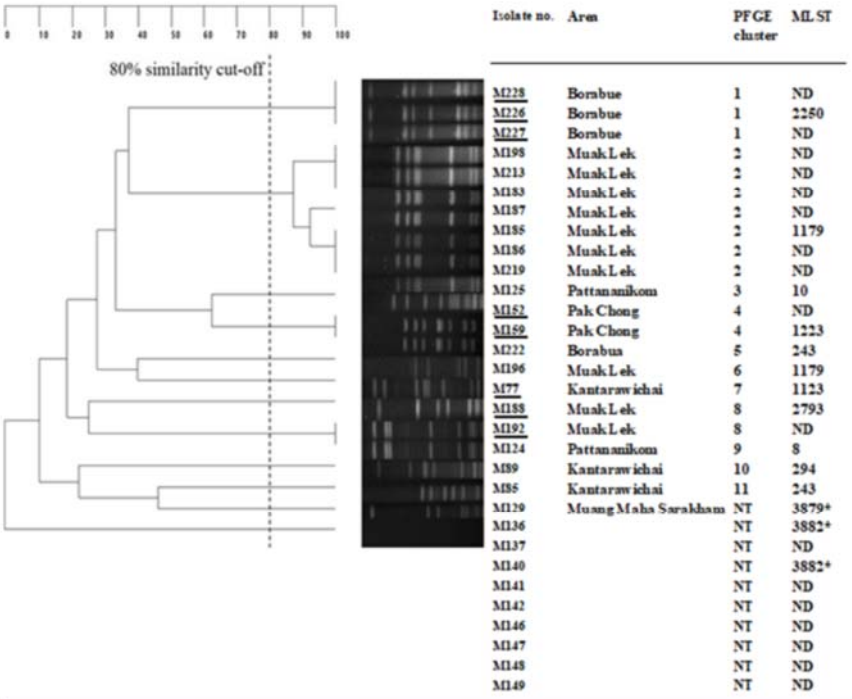

Figure 1 UPGMA Dendrogram derived from *SmaI*—pulsed field gel electrophoresis PFGE) and multilocus sequence types (MLST) of *Staphylococcus aureus* and *Staphylococcus argenteus* (underlined M226, M227, M228, M152, M159, M77, M188 and M192).
Full-size DOI: 10.7717/peerj.6587/fig-1

(they had also different drug resistant patterns), that is, M129, M136 and M140 (Fig. 1) were typed by MLST method to define the STs. The results for allelic numbers and allelic profiles of the STs were derived from the PubMLST database (https://pubmlst.org; University of Oxford, UK and the Wellcome Trust fund). Among the 14 isolates, 12 STs were identified including ST2250 (PFGE cluster 1), ST1179 (PFGE clusters 2 and 6), ST10 (PFGE cluster 3), ST1223 (PFGE cluster 4), ST243 (PFGE clusters 5 and 11), ST 1123 (PFGE cluster 7), ST2793 (PFGE cluster 8), ST8 (PFGE cluster 9), and ST294 (PFGE cluster 10); all of these isolates were susceptible to methicillin (MSSA) except one isolate, M152 (PFGE cluster 4) was resistent to methicillin methicillin-resistant *S. aureus* (MRSA). The three isolates which were PFGE non-typeable had three novel STs, that is, ST3879, ST3882 and ST3883; they were all MRSA. The allelic profiles with the STs and other details of the tested staphylococci are shown in Fig. 1.

NRPS gene amplification

Eight suspected *S. argenteus* isolates which were PFGE cluster 1: ST2250 (M226, M227, M228), PFGE cluster 4, 7: ST1223 (M152, M159, M77) and PFGE cluster 8: ST2793 (M188, M192) (Fig. 1), were confirmed as *S. argenteus* by NRPS gene amplification.

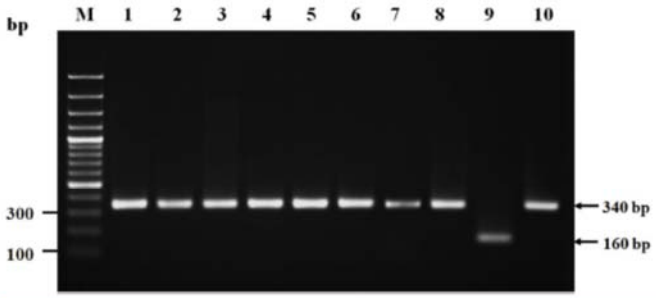

Figure 2 Nonribosomal peptide synthetase (NRPS) gene amplicons of isolated *Staphylococcus argenteus*. Lane M, DNA molecular size ladder; lanes 1–8, PCR amplicons of isolates (suspected to be *S. argenteus*) no. M226, M227, M228, M152, M159, M77, M188 and M192, respectively; lane 9, PCR amplicons of *Staphylococcus aureus* ATCC25923; and lane 10, PCR amplicon of *Staphylococcus argenteus* DS-003. Full-size DOI: 10.7717/peerj.6587/fig-2

The results showed that all of these eight isolates had PCR product of ~340 bp (Fig. 2) which were correlated to the amplicon of the *S. argenteus* control strain but different from the amplicon of *S. aureus* control (~160 bp), indicating that these four bacterial isolates were *S. argenteus*.

Antimicrobial phenotypes of the staphylococcal isolates

The antimicrobial phenotypes of all staphylococcal isolates were determined using the 15 antimicrobial agents. Among the 197 CoNS isolates, resistance to penicillin was the predominant antimicrobial phenotype (126/197; 64%). The percentages of other antimicrobial resistance were novobiocin (78/197; 40%), tetracycline and clindamycin (35/197; 18%), oxacillin (29/197; 15%), erythromycin (27/197; 14%), cefoxitin and kanamycin (25/197; 13%), gentamicin (15/197; 8%), rifampin and sulfamethoxazole plus trimethoprim (12/197; 6%), ciprofloxacin and levofloxacin (9/197; 5%), and linezolid (2/197; 1%) (Table 2). None of the CoNS isolates was resistant to teicoplanin. There were 25 (13%) of the 197 CoNS that were resistant to methicillin (MR-CoNS) while 172 (87%) were sensitive (MS-CoNS). Of the 25 MR-CoNS isolates, five were from Kaeng Khoi district and seven from Muak Lek district of Saraburi province, eight from Muang district and one from Kantarawichai district of Maha Sarakham province, two from Pak-Chong district of Nakorn Ratchasima province, and two from Pattananikom district of Lopburi province.

Penicillin resistance was also the most prevalent antimicrobial-resistance phenotype of the 24 *S. aureus* isolates (58%); followed in falling order of percentage by novobiocin (65%), gentamicin, cefoxitin, oxacillin, rifampin and tetracycline (43%), erythromycin, clindamycin and kanamycin (36%), and linezolid (11%). No bacterial isolates were resistant to ciprofloxacin, levofloxacin, sulfamethoxazole plus trimethoprim, or teicoplanin. There were 11/24 (46%) MRSA isolates.

Seven *S. argenteus* isolates were MSSA and one isolate was MRSA (M152). Among them, three isolates (M226, M227, M228) was susceptible to all antibiotics; four isolates

were resistant to penicillin (M77, M152, M188 and M198) and novobiocin (M152, M159, M188 and M192), and one isolate (M188) was resistant to tetracycline (Table 2).

Prevalence of virulence genes

Enterotoxin (SE) and TSST-1 genes were PCR-amplified for the 24 *S. aureus* and eight *S. argenteus* isolates. A total of 21 *S. aureus* isolates (88%) detected at least one SE gene and 11 isolates (55%) detected the *tsst*. The most prevalent SE gene was *sec* (79%), followed by *sed* (71%), *sea* (21%) and *see* (8%) (Table 2). No isolates detected the *seb* gene. Among the eight *S. argenteus* isolates, M77, M188 and M228 had *sed,* M226, M227 and M228 detected *sec*, M152 detected *see*, while M159 did not have any of the SE genes. One of the *S. argenteus* isolates detected *tsst* (M152) and three *S. argenteus* detected *pvl* (M226, M227 and M228).

All 24 *S. aureus* and eight *S. argenteus* isolates (100%) detected *coa, clfA* and *spa* (X-region). All *S. aureus* isolates detected *spa* (IgG biding region), 23 (96%) isolates detected *pvl* and *hla*, and 17 (71%) isolates detected *hlb*. Of note, all *S. aureus* isolates detected at least one type of hemolysin gene (Table 2). In *S. argenteus* group, M226, M228, M77 and M188 detected *hla*; M77 detected *hlb*; M226, M227, M228, M152 and M159 detected *spa* (IgG biding region).

Comparative analysis of the prevalence of virulence genes between MRSA and MSSA isolates using the Chi-square and Fisher's exact test revealed that MRSA isolates possessed significantly higher prevalence of *sed* and *tsst* than the MSSA counterpart ($p = 0.022$ and 0.004, respectively).

DISCUSSION

In recent years, livestock-associated MRSA has been recognized as a novel pathogen of worldwide public health concern, as the bacteria have become a rapidly emerging cause of human infections that are difficult to treat and may lead to fatality. (*Price et al., 2012*; *Kadariya, Smith & Thapaliya, 2014*). Wide focus on epidemiology and control measures of this pathogen are warranted. Staphylococcal bacteria are the predominant cause of CM and SCM in dairy cattle. Asymptomatically infected cows with SCM in the herd may not be recognized and hence left untreated; thus, they serve as a carriage of *the bacteria* that can be transmitted to the other cattle and susceptible persons, as well as creating contaminated environment. Milk from the infected cows impose a potential health hazard to consumers, as it may be a major source of enterotoxigenic *S. aureus* that cause food-borne disease (*Zschock et al., 2005*). *S. aureus* may also be the cause of a serious and potentially fatal invasive disease of humans (*Lowy, 1998*). In Thailand, data are limited concerning the prevalence and incidence of the staphylococcal-associated-SCM among dairy cattle. Limited data are available including one from small-holder dairy farms in a northern province, that is, Chiang-mai, which reported the 36% incidence of SCM, and *S. aureus* was the common bacteria associated with the SCM (*Suriyasathaporn, 2011*). Another study from a northeast province (Khon Kaen) reported that the CoNS-associated SCM was 69% (*Jarassaeng et al., 2012*). More data on the SCM incidence and the associated pathogens, particularly *S. aureus*, CoNS and the newly emerged

S. argenteus, in other provinces/regions of the country where many more dairy farms are located are required, not only for the livestock economic point of view, but also for human health as far as the One Health policy is concern.

This study investigated SCM and the associated staphylococci in as many as 52 dairy farms of the central and northeast provinces of Thailand; thus, making it the largest coverage ever reported in the country. The results showed the average incidence of SCM was 132 from 224 cows (59%), which was higher than the previously reported incidence in Chiang-mai, indicating that *Staphylococcus* spp. is still a problem of infectious BM in Thailand. Among the 229 staphylococcal isolates from the 132 cows with SCM, the majority were CoNS, that is, 197 isolates from 121 cows, suggesting that CoNS are the predominant bacterial pathogens associated with SCM in Thailand. This finding is in agreement with the previous findings in Thailand (*Jarassaeng et al., 2012*), Sweden (*Persson, Nyman & Andersson, 2011*), eastern Algeria (*Bakir, Sabrina & Toufik, 2011*), Dharwad, India (*Kaliwal et al., 2011*), Northwest Iran (*Hosseinzadeh & Saei, 2014*) and Jiangsu Province, China (*Xu et al., 2015*). Although CoNS usually cause infections with less severe symptoms compared to the *S. aureus* infections, they are highly contagious and can be spread readily to other cattle in the herd, other herds, as well as other animals and humans (*Xu et al., 2015*) through direct contact or via the contaminated environmental sources such as manure, bedding, vegetation, ground, forage, water. It is noteworthy also that cows with SCM may experience a reduction in milk yield due to the high SCC and their milk quality is poor also, that is, decreased calcium, inorganic phosphorous, potassium, α-lactalbumin and β-lactoglobulin (*Batavani, Asri & Naebzadeh, 2007*). Besides, the infected cows may turn to succumb severe illness and/or death, if the immune system happened to be affected by co-morbidity or imbalanced homeostasis by any reason.

The population of MRSA and MR-CoNS were found in higher percentage (38%) in this study than the 22% reported from northeast Thailand in 2011 (*Intrakamha et al., 2012*). In addition, the incidence rate of MR-CoNS in Chiang-mai, Northern Thailand, was 10% (*Suriyasathaporn et al., 2012*), while it is 13% in the present study. The increasing trend of MRSA and MR-CoNS in the livestock emphasizes that regular monitoring and surveillance along with developing appropriate preventative and control measures of these highly contagious zoonotic pathogens are warranted.

Multilocus sequence typing is a recognized DNA sequence-based genotyping technique that analyses polymorphisms among housekeeping/conserved genes, or alleles. This technique provides phylogenetic relationships, local diversity, as well as information on the global dissemination of *S. aureus* genes (*Urwin & Maiden, 2003*). In this study, MLST was used to type 11 representative coagulase-positive staphylococcal bacteria from individual PFGE clusters and three PFGE-non-typeable *S. aureus* from different areas of isolation. The four *S. argenteus* isolates that underwent MLST typing yielded ST1223 (isolate no. M77, M159), ST2250 (isolate no. M226) and ST2793 (isolate no. M188) that have previously been identified as *S. argenteus* (*Thaipadungpanit et al., 2015*; *Tong et al., 2015*; *Chantratita et al., 2016*). The results revealed high heterogeneity with 12 STs including nine previously reported STs and three novel STs,

and five clonal complexes (CC); the isolates with different STs and CCs were from different study areas. Some isolates with the same ST were unrelated by PFGE typing. For example, ST1179 isolates belonged to PFGE clusters 2 and 6; ST243 isolates were in clusters 5 and 11. The three novel STs found in this study were MRSA non-typeable PFGE isolates, indicating that molecular variation that gave rise to novel variants/strains occurred within this bacterial lineage (*O'Hara et al., 2016*).

Among the 15 antimicrobial agents tested, *S. aureus*, *S. argenteus* and CoNS showed resistance against 10 agents, that is, cefoxitin, clindamycin, erythromycin, gentamicin, kanamycin, oxacillin, novobiocin, penicillin G, tetracycline and rifampin. The penicillin G-resistance was the most common phenotype, most likely because of the frequent use of this antibiotic for BM therapy in the dairy farms. In contrast, *S. aureus* and *S. argenteus* isolates were 100% susceptible to teicoplanin, ciprofloxacin, levofloxacin and sulfamethoxazole plus trimethoprim, whereas teicoplanin was the only antimicrobial to which all CoNS were susceptible. The emergence of antimicrobial resistance of the *S. aureus*, *S. argenteus* and CoNS isolated from the cow milk may be caused by irresponsible and unnecessary use of antibiotics by farmers/veterinarians (*McKellar, 1998*; *Briyne, 2016*).

Several *S. aureus* isolates produces enterotoxins and TSST-1, which can cause staphylococcal food poisoning and human toxic shock syndrome, respectively (*Zschock et al., 2005*). The toxin may persist in contaminated milk after pasteurization (*Baird-Parker, 2000*; *Asperger & Zangerl, 2003*; *Necidova et al., 2016*). Therefore, even though the milk of these farms are usually pasteurized before sale, they still pose a health hazard risk to the consumers as far as their toxins are concern. From the results of virulence genes detection, *S. aureus* and seven of eight *S. argenteus* isolates carried enterotoxin gene(s), while the *tsst* was found in *S. aureus* and one *S. argenteus*; the situation poses a potential human health hazard.

All bacterial isolates carried *coa*, *clfA* and *spa* (X region). The *spa* is known to be the fundamental virulence gene for *S. aureus* regarding mastitis development and severity. Moreover, 94% of the isolates were positive for *spa* IgG-binding region, whereas *pvl*, *hla* and *hlb* were found in 96, 96 and 71%. These results are conformed to those reported from Germany (*Akineden et al., 2001*). Virulence genes in *S. aureus* and *S. argenteus* are relative to the levels of the bacterial pathogenicity in BM (*Akineden et al., 2001*; *Momtaz, Rahimi & Tajbakhsh, 2010*). Moreover, high prevalence of *pvl*, which has never been reported for *S. aureus* isolates from cow milk in Thailand, was found in this study. This gene encodes for PVL protein, which destroys leukocytes and causes severe necrotic lesions of soft tissues and skin (*Rankin et al., 2005*). This cytotoxin is an important virulence factor in human diseases, such as pneumonitis (*Prashanth et al., 2011*); nevertheless, the role of PVL in BM is not yet known.

The STs identified previously for *S. argenteus* (*Thaipadungpanit et al., 2015*; *Tong et al., 2015*; *Chantratita et al., 2016*) were found also among the *S. argenteus* isolates in this study. They were ST1223, ST2250 and ST2793. These bacterial isolates (seven out of eight) carried also enterotoxin genes, *coa*, *clfA*, *pvl*, *tsst* and *spa* (X and IgG-binding region) indicating their pathogenic potential. This is the first report of NRPS-confirmed *S. argenteus* isolated from BM.

CONCLUSIONS

Both coagulase-positive (*S. aureus* and *S. argenteus*) and coagulase-negative *Staphylococcus* spp. were isolated from 59% of milk samples of cows with SCM in four provinces in central and northeast Thailand, indicating that the staphylococci are still common cause of SCM in many areas of the country. The bacterial isolates showed an increasing trend of methicillin-resistance as well as refractoriness to several other antibiotics. *S. argenteus*, the newly emerged animal and human pathogens were isolated for the first time from milk samples of SCM cows. The coagulase-positive isolates had 11 different PFGE patterns and one non-typeable pattern, of which individual patterns are not related to the multilocus STs. Three new STs were found among the *S. aureus* isolates. All staphylococcal isolates carried several virulence genes indicating their pathogenic potential for both animals and humans. Data gained from this study emphasized the need of the One Health practice for combating and control of staphylococcal infections, which requires participation of many sectors including dairy farmers, veterinarians, medical and public health personnel, scientists, etc. Molecular characteristics of the bacterial isolates reported in this study should be useful for epidemiological tracing of the existing traits as well as for recognizing newly emerged variants.

ABBREVIATIONS

CC	Clonal complex
CIP	Ciprofloxacin
CMT	California Mastitis Test
CN	Gentamicin
CoNS	Coagulase-negative staphylococcus
DA	Clindamycin
E	Erythromycin
FOX	Cefoxitin
I	Intermediate sensitivity
K	Kanamycin
LZD	Linezolid
MLST	Multilocus sequence type(s)/typing
MR-CoNS	Methicillin-resistant coagulase-negative staphylococci
MRSA	Methicillin-resistant *Staphylococcus aureus*
MSSA	Methicillin-susceptible *Staphylococcus aureus*
ND	Not determine
NV	Novobiocin
OX	Oxacillin
P	Penicillin
PFGE	Pulsed-field gel electrophoresis
PVL	Panton-Valentine leucocidin
R	Resistant (-ce)
RA	Rifampin

S	Susceptible
SCC(s)	Somatic cell counts
SE(s)	Staphylococcal enterotoxin(s)
ST(s)	Sequence type(s)
TE	Tetracycline
TSST-1	Toxic shock syndrome toxin 1
tsst	TSST-1 gene
spa (x)	Spa (x-region)
spa (Ig)	spa IgG biding region
UPGMA	Unweighted pair group method with arithmetic average.

ACKNOWLEDGEMENTS

The authors thank Dr. Satitpong Promsatit, Saraburi Provincial Livestock Office, Department of Livestock Development, Ministry of Agriculture and Cooperatives, Saraburi province, Thailand, for his kind cooperation in the field work.

ADDITIONAL INFORMATION AND DECLARATIONS

Funding

This work was supported by the Thailand Research Fund (grant no. RSA5980048) to Nitaya Indrawattana. The funders had no role in study design, data collection and analysis, decision to publish, or preparation of the manuscript.

Grant Disclosure

The following grant information was disclosed by the authors:
Thailand Research Fund: RSA5980048.

Competing Interests

The authors declare that they have no competing interests.

Author Contributions

- Natapol Pumipuntu conceived and designed the experiments, performed the experiments, analyzed the data, prepared figures and/or tables.
- Witawat Tunyong performed the experiments.
- Narisara Chantratita contributed reagents/materials/analysis tools.
- Pornphan Diraphat analyzed the data.
- Pornpan Pumirat analyzed the data.
- Nitat Sookrung analyzed the data, contributed reagents/materials/analysis tools.
- Wanpen Chaicumpa analyzed the data, contributed reagents/materials/analysis tools, authored or reviewed drafts of the paper, approved the final draft.
- Nitaya Indrawattana conceived and designed the experiments, performed the experiments, analyzed the data, contributed reagents/materials/analysis tools, prepared figures and/or tables, authored or reviewed drafts of the paper, approved the final draft.

Animal Ethics

The following information was supplied relating to ethical approvals (i.e., approving body and any reference numbers):

All animal procedures were approved by the Faculty of Tropical Medicine–Animal Care and Use Committee (FTM-ACUC), Mahidol University, Thailand (Reference number FTM-ACUC 002/2016).

Data Availability

The following information was supplied regarding data availability:

The raw data of gel from PFGE analysis is provided in Figure S1.

Supplemental Information

Supplemental information for this article can be found online at http://dx.doi.org/10.7717/peerj.6587#supplemental-information.

REFERENCES

Abebe R, Hatiya H, Abera M, Megersa B, Asmare K. 2016. Bovine mastitis: prevalence, risk factors and isolation of *Staphylococcus aureus* in dairy herds at Hawassa milk shed, South Ethiopia. *BMC Veterinary Research* **12(1)**:270 DOI 10.1186/s12917-016-0905-3.

Akineden Ö, Annemüller C, Hassan AA, Lämmler C, Wolter W, Zschöck M. 2001. Toxin genes and other characteristics of *Staphylococcus aureus* isolates from milk of cows with mastitis. *Clinical and Vaccine Immunology* **8(5)**:959–964 DOI 10.1128/CDLI.8.5.959-964.2001.

Aslantas O, Demir C, Turutoglu H, Cantekin Z, Ergun Y, Dogruer G. 2007. Coagulase gene polymorphism of *Staphylococcus aureus* isolated form subclinical mastitis. *Turkish Journal of Veterinary and Animal Sciences* **31**:253–257.

Asperger H, Zangerl P. 2003. *Staphylococcus aureus*. In: Roginski H, Fuquay J, Fox P, eds. *Encyclopedia of Dairy Science*. San Diego: Academic Press, 2563–2569.

Baird-Parker T. 2000. *Staphylococcus aureus*. In: Lund B, Baird-Parker T, Gould G, eds. *The Microbiological Safety and Quality of Food*. Gaithersburg: Aspen Publishers, 1317–1330.

Bakir M, Sabrina R, Toufik M. 2011. Antibacterial susceptibility profiles of sub-clinical mastitis pathogens isolated from cows in Batna and Setif governorates (East of Algeria). *Veterinary World* **4(12)**:537–541 DOI 10.5455/vetworld.2011.537-541.

Batavani RA, Asri S, Naebzadeh H. 2007. The effect of subclinical mastitis on milk composition in dairy cows. *Iranian Journal of Veterinary Research* **8(3)**:205–211 DOI 10.22099/IJVR.2007.925.

Becker K, Friedrich AW, Lubritz G, Weilert M, Peters G, Von Eiff C. 2003. Prevalence of genes encoding pyrogenic toxin superantigens and exfoliative toxins among strains of *Staphylococcus aureus* isolated from blood and nasal specimens. *Journal of Clinical Microbiology* **41(4)**:1434–1439 DOI 10.1128/JCM.41.4.1434-1439.2003.

Briyne ND. 2016. Veterinary attitudes towards antimicrobial resistance. *Veterinary Record* **179(3)**:66–67 DOI 10.1136/vr.i3792.

Chantratita N, Wikraiphat C, Tandhavanant S, Wongsuvan G, Ariyaprasert P, Suntornsut P, Thaipadungpanit J, Teerawattanasook N, Jutrakul Y, Srisurat N, Chaimanee P, Anukunananchai J, Phiphitaporn S, Srisamang P, Chetchotisakd P, West TE, Peacock SJ. 2016. Comparison of community-onset *Staphylococcus argenteus* and *Staphylococcus aureus* sepsis in Thailand: a prospective multicentre observational study. *Clinical Microbiology and Infection* **22(5)**:458.e11–458.e19 DOI 10.1016/j.cmi.2016.01.008.

CLSI. 2016. *Performance standards for antimicrobial susceptibility testing; Twentieth informational supplement CLSI document M100-S20.* Wayne: Clinical and Laboratory Standard Institute.

Djabri B, Bareille N, Beaudeau F, Seegers H. 2002. Quarter milk somatic cell count in infected dairy cows: a meta-analysis. *Veterinary Research* **33(4)**:335–357 DOI 10.1051/vetres:2002021.

El-Sayed A, Alber J, Limmler C, Bonner B, Huhn A, Kaleta EF, Zschech M. 2005. PCR-based detection of genes encoding virulence determinants in *Staphylococcus aureus* from birds. *Journal of Veterinary Medicine, Series B* **52(1)**:38–44 DOI 10.1111/j.1439-0450.2004.00814.x.

Enright MC, Day NPJ, Davies CE, Peacock SJ, Spratt BG. 2000. Multilocus sequence typing for characterization of methicillin-resistant and methicillin-susceptible clones of *Staphylococcus aureus*. *Journal of Clinical Microbiology* **38(3)**:1008–1015.

Fre´nay HM, Bunschoten AE, Schouls LM, van Leeuwen WJ, Vandenbroucke-Grauls CM, Verhoef J, Mooi FR. 1996. Molecular typing of methicillin-resistant *Staphylococcus aureus* on the basis of protein a gene polymorphism. *European Journal of Clinical Microbiology & Infectious Diseases* **15(1)**:60–64 DOI 10.1007/BF01586186.

Harmon RJ. 1994. Physiology of mastitis and factors affecting somatic cell counts. *Journal of Dairy Science* **77**:2103–2112 DOI 10.3168/jds.S0022-0302(94)77153-8.

Holt DC, Holden MT, Tong SY, Castillo-Ramirez S, Clarke L, Quail MA, Currie BJ, Parkhill J, Bentley SD, Feil EJ, Giffard PM. 2011. A very early-branching *Staphylococcus aureus* lineage lacking the carotenoid pigment staphyloxanthin. *Genome Biology and Evolution* **3**:881–895 DOI 10.1093/gbe/evr078.

Hosseinzadeh S, Saei HD. 2014. Staphylococcal species associated with bovine mastitis in the North West of Iran: emerging of coagulase-negative staphylococci. *International Journal of Veterinary Science and Medicine* **2(1)**:27–34 DOI 10.1016/j.ijvsm.2014.02.001.

Indrawattana N, Pumipuntu N, Suriyakhun N, Jangsangthong A, Kulpeanprasit S, Chantratita N, Sookrung N, Chaicumpa W, Buranasinsup S. 2018. *Staphylococcus argenteus* from rabbits in Thailand. *Microbiology Open* **21**:e00665 DOI 10.1002/mbo3.665.

Indrawattana N, Sungkhachat O, Sookrung N, Chongsa-nguan M, Tungtrongchitr A, Voravuthikunchai SP, Kong-ngoen T, Kurazono H, Chaicumpa W. 2013. *Staphylococcus aureus* clinical isolates: antibiotic susceptibility, molecular characteristics, and ability to form biofilm. *Biomedical Research International* **2013**:314654 DOI 10.1155/2013/314654.

Intrakamha M, Komutarin T, Pimpakdee K, Aengwanich W. 2012. Incidence of enterotoxin-producing MRSA in bovine mastitis cases, bulk milk tanks and processing plants in Thailand. *Journal of Animal and Veterinary Advances* **11(5)**:655–661 DOI 10.3923/javaa.2012.655.661.

Islam MA, Islam MZ, Islam MA, Rahman MS, Islam MT. 2011. Prevalence of subclinical mastitis in dairy cows in selected areas of Bangladesh. *Bangladesh Journal of Veterinary Medicine* **9(1)**:73–78 DOI 10.3329/bjvm.v9i1.11216.

Jarassaeng CS, Aiumlamai C, Wachirapakorn M, Techakumphu Jos PTM, Noordhuizen AC, Beynen AC, Suadsong S. 2012. Risk factors of subclinical mastitis in small holder dairy cows in Kohn Kaen Province, Thailand. *Thai Journal of Veterinary Medicine* **42(2)**:143–151.

Jarraud S, Mougel C, Thioulouse J, Lina G, Meugnier H, Forey F, Nesme X, Etienne J, Vandenesch F. 2002. Relationships between *Staphylococcus aureus* genetic background, virulence factors, agr groups (alleles), and human disease. *Infection and Immunity* **70(2)**:631–641 DOI 10.1128/IAI.70.2.631-641.2002.

Kadariya J, Smith TC, Thapaliya D. 2014. *Staphylococcus aureus* and staphylococcal food-borne disease: an ongoing challenge in public health. *BioMed Research International* **2014**:827965 DOI 10.1155/2014/827965.

Kaliwal BB, Sadashiv SO, Kurjogi MM, Sanakal RD. 2011. Prevalence and antimicrobial susceptibility of coagulase-negative staphylococci isolated from bovine mastitis. *Veterinary World* **4**(**4**):158–161.

Kehrli ME Jr, Shuster DE. 1994. Factors affecting milk somatic cells and their role in health of the bovine mammary gland. *Journal of Dairy Science* **77**(**2**):619–627 DOI 10.3168/jds.S0022-0302(94)76992-7.

Kibebew K. 2017. Bovine mastitis: a review of causes and epidemiological point of view. *Journal of Biology, Agriculture and Healthcare* **7**(**2**):2017.

Lowy FD. 1998. Medical progress: *Staphylococcus aureus* infections. *New England Journal of Medicine* **339**(**8**):520–532.

McKellar QA. 1998. Antimicrobial resistance: a veterinary perspective: antimicrobials are important for animal welfare but need to be used prudently. *BMJ* **317**(**7159**):610–611 DOI 10.1136/bmj.317.7159.610.

Momtaz H, Rahimi E, Tajbakhsh E. 2010. Detection of some virulence factors in *Staphylococcus aureus* isolated from clinical and subclinical bovine mastitis in Iran. *African Journal of Biotechnology* **9**(**25**):3753–3758.

National Mastitis Council (U.S.), Research Committee, Oliver SP, National Mastitis Council (U.S.). 2004. *Microbiological procedures for the diagnosis of bovine udder infection and determination of milk quality.* Fourth Edition. Verona: NMC. *Available at https://trove.nla.gov.au/version/44357531.*

Necidova L, Bogdanovicova K, Harustiakova D, Bartova K. 2016. Short communication: pasteurization as a means of inactivating staphylococcal enterotoxins A, B, and C in milk. *Journal of Dairy Science* **99**(**11**):8638–8643 DOI 10.3168/jds.2016-11252.

O'Hara FP, Suaya JA, Ray GT, Baxter R, Brown ML, Mera RM, Close NM, Thomas E, Amrine-Madsen H. 2016. *spa* Typing and multilocus sequence typing show comparable performance in a macroepidemiologic study of *Staphylococcus aureus* in the United States. *Microbial Drug Resistance* **22**(**1**):88–96 DOI 10.1089/mdr.2014.0238.

Östensson K, Hageltorn M, Aström G. 1988. Differential cell couting in fraction-collected milk from dairy cows. *Acta Veterinaria Scandinavia* **29**:493–500 DOI 10.1016/j.smallrumres.2011.05.005.

Persson Y, Nyman AKJ, Andersson UG. 2011. Etiology and antimicrobial susceptibility of udder pathogens from cases of subclinical mastitis in dairy cows in Sweden. *Acta Veterinaria Scandinavica* **53**(**1**):36 DOI 10.1186/1751-0147-53-36.

Philpot WN, Nickerson SC. 1999. *Mastitis: Counter attack.* Illinois: Westfalia Surge LLC.

Prashanth K, Rao KR, Reddy PV, Saranathan R, Makki AR. 2011. Genotypic characterization of *Staphylococcus aureus* obtained from humans and bovine mastitis samples in India. *Journal of Global Infectious Diseases* **3**(**2**):115–122 DOI 10.4103/0974-777X.81686.

Price LB, Stegger M, Hasman H, Lance BP, Stegger M, Hasman H, Aziz M, Larsen J, Andersen PS, Pearson T, Waters AE, Foster JT, Schupp J, Gillece J, Driebe E, Liu CM, Springer B, Zdovc I, Battisti A, Franco A, Żmudzki J, Schwarz S, Butaye P, Jouy E, Pomba C, Porrero MC, Ruimy R, Smith TC, Robinson DA, Weese JS, Arriola CS, Yu F, Laurent F, Keim P, Skov R, Aarestrup FM. 2012. *Staphylococcus aureus* CC398: host adaptation and emergence of methicillin resistance in livestock. *MBio* **3**(**1**):pii:e00305-11 DOI 10.1128/mBio.00305-11.

Rankin S, Roberts S, O'Shea K, Maloney D, Lorenzo M, Benson CE. 2005. Panton Valentine leukocidin (PVL) toxin positive MRSA strains isolated from companion animals. *Veterinary Microbiology* **108(1–2)**:145–148 DOI 10.1016/j.vetmic.2005.02.013.

Rollin E, Dhuyvetter KC, Overton MW. 2015. The cost of clinical mastitis in the first 30 days of lactation: an economic modeling tool. *Preventive Veterinary Medicine* **122(3)**:254–264 DOI 10.1016/j.prevetmed.2015.11.006.

Schuster D, Rickmeyer J, Gajdiss M, Thye T, Lorenzen S, Reif M, Josten M, Szekat C, Melo LDR, Schmithausen RM, Liégeois F, Sahl HG, Gonzalez JJ, Nagel M, Bierbaum G. 2017. Differentiation of *Staphylococcus argenteus* (formerly: *Staphylococcus aureus* clonal complex 75) by mass spectrometry from *S. aureus* using the first strain isolated from a wild African great ape. *International Journal of Medical Microbiology* **307(1)**:57–63 DOI 10.1016/j.ijmm.2016.11.003.

Schwarz US, Diesterbeck K, Failing S, König K, Brügemann M, Zschöck W, Wolter W, Czerny CP. 2010. Somatic cell counts and bacteriological status in quarter foremilk samples of cows in Hesse, Germany—A longitudinal study. *Journal of Dairy Science* **93(12)**:5716–5728 DOI 10.3168/jds.2010-3223.

Seki K, Sakurada J, Seong HK, Murai M, Tachi H, Ishii H, Masuda S. 1998. Occurrence of coagulase serotype among *Staphylococcus aureus* strains isolated from healthy individuals-special reference to correlation with size of protein-A gene. *Microbiology and Immunology* **42(5)**:407–409 DOI 10.1111/j.1348-0421.1998.tb02302.x.

Suriyasathaporn W. 2011. Epidemiology of subclinical mastitis and their antibacterial susceptibility in small holder dairy farms, Chiang Mai province, Thailand. *Journal of Animal and Veterinary Advances* **10(3)**:316–321 DOI 10.3923/javaa.2011.316.321.

Suriyasathaporn W, Chupia V, Sing-Lah T, Wongsawan K, Mektrirat R, Chaisri W. 2012. Increases of antibiotic resistance in excessive use of antibiotics in smallholder dairy farms in northern Thailand. *Asian Australasian Journal of Animal Sciences* **25(9)**:1322–1328 DOI 10.5713/ajas.2012.12023.

Thaipadungpanit J, Amornchai P, Nickerson EK, Wongsuvan G, Wuthiekanun V, Limmathurotsakul D, Peacock SJ. 2015. Clinical and molecular epidemiology of *Staphylococcus argenteus* infections in Thailand. *Journal of Clinical Microbiology* **53(3)**:1005–1008 DOI 10.1128/JCM.03049-14.

Tong SYC, Schaumburg F, Ellington MJ, Corander J, Pichon B, Leendertz F, Bentley DS, Parkhill J, Holt CD, Peters G, Giffard MP. 2015. Novel staphylococcal species that form part of a *Staphylococcus aureus*-related complex: the non-pigmented *Staphylococcus argenteus* sp. nov. and the non-human primate-associated *Staphylococcus schweitzeri* sp. nov. *International Journal of Systematic and Evolutionary Microbiology* **65(Pt 1)**:15–22 DOI 10.1099/ijs.0.062752-0.

Tristan A, Ying L, Bes M, Etienne J, Vandenesch F, Lina G. 2003. Use of multiplex PCR to identify *Staphylococcus aureus* adhesins involved in human hematogenous infections. *Journal of Clinical Microbiology* **41(9)**:4465–4467 DOI 10.1128/JCM.41.9.4465-4467.2003.

Urwin R, Maiden MCJ. 2003. Multi-locus sequence typing: a tool for global epidemiology. *Trends in Microbiology* **11(10)**:479–487 DOI 10.1016/j.tim.2003.08.006.

White D, Walmsley M, Liew A, Claycomb R, Mein G. 2005. Chemical and rheological aspects of gel formation in the California Mastitis Test. *Journal of Dairy Research* **72(1)**:115–121 DOI 10.1017/s0022029904000561.

Wu D, Li X, Yang Y, Zheng Y, Wang C, Deng L, Liu L, Li C, Shang Y, Zhao C, Yu S, Shen X. 2011. Superantigen gene profiles and presence of exfoliative toxin genes in community-acquired

methicillin-resistant *Staphylococcus aureus* isolated from Chinese children. *Journal of Medical Microbiology* **60(1)**:35–45 DOI 10.1099/jmm.0.023465-0.

Xu J, Tan X, Zhang X, Xia X, Sun H. 2015. The diversities of staphylococcal species, virulence and antibiotic resistance genes in the subclinical mastitis milk from a single Chinese cow herd. *Microbial Pathogenesis* **88**:29–38 DOI 10.1016/j.micpath.2015.08.004.

Zhang D, Xu X, Song Q, Bai Y, Zhang Y, Song M, Shi C, Shi X. 2016. Identification of *Staphylococcus argenteus* in Eastern China based on nonribosomal peptide synthetase (NRPS) gene. *Future Microbiology* **11**:1113–1121 DOI 10.2217/fmb-2016-0017.

Zschock M, Kloppert B, Wolter W, Hamann HP, Lammler CH. 2005. Pattern of enterotoxin genes *seg, seh, sei* and *sej* positive *Staphylococcus aureus* isolated from bovine mastitis. *Veterinary Microbiology* **108(3–4)**:243–249 DOI 10.1016/j.vetmic.2005.02.012.

Received: 4 April 2018 | Revised: 6 May 2018 | Accepted: 8 May 2018

DOI: 10.1002/mbo3.665

ORIGINAL ARTICLE

WILEY MicrobiologyOpen

Staphylococcus argenteus from rabbits in Thailand

Nitaya Indrawattana[1] | Natapol Pumipuntu[2] | Nawarat Suriyakhun[3] | Arunee Jangsangthong[4] | Suphang Kulpeanprasit[1] | Narisara Chantratita[1] | Nitat Sookrung[5] | Wanpen Chaicumpa[6] | Shutipen Buranasinsup[4]

[1]Department of Microbiology and Immunology, Faculty of Tropical Medicine, Mahidol University, Bangkok, Thailand

[2]Office of Academic Affairs, Faculty of Veterinary Science, Mahasarakham University, Maha Sarakham, Thailand

[3]Prasu-Arthorn Animal Hospital, Faculty of Veterinary Science, Mahidol University, Nakhon Pathom, Thailand

[4]Department of Pre-Clinic and Applied Animal Science, Faculty of Veterinary Science, Mahidol University, Nakornpathom, Thailand

[5]Laboratory for Research and Technology Development, Faculty of Medicine, Siriraj Hospital, Mahidol University, Bangkok, Thailand

[6]Center of Excellence on Therapeutic Proteins and Antibody Engineering, Department of Parasitology, Faculty of Medicine, Siriraj Hospital, Mahidol University, Bangkok, Thailand

Correspondence
Shutipen Buranasinsup, Department of Pre-Clinic and Applied Animal Science, Faculty of Veterinary Science, Mahidol University, Nakornpathom 73710, Thailand.
Email: shutipen.bur@mahidol.ac.th

Funding Information
Annual Research Fund of the Faculty of Veterinary Science, Mahidol University 2014; Thailand Research Fund, Grant/Award Number: RSA5980048

Abstract

Staphylococcus argenteus, a novel species of the genus *Staphylococcus* or a member of the *S. aureus* complex, is closely related to *S. aureus* and is usually misidentified. In this study, the presence of *S. argenteus* in isolated *S. aureus* was investigated in 67 rabbits with abscess lesions during 2014–2016. Among 19 *S. aureus* complex isolates, three were confirmed to be *S. argenteus* by matrix-assisted laser desorption/ionization time-of-flight mass spectrometry, nonribosomal peptide synthetase gene amplification, and multilocus sequence type. All *S. aureus* complex isolates, including the *S. aureus* isolates, were examined for their antimicrobial resistance phenotype by disk diffusion and for their resistance genotype by PCR assays. Among the *S. argenteus* isolates, one was susceptible to all antimicrobial drugs and the other two were resistant to penicillin and doxycycline. In contrast, most *S. aureus* isolates were resistant to penicillin (37.5%), and gentamicin (12.5%). Moreover, *S. aureus* isolates harbored the *blaZ*, *mecA*, *aacA-aphD*, and *mrs(A)* as well as mutations of *gyrA* and *grlA*, but *S. argenteus* isolates carried solely the *blaZ*. *S. argenteus* isolates were investigated for enterotoxin (*sea-sed*) and virulence genes by PCR. One isolate carried *sea*, *sec*, and *sed*, whereas the other two isolates carried only *sea* or *sed*. No isolate carried *seb* and *see*. All three *S. argenteus* isolates carried *hla*, *hlb*, and *clfA*, followed by *pvl*, whereas *coa*, *spa* (IgG-binding region), and *spa* (x region) were not detected in the three isolates. This paper presents the first identification of *S. argenteus* from rabbits in Thailand. *S. argenteus* might be pathogenic because the isolates carried virulence genes. Moreover, antimicrobial resistance was observed. Investigations of this new bacterial species should be conducted in other animal species as well as in humans.

KEYWORDS
antimicrobial resistance, antimicrobial resistance genes, rabbit, *Staphylococcus argenteus*, *Staphylococcus aureus*, *Staphylococcus aureus* complex

1 | INTRODUCTION

The *Staphylococcus aureus* complex consists of opportunistic pathogens that can cause a wide spectrum of diseases in both humans and animals (Corpa et al., 2009). These pathogens are nonspore-forming, nonmotile, spherical organisms, appearing as grapelike clusters under a microscope. They are facultatively anaerobic, catalase-positive (Foster & Geoghegan, 2015), coagulase-positive and can produce

protein A. In rabbits, infection with the *S. aureus* complex usually results in small dermal lesions; the invasion of subcutaneous tissue and the development of pododermatitis, subcutaneous abscesses, and mastitis. Abscesses in internal organs are sometimes observed, such as in the lungs, liver, and uterus. This gives rise to poor reproductive results, infertility, and death (Corpa et al., 2009; Vancraeynest et al., 2004; Viana et al., 2007).

Recently, a novel coagulase-positive *Staphylococcus* species, *S. argenteus* (*S. aureus* complex), was identified from clinical human and animal sources (Argudín et al., 2016; Chantratita et al., 2016; Schuster et al., 2017; Thaipadungpanit et al., 2015; Tong et al., 2015). Bacterial colonies were characterised by a nonpigmented, creamy white appearance and showed β-hemolysis on blood agar. Moreover, the bacteria were shown to be gram-positive cocci in clusters and gave positive results in the catalase and coagulase tests, which are characteristic findings for *S. aureus* (Tong et al., 2015). Therefore, routine diagnostic analyses can lead to *S. argenteus* being misidentified as *S. aureus*. Moreover, identification by molecular methods, such as 16S rRNA sequencing, cannot differentiate *S. argenteus* from *S. aureus* (Tong et al., 2015). Other molecular techniques, such as matrix-assisted laser desorption/ionization time-of-flight mass spectrometry (MALDI-TOF MS), nonribosomal peptide synthetase (NRPS) gene amplification, and multilocus sequence type (MLST) determination, were thus recommended in many publications as tools for the identification of *S. argenteus* (Chantratita et al., 2016; Schuster et al., 2017; Zhang et al., 2016). Some sequencing types of *S. aureus* were previously confirmed to be *S. argenteus*, such as ST2793, ST1223, and ST2250 (Chantratita et al., 2016; Schuster et al., 2017; Thaipadungpanit et al., 2015; Tong et al., 2015).

The aim of this study was to characterize *S. argenteus* and *S. aureus* isolated from rabbits with clinical abscesses.

2 | MATERIALS AND METHODS

2.1 | Specimen collection and bacterial isolation

Sixty-seven pus samples were collected from rabbits with clinical abscesses by a veterinarian at Prasu-Arthorn Animal Hospital, Thailand, during 2014–2016. They were transported to a microbiological laboratory within 24 hr after collection. Individual samples were inoculated on sheep blood and mannitol salt agar (Oxoid, Basingstoke, UK) and incubated at 37°C for 24–48 hr. After incubation, the suspected bacterial colonies were selected and identified by conventional methods, including Gram staining, catalase, mannitol fermentation, coagulase (Ramel; Oxoid), and commercial latex agglutination (Dryspot Staphytect Plus; Oxoid), to detect protein A for *S. aureus* identification. This study was approved by The Faculty of Veterinary Science Animal Care and Use Committee, Mahidol University (protocol number MUVS-2013-35).

2.2 | *S. argenteus* identification

2.2.1 | MALDI-TOF MS

Mass spectra were generated using a MALDI Biotyper 3.0 Ultraflex platform (Bruker Daltonics, Massachusetts, USA). For individual suspected *S. argenteus* isolates, with white colonies, 1 ml of crude protein extract or one colony was deposited on a 96-spot polished steel target plate (Bruker Daltonics), air-dried and covered with 1 ml of HCCA matrix solution (Bruker Daltonics) (Kolecka et al., 2013). As a positive control and calibration reference, 1 ml of Bacterial Test Standard (Bruker Daltonics) was used. The main spectrum was acquired using the MALDI Biotyper Automated Flex Control software v.3.0 (Bruker Daltonics). The identification of isolates was performed using the Bruker database and in-house databases from Chantratita et al. (2016) and Moradigaravand et al. (2017).

2.2.2 | NRPS gene amplification

Primer sequences and the PCR protocol for NRPS gene indels were in accordance with those of Zhang et al. (2016). The NRPS gene was amplified in a total reaction volume of 25 μl. The PCR reaction was performed using the thermal cycles (Bio-Rad, California, USA) with initial denaturation at 94°C for 4 min, followed by 35 cycles of 94°C for 30 s, 53°C for 30 s, and 72°C for 40 s and then final extension at 72°C for 10 min. Individual PCR amplicons were purified using the GenepHlow™ Gel/PCR purification kit (Geneaid, New Taipei, Taiwan) and submitted for sequencing. DNA sequences were analyzed for similarity with the GenBank database.

2.2.3 | MLST

MLST was used to analyze the suspected *S. argenteus* isolates through the amplification of seven *S. aureus* housekeeping genes, by a method developed by Enright *et al.* (2000) at Imperial College London for analyzing a query profile for MLST. Before sequencing, individual PCR amplicons were purified using the GenepHlow™ Gel/PCR purification kit (Geneaid). The allelic number queries and sequence types (STs) obtained from trimmed DNA sequencing results for seven genes were determined using the online *S. aureus* MLST database (https://pubmlst.org/saureus/). The suspected novel alleles or queried allelic profiles of novel STs that did not match the database were submitted to the curator of PubMLST (https://pubmlst.org/saureus/) to check and assign a novel allele or novel ST number.

2.3 | Antimicrobial susceptibility testing

Antimicrobial susceptibility testing and interpretation were performed by the disk diffusion in according to the Clinical and Laboratory Standards Institute (2012). A total of 13 antimicrobial drugs were tested: amikacin (30 μg), azithromycin (15 μg), cefazolin (30 μg), cefoxitin (30 μg), ceftriaxone (30 μg), chloramphenicol (30 μg), ciprofloxacin (5 μg), doxycycline (30 μg), gentamicin (10 μg),

moxifloxacin (5 μg), norfloxacin (10 μg), penicillin (10 units), and trimethoprim/sulfamethoxazole (1.25 μg/23.75 μg). *S. aureus* ATTC®25923 was used as the control strain.

2.4 | Detection of 16s rRNA, antimicrobial resistance, and enterotoxin and virulence genes

All isolated *S. aureus* samples were prepared for genomic DNA extraction using a DNA extraction kit (Geneaid). The extraction protocol involved the measurement of the OD 260/280 nm ratio using a spectrophotometer. Amplification with specific oligonucleotide primers was performed for 16s rRNA of the *S. aureus* complex group (McClure et al., 2006) and eight antimicrobial resistance genes representative of each antibiotic drug group: *blaZ* (Gómez-Sanz et al., 2010) and *mecA* (Vancraeynest et al., 2004) for β-lactam resistance, *aacA-aphD* (Laplana et al., 2007) for aminoglycoside resistance, *msr(A)* (Gómez-Sanz et al., 2010) for macrolide resistance, *tet(K)* (Vancraeynest et al., 2004) for tetracycline resistance, *dfrG* (Lagier et al., 2009) for trimethoprim resistance, and *cfr* (Kehrenberg & Schwarz, 2006) for chloramphenicol resistance. PCR amplification for determined fluoroquinolone resistance, namely *gyrA* and *grlA* (Ihara et al., 2006) was performed. The PCR amplicon, namely the QRDR region, was sequenced and analyzed for resistance determining mutations. Deduced amino acid sequences of the PCR amplicons were analyzed using the GenBank database with accession numbers AAC31138.1 for *gyrA* and WP075108737.1 for *grlA*. The PCR reaction mixture was subjected to the following thermal cycling conditions using Flexcycler² (Analytik Jena, Überlingen, Germany): 5 min of 95°C; then 30 cycles of amplification with denaturing at 95°C for 30 s, annealing at a temperature specific for each primer for 30 s and extension at 72°C for 60 s; followed by a final extension at 72°C for 10 min.

In *S. argenteus* isolates, further identification of the virulence genes was performed, including classical enterotoxin (*sea*, *seb*, *sec*, *sed*, and *see*) (Wu et al., 2011), hemolysin (*hla* and *hlb*) (Jarraud et al., 2002), clumping factor (*clfA*) (Tristan et al., 2003), protein A [*spa* x region (Frénay et al., 1996) and *spa* IgG-binding region (Seki et al., 1998)], coagulase (*coa*) (Aslantas et al., 2007), and Panton-Valentine leukocidin (*pvl*) (Jarraud et al., 2002), with specific oligonucleotide primers. PCR reactions were performed, involving initial denaturation at 95°C for 10 min; 35 cycles of 95°C for 30 s, 55°C for 30 s, and 72°C for 30 s and a final extension at 72°C for 10 min.

PCR amplicons were analyzed using 1.5% agarose gel electrophoresis and SYBR safe (Invitrogen, New York, USA) staining. The DNA bands were observed under a UV tranzilluminator (UVP Bioimaging System; Invitrogen). Control bacteria for the PCR included the strains *S. aureus* ATCC 19095 (*sea* and *sec*), ATCC 14458 (*seb*), ATCC 23235 (*sed*), ATCC 27664 (*see*), ATCC 13565 (*coa*, *clfA*, *hla*, *hlb*, *spa* x region, and *spa* IgG-binding region) and laboratory control strains, which were sequenced and analyzed as accession numbers KX371630.1 (*pvl*). For gene amplification with no reference control, the PCR product from positive samples was subjected to nucleotide sequencing and sequence analysis for gene confirmation.

TABLE 1 Prevalence of enterotoxin and virulence genes, MLST and MALDI-TOF MS for suspected *Staphylococcus argenteus* identification

Isolate no.	Enterotoxin and virulence genes detection	MLST identification		Sequence results of NRPS PCR amplicon			MALDI-TOF MS identification
		ST	CC	Size (bp)	BLAST species	Sequence identities (%)	
U27 OC2.1	ND	ST4209[a]	Singleton	160	*S. aureus* strain K5 (CP020656.1)	97	*S. aureus*
U27 OC2.2	ND	ST4209[a]	Singleton	160	*S. aureus* strain FDAARGOS (CP007559.5)	99	*S. aureus*
U27 OC2.5	ND	ST4209[a]	Singleton	160	*S. aureus* strain K5 (CP020656.1)	96	*S. aureus*
U19 T10.1	*sed*, *hla*, *hlb*, *clfA*, *pvl*	ST4210[sa]	Singleton	640	*S. argenteus* strain XNO106 (CP015028.1)	99	*S. argenteus*
U46 S18.1	*sea*, *hla*, *hlb*, *clfA*	ST4211[sa]	Singleton	640	*S. argenteus* strain XNO106 (CP015028.1)	100	*S. argenteus*
U46 S18.5	*sea*, *sec*, *sed*, *hla*, *hlb*, *clfA*, *pvl*	ST4211[sa]	Singleton	640	*S. argenteus* strain XNO106 (CP015028.1)	100	*S. argenteus*
U14 T6.2	ND	ST4212[a]	Singleton	160	*S. aureus* strain FDAARGOS_159 (CP014064.2)	95	*S. aureus*
U65 S5	ND	ST4215[a]	Singleton	160	*S. aureus* strain NRS187 (CP016080.1)	91	*S. aureus*

Note. bp: base pair; BLAST: basic local alignment search tool; CC: clonal complex; MALDI-TOF MS: matrix-assisted laser desorption/ionization time-of-flight mass spectrometry; ND: not determine; MLST: multilocus sequence type; NRPS: nonribosomal peptide synthetase.

[a]Novel STs from this study.

[sa]*S. argenteus* ST.

3 | RESULTS

3.1 | Detection of *S. argenteus* by MALDI-TOF MS

From 67 samples (total of 19 bacterial isolates), we obtained 11 *S. aureus* isolates and 8 suspected *S. argenteus* isolates. These suspected *S. argenteus* isolates were analyzed by MALDI-TOF MS. After visual inspection and obtaining the spectral results of their ionizable cell surface components, which were compared for similarity with the spectral data in the Bruker and in-house databases. The results showed that there are five isolates that match with the *S. aureus* database and three isolates that match with the *S. argenteus* database, with a high score (>2.3) (isolate no. U19 T10.1, U43 S18.1, and U43 S18.3; Table 1).

3.2 | NRPS gene amplification of *S. argenteus*

The NRPS gene was amplified for eight suspected *S. argenteus* isolates, as shown in Figure 1. The results showed that three isolates (U19 T10.1, U43 S18.1, and U43 S18.3) have a PCR product of approximately 340 bp, which was correlated with *S. argenteus* as reported by Zhang et al. (2016). In contrast, the five other suspected isolates had a PCR product of nearly 160 bp, which was reported to correlate with *S. aureus* (Zhang et al., 2016). The sequences of NRPS amplicons were analyzed for similarity using the GenBank database, which showed that bacterial isolate no. U19 T10.1, U43 S18.1, and U43 S18.3 have 99% identity with *S. argenteus* strain XNO106 (accession number: CP025023.1). In contrast, the other five isolates showed high identity with *S. aureus* strain K5 (accession number: CP020656.1), *S. aureus* strain FDAARGOS (accession number: CP007539.3), *S. aureus* strain FDAARGOS_159 (accession number: CP014064.2), and *S. aureus* strain NRS137 (accession number: CP026080.1). These results correlated with the MALDI-TOF MS results (Table 1).

3.3 | MLST of *S. argenteus*

All eight suspected *S. argenteus* isolates were further analyzed by MLST to define STs. Several isolates were shown to be novel STs of the *Staphylococcus* complex, which included ST4209 (isolate no. U27 OC2.1, U27 OC2.2, and U27 OC2.3), ST4210 (isolate no. U19 T10.1), ST4211 (isolate no. U43 S18.1 and U43 S18.3), ST4212 (isolate no. U14 T6.2), and ST4213 (isolate no. U65 S3), derived from the curator of the PubMLST *S. aureus* database (https://pubmlst.org), University of Oxford, UK, and the Wellcome Trust fund. The results showed that three isolates (isolate no. U19 T10.1, ST4210; isolates no. U43 S18.1 and U43 S18.3, ST4211) were identified as *S. argenteus*, which correlated with the results of MALDI-TOF MS and the NRPS gene. The neighbor-joining and maximum likelihood analyses yielded similar phylogenetic trees. Based on *arcC*, *aroE*, *gmk*, and *pta*, three bacterial isolates, ST4210 (isolate no. U19 T10.1) and ST4211 (isolates no. U43 S18.1 and U43 S18.3), showed close similarity to the *S. argenteus* group (ST1223, ST2250, ST2854, and ST2198) (Figure 2).

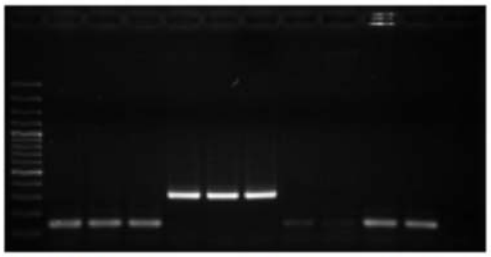

FIGURE 1 Non ribosomal peptide synthetase amplicon of eight suspected *Staphylococcus argenteus*. Lane M: DNA marker; lane 1: isolate no. U27 OC2.1; lane 2: isolate no. U27 OC2.2; lane 3: isolate no. U27 OC2.3; lane 4: isolate no. U19 T10.1; lane 5: isolate no. U43 S18.1; lane 6: isolate no. U43 S18.3; lane 7: isolate no. U14 T6.2; lane 8: isolate no. U65 S3; lane 9: *S. aureus* ATCC13565; lane 10: *S. aureus* ATCC25923; lane 11: negative control

3.4 | Enterotoxin and virulence genes

Five classical enterotoxin genes and seven virulence genes, as mentioned in the Materials and Methods section, were investigated in the three *S. argenteus* isolates by PCR, the results of which are shown in Table 1. The detected enterotoxin genes were *seo*, *sec*, and *sed*. No isolate carried *seb* and *see*. Regarding the virulence genes, the most prevalent ones were *hla*, *hlb*, and *clfA* present at a rate of 100%, followed by *pvl* at 66.67%, whereas *coa*, *spa* (IgG-binding region) and *spa* (X region) were not detected in the *S. argenteus* isolates.

3.5 | Antimicrobial susceptibility testing

From bacterial identification, we obtained 16 *S. aureus* isolates and three *S. argenteus* isolates. Among the three *S. argenteus* isolates, one (isolate no. U19 T10.1) was susceptible to all the tested antimicrobial drugs, whereas the remaining two (isolate no. U43 S18.1 and U43 S18.3) were resistant to penicillin and doxycycline. Meanwhile, among the *S. aureus* isolates, six were resistant to penicillin and two were resistant to gentamicin. One *S. aureus* isolate (isolate no. U14 T6.2) was resistant to several antimicrobial classes, namely, β-lactams, aminoglycosides, macrolides, tetracyclines, and fluoroquinolones.

3.6 | Antimicrobial resistance genes

In the *S. aureus* and *S. argenteus* isolates, the presence of antimicrobial resistance genes was tested. We found that all *S. aureus* isolates carried *blaZ*, *mecA*, *aacA-aphD*, and *mrs(A)*, but none carried *dfrG*, *tet(K)*, and *cfr*, whereas all three *S. argenteus* isolates carried only the *blaZ* (isolate no. U43 S18.1 and U43 S18.3). Mutations of *gyrA* and *grlA* were found in the *S. aureus* isolate no. U14 T6.2. The mutations of *gyrA* occurred at codons 88 [GAA (Glu) → GAT (Asn)] and 96 [GAT (Asp) → ACA (Thr)], whereas the mutation of *grlA* occurred at codon 80 [TCC (Ser) → TTA (Leu)]. The presence of antimicrobial resistance genes in *S. aureus* is shown in Table 2.

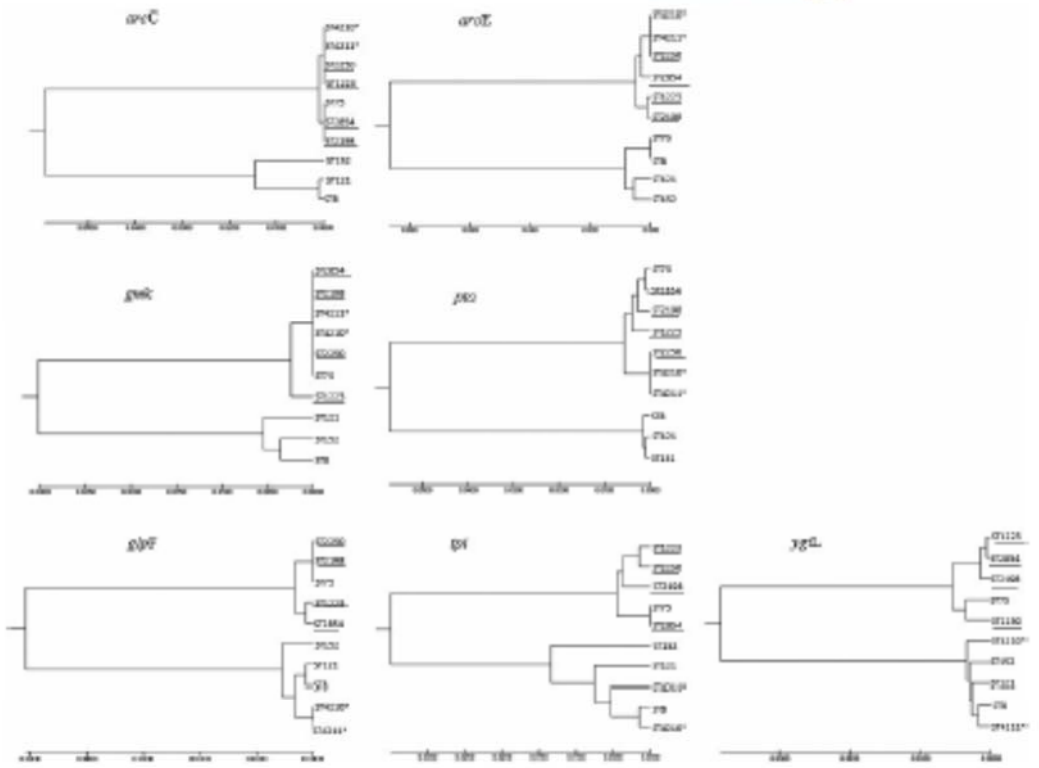

FIGURE 2 Phylogenetic neighbor-joining tree of suspected *Staphylococcus argenteus*. The tree is constructed from *arcC*, *aroE*, *gmk*, *glpF*, *pta*, *tpi*, and *ygiL* gene sequences from the suspected *S. argenteus* (ST4210*, ST4211*), *S. aureus* reference strain (ST75, ST152, ST121, ST8) and ST of published *S. argenteus* group (ST1223, ST2250, ST2854, ST2198). The phylogenetic analysis was performed using MEGA7

4 | DISCUSSION

Staphylococci are considered the most important veterinary bacterial pathogens because they cause a multiplicity of infections and a wide range of diseases in many host species, including humans and animals (Holmes et al., 2016). This virulent group of pathogens is not only important for livestock, causing conditions such as bovine mastitis or lameness in chickens, but also for causing skin infections resulting in abscesses in pets, such as dogs, cats, and rabbits (Drougka et al., 2016; Goffi et al., 2004; Loncaric et al., 2014; Youn et al., 2014). Pathogenic strains of staphylococci that cause skin infections have been well studied and characterized. Moreover, in farm rabbits, abscesses in the lungs, liver, and uterus lead to poor production, infertility, and death (Corpa et al., 2009). This study revealed the presence of *S. aureus*, including a new member of the *S. aureus* complex, *S. argenteus*, which caused skin infections producing abscesses in rabbits.

Intriguingly, from the 19 *S. aureus* isolates, eight had white colonies, which differs from the normal colony color of *S. aureus*, which is golden or yellowish. The suspected eight isolates were further analyzed using MALDI-TOF MS, and bacterial diversity discriminated by NRPS amplification and MLST. The MALDI-TOF MS results revealed three *S. argenteus* isolates, which were investigated for enterotoxin and virulence genes. The enterotoxins detected were *sea* and *sed*. All three isolates carried the common virulence *hla*, *hlb*, and *clfA*. Surprisingly, previous studies have reported that *S. argenteus* is negative for the *pvl* (Thaipadungpanit et al., 2015), but we found the *pvl* in two *S. argenteus* isolates in this study. These three *S. argenteus* isolates, isolated from rabbits, had the ability to cause severe illness in these animals, particularly via the presence of *clfA*, which usually contributes to abscess formation in rabbits, as previously reported (Malachowa et al., 2016). Although *S. argenteus* is regionally distributed in animals other than humans, they have been misidentified as *S. aureus*; this has been suggested in several previous publications (Chantratita et al., 2016; Schuster et al., 2017; Thaipadungpanit et al., 2015; Tong et al., 2015).

The NRPS gene has been identified in studies of a diverse array of related *S. aureus* and *S. argenteus*. This study found that NRPS amplification can differentiate *S. argenteus* from *S. aureus*, as also reported previously (Zhang et al., 2016). The sequences

TABLE 2 Antimicrobial drug resistance phenotypes and antimicrobial resistance genes of *Staphylococcus aureus* isolated from rabbit

Antimicrobial susceptibility testing				Antimicrobial resistance genes amplification	
Drug	S (%)	I (%)	R (%)	Gene	No. of isolates (%)
β-lactams					
Penicillin	62.5	0	37.5	blaZ	1 (6.25)
Cefoxitin	93.75	0	6.25	mecA	1 (6.25)
Cefazolin	93.75	0	6.25		
Ceftriaxone	75.0	18.75	6.25		
Aminoglycosides					
Gentamicin	87.5	0	12.5	aacA-	1 (6.25)
Amikacin	93.75	0	6.25	aphD	
Macrolides					
Azithromycin	93.75	0	6.25	mrz(A)	1 (6.25)
Tetracycline					
Doxycycline	93.75	0	6.25	tet(K)	0 (0)
Fluoroquinolones					
Ciprofloxacin	93.75	0	6.25	gyrA	1 (6.25)
Moxifloxacin	93.75	0	6.25	grlA	1 (6.25)
Norfloxacin	93.75	0	6.25		
Folate pathway inhibitors					
Trimethoprim/ sulfamethoxazole	100	0	0	dfrG	0 (0)
Phenicols					
Chloramphenicol	100	0	0	cfr	0 (0)

Note. S: susceptible; I: intermediate; R: resistance.

of NRPS amplicons analyzed using the GenBank database also corresponded to the MALDI-TOF MS results. Furthermore, when we performed molecular identification using MLST, all eight isolates were found to have diverse novel STs belonging to *S. aureus* (ST4209, ST4212, and ST4213) and *S. argenteus* (ST4210 and ST4211). The results showed high heterogeneity among these pathogenic bacterial isolates from rabbits. Moreover, this study revealed a new pathogenic member of the *S. aureus* complex, *S. argenteus*, for the first time. These bacteria form a genetically diverse lineage from *S. aureus* (Tong et al., 2015), being recently discovered in humans, in 2014. This study may be the first to report on *S. argenteus* originating from rabbits. We found that one *S. argenteus* isolate was susceptible to all the tested antibiotic agents and the other two *S. argenteus* isolates were resistant to penicillin and doxycycline. These results could be useful for veterinarians who have difficulty treating rabbits successfully with penicillin. In this study, we found one *S. aureus* isolate with mutations of gyrA and grlA, which indicated the possibility of quinolone resistance. Mutations in these genes have typically been found at codon 88 [GAA (Glu) → AAA (Lys)] in gyrA (Griggs et al., 2003; Iihara et al., 2006) and codon 80 [TCC (Ser) → TTC (Phe)] in grlA (Alighol et al., 2011; Iihara et al., 2006). Interestingly, the mutation of grlA at codon 80 found in our study was TCC (Ser) → TTA (Leu), and the mutation of gyrA at codon 88 was GAA (Glu) → GAT (Asp). Comparing the antibiotic resistance pattern, the isolated *S. argenteus* showed higher susceptibility to antibiotic agents than the isolated *S. aureus*. However, it is necessary to monitor the development of drug resistance in *S. argenteus* in the future. From the discovery of *S. argenteus* in rabbits, further study of its virulence factors, pathogenesis, clinical manifestations, antimicrobial resistance, and severity or outcome should be performed to improve our knowledge for treating, controlling, or preventing this novel pathogen in exotic pets.

ACKNOWLEDGMENTS

We thank Prasu-Arthorn Animal Hospital for help with specimen collection. We appreciative Mr. Paul Adams for correcting grammatical and typing errors in this manuscript. This work was supported by the Annual Research Fund of the Faculty of Veterinary Science, Mahidol University 2014; and Thailand Research Fund (RSA5980048).

CONFLICT OF INTEREST

The authors state that there are no conflicts of interest.

ORCID

Narisara Chantratita http://orcid.org/0000-0003-3906-7379

Shutipen Buranasinsup http://orcid.org/0000-0001-8299-8828

REFERENCES

Alighoil, M., Mirzaiehian, A., Halimi, S., Imaeini, H., Taherikalani, M., Jabalameli, F., … Emaneini, M. (2011). Phenotypic and genotypic evaluation of fluoroquinolone resistance in clinical isolates of *Staphylococcus aureus* in Tehran. *Medical Science Monitor*, *17*, PH71–PH74.

Argudín, M. A., Deplano, M., Vandendriessche, S., Rottiers, S., Tribes, C., Roisin, S., … Denis, O. (2016). Low occurrence of the new species *Staphylococcus argenteus* in a *Staphylococcus aureus* collection of human isolates from Belgium. *European Journal of Clinical Microbiology and Infectious Diseases*, *35*, 1017–1022. https://doi.org/10.1007/s10096-016-2662-x

Aslantaş, O., Demir, C., Turutoğlu, H., Cantekin, Z., Ergun, Y., & Doğruer, G. (2007). Coagulase gene polymorphism of *Staphylococcus aureus* isolated form subclinical mastitis. *Turkish Journal of Veterinary and Animal Science*, *31*, 255–257.

Chantratita, N., Wikraiphat, C., Tandhavanant, S., Wongsuvan, G., Ariyaprasert, P., Suntornsut, P., … Chaimanee, P. (2016). Comparison of community-onset *Staphylococcus argenteus* and *Staphylococcus aureus* sepsis in Thailand: A prospective multicenter observational study. *Clinical Microbiology and Infection*, *22*, 458e11–458e19. https://doi.org/10.1016/j.cmi.2016.01.008

Clinical and Laboratory Standards Institute. (2012). *Performance standards for antimicrobial susceptibility testing: twentieth informational supplement*. CLSI document M100-S20, Wayne, PA.

Corpa, J. M., Hermans, K., & Haesebrouck, F. (2009). Main pathologies associated with *Staphylococcus aureus* infections in rabbits: A review. *World Rabbit Science*, *17*, 115–125.

Drougka, E., Foka, A., Koutinas, C. K., Jelastopulu, E., Giormezis, N., Farmaki, O., … Spiliopoulou, I. (2016). Interspecies spread of *Staphylococcus aureus* clones among companion animals and human close contacts in a veterinary teaching hospital. Across-sectional study in Greece. *Preventive Veterinary Medicine*, *126*, 190–198. https://doi.org/10.1016/j.prevetmed.2016.02.004

Enright, M. C., Day, N. P. J., Davies, C. E., Peacock, S. J., & Spratt, B. G. (2000). Multilocus sequence typing for characterization of methicillin-resistant and methicillin-susceptible clones of *Staphylococcus aureus*. *Journal of Clinical Microbiology*, *38*, 1008–1015.

Foster, T. J., & Geoghegan, J. A. (2015). *Staphylococcus aureus*. *Medical Microbiology and Immunology*. https://doi.org/10.1016/B978-0-12-397169-2.00057-8

Frénay, H. M., Bunschoten, A. E., Schouls, L. M., Van Leeuwen, W. J., Vandenbroucke-Grauls, C. M., Verhoef, J., & Mooi, F. R. (1996). Molecular typing of methicillin-resistant *Staphylococcus aureus* on the basis of protein a gene polymorphism. *European Journal of Clinical Microbiology and Infectious Diseases*, *15*, 60–64. https://doi.org/10.1007/BF01586186

Gómez-Sanz, E., Torres, C., Lozano, C., Fernández-Pérez, R., Aspiroz, C., Ruiz-Larrea, F., & Zarazaga, M. (2010). Detection, molecular characterization, and clonal diversity of methicillin-resistant *Staphylococcus aureus* CC398 and CC97 in Spanish slaughter pigs of different age groups. *Foodborne Pathogens and Disease*, *7*, 1269–1277. https://doi.org/10.1089/fpd.2010.0610

Gohil, P., Vergara, Y., Ruiz, J., Albizu, I., Vila, J., & Gómez-Luz, R. (2004). Antibiotic resistance and epidemiological typing of *Staphylococcus aureus* strains from ovine and rabbit mastitis. *International Journal of Antimicrobial Agents*, *25*, 268–272.

Griggs, D. J., Morona, H., & Piddock, L. J. V. (2006). Selection of moxifloxacin-resistant *Staphylococcus aureus* compared with five other fluoroquinolones. *Journal of Antimicrobial Chemotherapy*, *57*, 1405–1407. https://doi.org/10.1093/jac/dkg241

Holmes, M. A., Harrison, E. M., Fisher, E. A., Graham, E. M., Parkhill, J., Foster, G., & Paterson, G. K. (2016). Genomic analysis of companion rabbit *Staphylococcus aureus*. *PLoS ONE*, *11*, e0151458. https://doi.org/10.1371/journal.pone.0151458

Ihara, H., Suzuki, T., Kawamura, Y., Ohkusu, K., Inoue, Y., Zhang, W., … Ezaki, T. (2006). Emerging multiple mutations and high-level fluoroquinolone resistance in methicillin-resistant *Staphylococcus aureus* isolated from ocular infections. *Diagnostic Microbiology and Infectious Disease*, *56*, 297–305. https://doi.org/10.1016/j.diagmicrobio.2006.04.017

Jarraud, S., Mougel, C., Thioulouse, J., Lina, G., Meugnier, H., Forey, F., … Vandenesch, F. (2002). Relationships between *Staphylococcus aureus* genetic background, virulence factors, agr groups (alleles), and human disease. *Infection and Immunity*, *70*, 631–641. https://doi.org/10.1128/IAI.70.2.631-641.2002

Kehrenberg, C., & Schwarz, S. (2006). Distribution of florfenicol resistance genes *fexA* and *cfr* among chloramphenicol-resistant *Staphylococcus* isolates. *Antimicrobial Agents and Chemotherapy*, *50*, 1156–1163. https://doi.org/10.1128/AAC.50.4.1156-1163.2006

Kolecka, A., Khayhan, K., Groenewald, M., Theelen, B., Arabatzis, M., Velegraki, A., … Boekhout, T. (2013). Identification of medically relevant species of arthroconidial yeasts by use of matrix-assisted laser desorption ionization-time offlight mass spectrometry. *Journal of Clinical Microbiology*, *51*, 2491–2500. https://doi.org/10.1128/JCM.00470-13

Lagier, J., Fenollar, F., Hallé, O., Lepidi, H., & Raoult, D. (2009). Letters to the editor: Trimethoprim resistance genes in vancomycin-resistant *Enterococcus faecium* clinical isolates from France. *International Journal of Antimicrobial Agents*, *34*, 590–591.

Laplana, L. M., Cepero, P. G., Ruiz, J., Zolezzi, P. C., Calvo, C. R., Erazo, M. C., & Gómez-Luz, R. (2007). Molecular typing of *Staphylococcus aureus* clinical isolates by pulsed-field gel electrophoresis, staphylococcal cassette chromosome *mec* type determination and dissemination of antibiotic resistance genes. *International Journal of Antimicrobial Agents*, *30*, 505–515. https://doi.org/10.1016/j.ijantimicag.2007.06.020

Loncaric, I., Künzel, F., Licka, T., Simhofer, H., Spergser, J., & Rosengarten, R. (2014). Identification and characterization of methicillin-resistant *Staphylococcus aureus* (MRSA) from Austrian companion animals and horses. *Veterinary Microbiology*, *168*, 381–387. https://doi.org/10.1016/j.vetmic.2013.11.022

Malachowa, N., Kobayashi, S. D., Porter, A. R., Braughton, K. R., Scott, D. P., & Gardner, D. J. (2016). Contribution of *Staphylococcus aureus* coagulases and clumping factor A to abscess formation in a rabbit model of skin and soft tissue infection. *PLoS ONE*, *11*, e0158295. https://doi.org/10.1371/journal.pone.0158295

McClure, J., Conly, J. M., Lau, V., Elsayed, S., Louie, T., Hutchins, W., & Zhang, K. (2006). Novel multiplex PCR assay for detection of the *Staphylococcal* virulence marker panton-valentine leukocidin genes and simultaneous discrimination of methicillin-susceptible from -resistant *Staphylococci*. *Journal of Clinical Microbiology*, *44*, 1141–1144. https://doi.org/10.1128/JCM.44.3.1141-1144.2006

Moradigaravand, D., Jamrozy, D., Mostowy, R., Anderson, A., Nickerson, E. K., Thaipadungpanit, J., … Wongsuvan, G. (2017). Evolution of the *Staphylococcus argenteus* ST2250 clone in Northeastern Thailand is linked with the acquisition of livestock-associated Staphylococcal genes. *MBio*, *8*, e00802-17. https://doi.org/10.1128/mbio.00802-17

Schuster, D., Rickmeyer, J., Gajdiss, M., Thye, T., Lorenzen, S., Reif, M., … Liégeois, F. (2017). Differentiation of *Staphylococcus argenteus* (formerly: *Staphylococcus aureus* complex 75) by mass spectrometry from *S. aureus* using the first strain isolated from a wild African great

ape. *International Journal of Medical Microbiology*, 307, 57–66. https://doi.org/10.1016/j.ijmm.2016.11.006

Seki, K., Sakurada, J., Seong, H. K., Murai, M., Tachi, H., Ishii, H., & Masuda, S. (1998). Occurrence of coagulase serotype among *Staphylococcus aureus* strains isolated from healthy individuals-special reference to correlation with size of protein-A gene. *Microbiology and Immunology*, 42, 407–409.

Thalpadungpanit, J., Amronchai, R., Nickerson, E. K., Wongsuvan, G., Wuthiekanun, V., Limmathurotsakul, D., … Peacock, S. J. (2015). Clinical and molecular epidemiology of *Staphylococcus argenteus* infections in Thailand. *Journal of Clinical Microbiology*, 53, 1005–1008. https://doi.org/10.1128/JCM.03049-14

Tong, S. Y. C., Schaumburg, F., Ellington, M. J., Corander, J., Pichon, B., Leendertz, F., … Gifford, D. M. (2015). Novel staphylococcal species that form part of a *Staphylococcus aureus*-related complex: The non-pigmented *Staphylococcus argenteus* sp. nov. and *Staphylococcus schweitzeri* sp. nov. *International Journal of Systematic and Evolutionary Microbiology*, 65, 15–22. https://doi.org/10.1099/ijs.0.062752-0

Tristan, A., Ying, L., Bes, M., Etienne, J., Vandenesch, F., & Lina, G. (2006). Use of multiplex PCR to identify *Staphylococcus aureus* adhesins involved in human hematogenous infections. *Journal of Clinical Microbiology*, 41, 4465–4467. https://doi.org/10.1128/JCM.41.9.4465-4467.2006

Vancraeynest, D., Hermans, K., Martel, A., Vaneechoutte, M., Devriese, L. A., & Haesebrouck, F. (2004). Antimicrobial resistance and resistance genes in *Staphylococcus aureus* strains from rabbits. *Veterinary Microbiology*, 101, 245–251. https://doi.org/10.1016/j.vetmic.2004.05.021

Viana, D., Selva, L., Segura, P., Penadés, J. R., & Corpa, J. M. (2007). Genotypic characterization of *Staphylococcus aureus* strains isolated from rabbit lesions. *Veterinary Microbiology*, 121, 288–298. https://doi.org/10.1016/j.vetmic.2006.12.006

Wu, D., Li, X., Yang, Y., Zhang, Y., Wang, C., Deng, L., … Yu, S. (2011). Superantigen gene profiles and presence of exfoliative toxin genes in community-acquired methicillin-resistant *Staphylococcus aureus* isolated from Chinese children. *Journal of Medical Microbiology*, 60, 55–65. https://doi.org/10.1099/jmm.0.025460-0

Youn, J., Park, Y. H., Hang'ombe, B., & Sugimoto, C. (2014). Prevalence and characterization of *Staphylococcus aureus* and *Staphylococcus pseudintermedius* isolated from companion animals and environment in the veterinary teaching hospital in Zambia, Africa. *Comparative Immunology, Microbiology and Infectious Diseases*, 37, 125–130. https://doi.org/10.1016/j.cimid.2014.01.006

Zhang, D., Xu, X., Song, Q., Bai, Y., Zhang, Y., Song, M., & Shi, X. (2016). Identification of *Staphylococcus argenteus* in Eastern China based on nonribosomal peptide synthetase (NRPS) gene. *Future Microbiology*, 11, 1115–1121.

How to cite this article: Indrawattana N, Pumipuntu N, Suriyakhun N, et al. *Staphylococcus argenteus* from rabbits in Thailand. MicrobiologyOpen. 2018;e665. https://doi.org/10.1002/mbo3.665

Chiang Mai J. Sci. 2018; 45(1) : 21-32
http://epg.science.cmu.ac.th/ejournal/
Contributed Paper

Prevalence of the Multi-drug Resistance of Shiga Toxin-producing *Escherichia coli* Isolated from Pigs in Central Thailand

Shutipen Buranasinsup [a], Suphang Kulpeanprasit [a, b], Thida Kong-ngoen [b], Arunee Jangsangthong [a], Nitat Sookrung [c], Wanpen Chaicumpa [d] and Nitaya Indrawattana* [b]

[a] Department of Pre-clinic and Applied Animal Science, Faculty of Veterinary Science, Mahidol University, Nakompathom, 73170, Thailand.

[b] Department of Microbiology and Immunology, Faculty of Tropical Medicine, Mahidol University, Bangkok, 10400, Thailand.

[c] Department of Research and Development, Faculty of Medicine Siriraj Hospital, Mahidol University, Bangkok, 10700, Thailand.

[d] Department of Parasitology and Center of Excellence on Therapeutic Proteins and Antibody Engineering, Faculty of Medicine Siriraj Hospital, Mahidol University, Bangkok, 10700, Thailand.

* Author for correspondence; e-mail: nitaya.ind@mahidol.ac.th

Received: 1 December 2016
Accepted: 28 March 2017

ABSTRACT

Shiga toxin-producing *E. coli* (STEC), a strain producing cytotoxins known as Shiga toxins (Stxs, encoded by EVS and EVC genes), can cause neonatal and post-weaning diarrhea (PWD) in pigs, leading to substantial economic loss in the form of medication costs, reduced growth rate, and increased morbidity and mortality. To tackle this, several antimicrobial agents are used in pig farms, although misuse may lead to occurrence of antimicrobial-resistant pathogens. In this study, 5,831 *E. coli* bacterial isolates were collected from 715 pigs. Of these, 206 bacterial isolates were STEC carrying EVS–EVC genes. A majority of the STECs were resistant to ampicillin (99.5%), carbenicillin (99%), and trimethoprim/sulfamethoxazole (60.2%). Among these isolates, 93.69% and 0.97% of STEC were carried class 1 (6.8% belong to *CS1*) and class 2 integrons, respectively. None isolate carried *CS2*. The predominant antimicrobial resistance genes were bla_{TEM}, *aadA*, *sul*II, *dhfr*V, and *int*I. The results of antimicrobial resistance phenotype and also genotype were correlated to antibiotics use in the swine farm such as amoxicillin and penicillin. Therefore, frequent use of antimicrobial drugs in pig farms may result in the occurrence of multi-drug resistant bacteria, and this should be taken into consideration prior to use.

Keywords: antimicrobial resistance, antimicrobial resistance genes, EVC-EVS, integrons, Shiga toxin-producing *E. coli*

1. INTRODUCTION

Shiga toxin producing *Escherichia coli* (STEC), a strain of bacteria known to produce cytotoxins known as Shiga toxins (Stxs), have been reported to cause enteric

infections in pigs as well as zoonotic disease symptoms in humans such as bloody diarrhea and hemolytic-uremic syndrome (HUS) [1,2]. Bacterial toxins may cause severe hemorrhagic and inflammatory responses in the intestinal mucosa, presenting as watery diarrhea with rapid dehydration, acidosis and death. Over the last decade, the cost of medication, reduction in growth rate and increased morbidity and mortality caused by these diseases in the animal population pose a substantial economic burden. In order to avoid this, various antimicrobials are commonly used in pig farms [3] particularly among young piglets in the post-weaning stage when the mortality rates are quite high [4]. However, the use of these antimicrobial agents as feed additive for growth promotion and/or prophylaxis, and their misuse or overuse can increase the occurrence of antimicrobial resistance [4-7]. Several mechanisms for the development of antimicrobial resistance present, example; bla_{TEM}, bla_{SHV}, bla_{CMY-2} genes for resistant to β-lactam via drug inactivation or alteration pathway, *tet*A, *tet*B, *tet*C, *tet*D, and *tet*G genes for tetracycline resistance through efflux pumps, *sul*I or *sul*II for genes encoded for sulfonamide resistance via metabolic pathway [8]. Recently, integrons, gene cassette of several antimicrobial resistance genes which carried by mobile genetic element, are presented as a key of the development of multi-drug resistance in gram-negative bacteria. The general structure of the integrons consist of a conserved region that codes integrase (*Int*) and a variable region (*5'CS-3'CS*) where various resistance cassettes can be integrated themselves. The common types of integrons identified are class 1, 2 and 3 according to the integrase gene (*intI*) [9]. Among the integrons classes, class 1 and 2 integrons are the most regular and extensively present in Enterobacteriaceae including *E. coli* and are responsible for the spread of MDR strain [10]. Tajbakhsh *et al.* investigated the prevalence of integrons in the multi-drug resistant *E. coli* isolated from aquaculture water in Chaharmahal Va Bakhtiari province, Iran. Among these bacterial isolates, they were positive for integrons class 1 (40%) and class 2 (10%) [11]. Recently, the prevalence of integrons in STEC increased as reported by Kheiri *et al.* They found 50, 38, 6 and 16 % were class I integrons and 26, 8, 0 and 4 % were class II in chicken, human, cattle and sheep isolates in Alborz province, respectively [12].

The prevalence of multi-drug resistant *E. coli* has become a critical problem globally, and poses a threat to human health as it acts as a reservoir and transfers resistance genes from animals to human beings via the food chain [13-16].

Currently, there is limited evidence on the antimicrobial resistance of *E. coli* isolated from pigs in Thailand. Therefore, the aim of this study was to investigate the prevalence of multi-drug resistance including antimicrobial resistance genes and integrons of STEC isolated from pigs in Nakornpathom and Ratchaburi provinces. These locations are the large area of swine farm in Thailand which also distributed pig or pork to another provinces and neighbor countries.

2. MATERIALS AND METHODS

2.1 Sample Collection and Bacterial Isolation

This study included 715 rectal swabs of pigs aged 2-8 weeks and belonging to 7 farms in the Nakornpathom (n = 323) and Ratchaburi (n = 392) provinces, Thailand where agriculture and livestock are the main source of income of the people. All samples were collected between 2012 and 2014.

They were transported to the laboratory within 24 h of collection, inoculated on MacConkey (MAC) (Becton, Dickinson and Company, MD, USA) agar, and incubated at 37°C for 24 h. After incubation, the suspected bacterial colonies (lactose fermenter colonies), twelve colonies randomly selected from individual sample, were subjected to Gram staining and conventional bacterial biochemical tests such as triple sugar iron agar (TSI), ornithine decarboxylation/motility/indole (OMI) and citrate for *E. coli* identification. The farm owners were interviewed to gather information regarding the antimicrobials used. The agents used included amoxicillin, penicillin, colistin, tiamulin, gentamycin, enrofloxacin, tetracycline, and ceftriaxone. This study was approved by The Faculty of Veterinary Science-Animal Care and Use Committee, Mahidol University (protocol number MUVS-2012-55).

2.2 *stx*1 and *stx*2 Family Amplification

The presence of the *stx*1 (EVS) and *stx*2 (EVC) genes encoding Shiga-like toxin in the *E. coli* isolates was determined by PCR using specific primers, as listed in Table 1. Bacterial genomic DNA was extracted by suspending the bacterial colonies in sterile distilled water and boiling them for 10 min. Thereafter, the supernatant was used as template for PCR. The total volume of the PCR mixture was 25 µL, including 1 µM of each primer, 2.5 µL of 10× Taq PCR buffer, 0.2 mM dNTP, 2 mM $MgCl_2$ and 1 U of Taq DNA polymerase (Fermentas, St. Leon-Rot, Germany). The PCR reaction mixture was subjected to the following thermal cycle: 5 min of initial denaturation at 95°C, 30 cycles of amplification at 94°C denaturation for 90 s, 55°C annealing for 90 s, 72°C extension for 90 s for both EVT1/EVT2 and EVS1/EVC2, and a final extension at 72°C for 8 min using the Lifecycler (Biorad, California, USA). The amplified products were analyzed using 1% agarose gel electrophoresis and ethidium bromide staining. The DNA bands were visualized under a UV trans-illuminator (Syngene, Cambridge, England).

Table 1. The PCR primer for amplification of *stx*, antimicrobial-resistant genes and integrons.

Target genes	Primer (5′-3′)	Reference
stx-1: EVT1/EVT2	CAACACTGGATGATCTCAG CCCCCTCAACTGCTAATA	Ali *et al.*, 2014
stx-2: EVS1/EVC2	ATCAGTCGTCACTCACTGGT CTGCTGTCACAGTGACAAA	Ali *et al.*, 2014
Sulfonamide		
*sul*I	CGACACAGAAATCGAGCGTA GTCTTGCACCGAATGCATAA	Use in this study
*sul*II	GGCAGATGTGATCGACCTCG ATGCCGGGATCAAGGACAAG	Leverstein-Van Hall *et al.*, 2002
*sul*III	GAGCAAGATTTTTGGAATCG AACTAACCTAGGGCTTTGGA	Boerlin *et al.*, 2005

Table 1. Continued.

Target genes	Primer (5′-3′)	Reference
Beta-lactams		
bla_{TEM}	TTAACTGGCGAACTACTTAC	Kozak *et al.*, 2009
	GTCTATTTCGTTCATCCATA	
bla_{SHV}	AGGATTGACTGCCTTTTTG	Kozak *et al.*, 2009
	ATTTGCTGATTTCGCTCG	
bla_{CMY-2}	GACAGCCTCTTTCTCCACA	Kozak *et al.*, 2009
	TGGACACGAAGGCTACGTA	
Trimethoprim		
*dhfr*I	AAGAATGGAGTTATCGGGAATG	Maynard *et al.*, 2003
	GGGTAAAAACTGGCCTAAAATTG	
*dhfr*V	CTGCAAAAGCGAAAAACGG	Maynard *et al.*, 2003
	AGCAATAGTTAATGTTTGAGCTAAAG	
*dhfr*VII	GGTAATGGCCCTGATATCCC	Maynard *et al.*, 2003
	TGTAGATTTGACCGCCACC	
Quinolone		
*qnr*A	AGAGGATTTCTCACGCCAGG	Huang *et al.*, 2012
	TGCCAGGCACAGATCTTGAC	
*qnr*B	GGCATTGAAATTCGCCACTG	Huang *et al.*, 2012
	TTTGCTGCTCGCCAGTCGAA	
*qnr*S	GCAAGTTCATTGAACAGGGT	Huang *et al.*, 2012
	TCTAAACCGTCGAGTTCGGCG	
Aminoglycosides		
aac(3)-IIa (*aac*C2)	CGGAAGGCAATAACGGAG	Maynard *et al.*, 2003
	TCGAACAGGTAGCACTGAG	
aac(3)-IV	GTGTGCTGCTGGTCCACAGC	Maynard *et al.*, 2003
	AGTTGACCCAGGGCTGTCGC	
*aad*B	GAGGAGTTGGACTATGGATT	Kozak *et al.*, 2009
	CTTCATCGGCATAGTAAAAG	
Class 1 integrons		
*Int*I	CCTCCCGCACGATGATC	Smith *et al.*, 2010
	TCCACGCATCGTCAGGC	
5′ *CS* class 1	GGCATCCAAGCAGCAAG	Smith *et al.*, 2010
3′ *CS* class 1	AAGCAGACTTGACCTGA	
Class 2 integrons		
IntI1	TTATTGCTGGGATTAGGC	Lapierre *et al.*, 2008
	ACGGCTACCCTCTGTTATC	
5′ *CS* class 2	GACGGCATGCACGATTTGTA	Lapierre *et al.*, 2008
3′ *CS* class 2	GATGCCATCGCAAGTACGAG	

2.3 Serotyping

The serotype of *E. coli* was analyzed using the agglutination method (S and A reagents lab LTD, Bangkok, Thailand). First, the isolated colonies were tested with 3 polyvalent antisera, namely, polyvalent I, II, and III. The

serospecific antisera present in polyvalent I are O25:K11, O26:K60, O44:K74, O55:K59, O78:K80, O111:K58, O114:K-, and O119:K69; polyvalent II comprises O86:K61, O124:K72, O125:K70, O126:K71, O127:K63, and O128:K67; and polyvalent III includes O18ac:K77, O20ab:K84, O28:K73, and O112ac:K66. Thereafter, the isolated colonies divided into serospecific groups and analyzed.

2.4 Antimicrobial Susceptibility Testing

The EVS-EVC positive *E. coli* or STECs were examined for resistance to 18 antimicrobial drugs via the disk diffusion test following the Clinical and Laboratory Standards Institute guidelines (CLSI), 2012 [17]. Those were ampicillin (10 µg), carbenicillin (100 µg), amoxicillin/clavulanic acid (20 µg/10 µg), sulbactam/cefoperazone (30 µg/75 µg), piperacillin/tazobactam (100 µg/10 µg), cefuroxime sodium (30 µg), cefepime (30 µg), ceftriaxone (30 µg), cefotaxime (30 µg), ceftazidime (30 µg), imipenem (10 µg), meropenem (10 µg), gentamicin (10 µg), amikacin (30 µg), tigecycline (15 µg), ciprofloxacin (5 µg), norfloxacin (10 µg), and trimethoprim/sulfamethoxazole (1.25 µg/23.75 µg) (Oxoid, Basingstoke, UK). *E. coli* ATCC 25922 was used as the control strain [17].

2.5 Detection of Antimicrobial Resistance Genes and Integrons

Bacterial genomic DNA of the STEC isolates were examined for the presence of antimicrobial resistance genes and integrons using PCR with specific primers for individual genes, as listed in Table 1.

3. RESULTS AND DISCUSSIONS

A total of 5,381 isolates of *E. coli* were obtained from the 715 swabs, of which 206 were positive for EVS-EVC (3.83%). Amongst these STEC isolates, 122 (59.22%) were typed to 16 serogroups which comprising 3 majors serogroups: O20ab:K84 (12.6%), O128:K67 (9.22%), and O28:K73 (9.22%) (Table 2). The prevalence of STEC may variable among different area and time duration. In 2000, Vuddhakul *et al.* reported the prevalence of STEC isolated from retail beef and bovine feces during May and October 1998 in Songkla Province, the southern part of Thailand. They found five (3.3%) bacterial isolates of were STEC which is similar to our study [18]. However, in 2010, Prapasarakul *et al.* reported a higher prevalence of STEC (11.2%) from pigs with PWD which collected from Chancherngsao, Nakornpathom and Ratchaburi provinces in central Thailand during January 2006 to December 2008 [19]. The differences in the prevalence of STEC among these studies are probably due to the fact that the patterns of STEC are relied on diet, age, environmental condition, and seasonal variation.

In this study, the isolated STECs were subjected to investigate antimicrobial susceptibility, and the results have been shown in Table 3. Ampicillin-resistant bacteria were the predominant isolates (99.5%), followed by isolates resistant to carbenicillin (99%) and trimethoprim/sulfamethoxazole (60.2%). None of the STEC isolates exhibited resistance to amoxicillin/clavulanic acid, sulbactam/cefoperazone, cefepime, imipenem, or meropenem. Multi-drug resistant STECs (4.85%) were also identified in this study, and showed the highest resistance to ampicillin, carbenicillin, ceftazidime, ciprofloxacin, ceftriaxone, cefotaxime, gentamicin, norfloxacin, trimethoprim-sulfamethoxazole, and tigecycline.

Table 2. Prevalence of STEC serotype.

Polyvalent	Group specific antisera	No. of isolates (%)
E. coli (O & K) polyvalent I	O25 : K11	4 (1.94)
	O26 : K60	7 (3.4)
	O44 : K74	7 (3.4)
	O55 : K59	2 (0.97)
	O78 : K80	10 (4.85)
	O111 : K58	3 (1.46)
	O114 : K-	3 (1.46)
	O119 : K69	2 (0.97)
E. coli (O & K) polyvalent II	O86 : K61	2 (0.97)
	O124 : K72	2 (0.97)
	O125 : K70	0 (0)
	O126 : K71	0 (0)
	O127 : K63	1 (0.5)
	O128 : K67	19 (9.22)
E. coli (O & K) polyvalent III	O18ac : K77	11 (5.34)
	O20ab : K84	26 (12.6)
	O28 : K73	19 (9.22)
	O112ac : K66	4 (1.94)
Non-typable		84 (40.78)

STEC: Shiga toxin-producing *E. coli*

Table 3. Antimicrobial drug resistance phenotypes, antimicrobial resistance genes, and integrons in STEC isolated from pigs.

Antimicrobial susceptibility testing				Antimicrobial resistance genes	No. of isolates (%)
Drug	S (%)	I (%)	R (%)		
Penicillins				bla_{TEM}	203 (98.07%)
Ampicillin	0.5	0	99.5	bla_{SHV}	0 (0%)
Carbenicillin	1	0	99	bla_{CMY-2}	0 (0%)
β-lactam/β-lactamase inhibitor combinations					
Amoxicillin/ Clavulanic acid	90.3	9.7	0		
Sulbactam/ Cefoperazone	97.1	2.9	0		
Piperacillin/ Tazobactam	93.2	1.9	4.9		
Cephems					
Cefuroxime sodium	99	0.5	0.5		
Cefepime	100	0	0		
Ceftriaxone	99.5	0	0.5		

Table 3. Continued.

Antimicrobial susceptibility testing				Antimicrobial resistance genes	No. of isolates (%)
Drug	S (%)	I (%)	R (%)		
Cefotaxime	99.5	0	0.5		
Ceftazidime	99.5	0	0.5		
Carbapenems					
Imipenem	100	0	0		
Meropenem	100	0	0		
Aminoglycosides				*aac*(3)-IIa	17 (8.21%)
Gentamicin	99	0.5	0.5	*aac*(3)-IV	6 (2.9%)
Amikacin	99.51	0	0.49	*aadA*	175 (84.54%)
				aadB	0 (0%)
Tetracycline				*tetA*	0 (0%)
Tigecycline	95.6	3.4	1	*tetB*	0 (0%)
				tetC	0 (0%)
Quinolones				*qnrA*	0 (0%)
Ciprofloxacin	98.1	0	1.9	*qnrB*	0 (0%)
Norfloxacin	98.1	0	1.9	*qnrS*	7 (3.38%)
Folate pathway				*dhfrI*	0 (0%)
inhibitors	38.8	1	60.2	*dhfrV*	139 (67.15%)
Trimethoprim/				*dhfrVII*	0 (0%)
Sulfamethoxazole				*sulI*	1 (0.48%)
				sulII	175 (84.54%)
				sulIII	0 (0%)
				intI	193 (93.69%)
				CS1	14 (6.8%)
				intII	2 (0.97%)
				CS2	0 (0%)

STEC = Shiga toxin-producing *E. coli*; S = Susceptible, I = Intermediate, R = Resistance

Among the β-lactam-resistant bacteria, most isolates were seen to carry only the bla_{TEM} gene (98.07%), whereas the bacteria in the aminoglycoside-resistant group carried *aadA* (84.54%), *aac*(3)-IIa (8.21%), and *aac*(3)-IV gene (2.9%). None isolates exhibited the presence of *aadB*. For quinolone-resistant isolates, the bacteria were seen to carry the *qnrS* gene (3.38%), but not *qnrA* or *qnrB*. While, the sulfamethoxazole resistant isolates, the *sulII* gene (84.54%) was most common, followed by the *sulI* gene (0.48%). No traces of the *sulIII* gene were observed. Trimethoprim-resistant STEC isolates exhibited the presence of *dhfrV* (67.15%), but not *dhfrI* or *dhfrVII*, and none of the isolates in the tetracycline-resistant group carried *tetA*, *tetB*, or *tetC*.

With regard to class 1 integrons, 93.69% (193/206 isolates) of STECs carried *intI* and 6.8% (14/206 isolates) carried *CS1* in 3 distinct fragments, namely, 300, 400, 500 and 2,000 bps (Figure 1). Among the class 2 integrons, only 0.97% (2/206 isolates) of

bacteria carried *intI*II and no isolates carried *CS2* (Table 3). The patterns of antimicrobial resistance among STEC isolates have been shown in Table 4. Base on the age and diarrhea symptom of swine group, 3 (1.5%) STECs isolated from Normal piglets (age: < 3 weeks) group which carried antimicrobial resistance genes bla_{TEM}, *aadA*, *IntI*; 1 (0.5%) STEC was isolated from diarrhea piglets, (age: < 3 weeks) group, carried *sul*I, *sul*II, bla_{TEM}; and 92 (44.6%) STECs, isolated from normal piglets (age: 3-8 weeks) group, carried *sul*II, bla_{TEM}, *aadA*, *dhfrV*, *aac*(3)IIa, *qnrS*, *IntI*, *IntI*I; and 110 (53.4%) STECs, isolated from diarrhea piglets (age: 3-8 weeks) carried *sul*II, bla_{TEM}, *aadA*, *dhfrV*, *aac*(3)IIa, *IntI*, and class I integrons.

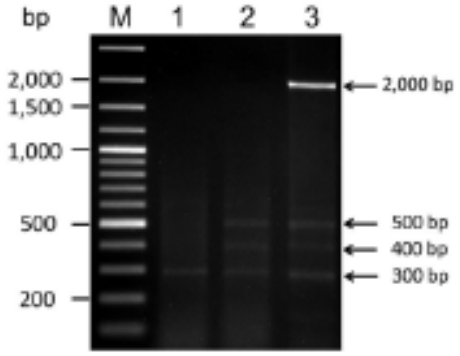

Figure 1. *CS* class I integrons expression. Lane M is 100 bp ladder marker, Lane 1 is *CS* class 1 gene expression (300 bp), Lane 2 is *CS* class 1 gene expression (300, 400, and 500 bp) and Lane 3 is *CS* class 1 gene expression (300, 400, 500, and 2,000 bp).

Table 4. Pattern of antimicrobial resistance among EVS-EVC-positive *Escherichia coli*.

Pattern of antimicrobial resistance	No. of isolates (%)
SXT	1 (0.49)
AMP, CAR	77 (37.38)
AMP, SXT	1 (0.49)
AMP, CAR, SXT	112 (54.37)
AMP, CAR, TZP	5 (2.43)
AMP, CAR, SXT, TGC	1 (0.49)
AMP, CAR, SXT, TZP	5 (2.43)
AMP, CAR, CIP, NOR, SXT	2 (0.97)
AK, AMP, CAR, CIP, NOR, SXT	1 (0.49)
AMP, CAR, CAZ, CIP, CN, CRO, CTX, NOR, SXT, TGC	1 (0.49)

AK = Amikacin, AMP = Ampicillin, CAR = Carbenicillin, CAZ = Ceftazidime, CIP = Ciprofloxacin, CN = Gentamicin, CRO = Ceftriaxone, CTX = Cefotaxime, NOR = Norfloxacin, SXT = Trimethoprim/Sulfamethoxazole, TGC = Tigecycline, TZP = Piperacillin/Tazobactam

Several studies have reported an increase in the prevalence of antimicrobial-resistant *E. coli* since 1950 [20]. A Canadian study reported that *E. coli* bacterial isolates from pigs frequently exhibited resistance to tetracycline, sulfonamide, and streptomycin [15, 21-23]. Similarly, *E. coli* isolated from pigs in the USA also exhibited resistance to tetracycline and spectinomycin, in addition to β-lactams [16]. Conversely, Asian studies conducted in China, Taiwan, Korea and Thailand reported that *E. coli* was resistant to aminoglycoside, tetracycline, sulfonamide, spectinomycin, chloramphenicol, quinolone, amoxicillin, ampicillin, streptomycin, carbenicillin, and trimethoprim-sulfamethoxazole [5, 14, 24]. These geographic differences in resistance patterns may be explained by differences in the drugs used in these regions. In this study, the isolated *E. coli* exhibited high levels of resistance to ampicillin and carbenicillin, which both are commonly antibiotics used in pig farms, and also carried the gene associated with drug resistance (bla_{TEM}). These results demonstrated that repeated use of antibiotics including amoxicillin and penicillin in pig farms may affect the antimicrobial resistance phenotype and genotype of isolated *E. coli*, which correspondence to the relationship between other antibiotics and pathogens.

The mechanisms leading to antimicrobial resistance include the production of enzymes to inactivate or modify the antibiotic drug, reduction of the binding capacity of antibiotics by alteration of its target site and reduction of intracellular antibiotic accumulation by decreasing permeability and/or increasing active efflux of the antibiotic. Additionally, bacteria can develop resistance to antibiotics by mutating existing genes (vertical evolution) or by acquiring new genes from other strains or species (horizontal gene transfer). The sharing of genes between bacteria by horizontal gene transfer occurs through several methods including plasmids, transposons, and integrons [6, 8].

The mechanisms used by bacteria for β-lactam antibiotic resistance include modification of porins (permeability barrier), alteration of target affinity (penicillin binding proteins; PBP's) and production of inactivating enzymes (β-lactamases). The last method is the most common among gram-negative bacteria [25]. The genes that encode β-lactamases resistance include bla_{TEM}, bla_{SHV}, and bla_{CMY-2}. In this study, although the resistance of STEC to penicillin was very high, only the presence of bla_{TEM} was observed and there was no evidence of bla_{SHV} and bla_{CMY-2}. This was in accordance with previous studies [15, 21].

The mechanisms of aminoglycoside resistance include reduction of drug uptake or decreased cell permeability, alteration of the ribosomal binding sites and production of aminoglycoside modifying enzymes. There are 3 types of aminoglycoside modifying reactions including acetylation, adenylation, and phosphorylation. Of these, modification of the drugs by bacterial enzymes is the most common mechanism [6]. The genes that encode aminoglycoside modifying enzymes include *aac*(3)-IIa (*aac*C2), *aac*(3)-IV, *aad*A, and *aad*B. In this study, although most STECs were susceptible to aminoglycosides, the presence of aminoglycosides resistance gene was observed. The *aad*A was the most frequently observed gene, followed by *aac*(3)-IIa and *aac*(3)-IV. None of the isolates exhibited the presence of *aad*B. These results were in accordance with a previous study that examined the prevalence of *aad*A and *aac* in 515 non-pathogenic *E. coli* isolated from food products of animal origin and fecal

samples of healthy animals [13].

The mechanisms of quinolone resistance include alteration of the targets of quinolones, decreased accumulation inside the bacteria due to decreased permeability of the membrane and/or overexpression of the efflux pump system, and plasmid mediated quinolone resistance [26-27]. Of these, the last mechanism is most commonly observed. The genes that encode quinolone resistance and transfer via plasmids include *qnr*A, *qnr*B, and *qnr*S. Of these, *qnr*S is more frequently detected than the other genes [28]. In this study, although most STECs were susceptible to quinolones, *qnr*S, a gene associated with quinolone resistance, was observed.

Resistance to sulfonamides is frequently observed in farm animals, and is brought about by the retrieval of *sul* genes (*sul*I, *sul*II, and *sul*III) via plasmid transfer [23]. The prevalence of *sul*I was high between 1995 and 2003, but this was replaced by *sul*II thereafter [1, 21-22, 29]. *Sul*III was detected for the first time in the year 2003 [30]. In this study, a high resistance of STEC to sulfonamides was observed, and the prevalence of sulfonamide resistance genes was common. The *sul*II gene was most frequently observed, and there was no evidence of the *sul*III gene in any of the isolates.

The mechanisms of bacterial resistance to trimethoprim (TMP) include reduced cell wall permeability, alternative metabolic pathways, production of a resistant chromosomal DHFR enzyme, overproduction of a chromosomal enzyme, and production of a plasmid-mediated TMP-resistant DHFR enzyme. The most important resistance mechanism is the acquisition of a TMP-insensitive DHFR variant resulting in high-level TMP resistance in various bacteria [31]. Several studies have reported observing genes associated with TMP resistance such as *dhfr*I, *dhfr*V, and *dhfr*XIII [1, 21]. In this study, although the STECs exhibited levels of trimethoprim resistance similar to that of sulfonamides, the prevalence of trimethoprim resistance genes was less. Additionally, of the TMP resistance genes, only the presence of *dhfr*V was observed.

The different mechanisms of tetracycline resistance include tetracycline efflux, ribosome protection and enzymatic inactivation of tetracycline. Of these, tetracycline efflux is the most common mechanism among gram-negative bacteria [32]. The genes that encode tetracycline resistance are *tet*A, *tet*B, and *tet*C, and studies reporting their prevalence are controversial. Some studies have reported the presence of *tet*B in tetracycline-resistant *E. coli* more frequently than *tet*A and *tet*C [1, 22, 29], whereas others observed *tet*A more commonly in tetracycline-resistant *E. coli* isolates than *tet*B [21]. In this study, none of the STECs that exhibited susceptibility to tetracycline (95.6%) were seen to carry any of the *tet* genes.

Integrons are mobile genetic elements that contribute to the development of multi-antimicrobial resistance in gram-negative bacteria. The general structure of the integrons consist of a conserved region that codes integrase (*Int*) and a variable region (*5'CS-3'CS*) where various resistance cassettes can be integrated themselves. Several studies have shown that the most common integrons in enterobacteria such as *E. coli* belong to class 1 and class 2 [9, 33]. *E. coli* isolated from pigs usually exhibit both class I and class II integrons, but the prevalence of class I is higher than class II [14]. Our results are consistent with previous reports.

4. CONCLUSION

In this study, we found STEC isolates from swine which belonging to 3 majors serogroups: O20ab:K84, O128:K67 and O28:K73. Resistance to ampicillin was the major problem following with carbenicillin and trimethoprim/sulfamethoxazole. The bacterial isolates usually resistance to 3 kinds of antimicrobial drug. Interestingly, they can be resist up to 10 kinds of antimicrobial drugs. The antimicrobial resistance genes that always found in this study comprise of bla_{TEM}, *aadA*, *sulII*, *dfrfV* and *IntI*. These finding indicate that a surveillance program is needed to monitor the antimicrobial resistance in bacterial isolated from animals. In addition, it is urgently to educate pig farmer, implement administrative regulations and guidelines for the rational use of drugs to prevent the spread of multi-drug resistant bacteria.

ACKNOWLEDGEMENTS

We thank Assoc. Prof. Kampon Kaeoket, Assist. Prof. Dusit Laohasinnarong, Assist. Prof. Panida Chanapiwat, and Siriporn Tantavej, DVM for helping with access to the pig farms and specimen collection. We are also very grateful to the Faculty of Veterinary Science and Faculty of Tropical Medicine, Mahidol University for providing us with a laboratory and suitable equipment. This work was supported by the capital budget of Mahidol University 2014-2015 [grant number 148894], National Research University (NRU), Mahidol University. Nitaya Indrawattana is a scholar of the Thailand Research Fund [grant number RSA5980048].

REFERENCES

[1] Smith M.G., Jordan D., Chapman T.A., Chin J.J., Barton M.D., Do T.N., Fahy V.A., Fairbrother J.M. and Trott D.J., *Vet. Microbiol.*, 2010; 145: 299-307. DOI 10.1016/j.vetmic.2010.04.004.

[2] Olaitan A.O., Thongmalayvong B., Akkhavong K., Somphavong S., Paboriboune P., Khounsy S., Morand S. and Rolain J.M., *J. Antimicrob. Chemother.*, 2015. DOI 70:3402-3404. 10.1093/jac/dkv252.

[3] Huang K., Xu C.W., Zeng B., Xia Q.Q., Zhang A.Y., Lei C.W., Guan Z.B., Cheng H. and Wang H.N., *J. Vet. Med. Sci.*, 2014; 76: 1213-1218.

[4] Mazurek J., Bok E., Stosik M. and Baldy-Chudzik K., *Int. J. Environ. Res. Public. Health*, 2015; 12: 2150-2163. DOI 10.3390/ijerph120202150.

[5] Hsu S.C., Chiu T.H., Pang J.C., Hsuan-Yuan C.H., Chang G.N. and Tsen H.Y., *Int. J. Antimicrob. Agents*, 2006; 27: 383-391. DOI 10.1016/j.ijantimicag.2005.11.020.

[6] Zhang X.Y., Ding L.J. and Yue J., *Microb. Drug Resist.*, 2009; 15: 323-328. DOI 10.1089/mdr.2009.0020.

[7] Chantziaras I., Boyen F., Callens B. and Dewulf J., *J. Antimicrob. Chemother.*, 2014; 69: 827-834. DOI 10.1093/jac/dkt443.

[8] Santajit S. and Indrawattana N., *Biomed. Res. Int.*, 2016; 2475067. DOI 10.1155/2016/2475067.

[9] Lapierre L., Cornejo J., Borie C., Toro C. and San Martin B., *Microb. Drug Resist.*, 2008; 14: 265-272. DOI 10.1089/mdr.2008.0810.

[10] Jones L.A., Melver C.J., Rawlinson W.D. and White P.A., *Commun. Dis. Intel.*, 2003; 27: 103-110.

[11] Tajbakhsh E., Khamesipour F., Ranjbar R. and Ugwu C.I., *Iran. Ann. Clin. Microbiol. Antimicrob.*, 2015; 14: 37. DOI 10.1186/s12941-015-0096-y.

[12] Kheiri R. and Akhtari L., *Gut Pathogens.*, 2016; 8: 40. DOI 10.1186/s13099-016-0123-3.

[13] Saenz Y., Brinas L., Dominguez E., Ruiz J., Zarazaga M., Vila J. and Torres C., *Antimicrob. Agents Chemother.*, 2004; **48**: 3996-4001. DOI 10.1128/AAC.48.10.3996-4001.2004.

[14] Kang H.Y., Jeong Y.S., Oh J.Y., Tae S.H., Choi C.H., Moon D.C., Lee W.K., Lee Y.C., Seol S.Y., Cho D.T. and Lee J.C., *J. Antimicrob. Chemother.*, 2005; **55**: 639-644. DOI 10.1093/jac/dki076.

[15] Rosengren L.B., Waldner C.L. and Reid-Smith R.J., *Appl. Environ. Microbiol.*, 2009; **75**: 1373-1380. DOI 10.1128/AEM.01253-08.

[16] Malik Y.S., Chander Y., Olsen K. and Goyal S.M., *Can. J. Vet. Res.*, 2011; **75**: 117-121.

[17] Clinical and Laboratory Standards Institute. 2012. Performance standards for antimicrobial susceptibility testing: twenty-two informational supplement. CLSI Document M100-S22. CLSI, Wayne, PA. 32.

[18] Vuddhakul V., Patararungrong N., Pungrassamee P., Jitsurong S., Morigaki T., Asai N. and Nishibuchi M., *FEMS Microbiol. Lett.*, 2000; **182**: 343-347.

[19] Prapasarakul N., Tummaruk P., Niyomtum W., Tripipati T. and Serichantalergs O., *J. Vet. Med. Sci.*, 2010; **72**: 1603-1608. DOI 10.1292/jvms.10-0124.

[20] Tadesse D.A., Zhao S., Tong E., Ayers S., Singh A., Bartholomew M.J. and McDermott P.F., *Emerg. Infect. Dis.*, 2012; **18**: 741-749. DOI 10.3201/eid1805.111153.

[21] Maynard C., Fairbrother J.M., Bekal S., Sanschagrin F., Levesque R.C., Brousseau R., Masson L., Lariviere S. and Harel J., *Antimicrob. Agents Chemother.*, 2013; **47**: 3214-3221.

[22] Boerlin P., Travis R., Gyles C.L., Reid-Smith R., Janecko N., Lim H., Nicholson V., McEwen S.A., Friendship R. and Archambault M., *Appl. Environ. Microbiol.*, 2005; **71**: 6753-6761. DOI 10.1128/AEM.71.11.6753-6761.2005.

[23] Kozak G.K., Pearl D.L., Parkman J., Reid-Smith R.J., Deckert A. and Boerlin P., *Appl. Environ. Microbiol.*, 2009; **75**: 5999-6001. DOI 10.1128/AEM.02844-08.

[24] Lu L., Dai L., Wang Y., Wu C., Chen X., Li L., Qi Y., Xia L. and Shen J., *Acta Trop.*, 2010; **113**: 20-25. DOI 10.1016/j.actatropica.2009.08.028.

[25] Rice L.B., *Mayo Clin. Proc.*, 2012; **87**: 198-208. DOI 10.1016/j.mayocp.2011.12.003.

[26] Ruiz J., *J. Antimicrob. Chemother.*, 2003; **51**: 1109-1117. DOI 10.1093/jac/dkg222.

[27] Jacoby G.A., *Clin. Infect. Dis.*, 2005; **41 Suppl 2**: S120-126. DOI 10.1086/428052.

[28] Huang S.Y., Zhu X.Q., Wang Y., Lin H.B., Dai L., He J.K., Li B.B., Wu C.M. and Shen J.Z., *Foodborne Pathog. Dis.*, 2012; **9**: 896-901. DOI 10.1089/fpd.2012.1131.

[29] Lanz R., Kuhnert P. and Boerlin P., *Vet. Microbiol.*, 2003; **91**: 73-84.

[30] Perreten V. and Boerlin P., *Antimicrob. Agents Chemother.*, 2003; **47**: 1169-1172.

[31] Seputiene V., Povilonis J., Ruzauskas M., Pavilonis A. and Suziedeliene E., *J. Med. Microbiol.*, 2010; **59**: 315-322. DOI 10.1099/jmm.0.015008-0.

[32] Chopra I. and Roberts M., *Microbiol. Mol. Biol. Rev.*, 2001; **65**: 232-260. DOI 10.1128/MMBR.65.2.232-260.2001.

[33] Su H.C., Ying G.G., Tao R., Zhang R.Q., Zhao J.L. and Liu Y.S., *Environ. Pollut.*, 2012; **169**: 42-49. DOI 10.1016/j.envpol.2012.05.007.

[34] Ali M.M., Ahmed S.F., Klena J.D., Mohamed Z.K., Moussa T.A. and Ghenghesh K.S., *J. Infect. Dev. Ctries.*, 2014; **8**: 589-596. DOI 10.3855/jidc.4077.

[35] Leverstein-Van Hall M.A., Paauw A., Box A.T., Blok H.E., Verhoef J. and Fluit A.C., *J. Clin. Microbiol.*, 2002; **40**: 3038-3040.

Veterinary World, EISSN: 2231-0916
Available at www.veterinaryworld.org/Vol.10/July-2017/1.pdf

RESEARCH ARTICLE
Open Access

Screening method for *Staphylococcus aureus* identification in subclinical bovine mastitis from dairy farms

Natapol Pumipuntu[1], Suphang Kulpeanprasit[1], Sirijan Santajit[1], Witawat Tunyong[1], Thida Kong-ngoen[1], Woranich Hinthong[2] and Nitaya Indrawattana[1]

1. Department of Microbiology and Immunology, Faculty of Tropical Medicine, Mahidol University, Bangkok, Thailand; 2. Faculty of Medicine and Allied Health, HRH Princess Chulabhorn College of Medical Science Bangkok, Thailand.
Corresponding author: Nitaya Indrawattana, e-mail: nitaya.ind@mahidol.ac.th
Co-authors: NP: film.natapol@gmail.com, SK: Suphang.kpt@gmail.com, SS: sirijan.santajit@gmail.com, WT: witawat.tun@mahidol.ac.th, TK: thida.kon@mahidol.ac.th, WH: p_prem85@yahoo.com
Received: 09-02-2017, **Accepted:** 12-05-2017, **Published online:** 01-07-2017

doi: 10.14202/vetworld.2017.721-726 **How to cite this article:** Pumipuntu N, Kulpeanprasit S, Santajit S, Tunyong W, Kong-ngoen T, Hinthong W, Indrawattana N (2017) Screening method for *Staphylococcus aureus* identification in subclinical bovine mastitis from dairy farms, *Veterinary World*, 10(7):721-726.

Abstract

Background: *Staphylococcus aureus* is one of the most important contagious bacteria causing subclinical bovine mastitis. This bacterial infection is commonly identified by determine the pathogen in bovine milk samples through conventional technique including coagulase test. However, this test has several disadvantages as low sensitivity, risk of biohazard, cost expensive, and limited preparation especially in local area.

Aim: Aim of this study was to compare and assess the screening method, Mannitol fermentation test (Mannitol salt agar [MSA]), and deoxyribonuclease (DNase) test, for *S. aureus* identification in milk samples.

Materials and Methods: A total of 224 subclinical bovine mastitis milk samples were collected from four provinces of Thailand and determined *S. aureus* using conventional method and also subjected to the screening test, MSA and DNase test. The sensitivity, specificity, positive predictive value (PPV), and negative predictive value (NPV) among both tests were analyzed and compared to the tube coagulase test (TCT), as reference method. Immunological test by latex agglutination and molecular assay by determined *spa* gene were also used to identify and differentiate *S. aureus*.

Results: A total of 130 staphylococci were isolated by selective media, Gram-stain, and catalase test. The number of *S. aureus* which identified using TCT, MSA and DNase test were 32, 102, and 74 isolates, respectively. All TCT results were correlated to results of latex agglutination and *spa* gene which were 32 *S. aureus*. MSA showed 100% sensitivity, 28.57% specificity, 31.37% PPV, and 100% NPV, whereas DNase showed 53.13% sensitivity, 41.84% specificity, 22.97% PPV, and 73.21% NPV. DNase test showed higher specificity value than MSA but the test presented 26.79% false negative results whereas no false-negative result from MSA when comparing to TCT.

Conclusion: MSA had a tendency to be a good preference for screening *S. aureus* because of its high sensitivity and NPV. The result from this study will improve a choice to use a screening test to diagnose *S. aureus* of veterinary field for prompt disease controlling and effective treatment.

Keywords: bovine mastitis, deoxyribonuclease test, mannitol fermentation test, screening methods, *Staphylococcus aureus*.

Introduction

Bovine mastitis is a disease of the most prevalence and costly diseases in dairy cows or some livestock milk industries with losses lead to reducing of milk production, changing in milk composition, discarding or low quality milk, increasing veterinary services, and increasing labor costs [1]. This inflammation of the mammary gland can be divided into two types that manifested by the appearance of inflammation at the udder of dairy cow; asymptomatic (subclinical mastitis) and symptomatic mastitis (clinical mastitis), whereas subclinical mastitis can be occurred up to 40 times more common than clinical cases [2]. Thus, this subclinical mastitis seems to be an important type of mastitis in dairy cow because it is a hidden mastitis or invisible problem in the herd [3] and needed to be more concern. *Staphylococcus* species are one of the main etiological bacteria that cause bovine mastitis especially for *Staphylococcus aureus* which is considered as a contagious pathogen that often cause bovine mastitis [4]. These bacteria can spread from infected cow to another cow in a herd by mainly through many routes as contaminated milking equipment or through hands of farmers. *S. aureus* infection in subclinical bovine mastitis becomes to be a large and important problem in dairy farm industry [5]. There are estimates that about 80-100% of all dairy herds have at least some *S. aureus* mastitis, with from 5% to 10% of infected cows [6]. In Thailand, the prevalence of *S. aureus* infection in dairy cattle subclinical mastitis is also different in each study site such as 8% and 3%

of the bacterial isolates in Chiang Mai [7] and Khon Kaen [8], respectively.

Conventional method is the gold standard for identification of staphylococcal infection from the clinical specimen. Tube coagulase test (TCT) is the one of biochemical tests that commonly used to differentiate *S. aureus* from coagulase-negative staphylococci for a reason that the bacteria can produce coagulase protein to promote coagulation [9-12]. This protein enzyme can activate the nonproteolytic activation of prothrombin and cleavage of fibrinogen [13]. In routine laboratory, TCT is normally prepared from plasma of human or rabbit or horse [14]. Nevertheless, the differentiation of *S. aureus* by TCT spent a times to monitor and interpret the results [15]. Moreover, the interpretation of TCT needs the expertise to clarify the results [16]. Risk of biohazard from TCT can be happen when the plasma derived from the infectious plasma whatever from human or animal [17]. Furthermore, some *S. aureus* may produce low amount of coagulase which render false negative result in TCT [18].

Beside the disadvantage of TCT, Mannitol salt agar (MSA) and deoxyribonuclease (DNase) testing are the other biochemical methods which can be used for screening the differentiation of *S. aureus* from other species. Due to *S. aureus* can ferment mannitol sugar and produces an acid at the end product when inoculated on MSA result in the phenol red indicator change the color from red to yellow [19]. Since *S. aureus* has an ability to produce enzyme DNase which can hydrolyze nucleic acid in DNase medium agar, then it will be seen a clear zone around bacterial colonies [20]. From the limitation in some laboratories which in short supply to find some plasma to perform the coagulase test by the reason of its expensive and risk of biohazard that we mentioned above. MSA and DNase are interested to use instead of TCT [21]. Therefore, this study aims to evaluate the efficiency of MSA and DNase for screening *S. aureus* in milks of subclinical bovine mastitis cases from four provinces in Thailand comparing to TCT. The sensitivity, specificity, positive predictive value (PPV), and negative predictive value (NPV) were determined. The result from this study will provide a choice of a screening test for diagnose *S. aureus* of veterinary field for further prompt disease controlling and effective treatment.

Materials and Methods

Ethical approval

All procedures performed in this study were approved by the Faculty of Tropical Medicine-Animal Care and Use Committee, Mahidol University, Thailand (protocol no. 002-2016).

Sample collection and preparation

Individual 224 milk samples were aseptically collected from subclinical bovine mastitis cases in from 52 dairy farms which 8 different areas Thailand, i.e.; Saraburi, Lopburi, Nakorn Ratchasima, and Maha Sarakham provinces during September 2015 to April 2016. All samples were inoculated on Columbia blood agar supplemented with nalidixic acid and colistin sulfate for *Staphylococcus* spp. and *Streptococcus* spp. (Oxoid, Hampshire, UK) and incubated at 35°C for 18 h. The suspected bacterial colonies were subjected to conventional methods such as Gram-stain, catalase test, coagulase test, MSA, and DNase.

Screening test for *S. aureus*

Staphylococcal isolates which showed positive result for catalase test were subcultured on human blood agar and incubated at 37°C for 24 h. Then, the single colonies were subjected to the screening test, i.e., MSA, DNase and TCT, respectively.

MSA

MSA contains 1% mannitol, 7.5% sodium chloride, phenol red indicator, and peptone. *S. aureus* can tolerate and survive in high salt condition in this medium and can grow on it whereas the other bacteria will be inhibited by the high salt concentration from the media. *S. aureus* can ferment the sugar mannitol and from this ability it produces an acid at the end product that changes phenol red indicator into yellow. In this experiment, the suspected single bacterial colony was inoculated on MSA plate (Oxoid, Basingstoke, UK), incubated at 35°C for 24 h and observed the indicator change (Figure-1).

DNase test

DNase agar contains 2% tryptose, 0.2% deoxyribonucleic acid, 0.5% sodium chloride, and methyl green indicator. *S. aureus* has ability to produce enzyme DNase which can hydrolyze nucleic acid in DNase medium and was seen a colorless zone around their colonies. In this study, the single bacterial colony was inoculated on DNase plate (Oxoid, Basingstoke, UK), incubated at 37°C for 18 h and observed the colorless zone around bacterial colony which indicated the colony of *S. aureus* (Figure-1).

TCT

TCT is prepared using human or animal plasma. The test aspired for detecting free coagulase of *S. aureus*. Free coagulase is secreted from extracellular specifically by *S. aureus* that reacted with the coagulase reacting factor in plasma that able to from a complex together, which called thrombin. The thrombin has ability to convert fibrinogen to fibrin resulting in clotting of plasma. This thrombin can be called staphylothrombin. In this study, TCT was done by adapted the protocol from Murray, 2003 [22]. The full loop of fresh suspected colonies with 1 ml of human plasma, then incubated the mixture at 37°C and observed for clotting formation by gently tilting it horizontal from the vertical after incubated for 4, 6 and 24 h. Plasma clotting was considered to be a positive result for coagulase test (Figure-1).

All methods have subjected with *S. aureus* ATCC 25923 as positive control and *Staphylococcus*

epidermidis ATCC 12228 was used as a negative control, respectively.

Verify assays for differentiate S. *aureus*

Latex agglutination

The suspected bacterial isolates, which showed gram positive cocci and positive for catalase test, were determined to be *S. aureus* by Staphaurex Plus kit (Remel Europe Ltd., Dartford, UK) based on immuno-agglutination technique. The latex particle was coated with rabbit immunoglobulin G (IgG) and fibrinogen which can render the interaction of fibrinogen and *S. aureus* clumping factor, the Fc portion of IgG and *S. aureus* protein A and specific IgG and *S. aureus* cell surface antigens. The experiment was done following to the manufacture's protocol [23]. Two drops of bacterial suspension was mixed with a drop of latex particle reagent on a reaction card. Then, the card was rotated smoothly for 30 seconds before observing noticeable agglutination. *S. aureus* strain ATCC 25923 was used as positive control which showed the mixture agglutination whereas no agglutination when tested with *S. epidermidis* strain ATCC 12228, a negative control. The staphaureux-positive isolates were determined the *spa* gene by polymerase chain reaction (PCR).

Amplification of spa gene

Several studies used the molecular method to determine *S. aureus* by amplify the *spa* gene that is encoded for protein A [24,25]. Bacterial genomic DNA was extracted using DNA extraction kit (Geneaid, Taiwan). The PCR mixture (25 µL) consisted of 1 µM of forward primer (5'-CAAGCACCAAAAGAGGAA-3') and reverse primer (5'-CACCAGGTTTAACGACAT-3'), 100 ng of DNA template, 2.5 µL of 10×Taq PCR buffer, 0.2 mM dNTP, 2 mM $MgCl_2$, and 1 unit of Taq DNA polymerase (Thermo Scientific, USA). The PCR mixture was subjected to the following thermal cycle conditions using the T100™ Thermal Cycler (BioRad, USA): 95 min of 95°C before 35 cycles of amplification at 95°C for 45 s, 58°C for 45 s, and 72°C for 45 s, followed by a final extension at 72°C for 10 min. The PCR products were analyzed by 1.5% agarose gel electrophoresis and ethidium bromide staining [26]. The DNA bands, size 300 base pairs (Figure-2), were observed under a Gel Doc™ XR+ System (Biorad, USA). *S. aureus* ATCC 25923 and *S. epidermidis* ATCC 12228 were used in this study as positive and negative control, respectively.

Efficiency analysis

The SPSS software (version 20.0) was used for statistical analysis. The sensitivity and specificity of MSA and DNase were analyzed using two × two tables as the followings formulas:

$$\text{Sensitivity (\%)} = \frac{\text{True positive}}{\text{All positive}} \times 100$$

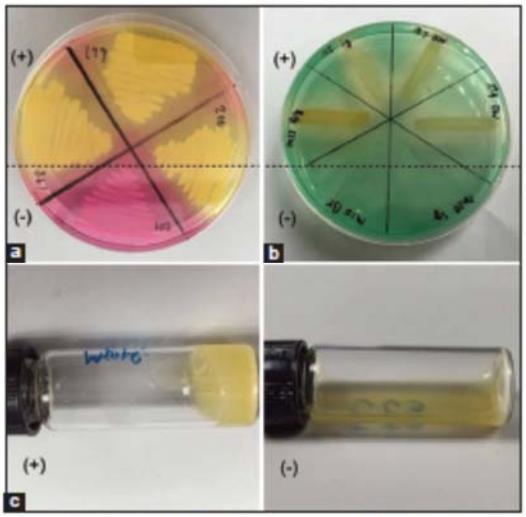

Figure-1: Screening tests for identification of *Staphylococcus aureus* from subclinical bovine mastitis milk sample. (a) Mannital salt agar; (b) deoxyribonuclease test and (c) tube coagulase test. (+) - positive result; (−) - negative result.

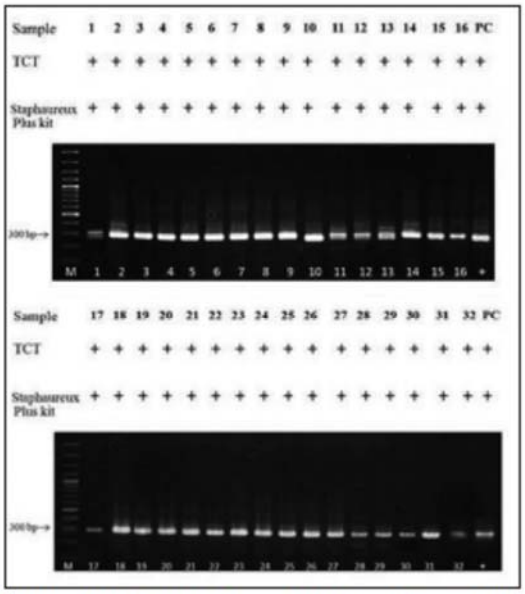

Figure-2: *Staphylococcus aureus* identification by using tube coagulase test, Staphareux Plus kit and *spa* gene amplification. Lane M, 100 bp DNA ladder; Lane 1-32, Staphylococal isolate DNA samples; Lane PC, *S. aureus* ATCC 25923 (positive control). *Spa* amplicon is 300 bp. (+) - positive result.

$$\text{Specificity (\%)} = \frac{\text{True negative}}{\text{All negative}} \times 100$$

$$\text{Positive predictive value (PPV) (\%)} = \frac{\text{True positive}}{\text{True positive} + \text{False positive}} \times 100$$

$$\text{Negative predictive value (NPV)}(\%) = \frac{\text{True negative}}{\text{True negative} + \text{False negative}} \times 100$$

Results

From total 224 milk samples, 130 *Staphylococcus* spp. were isolated by the selective media (Columbia supplemented with the inhibitors), Gram-stain and catalase test. As showed in Table-1, there were 78.46 % (102/130), 56.92% (74/130), and 24.65% (32/130) staphylococcal isolates showed positive result on MSA test, DNase test and TCT test, respectively. All 32-positive TCT isolates were also positive for both Staphaureux Plus and *spa* gene as showed in Figure-2.

The efficiency of MSA showed 100% sensitivity, 28.57% specificity, 31.37% PPV, and 100% NPV. Whereas, the efficiency of DNase showed 53.13% sensitivity, 41.84% specificity, 22.97% PPV, and 73.21% NPV (Table-2). DNase test showed higher specificity value than MSA but the test presented 26.79% (15/56) false negative results whereas no false-negative result from MSA when comparing to TCT. The efficiency of the combination tests, MSA and DNase, for screening *S. aureus* also determined (Table-2.). The combined test presented 100% sensitivity, 17.39% specificity, 30.9% PPV, and 100% NPV.

Discussion

Screening method for identification of *S. aureus* is important and necessary for prevention and control in dairy herd for veterinary field and animal health. There has less report about the evaluation of screening method for this pathogen especially with clinical sample from animal. Our study demonstrates that MSA show high sensitivity and can be used as screening test for differentiates *S. aureus* from animal specimen which possible infected with various species of *Staphylococcus*. The results similar to other reported from Kateete *et al.* [27] which screening clinical staphylococcal isolates from human by using MSA and combination method (MSA/DNase). They reported that MSA had higher sensitivity and NPV but lower specificity and PPV than DNase test. They also concluded that a combination of MSA and DNase which had highest sensitivity was the best choice for screening and identifying of *S. aureus* clinical isolates [27]. However, our study showed similar sensitivity value (100%) of MSA and the combination method (MSA and DNase test). Moreover, screening *S. aureus* from *Staphylococcus* isolates using MSA method showed higher specificity than the combination test. Consequently, MSA would be the best choice to screen and identify *S. aureus* isolated from bovine mastitis milk rather than the combined method even the PPV is very close (31.4% vs. 30.9%).While DNase test, presented low sensitivity and specificity, may not appropriate to use for screening and identifying as a single test. Furthermore, MSA had 100% NPV, it means that negative-MSA result can reliable as true negative result. MSA is appropriate to rule out the negative result as non-*S. aureus* isolates. Besides, many studies reported that DNase test showed lower sensitivity than MSA when compare the results with TCT [17,27,28]. Although DNase test showed higher sensitivity value than TCT, it may not suitable to use for screening *S. aureus* infection in dairy cows. Because of the DNase test showed high false negative results which render the infected cow (false negative-DNase test) will not treat and still be with the uninfected animal. Thus, the mastitis infection can disseminate in the dairy farm via this management. Therefore, it is extremely important to choose the appropriate screening test with provide the true negative result for quarantine *S. aureus* infected animal out from uninfected animal in order to medicate, prevent and limit the exposure and expansion of the infection in farms.

Furthermore, if we compared MSA, DNase and TCT in the terms of economic or cost of commercial media, they were found that MSA was very low priced. It was cheaper than DNase test 1.5 times and cheaper

Table-1: Screening for *Staphylococcus aureus* from subclinical bovine mastitis milk sample by MSA and DNase test comparing to tube coagulase test.

Biochemical test	Number isolates (n)	Tube coagulase test	
		Positive (n)	Negative (n)
MSA (+)	102	32	70
MSA (−)	28	0	28
DNase (+)	74	17	57
DNase (−)	56	15	41
MSA, DNase (+,+)	55	17	38
MSA, DNase (+,−)	47	16	31
MSA, DNase (−,+)	20	0	20
MSA, DNase (−,−)	8	0	8

Total 130 Staphylococcal isolates. MSA=Mannitol salt agar, DNase=Deoxyribonuclease test

Table-2: The calculated efficiency of MSA and DNase tests for screening of *Staphylococcus aureus* from subclinical bovine mastitis milk sample.

Biochemical tests	Sensitivity (%)	Specificity (%)	PPV (%)	NPV (%)
MSA	100	28.57	31.37	100
DNase	53.13	41.84	22.97	73.21
MSA and DNase*	100	19.15	30.9	100

*Only MSA, DNase (+,+) and MSA, DNase (−,−) were considered for this calculation. MSA=Mannitol salt agar, DNase=Deoxyribonuclease test, PPV=Positive predictive value, NPV=Negative predictive value

than TCT about 50 times. Therefore, MSA is a good choice to be an optimal choice for initial screening of *S. aureus* infection in dairy herd.

Conclusion

The use of MSA seems to be a valuable tool for initial screening and identifying of *S. aureus* clinical isolates in bovine milk sample. It can be used to screen *S. aureus* infection in local laboratories nearby agricultural fields in order to assist veterinarians for diagnosing and making a decision to readily medicate, control and prevention. However, if veterinarians suggest culling the infected cows out of the farm as *S. aureus* infection after MSA positive result, they need to be confirmed this bacterial infection by TCT or other molecular techniques before culling.

Authors' Contributions

NP and NI planed and designed of the study. The samples were collected in the fields by NP. Laboratory works were done by NP, SK, SS, WT, TK and WH. NI and NP analyzed the data and achieved statistical analysis. NP drafted and revised the manuscript under the advice from NI. Finally, all authors read and approved the final manuscript.

Acknowledgments

The work was supported by NSTDA Chair professor grant (P-1450624) funded by the Crown Property Bureau of Thailand and RSA5980048 of the Thailand Research Fund (TRF). Thanks are due to Professor Wanpen Chaicumpa, Center of Research Excellence on Therapeutic Proteins and Antibody Engineering, Department of Parasitology, Faculty of Medicine Siriraj Hospital, Mahidol University, Thailand, for her valuable advised and Satitpong Promsatit, DVM, Saraburi Provincial Livestock Office, Department of Livestock Development, Ministry of Agriculture and Cooperatives, Saraburi, Thailand, for his cooperation in the field.

Competing Interests

The authors declare that there is no conflict of interest in this research.

References

1. Hillerton, J.E. and Berry, E.A. (2005) Treating mastitis in the cow-a tradition or an archaism. *J. Appl. Microbiol.*, 98(6): 1250-1255.
2. Islam, M.R., Ahamed, M.S., Alam, M.S., Rahman, M.M., Sultana, T., Roh, Y.S. and Kim, B. (2011) Identification and antibiotic sensitivity of the causative organisms of sub-clinical mastitis in sheep and goats. *Pak. Vet. J.*, 32(2): 179-182.
3. Yadav, S., Sharma, M., Yadav, A. and Chaudhary, U.A. (2014) Study of biofilm production in *Staphylococcus aureus*. *Int. J. Pharm. Biol. Sci.*, 3(2): 61-63.
4. National Mastitis Council. (1996) Current Concepts of Bovine Mastitis. 4th ed. National Mastitis Council, Arlington, VA.
5. Piozza, K., Lievaart, J.J., Potts, G. and Barkema, H.W. (2011) Subclinical mastitis and associated risk factors on dairy farms in New South Wales. *Aust. Vet. J.*, 89(1-2): 41-46.
6. Jürgen, S., Bärbel, K., Wilfried, W., Michael, Z., Axel, S. and Klaus, F. (2003) The epidemiology of *Staphylococcus aureus* infections from subclinical mastitis in dairy cows during a control programme. *Vet. Microbiol.*, 96(1): 91-102.
7. Witaya, S. (2011) Epidemiology of subclinical mastitis and their antibacterial susceptibility in smallholder dairy farms, Chiang Mai province, Thailand. *J. Anim. Vet. Adv.*, 10(3): 316-321.
8. Jaruwan, K., Varaporn, S., Anantachai C., Sarinya, R. and Arunee, P. (2010) Chronic mastitis in small dairy cattle herds in Muang Khon Kaen. *Thai J. Vet. Med.*, 40(3): 265-272.
9. Balows, A., Hausler, W.J., Hermann, K.L., Isenberg, H.D. and Shadomy, H.J. (1991) Manual of Clinical Microbiology. 5th ed. American Society for Microbiology, Washington, DC.
10. McDonald, C.L. and Chapin, K. (1995) Rapid identification of *Staphylococcus aureus* from blood culture bottles by a classic 2-hour tube coagulase test. *J. Clin. Microbiol.*, 33(1): 50-52.
11. Moreillon, P., Entenza, J.M., Francioli, P., McDevitt, D., Foster, T.J. and Francois, P. (1995) Role of *Staphylococcus aureus* coagulase and clumping factor in pathogenesis of experimental endocarditis. *Infect. Immun.*, 63(12): 4738-4743.
12. Bello, C.S.S. and Qahtani, A. (2006) Pitfalls in the routine diagnosis of *Staphylococcus aureus*. *Afr. J. Biotechnol.*, 4(1): 83-86.
13. Cheng, A.G., McAdow, M., Kim, H.K., Bae, T., Missiakas, D.M. and Schneewind, O. (2010) Contribution of coagulases towards *Staphylococcus aureus* disease and protective immunity. *PLoS Pathog.*, 6(8): e1001036.
14. Yousef, A.E. and Carolyn, C. (2003) Food Microbiology: A Laboratory Manual. John Wiley & Sons, United States of America.
15. Sperber, W.H. and Tatini, S.R. (1975) Interpretation of the tube coagulase test for identification of *Staphylococcus aureus*. *Appl. Microbiol.*, 29(4): 502-505.
16. Berke, A. and Tilton, R.C. (1986) Evaluation of rapid coagulase methods for the identification of *Staphylococcus aureus*. *J. Clin. Microbiol.*, 23(5): 916-919.
17. Makwana, D.G.E., Gadhavi, D.H. and Sinha, D.M. (2012) Comparision of tube coagulase test with mannitol fermentation test for diagnosis of *Staphylococcus aureus*. *Natl. J. Integr. Res. Med.*, 3(4): 73-75.
18. Varettas, K., Mukerjee, C. and Taylor, P.C. (2005) Anticoagulant carryover may influence clot formation in direct tube coagulase tests from blood cultures. *J. Clin. Microbiol.*, 43(9): 4613-4615.
19. D'Souza, H.A. and Baron, E.J. (2005) BBL CHROMagar *Staphylococcus aureus* is superior to mannitol salt for detection of *Staphylococcus aureus* in complex mixed infections. *Am. J. Clin. Pathol.*, 123(6): 806-808.
20. Weckman, B.G. and Catlin, B.W. (1957) Deoxyribonuclease activity of micrococci from clinical sources. *J. Bacteriol.*, 73: 747-753.
21. Anyanwu, N.C.J. and John, W.C. (2013) Conventional and rapid methods for identification of *Staphylococcus aureus* from clinical specimens. *Sci. J. Microbiol.*, 2(9): 174-178.
22. Murray, P.R., Baron, E.J., Jorgensen, J.H., Pfaller, M.A. and Yolken, R.H. (2003) Manual of Clinical Microbiology. 8th ed. American Society for Microbiology, Washington, DC.
23. Remel Europe Ltd. (2011) Staphaurex™ Plus Latex Agglutination. Remel Europe Ltd., Dartford, UK.
24. Bhati, T., Nathawat, P., Sharma, S.K., Yadav, R., Bishnoi, J. and Kataria, A.K. (2016) Polymorphism in *spa* gene of *Staphylococcus aureus* from bovine subclinical mastitis. *Vet. World*, 9(4): 421-424.

25. Akineden, Ö., Annemüller, C., Hassan, A.A., Lämmler, C., Wolter, W. and Zschöck, M. (2001) Toxin genes and other characteristics of *Staphylococcus aureus* isolates from milk of cows with mastitis. *Clin. Diagn. Lab. Immunol.*, 8(5): 959-964.
26. Indrawattana, N., Sungkhachat, O., Sookrung, N., Chongsa-nguan, M., Tungtrongchitr, A. and Voravuthikunchai, S.P., Kong-Ngoen, T., Kurazono, H. and Chaicumpa, W. (2013) *Staphylococcus aureus* clinical isolates: Antibiotic susceptibility, molecular characteristics, and ability to form biofilm. *BioMed. Res. Int.*, 2013: 314654.
27. Kateete, D.P., Kimani, C.N., Katabazi, F.A., Okeng, A., Okee, M.S., Nanteza, A., Joloba, L.M. and Najjuka, C.F. (2010) Identification of *Staphylococcus aureus*: DNase and mannitol salt agar improve the efficiency of the tube coagulase test. *Ann. Clin. Microbiol. Antimicrob.*, 9: 23.
28. Lagacé-Wiens, P.R.S., Alfa, M.J., Manickam, K. and Karlowsky, J.A. (2007) Thermostable DNase is superior to tube coagulase for direct detection of *Staphylococcus aureus* in positive blood cultures. *J. Clin. Microbiol.*, 45(10): 3478-3479.

****

Received: 9 September 2016 | Revised: 3 April 2017 | Accepted: 10 April 2017

DOI: 10.1002/mbo3.493

ORIGINAL RESEARCH

WILEY MicrobiologyOpen

Effects of sodium chloride on heat resistance, oxidative susceptibility, motility, biofilm and plaque formation of *Burkholderia pseudomallei*

Pornpan Pumirat[1] | Muthita Vanaporn[1] | Usa Boonyuen[2] | Nitaya Indrawattana[1] | Amporn Rungruengkitkun[1] | Narisara Chantratita[1,3]

[1]Department of Microbiology and Immunology, Faculty of Tropical Medicine, Mahidol University, Bangkok, Thailand

[2]Department of Molecular Tropical Medicine and Genetics, Faculty of Tropical Medicine, Mahidol University, Bangkok, Thailand

[3]Mahidol-Oxford Tropical Medicine Research Unit, Faculty of Tropical Medicine, Mahidol University, Bangkok, Thailand

Correspondence
Narisara Chantratita, Department of Microbiology and Immunology, Faculty of Tropical Medicine, Mahidol University, Bangkok, Thailand.
Email: narisara@tropmedres.ac

Funding information
Thailand Research Fund, Grant/Award Number: MRG5580040; Faculty of Tropical Medicine, Mahidol University, Grant/Award Number: ICTM; RSA grant of Thailand Research Fund, Grant/Award Number: RSA5980048; National Institute of Allergy and Infectious Diseases of the National Institutes of Health, Grant/Award Number: U01AI115520

Abstract

Burkholderia pseudomallei is an environmental saprophyte and the causative agent of melioidosis, a severe infectious disease prevalent in tropical areas, including southeast Asia and northern Australia. In Thailand, the highest incidence of melioidosis is in the northeast region, where saline soil and water are abundant. We hypothesized that *B. pseudomallei* develops an ability to thrive in saline conditions and gains a selective ecological advantage over other soil-dwelling microorganisms. However, little is known about how an elevated NaCl concentration affects survival and adaptive changes in this pathogen. In this study, we examined the adaptive changes in six isolates of *B. pseudomallei* after growth in Luria-Bertani medium containing different concentrations of NaCl at 37°C for 6 hr. The bacteria were then investigated for resistance to heat at 50°C and killing by hydrogen peroxide (H_2O_2). In addition, flagellar production, biofilm formation, and the plaque formation efficiency of *B. pseudomallei* after culture in saline conditions were observed. In response to exposure to 150 and 300 mmol L^{-1} NaCl, all *B. pseudomallei* isolates showed significantly increased thermal tolerance, oxidative resistance, and plaque-forming efficiency. However, NaCl exposure notably decreased the number of *B. pseudomallei* flagella. Taken together, these results provide insight into the adaptations of *B. pseudomallei* that might be crucial for survival and persistence in the host and/or endemic environments with high salinity.

KEYWORDS
Burkholderia pseudomallei, melioidosis, salt stress, sodium chloride

1 | INTRODUCTION

Burkholderia pseudomallei is a Gram-negative pathogenic bacterium responsible for melioidosis in humans and animals. This saprophytic organism is found in soil, stagnant water, and rice paddies. Regions in which melioidosis is endemic include southeast Asia, particularly Thailand, and northern Australia (Cheng & Currie, 2005; Wuthiekanun, Smith, Dance, & White, 1995). Rice farmers are considered a high-risk group for exposure to *B. pseudomallei* especially during the monsoonal and rainy season when there is a lot of mud and surface water in the rice fields (Chaowagul et al., 1989; Cheng & Currie, 2005; Inglis & Sagripanti, 2006; Wiersinga, van der Poll, White, Day, & Peacock, 2006). Infection mainly occurs by inoculation through skin abrasions or inhalation. The clinical features of

melioidosis vary considerably, ranging from acute fulminant septicemia to chronic localized infection. In its acute form, death can occur within days of the onset of symptoms. However, the longest reported incubation period between initial acquisition of the organism and subsequent infection is a remarkable 62 years. Furthermore, a high rate of relapse has been recognized (Ngauy, Lemeshev, Sadkowski, & Crawford, 2005). Unfortunately, there is currently no effective vaccine available for the prevention of melioidosis. The treatment of melioidosis generally involves the antibiotics ceftazidime or carbapenem as *B. pseudomallei* exhibits resistance to several empiric antimicrobial therapies.

In Thailand, the highest prevalence of *B. pseudomallei* and the highest incidence of melioidosis are in the northeast region, where saline soil and water are plentiful. The electrical conductivity of soil samples from northeast Thailand ranges from 4 to 100 dS/m, which is higher than that of normal soil from other regions (approximately 2 dS/m) (Development Department of Thailand). We hypothesized that *B. pseudomallei* may develop an ability to adapt to saline conditions and gain cross-protection to other stress conditions. There is evidence of a link between high NaCl concentrations and an ability to survive in saline conditions in other closely related organisms, namely, the *Burkholderia cepacia* complex (BCC). These organisms are opportunistic pathogens of cystic fibrosis (CF) sufferers (Mahenthiralingam, Baldwin, & Vandamme, 2002; Vandamme et al., 1997) whose lung airways have an increased concentration of NaCl in the surface liquid (Widdicombe, 2001), approximately twofold higher than that of healthy lungs (Joris, Dab, & Quinton, 1993). The potential pathogenic role of *B. pseudomallei* in CF lung disease has also been reported (O'Carroll et al., 2003).

Several studies have shown that exposure to NaCl can influence the adaptive survival and virulence of pathogenic bacteria. The relevance of this has been shown in *Salmonella enterica* serovar Typhimurium (12), *Staphylococcus aureus* (Park et al., 2012), and *Listeria monocytogenes* (Garner, James, Callahan, Wiedmann, & Boor, 2006), whereby bacteria cultured in medium-containing high NaCl show increased heat tolerance (Park et al., 2012; Yoon, Park, Oh, Choi, & Yoon, 2013), antibiotic resistance (Yoon et al., 2013), and invasion ability into host cells (Garner et al., 2006; Yoon et al., 2013). Our previous study also showed that *B. pseudomallei* grown under salt stress displayed significantly greater resistance to the antibiotic ceftazidime (Pumirat et al., 2009). Salt-treated *B. pseudomallei* exhibited greater invasion efficiency into the lung epithelial cell line A549 (Pumirat et al., 2010). However, only one *B. pseudomallei* isolate was used in our previous study and adaptive responses of *B. pseudomallei* to high NaCl concentrations remain largely unknown.

In this study, we further investigated the adaptive response of six *B. pseudomallei* isolates grown in Luria–Bertani (LB) medium with different concentrations of NaCl for 6 hr at 37°C. The concentrations of NaCl used were 0, 150, and 300 mmol L^{-1} which are equivalent to 0, 15, and 30 dS/m, respectively. The bacteria under salt stress were then tested for heat resistance, oxidative susceptibility, swarm motility, flagellar production, and biofilm and plaque formation.

2 | METHODS

2.1 | Bacterial strains, growth, and salt treatment

Experiments were performed using six clinical isolates of *B. pseudomallei*: strains 153, 576, 1026b, 1530, 1634, and the reference strain K96243. All strains were obtained from clinical specimens of six patients presenting with melioidosis in northeast Thailand. The bacteria were generally maintained on LB agar at 37°C. To examine the effect of NaCl, *B. pseudomallei* was subcultured in NaCl-free LB broth and incubated at 37°C with shaking at 200 rpm overnight. The bacteria were then inoculated at a dilution of 1:10 into 10 ml of LB broth containing 0, 150, and 300 mmol L^{-1} NaCl and incubated at 37°C for 6 hr with shaking. The salt-treated and untreated *B. pseudomallei* were adjusted to an OD_{600} of 0.15. A serial dilution was performed to determine the number of colony-forming units (CFU) to obtain the starting number of bacteria.

2.2 | Heat resistance assay

A heat stress resistance assay was performed as described previously (Vanaporn, Vattanaviboon, Thongboonkerd, & Korbsrisate, 2008) with some modifications. Briefly, *B. pseudomallei* cultured in LB medium containing different salt concentrations (0, 150, and 300 mmol L^{-1} NaCl) at 37°C for 6 hr were washed with phosphate-buffered saline (PBS) and resuspended in PBS to an OD_{600} of 0.15. One milliliter of the bacterial suspension was then added into a prewarmed tube and incubated at 50°C for 15 min. Before and after heat challenge, bacterial survival was enumerated on LB agar plates after incubating at 37°C for 24 hr. The number of surviving bacteria was expressed as a percentage of the viable cells.

% Survival = CFU (heat exposure) × 100/CFU (without heat exposure)

2.3 | Oxidative stress assay

The survival of *B. pseudomallei* under oxidative conditions was determined by observing the number of viable bacteria after exposure to an oxidative agent. After 6 hr of culturing in LB medium containing different salt concentrations (0, 150, and 300 mmol L^{-1} NaCl), *B. pseudomallei* cells were harvested, washed, and resuspended in PBS. The bacterial concentration was adjusted to an OD_{600} of 0.15. Then, 100 µl of bacterial suspension was treated with H_2O_2 (at a final concentration of 1 µmol L^{-1}) or left untreated at room temperature for 15 min. A 10-fold dilution of treated and untreated bacteria was performed and plated on LB agar. After incubation at 37°C for 24 hr, colonies were counted. The number of colonies of treated bacteria was compared with that of untreated bacteria (without oxidant) and presented as the % bacterial survival.

% Survival = CFU (with oxidant) × 100/ CFU (without oxidant)

2.4 | Motility assay

A motility assay was undertaken using the swarm plate method as previously described (Deziel, Comeau, & Villemur, 2001). Briefly, *B.*

pseudomallei were grown in LB broth with 0, 150, or 300 mmol L^{-1} NaCl for 6 hr at 37°C. Bacterial pellets were collected, washed, and adjusted in PBS to approximately 10^8 CFU/ml. Swarm plates were inoculated by placing 2 µl of the prepared inoculum onto the agar surface at the center of the plate. The diameter of the swarming motility zone was measured from the point of inoculation after incubation at 37°C for 24 hr.

2.5 | Electron microscopic examination

The presence of *B. pseudomallei* flagella was examined using a transmission electron microscope. Fifty microliters of *B. pseudomallei* grown in LB broth with different salt concentrations was harvested and dropped onto parafilm. Formvar-coated carbon grids were placed on top of the parafilm for 10 min to transfer the bacterial cells. The liquid was then carefully removed with filter paper. The samples were stained with 1% uranyl acetate for 10 min, then the liquid was removed again. The grid was dried at room temperature overnight. Bacteria were observed under a Hitachi Electron Microscope H-7000 (Japan). The presence of bacterial flagella was recorded for 100 bacteria per condition.

2.6 | RNA preparation and real-time RT-PCR

RNA was isolated from 6 hr culture of *B. pseudomallei* grown at 37°C by adding 10 ml of RNAprotect bacterial reagent (QIAGEN) to 5 ml of bacteria culture and incubating for 5 min at room temperature. Subsequently, total RNA was extracted from bacterial pellets using Trizol (Invitrogen, Carlsbad, CA, USA) according to the manufacturer's instructions and treated with DNase (NEB, MA, USA) for 10 min at 37°C before use. Conventional PCR for 23S RNA gene was used to verify that there was no gDNA contamination in the DNase-treated RNA samples. Real-time RT-PCR was performed for six genes (*rpoE*, *groEL*, *htpG bopA*, *bopE*, and *bipD)* using Brilliant II SYBR® Green QPCR Master Mix, one step (Agilent Technologies, Santa Clara, CA, USA) with following conditions: reverse transcription at 50°C for 30 min, enzyme activation at 95°C for 10 min, then 40 cycles of denaturation at 95°C for 30 s, annealing at 55°C for 1 min, and melting curve analysis at 72°C for 1 min in a CFX96 Touch™ Real-Time PCR Detection System (CA, USA). Real-time RT-PCR primers are listed in Table 1. Relative mRNA levels were determined by fold change in expression, calculated by $2^{-\Delta\Delta CT}$ using the relative mRNA level of 23S RNA, representing a house-keeping gene expression, as a baseline for comparison.

2.7 | Biofilm formation assay

Quantification of biofilm formation was performed using a microtiter plate assay as previously described (Leriche & Carpentier, 2000; Stepanovic, Vukovic, Dakic, Savic, & Svabic-Vlahovic, 2000). Briefly, biofilm formation of *B. pseudomallei* was induced in trypticase soy broth at 37°C for 24 hr. After incubation, the adherent bacteria were washed using deionized water three times and fixed with 99% methanol for 15 min at room temperature. The bacteria were stained for 15 min with 1% crystal violet and solubilized with 33% (v/v) glacial acetic acid. The quantity of biofilm was measured at 630 nm using a microplate reader (Bio-Rad). Each *B. pseudomallei* isolate was assayed in duplicate, using eight wells per experiment.

TABLE 1 Oligonucleotide primers used in this study

Primers	Sequences (5′–3′)	Sources
RpoE 36	CTCCAAATACCACCGCAAGAT	(Korbsrisate et al., 2005)
RpoE 37	TATCCCTTAGTTGGTCCG	
Gro1	AGGACGGCGACTTGCTTGT	(Vanaporn et al., 2008)
Gro2	TTCCAAGACCAGTCGACAAC	
Htp1	TACAGCAACAAGGAAATCT	
Htp2	CACTCCTCCTTCTTCATCA	
BopA F	GTATTTCGGTCGTGGGAATG	(Pumirat et al., 2010)
BopA R	GCGATCGAAATGCTCCTTAC	
BopE F	CGGCAAGTCTACGAAGCGA	
BopE R	GCGGCGGTATGTGGCTTC G	
BipD F	GGACTACATCTCGGCCAAAG	
BipD R	ATCAGCTTGTCCGGATTGAT	
23s F	TTTCCCGCTTAGATGCTTT	
23s R	AAAGGTACTCTGGGGATAA	

2.8 | Plaque formation assay

Plaque-forming efficiency was assessed as previously described (Pumirat et al., 2014). HeLa cells were infected with *B. pseudomallei* at a multiplicity of infection of 20 and incubated at 37°C with 5% CO_2 for 2 hr. Thereafter, the infected cell monolayers were washed and replaced with medium-containing kanamycin (250 µg/ml). The plates were incubated at 37°C in a humidified 5% CO_2 atmosphere for 20 hr. Plaques were stained with 1% (w/v) crystal violet in 20% (v/v) methanol and counted by microscopy. Plaque-forming efficiency was calculated by determining the number of plaques per CFU of bacteria added per well.

2.9 | Statistical analysis

All assays were conducted in triplicate, and an unpaired *t*-test of independent experiments was performed using the GraphPad Prism 6 program (STATCON). Results were considered significant at a $p \leq .05$.

3 | RESULTS

3.1 | NaCl stress induces cross-protection against heat and oxidative agents

Different growth rates may affect the number of viable bacteria under NaCl stress conditions. Therefore, prior to observing the effect of NaCl stress on cross-protection against heat and oxidative agents, the

individual growth of six clinical *B. pseudomallei* isolates (K96243, 153, 576, 1026b, 1530, and 1634) from six patients in northeast Thailand was compared in LB broth containing different NaCl concentrations. Strains K96243, 153, 576, and 1026b were selected as these have been used extensively as reference isolates, and sequence type data are available (K96253, ST10; 153, ST15, 576; ST 501 and 1026b; ST102). Strains 1530 and 1634 were isolated from blood samples of two cases in northeast Thailand and used for comparison. In our previous study, *B. pseudomallei* K96243 demonstrated growth impairment during culture in LB containing 470 mmol L^{-1} NaCl (Pumirat et al., 2010). In this study, we investigated the growth kinetics of six *B. pseudomallei* isolates in LB media containing 0, 150, or 300 mmol L^{-1} NaCl for 6 hr after incubation at 37°C. Similar growth curves were observed for the six isolates under conditions of 0, 150, and 300 mmol L^{-1} NaCl (Figure S1). Therefore, salt concentrations ranging from 0 to 300 mmol L^{-1} and a culture time of 6 hr were chosen for further investigations.

To evaluate the effect of NaCl on heat resistance in *B. pseudomallei*, six *B. pseudomallei* isolates were cultured in LB broth with different concentrations of NaCl for 6 hr to reach the log phase of bacterial growth, followed by heating at 50°C for 15 min. Figure 1 shows the percentage of surviving bacteria and demonstrates a significant difference in heat resistance between *B. pseudomallei* isolates cultured in NaCl-free medium and those cultured in LB with 150 mmol L^{-1} NaCl ($p = .014$ for K96243, $p = .011$ for 153, $p = .028$ for 576, $p = .027$ for 1026b, $p = .011$ for 1530, and $p = .040$ for 1634) or those cultured in LB with 300 mmol L^{-1} NaCl ($p = .020$ for K96243, $p = .004$ for 153, $p < .001$ for 576, $p < .001$ for 1026b, $p < .001$ for 1530, and $p = .002$ for 1634). In addition, the data also showed a significant difference in the percentage of bacterial survival between *B. pseudomallei* isolates cultured in LB supplemented with 150 and 300 mmol L^{-1} NaCl ($p = .038$ for K96243, $p = .002$ for 153, $p = .001$ for 576, $p < .001$ for 1026b, $p = .002$ for 1530, and $p = .008$ for 1634). The mean and standard deviation (SD) of bacterial survival in NaCl-free medium of the six *B. pseudomallei* isolates after heat treatment were 2.2 ± 0.5%. By contrast, the mean and SDs of bacterial survival of the six isolates in medium containing 150 mmol L^{-1} and 300 mmol L^{-1} NaCl were 18.2 ± 2.9% and 67.9 ± 8.9%, respectively. These data clearly revealed that salinity is associated with increased resistance of *B. pseudomallei* to heat stress.

Activation of the oxidative response during survival in salt stress has been reported for various bacteria (den Besten, Mols, Moezelaar, Zwietering, & Abee, 2009; Metris, George, Mulholland, Carter, & Baranyi, 2014). We investigated the effect of NaCl on oxidative susceptibility of six *B. pseudomallei* isolates grown in different NaCl concentrations. Equal numbers of salt-treated and untreated *B. pseudomallei* were exposed to 1 μmol L^{-1} H_2O_2 for 15 min, and their survival on LB agar was determined (Figure 2). The percentage of surviving bacteria among the *B. pseudomallei* isolates grown in salt-free medium in the presence of H_2O_2 was significantly lower than the bacteria exposed to salt at a concentration of 150 mmol L^{-1} NaCl ($p = .046$ for K96243, $p = .039$ for 153, $p = .019$ for 576, $p = .027$ for 1026b, $p = .043$ for 1530, and $p = .014$ for 1634), or those exposed to 300 mmol L^{-1} NaCl ($p = .004$ for K96243, $p = .004$ for 153, $p < .001$ for 576, $p = .010$ for 1026b, $p = .011$ for 1530, and $p < .001$ for 1634). These data also showed a significant difference in the percentage of bacterial survival between *B. pseudomallei* isolates cultured in LB medium supplemented with 150 mmol L^{-1} and 300 mmol L^{-1} NaCl under oxidative stress conditions ($p = .010$ for K96243, $p = .004$ for 153, $p = .005$ for 576, $p = .046$ for 1026b, $p = .049$ for 1530, and $p < .001$ for 1634). In the presence of H_2O_2, the mean survival rate of untreated *B. pseudomallei* isolates was 1.7 ± 0.6%, compared with 5.6 ± 1.2% for those exposed to 150 mmol L^{-1} NaCl and 12.7 ± 2.3% for those exposed to 300 mmol L^{-1} NaCl. These data indicated that preexposing bacteria to salt stress reduced susceptibility to H_2O_2 in *B. pseudomallei*.

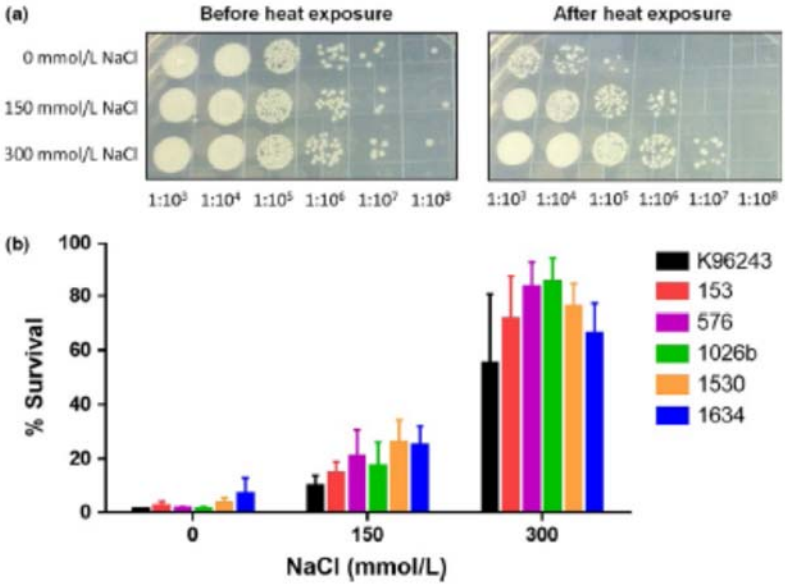

FIGURE 1 Resistance to heat of *Burkholderia pseudomallei* after growth in Luria–Bertani (LB) broth containing 0, 150, or 300 mmol L^{-1} NaCl. (a) Cell viability of *B. pseudomallei* K96243 before and after heat treatment at 50°C for 15 min. Colony-forming units were enumerated on LB agar plates after incubation at 37°C for 24 hr. (b) Percent survival of six *B. pseudomallei* isolates after heat treatment at 50°C for 15 min. 100% viability corresponds to the colony-forming unit count of unexposed bacteria. The data were obtained from at least three experiments. Error bars represent the standard deviation of the mean for experiments performed in triplicate

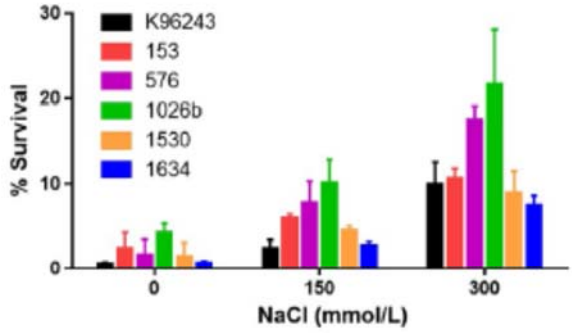

FIGURE 2 Susceptibility to oxidative stress of six *Burkholderia pseudomallei* isolates grown in Luria–Bertani (LB) broth containing 0, 150, and 300 mmol L^{-1} NaCl. Susceptibility to killing by 1 μmol L^{-1} H_2O_2 was determined at 15 min. Surviving bacteria were enumerated on LB agar plates after incubation at 37°C for 24 hr and were expressed as the % survival. The data were obtained from three experiments. Error bars represent the standard deviation of the mean for three experiments

The response of *B. pseudomallei* to heat and oxidative stress has been reported to be dependent on various cellular components, including transcription factors, heat shock proteins, and virulent proteins (Jitprasutwit et al., 2014; Korbsrisate et al., 2005; Vanaporn et al., 2008). We therefore investigated whether NaCl affects the expression of the *rpoE*, *groEL*, *htpG*, *bopA*, *bopE*, and *bipD*. The *rpoE*, *groEL*, and *htpG* genes were selected because they code transcription factors or heat shock proteins that have previously been reported to be involved in heat and oxidative stress (Jitprasutwit et al., 2014; Korbsrisate et al., 2005; Vanaporn et al., 2008). The *bopA*, *bopE*, and *bipD* were T3SS genes which may be important for cell invasion (Gong et al., 2011; Muangsombut et al., 2008; Stevens et al., 2003). Real-time RT-PCR results showed that *B. pseudomallei* K96243 when exposed to NaCl (150 and 300 mmol L^{-1}) exhibited increased expression of all tested genes, compared with bacteria grown under NaCl-free conditions (Figure 3). These data suggested that NaCl is involved in increasing the expression of stress response proteins, which might be responsible for the enhanced resistance of *B. pseudomallei* to heat and oxidative stress.

3.2 | NaCl decreases the expression of *B. pseudomallei* flagella

Motility is a crucial factor for bacterial pathogenesis. Using a microarray, we previously demonstrated that *B. pseudomallei* grown under high NaCl conditions exhibited downregulation of the flagella biosynthesis sigma factor gene "*fliA*" (*bpsl3291*) (Pumirat et al., 2010). Therefore, in this study, we further examined whether salt affects *B. pseudomallei* swarm motility. Six isolates of *B. pseudomallei* were grown in LB broth containing different concentrations of NaCl (0, 150, or 300 mmol L^{-1}) for 6 hr, then equal numbers of bacteria for each isolate were used to inoculate swarm agar medium. After incubation at 37°C for 24 hr, the

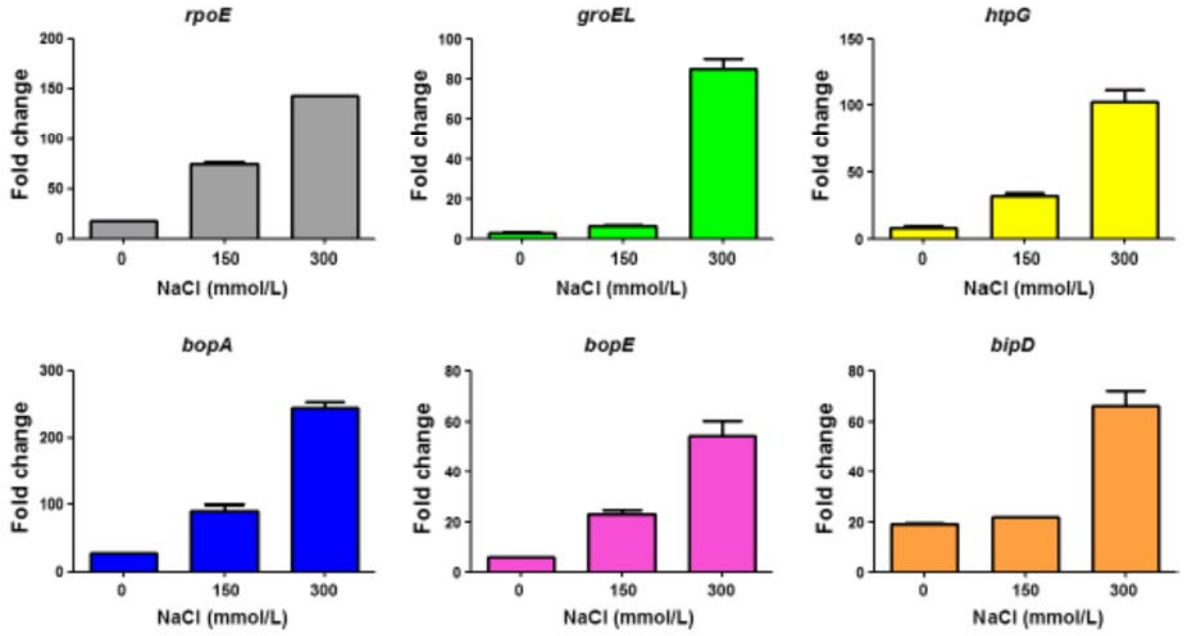

FIGURE 3 Fold change of *rpoE*, *groEL*, *htpG*, *bopA*, *bopE*, *and bipD* genes in *Burkholderia pseudomallei* K96243 grown in Luria–Bertani (LB) broth containing 0, 150, and 300 mmol L^{-1} NaCl. RNA of *B. pseudomallei* grown in LB broth with different NaCl concentrations for 6 hr was used for determination of gene expression by quantitative real-time RT-PCR using the Brilliant II SYBR® Green QPCR Master Mix, one step (Agilent Technologies, Santa Clara, CA, USA) according to the manufacturer's recommendation. Relative mRNA levels were determined by fold changes in expression, calculated by $2^{-\Delta\Delta CT}$. 23S rRNA gene was used for normalization. Error bars represent the standard deviation of the means for experiments performed in triplicate

diameter of the swarming zone was measured (Figure S2). The mean and SDs of the swarming zone diameters of the six *B. pseudomallei* isolates were 23.7 ± 0.9, 21.8 ± 1.2, and 17.4 ± 1.6 mmol L^{-1} for bacteria exposed to 0, 150, and 300 mmol L^{-1} NaCl, respectively (Table 2).

To determine whether altered expression of the *fliA* gene affects bacterial flagella, we examined the number of flagella on the six *B. pseudomallei* isolates during growth under different salt conditions using an electron microscope. The results showed that the number of flagella decreased with increasing concentrations of NaCl (Figure S3). The number of flagella counted on 100 bacteria for each of the six isolates is shown in Table 3. The majority of *B. pseudomallei* isolates (70.7 ± 3.5%) grown in LB with 300 mmol L^{-1} NaCl showed no flagella. By contrast, only 38.0 ± 3.8% and 49.3 ± 4.3% of *B. pseudomallei* cultured in NaCl-free and 150 mmol L^{-1} NaCl-supplemented media, respectively, had no flagella. The number of unflagellated bacteria among the *B. pseudomallei* isolates grown in 300 mmol L^{-1} NaCl-supplemented medium was therefore significantly higher than among those grown in salt-free ($p < .001$) or 150 mmol L^{-1} NaCl-supplemented medium ($p = .003$, respectively). This phenomenon indicated that salinity affects flagella production in *B. pseudomallei*.

TABLE 2 Effect of NaCl on the swarming motility of *B. pseudomallei*

B. pseudomallei isolates	Diameter of swarm zone (mmol L^{-1})		
	0 mmol L^{-1} NaCl	150 mmol L^{-1} NaCl	300 mmol L^{-1} NaCl
K96243	24.0 ± 7.0	21.3 ± 6.7	17.7 ± 7.2
153	27.3 ± 4.6	26.3 ± 5.5	23.5 ± 4.4
576	24.7 ± 7.6	24.0 ± 8.2	16.0 ± 9.5
1026b	22.0 ± 7.0	21.7 ± 7.2	19.0 ± 8.2
1530	23.3 ± 9.1	18.3 ± 5.5	16.3 ± 6.4
1634	20.7 ± 2.3	19.3 ± 3.1	11.7 ± 8.1

Data represent the mean ± SD of three experiments each performed in triplicate.

TABLE 3 Effect of NaCl on the number of flagella expressed on *Burkholderia pseudomallei*

B. pseudomallei isolates	NaCl (mmol L^{-1})	% Bacteria with flagella		
		0	1–3	>3
K96243	0	36	50	14
	150	52	36	12
	300	76	24	0
153	0	36	52	12
	150	52	28	20
	300	60	40	0
576	0	24	42	24
	150	32	60	8
	300	76	24	0
1026b	0	36	56	8
	150	44	56	0
	300	80	20	0
1530	0	52	44	4
	150	52	44	4
	300	60	40	0
1634	0	44	52	4
	150	64	32	4
	300	72	24	4

Data represent the mean ± SD of three experiments each performed in triplicate. One hundred bacterial cells were counted to determine the number of flagella.

3.3 | Effect of NaCl on *B. pseudomallei* biofilm formation

B. pseudomallei can produce biofilm, which may offer protection against hostile conditions such as antibiotic treatment, salinity, and immune responses (Cheng & Currie, 2005; Inglis & Sagripanti, 2006; Kamjumphol, Chareonsudjai, Chareonsudjai, Wongratanacheewin, & Taweechaisupapong, 2013). We therefore tested whether *B. pseudomallei* biofilm formation is affected by salt stress. Six isolates of *B. pseudomallei* were grown in LB broth with different concentrations of NaCl for 6 hr at 37°C prior to the induction of biofilm formation. The results in Table 4 demonstrate the biofilm formation capacity of each of the *B. pseudomallei* isolates. The mean OD values and SDs of the biofilm formation capacity of the *B. pseudomallei* isolates increased from 0.19 ± 0.01 to 0.24 ± 0.03 and then to 0.31 ± 0.03 when bacteria were grown in the presence of 0, 150, and 300 mmol L^{-1} NaCl, respectively. Although, each of the *B. pseudomallei* isolates tended to show increased biofilm formation when grown in the presence of NaCl compared with those grown in 0 mmol L^{-1} NaCl, we could not detect a significant difference in biofilm formation when comparing bacteria grown in the presence of 0, 150, and 300 mmol L^{-1} NaCl.

3.4 | NaCl affects *B. pseudomallei* plaque formation

B. pseudomallei is a facultative intracellular bacteria that harbors the ability for cell-to-cell spread (Kespichayawattana,

TABLE 4 Effect of NaCl on biofilm formation of *Burkholderia pseudomallei*

B. pseudomallei isolates	Corrected OD_{630} nm		
	0 mmol L^{-1} NaCl	150 mmol L^{-1} NaCl	300 mmol L^{-1} NaCl
K96243	0.16 ± 0.03	0.21 ± 0.07	0.23 ± 0.07
153	0.24 ± 0.12	0.33 ± 0.18	0.35 ± 0.18
576	0.14 ± 0.01	0.16 ± 0.02	0.22 ± 0.04
1026b	0.20 ± 0.07	0.35 ± 0.22	0.45 ± 0.27
1530	0.17 ± 0.04	0.18 ± 0.04	0.23 ± 0.03
1634	0.21 ± 0.03	0.23 ± 0.03	0.25 ± 0.01

Data represent the mean ± SD of three experiments each performed in triplicate.

Rattanachetkul, Wanun, Utaisincharoen, & Sirisinha, 2000), which is an important characteristic for pathogenesis. Previously, NaCl was found to increase expression of the *Burkholderia* secretion apparatus (Bsa) type III secretion system (T3SS), which involved a virulence-associated interaction with the host cell (Pumirat et al., 2010). In particular, the translocon "BipB" and the secreted effector protein "Cif" homolog in *B. pseudomallei* were reported to induce cell-to-cell dissemination (Pumirat et al., 2014; Suparak et al., 2005). Hence, we investigated whether salt stress affects cell-to-cell spread of *B. pseudomallei*. Six *B. pseudomallei* isolates grown in LB with different concentrations of NaCl for 6 hr at 37°C were assessed for plaque formation. Figure 4a demonstrates plaque formation in the HeLa cell line induced by *B. pseudomallei* K96243 when grown in 0, 150, and 300 mmol L^{-1} NaCl. The mean and SD of the plaque-forming efficiency of *B. pseudomallei* isolates grown in 300 mmol L^{-1} NaCl were 59.8 ± 2.8, compared with 41.7 ± 2.2 for bacteria grown in 150 mmol L^{-1} NaCl and 35.0 ± 2.7 for those grown in NaCl-free LB. All *B. pseudomallei* isolates grown in the presence of 300 mmol L^{-1} NaCl showed significantly increased plaque formation relative to bacteria cultured in NaCl-free medium ($p = .004$ for K96243, $p = .021$ for 153, $p = .002$ for 576, $p = .017$ for 1026b, $p = .032$ for 1530, and $p = .016$ for 1634). Moreover, we also observed a significant difference in the plaque-forming capacity of all *B. pseudomallei* isolates cultured in LB supplemented with 300 mmol L^{-1} NaCl compared with those cultured in 150 mmol L^{-1} NaCl ($p = .027$ for K96243, $p = .029$ for 153, $p = .019$ for 576, $p = .033$ for 1026b, $p = .048$ for 1530, and $p = .042$ for 1634). This finding indicated the influence of NaCl on *B. pseudomallei* pathogenesis.

4 | DISCUSSION

B. pseudomallei is a saprophyte that can survive and multiply under different environmental conditions (Cheng & Currie, 2005; Dharakul & Songsivilai, 1999; White, 2003). It is a difficult microorganism to kill. It can inhabit harsh environments for many years, especially in endemic areas, including northeast Thailand (Wuthiekanun et al., 1995) where saline soil and water are abundant. *B. pseudomallei* was reported as potential opportunist pathogens of CF patients (Mahenthiralingam et al., 2002; O'Carroll et al., 2003; O'Sullivan et al., 2011; Vandamme et al., 1997), who have a high concentration of NaCl in their lung airway surface liquid. Adaptive responses of *Burkholderia* species, including *B. pseudomallei*, to high salt conditions have been investigated previously (Inglis & Sagripanti, 2006; O'Quinn, Wiegand, & Jeddeloh, 2001; Pumirat et al., 2009, 2010), however, the mechanisms underlying these remain poorly understood. This study demonstrated the adaptive phenotypes of six *B. pseudomallei* isolates to NaCl in various concentrations. The concentrations of NaCl used in our experiments were in the range of salt concentrations found in the soil and water in northeast Thailand. We showed that adaptations under salt stress conditions were associated with cross-protection against other environmental stresses, as well as increased pathogenicity.

Our present study verified that the growth rate of six *B. pseudomallei* isolates in LB containing 0, 150, and 300 mmol L^{-1} NaCl remained constant. We therefore conducted our experiments within this range of concentrations. Although high salinity seems to be a disadvantage for *B. pseudomallei*, as high salt (≥470 mmol L^{-1} NaCl) diminished bacterial growth (Pumirat et al., 2010; Wang-Ngarm, Chareonsudjai, & Chareonsudjai, 2014), *B. pseudomallei* would regularly encounter a

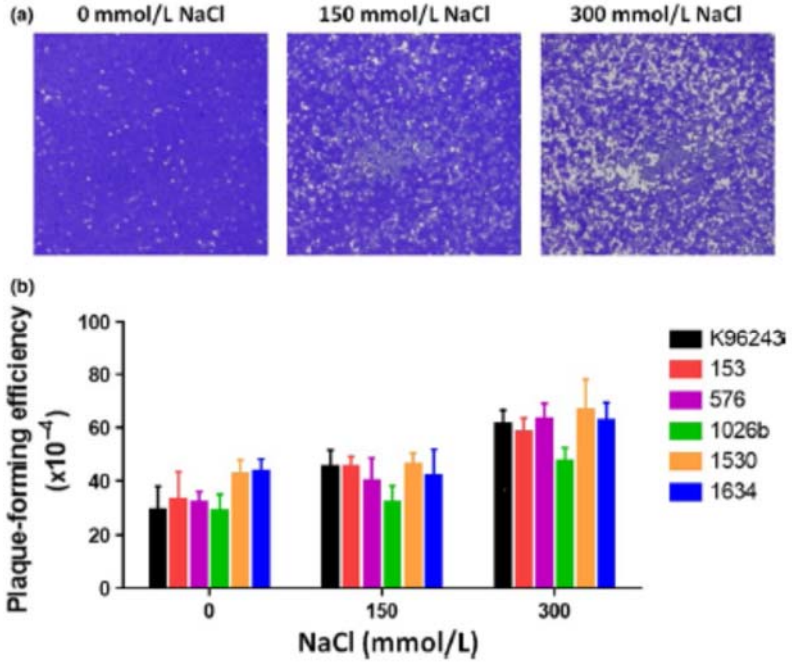

FIGURE 4 Plaque formation by *Burkholderia pseudomallei* after growth in Luria–Bertani (LB) broth containing 0, 150, and 300 mmol L^{-1} NaCl. (a) Images of plaques formed by *B. pseudomallei* K96243. Representative images of HeLa cell monolayers after infection with *B. pseudomallei* K96243, which had been grown in LB broth containing 0, 150, or 300 mmol L^{-1} NaCl for 20 hr. (b) Plaque-forming efficiency of six *B. pseudomallei* isolates. HeLa cells were infected with *B. pseudomallei* grown in LB broth containing 0, 150, or 300 mmol L^{-1} NaCl at a multiplicity of infection of 20. The infected cells were stained with crystal violet after 20 hr incubation. Plaque-forming efficiency was calculated as the number of plaques × 100/number of colony-forming units of bacteria added per well. Error bars represent the standard deviation of the means for experiments performed in triplicate

high salinity environment in its physiological habitat. In this study, we demonstrated that NaCl enhanced the ability of *B. pseudomallei* to survive under heat and oxidative stress. Several studies in other bacteria, such as *Bacillus cereus* (den Besten et al., 2009), *Bacillus subtilis* (Volker, Mach, Schmid, & Hecker, 1992), and *Escherichia coli* (Gunasekera, Csonka, & Paliy, 2008), have also reported that activation of the salt stress response conferred cross-protection against other stresses, that is, increased resistance to heat and H_2O_2. Recently, Yuan, Agoston, Lee, Lee, & Yuk, (2012) and Yoon et al., (2013) also showed that the heat resistance of *Salmonella enterica* was increased after exposure to NaCl. Moreover, it is evident that growing *Vibrio harveyi* in LB broth supplemented with 2% NaCl (34.2 mmol L^{-1}) resulted in increased resistance to menadione killing compared with the same organism grown in normal LB broth (Vattanaviboon, Panmanee, & Mongkolsuk, 2003). It is possible that the salt stress adaptation may reflect the ability of these bacteria, including *B. pseudomallei*, to survive under hostile environmental conditions, such as high temperature and oxidative stress.

As *B. pseudomallei* is an intracellular organism, it has the capability to survive in phagocytic cells (Allwood, Devenish, Prescott, Adler, & Boyce, 2011). While trafficking within macrophages, *B. pseudomallei* may be exposed to oxidative stress. Interestingly, Scott & Gruenberg (2011) reported that chloride and sodium ion channels play important roles in regulating the phagosomal environment through counter ion regulation and charge compensation of macrophages. Therefore, the salt content in the phagosome may promote bacterial resistance to oxidative stress and allow *B. pseudomallei* to survive within the host cell.

These oxidative and heat protective effects of NaCl could be a result of the increased expression of stress response cellular components. The increased expression of the *rpoE* and *groEL* genes detected in this study was in agreement with previous reports for the *B. pseudomallei* transcriptome (Pumirat et al., 2010) and secretome (Pumirat et al., 2009) under high salinity conditions. The expression of *groEL* (*bpss0477*) and *rpoE* (*bpsl2434*) was upregulated in *B. pseudomallei* cultured in LB containing 320 mmol L^{-1} NaCl, by approximately 1.2- and 1.4-fold, respectively, compared with *B. pseudomallei* cultured in 170 mmol L^{-1} NaCl at the 6-hr time point (Pumirat et al., 2010). Indeed, the secretomic profile confirmed the presence of GroEL in the culture supernatant only after exposure to 320 mmol L^{-1} NaCl (Pumirat et al., 2009). Moreover, our results were consistent with the observation that inactivation of the *rpoE* operon increased susceptibility of *B. pseudomallei* to killing by menadione and H_2O_2 and high osmolarity (Korbsrisate et al., 2005). Furthermore, it has been demonstrated that *rpoE* regulated a heat-inducible promoter of the *rpoH* gene in *B. pseudomallei* (Vanaporn et al., 2008). These data implied that RpoE plays an important role in the increased resistance of *B. pseudomallei* in response to heat and oxidative stress.

Among the salt-altered genes of *B. pseudomallei* K96243 (Pumirat et al., 2010), we previously detected downregulation of the flagella biosynthesis sigma factor *fliA* gene (*bpsl3291*), by approximately 1.5- and 1.2-fold (at 3 and 6 hr, respectively), when *B. pseudomallei* was grown in medium supplemented with 320 mmol L^{-1} NaCl compared with 170 mmol L^{-1} NaCl. This observation led us to examine whether growth of *B. pseudomallei* under high salt conditions affected the production of flagella. Under electron microscopic examination (Table 3), we found that most *B. pseudomallei* isolates grown under high salt conditions (300 mmol L^{-1} NaCl) did not produce flagella, whereas the majority of *B. pseudomallei* isolates grown under lower salt concentrations (0 and 150 mmol L^{-1} NaCl) presented at least one flagellum. The decreased expression of motility genes due to salt stress has also been documented for other bacteria such as *Sphingomonas* sp. strain LH128 (Fida et al., 2012) and *B. subtilis* (Hoper, Bernhardt, & Hecker, 2006; Steil, Hoffmann, Budde, Volker, & Bremer, 2003). All six *B. pseudomallei* isolates exhibited a smaller mean diameter for their motility zone when cultured under high salt conditions (300 mmol L^{-1} NaCl), compared with culturing under salt-free or low salt conditions (0 and 150 mmol L^{-1} NaCl). This observation implied that salt stress plays an important role in regulating the production of bacterial flagella. One possible explanation for this is that in order to cope with stressful environmental conditions the bacteria conserve energy by diminishing nonvital activities, such as motility, by reducing the production of flagella by decreasing the expression of the motility regulator gene.

The ability to form a biofilm is important for *B. pseudomallei* to gain resistance to numerous environmental factors, including certain antibiotics and stresses (Cheng & Currie, 2005; Inglis & Sagripanti, 2006; Kamjumphol et al., 2013). Our study detected the increased ability of *B. pseudomallei* to form a biofilm when bacterial isolates were grown in medium supplemented with NaCl, compared with salt-free medium (Table 4). This was consistent with the findings of Kamjumphol et al. who demonstrated that biofilm formation was increased when *B. pseudomallei* was grown in modified Vogel and Bonner's medium containing 0.85–1.7 mol L^{-1} NaCl (Kamjumphol et al., 2013). This indicated that *B. pseudomallei* responds to salt stress by producing a biofilm that could confer cross-protection against other environmental stresses.

Exposure to high salinity is likely to be associated with pathogenesis in *B. pseudomallei*. Previously, invasion of A549 cells was enhanced by culturing of *B. pseudomallei* K96243 in salt-supplemented LB medium (Pumirat et al., 2010). Our results showed that when grown in the presence of NaCl, all six *B. pseudomallei* isolates exhibited significantly increased plague formation in HeLa cells (Figure 4). The elevated rate of cellular invasion in response to NaCl may increase the load of intracellular bacteria, contributing to cell-to-cell spread or enhance cell cytotoxicity. Several studies have demonstrated the requirement of the Bsa T3SS and type VI secretion system (T6SS) for the intracellular pathogenicity of *B. pseudomallei* (Burtnick et al., 2008, 2011; Lim et al., 2015; Shalom, Shaw, & Thomas, 2007; Stevens et al., 2002; Warawa & Woods, 2005). We postulate that these systems may participate in the enhanced plaque formation of *B. pseudomallei* observed after exposure to NaCl. However, further experiments are required to investigate this possibility.

5 | CONCLUSIONS

In conclusion, our results demonstrated that high salt conditions modulate adaptive responses in *B. pseudomallei* isolates. These adaptive responses include increased thermal resistance, plaque formation, and

decreased flagella and oxidative susceptibility. Similar results were observed in all six isolates tested; suggesting that salt stress induces a general, conserved response in *B. pseudomallei*. Our findings provide insight into how these bacteria persist in endemic environments abundant in saline soil and water, and may indicate the link between the establishment and pathogenesis of *B. pseudomallei* infection in CF patients.

ACKNOWLEDGMENTS

This work was supported by the Thailand Research Fund (MRG5580040) and the ICTM grant from the Faculty of Tropical Medicine, Mahidol University. NI was supported by the RSA grant (RSA5980048) of Thailand Research Fund. NC was supported by the National Institute of Allergy and Infectious Diseases of the National Institutes of Health (U01AI115520).

CONFLICT OF INTEREST

The authors declare that they have no competing interests.

REFERENCES

Allwood, E. M., Devenish, R. J., Prescott, M., Adler, B., & Boyce, J. D. (2011). Strategies for Intracellular Survival of *Burkholderia pseudomallei*. *Frontiers in Microbiology*, *2*, 170.

den Besten, H. M., Mols, M., Moezelaar, R., Zwietering, M. H., & Abee, T. (2009). Phenotypic and transcriptomic analyses of mildly and severely salt-stressed *Bacillus cereus* ATCC 14579 cells. *Applied and Environment Microbiology*, *75*, 4111–4119.

Burtnick, M. N., Brett, P. J., Harding, S. V., Ngugi, S. A., Ribot, W. J., Chantratita, N., … Deshazer, D. (2011). The cluster 1 type VI secretion system is a major virulence determinant in *Burkholderia pseudomallei*. *Infection and Immunity*, *79*, 1512–1525.

Burtnick, M. N., Brett, P. J., Nair, V., Warawa, J. M., Woods, D. E., & Gherardini, F. C. (2008). *Burkholderia pseudomallei* type III secretion system mutants exhibit delayed vacuolar escape phenotypes in RAW 264.7 murine macrophages. *Infection and Immunity*, *76*, 2991–3000.

Chaowagul, W., White, N. J., Dance, D. A., Wattanagoon, Y., Naigowit, P., Davis, T. M., … Pitakwatchara, N. (1989). Melioidosis: A major cause of community-acquired septicemia in northeastern Thailand. *Journal of Infectious Diseases*, *159*, 890–899.

Cheng, A. C., & Currie, B. J. (2005). Melioidosis: Epidemiology, pathophysiology, and management. *Clinical Microbiology Reviews*, *18*, 383–416.

Deziel, E., Comeau, Y., & Villemur, R. (2001). Initiation of biofilm formation by *Pseudomonas aeruginosa* 57RP correlates with emergence of hyperpiliated and highly adherent phenotypic variants deficient in swimming, swarming, and twitching motilities. *Journal of Bacteriology*, *183*, 1195–1204.

Dharakul, T., & Songsivilai, S. (1999). The many facets of melioidosis. *Trends in Microbiology*, *7*, 138–140.

Fida, T. T., Breugelmans, P., Lavigne, R., Coronado, E., Johnson, D. R., van der Meer, J. R., … Springael, D. (2012). Exposure to solute stress affects genome-wide expression but not the polycyclic aromatic hydrocarbon-degrading activity of *Sphingomonas sp.* strain LH128 in biofilms. *Applied and Environment Microbiology*, *78*, 8311–8320.

Garner, M. R., James, K. E., Callahan, M. C., Wiedmann, M., & Boor, K. J. (2006). Exposure to salt and organic acids increases the ability of *Listeria monocytogenes* to invade Caco-2 cells but decreases its ability to survive gastric stress. *Applied and Environment Microbiology*, *72*, 5384–5395.

Gong, L., Cullinane, M., Treerat, P., Ramm, G., Prescott, M., Adler, B., … Devenish, R. J. (2011). The *Burkholderia pseudomallei* type III secretion system and BopA are required for evasion of LC3-associated phagocytosis. *PLoS ONE*, *6*, e17852.

Gunasekera, T. S., Csonka, L. N., & Paliy, O. (2008). Genome-wide transcriptional responses of *Escherichia coli* K-12 to continuous osmotic and heat stresses. *Journal of Bacteriology*, *190*, 3712–3720.

Hoper, D., Bernhardt, J., & Hecker, M. (2006). Salt stress adaptation of *Bacillus subtilis*: A physiological proteomics approach. *Proteomics*, *6*, 1550–1562.

Inglis, T. J., & Sagripanti, J. L. (2006). Environmental factors that affect the survival and persistence of *Burkholderia pseudomallei*. *Applied and Environment Microbiology*, *72*, 6865–6875.

Jitprasutwit, S., Ong, C., Juntawieng, N., Ooi, W. F., Hemsley, C. M., Vattanaviboon, P., … Korbsrisate, S. (2014). Transcriptional profiles of *Burkholderia pseudomallei* reveal the direct and indirect roles of Sigma E under oxidative stress conditions. *BMC Genomics*, *15*, 787.

Joris, L., Dab, I., & Quinton, P. M. (1993). Elemental composition of human airway surface fluid in healthy and diseased airways. *American Review of Respiratory Disease*, *148*, 1633–1637.

Kamjumphol, W., Chareonsudjai, S., Chareonsudjai, P., Wongratanacheewin, S., & Taweechaisupapong, S. (2013). Environmental factors affecting *Burkholderia pseudomallei* biofilm formation. *Southeast Asian Journal of Tropical Medicine and Public Health*, *44*, 72–81.

Kespichayawattana, W., Rattanachetkul, S., Wanun, T., Utaisincharoen, P., & Sirisinha, S. (2000). *Burkholderia pseudomallei* induces cell fusion and actin-associated membrane protrusion: A possible mechanism for cell-to-cell spreading. *Infection and Immunity*, *68*, 5377–5384.

Korbsrisate, S., Vanaporn, M., Kerdsuk, P., Kespichayawattana, W., Vattanaviboon, P., Kiatpapan, P., & Lertmemongkolchai, G. (2005). The *Burkholderia pseudomallei* RpoE (AlgU) operon is involved in environmental stress tolerance and biofilm formation. *FEMS Microbiology Letters*, *252*, 243–249.

Leriche, V., & Carpentier, B. (2000). Limitation of adhesion and growth of *Listeria monocytogenes* on stainless steel surfaces by *Staphylococcus sciuri* biofilms. *Journal of Applied Microbiology*, *88*, 594–605.

Lim, Y. T., Jobichen, C., Wong, J., Limmathurotsakul, D., Li, S., Chen, Y., … Gan, Y. H. (2015). Extended loop region of Hcp1 is critical for the assembly and function of type VI secretion system in *Burkholderia pseudomallei*. *Scientific Reports*, *5*, 8235.

Mahenthiralingam, E., Baldwin, A., & Vandamme, P. (2002). *Burkholderia cepacia* complex infection in patients with cystic fibrosis. *Journal of Medical Microbiology*, *51*, 533–538.

Metris, A., George, S. M., Mulholland, F., Carter, A. T., & Baranyi, J. (2014). Metabolic shift of *Escherichia coli* under salt stress in the presence of glycine betaine. *Applied and Environment Microbiology*, *80*, 4745–4756.

Muangsombut, V., Suparak, S., Pumirat, P., Damnin, S., Vattanaviboon, P., Thongboonkerd, V., & Korbsrisate, S. (2008). Inactivation of *Burkholderia pseudomallei bsaQ* results in decreased invasion efficiency and delayed escape of bacteria from endocytic vesicles. *Archives of Microbiology*, *190*, 623–631.

Ngauy, V., Lemeshev, Y., Sadkowski, L., & Crawford, G. (2005). Cutaneous melioidosis in a man who was taken as a prisoner of war by the Japanese during World War II. *Journal of Clinical Microbiology*, *43*, 970–972.

O'Carroll, M. R., Kidd, T. J., Coulter, C., Smith, H. V., Rose, B. R., Harbour, C., & Bell, S. C. (2003). *Burkholderia pseudomallei*: Another emerging pathogen in cystic fibrosis. *Thorax*, *58*, 1087–1091.

O'Quinn, A. L., Wiegand, E. M., & Jeddeloh, J. A. (2001). *Burkholderia pseudomallei* kills the nematode *Caenorhabditis elegans* using an endotoxin-mediated paralysis. *Cellular Microbiology*, *3*, 381–393.

O'Sullivan, B. P., Torres, B., Conidi, G., Smole, S., Gauthier, C., Stauffer, K. E., … Smith, T. L. (2011). *Burkholderia pseudomallei* infection in a child with cystic fibrosis: Acquisition in the Western Hemisphere. *Chest*, *140*, 239–242.

Park, A., Lee, J., Jeong, S., Cho, J., Lee, S., Lee, H., & Yoon, Y. (2012). Thermal Inactivation of Sodium-Habituated *Staphylococcus aureus* in Ready-to-Heat Sauces. *Korean Journal for Food Science of Animal Resources*, *32*, 713–717.

Pumirat, P., Broek, C. V., Juntawieng, N., Muangsombut, V., Kiratisin, P., Pattanapanyasat, K., … Korbsrisate, S. (2014). Analysis of the prevalence, secretion and function of a cell cycle-inhibiting factor in the melioidosis pathogen *Burkholderia pseudomallei*. *PLoS ONE*, *9*, e96298.

Pumirat, P., Cuccui, J., Stabler, R. A., Stevens, J. M., Muangsombut, V., Singsuksawat, E., … Korbsrisate, S. (2010). Global transcriptional profiling of *Burkholderia pseudomallei* under salt stress reveals differential effects on the Bsa type III secretion system. *BMC Microbiology*, *10*, 171.

Pumirat, P., Saetun, P., Sinchaikul, S., Chen, S. T., Korbsrisate, S., & Thongboonkerd, V. (2009). Altered secretome of *Burkholderia pseudomallei* induced by salt stress. *Biochimica et Biophysica Acta*, *1794*, 898–904.

Scott, C. C., & Gruenberg, J. (2011). Ion flux and the function of endosomes and lysosomes: pH is just the start: The flux of ions across endosomal membranes influences endosome function not only through regulation of the luminal pH. *BioEssays*, *33*, 103–110.

Shalom, G., Shaw, J. G., & Thomas, M. S. (2007). In vivo expression technology identifies a type VI secretion system locus in *Burkholderia pseudomallei* that is induced upon invasion of macrophages. *Microbiology*, *153*, 2689–2699.

Steil, L., Hoffmann, T., Budde, I., Volker, U., & Bremer, E. (2003). Genome-wide transcriptional profiling analysis of adaptation of *Bacillus subtilis* to high salinity. *Journal of Bacteriology*, *185*, 6358–6370.

Stepanovic, S., Vukovic, D., Dakic, I., Savic, B., & Svabic-Vlahovic, M. (2000). A modified microtiter-plate test for quantification of staphylococcal biofilm formation. *Journal of Microbial Methods*, *40*, 175–179.

Stevens, M. P., Friebel, A., Taylor, L. A., Wood, M. W., Brown, P. J., Hardt, W. D., & Galyov, E. E. (2003). A *Burkholderia pseudomallei* type III secreted protein, BopE, facilitates bacterial invasion of epithelial cells and exhibits guanine nucleotide exchange factor activity. *Journal of Bacteriology*, *185*, 4992–4996.

Stevens, M. P., Wood, M. W., Taylor, L. A., Monaghan, P., Hawes, P., Jones, P. W., … Galyov, E. E. (2002). An Inv/Mxi-Spa-like type III protein secretion system in *Burkholderia pseudomallei* modulates intracellular behaviour of the pathogen. *Molecular Microbiology*, *46*, 649–659.

Suparak, S., Kespichayawattana, W., Haque, A., Easton, A., Damnin, S., Lertmemongkolchai, G., … Korbsrisate, S. (2005). Multinucleated giant cell formation and apoptosis in infected host cells is mediated by *Burkholderia pseudomallei* type III secretion protein BipB. *Journal of Bacteriology*, *187*, 6556–6560.

Vanaporn, M., Vattanaviboon, P., Thongboonkerd, V., & Korbsrisate, S. (2008). The *rpoE* operon regulates heat stress response in *Burkholderia pseudomallei*. *FEMS Microbiology Letters*, *284*, 191–196.

Vandamme, P., Holmes, B., Vancanneyt, M., Coenye, T., Hoste, B., Coopman, R., … Govan, J. R. (1997). Occurrence of multiple genomovars of *Burkholderia cepacia* in cystic fibrosis patients and proposal of *Burkholderia multivorans* sp. nov. *International Journal of Systematic Bacteriology*, *47*, 1188–1200.

Vattanaviboon, P., Panmanee, W., & Mongkolsuk, S. (2003). Induction of peroxide and superoxide protective enzymes and physiological cross-protection against peroxide killing by a superoxide generator in Vibrio harveyi. *FEMS Microbiology Letters*, *221*, 89–95.

Volker, U., Mach, H., Schmid, R., & Hecker, M. (1992). Stress proteins and cross-protection by heat shock and salt stress in *Bacillus subtilis*. *Journal of General Microbiology*, *138*, 2125–2135.

Wang-Ngarm, S., Chareonsudjai, S., & Chareonsudjai, P. (2014). Physicochemical factors affecting the growth of *Burkholderia pseudomallei* in soil microcosm. *American Journal of Tropical Medicine and Hygiene*, *90*, 480–485.

Warawa, J., & Woods, D. E. (2005). Type III secretion system cluster 3 is required for maximal virulence of *Burkholderia pseudomallei* in a hamster infection model. *FEMS Microbiology Letters*, *242*, 101–108.

White, N. J. (2003). Melioidosis.*Lancet*, *361*, 1715–1722.

Widdicombe, J. H. (2001). Altered NaCl concentration of airway surface liquid in cystic fibrosis. *Pflugers Archiv. European Journal of Physiology*, *443*(Suppl 1), S8–S10.

Wiersinga, W. J., van der Poll, T., White, N. J., Day, N. P., & Peacock, S. J. (2006). Melioidosis: Insights into the pathogenicity of *Burkholderia pseudomallei*. *Nature Reviews Microbiology*, *4*, 272–282.

Wuthiekanun, V., Smith, M. D., Dance, D. A., & White, N. J. (1995). Isolation of *Pseudomonas pseudomallei* from soil in north-eastern Thailand. *Transactions of the Royal Society of Tropical Medicine and Hygiene*, *89*, 41–43.

Yoon, H., Park, B. Y., Oh, M. H., Choi, K. H., & Yoon, Y. (2013). Effect of NaCl on heat resistance, antibiotic susceptibility, and Caco-2 cell invasion of *Salmonella*. *BioMed Research International*, *2013*, 274096.

Yuan, W., Agoston, R., Lee, D., Lee, S. C., & Yuk, H. G. (2012). Influence of lactate and acetate salt adaptation on *Salmonella* Typhimurium acid and heat resistance. *Food Microbiology*, *30*, 448–452.

SUPPORTING INFORMATION

Additional Supporting Information may be found online in the supporting information tab for this article.

How to cite this article: Pumirat P, Vanaporn M, Boonyuen U, Indrawattana N, Rungruengkitkun A, Chantratita N. Effects of sodium chloride on heat resistance, oxidative susceptibility, motility, biofilm and plaque formation of *Burkholderia pseudomallei*. *MicrobiologyOpen*. 2017;00:e493. https://doi.org/10.1002/mbo3.493

PeerJ

Detection and drug resistance profile of *Escherichia coli* from subclinical mastitis cows and water supply in dairy farms in Saraburi Province, Thailand

Woranich Hinthong[1], Natapol Pumipuntu[2,3], Sirijan Santajit[2], Suphang Kulpeanprasit[2], Shutipen Buranasinsup[4], Nitat Sookrung[5], Wanpen Chaicumpa[6], Pisinee Aiumurai[5] and Nitaya Indrawattana[2]

[1] Faculty of Medicine and Allied Health, HRH Princess Chulabhorn College of Medical Science, Bangkok, Thailand

[2] Department of Microbiology and Immunology, Faculty of Tropical Medicine, Mahidol University, Bangkok, Thailand

[3] Faculty of Veterinary Sciences, Mahasarakham University, Mahasarakham, Thailand

[4] Department of Pre-clinic and Applied Animal Science, Faculty of Veterinary Medicine, Mahidol University, Nakornpathom, Thailand

[5] Department of Research and Development, Faculty of Medicine Siriraj Hospital, Mahidol University, Bangkok, Thailand

[6] Center of Excellence on Therapeutic Proteins and Antibody Engineering, Department of Parasitology, Faculty of Medicine Siriraj Hospital, Mahidol University, Bangkok, Thailand

ABSTRACT

Subclinical mastitis is a persistent problem in dairy farms worldwide. Environmental *Escherichia coli* is the bacterium predominantly responsible for this condition. In Thailand, subclinical mastitis in dairy cows is usually treated with various antibiotics, which could lead to antibiotic resistance in bacteria. *E. coli* is also a reservoir of many antibiotic resistance genes, which can be conveyed to other bacteria. In this study, the presence of *E. coli* in milk and water samples was reported, among which enteropathogenic *E. coli* was predominant, followed by enteroaggregative *E. coli* and enterohemorrhagic *E. coli*, which was found only in milk samples. Twenty-one patterns of antibiotic resistance were identified in this study. Ampicillin- and carbenicillin-resistant *E. coli* was the most common among the bacterial isolates from water samples. Meanwhile, resistance to ampicillin, carbenicillin, and sulfamethoxazole-trimethoprim was the pattern found most commonly in the *E. coli* from milk samples. Notably, only the *E. coli* from water samples possessed ESBL phenotype and carried antibiotic resistance genes, bla_{TEM} and bla_{CMY-2}. This indicates that pathogenic *E. coli* in dairy farms is also exposed to antibiotics and could potentially transfer these genes to other pathogenic bacteria under certain conditions.

Submitted 20 February 2017
Accepted 17 May 2017
Published 13 June 2017

Corresponding author
Nitaya Indrawattana,
nitaya.ind@mahidol.ac.th

Academic editor
Paul Tulkens

Additional Information and Declarations can be found on page 12

DOI 10.7717/peerj.3431

Subjects Microbiology, Infectious Diseases
Keywords Subclinical bovine mastitis, *Escherichia coli*, Antibiotic resistance, Extend spectrum beta-lactamase

How to cite this article Hinthong et al. (2017), Detection and drug resistance profile of *Escherichia coli* from subclinical mastitis cows and water supply in dairy farms in Saraburi Province, Thailand. **PeerJ** 5:e3431; **DOI 10.7717/peerj.3431**

INTRODUCTION

In dairy farms, mastitis is a persistent problem resulting in economic losses and premature culling of cows. *Staphylococcus aureus* (*S. aureus*) is considered a major causative pathogen which is a threat to farmers, although easily identifiable, whereas other gram negative bacteria is overlooked or not considered to be a cause for concern by farmers. Subclinical mastitis, which is defined as a somatic cell count (SCC) of >200,000 cells/mL in milk, is usually caused by gram negative bacteria, such as *Escherichia coli* (*E. coli*), *Klebsiella pneumoniae*, and *Serratia marcescens* (*Schukken et al., 2012*; *Azevedo et al., 2016*). These bacteria are commonly found in environmental settings, such as bedding, clothes, farmers' hands, and water used on farms (*Perkins et al., 2009*; *Iraguha, Hamudikuwanda & Mushonga, 2015*; *Azevedo et al., 2016*). Among gram negative bacteria, *E. coli* is the most notable cause of mastitis. *E. coli* was found to usually infected mammary gland of cows parturition and early lactation period which could lead to local and acute mastitis (*Burvenich et al., 2003*). In a study in Portugal, *E. coli* was found to be the second most common bacteria after non-coagulative staphylococci found in bulk tank milk (*Azevedo et al., 2016*). In Uruguay, *E. coli* was second only to *S. aureus* in bovine subclinical mastitis cases (*Gianneechini et al., 2002*), whereas in China, it was one of the leading types of coliform bacteria found in milk from cows with subclinical mastitis (*Memon et al., 2013*; *Wang et al., 2015*).

The treatment of bovine subclinical mastitis usually depends on the severity of the symptoms. In Thailand, the disease is usually treated with antibiotics or the infected cows are culled. Antibiotics are also used for prevention in some farms. However, this can lead to bacteria developing resistance to them. For example, increased resistance to antibiotics in *S. aureus* in the form of oxacillin- or gentamicin-resistant strains was reported in Thailand due to their excessive use (*Suriyasathaporn, 2011*; *Suriyasathaporn et al., 2012*). Despite this background, there is little information on antibiotic resistance and drug resistance genes in other bacteria related to bovine mastitis in Thailand. *E. coli* can be antibiotic-resistant as it is also exposed to antibiotics from wastewater from farms. Furthermore, *E. coli* that carries resistance genes can transfer those genes to other pathogenic bacteria (*Hu et al., 2016*). The discovery of antibiotic resistance in *E. coli* isolates from farms could possibly show the trend or specific characteristic of antibiotic resistance and facilitate better prevention or the more effective treatment for mastitis on dairy farm. This study was thus conducted to detect *E. coli* from water sources and milk from cows with subclinical mastitis, and their antibiotic resistance patterns.

MATERIALS AND METHODS

Sample collection

All procedures performed in this study are in accordance with the ethical standards of the Faculty of Tropical Medicine–Animal Care and Use Committee (FTM-ACUC), Mahidol University, Thailand (protocol no. 002-2016). Water and milk samples were collected from 17 dairy farms in Saraburi Province, Thailand, where agriculture and livestock are the main source of income of the people. A total of 35 water samples were collected in 500-ml

sterile bottles from drinking water for cows in a milking area and also from washing water. Thirty-eight milk samples were collected in sterile falcon tubes from cows with subclinical mastitis, which had an SCC of >200,000 cells/ml in milk, after the teats had been disinfected with 70% ethanol and 4–5 streams of milk had been removed. Both water and milk samples were stored at 4 °C and transported to the laboratory within 24 h for the experiment.

Bacterial isolation

Each water and milk sample was centrifuged at 6,000 rpm for 10 min, and the precipitant was subjected to 10-fold dilution and spread on MacConkey agar (Becton, Dickinson, and Company). Suspected *E. coli* lactose-fermenting colonies (pink colonies) were subjected to gram staining and standard biochemical tests, including triple sugar iron agar, lysine decarboxylase, ornithine decarboxylase/deaminase, motility, and indole production tests.

Antibiotic susceptibility tests

All *E. coli* isolates were subjected to antibiotic susceptibility tests following the Clinical and Laboratory Standards Institute (CLSI) guidelines (*Clinical and Laboratory Standards Institute, 2016*). The antimicrobial disks used in the experiment included 10 μg ampicillin (≤13 mm), 100 μg piperacillin (≤17 mm), 10 μg carbenicillin (≤17 mm), 20 μg amoxicillin-clavulanic acid (≤13 mm), 30 μg cefepime (≤14 mm), 30 μg cefotaxime (≤22 mm), 30 μg ceftriaxone (≤19 mm), 30 μg ceftazidime (≤17 mm), 75 μg cefoperazone (≤15 mm), 30 μg cefuroxime (≤14 mm), 10 μg imipenem (≤19 mm), 10 μg meropenem (≤19 mm), 10 μg gentamicin (≤12 mm), 30 μg amikacin (≤14 mm), 15 μg tigecycline (≤14 mm), 5 μg ciprofloxacin (≤15 mm), 10 μg norfloxacin (≤12 mm), and 23.75 μg trimethoprim–sulfamethoxazole (≤10 mm) (Oxoid). *E. coli* strain ATCC 25922 was used as a control in this experiment.

Extended spectrum β-lactamase (ESBL) production was tested by double disk synergy (DDS) method modified from *Clinical and Laboratory Standards Institute (2012)*. The test uses 30 μg antibiotic disks of cefepime, cefotaxime ceftriaxone, ceftazidime, and cefuroxime. The antibiotic disks were placed on the *E. coli* spreaded MHA culture plate, 30 mm (center to center) from the amoxicillin-clavulanic acid (30 μg) disk. Plates were incubated at 37 °C overnight and observed for the presence of an extended spectrum beta-lactamase (ESBL) phenotype by an extension of the edge of inhibition zone of antibiotic disks toward the amoxicillin-clavulanic acid.

Gene detection by polymerase chain reaction

All *E. coli* isolates from both water and milk samples were determined using specific gene and plasmid, and the isolates that showed resistance to antibiotics were selected and subjected to PCR to investigate their drug resistance genes. The bacteria were cultured in 1.5 ml of tryptic soy broth (Oxoid) and incubated overnight; they were then harvested and centrifuged for 10 min at 6,000 rpm. The pellet was resuspended with 800 μl of sterile distilled water, boiled for 10 min, centrifuged at 6,000 rpm for 10 min, and then the supernatant was collected for use as a DNA template in PCR. PCR primers, conditions, and positive control strains for the detection of target gene and drug resistance genes are presented in Tables 1 and 2. All PCR reactions with a total volume of 25 μl were performed

Table 1 Primers and PCR conditions used for virulence gene detection.

Target genes	Positive control	Sequences (5′–3′)	Annealing temperature (°C)	Product size (bp)	References
Heat-labile toxin (*lt*)	ETEC	tctctatgcatacggag ccatactgattgccgcaatt	55	322	*Deng et al. (1996)*
Hest-stable toxin (*st*)	ETEC	tgctaaaccagtagagtcttcaaaa gcaggcttacaacacaattcacagcag	55	138	*Mercado et al. (2011)*
Shiga-like enterotoxins 1 (*evt*)	EHEC	caacactggatgatctcag ccccctcaactgctaata	55	349	*Khan et al. (2002)*
Shiga-like enterotoxins 2 (*evs*)	EHEC	atcagtcgtcactcactggt ctgctgtcacagtgacaaa	55	110	*Khan et al. (2002)*
Transcriptional activator of the aggregative adherence fimbriae (*agg*R)	EAEC 17-2	ctaattgtacaatcgatgta atgaagtaattcttgaat	55	308	*Nataro et al. (1994)*
*pCVD*432 plasmid	EAEC 17-2	ctggcgaaagactgtatcat caatgtatagaaatccgctgtt	55	630	*Aranda, Fagundes-Neto & Scaletsky (2004)*
Intimin (*eae*A)	Plasmid-*eae*A	aaacaggtgaaactgttgcc tctcgcctgatagtgtttggta	55	350	*Yu & Kaper (1992)*
Bundle-forming pilus (*bfp*A)	–	aatggtgcttgcgcttgctgc gccgctttatccaacctggta	57	326	*Zhang et al. (2016)*

Notes.
ETEC, enterotoxigenic *E. coli*; EHEC, enterohemorrhagic *E. coli*; EAEC, enteroaggregative *E. coli*.

in 1× Taq buffer, 1 mM $MgCl_2$, 0.2 mM dNTP, 1 μM of each of the forward and reverse primers, and 2 units of *Taq* DNA polymerase (Thermo Scientific). The PCR amplicon was subjected to 1.5% agarose gel electrophoresis in TAE buffer. For gene amplification with no reference control, the PCR product from positive samples was subjected to nucleotide sequencing and sequence analysis for gene confirmation.

Serotyping

E. coli isolates with virulence genes were serotyped using Serosystem (Serosystem, Clinag, Thailand) to identify O and H antigens present on the surface of the pathogenic *E. coli* isolates with slide agglutination test. The experiment was performed following the manufacturer's protocol. EAEC, EHEC, EPEC, and ETEC strains were used as positive control in the experiment.

RESULTS

E. coli isolation and antibiotic resistance patterns

A total of 185 *E. coli* isolates were collected from water (116 isolates) and milk (69 isolates) samples and subjected to antibiotic susceptibility tests. Among these isolates, a total of 77 (51 isolates from water and 26 isolates from milk samples) showed resistance to at least one of the antibiotics use in the experiment. Penicillin-resistant *E. coli* (71/77, 92.2%) was found to be the largest group in this study followed by folate pathway inhibitor-resistant *E. coli* (20/77, 26%). *E. coli* resistant to cephems (14/77, 18.2%), aminoglycosides (14/77, 18.2%), β-lactamase inhibitor combination (4/77, 5.2%), fluoroquinolone (12/77, 14.3%), and carbapenem (1/77, 1.3%) were also found. Among antibiotic resistant *E. coli*, 84.31%

Table 2 Primers and PCR conditions used for antibiotic resistance gene detection.

Drug resistance genes	Positive control	Sequences (5′–3′)	Annealing temperature (°C)	Product size (bp)	References
Beta-lactams					
bla_{TEM}	–	ttaactggcgaactacttac gtctatttcgttcatccata	60	247	*Kozak et al. (2009)*
bla_{SHV}	–	aggattgactgccttttg atttgctgatttcgctcg	60	393	*Kozak et al. (2009)*
bla_{CMY-2}	–	gacagcctctttctccaca tggacacgaaggctacgta	60	1,000	*Kozak et al. (2009)*
Aminoglycosides					
aac(3)-IIa	–	cggaaggcaataacggag tcgaacaggtagcactgag	60	740	*Soleimani et al. (2014)*
aac(3)-IV	–	gtgtgctgctggtccacagc agttgacccagggctgtcgc	60	627	*Maynard et al. (2004)*
*aad*A	–	cccctggagagagcgagatt cgtggctggctcgaagatac	60	152	Our study
*aad*B	–	gaggagttggactatggatt cttcatcggcatagtaaaag	60	208	*Kozak et al. (2009)*
Quinolone					
*qnr*A	–	agaggatttctcacgccagg tgccaggcacagatcttgac	60	580	*Cattoir et al. (2007)*
*qnr*B	–	ggcattgaaattcgccactg tttgctgctcgccagtcgaa	60	264	*Cattoir et al. (2007)*
*qnr*S	–	gcaagttcattgaacagggt tctaaaccgtcgagttcggcg	60	428	*Cattoir et al. (2007)*

(43/51) of *E. coli* found in water samples are multidrug resistance and 84.61% (22/26) in milk samples (Table 3). The antibiotic patterns could be divided into 21 types, as shown in Table 3. We also found the ESBL phenotype (12/185, 6.5%) in six *E. coli* isolates each from water and milk samples. The antibiotics that the *E. coli* strains are susceptible to are as shown in Fig. 1.

Specific gene and drug resistance gene detection and serotyping

All 185 *E. coli* isolates from both water and milk samples were also subjected to an analysis of the virulence genes and plasmid for EAEC, EHEC, EPEC, and ETEC (*agg* R and *pCVD*432, *evt* and *evs*, *eae*A and *bfp*A, and *lt* and *st*, Fig. 2). Among the bacterial isolates, 24 (24/185, 12.97%) showed positive results for gene detection by PCR, with *bfp*A positive isolates, EPEC forming the majority (13/185, 7.02%) followed by *pCVD*432 positive isolates, EAEC (8/185, 4.32%) and *evt* positive isolates, EHEC (3/185, 1.62%) (Fig. 3). All EPEC *E. coli* isolates were from water samples. Among them, the bacteria presented different serotypes, namely, O124:K62 (2/13, 15.4%), O111:K58 (2/13, 15.4%), O128:K67 (1/13, 7.7%), O78:K80 (1/13, 7.7%), and O86:K61 (1/13, 7.7%). EAEC isolated from milk samples possessed the O18aO18C:K77 serotype (6/8, 75%) and those from water samples possessed the O112aO112c:K66 serotype (1/8, 12.5%), whereas one isolate could not be serotyped.

Table 3 Distribution of antibiotic resistance phenotypic patterns of *E. coli* isolates.

Resistance pattern	Phenotypic resistance	Number of resistant *E. coli* isolates	
		Water samples ($n = 51$)	Milk samples ($n = 26$)
I	AMC	1 (1.9%)	0 (0%)
II	AMC, AMP, CAR	2 (3.9%)	0 (0%)
III	AMC, AMP, CAR, IPM	1 (1.9%)	0 (0%)
IV	AMP	3 (5.8%)	2 (7.6%)
V	AMP, CAR	26 (50.9%)	0 (0%)
VI	AMP, CAR, CAZ, CN, CRO, CTX, CXM	2 (3.9%)	0 (0%)
VII	AMP, CAR, CAZ, CN, CRO, CTX, CXM, FEP	0 (0%)	6 (23.0%)
VIII	AMP, CAR, CAZ, CN, CRO, CTX, CXM, FEP, SCF	0 (0%)	1 (3.8%)
IX	AMP, CAR, CAZ, CN, CRO, CTX, CXM, FEP, SXT	1 (1.9%)	0 (0%)
X	AMP, CAR, CAZ, CN, CRO, CTX, CXM, SXT	1 (1.9%)	0 (0%)
XI	AMP, CAR, CIP, CN, CRO, CTX, CXM, FEP, SXT	1 (1.9%)	0 (0%)
XII	AMP, CAR, CIP, NOR	0 (0%)	7 (26.9%)
XIII	AMP, CAR, CIP, NOR, SXT	1 (1.9%)	0 (0%)
XIV	AMP, CAR, CN, CRO, CTX, CXM, SXT	1 (1.9%)	0 (0%)
XV	AMP, CAR, NOR	1 (1.9%)	0 (0%)
XVI	AMP, CAR, SXT	6 (11.7%)	7 (26.9%)
XVII	AMP, CAZ, CRO, CTX, CXM	0 (0%)	1 (3.8%)
XVIII	CN	1 (1.9%)	0 (0%)
XIX	NOR	1 (1.9%)	1 (3.8%)
XX	SXT	1 (1.9%)	1 (3.8%)
XXI	TZP	1 (1.9%)	0 (0%)

Notes.
AMP, ampicillin; TZP, piperacillin; CAR, carbenicillin; AMC, amoxicillin–clavulanic acid; FEP, cefepime; CTX, cefotaxime; CRO, ceftriaxone; CAZ, ceftazidime; SCF, cefoperazone; CXM, cefuroxime; IPM, imipenem; MEM, meropenem; CN, gentamicin; AK, amikacin; TGC, tigecycline; CIP, ciprofloxacin; NOR, norfloxacin; SXT, trimethoprim–sulfamethoxazole.

EHEC isolates from milk samples possessed the O114:K serotype (2/3, 66.7%), whereas positive isolates from water could not be serotyped (Table 4).

The bacterial antibiotic-resistant isolates (77 isolates) were investigated for drug resistance genes (β-lactam: bla_{TEM}, bla_{SHV}, bla_{CMY-2}; aminoglycoside: *aac*(3)-IIa, *aac*(3)-IV, *aad*A, *aad*B; quinolone: *qnr*A, *qnr*B, and *qnr*S) using PCR. The results showed that one *pCVD*432 positive *E. coli* and one *bfpA* positive *E. coli* isolates possessed bla_{CMY-2} and bla_{TEM}, respectively. We also found one *pCVD*432 positive isolate with the ESBL phenotype that carried both bla_{TEM} and bla_{CMY-2}. In non-pathogenic *E. coli* isolates, 43 (43/77, 55.9%) isolates were found to possess various antibiotic resistance genes (Table 5). The most common resistant gene found was bla_{TEM} (38/62, 61.3%) followed by bla_{CMY-2} (16/62, 25.8%) and *aac*(3)IIa (3/62, 4.9%). Other resistance genes carried by non-pathogenic isolates were *aad*A (2/62, 3.3%) and bla_{SHV}(2/62, 3.3%). None of the *E. coli* isolates carried quinolone resistance genes.

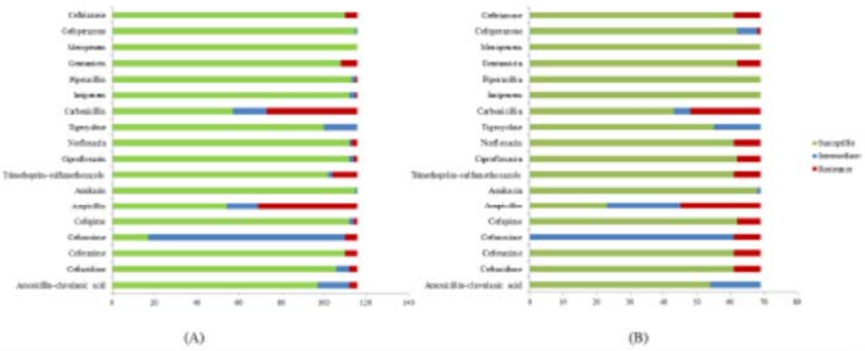

Figure 1 **Antibiotic susceptibility test results.** (A) *E. coli* isolates from water samples. (B) *E. coli* isolates from milk samples.

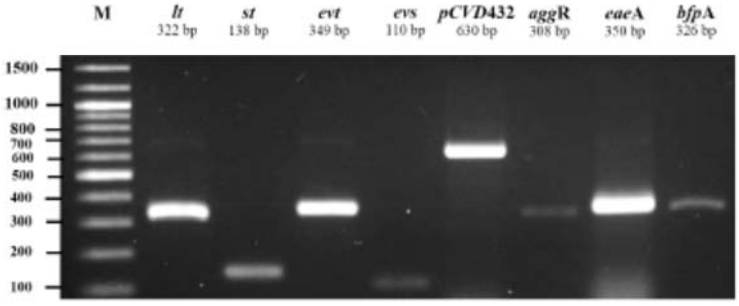

Figure 2 **Agarose gel electrophoresis of 1% agarose of the amplification products of virulence genes and plasmid for ETEC (*lt, st*), EHEC (*evt, evs*), EAEC (*pCVD*432, *agg*R), and EPEC (*eae*A, *bfp*A).** M, DNA Marker.

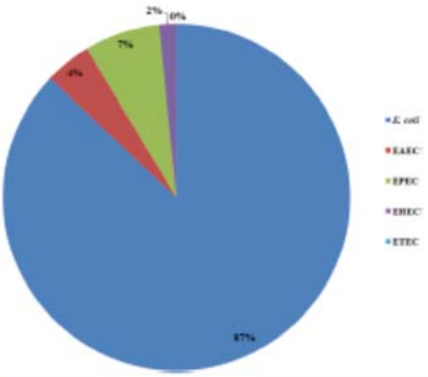

Figure 3 **Prevalence of pathogenic *E. coli* detected from water and milk samples.**

Table 4 Target genes, serotyping, antibiotic resistance pattern, resistant gene profile, and ESBL phenotype of pathogenic *E. coli* isolates.

Isolate number	Origin	Target gene	Serotype	Antibiotic resistance pattern	Resistance gene profile	ESBL phenotype
M-W910-1 LF1	Water	*bfp*A	[a]	[b]	–	–
M-W910-1 LF3	Water	*bfp*A	[a]	[b]	–	–
M-W1010-1 LF1	Water	*bfp*A	[a]	V	bla_{TEM}	–
M-W1110-1 LF3	Water	*bfp*A	[a]	XX	–	–
M-W1110-1 LF5	Water	*bfp*A	O124:K62	[b]	–	–
M-W1110-1 LF6	Water	*bfp*A	O111:K58	[b]	–	–
M-W12UD LFB6	Water	*bfp*A	O111:K58	I	–	–
M-W13UD LFB6	Water	*bfp*A	O128:K67	[b]	–	–
M-W13UD LFB7	Water	*bfp*A	O124:K62	[b]	–	–
M-W13UD LFB10	Water	*bfp*A	O78:K80	[b]	–	–
M-W15UD LFB4	Water	*bfp*A	[a]	V	–	–
M-W22UD LF9	Water	*pCVD*432	[a]	VI	bla_{CMY-2}, *aac*(3)IIa	–
M-W23UD LF2	Water	*pCVD*432	O112aO112c:K66	VI	bla_{TEM}, bla_{CMY-2}, *aac*(3)IIa, *aad*A	+
M-W32UD LF1	Water	*bfp*A	[a]	V	–	–
M-W33UD LF1	Water	*bfp*A	O86:K61	[b]	–	–
M-M10UD LFB4	Milk	*evt*	O114:K	[b]	–	–
M-M10UD LFB5	Milk	*evt*	O114:K	[b]	–	–
M-M35UD LFB2	Milk	*pCVD*432	O18aO18c:K77	VII	–	+
M-M35UD LFB3	Milk	*pCVD*432	O18aO18c:K77	VII	–	+
M-M35UD LFB4	Milk	*pCVD*432	O18aO18c:K77	VII	–	+
M-M35UD LFB5	Milk	*pCVD*432	O18aO18c:K77	VIII	–	+
M-M35UD LFB6	Milk	*pCVD*432	O18aO18c:K77	VII	–	+
M-M35UD LFB7	Milk	*pCVD*432	O18aO18c:K77	VII	–	+
M-M37UD LFB4	Milk	*evt*	[a]	XVI	–	–

Notes.
[a] Not typable.
[b] Susceptible.
+ Positive.
– Negative.

DISCUSSION

E. coli is known to be the most common gram negative bacteria that potentially causes subclinical mastitis and exhibits antibiotic resistance. However, pathogenic *E. coli* in the environment has often been overlooked. Many studies have reported the presence of *E. coli* among subclinical mastitis cases in dairy farms in many regions of the world, particularly in developing countries, such as Uruguay, Turkey, Brazil, Ethiopia, Mexico, and China (*Gianneechini et al., 2002*; *Guler & Gunduz, 2007*; *Fernandes et al., 2011*; *Haftu et al., 2012*; *Abera et al., 2012*; *Olivares-Perez et al., 2015*; *Wang et al., 2015*). This study demonstrated the existence of pathogenic *E. coli* in environmental sources and also in milk from cows with subclinical mastitis by detecting specific genes associated with the pathogenic types of this species. *bfp*A-positive *E. coli* was found to be the most common strain of pathogenic *E. coli* residing in water sources. *pCVD*432-positive isolate was found in both water and

Table 5 Target genes, serotyping, antibiotic resistance pattern, resistant gene profile, and ESBL phenotype of non-pathogenic *E. coli* isolates.

Isolate number	Origin	Target gene	Serotype	Antibiotic resistance pattern	Resistance gene profile	ESBL phenotype
M-W610-1 LF1	Water	–	b	V	bla_{TEM}	–
M-W910-1 LF2	Water	–	b	IV	bla_{CMY-2}	–
M-W1110-1 LF9	Water	–	b	XVI	bla_{TEM}	–
M-W12UD LFB6	Water	–	b	I	bla_{CMY-2}	–
M-W16UD LF1	Water		b	V	bla_{TEM}, bla_{SHY}, bla_{CMY-2}	–
M-W16UD LF2	Water	–	b	V	bla_{TEM}, bla_{CMY-2}	–
M-W1910-1 LF6	Water	–	b	V	bla_{TEM}	–
M-W20UD LF6	Water	–	b	V	bla_{TEM}, bla_{CMY-2}	–
M-W20UD LF9	Water	–	b	V	bla_{TEM}, bla_{CMY-2}	–
M-W22UD LF3	Water	–	b	XIV	bla_{TEM}, bla_{CMY-2}	+
M-W22UD LF7	Water	–	b	X	bla_{TEM}, bla_{CMY-2}, *aac*(3)IIa	+
M-W24UD LF1	Water	–	b	V	bla_{TEM}	–
M-W24UD LF3	Water	–	b	XI	bla_{TEM}, bla_{CMY-2}, *aac*(3)IIa, *aad*A	+
M-W24UD LF4	Water	–	b	V	bla_{TEM}	–
M-W24UD LF5	Water	–	b	XVI	bla_{TEM}	–
M-W24UD LF7	Water	–	b	*	bla_{TEM}, bla_{CMY-2}	–
M-W26UD LF8	Water	–	b	IV	bla_{TEM}	–
M-W27UD LF4	Water	–	b	XVI	bla_{TEM}	–
M-W28UD LF1	Water	–	b	XV	bla_{TEM}	–
M-W28UD LF5	Water	–	b	V	bla_{SHV}, bla_{CMY-2}	–
M-W28UD LF7	Water	–	b	V	bla_{TEM}, bla_{CMY-2}	–
M-W29UD LF1	Water	–	b	IX	bla_{TEM}, bla_{CMY-2}, *aac*(3)IIa, *aad*A	+
M-W29UD LF10	Water	–	b	XVI	bla_{TEM}	–
M-W31UD LF6	Water	–	b	V	bla_{TEM}	–
M-W33UD LF2	Water	–	b	V	bla_{TEM}	–
M-W33UD LF6	Water	–	b	V	bla_{TEM}	–
M-W33UD LF9	Water	–	b	V	bla_{TEM}	–
M-W33UD LF10	Water	–	b	V	bla_{TEM}	–
M-W34UD LF3	Water	–	b	V	bla_{TEM}	–
M-W34UD LF7	Water	–	b	XIII	bla_{TEM}	–
M-M1610-1 LFB2	Milk	–	b	IV	bla_{TEM}	–
M-M37UD LFB1	Milk	–	b	XVI	bla_{TEM}	–
M-M37UD LFB3	Milk	–	b	XVI	bla_{TEM}	–
M-M37UD LFB5	Milk	–	b	XVI	bla_{CMY-2}	–
M-M37UD LFB6	Milk	–	b	XVI	bla_{TEM}, bla_{CMY-2}	–
M-M37UD LFB8	Milk	–	b	XVI	bla_{CMY-2}	–
M-M38UD LFB1	Milk	–	b	XII	bla_{TEM}	–
M-M38UD LFB2	Milk	–	b	XII	bla_{TEM}	–
M-M38UD LFB3	Milk	–	b	XII	bla_{TEM}	–
M-M38UD LFB4	Milk	–	b	XII	bla_{TEM}	–

(*continued on next page*)

Table 5 (*continued*)

Isolate number	Origin	Target gene	Serotype	Antibiotic resistance pattern	Resistance gene profile	ESBL phenotype
M-M38UD LFS2	Milk	–	[b]	XII	bla_{TEM}	–
M-M38UD LFS3	Milk	–	[b]	XII	bla_{TEM}	–
M-M38UD LFS4	Milk	–	[b]	XII	bla_{TEM}	–

Notes.
[b] Not serotype.
[s] Susceptible.
[+] Positive.
[–] Negative.

milk samples. *evt*-positive *E. coli* was the least common and was only identified in milk samples; it was not present in any of the water samples. In this study, EPEC possessed only *bfp*A, which encodes bundle-forming pili that are a specific characteristic of EPEC (*Cleary et al., 2004*). The presence of EPEC in water sources in dairy farms could lead to intramammary infection of cows. A study by *Dopfer, Nederbragt & Almeida (2001)* also reported the isolation of *bfp*A-positive EPEC from persistent cases of bovine mastitis (*Dopfer, Nederbragt & Almeida, 2001*). Although none of the *E. coli* isolates was positive for *eae*A in this study, there are reports of the presence of *eae*A-positive EPEC among *E. coli* found in cows with mastitis in Brazil and Turkey (*Correa & Marin, 2002*; *Guler & Gunduz, 2007*). However, in Iran, *eae*A-positive *E. coli* was not found in clinical mastitis cases (*Ghanbarpour & Oswald, 2010*). This indicates that *bfp*A- and *eae*A-positive EPEC may be distributed unevenly across the globe. EAEC (*pCVD*432-positive isolates) was found in both water and milk samples. However, the serotypes of those isolates differed. This may indicated different sources of EAEC in water and infected cows. The results also designated that EAEC may be an epidemic strain in dairy farms in Saraburi Province, and EAEC and EPEC could be causative agents of mastitis considering their potential infection through water in farms. EHEC was the least common group found only in milk samples in this study and positive only for *evt* (shiga-toxin 1-encoding gene). These results raise concerns regarding the bacterial distribution to nearby areas via the contaminated water which workers should be aware of. Studies by *Lira, Macedo & Marin (2004)* and *Momtaz (2010)* also reported shiga-toxin 1-producing *E. coli* from cases of subclinical mastitis in cows in Brazil and Iran. *Momtaz et al. (2012)* later reported that shiga-toxin 1-producing *E. coli* was the most common type of *E. coli* in milk samples from cows with subclinical mastitis in Iran (*Momtaz et al., 2012*). These results also correlated with many studies on clinical cases of bovine mastitis. For example, *Momtaz et al. (2012)* reported the presence of EHEC with shiga-toxin 1-encoding gene as the most common virulence gene in milk samples from cases with subclinical and clinical mastitis (*Momtaz et al., 2012*), which also correlated with the study by *Suojala et al. (2011)*, in which shiga-toxin 1-encoding gene was among the most common virulence genes found in clinical cases of bovine mastitis (*Suojala et al., 2011*).

Among the 21 antibiotic resistance patterns, the most common pattern found in *E. coli* from water sources was pattern V (ampicillin and carbenicillin resistance), followed by pattern XVI (ampicillin, carbenicillin, gentamicin, ceftriaxone, cefotaxime, and trimethoprim/sulfamethoxazole resistance). Among the antibiotic patterns in the *E. coli*

from milk, pattern XII (ampicillin, carbenicillin, ciprofloxacin, and norfloxacin resistance) and XVI were the most common. This may indicate that *E. coli* in milk could potentially derive from water or other environmental sources. A study by *Sayah et al. (2005)* also reported the difference in antibiotic resistance patterns between *E. coli* isolated from farm water and fecal samples (*Sayah et al., 2005*). Our results call for a more cautious approach with antibiotics usage in dairy farms in the Saraburi province area, since the antibiotics that the *E. coli* isolates were susceptible to are from the high generation cephalosporin and β-lactam classes which are normally used for the treatment of drug-resistance bacteria.

In another study, *Geser, Stephan & Hachler (2012)* reported on ESBL-positive *E. coli* in milk from cows with mastitis *Geser, Stephan & Hachler (2012)*, and ESBL-producing *E. coli* was shown to be able to spread from infected animals to the environment, such as air and slurry, as reported in a pig farm in Germany (*Von Salviati et al., 2015*). In this study, EAEC was the only pathogenic strain that possessed the ESBL phenotype. Notably, only the ESBL-producing EAEC isolates from water samples contained antibiotic resistance genes (bla_{TEM} and $bla_{\text{CMY-2}}$). The results also correlate with the study by *Franz et al. (2015)*, who reported that EAEC found in surface water and wastewater dominates over other strains of pathogenic *E. coli* in terms of possessing the ESBL phenotype (*Franz et al., 2015*). In this study, we found that non-pathogenic *E. coli* isolates carried ESBL-associated genes (bla_{TEM}, bla_{SHV}, and $bla_{\text{CMY-2}}$. However, only four isolates (M-W22UD LF3, M-W22UD LF7, M-W24UD LF3, and M-W29UD LF1) presented the ESBL phenotype and all of these carried bla_{TEM} and $bla_{\text{CMY-2}}$. These results imply that the presence of drug-resistant strains of non-pathogenic *E. coli* isolates from the environment is possible. This can pose a threat to mastitis management programs for farm since one study also reported that non-pathogenic *E. coli* can serve as a reservoir of antibiotic resistance genes and could possibly transfer the genes to other pathogenic *E. coli* if conditions are suitable (*Hu et al., 2016*).

CONCLUSION

This study provides evidence that *E. coli* isolates from cows with subclinical mastitis and from water at dairy farms in Saraburi Province of Thailand consisted of pathogenic *E. coli* strains that are resistant to many groups of antibiotics, including the fluoroquinolone group, which should raise concerns regarding the improper use of antibiotics in this area. However, the information on which antibiotics are being used on the farms is very limited. Identification of the ESBL phenotype and β-lactamase genes was also a concern as these can be transferred to other *E. coli* strains, including pathogenic strains, and bacterial species. This could lead to more serious problems associated with antibiotic resistance in the future. It should be recommended that farms prevent mastitis by promote clean environments for cows such as frequently changing bedding at the stalls and milking areas by cleaning the areas thoroughly. The use of dry and clean cloths to clean the teats before milking and effective teat dips should reduce mastitis on farms. The use of antibiotics, mastitis control programs, and milking hygiene should be considered and supervised by veterinarians to improve mastitis status and treatment in this area.

ADDITIONAL INFORMATION AND DECLARATIONS

Funding

The work was supported by a NSTDA Chair professor grant (P-1450624) funded by the Crown Property Bureau of Thailand, Thailand Research Fund (RSA5980048) and Royal Golden Jubilee (RGJ) grant (PHD58K0073). The funders had no role in study design, data collection and analysis, decision to publish, or preparation of the manuscript.

Grant Disclosures

The following grant information was disclosed by the authors:
Crown Property Bureau of Thailand, NSTDA: P-1450624.
Thailand Research Fund: RSA5980048.
Royal Golden Jubilee (RGJ): PHD58K0073.

Competing Interests

The authors declare there are no competing interests.

Author Contributions

- Woranich Hinthong conceived and designed the experiments, performed the experiments, analyzed the data, wrote the paper, prepared figures and/or tables, reviewed drafts of the paper.
- Natapol Pumipuntu, Sirijan Santajit, Suphang Kulpeanprasit and Pisinee Aiumurai performed the experiments.
- Shutipen Buranasinsup analyzed the data, contributed reagents/materials/analysis tools, prepared figures and/or tables.
- Nitat Sookrung analyzed the data, contributed reagents/materials/analysis tools, reviewed drafts of the paper.
- Wanpen Chaicumpa analyzed the data, contributed reagents/materials/analysis tools.
- Nitaya Indrawattana conceived and designed the experiments, analyzed the data, contributed reagents/materials/analysis tools, wrote the paper, prepared figures and/or tables, reviewed drafts of the paper.

Animal Ethics

The following information was supplied relating to ethical approvals (i.e., approving body and any reference numbers):

The ethical standards of the Faculty of Tropical Medicine–Animal Care and Use Committee (FTM-ACUC), Mahidol University, Thailand.

Data Availability

The following information was supplied regarding data availability:

The raw data has been supplied as a Supplementary File.

Supplemental Information

Supplemental information for this article can be found online at http://dx.doi.org/10.7717/peerj.3431#supplemental-information.

REFERENCES

Abera M, Habte T, Aragaw K, Asmare K, Sheferaw D. 2012. Major causes of mastitis and associated risk factors in smallholder dairy farms in and around Hawassa, Southern Ethiopia. *Tropical Animal Health and Production* **44**:1175–1179 DOI 10.1007/s11250-011-0055-3.

Aranda KRS, Fagundes-Neto U, Scaletsky ICA. 2004. Evaluation of multiplex PCRs for diagnosis of infection with diarrheagenic *Escherichia coli* and *Shigella* spp. *Journal of Clinical Microbiology* **42**:5849–5853.

Azevedo C, Pacheco D, Soares L, Romao R, Moitoso M, Maldonado J, Guix R, Simoes J. 2016. Prevalence of contagious and environmental mastitis-causing bacteria in bulk tank milk and its relationships with milking practices of dairy cattle herds in Sao Miguel island (Azores). *Tropical Animal Health and Production* **48**:451–459 DOI 10.1007/s11250-015-0973-6.

Burvenich C, Merris VV, Mehrzad J, Diez-Fraile A, Duchateau L. 2003. Severity of *E. coli* mastitis is determined by cow factors. *Veterinary Research* **34**:521–564 DOI 10.1051/vetres:2003023.

Cattoir V, Poirel L, Rotimi V, Soussy C, Nordmann P. 2007. Multiplex PCR for detection of plasmid-mediated quinolone resistance *qnr* genes in ESBL-producing enterobacterial isolates. *Journal of Antimicrobial Chemotherapy* **60**:394–397 DOI 10.1093/jac/dkm204.

Cleary J, Lai LC, Shaw RK, Straatman-Iwanowska A, Donnegberg MS, Frankel G, Knutton S. 2004. Enteropathogenic *Escherichia coli* (EPEC) adhesion to intestinal epithelial cells: role of bundle-forming pili (BFP), EspA filaments and intimin. *Microbiology* **150**:527–538 DOI 10.1099/mic.0.26740-0.

Clinical and Laboratory Standards Institute. 2012. Performance standards for antimicrobial susceptibility testing; Twenty second informational supplement. In: *CLSI document M100-S22*. Wayne: Clinical and Laboratory Standards Institute.

Clinical and Laboratory Standards Institute. 2016. Performance standards for antimicrobial susceptibility testing. In: *CLSI document M100S*. 26th edition. Wayne: Clinical and Laboratory Standards Institute.

Correa MGP, Marin JM. 2002. O-serogroups, *eae* gene and EAF plasmid in *Escherichia coli* isolates from cases of bovine mastitis in Brazil. *Veterinary Microbiology* **85**:125–132 DOI 10.1016/S0378-1135(01)00413-8.

Deng MY, Cliver DO, Day SP, Fratamico PM. 1996. Enterotoxigenic *Escherichia coli* detected in foods by PCR and an enzyme-linked oligonucleotide probe. *International Journal of Food Microbiology* **30**:217–329 DOI 10.1016/0168-1605(96)00942-7.

Dopfer D, Nederbragt H, Almeida RA. 2001. Studies about the mechanism of internalization by mammary epithelial cells of *Escherichia coli* isolated from persistent bovine mastitis. *Veterinary Microbiology* **80**:285–296 DOI 10.1016/S0378-1135(01)00307-8.

Fernandes JBC, Zanardo LG, Galvao NN, Carvalho IA, Nero LA, Moreira MAS. 2011. *Escherichia coli* from clinical mastitis: serotypes and virulence factors. *Journal of Veterinary Diagnostic Investigation* **23**:1146–1152 DOI 10.1177/1040638711425581.

Franz E, Veenman C, Van Hoek AHAM, De Roda Husman A, Blaak H. 2015. Pathogenic *Escherichia coli* producing Extended-Spectrum β-Lactamases isolated from surface water and wastewater. *Scientific Reports* **5**:14372 DOI 10.1038/srep14372.

Geser N, Stephan R, Hachler H. 2012. Occurrence and characteristics of extended-spectrum β-lactamase (ESBL) producing *Enterobacteriaceae* in food producing animals, minced meat and raw milk. *BMC Veterinary Research* **8**:21 DOI 10.1186/1746-6148-8-21.

Ghanbarpour R, Oswald E. 2010. Phylogenetic distribution of virulence genes in *Escherichia coli* isolated from bovine mastitis in Iran. *Research in Veterinary Science* **88**:6–10 DOI 10.1016/j.rvsc.2009.06.003.

Gianneechini R, Concha C, Rivero R, Delucci I, Moreno Lopez J. 2002. Occurrence of clinical and sub-clinical mastitis in dairy herds in the West Littoral Region in Uruguay. *Acta Veterinaria Scandinavica* **43**:221–230 DOI 10.1186/1751-0147-43-221.

Guler L, Gunduz K. 2007. Virulence properties of *Escherichia coli* isolated from clinical bovine mastitis. *Turkish Journal of Veterinary and Animal Science* **31**:361–365.

Haftu R, Taddele H, Gugsa G, Kalayou S. 2012. Prevalence, bacterial causes, and antimicrobial susceptibility profile of mastitis isolates from cows in large-scale dairy farms of Northern Ehtiopia. *Tropical Animal Health and Production* **44**:1765–1771 DOI 10.1007/s11250-012-0135-z.

Hu Y, Yang X, Li J, Lv N, Liu F, Wu J, Lin IYC, Wu N, Weimer BC, Gao GF, Liu Y, Zhu B. 2016. The transfer network of bacterial mobile resistome connecting animal and human microbiome. *Applied and Environmental Microbiology* **82**:6672–6681 DOI 10.1128/AEM.01802-16.

Iraguha B, Hamudikuwanda H, Mushonga B. 2015. Bovine mastitis prevalence and associated risk factors in dairy cows in Nyagatare District, Rwanda. *Journal of the South African Veterinary Association* **86(1)** DOI 10.4102/jsava.v86i1.1228.

Khan A, Yamasaki S, Sata T, Ramamurthy T, Pal A, Datta S, Chowdhury NR, Das SC, Sikdar A, Tsukamoto T, Bhattacharya SK, Takeda Y, Nair GB. 2002. Prevalence and genetic profiling of virulence determinants of non-O157 shiga toxin-producing *Escherichia coli* isolated from cattle, beef, and humans, Calcutta, India. *Emerging Infectious Diseases* **8**:54–62 DOI 10.3201/eid0801.010104.

Kozak GK, Boerlin P, Janecko N, Reid-Smith RJ, Jardine C. 2009. Antimicrobial resistance in *Escherichia coli* isolates from swine and wild animal mammals in the proximity of swine farms and in natural environments in Ontario, Canada. *Applied and Environmental Microbiology* **75**:559–566 DOI 10.1128/AEM.01821-08.

Lira WM, Macedo C, Marin JM. 2004. The incidence of shiga toxin-producing *Escherichia coli* in cattle with mastitis in Brazil. *Journal of Applied Microbiology* **97**:861–866 DOI 10.1111/j.1365-2672.2004.02384.x.

Maynard C, Bekal S, Sanschagrin F, Levesque RC, Brousseau R, Masson L, Lariviere S, Harel J. 2004. Heterogeneity among virulence and antimicrobial resistance gene profiles of extraintestinal *Escherichia coli* isolates of animal and human origin. *Journal of Clinical Microbiology* **42**:5444–5452 DOI 10.1128/JCM.42.12.5444-5452.2004.

Memon J, Kashif J, Yaqoob M, Liping W, Yang Y, Hongjie F. 2013. Molecular characterization and antimicrobial sensitivity of pathogens from sub-clinical and clinical mastitis in eastern China. *Pakistan Veterinary Journal* **33**:170–174.

Mercado EH, Ochoa TJ, Eckar L, Cabello M, Durand D, Barletta F, Molina M, Gil AI, Huicho L, Lanata CF, Cleary TG. 2011. Fecal leukocytes in children infected with diarrheagenic *Escherichia coli*. *Journal of Clinical Microbiology* **49**:1376–1381 DOI 10.1128/JCM.02199-10.

Momtaz H. 2010. Investigation of virulence factors in *Escherichia coli* isolated from clinical and subclinical bovine mastitis. *Bulgarian Journal of Veterinary Medicine* **13**:122–126.

Momtaz H, Dehkordi FS, Taktaz T, Rezvani A, Yarali S. 2012. Shiga toxin-producing *Escherichia coli* isolated from bovine mastitic milk: serogroups, virulence factors, and antibiotic resistance properties. *The Scientific World Journal* **2012**:618709 DOI 10.1100/2012/618709.

Nataro JP, Yikang D, Yingkang D, Walker K. 1994. AggR, a transcriptional activator of aggregative adherence fimbria I expression in enteroaggregative *Escherichia coli*. *Journal of Bacteriology* **176**:4691–4699 DOI 10.1128/jb.176.15.4691-4699.1994.

Olivares-Perez J, Kholif AE, Rojas-Hernandez S, Elghandour MMMY, Salem AZMS, Bastida AZ, Velazquez-Reynoso D, Cipriano-Salazar M, Camacho-Diaz LM, Alonso-Fresan MU, DiLorenzo N. 2015. Prevalence of bovine subclinical mastitis, its etiology and diagnosis of antibiotic resistance of dairy farms in four municipalities of a tropical region of Mexico. *Tropical Animal Health and Production* **47**:1497–1504 DOI 10.1007/s11250-015-0890-8.

Perkins NR, Kelton DF, Hand KJ, MacNaughton G, Berke O, Leslie KE. 2009. An analysis of the relationship between bulk tank milk quality and wash water quality on dairy farms in Ontario, Canada. *Journal of Dairy Science* **92**:2009–2030.

Sayah RS, Kaneene JB, Johnson Y, Miller R. 2005. Patterns of antimicrobial resistance observed in *Escherichia coli* isolates obtained from domestic- and wild-animal fecal samples, human septage, and surface water. *Applied and Environmental Microbiology* **71**:1394–1404 DOI 10.1128/AEM.71.3.1394-1404.2005.

Schukken Y, Chuff M, Moroni P, Gurjar A, Santisteban C, Welcome F, Zadoks R. 2012. The "other" gram-negative bacteria in mastitis: *Klebseilla*, *Serratia*, and more. *Veterinary Clinics of North America: Food Animal Practice* **28**:239–256.

Soleimani N, Aganj M, Ali L, Shokoohizadeh L, Sakinc T. 2014. Frequency distribution of genes encoding aminoglycoside modifying enzymes in uropathogenic *E. coli* isolates from Iranian hospital. *BMC Research Notes* **7**:842 DOI 10.1186/1756-0500-7-842.

Suojala L, Pohjanvirta T, Simojoki H, Myllyniemi AL, Pitkala A, Pelkonen S, Pyorala S. 2011. Phylogeny, virulence factors and antimicrobial susceptibility of *Escherichia coli* isolated in clinical bovine mastitis. *Veterinary Microbiology* **147**:383–388 DOI 10.1016/j.vetmic.2010.07.011.

Suriyasathaporn W. 2011. Epidemiology of subclinical mastitis and their antibacterial susceptibility in smallholder dairy farm, Chiang Mai province, Thailand. *Journal of Animal and Veterinary Advances* **10**:316–321 DOI 10.3923/javaa.2011.316.321.

Suriyasathaporn W, Chupia V, Sing-Lah T, Wongsawan K, Mektrirat R, Chaisri W. 2012. Increases of antibiotic resistance in excessive use of antibiotics in smallholder dairy farms in northern Thailand. *Asian-Australasian Journal of Animal Sciences* **25**:1322–1328 DOI 10.5713/ajas.2012.12023.

Von Salviati C, Laube H, Guerra B, Roesler U, Friese A. 2015. Emission of ESBL/AmpC producing *Escherichia coli* from pig fattening farms to surrounding areas. *Veterinary Microbiology* **30**:77–84 DOI 10.1016/j.vetmic.2014.10.010.

Wang L, Yang F, Wei X, Luo Y, Zhou X, Gua W, Niu J, Guo Z. 2015. Investigation of bovine mastitis pathogen in two northwestern provinces of China from 2012–2014. *Journal of Animal and Veterinary Advances* **14**:237–243 DOI 10.3923/javaa.2015.237.243.

Yu J, Kaper JB. 1992. Cloning and characterization of the eae gene of enterohemorrhagic *Escherichia coli* O157:H7. *Molecular Microbiology* **6**:411–417.

Zhang S, Wu Q, Zhang J, Zhu X. 2016. Occurrence and characterization of enteropathogenic *Escherichia coli* (EPEC) in retail ready-to-eat foods in China. *Foodborne Pathogen and Diseases* **13**:49–55 DOI 10.1089/fpd.2015.2020.

toxins

MDPI

Article

Human scFvs That Counteract Bioactivities of *Staphylococcus aureus* TSST-1

Thunchanok Rukkawattanakul [1,2], Nitat Sookrung [2,3], Watee Seesuay [2], Nattawat Onlamoon [3], Pornphan Diraphat [4], Wanpen Chaicumpa [2] and Nitaya Indrawattana [5,*]

1 Graduate Program in Immunology, Department of Immunology, Faculty of Medicine Siriraj Hospital, Mahidol University, Bangkok 10700, Thailand; ruk.thunchanok@gmail.com
2 Center of Research Excellence on Therapeutic Proteins and Antibody Engineering, Department of Parasitology, Faculty of Medicine Siriraj Hospital, Mahidol University, Bangkok 10700, Thailand; nitat.soo@mahidol.ac.th (N.S.); watee.see@gmail.com (W.S.); wanpen.cha@mahidol.ac.th (W.C.)
3 Department of Research and Development, Faculty of Medicine Siriraj Hospital, Mahidol University, Bangkok 10700, Thailand; nattawat.onl@mahidol.ac.th (N.O.)
4 Department of Microbiology, Faculty of Public Health, Mahidol University, Bangkok 10400, Thailand; pornphan.dir@mahidol.ac.th
5 Department of Microbiology and Immunology, Faculty of Tropical Medicine, Mahidol University, Bangkok 10400, Thailand
* Correspondence: nitaya.ind@mahidol.ac.th; Tel.: +66-2-354-9100 (ext. 1598); Fax: +66-2-643-5583

Academic Editor: Andreas Rummel
Received: 7 November 2016; Accepted: 9 February 2017; Published: 17 February 2017

Abstract: Some *Staphylococcus aureus* isolates produced toxic shock syndrome toxin-1 (TSST-1) which is a pyrogenic toxin superantigen (PTSAg). The toxin activates a large fraction of peripheral blood T lymphocytes causing the cells to proliferate and release massive amounts of pro-inflammatory cytokines leading to a life-threatening multisystem disorder: toxic shock syndrome (TSS). PTSAg-mediated-T cell stimulation circumvents the conventional antigenic peptide presentation to T cell receptor (TCR) by the antigen-presenting cell (APC). Instead, intact PTSAg binds directly to MHC-II molecule outside peptide binding cleft and simultaneously cross-links TCR-Vβ region. Currently, there is neither specific TSS treatment nor drug that directly inactivates TSST-1. In this study, human single chain antibodies (HuscFvs) that bound to and neutralized bioactivities of the TSST-1 were generated using phage display technology. Three *E. coli* clones transfected with TSST-1-bound phages fished-out from the human scFv library using recombinant TSST-1 as bait expressed TSST-1-bound-HuscFvs that inhibited the TSST-1-mediated T cell activation and pro-inflammatory cytokine gene expressions and productions.Computerized simulation, verified by mutations of the residues of HuscFv complementarity determining regions (CDRs),predicted to involve in target binding indicated that the HuscFvs formed interface contact with the toxin residues important for immunopathogenesis. The HuscFvs have high potential for future therapeutic application.

Keywords: direct acting anti-TSST-1; human scFv; *Staphylococcus aureus*; superantigen; Toxic shock syndrome (TSS)

1. Introduction

Superantigens (SAgs) are proteins produced by some bacterial and viral strains that mediate T cell activation by bypassing the conventional peptide-MHC-II presentation to T cell receptor (TCR) [1]. Instead, intact (unprocessed) SAgs bind directly to MHC-II molecules on the antigen presenting cells (APC)and simultaneously cross-link TCR-Vβ domains shared by about 5%–20% of circulating $CD4^+$

and CD8$^+$ T lymphocytes [1,2]. T cell stimulation by SAgs is Lck pathway-independent [3], initiated at the Gα11 (a membrane raft-enriched heterotrimeric G-protein) that stimulates PLCβ and PKC to activate mitogen-activated protein kinases (ERKs) causing nuclear translocation of NF-AT and NF-κB and cytokine gene expressions [3]. Massive amounts of cytokines including IL-1β, IL-2, IL-6,TNFα and IFNγ are released from the activated cells into the circulation [1] leading to high fever, rash, skin desquamation (peeling), plasma leakage, obstinate hypotension, and life-threatening multisystem organ failure called toxic shock syndrome (TSS) [2,4]. SAgs potentiate host sensitivity to bacterial endotoxin resulting in TNFα-mediated capillary leakage which is the major contributor of the TSS [5,6].

Staphylococcus aureus secretes several pyrogenic toxin superantigens (PTSAgs) including toxic shock syndrome toxin-1 (TSST-1) and many enterotoxins [1,7]. TSST-1 is a prototype of group I PTSAgs responsible for most cases of menstrually-related-TSS and a large proportion of non-menstrual cases, i.e., patients with surgical wound and cutaneous infections, osteomyelitis, arthritis, burns, post-partum infection, and barrier contraceptive users [8,9]. Although PTSAgs share nearly identical tertiary structure, their primary sequences are diverse (only 20%–30% identity) and the way they interact with the host receptors (MHC-II and TCR) are different [10–16]. For examples, *S. aureus* TSST-1 occupies almost one-half of the HLA-DR1 and contact with α-helices of the MHC-II and the bound peptide while *S. aureus* enterotoxin B binds to only one edge of the peptide binding cleft of the DR1 [10]. TSST-1 is encoded by *tst*H gene in the *S. aureus* mobile genetic element [17]. TSST-1 structure and regions that interacted with MHC-II and TCR have been investigated extensively [10,18–20]. Mature toxin (194 residues; ~22 kDa) is monomeric in solution and comprises two tightly packed-distinct domains [18,20]. The N-terminal domain (small domain B) acquires α-helix configuration (α1; residues 1–17) that is surrounded by five β-strands (β1-β5; residues 18–89). The C-terminal domain (large domain A) is connected to the N-domain and contains a long α-helix (α2 or the toxin backbone; residues 125-141) packed against fiveβ strands; residues 90–194) that form a β-grasp motif [18–20]. N-terminal domain of TSST-1 binds MHC-II, while C-terminal domainis implicated in binding to TCR-Vβ [10,16,18,21].

TSS management includes supportive and symptomatic treatment. Antimicrobials and surgical debridement to remove the toxin-producing microorganisms are important. Maintaining blood pressure by fluid therapy is necessary [22,23]. Intravenous immunoglobulin (IVIG) confers some benefit to the patients [24].Murine monoclonal antibodies that neutralized endotoxin prevented rabbits from lethal TSS and endotoxin challenge [6]. Symptom severity of TSS was mitigated in a rabbit model after giving a mouse monoclonal antibody that neutralized TSST-1 activities [25]. Rabbit polyclonal antisera against wild type and TSST-1 mutants (G31R and H135A which affected MHC-II and TCR bindings) protected rabbits even when given late in the course of the TSST-1 challenge [26]. In this study, human monoclonal single chain antibodies (HuscFvs) that bound to functionally important residues of TSST-1 were produced by phage display technology. HuscFvs of three phage-transformed *Escherichia coli* clones inhibited TSST-1 mitogenicity (activation of T cell proliferation) and pyrogenicity (induction of pro-inflammatory cytokine gene expressions and the cytokine secretions). The human scFvs have high potential for testing further as a safe, direct acting anti-TSST-1 remedy.

2. Results and Discussion

2.1. Recombinant TSST-1 and Activities

Recombinant pET21a$^+$ with TSST-1 gene insert was synthesized (GenScript) and used to transform NiCo21 (DE3) *E. coli*. Amplicon of the gene is shown in Figure 1A. From 1 L culture of the transformed *E. coli* grown under 1 mM isopropyl β-D-1-thiogalactopyranoside (IPTG) induction, 1.46 grams of purified recombinant protein was obtained. The purified preparation revealed only one protein band in SDS-PAGE and protein staining (lane 1, left panel of Figure 1B) and Western blotting (lane 1, right panel of Figure 1B). The LPS content of the purified preparation was 0.15 endotoxin unit (EU)/microgram. One endotoxin unit was approximately 0.1–0.2 ng [27]. Mass spectrometry verified that the recombinant protein was TSST-1 (Table 1). Figure S1A shows codon-optimized nucleotide sequence of the TSST-1 of

this study. *BamH*I and *Hind*III restriction sites were placed at the 5′ and 3′ ends of the gene sequence, respectively; a stop codon of the TSST-1 gene was removed from the 3′ end upstream of the *Hind*III site. The deduced amino acid sequence, which has 100% amino acid identity to the TSST-1 of the database (accession J02615), is shown in Figure S1B.

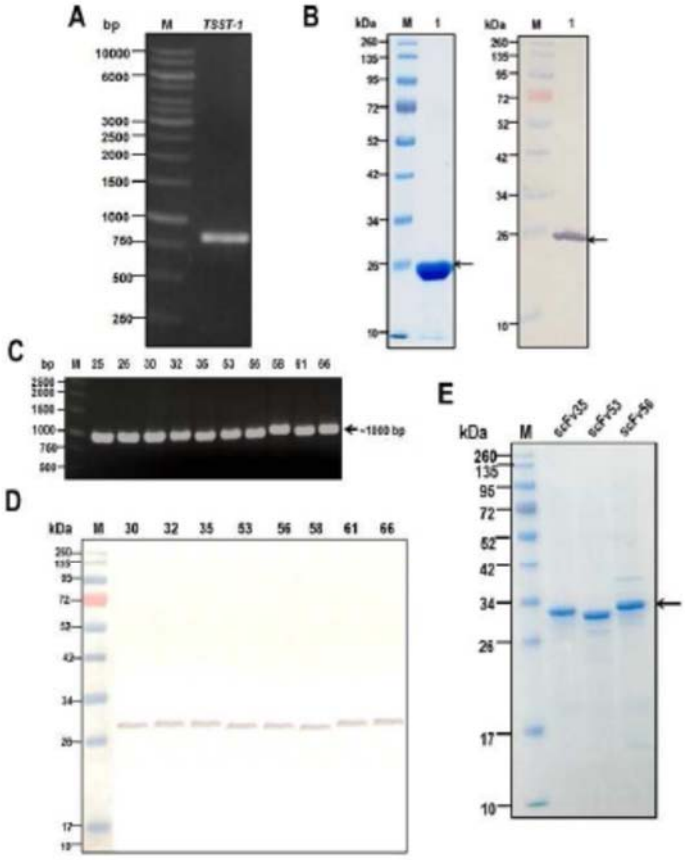

Figure 1. (**A**) Amplicon of TSST-1 gene. (**B**) Stained-SDS-PAGE-separated-rTSST-1 (1 µg per lane) (lane 1 of left panel)and Western blot pattern (lane 1 of right panel). In the Western blotting, mouse monoclonal anti-6× His (AbDSerotec) at 1:3000 was used as the primary antibody; goat-anti-mouse isotype-alkaline phosphatase conjugate (Southern Biotech) at 1:3000 as secondary antibody and BCIP/NBT substrate (KPL). (**C**) Amplicons of *huscfvs* (~1000 bp) from 10 phage-transformed HB2151 *E. coli* clones. (**D**) Binding of HuscFvs in lysates of 8 HB2151 *E. coli* clones to SDS-PAGE-separated-rTSST-1 (1 µg per lane). (**E**) SDS-PAGE-separated- purified and refolded HuscFv35, HuscFv53, and HuscFv56 from transformed NiCo21 (DE3) *E. coli*. M in (**A**,**C**) DNA ladders in base-pairs (bp); M in (**B**,**D**,**E**) protein markers in kDa.

The rTSST-1 at 10, 100, and 1000 ng/mL activated T cells to express CD69 (T cell activation marker) by 5.2%, 6.3%, and 7.2%, respectively, compared with 0.6% of the negative control (cells in medium alone) and 24.8% of the cells stimulated by 1000 ng/mL PHA (pan T cell mitogen) which served as positive control (Figure 2A). At 72 h after exposure to rTSST-1 (10, 100, and 1000 ng/mL) and PHA (1000 ng/mL), the percentages of proliferated cells were 5.1%, 6.2%, 7.5%, and 26.8%, respectively, compared with 0.5% of the cells in medium alone (Figure 2B).

Table 1. LC-MS/MS Mascot results of peptides generated from recombinant TSST-1 of this study with 30% sequence coverage.

Proteins	Orthologous Protein	Accession No.	Number of Matched Peptides	Score	Matched Peptide Sequence (Score)
TSST-1	Toxic shock syndrome toxin-1 of *S. aureus*	Gi 136457	9	239	DSPLKYGPK (44) LPTPIELPLKVK (38) HQLTQIHGLYR (36) ITMNDGSTYQSDLSK (91) ITMNDGSTYQSDLSK (35) ITMNDGSTYQSDLSK (28) ITMNDGSTYQSDLSK (28) NTDGSISLIIPSPYYSPAFTKGEK (32) NTDGSISLIIPSPYYSPAFTKGEK (23)

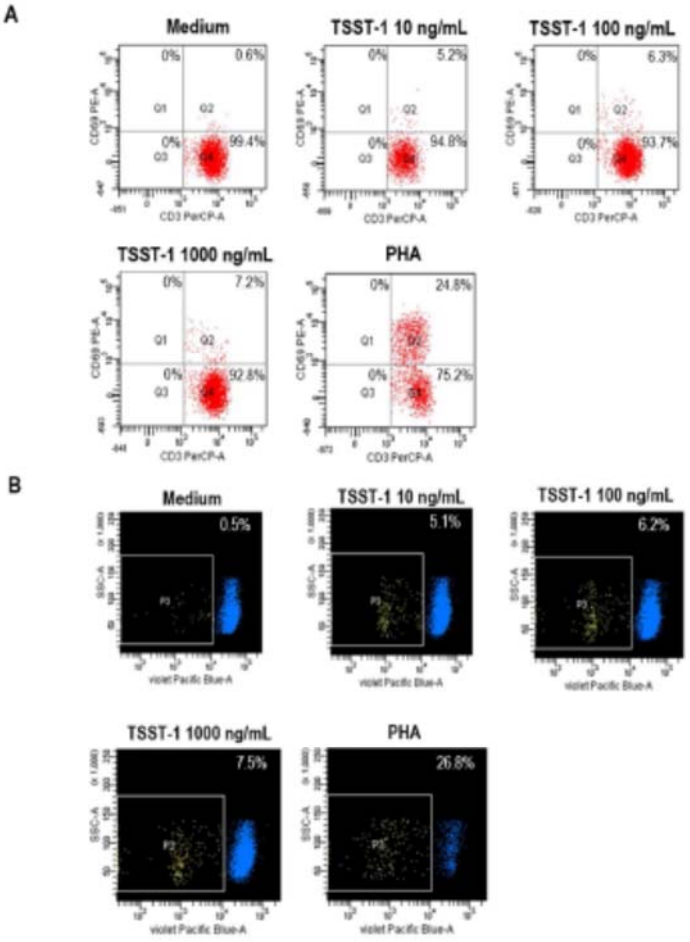

Figure 2. Mitogenicity of the rTSST-1 (ability of the TSST-1 to induce T cell proliferation). (**A**) TSST-1 at 10, 100, and 1000 ng/mL activated T cells to express CD69 (activation marker) by 5.2%, 6.3%, and 7.2%, respectively, compared with the cells in medium alone (0.6%) and PHA (1000 ng/mL)-stimulated cells (24.8%). (**B**) At 72 h after exposure to rTSST-1 (10, 100, and 1000 ng/mL) and PHA (1000 ng/mL), the percentages of proliferated cells were 5.1%, 6.2%, 7.5%, and 26.8%, respectively, compared with 0.5% of the cells in medium alone.

The rTSST-1 at 10, 100, and 1000 ng/mL were tested for pyrogenicity (ability to induce pro-inflammatory cytokine gene expressions in stimulated cells). Figure 3 shows fold-increase of IL-1β, IL-6, and TNFαgene expressions, respectively, in the human PBMCs after stimulation with rTSST-1 and PHA (positive control) in comparison with non-stimulated cells. Pyrogenicity of the rTSST-1 was not concentration dependent which was conformed to the results reported previously [28].

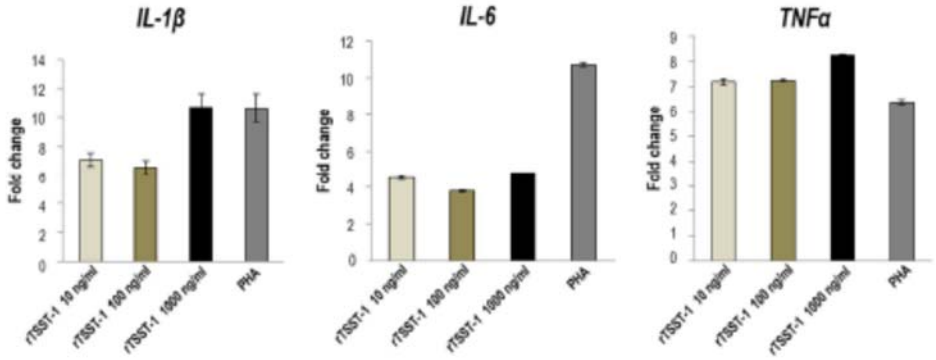

Figure 3. Pyrogenicity of the rTSST-1 (ability to induce stimulated cells to express pro-inflammatory cytokine genes). Fold increase of *IL-1β*, *IL-6*, and *TNFα* expressions in the human PBMCs after stimulation with rTSST-1 at 10, 100, and 1000 ng/mL and 1000 ng/mL PHA (positive control) in relation to non-stimulated cells (negative control).

To exclude the effect of contaminated LPS in the TSST-1 preparation, an experiment in which 1 µg/mL of LPS (Sigma-Aldrich, St. Louis, MO, USA) was used to stimulate the PBMCs was performed. It was found that the LPS induced only 28% of the cell proliferation compared to 100% stimulation by 1000 ng/mL of TSST-1 (Figure S2). Overall results indicated that the bacterially derived-rTSST-1 acquired the inherent activities of the native counterpart. Thus, the active protein was used further.

2.2. Production of HuscFvs

Ten colonies of the HB2151 *E. coli* transfected with rTSST-1-bound phages derived from the human scFv phage display library by means of phage bio-panning using the rTSST-1 as bait (see Materials and Methods) revealed amplicons of HuscFv coding genes (*huscfv*; ~1000 bp) (Figure 1C). Only eight clones produced soluble HuscFvs that bound to SDS-PAGE-separated-rTSST-1 (Figure 1D). Even though the HuscFvs bound to the rTSST-1 which was prepared in buffer containing reducing agents (SDS and mercaptoethanol) in the Western blotting, conclusion cannot be made at this stage that the rTSST-1 epitopes are linear sequences [29]. After nucleotide sequencing, three clones (nos. 35, 53, and 56) showed complete HuscFv sequences, i.e., contiguous sequence coding for IgVH, peptide linker $(Gly_4Ser_1)_3$, and IgVL. Therefore, *huscfvs* of these three clones were subcloned into pLATE52 vector and the recombinant vector was used to transform NiCo21 (DE3) *E. coli* for large scale production of the antibodies. Inclusion bodies were purified from homogenates of the *E. coli* grown under IPTG induction condition and the HuscFvs were refolded. Figure 1E shows SDS-PAGE-separated purified and refolded HuscFvs. The refolded antibodies retained their binding specificity to the TSST-1 coated on the ELISA well surface with and without BSA as determined by indirect ELISA (Figure S3); indicating that the antibodies were refolded properly. The HuscFvs also bound to *S. aureus* enterotoxin A (SEA) (Figure S3).

2.3. Presumptive Residues and Regions of TSST-1 Bound by the HuscFvs

TSST-1 3D structure (PDB 2IJO) and modeled HuscFvs (Table S1) were subjected to intermolecular docking. Interactive modes: salt-bridge, hydrogen, hydrophobic, and van der Waals, were selected from molecular dynamic results. The lowest energy scores for TSST-1 complexed with HuscFv35, HuscFv53, and HuscFv56 were −304± 75.4, −243.3± 23.7, and −371.6± 15.3 kcal/mol, respectively. Tables 2–4, Figure S4A–C, and Figure S5 show TSST-1 residues and motives that were predicted to form contact interface with HuscFv35, HuscFv53, and HuscFv56. Epitopes of the HuscFv35 and HuscFv56 tend to be conformational, i.e., formed by residues in the separated portions of the TSST-1 molecule that are spatially juxtapose upon the active protein folding, while residues that formed predicted HuscFv53 epitope located mainly between β4 and β5 of the TSST-1 N-terminal domain,suggesting that the epitope might be linear (Figure S5).

HuscFv35 was predicted to interact with TSST-1 at S1, D4, I6, K7, W12 and S15 of α1-helix, G16 before β1-strand, K67, R68, K71, S72, and Q73 of β4-strand, and β5 Y80 (Table 2). Rabbit immune sera predominantly reacted with residues 1–15 of the TSST-1 N-terminal domain was shown previously to neutralize TSST-1 mitogenicity [30]. Blocking of α1-helix impaired interaction between TSST-1 and MHC-II molecules [30]. S15-G16 peptide bond has been shown to play a role in modulating TSST-1 mitogenicity [31]. A side chain on residue 16 geometrically stabilizes the wild type TSST-1 [32]. G16 (located in the last turn of α1) and S15 were affected when H135 was mutated to alanine and this impaired TSST-1-TCR interaction [30]. Y80W TSST-1 had reduced mitogenicity in a rabbit model [33]. TSST-1 with R68A and S72A mutations failed to activate T cells carrying Vβ2 TCR [34]. Functions of K67, K71, and Q73 are elusive. Results of computerized simulation suggested that HuscFv35 should be able to reduce TSST-1 mitogenicity by interfering with TSST-1 binding to TCR-vβ and cause reduction of TSST-1-mediated cellular cytokine release by interfering with several important residues of the toxin.

Table 2. TSST-1 residues and motives predicted to be bound by residues and domains ofHuscFv35. After residues labeled in red were mutated to alanines, the HuscFv35 lost ability to suppress TSST-1 mitogenicity and pyrogenicity.

TSST-1		HuscFv35		Intermolecular Bond
Residue	Motif	Residue(s)	Domain	
S1	α1-helix	T165	VL-CDR1	Van de Waals
D4	Before α1-helix	T165	VL-CDR1	Van de Waals
D4	Before α1-helix	N166	VL-CDR1	H-bond
I6	α1-helix	N166	VL-CDR1	H-bond
K7	α1-helix	Y168	VL-CDR1	Water bridge
K7	α1-helix	Y227	VL-CDR3	H-bond
K7	α1-helix	D228	VL-CDR3	H-bond
D8	α1-helix	Y103	VL-CDR3	OH-π
D8	Before α1-helix	N166	VL-CDR1	Van de Waals
W12	α1-helix	L102	VH-CDR3	CH-π
S15	α1-helix	Q101	VL-CDR3	H-bond
G16	Before β1-strand	Q101	VH-CDR3	Hydrophobic
K67	β4-strand	Q101	VH-CDR3	Water bridge
R68	β4-strand	D31	VH-CDR1	H-bond
R68	β4-strand	H100	VH-CDR3	CH-π
R68	β4-strand	Q101	VH-CDR3	Van de Waals
K71	β4-strand	H100	VH-CDR3	CH-π
K71	β4-strand	D108	VH-CDR3	H-bond
K71	β4-strand	Y185	VL-FR2	H-bond
S72	β4-strand	H100	VH-CDR3	H-bond
Q73	β4-strand	T192	VL-FR3	H bond
Y80	β5-strand	Y27	VH-FR1	H bond
Y80	β5-strand	D31	VH-CDR1	OH-π

By the *in silico* docking, HuscFv53 contacted with D18 (before β1-strand), D39 (before β3-strand), and R68; K71 and H74 (β4-strand); S76 and E77 (before β5-strand); and Y80 (β5-strand) of the TSST-1 N-terminal domain (Table 3, Figures S4B and S5). R68A rendered TSST-1 inability to bind to the HLA-DR2 [34]. Y80W TSST-1 had reduced mitogenicity in a rabbit model [35]. Functions of other residues predicted to form contact interface with the HuscFv53 are unknown. Based on the computerized results, the HuscFv53 should not be as effective as the HuscFv35 in mitigation/amelioration of the TSST-1 bioactivities.

HuscFv56 was predicted to interact with TSST-1 K7, L10, D11 and S15 of α1-helix; S17 and D18 before β1-strand; T19 and F20 of β1-strand; D39 before β3-strand; N65, R68, K71, S72 and H74 of β4-strand; Y80 of β5-strand; K114, Y115, and P117 before β8-strand; K118 and F119 of β8-strand; E132, H135, T138, Q139 and I140 of α2-helix; and R145 before β9-strand (Table 4, Figures S4C and S5). Importance of TSST-1 R68 and S72 on the TCR-Vβ binding and N-terminal residues 1–15 (which include K7, D11, and S15) and Y80 on T cell mitogenicity has been mentioned above. H135 and Q139 on the α2-helix have been shown to be important for the TSST-1 superantigenicity [18,32,35–37]. Previous data indicated that H135A TSST-1 mutant possessed only 5%–10% mitogenicity of the wild type [35]. H135 and Q139 are individually critical for functional activity and direct interaction of TSST-1 with TCR-vβ [37]. TSST-1 with H135 mutated to alanine had abolished capacity to induce TNF-α and IL-6 mRNA expressions and protein production [35]. Y115 is a pronounced inducer of IL-6 and TNFα as well as IL-8 [36]. Y115A mutant of TSST-1 had much reduced mitogenicity on T cells and did not express significant toxicity in the rabbit model of TSS [35]. Because the HuscFv56 formed interface contact with several important TSST-1 residues, this antibody should be able to neutralize the TSST-1 activities.

Table 3. TSST-1 residues and motives predicted to be bound by residues and domains of HuscFv53. After residues labeled in red were mutated to alanines, the HuscFv53 lost ability to suppress TSST-1 mitogenicity and pyrogenicity.

TSST-1		HuscFv53		Intermolecular Bond
Residue	Motif	Residue(s)	Domain	
D18	Before β1-strand	R31	VH-CDR1	H-bond
D39	Before β3-strand	R31	VH-CDR1	H-bond
R68	β4-strand	T52	VH-CDR2	Van de Waals
R68	β4-strand	D57	VH-CDR2	H-bond
K71	β4-strand	W33	VH-CDR1	NH-π
K71	β4-strand	T52	VH-CDR2	H-bond
K71	β4-strand	D57	VH-CDR2	H-bond
Q73	β4-strand	W33	VH-CDR1	Van de Waals
Q73	β4-strand	W230	VL-CDR3	Van de Waals
H74	β4-strand	W33	VH-CDR3	π-stacking
H74	β4-strand	R100	VH-CDR3	NH-π
H74	β4-strand	F101	VL-CDR1	π-stacking
S76	Before β5-strand	D166	VL-CDR1	H bond
S76	Before β5-strand	Y168	VL-CDR1	H bond
S76	Before β5-strand	K186	VL-CDR2	H bond
E77	Before β5-strand	K186	VL-CDR2	Water bridge
Y80	β5-strand	W33	VH-CDR1	H-bond
Y80	β5-strand	R100	VH-CDR3	NH-π

Table 4. TSST-1 residues and motives predicted to be bound by residues and domains ofHuscFv56. After residues labeled in red were mutated to alanines, the HuscFv56 lost ability to suppress TSST-1 mitogenicity and pyrogenicity.

TSST-1		HuscFv56		Intermolecular Bond
Residue	Motif	Residue(s)	Domain	
K7	α1-helix	S162	VL-CDR1	H-bond
K7	α1-helix	I163	VL-CDR1	Van der Waals
L10	α1-helix	I163	VL-CDR1	Hydrophobic
D11	α1-helix	I163	VL-CDR1	Van de Waals
D11	α1-helix	R164	VL-CDR1	H-bond
D11	α1-helix	Y165	VL-CDR1	OH-π
S15	α1-helix	Y165	VL-CDR1	H-bond
S17	Before β1-strand	Y102	VL-CDR3	H-bond
D18	Before β1-strand	R103	VH-CDR3	Water bridge
T19	β1-strand	Y102	VH-CDR3	CH-π
T19	β1-strand	R103	VH-CDR3	Van de Waals
F20	β1-strand	R103	VH-CDR3	CH-π
D39	Before β3-strand	Y182	VL-FR2	Water bridge
D39	Before β3-strand	P189	VL-CDR2	Van de Waals
N65	β4-strand	Y102	VH-CDR3	OH-π
R68	β4-strand	Y182	VL-FR2	H bond
R68	β4-strand	N186	VL-CDR2	Van de Waals
K71	β4-strand	S185	VL-CDR2	Van de Waals
K71	β4-strand	N186	VL-CDR2	Van de Waals
S72	β4-strand	N186	VL-CDR2	H bond
H74	β4-strand	F193	VL-FR3	π-stacking
Y80	B5-strand	Y182	VL-FR2	π-stacking
Y80	B5-strand	N186	VL-CDR2	Van de Waals
Y80	B5-strand	V187	VL-CDR2	H bond
Y80	B5-strand	F193	VL-FR3	π-stacking
K114	Before β8-strand	S57	VH-CDR2	Van de Waals
K114	Before β8-strand	T58	VH-CDR2	H bond
K114	Before β8-strand	E59	VH-CDR2	Salt bridge
Y115	Before β8-strand	W50	VH-CDR2	π-stacking
Y115	Before β8-strand	F52	VH-CDR2	π-stacking
Y115	Before β8-strand	Y101	VH-CDR3	H-bond
P117	Before β8-strand	F52	VH-CDR2	CH-π
P117	Before β8-strand	Y101	VH-CDR3	CH-π
P117	Before β8-strand	Y102	VH-CDR3	CH-π
K118	β8-strand	S31	VH-CDR1	H bond
K118	β8-strand	E55	VH-CDR2	H bond
K118	β8-strand	Y102	VH-CDR3	H bond
F119	β8-strand	Y102	VH-CDR3	π-stacking
E132	α2-helix	Y101	VH-CDR3	OH-π
E132	α2-helix	Y102	VH-CDR3	CH-π
E132	α2-helix	R104	VH-CDR3	Salt bridge
H135	α2-helix	R104	VH-CDR3	NH-π
H135	α2-helix	W224	VL-CDR3	π-stacking
Q139	α2-helix	W224	VL-CDR3	CH-π
Q139	α2-helix	Y227	VL-CDR3	CH-π
Q139	α2-helix	Y229	VL-CDR3	H bond
I140	α2-helix	Y227	VL-CDR3	CH-π
R145	Before β9-strand	S225	VL-CDR3	H-bond

2.4. Inhibition of TSST-1 Activities by HuscFvs

Experiments were performed to verify the computerized intermolecular docking results. TSST-1-mediated 7.8% T cell activation (Figure 4). After treatment with HuscFv35, HuscFv53, and

HuscFv56, percent activated T cells were reduced to 1.2%, 1.7%, and 0.9%, respectively (Figure 4). The inhibitory activities of the HuscFv35 and HuscFv56 were higher than the HuscFv53 which conformed to the computerized prediction that the former interacted with several TSST-1 residues important for superantigenicity. The HuscFvs did not cause percent $CD69^+$ cell reduction among the PHA-exposed-$CD3^+$ cells, indicating their target specificity. Control HuscFv showed modest inhibitory (placebo) effect on the percent $CD69^+$ cells (6.5%). Normal PBMCs contained 0.2% $CD3^+CD69^+$ cells.

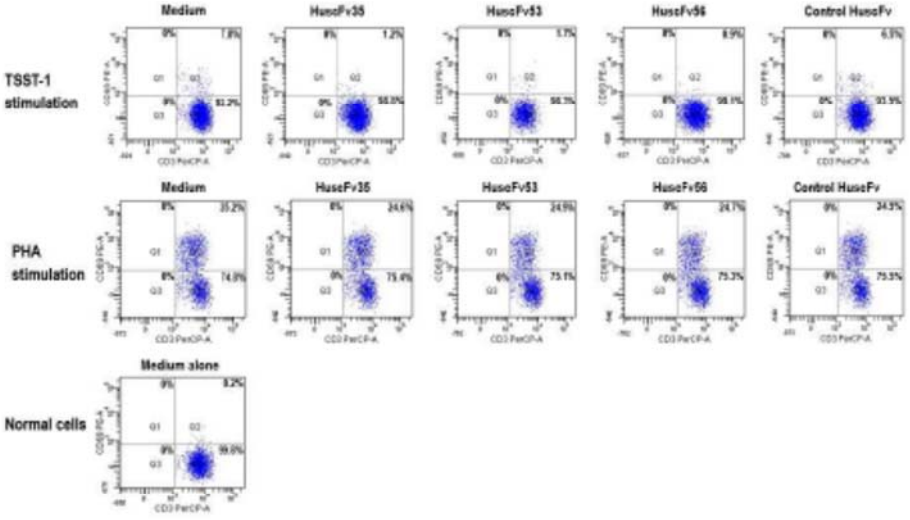

Figure 4. Percent activated $CD3^+CD69^+$ among the $CD3^+$ cells exposed to TSST-1 (1000 ng/mL) after treatment with individual HuscFvs (4 µg), control HuscFv (4 µg), and medium for 24 h. The percent TSST-1-activated T cells (7.8%) was markedly reduced after exposure to HuscFv35 (1.2%), HuscFv53 (1.7%), and HuscFv56 (0.9%). The control HuscFv had some inhibitory activity (placebo effect) on the TSST-1-activated cells (6.5%). The TSST-1-specific-HuscFvs did not affect the PHA-stimulated cells indicating their target specificity.

TSST-1-exposed-human PBMCs added with the HuscFvs had markedly reduced cytokine gene expressions (Figure 5) and the respective cytokine levels (Figure 6), compared to the control HuscFv-treated and non-treated cells ($p < 0.05$). Both HuscFv35 and HuscFv56 performed better than the HuscFv53. Noantibodies had an effect on the PHA-exposed cells, indicating that the HuscFv inhibitory effect on the TSST-1 pyrogenicity was target specific. The data obtained from PBMCs exposed to rTSST-1 and PHA of Figure 5 do not fit with the data of Figure 3. The reason should be that the experiments were performed on blood samples taken a few months apart, although from the same blood donor. However data of duplicate experiments performed on blood samples taken from the blood donor one or two days apart were not statistically different, as shown by the small error bars of both Figures.

Tables 2–4 provide information on the amino acids, their positions, CDRs, and domains of the scFvs that have been predicted to involve in target binding. In order to demonstrate the relevance of the predicted HuscFv residues that formed interface contact with the TSST-1, many of the HuscFv residues which their side chains interacted with TSST-1 were substituted by alanines (marked red in Tables 2–4). The mutated residues for HuscFv35 were Y27A of VH-FR1; D31A of VH-CDR1; H100A, Q101A, and D108A of VH-CDR3; T165, N166A and Y168A of VL-CDR1; Y185A of VL-FR2; and T192A of VL-FR3; for HuscFv53 were R31A of VH-CDR1; T52A and D57A of VH-CDR2; Y168A of VL-CDR1; and K186 of VL-CDR2; and for HuscFv56 were S31A of VH-CDR1; E55A and E59A of

VH-CDR2; Y101A, Y102A, and R104 of VH-CDR3; Y165A of VL-CDR1; Y182 of VL-FR2; N186 of VL-CDR2; and S225 and Y229 of VL-CDR3. The inhibitory activities of the wild type HuscFvs on the TSST-1-mediated cell proliferation and pro-inflammatory cytokine production were abrogated after the residue mutations, i.e., the mHuscFvs could not reduce mitogenicity and pyrogenicity of the TSST-1, as shown in Figures 6 and 7, respectively.

Antibodies of heterologous source have been shown to mitigate symptom severity and rescued animals from the TSS-mediated lethality [30,31]. Treatment of human TSS cases is usually performed in the intensive care unit and includes supportive and symptomatic measures, removal of bacteria producing the causative toxin as well as infusion of IVIG thought to contain antibodies to bacterial endotoxin. However, passive immunization and immunotherapy by using homologous (human) antibodies directed to the TSST-1 functionally critical residues has never been performed. Human scFvshave potential applications for immunotherapy of diseases [38–40]. Thus, the fully human scFvs produced in this study, especially the HuscFv35 and HuscFv56 have high potential for testing further as a safe, direct acting anti-TSST-1 remedy.

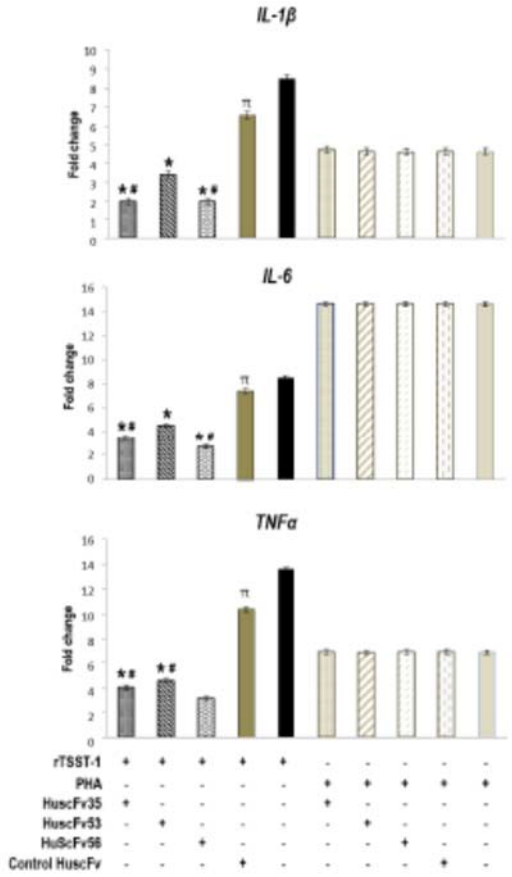

Figure 5. Fold change of IL-1β, IL-6, and TNFα gene expressions in human PBMCs that had been exposed to 1000 ng/mLof TSST-1 and treated with 4 µgof HuscFv35, HuscFv53, and HuscFv56 and controls for 24 h. *, significantly different from (lower than) both controls ($p < 0.05$); #, significantly different from HuscFv53-treated, TSST-1-exposed cells ($p < 0.05$);π, significantly different from TSST-1-exposed cells in medium alone, indicating a placebo effect of the control HuscFv.

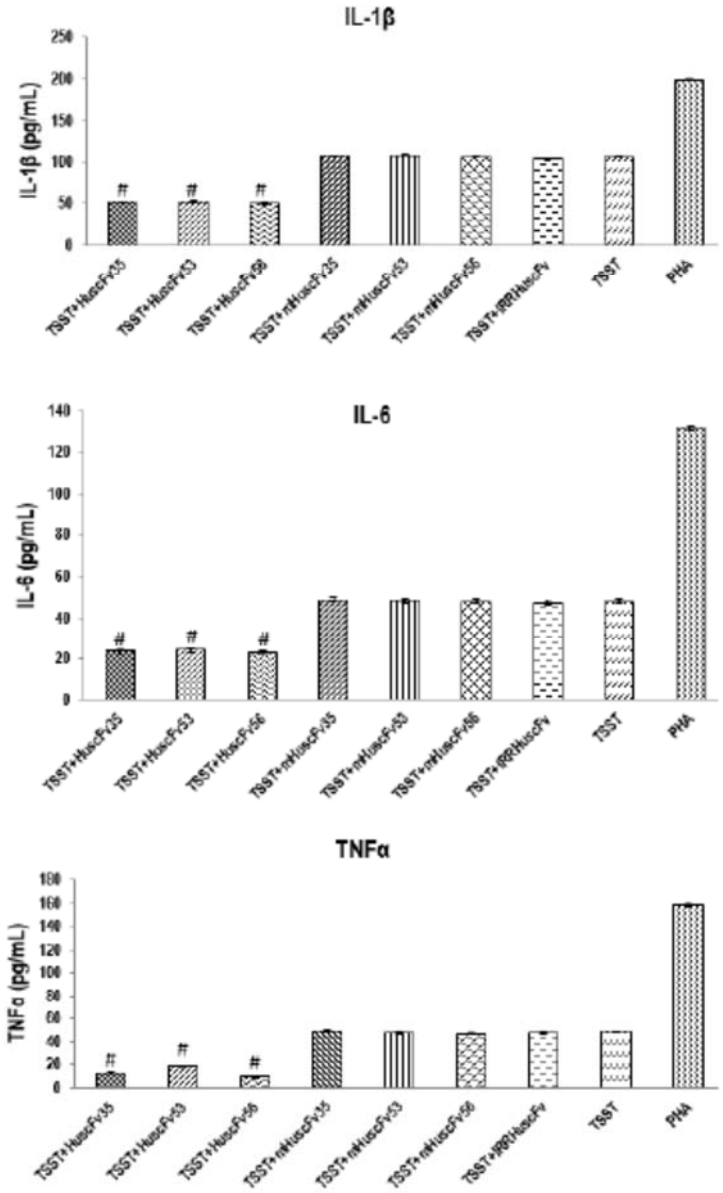

Figure 6. Levels of IL-1β, IL-6, and TNFα cytokines in culture supernatants of PBMCs exposed to 1000 ng/mL of rTSST-1after treatment with 4 µg of TSST-1-bound-HuscFvs, 4 µg CDR mutated-HuscFvs, negative control (TSST-1-exposed cells in medium alone), and positive control (cells stimulated with 1000 ng/mL PHA). #, significantly lower than the groups treated with mHuscFvs and TSST-1- and PHA-stimulated cells.

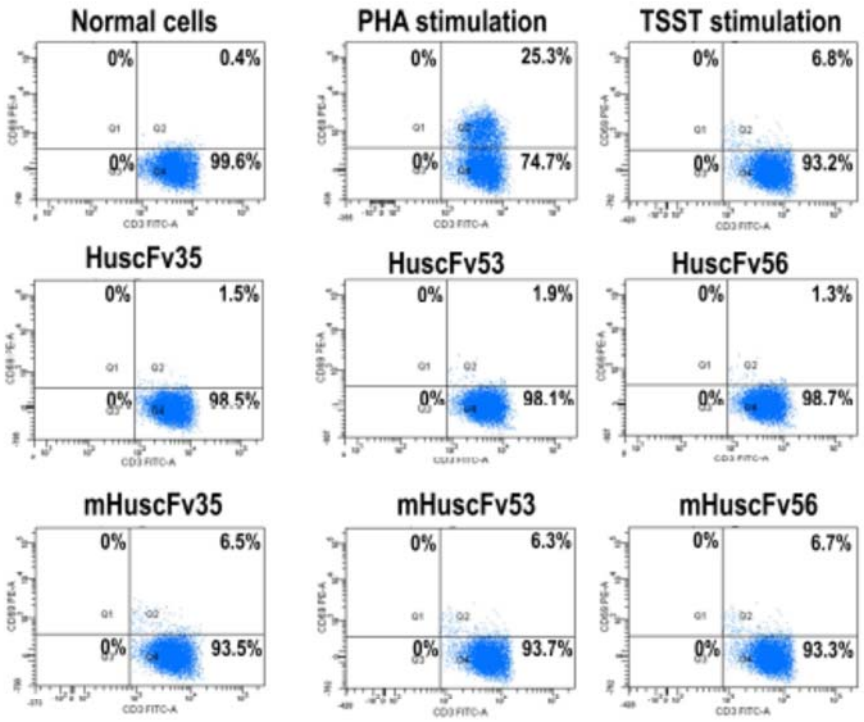

Figure 7. Percent activated T cells ($CD3^+CD69^+$) among the TSST-1-exposed PBMCs after treatment with HuscFv35, HuscFv53, and HuscFv56, mutated-HuscFvs (mHuscFv35, mHuscFv53, and mHuscFv56), control HuscFv, and medium. The mutated-HuscFvs could not reduce TSST-1 mitogenicity on the human PBMCs (percent activated T cells were not different from the TSST-1-exposed PBMCs cultured in the medium alone).

3. Materials and Methods

3.1. Recombinant TSST-1 (rTSST-1) Production

TSST-1 gene was retrieved from GenBank no. J02615. Synthetic TSST-1 gene sequence with stop codondeletion and *BamH*1 and *Hind*III restriction sites incorporation at the 5′ and 3′ ends, respectively, was inserted into pET21a$^+$ DNA (GenScript). The recombinant plasmid was used to transform NiCo21 (DE3) *E. coli* by means of a highly efficient transformation protocol (New England Biolabs, UK). Appropriately transformed *E. coli* colony was grown in LB-A broth containing 1 mM IPTG and the 6× His-tagged-rTSST-1 was purified from the bacterial lysate by using Ni-NTA resin (Invitrogen, Waltham, MA, USA).

3.2. Mitogenic and Pyrogenic Activities of rTSST-1

Because activated T cells expressed surface CD69 molecules [41]; thus, mitogenicity testing of the rTSST-1 was performed by detecting percentages of $CD3^+CD69^+$ in human PBMCs after exposure to the toxin and controls. Human PBMCs (3×10^5 cells/well) were cultured in 48-well round-bottom tissue culture plate (Corning) in RPMI-1640 medium (Gibco^{TM}) supplemented with 10% fetal bovine serum, 2 mM L-glutamine, 100 units/mL penicillin, and 100 µg/mL streptomycin (complete medium) at 37 °C in 5% CO_2 atmosphere. Various concentrations of rTSST-1 (10–1000 ng/mL) were added appropriately to the cells. Positive control was cells stimulated with 1000 ng/mL phytohemagglutinin (PHA) (Sigma)

which is a pan T cell mitogen and negative control was cells in culture medium alone. After 24 h, cells were washed twice with cell washing/blocking reagent (1% heat-inactivated normal serum in PBS), re-suspended in fresh culture medium, added with anti-CD3-PerCP and anti-CD69-PE, and subjected to FACScan flow cytometry with BD Diva software for data acquisition and analysis. Lymphocyte population was identified using forward and side scattered property. T cell population was identified by cells that were $CD3^+$. The percentage of activated T cells ($CD3^+CD69^+$) was determined from an upper-right quadrant (Q2) where as Q4 was $CD3^+$ cells. The Q1 and Q3 were non-activated cell population ($CD3^-CD69^-$). Results are expressed as percentages of $CD3^+CD69^+$ cells.

For testing rTSST-1-mediated cell proliferation, human PBMCs were incubated with violet CellTrace™ for 20 min in complete medium before stimulating with rTSST-1 as above. Similar controls were included. After 72 h, cells were washed, stained with anti-CD3-PerCP, and subjecting to FACScan flow cytometry. Results were expressed as percentages of violet/pacific blue stained-$CD3^+$ cells.

Pyrogenicity of rTSST-1 was tested. Human PBMCs (1×10^5 cells/well) were cultured and stimulated with various concentrations of rTSST-1 as above. Similar controls were included. After 24 h, total RNAs were extracted from cells in individual wells. Expressions of pro-inflammatory cytokine genes including *IL-1β*, *IL-6*, and *TNFα* were determined by quantitative real-time RT-PCR (qRT-PCR) using primers listed in Table S2. One microliter cDNA(50 ng) and 100 nM each PCR primer was put in SYBR Green Master Mix (Applied Biosystems) and subjected to PCR reaction: 95 °C, 10 min then 36 cycles of denaturation at 95 °C for 30 s, annealing at 60 °C for 1 min, extension at 72 °C for 30 s, and hold at 72 °C for 5 min in Strategene Mx3005P QPCR System (Agilent Technologies). Data were analyzed using MxPro QPCR software. β-actin gene was used for normalization. Levels of the pro-inflammatory cytokines in cell culture supernatants were determined by using ELISA kit (Thermo Fisher Scientific, Waltham, MA, USA).

3.3. Production of TSST-1-bound HuscFvs

Human scFv phage display library used in this study was constructed previously [42]. Briefly, cDNAs were prepared from mRNAs of peripheral blood lymphocytes of multiple human blood donors and used as templates for amplification of immunoglobulin VH and Vκ coding sequences by PCR. The oligonucleotide primers used for the PCR were human degenerate primers designed from all families of human immunoglobulin variable sequences [42]. The PCR amplified *vh* and *vl* sequences were ligated randomly via a polynucleotide linker (coding for $(Gly_4Ser)_3$) to generate a repertoire of *vh*-linker-*vl* sequences or *scfv* sequences. The *scfvs* were ligated with pCANTAB5E phagemid DNAs and the recombinant phagemids were used to transfect TG1 *E. coli*. After growing the recombinant phagemid-transformed *E. coli* in the presence of helper phage (M13KO7), complete phage particles which displayed human scFvs as fusion proteins with the phage coat protein (p3) and also carried the respective *scfvs* in the phage genomes could be obtained from the *E. coli* culture supernatant.

HuscFv-displayed phage clones that bound to the rTSST-1 were fished-out from the library using the recombinant protein as bait in the biopanning process [42]. The phage library was added to an ELISA well pre-coated with 1 µg of purified rTSST-1 and the plate was incubated at 37 °C for 1 h. Unbound phages were removed by washing with buffer and a log phase-grown HB2151 *E. coli* culture was added to the well containing the antigen-bound phages.The phage transformed bacterial coloniesthat grew on selective agar plates after overnight incubation were screened for the HuscFv genes (*huscfvs*) by PCR [42]. The *huscfv*-positive clones were grown in 0.2 mMIPTG-conditioned broth to induce HuscFv expressions. Binding of soluble HuscFvs in the bacterial lysates to the SDS-PAGE-separated-rTSST-1 were tested by Western blotting. Nucleotides of the *huscfvs* coding for rTSST-1-bound-HuscFvs were sequenced, deduced, and canonical complementarity determining regions (CDRs) and immunoglobulin framework regions (FRs) were determined using the IMGT® Information System [43].

For large scale production of HuscFvs, *huscfvs* of HB2151 *E. coli* clones of interest were subcloned from the phagemids to pLATE52™ expression vector by using ligation independent cloning (LIC)

system (Thermo Fisher Scientific). The pLATE52-*huscfv* plasmids were used to transfect NiCo21 (DE3) *E. coli*. Selected transformed bacterial colonies were grown under IPTG induction; the bacterial pellet was suspended in BugBuster®Protein Extraction buffer (5 mL/g bacterial wet weight) and kept at 25 °C with agitation. The preparation was added with Lysonase™ Bioprocessing reagent (10 µL/g of bacteria) and agitated further for 20 min. *E. coli* inclusion body was harvested by centrifugation, washed twice with Wash-100 Solution (50 mM sodium phosphate buffer, pH 8.0; 500 mM NaCl; 5 mM EDTA; 8% (*w*/*v*) glycerol; 1% (*v*/*v*) TritonX-100); twice with Wash-114 Reagent (50 mM Tris buffer, pH 8.0; 300 mM NaCl; 1% (*v*/*v*) Triton X-114), and once with Wash-Solvent (50 mM Tris buffer, pH 8.0; 60% (*v*/*v*) isopropanol) by shaking the preparation vigorously followed by centrifugation. For HuscFv refolding, the inclusion body was solubilized (*w*/*v*) in buffer (50 mM CAPS, pH 11.0; 0.3% (*w*/*v*) N-lauryl sarcosine; 1 mM DTT) and kept at 4 °C for 16 h. The preparation was loaded into the Slide-A-Lyzer® 2K Dialysis Cassettes G2 (Thermo Fisher Scientific), dialyzed at 4 °C with slow stirring against refolding buffer (20 mM imidazole, pH 8.5 supplemented with 0.1 mM DTT), filtered through 0.02 µm low protein binding Acrodisc® syringe filter (Pall, Port Washington, NY, USA), and kept in water-bath at 30 °C for 2 h before adding with 60 mM trehalose. Protein content was determined. The refolded-HuscFvs were retested for binding to rTSST-1 by indirect ELISA.

3.4. Computerized Simulation for Determining Interactive Residues between TSST-1 and HuscFvs

TSST-1 3D structure was retrieved from RCSB PDB 2IJO. The *huscfv* 3D structures were modeled by the I-TASSER server [44,45]. The I-TASSER-predicted structures were further refined [46,47] and improved to near native states on the automated ClusPro 2.0 antibody-protein docking server. The models from the docking were simulated with NAMD Molecular Dynamics [48]. The TSST-1-HuscFv complexes were built and visualized by using PyMol software (PyMol Molecular Graphics System, Version 2 edu, Schrodinger, LLC).

3.5. Preparation of Mutated-HuscFvs (mHuscFvs)

Gene sequences coding for HuscFvs which side chains of their residues interacted with TSST-1 (data from molecular dynamics) were substituted by alanines and synthesized (Integrated DNA Technologies, Coralville, IA, USA). The DNA fragments were cloned into pLATE52 and the recombinant vector was used to transform NiCo21 (DE3) *E. coli*. The HuscFvs were prepared from appropriately transformed *E. coli* as for the wild type HuscFvs. The mutated HuscFvs (mHuscFvs) were tested for their ability to inhibit TSST-1 activities (mitogenicity and pyrogenicity).

3.6. HuscFvs-mediated Inhibition of TSST-1 Activities

For inhibition of TSST-1-mediated T cell activation by the HuscFvs, human PBMCs were added with mixture of rTSST-1 and HuscFvs/mHuscFvs or control HuscFv and kept for 24 h. TSST-1-stimulated cells without antibody treatment, PHA-stimulated cells treated similarly with TSSTS-1-bound-HuscFvs, and normal cells in medium were included in the experiment. After washing, cells were labeled with CD3-PerCP and CD69-PE and analyzed by FACScan Flow cytometry. Total viable lymphocytes were gated by SSC and FSC and $CD3^+$ cells were gated for $CD69^+$ cells. Results were expressed as percentages of $CD3^+CD69^+$ cells.

For inhibiting rTSST-1 pyrogenicity by the HuscFvs/mHuscFv, human PBMCs (5×10^4 cells/well) in complete medium were added with 1000 ng/mL rTSST-1. The TSST-1-stimulated cells were treated either with TSST-1-bound-HuscFvs/mHuscFv, control/irrelevant HuscFv (did not bind to TSST-1), or medium alone. The antibody:TSST-1 molar ratios were 4:1 (optimal from titration). Triplicate wells were set for each treatment. Cells added with 1000 ng/mL PHA with and without HuscFv-treatments, and cells in medium alone (normal cells) were included. After 24 h, total RNAs were extracted from cells in individual wells and quantified by using NanoDrop instrument. Complementary DNAs were synthesized (RevertAid First Strand cDNA Synthesis kit) and used as templates for quantification of mRNAs of pro-inflammatory cytokines including TNF-α, IL-1B, and IL-6. The quantitative

real-time PCR primers for the mRNA quantification are listed in Table S2. β-actin gene was used for normalization. Moreover, cell culture supernatants in all wells were collected and the levels of the pro-inflammatory cytokines were measured using commercial ELISA kits (Thermo Fisher Scientific). Results are the average of the two reproducible experiments.

3.7. Statistical Analysis

One way ANOVA followed by post hoc comparison using least significant difference (LSD) and independent *t*-test were performed for data comparison using SPSS 18.0 statistical software. Significant difference was $p < 0.05$.

4. Conclusions

Human single chain antibodies (HuscFvs) to *S. aureus* TSST-1 that inhibited the TSST-1-mediated T cell activation and pro-inflammatory cytokine gene expressions and productions were generated. The HuscFvs formed interface contact with the TSST-1 residues important for immunopathogenesis of toxic shock syndrome. The HuscFvs have high potential for testing further as a direct acting anti-TSST-1 agent for future clinical use.

Supplementary Materials: The following are available online at www.mdpi.com/2072-6651/9/2/50/s1, Figure S1: Codon-optimized nucleotide and deduced amino acid sequences of the TSST-1 of this study. Figure S2: Effect of lipopolysaccharide (LPS) on PBMC stimulation compared to TSST-1. Figure S3: Binding of the purified, refolded HuscFv35 (T35), HuscFv53 (T53) and HuscFv56 (T56) to rTSSt-1 and SEA immobilized on the ELISA well surface with and without BSA. Figure S4: Computerized bindingof TSST-1 (cyan) and HuscFvs (green). Figure S5: Residues and motives of TSST-1. Table S1: Estimated accuracy of the modeled HuscFv35, HuscFv53, and HuscFv56. Table S2: Oligonucleotide primers used in quantitative real-time RT-PCR for monitoring cytokine gene expressions.

Acknowledgments: The work was supported by NSTDA Chair professor grant (P-1450624) funded by the Crown Property Bureau of Thailand, RSA5980048 of the Thailand Research Fund (TRF) and the NRU Project, Office of Commission on Higher Education. Nitaya Indrawattana and Nitat Sookrung are RSA scholars of the TRF.

Author Contributions: N.S., W.C. and N.I. conceived and designed the experiments. T.R. and W.S. performed the experiments. N.O., P.D., N.S., W.C. and N.I. analyzed the data. W.C. and N.I. reviewed and wrote the manuscript.

Conflicts of Interest: The authors declare no conflict of interest.

References

1. Kotb, M. Bacterial pyrogenic exotoxins as superantigens. *Clin. Microbiol. Rev.* **1995**, *8*, 411–426. [PubMed]
2. Todd, J.; Fishaut, M.; Kapral, F.; Welch, T. Toxic-shock syndrome associated with phage-group-I Staphylococci. *Lancet* **1978**, *2*, 1116–1118. [CrossRef]
3. Bueno, C.; Lemke, C.D.; Criado, G.; Baroja, M.L.; Ferguson, S.S.; Rahman, A.K.; Tsoukas, C.D.; McCormick, J.K.; Madrenas, J. Bacterial superantigens bypass Lck-dependent T cell receptor signaling by activating a Gα11-dependent, PLC-β-mediated pathway. *Immunity* **2006**, *25*, 67–78. [CrossRef] [PubMed]
4. Tofte, R.W.; Williams, D.N. Toxic shock syndrome: Clinical and laboratory features in 15 patients. *Ann. Intern. Med.* **1981**, *94*, 149–156. [CrossRef] [PubMed]
5. Priest, B.P.; Schlievert, P.M.; Dunn, D.L. Treatment of toxic shock syndrome with endotoxin-neutralizing antibody. *J. Surg. Res.* **1989**, *46*, 527–531. [CrossRef]
6. Kulhankova, K.; King, J.; Salgado-Pabón, W. Staphylococcal toxic shock syndrome: Superantigen-mediated enhancement of endotoxin shock and adaptive immune suppression. *Immunol. Rev.* **2014**, *59*, 182–187. [CrossRef] [PubMed]
7. Proft, T.; Frazer, J.D. Bacterial superantigens. *Clin. Exp. Immunol.* **2003**, *133*, 299–306. [CrossRef] [PubMed]
8. Kass, E.H.; Parsonnet, J. On the pathogenesis of toxic shock syndrome. *Rev. Infect. Dis.* **1987**, *9*, S482–S489. [CrossRef] [PubMed]
9. Shands, K.N.; Schmid, G.P.; Dan, B.B.; Blum, D.; Guidotti, R.J.; Hargrett, N.T.; Anderson, R.L.; Hill, D.L.; Broome, C.V.; Band, J.D.; et al. Toxic shock syndrome in menstruating women: Association with tampon use and *Staphylococcus aureus* and clinical features in 52 cases. *N. Engl. J. Med.* **1980**, *303*, 1438–1442. [CrossRef] [PubMed]

10. Kim, J.; Urban, R.G.; Strominger, J.L.; Wiley, D.C. Toxic shock syndrome toxin-1 complexed with a class II major histocompatibility molecules HLA-DR1. *Science* **1994**, *266*, 1870–1874. [CrossRef] [PubMed]
11. Petersson, K.; Håkansson, M.; Nilsson, H.; Forsberg, G.; Anders Svensson, L.; Liljas, A.; Walse, B. Crystal structure of a superantigen bound to MHC class II displays zinc and peptide dependence. *EMBO J.* **2001**, *20*, 3306–3312. [CrossRef] [PubMed]
12. Li, H.; Llera, A.; Tsuchiya, D.; Leder, L.; Ysern, X.; Schlievert, P.M.; Karjalainen, K.; Mariuzza, R.A. Three dimensional structure of the complex between a T cell receptor beta chain and the superantigen staphylococcal enterotoxin B. *Immunity* **1998**, *9*, 807–816. [CrossRef]
13. Li, H.; Llera, A.; Malchiodi, E.L.; Mariuzza, R.A. The structural basis of T cell activation by superantigens. *Annu. Rev. Immunol.* **1999**, *17*, 435–466. [CrossRef] [PubMed]
14. Günther, S.; Varma, A.K.; Moza, B.; Kasper, K.J.; Wyatt, A.W.; Zhu, P.; Nur-urRahman, A.K.M.; Li, Y.; Mariuzza, R.A.; McCormick, J.K.; et al. A novel loop domain in superantigens extends their T cell receptor recognition site. *J. Mol. Biol.* **2007**, *371*, 210–221. [CrossRef] [PubMed]
15. Murray, D.L.; Earhart, C.A.; Mitchell, D.T.; Ohlendorf, D.H.; Novick, R.P.; Schlievert, P.M. Localization of biologically important regions on toxic shock syndrome toxin 1. *Infect. Immun.* **1996**, *64*, 371–374. [PubMed]
16. McCormick, J.K.; Yarwood, J.M.; Schlievert, P.M. Toxic shock syndrome and bacterial superantigens: An update. *Annu. Rev. Microbiol.* **2001**, *55*, 77–104. [CrossRef] [PubMed]
17. Lindsay, J.A.; Ruzin, A.; Ross, H.F.; Kurepina, N.; Novick, R.P. The gene for toxic shock toxin is carried by a family of mobile pathogenicity islands in *Staphylococcus aureus*. *Mol. Microbiol.* **1998**, *29*, 527–543. [CrossRef] [PubMed]
18. Acharya, K.R.; Passalacqua, E.F.; Jones, F.Y.; Harlos, K.; Stuart, D.I.; Brehm, R.D.; Tranter, H.S. Structural basis of superantigen action inferred from crystal structure of toxic shock syndrome toxin-1. *Nature* **1994**, *367*, 94–97. [CrossRef] [PubMed]
19. Prasad, G.S.; Radhakrishnan, R.; Mitchell, D.T.; Earhart, C.A.; Dinges, M.M.; Cook, W.J.; Schlievert, P.M.; Ohlendorf, D.H. Refined structures of three crystal forms of toxic shock syndrome toxin-1 and of a tetramutant with reduced activity. *Prot. Sci.* **1997**, *6*, 1220–1227. [CrossRef] [PubMed]
20. Jardetzky, T.S.; Brown, J.H.; Gorga, J.C.; Stern, L.J.; Urban, R.G.; Chi, Y.I.; Stauffacher, C.; Strominger, J.L.; Wiley, D.C. Three dimensional structure of a human class II histocompatibility molecule complexed with superantigen. *Nature* **1994**, *368*, 711–718. [CrossRef] [PubMed]
21. Wahlsten, J.L.; Ramakrishnan, S. Separation of function between the domains of toxic shock syndrome toxin-1. *J. Immunol.* **1998**, *160*, 854–859. [PubMed]
22. Wu, C.C. Possible therapies of septic shock: Based on animal studies and clinical trials. *Curr. Pharm. Des.* **2006**, *27*, 3535–3541. [CrossRef]
23. Mellish, M.E.; Cherry, J.D. Staphylococcal infections. In *Pediatric Infectious Diseases*; Feigin, R.D., Ed.; WB Saunders and Company: Philadelphia, PA, USA, 1992.
24. Shankar-Hari, M.; Spencer, J.; Sewell, W.A.; Rowan, K.M.; Singer, M. Bench-to-bedside review: Immunoglobulin therapy for sepsis-biological plausibility from a critical perspective. *Crit. Care* **2002**, *16*, 206–220. [CrossRef] [PubMed]
25. Bonventre, P.F.; Thompson, M.R.; Adinolfi, L.E.; Gillis, Z.A.; Parsonnet, J. Neutralization of toxic shock syndrome toxin-1 by monoclonal antibodies in vitro and in vivo. *Infect. Immun.* **1988**, *56*, 135–141. [PubMed]
26. Stich, N.; Model, N.; Samstag, A.; Gruener, C.S.; Wolf, H.M.; Eibl, M.M. Toxic shock syndrome toxin-1 mediated toxicity inhibited by neutralizing antibodies late in the course of continual in vivo and in vitro exposure. *Toxins* **2014**, *6*, 1724–1741. [CrossRef] [PubMed]
27. Ryan, J. *Endotoxin and Cell Culture Technical Bulletin*; Corning Incorporated Life-Science: Lowell, MA, USA, 2008.
28. Stich, N.; Waclavicek, M.; Model, N.; Eibl, M.M. Staphylococcal superantigen (TSST-1) mutant analysis reveals that T cell activation is required for biological effect in the rabbit including the cytokine storm. *Toxins* **2010**, *2*, 2272–2288. [CrossRef] [PubMed]
29. Zhou, Y.H.; Chen, Z.; Purcell, R.H.; Emerson, S.U. Positive reactions on Western blots do not necessarily indicate the epitopes on antigens are continuous. *Immunol. Cell Biol.* **2007**, *85*, 73–78. [CrossRef] [PubMed]
30. Gampfer, J.M.; Samstag, A.; Waclavicek, M.; Wolf, H.M.; Eibl, M.M.; Gulle, H. Epitope mapping of neutralizing TSST-1 specific antibodies induced by immunization with toxin and toxoid. *Vaccine* **2002**, *20*, 3675–3684. [CrossRef]

31. Papageorgiou, A.C.; Brehm, R.D.; Leonidas, D.D.; Tranter, H.S.; Acharya, K.R. The refined crystal structure of toxic shock syndrome toxin-1 at 2.07 Å resolution. *J. Mol. Biol.* **1996**, *260*, 553–569. [CrossRef] [PubMed]
32. Earhart, C.A.; Mitchell, D.T.; Murray, D.L.; Pinheiro, D.M.; Matsumura, M.; Schlievert, P.M.; Ohlendorf, D.H. Structures of five mutants of toxic shock syndrome toxin-1 with reduced biological activity. *Biochemistry* **1998**, *37*, 7194–7202. [CrossRef] [PubMed]
33. Dereszewicz, R.L.; Woo, J.; Chan, M.; Finberg, R.W.; Kasper, D.L. Mutations affecting the activity of toxic shock syndrome toxin-1. *Biochemistry* **1994**, *33*, 12844–12851. [CrossRef] [PubMed]
34. Moza, B.; Buonpane, R.A.; Zhu, P.; Herfst, C.A.; Nur-urRahman, A.K.M.; McCormick, J.K.; Kranz, D.M.; Sundberg, E.J. Long-range cooperative binding effects in a T cell receptor variable domain. *Proc. Natl. Acad. Sci. USA* **2006**, *103*, 9867–9872. [CrossRef] [PubMed]
35. Bonventre, P.F.; Heeg, H.; Cullen, C.; Lian, C.J. Toxicity of recombinant toxic shock syndrome toxin 1 and mutant toxins produced by *Staphylococcus aureus* in a rabbit infection model of toxic shock syndrome. *Infect. Immun.* **1993**, *61*, 793–799. [PubMed]
36. Drynda, A.; König, B.; Bonventre, P.F.; König, W. Role of a carboxy-terminal site of toxic shock syndrome toxin 1 in eliciting immune responses of human peripheral blood mononuclear cells. *Infect. Immun.* **1995**, *63*, 1095–1101. [PubMed]
37. McCormick, J.K.; Tripp, T.J.; Llera, A.S.; Sundberg, E.J.; Dinges, M.M.; Mariuzza, R.A.; Schlievert, P.M. Functional analysis of the TCR binding domain of toxic shock syndrome toxin-1 predicts further diversity in MHC class II/superantigen/TCR ternary complexes. *J. Immunol.* **2003**, *171*, 1385–1392. [CrossRef] [PubMed]
38. Ahmad, Z.A.; Yeap, S.K.; Ali, A.M.; Ho, W.Y.; Alitheen, N.B.; Hamid, M. scFv antibody: Principles and clinical application. *Clin. Dev. Immunol.* **2012**, *2012*, 980250. [CrossRef] [PubMed]
39. Pucca, M.B.; Zoccal, K.F.; Roncolato, E.C.; Bertolini, T.B.; Campos, L.B.; Cologna, C.T.; Faccioli, L.H.; Arantes, E.C.; Barbosa, J.E. Serrumab: A human monoclonal antibody that counters the biochemical and immunological effects of *Tityusserrulatus* venom. *J. Immunotoxicol.* **2012**, *9*, 173–183. [CrossRef] [PubMed]
40. Jittavisutthikul, S.; Seesuay, W.; Thanongsaksrikul, J.; Thueng-in, K.; Srimanote, P.; Werner, R.G.; Chaicumpa, W. Human transbodies to HCV NS3/4A protease inhibit viral replication and restore host innate immunity. *Front. Immunol.* **2016**, *7*, 318. [CrossRef] [PubMed]
41. Lina, G.; Cozon, G.; Ferrandiz, J.; Greenland, T.; Vandenesch, F.; Etienne, J. Detection of staphylococcal superantigenic toxin by a CD69-specific cytofluorimetric assay measuring T-cell activation. *J. Clin. Microbiol.* **1998**, *36*, 1042–1045. [PubMed]
42. Kulkeaw, K.; Sakolvaree, Y.; Srimanote, P.; Tongtawe, P.; Maneewatch, S.; Sookrung, N.; Tungthrongchitr, A.; Tapchaisri, P.; Kurazono, H.; Chaicumpa, W. Human monoclonal ScFv neutralize lethal Thai cobra, Najakaouthia, neurotoxin. *J. Proteom.* **2009**, *72*, 270–282. [CrossRef] [PubMed]
43. Giudicelli, V.; Brochet, X.; Lefranc, M.P. IMGT/V-QUEST: IMGT standardized analysis of the immunoglobulin (IG) and T cell receptor (TR) nucleotide sequences. *Cold Spring Harb. Protoc.* **2011**, *2011*, 695–715. [CrossRef] [PubMed]
44. Zhang, Y. I-TASSER server for protein 3D structure prediction. *BMC Bioinform.* **2008**, *9*, 40. [CrossRef] [PubMed]
45. Roy, A.; Kucukural, A.; Zhang, Y. I-TASSER: A unified platform for automated protein structure and function prediction. *Nat. Protoc.* **2010**, *5*, 725–738. [CrossRef] [PubMed]
46. Xu, D.; Zhang, Y. Improving the physical realism and structural accuracy of protein models by a two-step atomic-level energy minimization. *Biophys. J.* **2011**, *101*, 2525–2534. [CrossRef] [PubMed]
47. Zhang, J.; Liang, Y.; Zhang, Y. Atomic-level protein structure refinement using fragment-guided molecular dynamics conformation sampling. *Structure* **2011**, *19*, 1784–1795. [CrossRef] [PubMed]
48. Hospital, A.; Andrio, P.; Fenollosa, C.; Cicin-Sain, D.; Orozco, M.; Gelpí, J.L. MDWeb and MDMoby: An integrated web-based platform for molecular dynamics simulations. *Bioinformatics* **2012**, *28*, 1278–1279. [CrossRef] [PubMed]

Hindawi Publishing Corporation
BioMed Research International
Volume 2016, Article ID 2475067, 8 pages
http://dx.doi.org/10.1155/2016/2475067

Hindawi

Review Article

Mechanisms of Antimicrobial Resistance in ESKAPE Pathogens

Sirijan Santajit and Nitaya Indrawattana

Department of Microbiology and Immunology, Faculty of Tropical Medicine, Mahidol University, Bangkok 10400, Thailand

Correspondence should be addressed to Nitaya Indrawattana; nitaya.ind@mahidol.ac.th

Received 7 January 2016; Revised 23 February 2016; Accepted 17 April 2016

Academic Editor: Paul M. Tulkens

The ESKAPE pathogens (*Enterococcus faecium*, *Staphylococcus aureus*, *Klebsiella pneumoniae*, *Acinetobacter baumannii*, *Pseudomonas aeruginosa*, and *Enterobacter* species) are the leading cause of nosocomial infections throughout the world. Most of them are multidrug resistant isolates, which is one of the greatest challenges in clinical practice. Multidrug resistance is amongst the top three threats to global public health and is usually caused by excessive drug usage or prescription, inappropriate use of antimicrobials, and substandard pharmaceuticals. Understanding the resistance mechanisms of these bacteria is crucial for the development of novel antimicrobial agents or other alternative tools to combat these public health challenges. Greater mechanistic understanding would also aid in the prediction of underlying or even unknown mechanisms of resistance, which could be applied to other emerging multidrug resistant pathogens. In this review, we summarize the known antimicrobial resistance mechanisms of ESKAPE pathogens.

1. Introduction

Nosocomial infections are caused by a variety of organisms, including bacteria, fungi, viruses, parasites, and other agents. Infections can be derived from exogenous or endogenous sources and are transferred by either direct or indirect contact between patients, healthcare workers, contaminated objects, visitors, or even various environmental sources. A survey of hospital-acquired infections (HAI) in the United States in 2011 reported a total of about 722,000 reported cases, with 75,000 deaths associated with nosocomial infections [1]. A second study conducted in 2002 estimated that when taking into account all types of bacterial infections, approximately 1.7 million patients suffered from HAIs, which contributed to the deaths of 99,000 patients per year [2].

The growing numbers of antimicrobial-resistant pathogens, which are increasingly associated with nosocomial infection, place a significant burden on healthcare systems and have important global economic costs. Effects include high mortality and morbidity rates, increased treatment costs, diagnostic uncertainties, and lack of trust in orthodox medicine. Recent reports using data from hospital-based surveillance studies as well as from the Infectious Diseases Society of America have begun to refer to a group of nosocomial pathogens as "ESKAPE pathogens" [3, 4]. ESKAPE is an acronym for the group of bacteria, encompassing both Gram-positive and Gram-negative species, made up of *Enterococcus faecium*, *Staphylococcus aureus*, *Klebsiella pneumoniae*, *Acinetobacter baumannii*, *Pseudomonas aeruginosa*, and *Enterobacter* species. These bacteria are common causes of life-threatening nosocomial infections amongst critically ill and immunocompromised individuals and are characterized by potential drug resistance mechanisms [5].

2. Antimicrobial Resistance Mechanisms of ESKAPE Pathogens

Antimicrobial resistance genes may be carried on the bacterial chromosome, plasmid, or transposons [6]. Mechanisms of drug resistance fall into several broad categories, including drug inactivation/alteration, modification of drug binding sites/targets, changes in cell permeability resulting in reduced intracellular drug accumulation, and biofilm formation [7–9].

2.1. Drug Inactivation or Alteration. Many bacteria produce enzymes that irreversibly modify and inactivate the antibiotics, such as β-lactamases, aminoglycoside-modifying enzymes, or chloramphenicol acetyltransferases. One of the well-characterized enzymes is β-lactamases. They are highly prevalent and act by hydrolyzing the β-lactam ring which is present in all β-lactams; thus, all penicillins, cephalosporins, monobactams, and carbapenems are essential to their activity [10]. β-lactamases are classified using two main classification systems: the Ambler scheme (molecular classification) and the Bush-Jacoby-Medeiros system, which classifies the most clinically important β-lactamases as those produced by Gram-negative bacteria [4]. Ambler class A enzymes consist of penicillinase, cephalosporinase, broad-spectrum β-lactamases, extended-spectrum β-lactamases (ESBLs), and carbapenemases. They can inactivate penicillins (except temocillin), third-generation oxyiminocephalosporins (e.g., ceftazidime, cefotaxime, and ceftriaxone), aztreonam, cefamandole, cefoperazone, and methoxycephalosporins (e.g., cephamycins and carbapenems). Class A enzymes can also be inhibited by β-lactamase inhibitors, such as clavulanic acid, sulbactam, or tazobactam [5, 6].

The Ambler class A group contains a number of significant enzymes including ESBLs (mainly TEM, SHV, and CTX-M type) and KPCs. TEM-type enzymes were first identified in 1965 in *Escherichia coli* from Greek patients, with TEM taken from a patient's name, Temoniera. TEM-1 is widespread not only amongst bacteria of the family Enterobacteriaceae (e.g., *K. pneumoniae*, *Enterobacter* spp.), but also in nonfermentative bacteria such as *P. aeruginosa*. Currently, TEM enzymes are the most common group in *E. coli*. Amongst sulfhydryl variable (SHV) enzymes, SHV-1 is the most clinically relevant and represents the most common *K. pneumoniae* [11]. The genes coding for TEM and SHV enzymes have quite high mutation rates, resulting in a high level of diversity in enzyme types and thus increasing the scope of antibiotic resistance. CTX-Ms have been identified in ESKAPE pathogens including *K. pneumoniae*, *A. baumannii*, *P. aeruginosa*, and *Enterobacter* species. Some of the highest prevalence and significant clinical impact are associated with the extended-spectrum β-lactamases in *K. pneumoniae* [12, 13]. Carbapenemases are also prevalent in clinical bacterial isolates such as *K. pneumonia* such as KPC-1 that results in resistance to imipenem, meropenem, amoxicillin/clavulanate, piperacillin/tazobactam, ceftazidime, aztreonam, and ceftriaxone [14].

Ambler class B enzymes, or group 3 enzymes as classified by the Bush-Jacoby system (Table 1), include metallo-β-lactamases (MBLs), which require Zn^{2+} as a cofactor. Bacteria that produce these enzymes show resistance to all β-lactams, including penicillins, cephalosporins, carbapenems, and β-lactamase inhibitors, except aztreonam. Genes encoding MBLs are found on plasmids; hence, they are easily transmitted to other microorganisms. The most common metallo-β-lactamases (MBLs) are imipenemase metallo-β-lactamases (IMP), Verona integron encoded metallo-β-lactamases (VIM), and the newly described New Delhi metallo-beta-lactamase-1 (NDM-1) enzymes [5, 15]. IMP-type MBLs have mainly been found in *P. aeruginosa*, *K. pneumoniae*, *A. baumannii*, and *Enterobacter cloacae*, whereas VIM-type enzymes have been detected mostly in *P. aeruginosa* and *A. baumannii*. NDM-1-type enzymes have been isolated from *K. pneumoniae* and *E. cloacae* [5, 16].

The Ambler class C group consists of several important enzymes, including penicillinase and cephalosporinase, such as AmpC β-lactamase, which results in low level resistance to narrow-spectrum cephalosporin drugs. Chromosomally encoded AmpC are usually identified in *P. aeruginosa* and bacteria in the Enterobacteriaceae family such as *Enterobacter* species where their production is typically very low level and does not elicit any clinically relevant resistance but can be inducible during drug therapy. Nevertheless, the acquisition of transmissible plasmids from other bacteria can lead to the overproduction of AmpC β-lactamase in some organisms ordinarily lacking the gene encoding for chromosomal AmpC, for example, *K. pneumonia* [17]. The AmpC β-lactamases inactivate aztreonam, all penicillin, and most cephalosporins and are not susceptible to inhibition by most β-lactamases inhibitors except avibactam, a new non-β-lactam β-lactamase inhibitor antibiotic [4].

Ambler class D consists of a variety of enzymes, such as oxacillin hydrolyzing enzymes (OXA). The most common members of this class, such as OXA-11, OXA-14, and OXA-16, demonstrate ESBL properties and are normally found in *P. aeruginosa* [11, 18, 19]. OXA enzymes are classified as group 2d following the Bush-Jacoby scheme, and almost all of these enzymes, except OXA-18, are resistant to β-lactamase inhibitors [20]. Furthermore, OXA-type carbapenemases are commonly found in *Acinetobacter* spp. Specific *A. baumannii* carbapenem-hydrolyzing OXA enzymes, which have low catalytic efficiency, together with porin deletion and other antibiotic resistance mechanisms, can cause high resistance to carbapenems [21].

2.2. Modification of Drug Binding Sites. Some resistant bacteria avoid recognition by antimicrobial agents by modifying their target sites. The mutation of gene encoding for penicillin-binding proteins (PBPs), which are enzymes typically anchored on the cytoplasmic membrane of the bacterial cell wall and function in assembly and control of the latter stages of the cell wall building, results in the expression of unique penicillin-binding proteins, for example, the expression of a unique PBP2a in *S. aureus*, which is the most dominant PBP in the MRSA cell compared to the native PBPs (PBP1–4) [22]. PBP2a has low affinity for all β-lactam antibiotics and acts as a substitute for the other PBPs, thus enabling the survival of *S. aureus* in the presence of high concentrations of β-lactam drugs including methicillin acting on cell wall biosynthesis [23]. Bacterial cell wall synthesis in methicillin-resistant Gram-positive organisms can be inhibited by glycopeptides, which target acyl-D-alanyl-D-alanine (acyl D-Ala-D-Ala) residues of peptidoglycan precursors. However, by changing the peptidoglycan cross-link target (D-Ala-D-Ala to D-Ala-D-Lac or D-Ala-D-Ser), encoded by a complex gene cluster (*Van*-A, *Van*-B, *Van*-D, *Van*-C, *Van*-E, and *Van*-G), *E. faecium* and *E. faecalis* can

Table 1: Categorization of bacterial β-lactamase enzymes by the Bush-Jacoby and Ambler systems.

Classification		Antimicrobial agents	Enzymes	Description	ESKAPE pathogens
Bush-Jacoby	Ambler				
1	C	Narrow and extended-spectrum cephalosporins, including cephamycins	ACT-1, FOX-1, MIR-1, CMY	Cephalosporinases not inactivated by clavulanic acid	*Enterobacter* spp.
2a	A	Penicillins	PC1	Penicillinases inactivated by clavulanic acid	Enterobacteriaceae (e.g., *K. pneumoniae*, *Enterobacter* spp.) and nonfermenters (i.e., *P. aeruginosa*, *A. baumannii*)
2b	A	Penicillins, cephalothin	TEM-1, TEM-2, TEM-13, SHV-1, SHV-11	Broad-spectrum enzymes inactivated by clavulanic acid	
2be	A	Penicillins, oxyimino-cephalosporins (cefotaxime, ceftazidime, ceftriaxone, cefepime), monobactams	TEM-3, TEM-10, TEM-26, SHV-2, SHV-3, *Klebsiella oxytoca* K1, CTX-M, PER, VEB	Extended broad-spectrum enzymes inactivated by clavulanic acid	
2br	A	Penicillins, resistant to clavulanic acid, tazobactam, sulbactam	TEM-30, TEM-31, SHV-10, SHV-72	Broad-spectrum enzymes with reduced binding to clavulanic acid (inhibitor-resistant TEMs)	
2ber	A	Penicillins, oxyimino-cephalosporins, monobactams, resistant to clavulanic acid, tazobactam, sulbactam	TEM-50, TEM-158	Extended-spectrum enzymes with relative resistance to clavulanic acid	
2c	A	Penicillins, carbenicillin	PSE-1, CARB-3	Carbenicillin-hydrolyzing enzymes inactivated by clavulanic acid	
2ce	A	Carbenicillin, cefepime	RTG-4 (CARB-10)	Extended-spectrum carbenicillinase	
2d	D	Cloxacillin, oxacillin	OXA-1, OXA-2, OXA-10	Cloxacillin-hydrolyzing enzymes with variable inactivation by clavulanic acid	
2de	D	Cloxacillin, oxacillin, oxyimino-cephalosporins, monobactams	OXA-11, OXA-15		
2df	D	Cloxacillin, oxacillin, carbapenems	OXA-23, OXA-51, OXA-58		
2e	A	Cephalosporins	CepA	Cephalosporinases inactivated by clavulanic acid	
2f	A	All β-lactams, including carbapenems	KPC, SME, GES, IMI-1	Carbapenem-hydrolyzing non-metallo-β-lactamases	
3	B	All β-lactams, including carbapenems, with exception of monobactams	IMP, VIM, IND	Metallo-β-lactamases	
4	—	Penicillins	Penicillinases from *Burkholderia cepacia*	Penicillinases not inactivated by clavulanic acid	

— no classification in Ambler system.

increase their resistance to glycopeptides in current clinical use (vancomycin and teicoplanin) [6].

2.3. Reduced Intracellular Drug Accumulation. The balance of antibiotic uptake and elimination determines the susceptibility of bacteria to a particular drug. Thus, reducing the amount of antibiotic able to pass through the bacterial cell membrane is one strategy used by bacteria to develop antibiotic resistance. Mechanisms by which bacteria achieve this include the occurrence of diminished protein channels on the bacterial outer membrane to decrease drug entry and/or the presence of efflux pumps to decrease the amount of drug accumulated within the cells.

2.3.1. Porin Loss. The outer membranes of Gram-negative bacteria contain proteins called porins that form channels that allow the passage of many hydrophilic substances, including antibiotics. A reduction in the amount of *P. aeruginosa* porin protein OprD results in decreased drug influx into the cell, allowing the bacterium to develop resistance to imipenem [24]. Loss of a 29-kDa outer membrane protein (OMP) in other Gram-negative bacteria, such as *A. baumannii*, allows them to become insensitive to imipenem and meropenem drugs. Multiple-drug resistant *K. pneumoniae* strains also exhibit resistant/reduced susceptibility to β-lactams (such as cephalosporins and carbapenems) by the loss of outer membrane proteins known as OmpK35 and OmpK36 together with the production of resistance enzymes, including AmpC β-lactamase and new-generation carbapenemase A, KPC [21].

2.3.2. Efflux Pumps. To increase the removal of antibiotics from the intracellular compartment (or the intermembrane space in Gram-negative bacteria), some bacteria contain membrane proteins that function as exporters, called efflux pumps, for certain antimicrobial agents. These pumps expel the drug from the cell at a high rate, meaning that the drug concentrations are never sufficiently high to elicit an antibacterial effect. Most efflux pumps are multidrug transporters that efficiently pump a wide range of antibiotics, contributing to multidrug resistance. Up to date, there are five super families of efflux pumps that have been described. These include the ATP-binding cassette (ABC) family, the small multidrug resistance family, the major facilitator super family, the resistance-nodulation-division (RND) family, and the multidrug and toxic compound extrusion family [25].

The most common type of efflux pump in Gram-negative bacteria is the polyselective efflux pump, belonging to the RND superfamily, which plays a key role in the multidrug resistance (MDR) bacterial phenotype. This type of pump expels a variety of antibiotics and structurally unrelated molecules, such as dyes and bile salts, but also detergents and biocides that are frequently used in medical practice [26]. AcrAB-TolC and MexAB-OprM are multidrug efflux pumps typically belonging to the RND superfamily. They are usually chromosomally encoded. These two efflux pumps are essential for bacterial survival, particularly in the presence of toxic agents. *P. aeruginosa* contains a large number of efflux pumps, with four potent RND-type multidrug resistance efflux pumps (Mex) capable of eliminating toxic compounds from the periplasm and cytoplasm. Two of these efflux pumps, MexAB-OprM and MexCD-OprJ, are responsible for resistance to at least three main classes of antibiotics, namely, carbapenems, fluoroquinolones, and aminoglycosides [27, 28]. Studies have shown that overexpression of MexXY-OprM from *P. aeruginosa* results in resistance to aminoglycosides, fluoroquinolones, and specific antipseudomonal cephalosporins. Furthermore, many clinical *P. aeruginosa* isolates also express MexCD-OprJ and MexEF-OprN.

An increase in the prevalence of strains overproducing these efflux pumps has also been reported in *Enterobacter aerogenes* and *K. pneumoniae* clinical isolates. Overexpression of the AcrAB efflux pump, together with decreased expression of porins, is characteristic of imipenem-resistant *E. aerogenes* MDR strains. In these bacteria, the efflux pump also ejects other unrelated antibiotics, such as fluoroquinolones, tetracycline, and chloramphenicol. *A. baumannii* isolates can also demonstrate a MDR phenotype through the presence and overexpression of RND efflux pump AdeABC. This pump is associated with resistance to a broad range of antibiotics, including fluoroquinolones, β-lactams, tetracyclines (including tigecycline), macrolides/lincosamides, chloramphenicol, and aminoglycosides. Like *P. aeruginosa*, *A. baumannii* porins also show very low permeability. The RND-type efflux pumps AdeABC, AdeDE, AdeFGH, and AdeIJK play a role in resistance to aminoglycosides, fluoroquinolones, erythromycin, tetracycline, and chloramphenicol in all bacterial species reported to date. Finally, the synergistic effect of multidrug efflux pumps and the outer membrane barrier is important for resistance to many agents. For example, the main porin expressed by *P. aeruginosa* is OprF, which has much lower permeability than *E. coli* OmpF, making the efflux pump activity more effective in resistant strains [26].

2.4. Biofilm Formation. Biofilms are complex microbial communities living as a thin layer on biotic or abiotic surfaces, implanted in a matrix of extracellular polymeric substances created by the biofilms themselves. Microorganisms within the biofilm can interact with each other, as well as the environment. The major component of the matrix is secreted extracellular polymeric substances, mainly consisting of polysaccharides, proteins, lipids, and extracellular DNA from the microbes [29]. There are three key steps for biofilm formation. The first step is adhesion, which occurs as cells reach a surface and anchor to the site. The second step is growth and maturation, which happens as the microbes begin to generate the exopolysaccharide that establishes the matrix and then mature from microcolonies to multilayered cell bunches. The final step is detachment, which can be divided into two types: active and passive. Active detachment is initiated by bacteria themselves, for example, by quorum sensing and enzymatic degradation of the biofilm matrix. In contrast, passive detachment is caused by external forces, such as fluid shear, scraping, and human intervention [30].

It could be argued that the main causes of antimicrobial resistance are not classical drug resistance mechanisms, that is, efflux pumps, target site modification, or enzymatic

degradation. It is likely that the matrix of biofilms provides a mechanical and biochemical shield that provides the conditions needed to attenuate the activity of the drugs (e.g., low O_2, low pH, high CO_2, and low water availability). Under these conditions it is difficult to eliminate bacteria using conventional antibiotics. Moreover, when the bacteria experience nutrient scarcity, they could become tolerant to antibiotics. This may explain the apparent greater antibiotic resistance of cells in the deep layers of a biofilm (bacteria extracted from the biofilms and grown in broth recover their full susceptibility, indicating that the resistance is phenotypic and not genotypic) [31]. The most common pathogens found in biofilms in a healthcare setting are *S. aureus*, *P. aeruginosa*, *A. baumannii*, and *K. pneumonia* [32].

3. Antibiotic Resistance in ESKAPE Pathogens

3.1. Enterococcus faecium. *Enterococcus* species were formerly classified as part of the genus *Streptococcus*. They are Gram-positive facultative anaerobes, which are often found in pairs or chains. Their normal habitat is the gut of humans and animals. There are more than 20 *Enterococcus* species, but *Enterococcus faecium* and *Enterococcus faecalis* are the most clinically relevant. Most *Enterococcus* infections are endogenously acquired, but cross-infection may occur in hospitalized patients [33]. Over the past decade, some reports have revealed a rise in ampicillin- and vancomycin-resistant enterococcal infections in healthcare facilities. For instance, in Netherlands, the average number of invasive ampicillin-resistant enterococcal infections in university hospitals escalated from approximately 10 infections in 1999 to 50 infections in 2005 per hospital [34]. Rates of antimicrobial resistance amongst enterococci are particularly concerning, especially the incidence of vancomycin-resistant *Enterococcus* (VRE), which is mainly associated with *E. faecium*. VRE emerged in North America during the late 1980s, with 61% of *E. faecium* isolates estimated to be vancomycin resistant by 2002. While the incidence of VRE is much lower in European countries, including Ireland and the United Kingdom, a survey by the British Society for Antimicrobial Chemotherapy from 2001 to 2006 found that the incidence of VRE in Europe had risen from approximately 20% to more than 30% [35, 36]. Despite the high global rates of VRE, there is some geographical variation. There are six types of VRE (Van-A–E and Van-G), with *van-A* being the most prevalent and showing the highest levels of resistance to all glycopeptide antibiotics [37]. In 2011, Galloway-Pena and her colleagues demonstrated two diverse clades of *E. faecium* which differ genetically. Clade A clinical isolates were found to associate predominantly with hospitals, whereas clade B isolates were associated with community origin. Both clades express low-affinity penicillin-binding proteins (called PBP5) which bind weakly to β-lactam drugs. In addition, clade A has acquired several virulence determinants and resistance genes from the presence of insertion sequence 16 (IS16) and a gene encoding the ampicillin-resistant PBP5 (pbp5R) while clade B has been shown to have a gene encoding for ampicillin-sensitive PBP5 (pbp5S) [38].

3.2. Staphylococcus aureus. *S. aureus* is a Gram-positive coccal bacterium, with cells arranged in characteristic grape-like clusters. With nonfastidious growth requirements, *S. aureus* is part of the normal skin flora, especially of the nose and perineum of humans and animals. Carriage rates are high in the general population, and transmission can occur by direct contact or airborne routes. Traditionally, infections caused by *Staphylococcus* species have responded well to penicillin treatment; however, excessive use of these antibiotics led to the emergence of β-lactamase-producing *Staphylococcus* isolates in 1948, with 65–85% of staphylococcal clinical isolates now also resistant to penicillin G. In two decades, the incident of β-lactamase-producing *Staphylococcus* species increased more than 80% in both community and hospital associated infections as reported by Bodonakik et al., 1984; Appelbaum and Brown, 2007; and Wu et al., 2010 [39–42]. Reports of methicillin-resistant *Staphylococcus aureus* (MRSA) emerged in the 1960s, and currently, MRSA isolates are estimated to account for 25% of *S. aureus* isolates, with a prevalence of up to 50% or more in some areas. Researchers from the Prince of Songkhla Hospital, Prasat Neurological Institute, and Hospital for Tropical Diseases, Thailand, studied the prevalence of methicillin resistance amongst 92 clinical *S. aureus* isolates. Of these isolates, 60.9% were MRSA, and all were sensitive to vancomycin [43]. Tackling the problem of MRSA is a top priority for public health systems worldwide, with much current research focused on future intervention strategies.

In most cases, glycopeptide antibiotics, for example, vancomycin and teicoplanin, are used as first-line antibiotics for treatment of MRSA infections. However, the selective pressure of these antibiotics has induced some strains to become intermediate-susceptible to vancomycin *in vitro*, with cases of clinical vancomycin-intermediate and vancomycin-resistant *S. aureus* (VISA and VRSA, resp.) becoming more common [44]. Unfortunately, most VISA isolates are also less susceptible to teicoplanin, with the term glycopeptide-intermediate *S. aureus* used to identify these isolates. VISA was first reported in Japan in the mid-1990s, and the strains have now emerged in other countries across Asia, the USA, and Europe. VRSA is of particular concern because of the interspecies exchange of genetic resistance genes from VRE. VRSA isolates contain both the *van-A* and *mec-A* resistance determinants of VRE and MRSA, which result in resistance to multiple drugs, including methicillin and vancomycin [45].

3.3. Klebsiella pneumonia. *K. pneumoniae* is a member of the family Enterobacteriaceae. It is a nonfastidious, Gram-negative bacillus, which is usually encapsulated. Species of the genus *Klebsiella* are the bacterial pathogens most often found associated with infections in healthcare settings and infections may be endogenous or acquired through direct contact with an infected host. In recent years, many *K. pneumoniae* strains have acquired a massive variety of β-lactamase enzymes, which can destroy the chemical structure of β-lactam antibiotics such as penicillins, cephalosporins, and carbapenems. Because carbapenems are conventionally used to treat persistent infections caused by Gram-negative bacteria, the increasing prevalence of carbapenem-resistant

K. pneumoniae (CRKP), with resistance encoded by bla_{KPC}, presents a significant challenge for physicians [46, 47]. In addition, the emergence of the *K. pneumoniae* super enzyme, known as NDM-1 and encoded by bla_{NDM-1}, has increased the proportion of carbapenem-resistant *K. pneumoniae* isolates and may pose a threat to other antibiotics such as β-lactams, aminoglycosides, and fluoroquinolones [15, 16]. Even if several intensive infection control practices are used, outbreaks of carbapenemase-mediated multidrug resistant (MDR) strains are only reduced and cannot be completely eradicated. An effective treatment is therefore needed to overcome these pathogens.

3.4. Acinetobacter baumannii. Acinetobacter species are widely distributed in the environment and readily contaminate the hospital environment. The most important human pathogen is *A. baumannii*, which has a relatively long survival time on human hands, which can lead to high rates of cross contamination in nosocomial infections [48]. *A. baumannii* is a nonfermentative Gram-negative coccobacillus and causes infections at a variety of sites, including the respiratory and urinary tracts. Strains are frequently antibiotic resistant, which is a particular problem in surgical wards and intensive care units [49]. Recently, the emergence of carbapenemase-producing *A. baumannii* strains carrying imipenem metallo-β-lactamases, encoded by bla_{IMP}, and oxacillinase serine β-lactamases, encoded by bla_{OXA}, has been reported. These strains show resistance to both colistin and imipenem, and the combination of resistance genes makes them capable of evading the action of most traditional antibiotic compounds [50, 51].

3.5. Pseudomonas aeruginosa. P. aeruginosa is a Gram-negative, rod-shaped, facultative anaerobe that is part of the normal gut flora. Carriage rates are fairly low in the general population but are higher in hospital inpatients, especially immunocompromised hosts. Patients become infected through an exogenous source, such as by direct/indirect contact with the environment, but endogenous sources are also possible. Many *P. aeruginosa* strains show an intrinsic reduced susceptibility to several antibacterial agents, as well as a propensity to develop resistance during therapy especially in carbapenem-resistant (chiefly imipenem) strains. The most common mechanism of imipenem resistance in *P. aeruginosa* is a combination of chromosomal AmpC production and porin change. Indeed, low level of AmpC enzymes production does not result in high-level carbapenem resistance due to their low potential to hydrolyze carbapenem drugs but their overproduction together with reduced outer membrane porin permeability and/or efflux pump overexpression contribute to high-level carbapenem resistance in this pathogen [24, 33]. *P. aeruginosa* also produces ESBLs and can harbor other antibiotic resistance enzymes such as *K. pneumoniae* carbapenemases (KPC), VIM encoded by bla_{VIM}, and imipenem metallo-β-lactamases. The combination of these enzymes leads to high rates of carbapenem resistance amongst *P. aeruginosa* isolates and also to the emergence of fluoroquinolone-resistant strains as the corresponding mechanisms of resistance may be carried by the same plasmid [46, 52]. The continuous increase of MDR isolates presents a complicated situation for antimicrobial therapy; however, colistin is still effective in most cases [51].

3.6. Enterobacter spp. Enterobacter species are nonfastidious Gram-negative rods that are sometimes encapsulated. They can cause opportunistic infections in immunocompromised, usually hospitalized, patients and contain a wide range of antibiotic resistance mechanisms. Many *Enterobacter* strains contain ESBLs and carbapenemases, including VIM, OXA, metallo-β-lactamase-1, and KPC [53]. Furthermore, stable derepression of the AmpC β-lactamases that can be expressed at high levels by mutation in this bacterial group is important also. These MDR strains are resistant to almost all available antimicrobial drugs, except tigecycline and colistin [51].

In conclusion, nosocomial ESKAPE bacteria represent paradigms of resistance, pathogenesis, and disease transmission. There are a range of antimicrobial resistance mechanisms used by the nosocomial ESKAPE pathogens, including enzymatic inactivation, modification of drug targets, changing cell permeability through porin loss or increase in expression of efflux pumps, and mechanical protection provided by biofilm formation. Antimicrobial resistance in these pathogens is a major menace to public health systems worldwide and seems likely to increase in the near future as resistance profiles change. This results in the dearth of potential therapeutic agents in the pipeline that causes real concerns but should trigger research and development of new antibiotics or new approaches to control the infections they cause. In this context, there are current research efforts which are focused on the introduction of new therapeutic schemes to circumvent these pathogens, including antivirulence strategies, bacteriophage therapy, probiotics, therapeutic antibodies, synthetic inhibitors specific to resistance enzymes or bacterial efflux pumps, and inhibition of biofilm formation. These novel tools provide hope for prevention and treatment of infectious diseases caused by these ESKAPE organisms.

Competing Interests

The authors have declared that no competing interests exist.

Acknowledgments

The work was supported by the National Research University (NRU) project of the Office of the Commission on Higher Education, Ministry of Education, Thailand, through the Center of Biopharmaceutical Development and Innovative Therapy, Mahidol University, Thailand. Sirijan Santajit is a scholar of Royal Golden Jubilee (RGJ) grant and Nitaya Indrawattana is a scholar of the RSA grant of the Thailand Research Fund.

References

[1] S. S. Magill, J. R. Edwards, W. Bamberg et al., "Multistate point-prevalence survey of health care-associated infections," *The New England Journal of Medicine*, vol. 370, no. 13, pp. 1198–1208, 2014.

[2] R. M. Klevens, J. R. Edwards, C. L. Richards Jr. et al., "Estimating health care-associated infections and deaths in U.S. Hospitals, 2002," *Public Health Reports*, vol. 122, no. 2, pp. 160–166, 2007.

[3] L. B. Rice, "Federal funding for the study of antimicrobial resistance in nosocomial pathogens: no ESKAPE," *Journal of Infectious Diseases*, vol. 197, no. 8, pp. 1079–1081, 2008.

[4] K. Bush and G. A. Jacoby, "Updated functional classification of β-lactamases," *Antimicrobial Agents and Chemotherapy*, vol. 54, no. 3, pp. 969–976, 2010.

[5] L. B. Rice, "Progress and challenges in implementing the research on ESKAPE pathogens," *Infection Control and Hospital Epidemiology*, vol. 31, supplement 1, pp. S7–S10, 2010.

[6] A. Giedraitienė, A. Vitkauskienė, R. Naginienė, and A. Pavilonis, "Antibiotic resistance mechanisms of clinically important bacteria," *Medicina*, vol. 47, no. 3, pp. 137–146, 2011.

[7] G. D. Wright, "Bacterial resistance to antibiotics: enzymatic degradation and modification," *Advanced Drug Delivery Reviews*, vol. 57, no. 10, pp. 1451–1470, 2005.

[8] X.-Z. Li and H. Nikaido, "Efflux-mediated drug resistance in bacteria," *Drugs*, vol. 64, no. 2, pp. 159–204, 2004.

[9] D. N. Wilson, "Ribosome-targeting antibiotics and mechanisms of bacterial resistance," *Nature Reviews Microbiology*, vol. 12, no. 1, pp. 35–48, 2014.

[10] G. A. Jacoby and L. S. Munoz-Price, "The new beta-lactamases," *The New England Journal of medicine*, vol. 352, no. 4, pp. 380–391, 2005.

[11] S. Džidić, J. Šušković, and B. Kos, "Antibiotic resistance mechanisms in bacteria: biochemical and genetic aspects," *Food Technology and Biotechnology*, vol. 46, no. 1, pp. 11–21, 2008.

[12] W.-H. Zhao and Z.-Q. Hu, "Epidemiology and genetics of CTX-M extended-spectrum β-lactamases in Gram-negative bacteria," *Critical Reviews in Microbiology*, vol. 39, no. 1, pp. 79–101, 2013.

[13] R. Bonnet, "Growing group of extended-spectrum β-lactamases: The CTX-M Enzymes," *Antimicrobial Agents and Chemotherapy*, vol. 48, no. 1, pp. 1–14, 2004.

[14] M. Babic, A. M. Hujer, and R. A. Bonomo, "What's new in antibiotic resistance? Focus on beta-lactamases," *Drug Resistance Updates*, vol. 9, no. 3, pp. 142–156, 2006.

[15] K. K. Kumarasamy, M. A. Toleman, T. R. Walsh et al., "Emergence of a new antibiotic resistance mechanism in India, Pakistan, and the UK: a molecular, biological, and epidemiological study," *The Lancet Infectious Diseases*, vol. 10, no. 9, pp. 597–602, 2010.

[16] D. Yong, M. A. Toleman, C. G. Giske et al., "Characterization of a new metallo-β-lactamase gene, *bla* NDM-1, and a novel erythromycin esterase gene carried on a unique genetic structure in *Klebsiella pneumoniae* sequence type 14 from India," *Antimicrobial Agents and Chemotherapy*, vol. 53, no. 12, pp. 5046–5054, 2009.

[17] G. A. Jacoby, "AmpC β-lactamases," *Clinical Microbiology Reviews*, vol. 22, no. 1, pp. 161–182, 2009.

[18] L. M. C. Hall, D. M. Livermore, D. Gur, M. Akova, and H. E. Akalin, "OXA-11, an extended-spectrum variant of OXA-10 (PSE-2) β-lactamase from *Pseudomonas aeruginosa*," *Antimicrobial Agents and Chemotherapy*, vol. 37, no. 8, pp. 1637–1644, 1993.

[19] F. Danel, L. M. C. Hall, D. Gur, and D. M. Livermore, "OXA-14, another extended-spectrum variant of OXA-10 (PSE-2) β-lactamase from *Pseudomonas aeruginosa*," *Antimicrobial Agents and Chemotherapy*, vol. 39, no. 8, pp. 1881–1884, 1995.

[20] L. N. Philippon, T. Naas, A.-T. Bouthors, V. Barakett, and P. Nordmann, "OXA-18, a class D clavulanic acid-inhibited extended-spectrum β-lactamase from *Pseudomonas aeruginosa*," *Antimicrobial Agents and Chemotherapy*, vol. 41, no. 10, pp. 2188–2195, 1997.

[21] J. M. Thomson and R. A. Bonomo, "The threat of antibiotic resistance in Gram-negative pathogenic bacteria: β-lactams in peril!," *Current Opinion in Microbiology*, vol. 8, no. 5, pp. 518–524, 2005.

[22] M. J. Pucci and T. J. Dougherty, "Direct quantitation of the numbers of individual penicillin-binding proteins per cell in *Staphylococcus aureus*," *Journal of Bacteriology*, vol. 184, no. 2, pp. 588–591, 2002.

[23] S. S. Tang, A. Apisarnthanarak, and L. Y. Hsu, "Mechanisms of β-lactam antimicrobial resistance and epidemiology of major community- and healthcare-associated multidrug-resistant bacteria," *Advanced Drug Delivery Reviews*, vol. 78, pp. 3–13, 2014.

[24] T. Fukuoka, S. Ohya, T. Narita et al., "Activity of the carbapenem panipenem and role of the OprD (D2) protein in its diffusion through the *Pseudomonas aeruginosa* outer membrane," *Antimicrobial Agents and Chemotherapy*, vol. 37, no. 2, pp. 322–327, 1993.

[25] J. Sun, Z. Deng, and A. Yan, "Bacterial multidrug efflux pumps: mechanisms, physiology and pharmacological exploitations," *Biochemical and Biophysical Research Communications*, vol. 453, no. 2, pp. 254–267, 2014.

[26] H. Nikaido and J.-M. Pagès, "Broad-specificity efflux pumps and their role in multidrug resistance of Gram-negative bacteria," *FEMS Microbiology Reviews*, vol. 36, no. 2, pp. 340–363, 2012.

[27] H. P. Schweizer, "Efflux as a mechanism of resistance to antimicrobials in *Pseudomonas aeruginosa* and related bacteria: unanswered questions," *Genetics and Molecular Research*, vol. 2, no. 1, pp. 48–62, 2003.

[28] H. Vaez, J. Faghri, B. N. Isfahani et al., "Efflux pump regulatory genes mutations in multidrug resistance *Pseudomonas aeruginosa* isolated from wound infections in Isfahan hospitals," *Advanced Biomedical Research*, vol. 3, article 117, 2014.

[29] G. Sharma, S. Rao, A. Bansal, S. Dang, S. Gupta, and R. Gabrani, "*Pseudomonas aeruginosa* biofilm: potential therapeutic targets," *Biologicals*, vol. 42, no. 1, pp. 1–7, 2014.

[30] G. Laverty, S. P. Gorman, and B. F. Gilmore, "Biomolecular mechanisms of *Pseudomonas aeruginosa* and *Escherichia coli* biofilm formation," *Pathogens*, vol. 3, no. 3, pp. 596–632, 2014.

[31] J. L. del Pozo and R. Patel, "The challenge of treating biofilm-associated bacterial infections," *Clinical Pharmacology and Therapeutics*, vol. 82, no. 2, pp. 204–209, 2007.

[32] N. Høiby, T. Bjarnsholt, M. Givskov, S. Molin, and O. Ciofu, "Antibiotic resistance of bacterial biofilms," *International Journal of Antimicrobial Agents*, vol. 35, no. 4, pp. 322–332, 2010.

[33] H.-A. Elsner, I. Sobottka, D. Mack, M. Claussen, R. Laufs, and R. Wirth, "Virulence factors of *Enterococcus faecalis* and *Enterococcus faecium* blood culture isolates," *European Journal of Clinical Microbiology and Infectious Diseases*, vol. 19, no. 1, pp. 39–42, 2000.

[34] J. Top, R. Willems, S. van der Velden, M. Asbroek, and M. Bonten, "Emergence of clonal complex 17 *Enterococcus faecium* in the Netherlands," *Journal of Clinical Microbiology*, vol. 46, no. 1, pp. 214–219, 2008.

[35] A. H. C. Uttley, N. Woodford, A. P. Johnson et al., "Vancomycin-resistant enterococci," *The Lancet*, vol. 342, no. 8871, pp. 615–617, 1993.

[36] R. Hope, D. M. Livermore, G. Brick, M. Lillie, and R. Reynolds, "BSAC working parties on resistance surveillance non-susceptibility trends among staphylococci from bacteraemias in the UK and Ireland, 2001–06," *Journal of Antimicrobial Chemotherapy*, vol. 62, supplement 2, pp. 165–174, 2001.

[37] A. Smith, "Bacterial resistance to antibiotics," in *Hugo and Russell's Pharmaceutical Microbiology*, pp. 220–232, John Wiley & Sons, 2009.

[38] C. A. Arias and B. E. Murray, "The rise of the *Enterococcus*: beyond vancomycin resistance," *Nature Reviews Microbiology*, vol. 10, no. 4, pp. 266–278, 2012.

[39] N. C. Bodonaktik, S. D. King, and V. R. Narla, "Antimicrobial resistance in clinical isolates of *Staphylococcus aureus* at the University Hospital of the West Indies," *The West Indian Medical Journal*, vol. 33, no. 1, pp. 8–13, 1984.

[40] P. C. Appelbaum, "Microbiology of antibiotic resistance in *Staphylococcus aureus*," *Clinical Infectious Diseases*, vol. 45, no. 3, pp. S165–S170, 2007.

[41] P. D. Brown and C. Ngeno, "Antimicrobial resistance in clinical isolates of *Staphylococcus aureus* from hospital and community sources in southern Jamaica," *International Journal of Infectious Diseases*, vol. 11, no. 3, pp. 220–225, 2007.

[42] D. Wu, Q. Wang, Y. Yang et al., "Epidemiology and molecular characteristics of community-associated methicillin-resistant and methicillin-susceptible *Staphylococcus aureus* from skin/soft tissue infections in a children's hospital in Beijing, China," *Diagnostic Microbiology and Infectious Disease*, vol. 67, no. 1, pp. 1–8, 2010.

[43] N. Indrawattana, O. Sungkhachat, N. Sookrung et al., "*Staphylococcus aureus* clinical isolates: antibiotic susceptibility, molecular characteristics, and ability to form biofilm," *BioMed Research International*, vol. 2013, Article ID 314654, 11 pages, 2013.

[44] H. F. Chambers and F. R. DeLeo, "Waves of resistance: *Staphylococcus aureus* in the antibiotic era," *Nature Reviews Microbiology*, vol. 7, no. 9, pp. 629–641, 2009.

[45] P. C. Appelbaum, "Reduced glycopeptide susceptibility in methicillin-resistant *Staphylococcus aureus* (MRSA)," *International Journal of Antimicrobial Agents*, vol. 30, no. 5, pp. 398–408, 2007.

[46] K. Bush, G. A. Jacoby, and A. A. Medeiros, "A functional classification scheme for β-lactamases and its correlation with molecular structure," *Antimicrobial Agents and Chemotherapy*, vol. 39, no. 6, pp. 1211–1233, 1995.

[47] A. M. Queenan and K. Bush, "Carbapenemases: the versatile β-lactamases," *Clinical Microbiology Reviews*, vol. 20, no. 3, pp. 440–458, 2007.

[48] E. T. S. Houang, R. T. Sormunen, L. Lai, C. Y. Chan, and A. S.-Y. Leong, "Effect of desiccation on the ultrastructural appearances of *Acinetobacter baumannii* and *Acinetobacter lwoffii*," *Journal of Clinical Pathology*, vol. 51, no. 10, pp. 786–788, 1998.

[49] M. Biendo, G. Laurans, J. F. Lefebvre, F. Daoudi, and F. Eb, "Epidemiological study of an *Acinetobacter baumannii* outbreak by using a combination of antibiotyping and ribotyping," *Journal of Clinical Microbiology*, vol. 37, no. 7, pp. 2170–2175, 1999.

[50] J. Vila, S. Martí, and J. Sánchez-Céspedes, "Porins, efflux pumps and multidrug resistance in *Acinetobacter baumannii*," *Journal of Antimicrobial Chemotherapy*, vol. 59, no. 6, pp. 1210–1215, 2007.

[51] H. W. Boucher, G. H. Talbot, J. S. Bradley et al., "Bad bugs, no drugs: no ESKAPE! An update from the Infectious Diseases Society of America," *Clinical Infectious Diseases*, vol. 48, no. 1, pp. 1–12, 2009.

[52] D. M. Livermore, "Multiple mechanisms of antimicrobial resistance in *Pseudomonas aeruginosa*: our worst nightmare?" *Clinical Infectious Diseases*, vol. 34, no. 5, pp. 634–640, 2002.

[53] M. Castanheira, L. M. Deshpande, D. Mathai, J. M. Bell, R. N. Jones, and R. E. Mendes, "Early dissemination of NDM-1- and OXA-181-producing *Enterobacteriaceae* in Indian hospitals: Report from the SENTRY Antimicrobial Surveillance Program, 2006-2007," *Antimicrobial Agents and Chemotherapy*, vol. 55, no. 3, pp. 1274–1278, 2011.